National Research
Council Canada

Conseil national
de recherches Canada

NRC · CNRC

Canadian Journal of Fisheries and Aquatic Sciences

Journal canadien des sciences halieutiques et aquatiques

ISSN 0706-652X / CJFSDX 52(10) 2063–2304 (1995)

The *Canadian Journal of Fisheries and Aquatic Sciences*, previously published as *Contributions to Canadian Biology* 1901–1925, *Contributions to Canadian Biology and Fisheries* 1926–1934, *Journal of the Biological Board of Canada* 1934–1937, and *Journal of the Fisheries Research Board of Canada* 1938–1979, is issued monthly to form annual volumes of 12 numbers plus Supplements.

Editorial policy: The *Journal* publishes original research articles, critical reviews, perspectives (essays of opinion or hypothesis), and comments. Papers may concern cells, organisms, populations, ecosystems, or processes that affect aquatic production systems, and they should lead to identifiable conclusions or synthesis, which variously may amplify, modify, question, or redirect accumulated knowledge embodied in contemporary perceptions of a particular state of fisheries and aquatic sciences. They should demonstrate clearly a contribution to knowledge beyond the confirmation state. Originality should relate to more than the particular (a certain year, place, taxon, or chemical compound) such that existing understanding is reformulated or extended.

Manuscripts for publication should be submitted to **Dr. D.G. Cook**, Canadian Journal of Fisheries and Aquatic Sciences, NRC Research Press, National Research Council of Canada, Ottawa, ON K1A 0R6, Canada (613-993-2209; fax: 613-952-7656; e-mail: cjfas@journals.lan.nrc.ca).

Submissions in English or French are acceptable. The information must be original, that is, not copyrighted, published, or submitted elsewhere except in abstract form or unless by written consent of the Editor. NRC accepts no responsibility for statements or opinions expressed by a contributor. Acceptance of an advertisement, announcement, or other material does not imply endorsement by either the *Journal*'s Editors or NRC. The use of proprietary names does not imply endorsement of the product or company.

Correspondence concerning accepted manuscripts and corrected proofs should be sent to NRC Research Press, National Research Council of Canada, Ottawa, ON K1A 0R6, Canada.

Instructions to Authors are published once a year in the first issue of each volume; copies can be obtained from the Publishing Office.

Microfilm: Issues from 1934 through the current volume can be purchased on 16- or 35-mm microfilm. Photocopies of individual articles or issues can be purchased from University Microfilms International, 330 North Zeeb Road, Ann Arbor, MI 48106, U.S.A.

Publié sans interruption depuis 1901, le *Journal canadien des sciences halieutiques et aquatiques* a paru sous plusieurs titres : *Contributions to Canadian Biology* 1901–1925, *Contributions to Canadian Biology and Fisheries* 1926–1934, *Journal of the Biological Board of Canada* 1934–1937, et *Journal of the Fisheries Research Board of Canada* 1938–1979. Le *Journal* paraît tous les mois, formant ainsi un volume de 12 numéros, et offre en plus jusqu'à deux suppléments par année.

Politique de rédaction : Le *Journal* publie des articles fondés sur une recherche originale, des critiques, des essais portant sur une opinion ou une hypothèse (perspectives) et des commentaires. Les textes peuvent avoir trait aux cellules, aux organismes, aux populations, aux écosystèmes ou aux processus qui influent sur les systèmes de production aquatique. Ils doivent aboutir à des conclusions ou synthèses précises qui, de diverses façons, peuvent accroître, modifier, remettre en question ou réorienter le bagage actuel des connaissances et perceptions dans une discipline donnée des sciences aquatiques. Ils doivent clairement démontrer qu'ils contribuent aux connaissances en faisant plus que corroborer des faits. L'originalité doit dépasser le caractère particulier (une année, un endroit, un taxon ou un composé chimique donné) et tenir à une épuration ou à une reformulation des connaissances actuelles.

Les auteurs doivent adresser leurs **manuscrits** à **D.G. Cook**, Journal canadien des sciences halieutiques et aquatiques, Presses scientifiques du CNRC, Conseil national de recherches du Canada, Ottawa, ON K1A 0R6, Canada (613-993-2209); télécopieur : 613-952-7656; courrier électronique : cjfas@journals.lan.nrc.ca).

Les contributions peuvent être en anglais ou en français. Elles doivent être originales, c.-à.-d. qu'elles ne doivent pas avoir fait l'objet d'un copyright, avoir été publiées ou soumises ailleurs, sauf sous forme abrégée ou avec le consentement du rédacteur. Le CNRC ne se tient en aucune façon responsable des opinions exprimées par un collaborateur ou des déclarations que pourrait faire ce dernier. La publication d'annonces publicitaires, d'avis et autres n'implique pas l'endossement de leur contenu par les directeurs du *Journal* ou du CNRC. L'utilisation des noms de marques de commerce ne signifie aucunement une sanction du produit en question ou de la compagnie qui le fabrique.

La correspondance ayant trait aux manuscrits acceptés et les **épreuves corrigées** doivent être envoyées aux Presses scientifiques du CNRC, Conseil national de recherches du Canada, Ottawa, ON K1A 0R6, Canada.

Des recommandations aux auteurs sont publiées une fois par année dans le premier numéro de chaque volume. On peut s'en procurer une copie, sur demande, au Bureau des publications.

Microfilms : On peut acheter sur microfilms de 16 ou 35 mm tous les numéros parus depuis 1934. Des photocopies d'articles ou de numéros individuels sont aussi en vente auprès de University Microfilms International, 330 North Zeeb Road, Ann Arbor, MI 48106, É.-U.

U.S. second-class postage paid at Champlain, N.Y., and at additional mailing offices. U.S. POSTMASTER: Send address changes to **Canadian Journal of Fisheries and Aquatic Sciences**, c/o USACAN Media Distribution Center, P.O. Box 2888, Plattsburg, NY 12901, U.S.A.

Courrier de seconde classe des É.-U. payé à Champlain, N.Y., et d'autres centres de courrier. MAÎTRE DE POSTE des É.-U. : Faire parvenir les corrections d'adresse à **Journal canadien des sciences halieutiques et aquatiques**, a/s du Service de distribution médias USACAN Inc., C.P. 2888, Plattsburg, NY 12901, É.-U.

Volume 52, Number 10, October 1995

Canadian Journal of Fisheries and Aquatic Sciences

Published by the National Research Council of Canada

Volume 52, numéro 10, octobre 1995

Journal canadien des sciences halieutiques et aquatiques

Publié par le Conseil national de recherches du Canada

Editor / directeur scientifique D.G. Cook
Assistant to the Editor / adjointe au directeur scientifique **M.M. Milne**
Consulting Editor / rédacteur-conseil **P.E.K. Symons** (Victoria, B.C.)
Consulting Editor / rédactrice-conseil **N. Moir** (Nepean, Ont.)

Editorial Board / conseil de rédaction
S.E. Campana, *DFO/MPO, Dartmouth*
E.M.P. Chadwick, *DFO/MPO, Moncton*
L.M. Dickie, *DFO/MPO, Dartmouth*
G.S. Jamieson, *DFO/MPO, Nanaimo*
J.R.M. Kelso, *DFO/MPO, Sault Ste. Marie*
J.D. Neilson, *DFO/MPO, St. Andrews*
L.S. Parsons, *DFO/MPO, Ottawa*
R.M. Peterman, *Simon Fraser University*
J.C. Roff, *University of Guelph*
D.M. Rosenberg, *DFO/MPO, Winnipeg*
P. Schwinghamer, *DFO/MPO, St. John's*
(Deputy editor / rédacteur adjoint)
C.J. Walters, *University of British Columbia*
W.G. Warren, *DFO/MPO, St. John's*
N.H.F. Watson, *DFO/MPO, Halifax*

NRC Research Press / Presses scientifiques du CNRC
Editor-in-chief / directeur général **Bruce P. Dancik**
Assistant Editor-in-chief / directeur général adjoint **Iain E.P. Taylor**

Publishing Office / Bureau des publications
(Fax / télécopieur : 613-952-7656; e-mail / courrier électronique : research.journals@nrc.ca;
URL : http://www.cisti.nrc.ca/cisti/journals/)
Director / directrice **Aldyth Holmes**
Business Manager / gestionnaire des affaires **Paul McClymont**
Production Manager / gestionnaire de la production **Susan R. Strahlendorf**
Senior Publication Officer / agent principal de publication **Mike Boroczki**
Publication Officers / agentes de publication **Jennifer Douglas, Sharon Smith**
Advertising / annonces publicitaires **Hoda Jabbour (613-993-9085)**
Reprints / tirés à part **Eileen Fink (613-993-0151)**
Subscriptions / abonnements **Helen Goulet (613-993-9084)**

© National Research Council of Canada 1995. All rights reserved.

No part of this publication may be reproduced, stored, or transmitted in any form or by any means, without the written permission of the publisher, except as stated below.

The National Research Council of Canada grants permission to individuals to make single copies of articles for personal use. Any person may reproduce short excerpts from articles in the journal for any purpose that respects the moral rights of authors, provided that the source is fully acknowledged. As a courtesy, the consent of authors of such material should be obtained directly from the author.

Authorization to reproduce items for other than personal use, as stated above, is granted by the National Research Council of Canada provided that the copyright fee of $3.00 per copy is paid directly to the Copyright Clearance Center (CCC) Transactional Reporting Service, 21 Congress Street, Salem, MA 01970, U.S.A. 0315-1468/95.

The above permission does not extend to other kinds of copying, such as copying for general distribution, for advertising, or promotional purposes, for creating new collective works, or for resale. For such copying, arrangements must be made with the publisher, National Research Council of Canada, Ottawa, ON K1A 0R6, Canada.

© Conseil national de recherches du Canada 1995. Tous droits réservés.

Il est interdit de reproduire, de sauvegarder ou de transmettre quelque partie de la présente publication dans quelque format ou de quelque façon sans le consentement écrit de l'éditeur, à l'exception des conditions suivantes.

Le Conseil national de recherches du Canada accorde aux particuliers le droit de faire des copies individuelles pour leur usage personnel. Toute personne peut reproduire de courts extraits des articles de la Revue pour autant que les droits moraux de l'auteur soient respectés et que la mention de provenance soit clairement indiquée. Il est de convenance de demander le consentement de l'auteur avant de faire mention de son travail.

On obtiendra l'autorisation de reproduire des articles à d'autres fins que l'usage personnel (tel qu'on l'a décrit ci-dessus) auprès du Conseil national de recherches du Canada pour autant que des redevances de droits d'auteurs de 3,00 $/copie soient versées au Copyright Clearance Center (CCC) Tranactional Reporting Service, 21 Congress Street, Salem, MA 01970, U.S.A. 0315-1468/95.

La permissoin ci-dessus ne s'applique pas à la reproduction à grande échelle, telle que la reproduction aux fins de distribution générale, publicitaire ou promotionnelle, de compilation de nouveaux ouvrages collectifs ou de revente. Dans de tels cas, il faudra ratifier une entente particulière avec l'éditeur, le Conseil national de recherches du Canada, Ottawa, ON K1A 0R6, Canada.

This journal is indexed or abstracted in / Ce journal est signalé ou résumé dans
Aquatic Sciences and Fisheries Abstracts, Biological & Agricultural Index, CAB Abstracts (Centre for Agriculture and Biosciences), Chemical Abstracts, Current Awareness in Biological Sciences, Current Contents, FAO Freshwater and Aquaculture Contents Tables, FAO Marine Science Contents Tables, Geo Abstracts, GEOBASE, Meteorological and Geoastrophysical Abstracts, Oceanic Abstracts, and Science Citation Index

The influence of error on population estimates from catch-age models

Jon T. Schnute and Laura J. Richards

Abstract: Catch-age analysis has become a standard tool for modern stock assessment, where it is recognized that population estimates are linked to estimates of the natural mortality rate M. We use state space models and simulation–estimation cycles to evaluate the performance of catch-age analysis. In particular, we design a simulation model with realistic measurement and process error. We then examine how effectively unknown parameters and population sizes can be obtained from an estimation model simplified to conform with common assumptions. We describe circumstances in which, simultaneously with all other parameters, M is estimable from traditional catch-age data. Increased fishing contrast improves estimates of some model parameters, but not M. The variance ratio ρ relating process error in recruitments with measurement error in the abundance index must be specified in the estimation. We consider both true and ad hoc choices for ρ. In general, estimation models perform better when the true ρ is specified and measurement error is low, so that recruitment error is the dominant source of model variability. Thus, well-designed data collection programs are critical to the correct interpretation of actual fishery data.

Résumé : De nos jours, l'analyse de l'âge à la capture est devenue un outil standard d'évaluation des stocks, qui reconnaît que les estimations de la population sont liées aux estimations du taux de mortalité naturelle, M. Nous avons recours à des modèles d'espace d'états et à des cycles de simulation–estimation pour évaluer la performance de la méthode d'analyse de l'âge à la capture. De façon plus particulière, nous avons conçu un modèle de simulation intégrant une erreur réaliste dans les mesures et les traitements. Nous examinons ensuite le degré d'efficacité dans le calcul des paramètres inconnus et de la taille des populations à partir d'un modèle d'estimation simplifié compatible avec les hypothèses courantes. Nous décrivons les circonstances dans lesquelles, parallèlement à tous les autres paramètres, M peut être estimé à partir de données traditionnelles sur l'âge à la capture. L'accroissement du contraste relatif à la pêche améliore l'estimation de certains paramètres des modèles, mais pas du taux de mortalité naturelle M. On doit préciser dans l'estimation le rapport de variance ρ établissant une corrélation entre l'erreur due au traitement dans le recrutement et l'erreur de mesure dans l'indice d'abondance. Nous avons envisagé des valeurs réelles et spéciales pour ρ. En général, les modèles d'estimation donnent de meilleurs résultats lorsque le ρ réel est précisé et que l'erreur de mesure est faible, de sorte que l'erreur dans le recrutement représente le principal facteur de variabilité du modèle. Ainsi, des programmes de collecte de données bien conçus sont essentiels à une bonne interprétation des données réelles sur les pêches.

[Traduit par la Rédaction]

Introduction

Stock assessments of many marine fish species depend on catch-age data. In Megrey's (1989) extensive literature review, assessment models range from deterministic back calculations, such as sequential population analysis (Gulland 1965) and cohort analysis (Pope 1972), to the statistical models of Fournier and Archibald (1982) and Deriso et al. (1985). More recent models contemplate numerous error sources that can be addressed statistically with the aid of Kalman filters (Sullivan 1992; Gudmundsson 1994). These diverse approaches can be unified within the framework of state space models, which are characterized by noisy observations extracted from a hidden dynamic system (Harvey 1989; Schnute 1994). In the context of catch-age data, observations typically include age proportions, and state variables in the hidden dynamic system correspond to numbers of fish at age in each year.

State space models also provide a framework for evaluating the performance of an assessment method. For example, a simulation model can be designed to include realistic sources of measurement and process error. Following standard methods (Schnute 1994), the model implies a corresponding statistical inference function, such as the likelihood or Bayes posterior, that provides the basis for estimating unknown parameters and hidden state variables from available data. Cycles of simulation and estimation then show how well the estimation method performs.

Received February 3, 1995. Accepted May 17, 1995.
J12754

J.T. Schnute and L.J. Richards. Department of Fisheries and Oceans, Science Branch, Pacific Region, Pacific Biological Station, Nanaimo, BC V9R 5K6, Canada.

A useful variant of this evaluation scheme involves choosing different simulation and estimation models. Estimation is generally much more complex than simulation, and this approach can be used to evaluate simplifying assumptions introduced during the estimation phase. For example, the simulator might include sources of error not considered in the estimation.

In this paper, we apply such an evaluation process to catch-age analysis. Many estimation methods, including most of those discussed by Megrey (1989), assume that each cohort follows a deterministic progression from initial recruitment; thus, no error is built into the survival process. We investigate the consequences of using this assumption in the estimator, but not the simulator. More generally, we design a simulator with realistic measurement and process error, and we examine how effectively unknown parameters and states can be estimated from a model simplified to conform with widely used methods. Our simulation model is similar to that proposed by Schnute (1994), although we show that some of his error assumptions must be modified to meet realistic requirements for fish populations.

For most marine populations it is difficult, if not impossible, to obtain an absolute measure of stock biomass. We base our models on the more common situation in which an observed index provides a relative measure. Intuitively, absolute biomass can be inferred from the index because removal of fish in the catch causes a corresponding reduction in the index. Deliberate variations in catch size may thus produce data necessary for a quantitative estimate of the relationship between index and biomass. State space models systematically include controls, such as catch removals, as a component of system dynamics. Thus, they provide a convenient framework for investigating information gains that might be achieved by manipulating the fishery.

We emphasize that the models developed here contemplate a reasonably reliable index, such as that obtained from a carefully planned research survey. By contrast, commercial catch per unit effort (CPUE) data often provide a notoriously poor index that can fail to indicate low population sizes (Hilborn and Walters 1992, pp.175–176; Schnute and Hilborn 1993; Richards 1994). Although the state space model framework can accommodate nonlinear relationships between the index and the underlying population size, we do not investigate such possibilities here. Thus, we identify some of the major features of age-structured analysis, while recognizing that similar methods could be used to investigate a large number of possible model variations.

Natural mortality M acts as a pivotal parameter in any age-structured analysis. For a specified data set, estimates of population size and natural mortality tend to be positively correlated. For example, as the estimate of M increases, the estimated population must also increase to account for higher mortality. Classical catch-age analyses often assume that M is known a priori, and thus implicitly determine abundance from the choice of M. We wish to avoid any approach that fails to capture the uncertainty owing to an unknown M. For instance, it would be illogical to (1) obtain an estimate $\hat{M}$ from age structure data and then (2) treat $\hat{M}$ as a known parameter in a subsequent catch-at-age analysis that depends on the data used in step 1. Even if M is estimated from external data sources, a Bayes prior for M could be used to represent uncertainty.

In this paper, we investigate cases in which M is one of the parameters to be estimated from available data. We show that estimation is feasible in some circumstances where age structure data are available back to the beginning of the fishery on an unexploited stock. Higher levels of measurement error in the abundance index weaken estimability. For example, it must be possible to distinguish high and low population levels against the background of index error. More precisely, variability in recruitment and population sizes must dominate measurement error in the index.

Section 1 defines a deterministic catch-age model, and section 2 extends this to a stochastic model with both measurement and process error. Section 3 defines the likelihood function corresponding to the model without process error in survival. We discuss various model features in section 4, where we provide intuitive arguments suggesting conditions in which the parameter M might be estimable. Section 5 presents results from a group of simulation–estimation experiments designed to examine various ranges of error and fishery controls. We discuss the practical implications of these results in section 6.

1. Deterministic model

State space models typically involves a state vector $\mathbf{X}_t$, an observation vector $\mathbf{Y}_t$, and a control vector $\mathbf{Z}_t$ for each time period t (Schnute 1994). In the model here, components of the state vector

$$(1.1) \qquad \mathbf{X}_t = \{N_{at}\}_{a=1}^{A}$$

include the numbers N_{at} of fish in age-class a at the start of each fishing year t. Age-classes range from 1 to A, where 'age-class' and 'age' need not be the same. Thus, if r denotes the age of first recruitment, then age-class 1 includes fish of age r and age-class A represents fish of age $r + A - 1$ or older. We assume that the observation vector

$$(1.2) \qquad \mathbf{Y}_t = \begin{pmatrix} I_t \\ p_{2t} \\ \vdots \\ p_{At} \end{pmatrix}$$

consists of an observed index I_t related to the population in year t and observed proportions p_{at} of fish at age a in year t. The proportion p_{1t} in age-class 1 is implicit in (1.2) because

$$(1.3) \qquad p_{1t} = 1 - \sum_{a=2}^{A} p_{at}.$$

Finally, the control vector

$$(1.4) \qquad \mathbf{Z}_t = \begin{pmatrix} C_{t-1} \\ C_t \end{pmatrix}$$

reflects actions in the fishery, where C_t is the number of fish caught in year t. We discuss below the reason for including both C_{t-1} and C_t in (1.4).

Table 1. Deterministic catch-at-age model. Calculations begin with the parameter vector Θ_D and proceed recursively to define all states, observations, and controls, as in (1.5).

Parameters

(D.1) $\Theta_D = (\alpha, \beta_1, M, q, \{R_t\}_{t=2-A}^{T}, h_1, h_2)$

Selectivity

(D.2) $\beta_a = 1 - (1 - \beta_1)\left(\frac{A-a}{A-1}\right)^{\alpha}$

State moments

(D.3) $P_t = \sum_{a=1}^{A} \beta_a N_{at}$

(D.4) $u_{at} = \beta_a N_{at} / P_t$

Initial states ($t = 1$)

(D.5) $N_{a1} = R_{2-a} e^{-M(a-1)}, \quad 1 \le a < A$

(D.6) $N_{A1} = R_{2-A} \frac{e^{-M(A-1)}}{1 - e^{-M}}$

State dynamics ($2 \le t \le T$)

(D.7) $N_{1t} = R_t$

(D.8) $N_{at} = e^{-M}[N_{a-1,t-1} - u_{a-1,t-1} C_{t-1}], \quad 2 \le a < A$

(D.9) $N_{At} = e^{-M}[N_{A-1,t-1} + N_{A,t-1} - (u_{A-1,t-1} + u_{A,t-1}) C_{t-1}]$

Observations ($1 \le t \le T$)

(D.10) $I_t = q\left(P_t - \frac{C_t}{2}\right)$

(D.11) $p_{at} = u_{at}, \quad 2 \le a \le A$

Controls ($1 \le t \le T$)

(D.12) $F_t = \frac{M}{2T}\left[2h_1(T - |2t - T|) + h_2(|2t - T| + 2t - T)\right]$

(D.13) $C_t = (1 - e^{-F_t}) P_t$

Table 1 presents a deterministic model for the states (1.1), observations (1.2), and controls (1.4) defined above. Essentially, the table has components that specify (1) the initial state $\mathbf{X}_1$, (2) the transition $\mathbf{X}_{t-1} \to \mathbf{X}_t$ from year $t-1$ to year t, (3) the relationship between states $\mathbf{X}_t$ and observations $\mathbf{Y}_t$, and (4) the policy that generates controls $\mathbf{Z}_t$. A recursive application of these four components produces values of all states, observations, and controls from the parameter vector Θ_D in (D.1). Symbolically, Table 1 defines the calculation

(1.5) $\Theta_D \to \mathbf{X}^T, \mathbf{Y}^T, \mathbf{Z}^T,$

where T is the number of years of simulated data and the superscript denotes cumulative vectors; for example,

(1.6) $\mathbf{X}^T = \{\mathbf{X}_t\}_{t=1}^{T}.$

We describe below how Table 1 defines the calculation (1.5), that is, how all states, observations, and controls are determined by the parameter vector Θ_D. However, we first provide a biological interpretation for each equation in the table.

The parameter vector (D.1) includes two selectivity parameters (α, β_1), natural mortality (M), an index coefficient (q), and a sequence of historic recruitments from years $t = 2 - A, \ldots, T$, where R_t is the recruitment of fish into age-class 1 at the start of year t. Two additional parameters (h_1, h_2) define the fishery management policy. Equation (D.2) defines the fishery selectivity β_a for age-class a, on the basis of an exponent α and initial selectivity β_1 with

(1.7) $\alpha > 0, \beta_1 \le 1.$

According to this relatively simple model, β_a increases from β_1 to 1 as a ranges from 1 to A; thus, the final age-class is always fully selected. The progression from β_1 to 1 is linear when $\alpha = 1$ and quadratic when $\alpha = 2$; when $\alpha > 1$, the curve (D.2) is convex downward with slope 0 at age $a = A$.

Given the state vector $\mathbf{X}_t$ in (1.1) and the selectivities (D.2), (D.3) defines the population P_t of fish available to the fishery in year t. Similarly, (D.4) defines the proportion u_{at} of these fish in each age-class a. Conceptually, P_t and u_{at} are moments that can be calculated from weighted sums of the components of the state vector $\mathbf{X}_t$.

Equations (D.5) and (D.6) define the initial state $\mathbf{X}_1$ in terms of natural mortality M and recruitments R_t with $t = 2 - A, \ldots, 1$. We assume no fishing mortality prior to year $t = 1$, the first year of the data series. Consequently, the initial population N_{a1} of age-class a is the recruitment R_{2-a} from year $1 - (a - 1)$ times the factor $\exp(-M(a-1))$ corresponding to $a - 1$ years of natural mortality. Fish in the final age-class come from all years $t \le 2 - A$; thus, assuming constant recruitment R_{2-a} during the prehistoric period, we obtain

$$N_{A1} = R_{2-A} \sum_{a=A-1}^{\infty} e^{-Ma},$$

a result that reduces to (D.6).

Equations (D.7)–(D.9) describe the transition $\mathbf{X}_{t-1} \to \mathbf{X}_t$. By (D.7), the number $N_{1t} = R_t$ of fish in the first age-class is determined by the parameter vector (D.1), independent of $\mathbf{X}_{t-1}$. Age-classes $a > 1$ result from fish in the previous year. For example, (D.8) relates the population N_{at} to $N_{a-1,t-1}$ via a two-step process. First, the catch C_{t-1} is allocated to age class $a - 1$ according to the available proportion (D.4) and the result is subtracted from the population $N_{a-1,t-1}$. Second, fish that survive the fishery experience natural mortality. A similar interpretation applies to (D.9), except that the population N_{At} comes from both age classes $A - 1$ and A in year $t - 1$.

The observation vector $\mathbf{Y}_t$ in (1.2) results from the state vector $\mathbf{X}_t$, as described by (D.10)–(D.11). First, the abundance index I_t is assumed to be proportional to the mean population

$$\frac{P_t + (P_t - C_t)}{2} = P_t - \frac{C_t}{2}$$

of available fish before and after the fishery. Second, the observed proportion p_{at} is presumed to agree with the actual proportion u_{at}.

Fig. 1. Time series of fishing mortality rates F_t ($t = 0, \ldots, T$) from (D.12). Six control policies (Table 5) are illustrated with $T = 20$, $M = 0.2$, and $h_2 = 0.5$. Labels indicate the six choices $h_1 = 0.5, 1.0, \ldots, 3.0$.

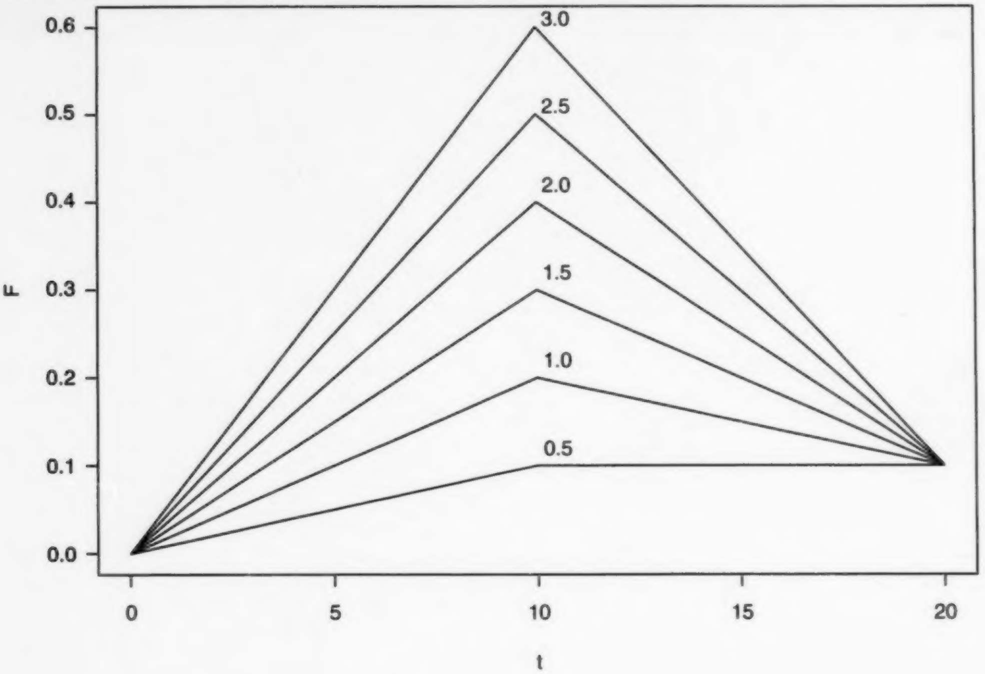

The final equations in Table 1 describe a control policy that determines the sequence of catches C_t ($t = 0, \ldots, T$). To examine the importance of contrast in fishery management, we consider the policy (D.12) in which the fishing mortality F_t takes the values 0, h_1M, and h_2M, respectively, in years $t = 0$, $T/2$, and T. Thus, fishing mortality is 0 prior to the first year of the data series, rises to h_1M halfway through the series, and ends at h_2M in the final year (Fig. 1). The control parameters h_1 and h_2 scale fishing mortality to natural mortality. The fishing mortality F_t and the available population P_t determine the catch C_t, as in (D.13). The control vector $\mathbf{Z}_t$ in (1.4) has two components because the process (D.8)–(D.9) and the observation (D.10) involve the catches C_{t-1} and C_t, respectively.

To complete the calculation (1.5), equations in Table 1 must be applied in a specific order. The following algorithm defines this process precisely.

- Step 1. Set values for all parameters (D.1) and compute selectivities $\{\beta_a\}_{a=1}^{A}$ from (D.2).
- Step 2. Compute the initial state vector $\mathbf{X}_1$ from (D.5)–(D.6). Set the year $t = 1$.
- Step 3. Based on the state vector $\mathbf{X}_t$ for the current year t, compute the moments P_t and $\{u_{at}\}_{a=1}^{A}$ from (D.3)–(D.4). Then compute the catch C_t from (D.12)–(D.13) and the observation vector $\mathbf{Y}_t$ from (D.10)–(D.11).
- Step 4. Reset the year t to $t + 1$. Compute the state vector $\mathbf{X}_t$ from the previous vector $\mathbf{X}_{t-1}$ using (D.7)–(D.9).
- Step 5. If $t < T$, repeat steps 3 and 4. If $t = T$, repeat step 3 and stop.

2. Stochastic model

To be useful statistically, the deterministic model in Table 1 must be rendered stochastic. We consider four sources of random variability, two connected with the system dynamics (process error) and two related to the observations (measurement error). Specifically, we assign process error to both recruitment and survival. We also incorporate measurement error into both the index I_t and the observed proportions p_{at}.

Table 2 presents modifications to Table 1 that define the stochastic model applied in our simulations. The parameter vector $\mathbf{\Theta}_S$ in (S.1) is similar to $\mathbf{\Theta}_D$ in (D.1), except that two parameters (R, γ) in $\mathbf{\Theta}_S$ replace the recruitment sequence $\{R_t\}_{t=2-A}^{T}$. Also, $\mathbf{\Theta}_S$ includes four standard errors (σ_1, σ_2, τ_1, τ_2) associated with the four random components described above.

Recruitment equations in Table 2 are derived from the lognormal autoregressive process

$$(2.1)\qquad \log R_t = \log R + \gamma(\log R_{t-1} - \log R) + \sigma_1\delta_{1t}$$

with parameters (R,γ,σ_1), where noise is introduced by the independent standard normal variates δ_{1t}. The process (2.1) implies that log R_t has the following conditional and unconditional means and variances:

$$(2.2)\qquad E[\log R_t|R_{t-1}] = (1 - \gamma)\log R + \gamma \log R_{t-1}$$

$$(2.3)\qquad \mathrm{Var}[\log R_t|R_{t-1}] = \sigma_1^2$$

$$(2.4)\qquad E[\log R_t] = \log R$$

Table 2. Stochastic counterpart of the deterministic model in Table 1. A bar over a quantity indicates its predicted value from Table 1; for example $\overline{N_{at}}$ denotes the prediction from (D.5)–(D.6) when $t = 1$ or (D.8)–(D.9) when $2 \le t \le T$. The standard normal variates δ_{at} and ϵ_{at} are mutually independent.

Parameters

$$\text{(S.1)}\quad \boldsymbol{\Theta}_S = (\alpha, \beta_1, M, q, R, \gamma, h_1, h_2, \sigma_1, \sigma_2, \tau_1, \tau_2)$$

Recruitment ($2 - A \le t \le T$)

$$\text{(S.2)}\quad R_{2-A} = Re^{\left(\sigma_1/\sqrt{1-\gamma^2}\right)\delta_{1,2-A}}$$

$$\text{(S.3)}\quad R_t = R^{1-\gamma}R_{t-1}^{\gamma}e^{\sigma_1\delta_{1t}}, \quad 2 - A < t \le T$$

Initial states ($t = 1$)

$$\text{(S.4)}\quad N_{11} = R_1$$

$$\text{(S.5)}\quad N_{a1} = \overline{N_{a1}}\prod_{b=2}^{a}\frac{e^{\sigma_2\delta_{b,b-a+1}}}{1-e^{-M}+e^{-M}e^{\sigma_2\delta_{b,b-a+1}}}, \quad 2 \le a \le A$$

State dynamics ($t \ge 2$)

$$\text{(S.6)}\quad N_{1t} = R_t$$

$$\text{(S.7)}\quad N_{at} = \overline{N_{at}}\,\frac{e^{\sigma_2\delta_{at}}}{1-e^{-M}+e^{-M}e^{\sigma_2\delta_{at}}}, \quad 2 \le a \le A$$

Observations

$$\text{(S.8)}\quad I_t = \overline{I}_t e^{\tau_1\epsilon_{0t}}$$

$$\text{(S.9)}\quad x_{at} = \log(\overline{p_{at}}) + \tau_2\epsilon_{at} - \frac{1}{A}\sum_{a=1}^{A}\left[\log(\overline{p_{at}}) + \tau_2\epsilon_{at}\right]$$

$$\text{(S.10)}\quad p_{at} = \frac{e^{x_{at}}}{\sum_{a=1}^{A} e^{x_{at}}}$$

$$\text{(2.5)}\quad \mathrm{Var}[\log R_t] = \sigma_1^2/(1 - \gamma^2).$$

In particular, when $\gamma = 0$, $\log R_t$ is normal with mean $\log R$ and variance σ^2, independent of R_{t-1}. When $\gamma = 1$, (2.1) corresponds to a random walk with finite conditional moments (2.2)–(2.3) but infinite unconditional variance (2.5). We adopt (2.1) in our simulation model because it provides a simple process for generating correlated recruitments; the nonstationary case $\gamma = 1$ allows recruitments to drift toward high or low levels over long time periods, as observed in some marine populations. Equation (S.2) follows from (2.4)–(2.5), where the historic recruitment level R_{2-A} is treated as an unconditional variate. The conditional process (S.3) for $t > 2 - A$ is equivalent to (2.1). In the special case $\gamma = 1$, the parameter R drops out of (S.3) and is replaced by R_{2-A} in the parameter vector (S.1).

We introduce error into the survival process with variates

$$\text{(2.6)}\quad \eta_{at} = \frac{e^{\sigma_2\delta_{at}}}{1-e^{-M}+e^{-M}e^{\sigma_2\delta_{at}}}$$

derived from independent standard normal variates δ_{at} with $a \ge 2$, the natural mortality M, and a parameter σ_2 related to the variance of η_{at}. It follows from (2.6) that

$$\text{(2.7)}\quad 0 < \eta_{at} < e^{M},$$

where left and right extremes of the range (2.7) correspond to the limiting values $\delta_{at} = -\infty$ and $\delta_{at} = \infty$, respectively. Furthermore, the median value $\delta_{at} = 0$ determines the median $\eta_{at} = 1$. The role of η_{at} in Table 2 is particularly evident in (S.7) when $2 \le a < A$, which can be written as

$$\text{(2.8)}\quad N_{at} = \{e^{-M}(N_{a-1,t-1} - u_{a-1,t-1}C_{t-1})\}\eta_{at}$$

where the expression in braces is the prediction $\overline{N_{at}}$ from (D.8). Because η_{at} has median 1, the median value of N_{at} in (2.8) is precisely $\overline{N_{at}}$. Furthermore, the range (2.7) guarantees that

$$\text{(2.9)}\quad 0 < N_{at} < N_{a-1,t-1} - u_{a-1,t-1}C_{t-1};$$

in particular, the simulated N_{at} cannot exceed the population available after the fishery is completed in the previous year $t - 1$. Obviously, a realistic fishery model must satisfy this constraint. In effect, the product $e^{-M}\eta_{at}$ acts as a stochastic survival coefficient in (2.8), and (2.7) guarantees that the survival cannot exceed 1:

$$\text{(2.10)}\quad e^{-M}\eta_{at} < 1.$$

Table 2 incorporates the variates (2.6) into not only the survival equation (S.7) but also the initial state calculation (S.5). As discussed earlier in connection with (D.5), the initial population N_{a1} with $2 < a < A$ comes from the recruitment R_{2-a} in year $2 - a$ after $a - 1$ years of natural mortality. The $a - 1$ stochastic factors in (S.5) simply build randomness into the deterministic survival coefficient $e^{-M(a-1)}$ in (D.5). The notation $\overline{N_{a1}}$ refers to the prediction in (D.5) or (D.6), depending on the value of a; thus, (S.5) provides the stochastic counterpart of both (D.5) and (D.6). Similarly, $\overline{N_{at}}$ in (S.7) denotes the prediction (D.8) when $2 \le a < A$ or (D.9) when $a = A$.

Equations (S.8)–(S.10) build observation error into the vector (1.2). Because I_t need only be constrained to be positive, it seems reasonable to assume lognormal error, as in (S.8), with standard normal variates ϵ_{0t} and standard error τ_1. The observed proportions p_{at} are somewhat more difficult to simulate because they must be positive and satisfy the constraint

$$\text{(2.11)}\quad \sum_{a=1}^{A} p_{at} = 1$$

for each year t. Although sampling theory suggests proportions derived from a multinomial distribution, we believe that errors obtained by this approach are unrealistically small for most fisheries data. Consequently, we depart from various historical analyses (e.g., Fournier and Archibald 1982; Methot 1989, 1990) and use the multivariate logistic distribution defined in (S.9)–(S.10). The proportions in (S.10) automatically satisfy the constraint (2.11), and large errors can be introduced through the parameter τ_2. For a given year t, the calculation proceeds as follows: (1) generate independent standard normal variates ϵ_{at} ($a = 1, \ldots, A$); (2) compute x_{at} from (S.9); and (3) compute p_{at} from (S.10). Inspection shows that the observation p_{at} equals the prediction $\overline{p_{at}}$ when $\tau_2 = 0$; however, as $\tau_2 \to \infty$, the observations become random and unrelated to the predictions. Notice that A variates ϵ_{at} are

Table 3. Likelihood function for the model in Table 2, assuming deterministic survival ($\sigma_2 = 0$). Calculations begin with the parameter vector $\boldsymbol{\Theta}_L$ and proceed sequentially to define $L(\boldsymbol{\Theta}_L)$ in (L.10).

Parameters

$$\text{(L.1)} \quad \boldsymbol{\Theta}_L = (\alpha, \beta_1, M, q, R, \gamma, \{R_t\}_{t=2-A}^{T}, \sigma_1, \tau_1, \tau_2)$$

Predicted states

$$\text{(L.2)} \quad N_{at} = \overline{N_{at}}, \quad 1 \le a \le A \text{ and } 1 \le t \le T$$

Residuals

$$\text{(L.3)} \quad \xi_{2-A} = \log R_{2-A} - \log R$$

$$\text{(L.4)} \quad \xi_t = \log R_t - (1 - \gamma) \log R - \gamma \log R_{t-1}, \quad 2 - A < t \le T$$

$$\text{(L.5)} \quad \eta_{0t} = \log I_t - \log \overline{I}_t$$

$$\text{(L.6)} \quad \eta_{at} = \log(p_{at}) - \log(\overline{p_{at}}) - \frac{1}{A}\sum_{a=1}^{A}\left[\log p_{at} - \log \overline{p_{at}}\right]$$

Likelihoods

$$\text{(L.7)} \quad L_1 = \sqrt{1-\gamma^2}\left(\sqrt{2\pi}\,\sigma_1\right)^{2-A-T} \exp\left[-\frac{1}{2\sigma_1^2}\left((1-\gamma^2)\xi_{2-A}^2 + \sum_{t=3-A}^{T} \xi_t^2\right)\right]$$

$$\text{(L.8)} \quad L_2 = \left(\sqrt{2\pi}\,\tau_1\right)^{-T} \exp\left[-\frac{1}{2\tau_1^2}\sum_{t=1}^{T}\eta_{0t}^2\right]$$

$$\text{(L.9)} \quad L_3 = \left(\sqrt{2\pi}\,\tau_2\right)^{-T(A-1)} A^{T/2} \exp\left[-\frac{1}{2\tau_2^2}\sum_{a=1}^{A}\sum_{t=1}^{T}\eta_{0t}^2\right]$$

$$\text{(L.10)} \quad L = L_1 L_2 L_3$$

used to generate effectively $A - 1$ proportions p_{at}, where the final proportion is determined by the constraint (2.11). In effect, correlated normal variates x_{at} act as surrogates for p_{at}, where the constraints (2.11) and

$$\text{(2.12)} \quad \sum_{a=1}^{A} x_{at} = 0$$

restrict each set of variates to $A - 1$ degrees of freedom for a given year t.

Table 1 defines the deterministic calculation (1.5) via the stepwise algorithm listed at the end of section 1. Similarly, Table 2 specifies the stochastic simulation

$$\text{(2.13)} \quad \boldsymbol{\Theta}_S \rightarrow \mathbf{X}^T, \mathbf{Y}^T, \mathbf{Z}^T$$

by the following modified algorithm.

- Step 1. Set values for all parameters $\boldsymbol{\Theta}_S$, compute selectivities $\{\beta_a\}_{a=1}^{A}$ from (D.2), and obtain stochastic recruitments $\{R_t\}_{t=2-A}^{T}$ from (S.2)–(S.3). All parameters $\boldsymbol{\Theta}_D$ in (D.1) are now available.
- Step 2. Compute the predicted initial state $\overline{\mathbf{X}}_1$ from (D.5)–(D.6) and the stochastic initial state $\mathbf{X}_1$ from (S.4)–(S.5). Set the year $t = 1$.
- Step 3. Based on the stochastic state $\mathbf{X}_t$ for the current year t, compute the moments P_t and $\{u_{at}\}_{a=1}^{A}$ from (D.3)–(D.4). Then compute the catch C_t from (D.12)–(D.13), the predicted observation $\overline{\mathbf{Y}}_t$ from (D.10)–(D.11), and the stochastic observation $\mathbf{Y}_t$ from (S.8)–(S.10).
- Step 4. Reset the year t to $t + 1$. Compute the predicted state $\overline{\mathbf{X}}_t$ from the previous stochastic state $\mathbf{X}_{t-1}$ using (D.7)–(D.9). Then compute the stochastic state $\mathbf{X}_t$ from (S.6)–(S.7).
- Step 5. If $t < T$, repeat steps 3 and 4. If $t = T$, repeat step 3 and stop.

3. Likelihood

Tables 1 and 2 define the process (2.13), in which specified parameters lead to observed data through the mechanism of an underlying population. Statistical inference requires reversing this process, that is, estimating parameters from the data. Symbolically, the estimation problem can be represented by

$$\text{(3.1)} \quad \mathbf{Y}^T, \mathbf{Z}^T \rightarrow \boldsymbol{\Theta}_L, \mathbf{X}^T,$$

where the superscript T denotes cumulative vectors as in (1.6). The inference (3.1) requires the following data: (1) the cumulative data vector $\mathbf{Y}^T$ of observed indices I_t and proportions p_{at} and (2) the cumulative control vector $\mathbf{Z}^T$ defined by catches C_t. From these data, we must obtain estimates of a parameter vector $\boldsymbol{\Theta}_L$ and the cumulative state vector $\mathbf{X}^T$, which includes the entire history of unknown populations N_{at} for years $t = 1, \ldots, T$.

Table 3 specifies the likelihood function corresponding to (3.1) for the model in Table 2 under the common assumption that there is no survival error:

(3.2) $\sigma_2 = 0.$

Given (3.2), equations (S.5) and (S.7) in Table 2 reduce to

$$N_{at} = \overline{N_{at}}$$

for all ages a and years t. Thus, (3.2) implies that the dynamic component (S.4)–(S.7) of the stochastic model in Table 2 reduces to the deterministic dynamics (D.5)–(D.9) in Table 1. Furthermore, the parameters $\mathbf{\Theta}_L$ in (L.1) include all parameters $\mathbf{\Theta}_D$ in (D.1), except the control parameters h_1 and h_2. These are not needed for the calculation in Table 1 when the catches C_t are specified, as in (3.1). Consequently, given the assumption (3.2), Table 1 determines the entire population history $\mathbf{X}^T$ from the parameter vector $\mathbf{\Theta}_L$, as indicated by (L.2) in Table 3. In summary, if $\sigma_2 = 0$, (3.1) reduces to the simpler estimation problem

(3.3) $\mathbf{Y}^T, \mathbf{Z}^T \rightarrow \mathbf{\Theta}_L,$

where in this case $\mathbf{X}^T = \mathbf{X}^T(\mathbf{\Theta}_L)$. The simplification from (3.1) to (3.3) provides a compelling reason for adopting (3.2) and perhaps explains why this assumption implicitly enters much of the literature on catch-age analysis.

The restriction (3.2) eliminates one of the four sources of model error. Table 3 defines residuals for each of the three remaining error components. Recruitment residuals ξ_t in (L.3)–(L.4) correspond to unconditional recruitment (S.2) or conditional recruitment (S.3) when $t = 2 - A$ or $t > 2 - A$, respectively. Residuals η_{0t} in (L.5) for the indices I_t derive from lognormal measurement error (S.8). Residuals η_{at} in (L.6) associated with measurement error in p_{at} correspond to the correlated normal variates x_{at} in (S.9), where a constraint analogous to (2.12) applies to η_{at}.

From the model in Table 2, the residuals (L.3)–(L.6) conform to multinormal distributions. In particular, ξ_t, η_{0t}, and η_{at} have the distributions (L.7)–(L.9), respectively, where the derivation of (L.9) takes account of linear dependencies among the residuals η_{at} (Appendix). The overall model likelihood is thus the product L in (L.10). In summary, $L(\mathbf{\Theta}_L)$ can be computed from the parameter vector $\mathbf{\Theta}_L$ by the following algorithm.

- Step 1. Compute states $N_{at}(\mathbf{\Theta}_L)$ from the deterministic algorithm of Table 1, as indicated in (L.2), where (D.12)–(D.13) are not used because the catches C_t are specified.
- Step 2. Compute the residuals $\xi_t(\mathbf{\Theta}_L)$ and $\eta_{at}(\mathbf{\Theta}_L)$ with $a \geq 0$ from the states $N_{at}(\mathbf{\Theta}_L)$ by (L.3)–(L.6).
- Step 3. Compute the functions $L_i(\mathbf{\Theta}_L)$ (i = 1, 2, 3) and their product $L(\mathbf{\Theta}_L)$ from the residuals in step 2 using (L.7)–(L.10).

The likelihood defined in Table 3 conforms to the errors-in-variables (EV) paradigm discussed by Schnute (1994). In this case, the recruitments R_t act as hidden state variables dependent on the underlying parameters R and γ. Not all parameters $\mathbf{\Theta}_L$ in (L.1) are estimable by maximum likelihood because the function $L(\mathbf{\Theta}_L)$ in (L.10) has two inherent singularities where $L \rightarrow \infty$. One of these is achieved by selecting parameters R_t that conform to a deterministic version of (S.4)–(S.5) with $\sigma_1 = 0$. For these parameters, $\xi_t = 0$ in (L.3)–(L.4), and the function (L.7) reduces to

$$L_1 = \sqrt{1-\gamma^2}\left(\sqrt{2\pi}\,\sigma_1\right)^{2-A-T},$$

which approaches ∞ as $\sigma_1 \rightarrow 0$. A similar singularity can generally be achieved in L_2 as $\tau_1 \rightarrow 0$ by adjusting the parameters R_t so that the predictions $\overline{I_t}$ equal the observations I_t and, consequently, $\eta_{0t} = 0$. This is theoretically possible because the number of adjustable parameters R_t ($t = 2 - A, \ldots, T$) exceeds the number of observations I_t ($t = 1, \ldots, T$).

To avoid these singularities, we must adopt the usual approach to EV estimation in which a variance ratio is presumed known (Kendall and Stuart 1979, pp. 407–410). For this purpose, define the parameters κ and ρ by

(3.4) $\kappa^2 = \sigma_1^2 + \tau_1^2, \quad \rho = \dfrac{\sigma_1^2}{\sigma_1^2 + \tau_1^2}.$

Thus, κ^2 is the total variance owing to recruitment process error and index measurement error, and ρ is the proportion of this variance owing to recruitment. Mathematically, (3.4) defines a transformation from the parameters (σ_1, τ_1) to alternative parameters (κ, ρ). The reverse transformation is given by

(3.5) $\sigma_1^2 = \rho\kappa^2, \quad \tau_1^2 = (1 - \rho)\kappa^2.$

The definition of κ^2 is reasonable biologically because errors in (S.2)–(S.3) and (S.8) are lognormal, σ_1 and τ_1 are dimensionless, and the sums in (3.4) involve comparable quantities. A specified parameter ρ corresponds to the variance ratio

(3.6) $\dfrac{\sigma_1^2}{\tau_1^2} = \dfrac{\rho}{1-\rho}.$

In particular, the three choices $\rho = 0$, $\rho = 0.5$, and $\rho = 1$ correspond to deterministic recruitment ($\sigma_1 = 0$), equal variation in recruitment and index measurement ($\sigma_1 = \tau_1$), and no measurement error ($\tau_1 = 0$), respectively.

If $\rho = 0$ (i.e., $\sigma_1 = 0$), equations (S.2)–(S.3) recursively imply constant recruitment

(3.7) $R_t = R$

for $t = 2 - A, \ldots, T$, independent of γ. Thus, the parameter vector $\mathbf{\Theta}_L$ for this case reduces to

(3.8) $(\mathbf{\Theta}_L|\sigma_1 = 0) = (\alpha, \beta_1, M, q, R, \tau_1, \tau_2),$

which includes five key biological parameters and two standard errors. Similarly, the likelihood L in (L.10) is replaced by the product

(3.9) $L(\mathbf{\Theta}_L|\sigma_1 = 0) = L_2 L_3.$

This simple case may provide a useful starting point for more detailed analyses with $\rho > 0$.

Given a specified value ρ, maximum likelihood estimates of κ and τ_2 can be computed analytically (Appendix). Table 4 presents these results, along with corresponding values of the inference function

(3.10) $\ell(\mathbf{\Phi}_L) = -2 \log L(\mathbf{\Phi}_L, \rho, \hat{\kappa}, \hat{\tau}_2) + K,$

where K is a constant independent of parameters and $\mathbf{\Phi}_L$ is the parameter vector obtained by dropping standard errors from $\mathbf{\Theta}_L$. Essentially, ℓ is twice the negative log likelihood minimized across the parameters κ and τ_2 at a specified value ρ. Because (κ, τ_2) are treated as nuisance parameters

Table 4. Maximum likelihood estimates $(\hat{\kappa}^2, \hat{\tau}_2^2)$ and the inference function ℓ defined by (3.10), where parameters (κ, ρ) are related to (σ_1, τ_1) by (3.4)–(3.5). For a specified value ρ, these quantities all depend on the subset $\mathbf{\Phi}_L$ of the parameters $\mathbf{\Theta}_L$. Results are shown for two cases: $\rho = 0$ and $0 < \rho < 1$.

$\rho = 0$

$$\text{(L.11)}\quad \mathbf{\Phi}_L = (\alpha, \beta_1, M, q, R)$$

$$\text{(L.12)}\quad \hat{\kappa}^2 = \hat{\tau}_1^2 = \frac{1}{T}\sum_{t=1}^{T} \eta_{0t}^2$$

$$\text{(L.13)}\quad \hat{\tau}_2^2 = \frac{1}{(A-1)T}\sum_{a=1}^{A}\sum_{t=1}^{T} \eta_{at}^2$$

$$\text{(L.14)}\quad \ell = T \log \hat{\kappa}^2 + (A-1)T \log \hat{\tau}_2^2$$

$0 < \rho < 1$

$$\text{(L.15)}\quad \mathbf{\Phi}_L = (\alpha, \beta_1, M, q, R, \gamma, \{R_t\}_{t=2-A}^{T})$$

$$\text{(L.16)}\quad \hat{\kappa}^2 = \frac{1}{A+2T-2}\left[\frac{1}{\rho}\left((1-\gamma^2)\xi_{2-A}^2 + \sum_{t=3-A}^{T} \xi_t^2\right) + \frac{1}{1-\rho}\sum_{t=1}^{T} \eta_{0t}^2\right]$$

$$\text{(L.17)}\quad \hat{\tau}_2^2 = \frac{1}{(A-1)T}\sum_{a=1}^{A}\sum_{t=1}^{T} \eta_{at}^2$$

$$\text{(L.18)}\quad \ell = (A + T - 2)\log \rho + T \log(1-\rho) - \log(1-\gamma^2) + (A + 2T - 2)\log \hat{\kappa}^2 + (A-1)T \log \hat{\tau}_2^2$$

and ρ is specified, all quantities computed in Table 4 depend only on the subset $\mathbf{\Phi}_L$ of the parameters $\mathbf{\Theta}_L$. The function $\ell(\mathbf{\Phi}_L)$ provides statistical inferences about $\mathbf{\Theta}_L$; for example, the maximum likelihood estimate $\hat{\mathbf{\Phi}}_L$ is obtained by minimizing ℓ. The table shows results both for the general case $0 < \rho < 1$ and the special case $\rho = 0$, in which recruitment (3.7) is constant.

4. Model features

We have developed our model from a similar one proposed by Schnute (1994), although we have excluded a few features to simplify the analysis. For example, our model is based entirely on population numbers; we do not consider conversions between fish weights and stock biomass. Similarly, our model contemplates ageing error, but we do not incorporate a known classification matrix (Richards et al. 1992; Schnute 1994).

Our model does, however, consider error structures more complex than those proposed by Schnute (1994). For example, lognormal survival error sometimes leads to a simulated population N_{at} that exceeds the upper limit (2.9). If the natural mortality M is small, a realistic lognormal survival coefficient $e^{-M}e^{\sigma_2\delta_{at}} = e^{-M+\sigma_2\delta_{at}}$ may have a significant probability of exceeding 1. For this reason, we adopted the logistic error (2.6). A generalization of this approach might utilize variates

$$\text{(4.1)}\qquad \eta_{at} = \frac{e^{\sigma_2\delta_{at}+\sigma_3\delta_t'}}{1 - e^{-M} + e^{-M}e^{\sigma_2\delta_{at}+\sigma_3\delta_t'}},$$

in which an overall survival effect δ_t' for each year t is added to the independent effect δ_{at} on each age-class. Unlike (2.6), the variates (4.1) are not independent; however, for simplicity, we confine our analyses to (2.6).

In many fisheries, information on natural mortality comes primarily from the population's age structure. For this reason, as discussed in the Introduction, we have constructed our model specifically to examine the prospect for estimating M along with other model parameters. To understand our approach intuitively, consider the population matrix

$$\text{(4.2)}\qquad \{N_{at}\} = \begin{pmatrix} R_1 & R_2 & \cdots & R_T \\ R_0 e^{-M} & N_{22} & \cdots & N_{2T} \\ \vdots & \vdots & \ddots & \vdots \\ R_{2-A}\dfrac{e^{-M(A-1)}}{1-e^{-M}} & N_{A2} & \cdots & N_{AT} \end{pmatrix}$$

for ages $a = 1, \ldots, A$ and years $t = 1, \ldots, T$, where the first row and column are specified by the deterministic model (D.5)–(D.7). Thus, the first row depends on recruitments R_t with $1 \le t \le T$. Similarly, because we have assumed no fishing mortality prior to year $t = 1$, the first column depends on M and R_t with $2 - A \le t \le 1$. This suggests that information on M should be available from the age structure in the first column, provided that recruitment variability follows a consistent pattern throughout the entire time period $t = 2 - A, \ldots, T$. To capture such a pattern, we have adopted the generic autoregressive model (S.2)–(S.3). In the limiting case

$$\text{(4.3)}\qquad \sigma_1 = \infty,$$

the recruitments R_t become independent parameters, there is no consistency among entries in the first column of (4.2) and M is no longer estimable. Many catch-at-age analyses implicitly assume (4.3); consequently, they offer no hope of estimating M.

Because likelihood estimation requires prior knowledge of the variance ratio ρ, we must examine the sensitivity of the estimate $\hat{M}$ to the choice of ρ during the estimation phase. In general, we test the validity of estimation models that differ from the model used for simulation. Because of its simplicity, the estimation model with $\rho = 0$ (i.e., $\sigma_1 = 0$) warrants particular interest, as discussed with (3.7)–(3.9). Another possible ad hoc choice for estimation involves the following compromise between (4.3) and $\sigma_1 = 0$:

$$\text{(4.4)}\qquad \sigma_1 = \begin{cases} 0, & 2 - A \le t \le 1 \\ \infty, & 2 \le t \le T \end{cases}$$

A model with (4.4) has time-dependent σ_1 in (S.2)–(S.3). Consequently, recruitment is constant ($R_t = R$) for the initial period $2 - A \le t \le 1$, and M is estimable from initial proportions. For the final period $2 \le t \le T$, recruitments R_t are treated as free parameters. Likelihood for the compromise model (4.4) is computed as in Table 3 from parameters

$$\text{(4.5)}\qquad \mathbf{\Theta}_L = (\alpha, \beta_1, M, q, R, \{R_t\}_{t=2}^{T}, \tau_1, \tau_2),$$

except that the component L_1 is omitted. A calculation similar to (L.11)–(L.14) is also appropriate for this case.

We have already discussed our reasons for adopting the measurement error (S.9)–(S.10) in the proportions p_{at}. This induces correlations among observed proportions consistent with the constraint (2.11) that they must sum to 1 in each year t. Furthermore, proportions near 0 or 1 have smaller variance than proportions near 0.5, consistent with constraints imposed by endpoints of the probability interval [0,1].

The model in Tables 1 and 2 assumes that the true catch by age reflects true proportions by age in the underlying population. Thus, in (D.8) the number of fish caught is determined by the true proportion $u_{a-1,t-1}$. By (S.9)–(S.10), variation in the observed proportion p_{at} comes entirely from measurement error. The simulation model could include another component of process error that allows random selectivity by the fishery, although we do not explore this possibility in the analyses that follow.

5. Results

We illustrate our model's utility by examining estimates $\hat{\Phi}_L$ of the parameters Φ_L obtained in various simulation–estimation experiments. To demonstrate how measurement error complicates the estimation process, we conduct simulations using both low and moderate values (τ_1, τ_2) over a range of control policies (Fig. 1). We also examine estimates of M and other model parameters under different choices ρ in the estimation phase. In particular, for each simulated data set, we obtain parameter estimates under the assumptions (1) $\rho = 0$, (2) $\rho = 0.5$, (3) ρ equals its true value in the simulation, and (4) the compromise (4.4) that we term the mixed ρ case. With 50 simulations for each of two error levels and six control policies, we generate a total of $50 \times 2 \times 6 = 600$ simulated data sets. Given four assumptions for ρ, our experiment requires $4 \times 600 = 2400$ estimations.

We constructed the simulated data sets from parameter values Θ_S in Table 5, using dimensions of $A = 10$ age-classes and $T = 20$ years. We attempted to select typical values for marine fisheries data. For example, we based values γ and σ_1 on an examination of historical recruitment time series (Myers et al. 1990). Interested readers may wish to verify that series $\{R_t\}$ generated by (S.2)–(S.3) with the parameters $(R,\gamma,\sigma_1) = (1.0, 0.5, 0.7)$ exhibit patterns typical of actual recruitments. The choice $R = 1$ sets the scale for population levels; effectively, the population is measured in units of R. Similarly, the choice $q = 1$ determines units of measurement for the index I_t. Thus, we can set $(R,q) = (1,1)$ without loss of generality, provided that these are treated as unknown parameters in the estimation phase.

Our simulations used the six control policies (Fig. 1) corresponding to the six values h_1 and fixed h_2 in Table 5. The maximum value F_t (reached at the middle year of each series) ranged from 0.1 to 0.6 , or from $0.5M$ to $3.0M$. The final value F_T was always 0.1, or $0.5M$.

To simulate low levels of measurement error, we chose $(\tau_1,\tau_2) = (0.05,0)$, so that the stochastic index typically fell within 10% of its deterministic value and age proportions were perfectly known. Although such precise measurements are obviously unrealistic, they provide a baseline against which to compare more reasonable values. For moderate measurement error, i.e., $(\tau_1,\tau_2) = (0.2,0.2)$, typical stochastic and deterministic values differed by less than 50% for the index and 30% for a proportion $p_{at} = 0.5$. By contrast, the choices $(\sigma_1,\sigma_2) = (0.7,0.2)$ allowed stochastic recruitments to vary more than 15-fold and stochastic survivals to vary more than 4-fold from their respective deterministic predictions. By (3.4), these choices lead to values $\kappa^2 = 0.49$ for low measurement error and $\kappa^2 = 0.53$ for moderate measurement error, with corresponding values $\rho = 0.99$ and 0.92, respectively. Because we expect recruitment variance to be much greater than index variance in fisheries data sets, ρ will take values near 1.0 in most cases.

Table 5. Values of parameters Θ_S in (S.1) used for model simulation, along with parameter bounds applied in model estimation. The six values for h_1 correspond to the control policies examined (Fig. 1). Two cases were explored for measurement error parameters (τ_1,τ_2), representing low or moderate measurement error.

Simulation parameters		Estimation bounds	
Θ_S	Value(s)	Minimum	Maximum
α	2	0.02	50
β	0.2	0	1
M	0.2	0.05	0.40
q	1	0.1	10
R	1	0.1	10
γ	0.5	−1	1
h_1	0.5, 1.0, 1.5, 2.0, 2.5, 3.0		
h_2	0.5		
σ_1	0.7		
σ_2	0.2		
(τ_1,τ_2)	(0.05, 0), (0.2, 0.2)		

The number of parameters to be estimated depends on the choice of ρ and the data set dimensions $(A,T) = (10,20)$. For the mixed ρ assumption, we require estimates of 24 parameters in (4.5), where $\hat{\tau}_1$ and $\hat{\tau}_2$ are given by (L.12)–(L.13). When $\rho = 0$, we must estimate the five parameters in (L.11). Finally, when $\rho > 0$ is specified, the 35 parameters in (L.15) must be estimated.

We obtained all estimates by minimizing the inference function $\ell(\Phi_L)$ through automatic differentiation (Griewank and Corliss 1991; Otter Research 1991) in conjunction with a quasi-Newton search algorithm (Press et al. 1992, pp. 425–430). Specifically, we used the combined function minimizer and C++ class library supplied in binary form by Otter Research Ltd. Although details of this minimization algorithm are not documented, convergence can be assessed by checking for small gradients, which are reliably computed by automatic differentiation to within machine precision. Several hours of computing time on a UNIX workstation were required to produce all analyses reported here.

We used true parameter values to initialize the minimization. Parameter estimates appeared robust to alternative initial points, but true parameter values provided a

Table 6. Percentage convergence of the estimator for 48 cases defined by two levels of measurement error (τ_1,τ_2), four assumptions for ρ, and six cases of the control parameter h_1. Each case represents 50 simulation–estimation cycles, for a total of 48 × 50 = 2400 runs with an overall 96% convergence rate.

				h_1					
Error level	τ_1	τ_2	ρ	0.5	1.0	1.5	2.0	2.5	3.0
Low	0.05	0	Mixed	90	96	98	100	96	94
Low	0.05	0	0	100	98	94	94	92	88
Low	0.05	0	0.5	92	98	100	94	98	94
Low	0.05	0	True	98	96	100	96	96	96
Moderate	0.2	0.2	Mixed	100	100	100	100	94	96
Moderate	0.2	0.2	0	100	98	94	94	92	90
Moderate	0.2	0.2	0.5	100	94	98	100	98	98
Moderate	0.2	0.2	True	96	98	98	96	98	98

convenient choice for automating cycles of simulation and estimation. Small gradients indicated that we had reached local minima, although we made no concerted effort to seek global minima except in a few trial cases. Techniques such as simulated annealing (Press et al. 1992, pp. 451–455) could be applied, but our experience suggested that these would not be necessary for the analysis here.

We opted to guide the estimation process by imposing biologically meaningful bounds (Table 5) on all parameters except the recruitments $\{R_t\}$. To bound a specified parameter θ within the interval $[a,b]$, we used the surrogate parameter x defined by the transformation

$$(5.1) \qquad \theta = a + (b-a)\frac{1-\cos(\pi x)}{2}.$$

By (5.1), a parameter θ computed from the surrogate x automatically honours the constraint $a \le \theta \le b$. The minimization procedure was generally well behaved with these bounds in effect (Table 6). Overall, we achieved 96 and 97% convergence for the low and moderate error cases, respectively. Although parameter bounds give stability to the minimization, we emphasize that estimates on the boundary should be interpreted as failure to capture biological reality.

From a fisheries management perspective, the most important outputs from a catch-age model are estimates of current population size P_T and the corresponding recommended harvest. For simplicity, we consider the quota

$$(5.2) \qquad Q = (1 - e^{-M})P_T$$

obtained by applying the harvest rate M to the current stock P_T (e.g., Leaman 1993). We estimate Q in (5.2) using the model estimates $\hat{M}$ and $\hat{P}_T$; consequently, $\hat{Q}$ acts as a composite quantity with which to gauge the success of estimation.

Figures 2–4 display the major simulation–estimation results, where parameter values are represented by the ratio of estimated to true values on a log (base 2) scale. Thus, a value of 0 indicates perfect fit and the illustrated range (−2,2) represents a fourfold deviation below or above the true parameter value. Because γ potentially takes negative values, we first applied the transformation

$$(5.3) \qquad \gamma' = \frac{1+\gamma}{1-\gamma}$$

to enable comparable scaling for all parameters.

With estimations combined across all six control policies, Fig. 2 represents the precision and bias of parameter estimates in relation to the simulated measurement error level and the choice of ρ for estimation. Parameter estimates tend to be unbiased under low measurement error, except for the choice $\rho = 0$, and precision tends to increase as ρ increases toward the true value. By contrast, given moderate measurement error, only the mixed ρ assumption provides unbiased estimates. The choices $\rho = 0.5$ and $\rho = 0.92$ (true) both lead to underestimates of (M,R,γ,P_T,Q) and overestimates of other parameters, while the choice $\rho = 0$ leads to the reverse pattern. In particular, with $\rho = 0.5$, the median estimate of M falls on the lower bound $M = 0.05$. Because $\hat{Q}$ in (5.2) depends on both $\hat{M}$ and $\hat{P}_T$, the bias in $\hat{Q}$ is correspondingly large.

When measurement error is low, a wide range of reasonable choices for the unknown ρ could lead to better estimates than alternative mixed ρ or $\rho = 0$ assumptions (Fig. 2). Higher levels of measurement error necessitate a trade-off between bias and precision. If true ρ can be closely approximated, then this choice for ρ in the estimation could provide a risk-averse fishing policy. The quota Q will be underestimated but have greater precision. Uncertainty in the choice of true ρ could lead to even more conservative fishing policies. The mixed ρ assumption provides a possible compromise with unbiased but less precise estimates $\hat{Q}$.

One feature of catch-age analysis is the tendency for parameter estimates to be highly correlated. Using the true ρ with moderate error for illustration (Fig. 3), estimates $(\hat{M},\hat{R},\hat{P}_T,\hat{Q})$ are positively correlated because they are all scaled to population size. In particular, higher estimates $\hat{M}$ imply that a larger population is required to achieve a given catch. Conversely, higher estimates $\hat{q}$ or $\hat{\beta}_1$ imply that fewer fish are required to achieve a given catch. The set of border points in plots that include $\hat{M}$ or $\hat{Q}$ represents estimates constrained by the lower bound $M = 0.05$. Although not illustrated in Fig. 3, estimates $\hat{\alpha}$ are positively

Fig. 2. Boxplots of the estimates ($\hat{M}, \hat{q}, \hat{\alpha}, \hat{\beta}_1, \hat{R}, \hat{\gamma}, \hat{P}_T, \hat{Q}$). Combined results for six control policies are shown in relation to two levels of simulated measurement error (low, moderate) and four choices for ρ in the estimation model (mixed (Mx) 0, 0.5, true (T)). Each panel represents the ratio of estimated to true values for the specified parameter on a $\log_2$ scale, where $\hat{\gamma}$ and γ are first transformed by (5.3). Boxes illustrate the interquartile range (25 to 75% quantiles) of the ratio, where a dot indicates the median. Whiskers are drawn to the nearest value not beyond 1.5 times the interquartile range. Points beyond this range are illustrated individually.

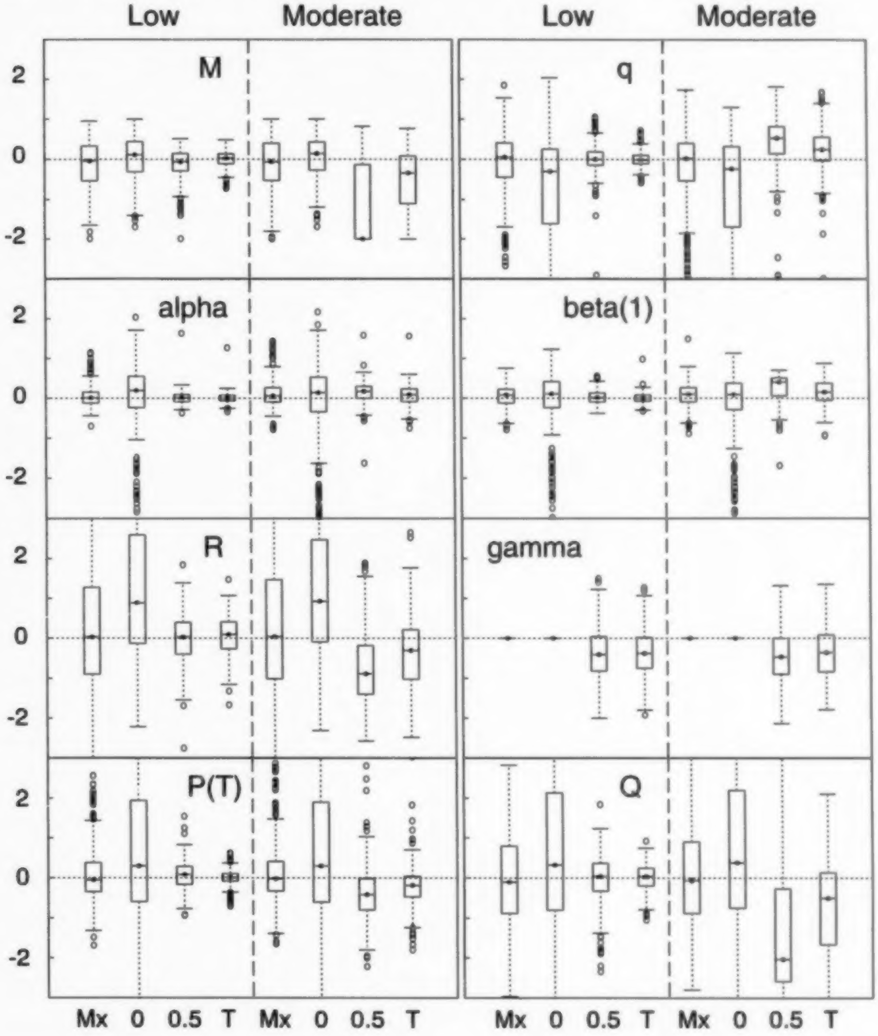

correlated with $\hat{\beta}_1$, while $\hat{\gamma}$ appears uncorrelated with other parameter estimates.

Figures 2 and 3 combine results across all six control policies. Figure 4 represents the behaviour of $\hat{M}$ and $\hat{q}$ in relation to the controls and three choices for ρ. Consistent with Fig. 2, under low measurement error both $\hat{M}$ and $\hat{q}$ appear relatively unbiased and their precision increases as the choice of ρ moves toward the true value. Furthermore, the precision of $\hat{q}$ increases markedly for controls with greater contrast (larger maximum values of F_t). Under moderate measurement error, both the precision and bias in $\hat{q}$ improve with larger fishery removals and more accurate choices for ρ. Thus, fishing contrast becomes more important with higher levels of measurement error. Estimates $\hat{M}$ appear to be more dependent on the choice of ρ than on the fishing policy. In particular, estimates $\hat{M}$ frequently fall on the lower bound $M = 0.05$ under moderate measurement error when $\rho = 0.5$.

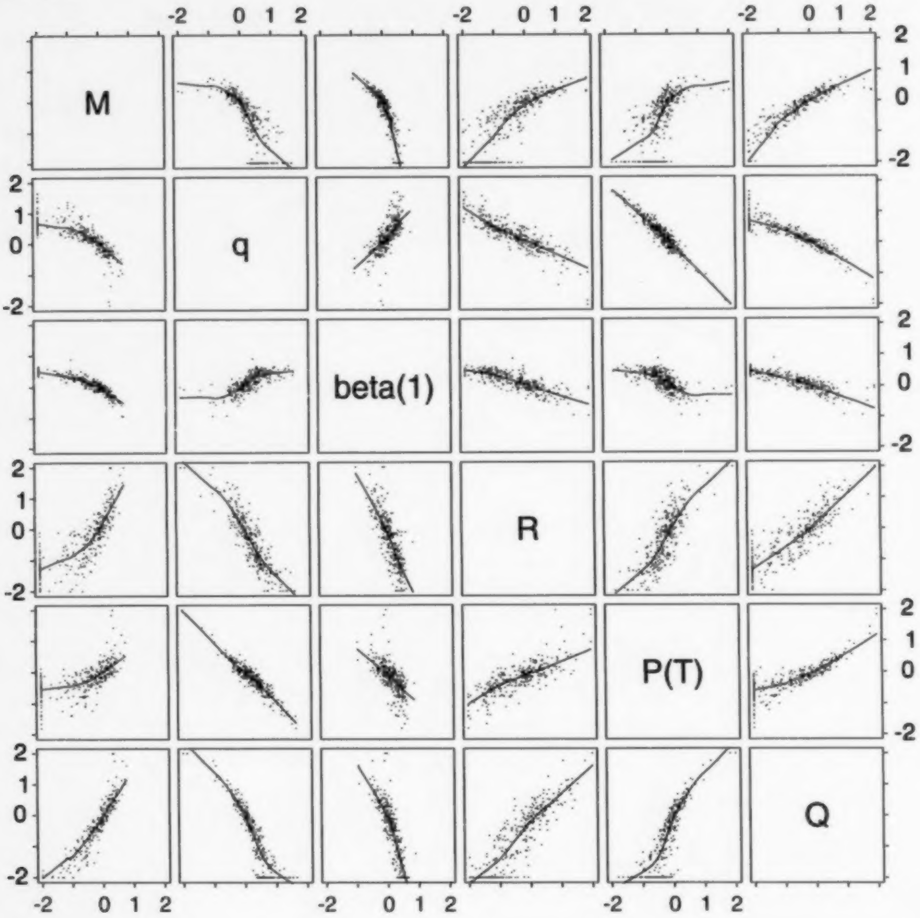

Fig. 3. Pairwise plots for the estimates ($\hat{M}, \hat{q}, \hat{\beta}_1, \hat{R}, \hat{P}_T, \hat{Q}$) obtained with moderate measurement error and the true choice of ρ. Results are combined across six control policies and scaled as in Fig. 2. The solid curve in each panel represents a locally weighted regression smoother through the data.

6. Discussion

Catch-age analysis has become a standard component of the stock assessment tool kit, where most applications assume that *M* is known. Our results confirm a high correlation between *M* and other model parameters, consistent with the usual requirement for a prescribed *M*. We have argued that realistic analyses must take account of uncertainty in *M*. For example, a Bayes prior (McAllister et al. 1994) could be used to summarize a range of possible values *M* obtained from the literature.

We have provided intuitive arguments in connection with the population matrix (4.2) suggesting that *M* might be estimable along with other parameters when catch-age data are available back to the first year of the fishery. Such an analysis depends on the pattern of recruitment variability, which we have captured through a simple autoregressive process. Alternatively, stock-recruitment relationships could be used to describe recruitment patterns, although we have not developed this approach here. Our results confirm the prospects for estimating *M*. Furthermore, our intuitive arguments find support in Fig. 4, where increased fishing contrast improves the estimate of *q*, but not of *M*. Presumably, this occurs because information on *M* is obtained primarily from the initial age structure.

Our analysis has examined the validity of estimation models that differ from the simulation model. In particular, we explored the use of different process error assumptions in the simulator and the estimator. We have shown that the simplified estimation assumption $\sigma_2 = 0$ appears workable, at least with small measurement error. We have followed this approach because it represents common practice in most catch-age analyses where the estimated population matrix (4.2) is determined from recruitments and other model parameters. We have not, however, investigated the full potential of estimators that contemplate both measurement and process error (Sullivan 1992; Schnute 1994).

Fig. 4. Boxplots of the estimates $(\hat{M}, \hat{q})$ scaled as in Fig. 2. Results are shown for each of the six control policies in relation to two levels of measurement error (low, moderate) and three choices for ρ (mixed, 0.5, true). Control policies are identified by the maximum fishing mortality $F_{T/2} = h_1 M$, obtained in the middle year of the time series.

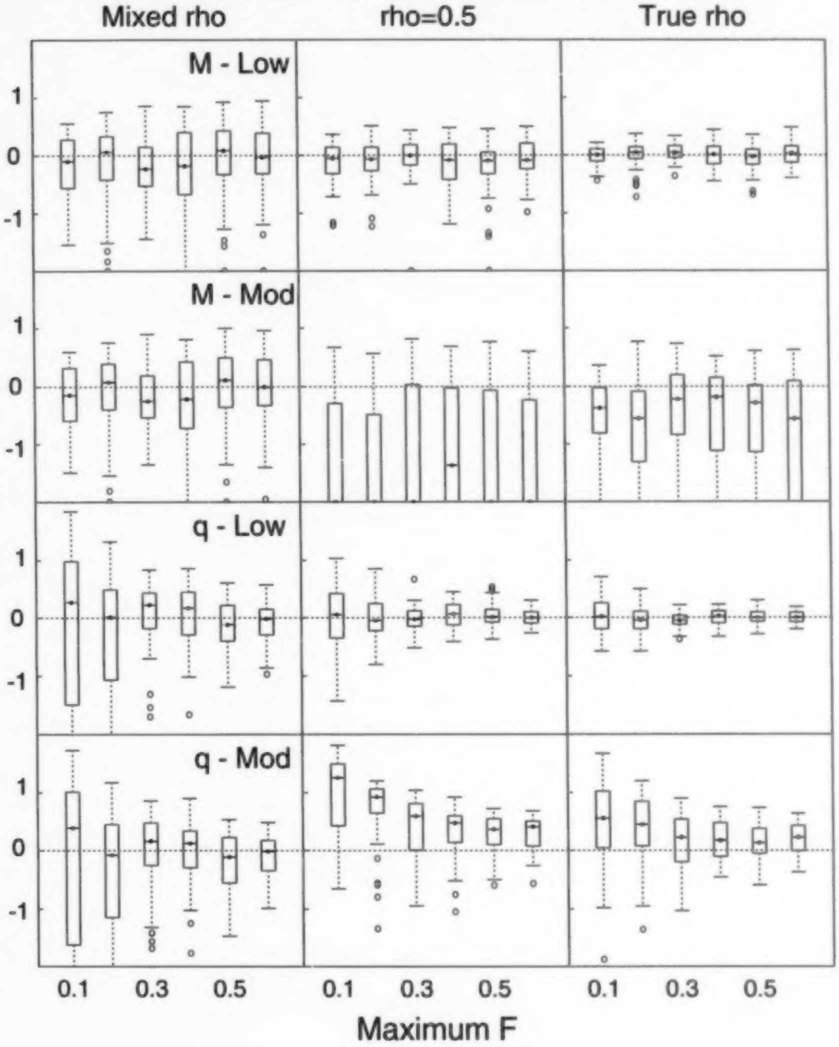

Our results suggest that the mixed ρ case can be helpful as an alternative to assuming a specified $\rho > 0$. We did not find the simplifying assumption $\rho = 0$ to be particularly useful, in spite of the low number of parameters, because of high variance in the corresponding estimates $\hat{\Phi}_L$. More complex estimation models performed better here than the simpler one, in contrast to other reported analyses (Ludwig and Walters 1985, 1989; Hilborn and Walters 1992, p. 76). Thus, additional complexity with the mixed ρ or specified $\rho > 0$ assumptions appears justified. We recognize, however, that choosing $\rho = 0$ is a naive approach to achieving simplicity. Perhaps a simple estimation model designed more intelligently would be able to capture major features of the dynamic system.

Estimation models generally perform better when measurement error is reduced and the correct ρ is specified (Fig. 2). In practice, reduced measurement error implies that ρ is near 1. These results indicate the importance of well-designed programs for data collection. Furthermore, the simplifying assumption $\rho = 0$ is particularly inappropriate for high-quality data with ρ near 1.

We have attempted to design a simulator with reasonable measurement and process errors. However, our results could easily be generalized to contemplate even more realistic scenarios. For example, stochastic components could be added to model random fishery selectivity, time-dependent survival, or other trends in the population dynamics. Fishing could be allowed prior to the first year, and more complex selectivity patterns could be introduced. In all such cases, the problem would be to design an estimator, perhaps with simpler error assumptions than in the simulator, capable of detecting such structural changes. Our results are not intended to be definitive. Rather, they illustrate a simulation–estimation framework within which to examine the possibilities and limitations of catch-age analysis.

Acknowledgements

We thank reviewers R. Deriso and D. Ludwig for thoughtful comments leading to an improved final draft. P. Aubry assisted the process of implementing our computer code on a UNIX workstation.

References

Deriso, R.B., T.J. Quinn II, and P.R. Neal. 1985. Catch–age analysis with auxiliary information. Can. J. Fish. Aquat. Sci. 42: 815–824.

Fournier, D., and C.P. Archibald. 1982. A general theory for analyzing catch at age data. Can. J. Fish. Aquat. Sci. 39: 1195–1207.

Griewank, A., and G.F. Corliss (*Editors*). 1991. Automatic differentiation of algorithms: theory, implementation, and application. Society for Industrial and Applied Mathematics, Philadelphia, Pa.

Gudmundsson, G. 1994. Time series analysis of catch-at-age observations. Appl. Stat. 43: 117–126.

Gulland, J.A. 1965. Estimation of mortality rates. Annex to Arctic Fisheries Working Group Report. ICES C.M. 1965. Doc. No. 3.

Harvey, A.C. 1989. Forecasting, structural time series models and the Kalman filter. Cambridge University Press, Cambridge, U.K.

Hilborn, R., and C.J. Walters. 1992. Quantitative fisheries stock assessment: choice, dynamics and uncertainty. Chapman & Hall, New York.

Kendall, M., and A. Stuart. 1979. The advanced theory of statistics. Vol. 2. 4th ed. MacMillan Publishing Co., New York.

Leaman, B.M. 1993. Reference points for fisheries management: the western Canadian experience. *In* Risk evaluation and biological reference points for fisheries management. *Edited by* S.J. Smith, J.J. Hunt, and D. Rivard. Can. Spec. Publ. Fish. Aquat. Sci. No. 120. pp. 15–30.

Ludwig, D., and C.J. Walters. 1985. Are age structured models appropriate for catch-effort data? Can. J. Fish. Aquat. Sci. 42: 1066–1072.

Ludwig, D., and C.J. Walters. 1989. A robust method for parameter estimation from catch and effort data. Can. J. Fish. Aquat. Sci. 46: 137–144.

McAllister, M.K., E.K. Pikitch, A.E. Punt, and R. Hilborn. 1994. A Bayesian approach to stock assessment and harvest decisions using the sampling/importance resampling algorithm. Can. J. Fish. Aquat. Sci. 51: 2673–2687.

Methot, R.D. 1989. Synthetic estimates of historical abundance and mortality for northern anchovy. Am. Fish. Soc. Symp. 6: 66–82.

Methot, R.D. 1990. Synthesis model: an adaptable framework for analysis of diverse stock assessment data. *In* Proceedings of the symposium on application of stock assessment techniques to gadids. *Edited by* L.-L. Low. Int. North Pac. Fish. Comm. Bull. No. 50. pp. 259–277.

Megrey, A. 1989. Review and comparison of age-structured stock assessment models from theoretical and applied points of view. Am. Fish. Soc. Symp. 6: 8–48.

Myers, R.A., W. Blanchard, and K.R. Thompson. 1990. Summary of North Atlantic fish recruitment 1942–1987. Can. Tech. Rep. Fish. Aquat. Sci. No. 1743.

Otter Research Ltd. 1991. AUTODIF: a C++ array language extension with automatic differentiation for use in nonlinear modeling and statistics. Otter Research Ltd., Nanaimo, B.C.

Pope, J.G. 1972. An investigation of the accuracy of virtual population analysis using cohort analysis. Int. Comm. Northwest Atl. Fish. Res. Bull. No. 9. pp. 65–74.

Press, W.H., S.A. Teukolsky, V.T. Vetterling, and B.P. Flannery. 1992. Numerical recipes in C: the art of scientific computing. 2nd ed. Cambridge University Press. Cambridge. U.K.

Richards, L.J. 1994. Trip limits, catch, and effort in the British Columbia rockfish trawl fishery. N. Am. J. Fish. Manage. 14: 742–750.

Richards, L.J., J.T. Schnute, A.R. Kronlund, and R.J. Beamish. 1992. Statistical models for the analysis of ageing error. Can. J. Fish. Aquat. Sci. 49: 1801–1815.

Schnute, J.T. 1994. A general framework for developing sequential fisheries models. Can. J. Fish. Aquat. Sci. 51: 1676–1688.

Schnute, J.T., and R. Hilborn. 1993. Analysis of contradictory data sources in fish stock assessment. Can. J. Fish. Aquat. Sci. 50: 1916–1923.

Sullivan, P.J. 1992. A Kalman filter approach to catch-at-length analysis. Biometrics, 48: 237–257.

Appendix. Likelihood derivations

The likelihood L_2 in (L.8) is the usual product of normal probability distributions for the residuals $\eta_{0t} = \tau_1\epsilon_{0t}$ ($t = 1, \ldots, T$) obtained from (L.5) and (S.8). Similarly, L_1 in (L.7) is the product of normal distributions for residuals ξ_t ($t = 2 - A, \ldots, T$) defined by (L.3)–(L.4) and (S.2)–(S.3), where the first residual ξ_{2-A} in this sequence has a larger variance than the others.

The derivation of L_3 in (L.9) is somewhat more complicated because, for a fixed t, the residuals η_{at} are linearly dependent. For convenience in this discussion, temporarily drop the index t from all variables. It follows from (2.12) and (S.10) that

$$\text{(A.1)} \qquad x_a = \log p_a - \frac{1}{A}\sum_{a=1}^{A} \log p_a .$$

Thus, x_a and p_a ($a = 1, \ldots, A$) are equivalent vectors, constrained by (2.11)–(2.12), where (A.1) transforms p_a to x_a and (S.10) defines the reverse transformation. Combining (A.1), (S.9), and (L.6) gives

$$\text{(A.2)} \qquad \eta_a = \tau_2\left(\epsilon_a - \frac{1}{A}\sum_{a=1}^{A}\epsilon_a\right).$$

It follows from (A.2) that the residuals η_a are multinormal, subject to the linear constraint

$$\text{(A.3)} \qquad \sum_{a=1}^{A} \eta_a = 0.$$

The likelihood for η_a is the probability density for the $A - 1$ dimensional vector $\mathbf{E} = (\eta_2, \eta_3, \ldots, \eta_A)$, where η_1 is determined by the constraint (A.3). The reader can verify from (A.2) that the covariance matrix of **E** is

$$\text{(A.4)} \quad \mathbf{V} = \tau_2^2\left(\mathbf{I}_{A-1} - \frac{1}{A}\mathbf{U}_{A-1}\right),$$

where $\mathbf{I}_k$ denotes a $k \times k$ identity matrix and $\mathbf{U}_k$ is a $k \times k$ 'unit' matrix with all entries 1. Furthermore, the inverse and determinant of **V** are

$$\text{(A.5)} \quad \mathbf{V}^{-1} = \tau_2^{-2}(\mathbf{I}_{A-1} + \mathbf{U}_{A-1})$$

$$\text{(A.6)} \quad |\mathbf{V}| = \frac{1}{A}\tau_2^{2(A-1)}.$$

The multinormal likelihood for **E** is

$$\text{(A.7)} \quad L = \left(\sqrt{2\pi}\right)^{-(A-1)}|\mathbf{V}|^{-1/2}\exp\left[-\frac{1}{2}\mathbf{E}'\mathbf{V}^{-1}\mathbf{E}\right],$$

where $\mathbf{E}'$ denotes the transpose of **E**. Combining (A.5)–(A.7) gives (after some algebra)

$$\text{(A.8)} \quad L = \left(\sqrt{2\pi}\,\tau_2\right)^{-(A-1)}\sqrt{A}\exp\left[-\frac{1}{2\tau_2^2}\sum_{a=1}^{A}\eta_a^2\right],$$

where η_1 in (A.8) is implicitly defined by (A.3). Finally, after reintroducing the index t, L_3 in (L.9) results from T factors of the form (A.8).

In deriving L_1 in (L.7), we assume that the index data consist of logarithmic measurements log I_t, rather than I_t directly. Consequently, the Jacobians $\partial\eta_{0t}/\partial(\log I_t)$ are equal to 1 and make no extra contribution to L_1. Similarly, Jacobians make no contribution to L_2 and L_3 because we deal with logarithmic recruitment parameters (log R_t) and regard the quantities x_a in (A.1) as raw measurements equivalent to the proportions p_a.

Substituting (3.5) into the combined likelihood (L.10) and reducing algebraically gives

$$\text{(A.9)} \quad -2\log L = K' - \log(1-\gamma^2) + (A+T-2)\log\rho + T\log(1-\rho) + (A+2T-2)\left(\frac{\hat{\kappa}^2}{\kappa^2} + \log\kappa^2\right) + (A-1)T\left(\frac{\hat{\tau}_2^2}{\tau_2^2} + \log\tau_2^2\right),$$

where $\hat{\kappa}^2$ and $\hat{\tau}_2^2$ are the formal expressions in (L.16)–(L.17) and K' is a constant independent of parameters (different from K in (3.10)). As a function of (κ,τ_2), the right side of (A.9) is minimized (i.e., L is maximized) when

$$\text{(A.10)} \quad (\kappa^2,\tau_2^2) = (\hat{\kappa}^2,\hat{\tau}_2^2).$$

Substituting (A.10) into (A.9) and dropping constants independent of parameters gives (L.18). A similar proof gives (L.14).

Influence of pH and hardness on toxicity of ammonia to the amphipod *Hyalella azteca*

G.T. Ankley, M.K. Schubauer-Berigan, and P.D. Monson

Abstract: The amphipod *Hyalella azteca* is frequently used for freshwater sediment tests throughout North America. A common potential toxicant in sediments is ammonia. Our objective was to characterize the influence of two key water quality variables, pH and hardness, on toxicity of ammonia to the amphipod. Ninety-six hour, water-only exposures of *H. azteca* to ammonia were conducted using three different water types with hardnesses of 42, 100, and 270 mg/L as $CaCO_3$ and three levels of pH (ca. 6.5, 7.5, and 8.5). In the soft water, toxicity of total ammonia was constant across test pH. As water hardness increased, toxicity of ammonia (on a total basis) to the amphipod decreased and became more pH dependent. Our data suggest that in softer water the amphipod was quite sensitive to the ionized (NH_4^+) form of ammonia. This contrasts with most other species that have been tested, which typically are more sensitive to un-ionized (NH_3) ammonia than to NH_4^+. These data provide baseline values for interpreting the possible contribution of ammonia to sediment toxicity in tests conducted with *H. azteca* and also indicate that in some situations NH_4^+ may be important in determining ammonia toxicity.

Résumé : L'amphipode *Hyalella azteca* est fréquemment utilisé pour les essais sur les sédiments d'eau douce partout en Amérique du Nord. L'ammoniac est un toxique potentiel commun dans ces sédiments. Le but de notre étude était de déterminer l'incidence de deux variables importantes liées à la qualité de l'eau, le pH et la dureté, sur la toxicité de l'ammoniac pour l'amphipode. *Hyalella azteca* a été exposé à l'ammoniac pendant 96 h, dans l'eau seulement, avec trois types d'eaux différents, ayant une dureté de 42, 100 et 200 $mg \cdot L^{-1}$ de $CacO_3$, et trois niveaux de pH (environ 6,5, 7,5 et 8,5). Dans l'eau douce, la toxicité de l'ammoniac total est constante, peu importe le pH. À mesure que la dureté de l'eau augmente, la toxicité de l'ammoniac (total) pour l'amphipode diminue et devient davantage liée au pH. Nos données laissent penser que, dans l'eau de dureté inférieure, l'amphipode est relativement sensible à la forme ionisée (NH_4^+) de l'ammoniac. Ces résultats vont à l'encontre de ceux qui ont été obtenus avec la plupart des autres espèces mises à l'essai, qui sont généralement plus sensibles à la forme non ionisée (NH_3) qu'à la forme ionisée (NH_4^+) de l'ammoniac. Ces données fournissent des valeurs de base pour l'interprétation de la contribution possible de l'ammoniac à la toxicité des sédiments dans les tests menés à l'aide de *H. azteca*; elles indiquent également que dans certaines conditions, NH_4^+ pourrait être un facteur important pour déterminer la toxicité de l'ammoniac.

[Traduit par la Rédaction]

Introduction

Assessments of contaminated sediments typically include biological assays with a variety of benthic macroinvertebrates. Although some assessments require only that a sediment be classified as toxic or nontoxic, it is usually desirable to identify the contaminants responsible for toxicity. This is often done by evaluating contaminants in sediment interstitial (pore) water, since chemicals present in pore water appear to represent that fraction of the total contaminant which is biologically available and free to exert toxicity (Adams et al. 1985; Swartz et al. 1985, 1990; Di Toro et al. 1990, 1991; Ankley et al. 1993, 1994). In situations where there are several potentially toxic contaminants, toxicity-based fractionation schemes that utilize pore water as a test medium can be useful for defining specific compounds or classes of compounds responsible for sediment toxicity (Ankley et al. 1990; U.S. EPA 1991; Schubauer-Berigan and Ankley 1991; Schubauer-Berigan et al. 1993*a*, 1993*b*; Burgess et al. 1993). In other instances, the list of suspect contaminants may be small, or it may be necessary to know only whether a particular compound is contributing to toxicity. In these cases, pore water contaminant

Received December 12, 1994. Accepted April 28, 1995.
J12677

G.T. Ankley.[1] U.S. Environmental Protection Agency, 6201 Congdon Boulevard, Duluth, MN 55804, U.S.A.
M.K. Schubauer-Berigan. Minnesota Pollution Control Agency, 320 West Second Street, Duluth, MN 55802, U.S.A.
P.D. Monson. Lake Superior Research Institute, 6201 Congdon Boulevard, Duluth, MN 55804, U.S.A.

[1] Author to whom all correspondence should be addressed.

Can. J. Fish. Aquat. Sci. **52**: 2078–2083 (1995). Printed in Canada / Imprimé au Canada

concentrations can be compared directly to corresponding water-only toxicity data for the species of concern to determine whether or not a particular contaminant may be responsible for toxicity (Adams et al. 1985; Swartz et al. 1985, 1990; Di Toro et al. 1991; Ankley et al. 1993, 1994). To make this type of comparison, it is necessary to have water-only toxicity databases for commonly tested species and sediment contaminants of concern.

One potentially toxic compound frequently present in sediment pore water is ammonia. Ammonia typically is found in sediments as a result of the diagenesis of nitrogen-containing compounds (Berner 1980), and occasionally it can be elevated to concentrations great enough to cause toxicity to commonly tested macroinvertebrates (Jones and Lee 1988; Ankley et al. 1990; Schubauer-Berigan and Ankley 1991; Burgess et al. 1993). Elevated ammonia concentrations in sediments may be natural or related to anthropogenic inputs of nutrients and (or) contaminants (Roy and Knowles 1994). Regardless of its origin, we often need to know whether ammonia is or is not responsible for toxicity observed in sediment bioassays. This is particularly true for dredged material assessments, where there has been a tendency to regard ammonia toxicity essentially as a test "artifact" (U.S. EPA/ACOE 1991, 1994).

Attributing sediment toxicity to ammonia, even through analysis and testing of pore water, is a challenging proposition (Ankley et al. 1992). For example, there is a general lack of high quality, water-only ammonia toxicity data for many of the invertebrates used in sediment toxicity assays. This problem is compounded by the fact that existing data often were collected under test conditions that preclude ready extrapolation to exposure scenarios of differing water quality. Because ammonia is present in ionized (NH_4^+) and un-ionized (NH_3) forms at ambient pH values, one of the most prominent water quality variables that may affect its toxicity to freshwater species is pH (U.S. EPA 1985*a*). For most species for which there are adequate data, ammonia toxicity (expressed on a total basis) increases at greater pH values as a result of increases in the relative concentration of the un-ionized form of ammonia, which is thought to be more toxic than the ionized form. This observation has led some aquatic toxicologists to assume that only un-ionized ammonia is toxic, when in fact the toxicity of ammonia may be best explained by a joint model that also considers the contribution of the ionized species (Erickson 1985).

Over the past 3 years, we have sought to develop a database to better define the toxicity of ammonia to three species of freshwater benthic macroinvertebrates commonly used for sediment testing in North America: *Lumbriculus variegatus* (oligochaetes), *Chironomus tentans* (midges), and *Hyalella azteca* (amphipods) (U.S. EPA 1992, 1994; ASTM 1995; Environment Canada 1994*a*, 1994*b*). To enhance extrapolation to variable exposure conditions, our tests were conducted both at multiple pH values and different hardnesses, as the latter can also affect ammonia toxicity (U.S. EPA 1985*a*). The results of these tests serve not only to enhance interpretation of sediment toxicity assays where ammonia may be present, but they also provide data for the planned derivation of sediment quality criteria and (or) future adjustments to existing water quality criteria for ammonia. Test results with *L. variegatus* and *C. tentans* were reasonably consistent with existing pH – ammonia toxicity models (Schubauer-Berigan et al. 1995), but results with amphipods were not. These latter data are presented here.

Materials and methods

Tests were conducted with 7- to 14-d-old *H. azteca* from on-site cultures maintained in Lake Superior water (initial hardness, 42 mg/L as $CaCO_3$) that had been increased in hardness to about 100 mg/L as $CaCO_3$ through the addition of a mixture of $CaSO_4$, $CaCl_2$, $MgSO_4$, $NaHCO_3$, and KCl (U.S. EPA 1985*b*, 1994). For the ammonia toxicity tests, the soft water (SW) was unadulterated Lake Superior water, moderately hard water (MW) was the "hardened" Lake Superior water described above, and the hard water (HW; ca. 240 mg/L as $CaCO_3$) was formulated from ultrapure (Millipore®) water and various metal salts (U.S. EPA 1985*b*). It should be noted that the three waters differed not only in hardness but in concentrations of specific anions. Thus, we cannot conclusively state that effects of water type on ammonia toxicity were caused solely by hardness.

Target pH values of 6.5, 7.5, and 8.5 for the toxicity tests were achieved through the use of a CO_2 head space technique described by Mount and Mount (1992). The pH of aliquots of the various test solutions was adjusted to the desired pH through additions of concentrated HCl or NaOH. The highest pH (i.e., 8.5) tended to remain relatively stable over the course of the 24-h period between test solution renewals. The pH values in the 6.5 and 7.5 treatments were maintained by placing the test chambers in 1.4-L glass canning jars that were flushed with a CO_2–air mixture and sealed until the next daily renewal. The precise amount of CO_2 necessary to stabilize pH at 6.5 or 7.5 for the different water types was determined through empirical observations made prior to performing the toxicity tests (Mount and Mount 1992).

Toxicity tests were conducted in disposable polystyrene cups containing 10 amphipods in 50 mL of test solution. Each cup contained a 1 × 3 cm piece of Nitex® screen for substrate, and the organisms were fed 400 μL of a yeast–Cerophyll®–trout chow mixture daily (Collyard et al. 1994; U.S. EPA 1994). Tests were conducted at 25 ± 1°C with a 16 h light : 8 h dark photoperiod. Four ammonia concentrations (50% serial dilutions) and a control were tested in duplicate at each hardness–pH combination. Separate canning jars were used for the different treatments because previous studies had indicated that ammonia was volatile enough to be transferred among test cups in the closed system (G.T. Ankley, unpublished data). Test solutions were renewed daily during the 96-h exposure using a freshly prepared ammonium chloride stock solution. Mortality of the amphipods was recorded at each test renewal and at the conclusion of the 96-h exposure.

Dissolved oxygen and pH were measured in all test solutions at test initiation and before and after each 24-h renewal. The pH was measured using a Beckman 40 pH meter and Orion combination probe. Dissolved oxygen, measured using a YSI model 57 meter, remained at acceptable levels

Table 1. Toxicity of ammonia to *Hyalella azteca* in 96-h tests at varying pH in soft, moderately hard, and hard water (SW, MW, and HW, respectively).

Water type	Nominal pH	Measured pH	LC_{50} (95% CI)	
			Total ammonia (mg N/L)	Un-ionized ammonia (mg NH_3-N/L)
SW	6.5	6.5±0.04	22.8 (15.1–34.4)	0.04 (0.03–0.06)
	7.5	7.49±0.22	17.5 (14.8–20.7)	0.31 (0.26–0.37)
	8.5	8.21±0.31	24.0 (NC)[a]	2.24 (NC)
MW	6.5	6.43±0.09	105 (53.7–203)	0.19 (0.10–0.36)
	7.5	7.31±0.25	64.0 (47.8–85.7)	0.83 (0.62–1.11)
	8.5	8.30±0.22	39.8 (34.4–46.0)	6.09 (5.26–7.04)
HW	6.5	6.55±0.06	>204	>0.37
	7.5	7.41±0.16	140 (110–177)	2.14 (1.68–2.71)
	8.5	8.45±0.06	35.2 (31.5–39.5)	5.38 (4.82–6.04)

Note: Measured pH values are the $\bar{x} \pm$ SD calculated from daily analyses performed on the new and old test solutions at the ammonia concentrations bracketing the final LC_{50} values.

[a] 95% CI could not be calculated using the trimmed Spearman–Karber method, as no partial kills occurred.

throughout the test at an average value of 7.8 mg/L. Ammonia concentrations were measured daily in each new stock solution using a Fisher Accunet 950 meter and a specific ion electrode, with a minimum detection limit of 0.1 mg/L.

The criterion for an acceptable test with the amphipod was ≥80% control survival (U.S. EPA 1994). Median lethal (LC_{50}) concentrations were calculated using the Spearman–Karber technique (Hamilton et al. 1977) and were based either on total ammonia or un-ionized ammonia. The latter was calculated from total ammonia values and mean test pH (averaged across the 96-h exposure) at a temperature of 25°C (Emerson et al. 1975). The pH values used for this conversion were those from serial dilutions bracketing the ultimate 96-h LC_{50}.

Results

Values of pH in the test system remained relatively constant and close to nominal values over the course of the 96-h exposure (Table 1). The greatest variation in pH, as well as deviation from the target nominal value, occurred in the SW initially adjusted to pH 8.5. The coefficients of variation in ammonia concentrations in stock solutions (measured daily) for the SW, MW, and HW were 1.6, 1.1, and 7.3%, respectively. Although ammonia concentrations were not measured after the 24-h holding period in these experiments (i.e., before the next daily renewal), previous experiments in our laboratory have shown that ammonia concentrations decrease by ≤10% over the course of 24 h in a static system (G.T. Ankley, unpublished data). Thus, LC_{50} values were calculated on the basis of the mean measured concentrations of ammonia in the stock solutions.

In the SW, LC_{50} values expressed on a total ammonia basis were essentially constant at 22.8, 17.5, and 24.0 mg N/L at nominal pH values of 6.5, 7.5, and 8.5, respectively (Table 1). However, when toxicity data were based on un-ionized ammonia, LC_{50} values varied by approximately 56-fold across the range of pH tested. There was nearly an order of magnitude difference in the LC_{50} values between each nominal test pH (Table 1).

At any tested pH, ammonia toxicity, expressed either on a total or un-ionized basis, was less in the MW than in the SW (Table 1). The LC_{50} values, expressed on a total basis, varied by a factor of around 2.5, ranging from 39.8 mg N/L at the nominal pH of 8.5 to 105 mg N/L at pH 6.5 (Table 1). As was true for the SW tests, when ammonia toxicity was expressed on the basis of un-ionized ammonia, the LC_{50} values were far more variable, ranging from 0.19 mg NH_3-N/L in the pH 6.5 treatment to 6.09 mg NH_3-N/L at the target pH of 8.5.

Ammonia toxicity, expressed either on a total or un-ionized basis, further decreased in the HW at nominal pH values of 6.5 and 7.5 (Table 1). There was more of an effect of pH on ammonia toxicity in the HW when LC_{50} values were based on total ammonia; the LC_{50} values ranged from 35.2 to >204 mg N/L at nominal pH values of 8.5 and 6.5, respectively. When LC_{50} values were based on un-ionized ammonia, they were still more variable than when based on total ammonia, but this variation was less than that observed in either the SW or MW.

Discussion

Preliminary studies in our laboratory suggested that the toxicity of ammonia to *H. azteca* in 4-d exposures was relatively constant over a pH range of approximately 2 units when LC_{50} values were expressed on the basis of total ammonia (U.S. EPA 1991). This result was somewhat unexpected. However, Borgmann (1994) confirmed our observations; in chronic tests with the amphipod at two pH values (ca. 7.4 and 8.4) he found that ammonia toxicity, expressed on a total basis, was more constant than when expressed as un-ionized ammonia. This led Borgmann (1994) to suggest that *H. azteca* was responding predominantly to ionized rather than un-ionized ammonia. Borgmann (1994) also indicated that hardness decreased toxicity of ammonia to the amphipod; however, this interpretation was made in tests conducted at only one pH and two hardnesses. The results of the present study confirm those described by U.S. EPA (1991) and Borgmann (1994) and, through use of a complete 3 × 3 pH × hardness test matrix, extend their observations one step further. At the low water hardness, ammonia toxicity appeared to be completely independent of pH, i.e., on a total ammonia basis, LC_{50} values were essentially the same over a pH range of 1.7 units, while LC_{50}s based on the un-ionized ammonia varied by more than 50-fold. As water hardness increased, toxicity expressed as total or un-ionized ammonia generally decreased, consistent with observations made with other species (U.S. EPA 1985*a*). Of more interest is the observation that as hardness increased the effects of pH on ammonia toxicity changed. At the intermediate water hardness, ammonia toxicity on a total basis varied by a factor of about 2.5-fold over 2 pH units, while on an un-ionized basis ammonia toxicity varied by 30-fold. In the hardest water, ammonia toxicity on a total basis varied by at least 6-fold, while on an un-ionized basis, toxicity varied by less than 14-fold. At the pH values in our tests the majority of the ammonia was ionized, so given the relative constancy in ammonia toxicity (expressed on a total basis) across pH, particularly in the SW and MW, we are in agreement with the assessment of Borgmann (1994) that the amphipod may be responding more to NH_4^+ than to NH_3.

Many studies have focused on the effects of pH on ammonia toxicity to aquatic organisms. Early studies with fishes (e.g., Chipman 1934) indicated a marked increase in ammonia toxicity with increased pH; this finding prompted researchers to suggest that toxicity of ammonia was due solely to NH_3 rather than NH_4^+. However, more careful studies with fishes at a wider range of pH values (e.g., Thurston et al. 1981) indicated that ammonia toxicity, expressed on the basis of un-ionized ammonia, was not constant across pH; at low pH values, the toxicity of un-ionized ammonia appeared to increase. This type of response seemed to be even more pronounced for some invertebrate species (Armstrong et al. 1978; Miller et al. 1990; Landau and Sanchez 1991). Two possible explanations have been advanced for the observed trends in ammonia toxicity with pH: (*i*) NH_3 is more potent at low pH values than at high pH values, and (*ii*) at low pH values, NH_4^+ exerts toxicity that is not apparent at higher pH values where comparatively greater concentrations of the more potent NH_3 are present. On the basis of the latter hypothesis, Erickson (1985) proposed a joint toxicity model for NH_3 and NH_4^+, with NH_3 causing most toxicity at high pH values and NH_4^+ contributing to toxicity at lower pH values. The analysis presented by Erickson (1985) for a joint toxicity model is compelling, on the basis of toxicological observations made at low pH values with fishes and invertebrates as well as the fact that it has been demonstrated that under low pH conditions a net inward flux of NH_4^+ can occur across the gills of aquatic species (Evans and Cameron 1986). Regardless of this evidence, it is not uncommon for ammonia toxicity to be reported solely on an un-ionized basis (e.g., Miller et al. 1990). Our studies (U.S. EPA 1991; present work) and those of Borgmann (1994) indicate that *H. azteca* likely is sensitive to both un-ionized and ionized forms of ammonia thus directly supporting the concept of a joint toxicity model for mixtures of NH_3 and NH_4^+.

There has been extensive research concerning mechanisms through which freshwater organisms excrete ammonia (Evans and Cameron 1986). Blood ammonia concentrations are controlled through a combination of passive diffusion of NH_3 (and to a lesser degree, NH_4^+) and active exchange of NH_4^+ for Na^+ from the external environment. A number of internal and external factors, including NH_3 and NH_4^+ gradients (which are determined in part by pH), salinity, and hardness, control which routes of excretion predominate. The general decrease that we observed in sensitivity to ammonia (either on a total or ionized basis) with increasing hardness (and, subsequently, Na^+) could logically be explained by an enhanced ability of the amphipod to excrete NH_4^+ via Na^+–NH_4^+ exchange. Unfortunately, many of the mechanistic studies concerning ammonia excretion (and osmoregulation) have been conducted using external ammonia concentrations far smaller than those typically used for toxicity tests. Thus, it is more difficult to formulate a mechanistic explanation concerning the sensitivity of *H. azteca* to NH_4^+ and the apparent interaction between pH and hardness on sensitivity of the amphipod to ammonia. This difficulty is further confounded in that the anionic composition (e.g., alkalinity) of our test waters covaried with hardness; hence, effects that we observed cannot be unequivocally attributed to cations in the water. In any case, additional studies focused on the physiological basis of *H. azteca* sensitivity to ammonia would be useful in terms of identifying other species potentially sensitive to NH_4^+.

There are a number of practical implications that arise concerning the observed trends in sensitivity of *H. azteca* to ammonia. For example, the most common expression of the U.S. EPA (1985*a*) water quality criterion (WQC) for ammonia is based on NH_3, under the premise that this is the form principally responsible for toxicity. This clearly may not be an appropriate assumption in the case of *H. azteca*, and hence, quite probably for other species as well. This premise is particularly problematic for WQC derived at low pH values where NH_3 concentrations (compared with total ammonia) can be exceedingly small, yet the organisms continue to be relatively sensitive to NH_4^+. For example, the *H. azteca* 96-h LC_{50} value of 0.04 mg NH_3/L at pH 6.5 in the SW is below the 1-h average WQC concentration (at a pH of 6.5 at 25°C) for non-salmonid species of 0.051 mg NH_3/L (U.S. EPA 1985*a*). Thus, our data suggest that WQC expressed solely on the basis of NH_3 have the potential to be underprotective of species sensitive to NH_4^+, in particular at low pH values.

One of the primary reasons for undertaking this research was to define an effect – no effect ammonia concentration to aid in the interpretation of results of sediment toxicity tests with *H. azteca*. Our strategy was to measure pore-water concentrations of ammonia during sediment toxicity tests and compare these with effect concentrations (e.g., LC_{50} values) derived from water-only tests to determine whether ammonia may be responsible for any observed toxicity (Ankley et al. 1992). It appears that this type of approach may not be as straightforward as initially envisioned given the seeming interaction observed between pH and hardness in determining ammonia toxicity. One conclusion that can be made from our study is that even under a worst case scenario (i.e., in soft water), at least 15–20 mg total ammonia/L would be required to cause appreciable mortality (≥50%) to *H. azteca* in a 96-h exposure. This, coupled with the observation that we find little difference between 4- and 10-d LC_{50} values for *H. azteca* exposed to ammonia (G.T. Ankley, unpublished data), suggests that pore-water ammonia concentrations of less than 10 mg/L in standard 10-d whole-sediment tests should not result in significant toxicity to the amphipod. This interpretation is important, because the majority of freshwater sediments we have tested at the Duluth EPA facility typically contain less than 10 mg total ammonia/L, which suggests that little, if any, ammonia toxicity to *H. azteca* would be predicted in assays with these sediments.

Acknowledgements

This work was supported by the Office of Research and Development and the Office of Water of the U.S. EPA, in part through a cooperative agreement CR 820433 to Dr. D. Call at the University of Wisconsin—Superior. We are indebted to Dr. R. Erickson for helpful comments and discussions during development of the manuscript, and to Dr. D. Mount, Dr. P. Chapman, Dr. S. Hedtke, Dr. P. Sibley, and Ms. P. Grittner for technical and editorial comments. The manuscript has been reviewed in accordance with official EPA policy. Mention of trade names does not indicate endorsement by the Federal government.

References

Adams, W.J., R.A. Kimerle, and R.G. Mosher. 1985. Aquatic safety assessment of chemicals sorbed to sediments. *In* Aquatic toxicology and hazard assessment: seventh symposium. *Edited by* R.D. Cardwell, R. Purdy, and R.C. Bahner. STP 854. American Society for Testing and Materials, Philadelphia, Pa. pp. 429–453.

Ankley, G.T., A. Katko, and J.W. Arthur. 1990. Identification of ammonia as an important sediment-associated toxicant in the lower Fox River and Green Bay, Wisconsin. Environ. Toxicol. Chem. 9: 313–322.

Ankley, G.T., M.K. Schubauer-Berigan, and R.A. Hoke. 1992. Use of toxicity identification evaluation techniques to identify dredged material disposal options: a proposed approach. Environ. Manage. 16: 1–6.

Ankley, G.T., V.R. Mattson, E.N. Leonard, C.W. West, and J.L. Bennett. 1993. Predicting the acute toxicity of copper in freshwater sediments: evaluation of the role of acid volatile sulfide. Environ. Toxicol. Chem. 12: 315–320.

Ankley, G.T., D.J. Call, J.S. Cox, M.D. Kahl, R.A. Hoke, and P.A. Kosian. 1994. Organic carbon partitioning as a basis for predicting the toxicity of chlorpyrifos in sediments. Environ. Toxicol. Chem. 13: 621–626.

Armstrong, D.A., D. Chippendale, A.W. Knight, and J.E. Colt. 1978. Interaction of ionized and un-ionized ammonia on short-term survival and growth of prawn larvae, *Macrobrachium rosenbergii*. Biol. Bull. (Woods Hole, Mass.), 154: 15–34.

ASTM. 1995. Standard test methods for measuring the toxicity of sediment-associated contaminants with freshwater invertebrates. E1706-95. American Society for Testing and Materials, Philadelphia, Pa.

Berner, R.A. 1980. Early diagenesis: a theoretical approach. Princeton University Press, Princeton, N.J.

Borgmann, U. 1994. Chronic toxicity of ammonia to the amphipod *Hyalella azteca*: importance of ammonium ion and water hardness. Environ. Pollut. 86: 329–335.

Burgess, R.M., K.A. Schweitzer, R.A. McKinney, and D.K. Phelps. 1993. Contaminated marine sediments: water column and interstitial toxic effects. Environ. Toxicol. Chem. 12: 127–138.

Chipman, W.A., Jr. 1934. The role of pH in determining the toxicity of ammonia compounds. Ph.D. thesis, University of Missouri, Columbia, Mo.

Collyard, S.A., G.T. Ankley, R.A. Hoke, and T. Goldenstein. 1994. Influence of age on the relative sensitivity of *Hyalella azteca* to diazinon, alkyphenol ethoxylates, copper, cadmium, and zinc. Arch. Environ. Contam. Toxicol. 26: 110–113.

Di Toro, D.M., J.D. Mahony, D.J. Hansen, K.J. Scott, B.B. Hicks, S.M. Mayr, and M.S. Redmond. 1990. Toxicity of cadmium in sediments: the role of acid volatile sulfide. Environ. Toxicol. Chem. 7: 483–498.

Di Toro, D.M., C.S. Zarba, D.J. Hansen, W.J. Berry, R.C. Swartz, C.E. Cowan, S.P. Pavlou, H.E. Allen, N.A. Thomas, and P.R. Paquin. 1991. Technical basis for establishing sediment quality criteria for nonionic organic chemicals using equilibrium partitioning. Environ. Toxicol. Chem. 10: 1541–1583.

Emerson, K., R.C. Russo, R. Lund, and R.V. Thurston. 1975. Aqueous ammonia equilibrium calculations: effects of pH and temperature. J. Fish. Res. Board Can. 32: 2379–2383.

Environment Canada. 1994*a*. Test for growth and survival in sediment using the freshwater amphipod *Hyalella azteca*. Draft Guidance Manual. Environment Canada, Ottawa, Ont.

Environment Canada. 1994*b*. Test for growth and survival in sediment using the freshwater midges *Chironomus tentans* and *C. riparius*. Draft Guidance Document. Environment Canada, Ottawa, Ont.

Erickson, R.J. 1985. An evaluation of mathematical models for the effects of pH and temperature on ammonia toxicity to aquatic organisms. Water Res. 19: 1047–1058.

Evans, D.E., and J.N. Cameron. 1986. Gill ammonia transport. J. Exp. Zool. 239: 17–23.

Hamilton, M.A., R.C. Russo, and R.V. Thurston. 1977. Trimmed Spearman–Karber method for estimating median lethal concentrations in toxicity bioassays. Environ. Sci. Technol. 11: 714–719. (Correction, Environ. Sci. Technol. 12: 417.)

Jones, R.A., and G.F. Lee. 1988. Toxicity of U.S. waterway sediments with particular reference to the New York Harbor area. *In* Chemical and biological characterization of sludges, sediments, dredge spoils and drilling muds. *Edited by* J.J. Lichtenberg, F.A. Winter, C.I. Weber, and L. Fradkin. STP 976. American Society for Testing and Materials, Philadelphia, Pa. pp. 403–417.

Landau, M., and V. Sanchez. 1991. Effect of pH and decapsulation on the toxicity of ammonia to the brine shrimp *Artemia franciscana*. J. World Aquacult. Soc. 22: 178–182.

Miller, D.C., S. Poucher, J.A. Cardin, and D. Hansen. 1990. The acute and chronic toxicity of ammonia to marine fish and a mysid. Arch. Environ. Contam. Toxicol. 19: 40–48.

Mount, D.I., and D.R. Mount. 1992. A simple method of pH control for static and static-renewal aquatic toxicity tests. Environ. Toxicol. Chem. 11: 609–614.

Roy, R., and R. Knowles. 1994. Effects of methane metabolism on nitrification and nitrous oxide production in polluted freshwater sediment. Appl. Environ. Microbiol. 60: 3307–3314.

Schubauer-Berigan, M.K., and G.T. Ankley. 1991. The contribution of ammonia, metals and nonpolar organic compounds to the toxicity of sediment interstitial water from an Illinois River tributary. Environ. Toxicol. Chem. 10: 925–940.

Schubauer-Berigan, M.K., J.R. Amato, G.T. Ankley, S.E. Baker, L.P. Burkhard, J.R. Dierkes, J.J. Jenson, M.T. Lukasewycz, and T.J. Norberg-King. 1993*a*. The behavior and identification of toxic metals in complex mixtures: examples from effluent and sediment pore water toxicity identification evaluations. Arch. Environ. Contam. Toxicol. 24: 298–306.

Schubauer-Berigan, M.K., J.R. Dierkes, P.D. Monson, and G.T. Ankley. 1993*b*. The pH-dependent toxicity of Cd, Cu, Ni, Pb and Zn to *Ceriodaphnia dubia*, *Pimephales promelas*, *Hyalella azteca*, and *Lumbriculus variegatus*. Environ. Toxicol. Chem. 12: 1261–1266.

Schubauer-Berigan, M.K., P.D. Monson, C.W. West and G.T. Ankley. 1995. Influence of pH on the toxicity of ammonia to *Chironomus tentans* and *Lumbriculus variegatus*. Environ. Toxicol. Chem. 14: 713–717.

Swartz, R.C., G.R. Ditsworth, D.W. Schults, and J.O. Lamberson. 1985. Sediment toxicity to a marine infaunal amphipod: cadmium and its interaction with sewage sludge. Mar. Environ. Res 18: 133–153.

Swartz, R.C., D.W. Schults, T.H. DeWitt, G.R. Ditsworth, and J.O. Lamberson. 1990. Toxicity of fluoranthene in sediment to marine amphipods: a test of the equilibrium partitioning approach to sediment quality criteria. Environ. Toxicol. Chem. 9: 1071–1080.

Thurston, R.V., R.C. Russo, and G.A. Vinogradov. 1981. Ammonia toxicity to fishes: effect of pH on the toxicity of un-ionized ammonia species. Environ. Sci. Technol. 15: 837–840.

U.S. Environmental Protection Agency. 1985*a*. Ambient water quality criteria for ammonia. EPA-440/05-85/001. Environmental Protection Agency, Washington, D.C.

U.S. Environmental Protection Agency. 1985*b*. Methods for measuring the acute toxicity of effluents to freshwater and marine organisms. EPA-600/04-85/013. Environmental Protection Agency, Cincinnati, Ohio.

U.S. Environmental Protection Agency. 1991. Sediment toxicity identification evaluation: phase I (characterization), phase II (identification) and phase III (confirmation) modifications of effluent procedures. EPA-600/6-91/007. Environmental Protection Agency, Duluth, Minn.

U.S. Environmental Protection Agency. 1992. Tiered testing issues for freshwater and marine sediments—workshop proceedings. Environmental Protection Agency, Washington, D.C.

U.S. Environmental Protection Agency. 1994. Methods for measuring the toxicity and bioaccumulation of sediment-associated contaminants with freshwater invertebrates. EPA-600/R-94/024. Environmental Protection Agency, Duluth, Minn.

U.S. Environmental Protection Agency/Army Corps of Engineers. 1991. Evaluation of dredged material proposed for ocean disposal—testing manual. EPA-503/8-91/001. Environmental Protection Agency. Washington, D.C.

U.S. Environmental Protection Agency/Army Corps of Engineers. 1994. Evaluation of dredged material proposed for discharge in waters of the U.S.—testing manual. EPA-823/B-94/002. Environmental Protection Agency, Washington, D.C.

Hydrological exchange and sediment characteristics in a riverbank: relationship between heavy metals and invertebrate community structure

Janine Gibert, Pierre Marmonier, Vladimir Vanek, and Sandrine Plénet

Abstract: The first metre of bed sediments of the Rhône River functions as a filter for fluxes of heavy metals and epigean organisms between surface and interstitial environments. To study the efficacy of this bank filtration, three sampling stations were established at increasing distances from pumping wells, resulting in a gradient of hydraulic characteristics. Station A, a permanent downwelling area with very high hydraulic gradients, low hydraulic conductivity, low oxygen content, and rather high metal concentrations contained a fauna exclusively composed of epigean organisms. At station B, intermediate hydraulic gradients, high hydraulic conductivity near the surface, and variable direction of water exchanges resulted in well-oxygenated pore water and a diversified fauna with hypogean and epigean species. Finally, at station C, low hydraulic gradient, low hydraulic conductivity, low water exchange, and high sediment metal concentrations resulted in low pore-water oxygen concentrations and low interstitial fauna density and diversity. At this site, low oxygen content and low biodiversity were related to the clogging of shallow sediments and low filtration efficiency. Thus, bank filtration efficiency, a property that depends mainly on natural or human-induced hydraulic gradients and sediment granulometry, determines pore-water chemistry, metal distribution, and faunal composition in the shallow interstitial environments of the Rhône River.

Résumé : Le premier mètre de sédiments du lit du Rhône fonctionne comme un filtre pour les flux de métaux lourds et d'organismes épigés entre les milieux superficiel et interstitiel. Afin d'étudier l'efficacité de cet effet filtre des berges, trois stations d'échantillonnage ont été choisies en bordure d'une zone de pompage, à des distances croissantes des puits le long d'un gradient des caractéristiques hydrauliques. La station A, une zone d'infiltration permanente caractérisée par de forts gradients hydrauliques, une conductivité hydraulique faible, des teneurs en oxygène basses et des concentrations en métal plutôt élevées, présente une faune composée exclusivement d'organismes épigés. À la station B, les gradients hydrauliques sont intermédiaires, la conductivité hydraulique est élevée près de la surface et les échanges d'eau sont de direction variable. Dans cette station, l'eau interstitielle est bien oxygénée et la faune est bien diversifiée en espèces épigées et hypogées. Enfin, à la station C, le gradient hydraulique et la conductivité hydraulique sont faibles, les échanges d'eau limités et les concentrations en métal élevées. À cette station, les concentrations en oxygène de l'eau interstitielle sont faibles, et la faune interstitielle est peu dense et peu diversifiée. Ces derniers résultats semblent être liés au colmatage des sédiments les plus superficiels et à l'efficacité de filtration. Ainsi, l'efficacité de cet effet filtre des berges dépend principalement des gradients hydrauliques (naturels ou induits par l'homme) et de la granulométrie des sédiments. Elle influence directement la chimie de l'eau interstitielle, la distribution des métaux et la composition faunistique des communautés présentes dans les habitats interstitiels peu profonds du Rhône.

Received November 17, 1994. Accepted April 28, 1995.
J12635

J. Gibert and S. Plénet. Université Claude Bernard Lyon I, Unité de recherche associée n° 1974 du Centre national de la recherche scientifique, Écologie des eaux douces et des grands fleuves, Hydrobiologie et écologie souterraines, 43, boulevard du 11/11/1918, 69622 Villeurbanne Cédex, France.
P. Marmonier. Université de Savoie, GRETI, Unité de recherche associée n° 1974 du Centre national de la recherche scientifique, Écologie des eaux douces et des grands fleuves, 73376 LeBourget-du-Lac, France.
V. Vanek. University of Lund and VBB Viak, Geijersgatan 8, 216 18 Malmö, Sweden.

Can. J. Fish. Aquat. Sci. **52**: 2084–2097 (1995). Printed in Canada / Imprimé au Canada

Introduction

Boundaries (ecotones) between various environments are important in controlling fluxes of mass and energy in the landscape and might, to some extent, be used to counteract the increasing pressures on aquatic systems from various human activities (Naiman and Décamps 1990; Holland et al. 1991). Previous studies dealing with surface water – interstitial water interfaces were usually focused on hydraulic, hydrogeologic, and hydrochemical processes (Wright 1980; Dahlblom and Lindh 1988). There is growing evidence that the composition of the invertebrate community can contribute to understanding the exchange mechanisms between rivers and their floodplains (Marmonier and Dole 1986; Dole-Olivier and Marmonier 1992*a*; Boulton et al. 1992; Hakenkamp et al. 1993). Unfortunately, biologically oriented studies were often isolated from those dealing with physical processes. Realizing the necessity of linking the physical and biological approaches, some authors (Danielopol 1980; Gibert 1990; Gibert et al. 1990; Lafont et al. 1992; Valett et al. 1993) and organizations (UNESCO-ICGW Working Group 1992; U.S. Environmental Protection Agency 1992) have encouraged the initiation of combined studies. The first such reports were from the floodplains of the Danube River (Danielopol 1984) and from the Rhine River and its basin (Stuyfzand 1989; Carbiener and Tremolières 1990). Because of the threat of contamination (e.g., heavy metals) from industry and land use, this type of multidisciplinary study has also been initiated on the Rhône River at the Grand Gravier site (Givors, Rhône). Hydrologic investigations including regional groundwater models (Durbec and Leduc 1989; Ille et al. 1991), local tracer tests (Gaillard et al. 1990, 1991), chemical and biological studies (Gibert 1992, 1994), and studies of the vertical distribution of organic matter and microbes (Marmonier et al. 1995) suggest that self-purification processes within the surface water – interstitial water ecotone are important controls on groundwater quality. However, this buffering potential or purification capacity of the system remains poorly understood (Ille et al. 1991; Lafont and Durbec 1990).

Artificial groundwater recharge (induced infiltration of surface water into river or lake shores and bottom sediments) is a common method of amending natural groundwater resources (Asano 1985; Freeze and Cherry 1979). Moreover, infiltration of surface water through the bankside is a natural method to enhance water quality. The exchanges between groundwater and surface water associated with this artificial recharge often result in a higher variability and wider range of process velocities than what is common under natural conditions (Fetter 1988). By studying such systems we can learn more about the nature of ecotone processes and their limits (Vanek 1995). Such knowledge is crucial when establishing management policies for these strategic areas and other human-influenced ecotones.

Here we study bank filtration and evaluate the relative importance of granulometry (composition and characteristics of the sediment) and water flow effects in influencing the chemistry of the ecotone and its biological communities. Two questions arise. (*i*) How do sediment properties and water flow rates influence water chemistry and the spatial distribution of heavy metals? (*ii*) How do interstitial communities react to sediment properties, flow rates, and water chemistry? Because the surface water – groundwater ecotone is three dimensional, its functioning may be influenced by longitudinal, lateral, and vertical gradients. This research, therefore, addresses the above questions in all three dimensions.

Site description

The Rhône River is a submontane river 522 km long that is characterized by extensive floodplains where water is exchanged between the river and its associated alluvial aquifer (Bravard 1987). The study sector, the Grand Gravier (Givors, Rhône), is a braided portion of the flooplain located approximately 20 km downstream from Lyon (Figs. 1*a* and 1*b*). It has a slope of ≤0.5 $m\cdot km^{-1}$ and a mean annual discharge of 1033 $m^3\cdot s^{-1}$ (Bravard 1987; Poinsart 1992).

The study area is covered by a 15–20 m thick sequence of glaciofluvial sediments of Wurmian age consisting of several layers of sand, gravel, and pebbles. The typical hydraulic conductivity (permeability) of the aquifer ranges from 1 to 3×10^{-3} $m\cdot s^{-1}$ (Durbec and Leduc 1989) but is assumed to be lower within the permanently submerged, partly clogged, river bottom sediments (Ille et al. 1991). Since the early 1950s, the site has been used as a groundwater extraction region by Grigny Waterworks to supply drinking water to southwestern areas of Lyon. At present, it harbours eight production wells located 60–120 m from the river (Fig. 1*c*) that yield ca. 13 000 $m^3\cdot day^{-1}$. Some 70–90% of the extracted water corresponds to infiltrated Rhône River water (Ille et al. 1991), and tracer tests performed in the upstream part of the study site have shown that the infiltrated river water reaches the nearest production well in less than 4 days (Gaillard et al. 1990, 1991).

Besides the municipality of Lyon and associated communities, various chemical, metallurgic, and other industries are located along the Rhône River and its tributaries upstream of the site. Permanent loading of the Rhône River by the effluents from numerous industrial and municipal wastewater treatment plant causes chronic pollution of river water in the area (Comité de Bassin Rhône–Méditerranée–Corse 1993). River pollutants occasionally reach high levels, for example, in connection with industrial accidents or malfunctioning of some of the treatment plants. In spite of high pollution levels in the river, the water extracted by the production wells usually has an acceptable drinking water quality (Ille 1992).

Material and methods

Three sampling stations were established near the river shore along a 450-m reach of the Grand Gravier sector (Fig. 1*c*). Each station consisted of three sampling locations, or substations, located 1.5 m into the river, at the river shoreline, and 1.5 m inland from the shore (Fig. 1*d*). These substations were designated river (R), shoreline (SL), and shore (S), respectively. Each substation was sampled at three submerged sediment depths (20, 50, and 100 cm, measured from the surface of the water table in the case of the shore substation) using the Bou–Rouch pumping

Fig. 1. The study site at the Grand Gravier, Rhône, France, showing the study reach location (*a* and *b*), sampling station locations at the reach scale (*c*), and vertical and horizontal distributions of sampling at each station (*d*).

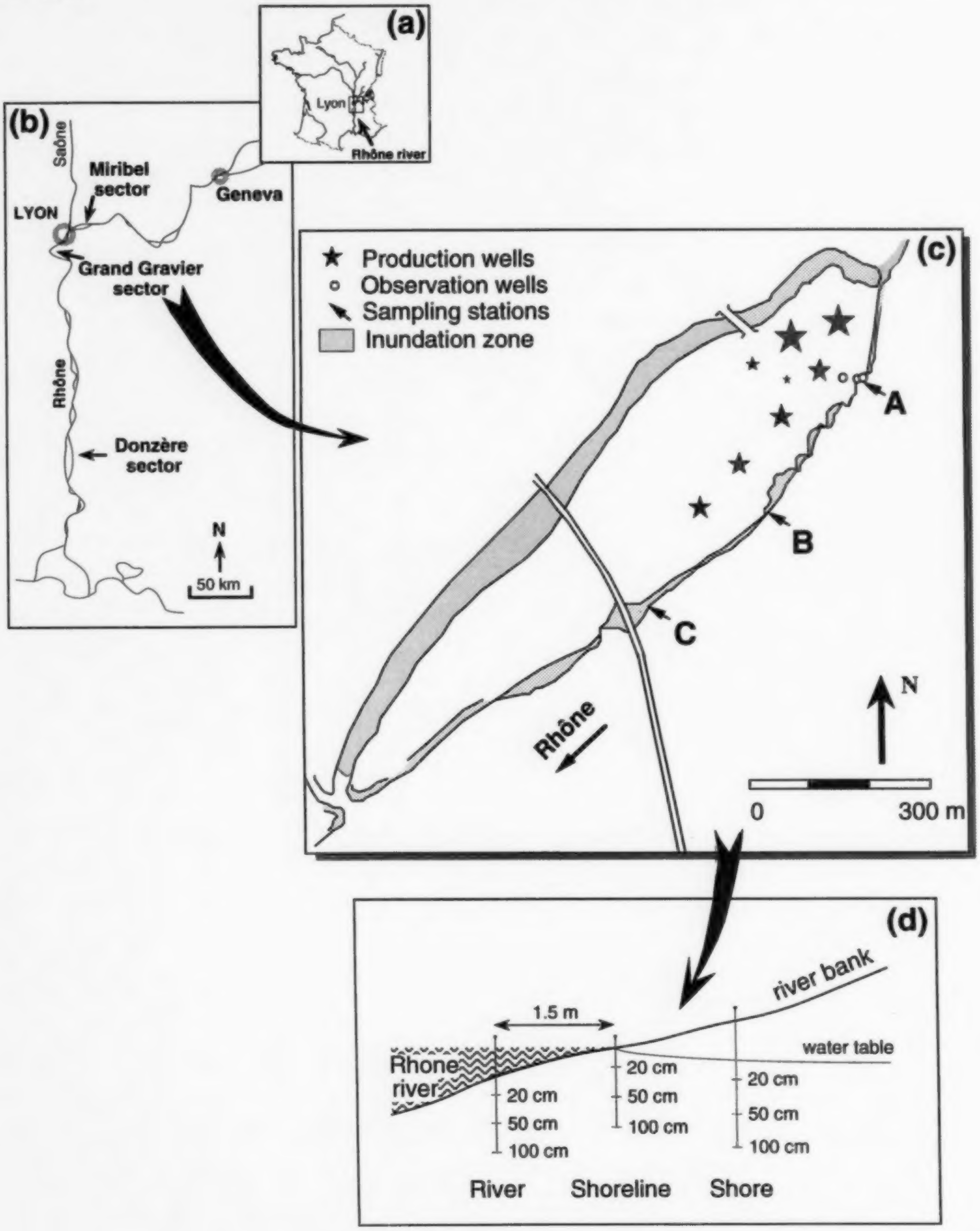
(a)
Lyon
Rhône river
(b)
Saône
Miribel sector
LYON
Geneva
Grand Gravier sector
Rhône
Donzère sector
N
50 km
(c)
Production wells
Observation wells
Sampling stations
Inundation zone
A
B
C
Rhône
N
0
300 m
(d)
river bank
1.5 m
water table
Rhone river
20 cm
50 cm
100 cm
20 cm
50 cm
100 cm
20 cm
50 cm
100 cm
River
Shoreline
Shore

technique (Bou and Rouch 1967). A perforated pipe (36 holes of 5 mm diameter located between 4 and 17 cm from the distal end) was driven to the desired sediment depth and a manual pump was used to collect 10 L of a mixture of fine sediments, water, and fauna. Samples were filtered through a 200-μm mesh net and interstitial fauna was preserved in a 4% formaldehyde solution. Fauna was surveyed on 1 day in each of the four seasons: 23 July 1991,

Table 1. Average values (January 1993 – May 1994) of various parameters at stations A, B, C; substations river (R), shoreline, (SL) and shore (S); and in river water near station (A) (R_A): water specific conductivity, dissolved oxygen (O_2), pH, and hydraulic conductivity (*K*) measured at two different sediments depths (20 and 80–100 cm), and vertical hydraulic gradient against the Rhône River (*i*) measured between 0 and 20 cm and between 0 and 100 cm depth.

	Depth (cm)	A			B			C			
		R	SL	S	R	SL	S	R	SL	S	R_A
Conductivity ($\mu S \cdot cm^{-1}$)	20	323	317	331	324	325	345	353	327	354	317
		(11)	(11)	(9)	(23)	(19)	(20)	(13)	(14)	(20)	(12)
	80–100	336	329	322	344	334	341	383	338	361	
		(14)	(12)	(10)	(16)	(17)	(16)	(24)	(11)	(13)	
O_2 ($mg \cdot L^{-1}$)	20	2.1	2.7	4.9	3.8	5.3	2.0	1.2	2.3	1.0	9.2
		(1.0)	(1.0)	(0.4)	(1.1)	(0.9)	(0.5)	(0.8)	(0.8)	(0.5)	(0.5)
	80–100	0.8	1.2	2.2	1.0	2.5	1.8	0.5	0.7	0.6	
		(0.2)	(0.3)	(0.4)	(0.4)	(0.5)	(0.6)	(0.8)	(0.2)	(0.2)	
pH	20	7.53	7.41	7.49	7.57	7.60	7.40	7.31	7.28	7.44	7.62
		(0.04)	(0.06)	(0.05)	(0.06)	(0.17)	(0.08)	(0.14)	(0.08)	(0.12)	(0.07)
	80–100	7.25	7.30	7.37	7.36	7.39	7.35	7.24	7.27	7.23	
		(0.06)	(0.06)	(0.08)	(0.08)	(0.08)	(0.10)	(0.06)	(0.04)	(0.04)	
i (%)	0–20	−23.9	−40.3	−54.0	−13.0	−17.5	−23.7	−1.9	−5.2	−1.0	0
		(6.5)	(8.0)	(17.9)	(4.9)	(10.2)	(8.3)	(0.5)	(2.6)	(0.5)	
	0–100	−22.2	−21.6	−22.7	−5.5	−5.7	−5.7	−0.4	−0.5	−1.5	
		(2.5)	(2.6)	(3.0)	(1.1)	(1.2)	(1.0)	(0.1)	(0.2)	(0.3)	
K ($mm \cdot s^{-1}$)	ca. 20	0.5	1.9	1.0	4.3	7.7	6.5	4.5	1.0	1.1	
	80–100	1.8	1.2	2.0	1.6	1.1	9.0	1.9	1.7	4.2	

Note: Values in parentheses are standard errors; $n = 25$.

24 November 1991, 27 January 1992, and 19 May 1992. To evaluate the invertebrate community structure the numbers of individuals and taxa were determined.

In the laboratory, collected sediment (<200 μm) was oven dried at 60°C to constant weight and homogenized for measurements of sediment metal concentrations. A 1-g sample was digested for 1.5 h in a Pyrex flask with a HNO_3–HCl mixture (7.5 and 2.5 mL, respectively), cooled to room temperature, filtered, and diluted with double deionized water to a final volume of 50 mL (Plénet 1995). Metals were analyzed by inductively coupled plasma – atomic emission spectrometry (ICP-AES) at the Analytical Institute of the Centre national de la recherche scientifique in Solaize, France. A pollution factor (*F*) was calculated as the observed sediment metal concentration divided by a standard concentration considered typical of unpolluted sediments. Standard background values provided by Agence de l'eau Rhône–Méditerranée–Corse (1993) were as follows: Cr, 22 $\mu g \cdot g^{-1}$; Cu, 26 $\mu g \cdot g^{-1}$; Ni, 20 $\mu g \cdot g^{-1}$; Pb, 50 $\mu g \cdot g^{-1}$; Zn, 94 $\mu g \cdot g^{-1}$. Two heavy metal surveys were carried out on 27 January and 19 May 1992. On these two dates, dissolved organic carbon (DOC) was measured in the interstitial water of station A. The water was filtered through a 0.22-μm acetate filter (washed with 50 mL of distilled water) and analyzed for DOC using a Dohrman DC80 total carbon analyzer. This procedure is based on UV-promoted potassium persulfate oxidation (precision ±1%) following elimination of mineral carbon by orthophosphoric acid (1 $\mu L \cdot mL^{-1}$) and CO_2 stripping under a 10-min oxygen flow.

Subsamples of the collected sediment (<200 μm) (from 27 January and 19 May 1992) were used for grain-size analysis. Each sample was dispersed and divided into 14 particle size-classes by a Coulter counter method. Eight grain-size characteristics were determined according to Håkanson and Jansson (1983): D_5, D_{25}, D_{50}, D_{75}, and D_{95} grain diameter quartiles (which were estimated from cumulative semilogarithmic curves and corresponded to the grain size diameter (in micrometres) at which *x*% of the particles were finer), percentages of particles with diameter <63 μm (size limit between sand and silt) and <100 μm (mean values of the collected sediments of <200 μm), and sorting coefficient (the dispersion of the particle sizes from the mean, which corresponded to the selection of particles during transport according to their sizes, specific gravities, and shapes). The sorting coefficient was calculated using

$$S_0 = (\log D_{95} - \log D_5) / \log 4$$

In well-sorted sediments, S_0 values of 0–1 were found, while values of $S_0 > 1$ were typical of poorly sorted sediment.

In interstitial water, most physical and chemical data were obtained by sampling water from minipiezometers. Each minipiezometer consisted of an aluminium tip equipped with 0.25-mm slots and attached to 1.2-m hard polyvinyl chloride (PVC) tubing (i.d. 4 mm). The minipiezometers were installed permanently at 80–100 cm sediment depth, by pushing them into a predrilled hole of slightly larger diameter (Vanek 1993). They were sampled, on average, twice every month during April–September

Fig. 2. Distribution of the sediment fraction <63 μm and sorting coefficient at different depths (20, 50, and 100 cm) for substations river (R; ■), shoreline (SL; ○), and shore (S; ◆) and at different stations (A, B, and C) of the riverbank of the Rhône River.

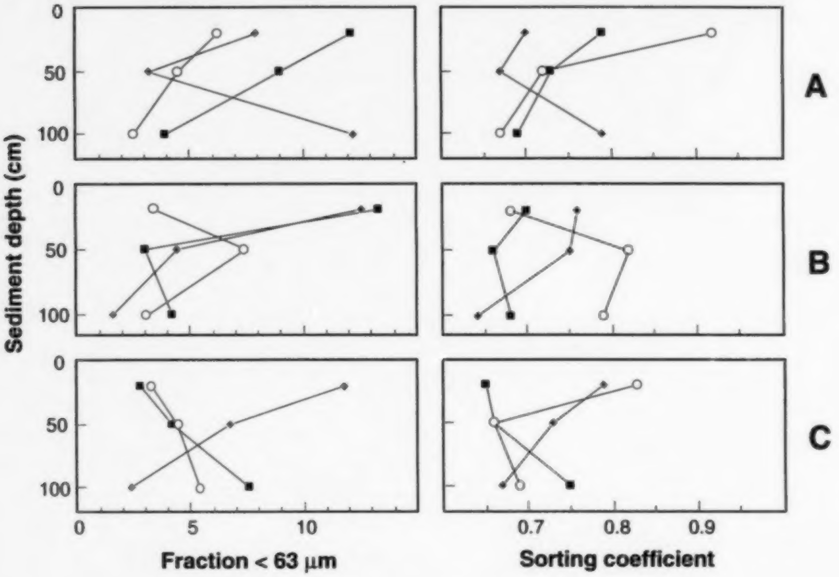

1993 and once every second month in January–March 1993 and October 1993 – May 1994 (total of 25 surveys). At 20-cm sediment depth, a portable sampler equipped with a minipiezometer tip was used. Samples at this depth were obtained on eight occasions during June 1993 – May 1994. Minipiezometers were used to measure a pressure difference between piezometric level and river water that, when divided by the sediment depth, gave the vertical hydraulic gradient (VHG; Lee and Cherry 1978). Hydraulic conductivity of the sediments was determined by falling-head tests (Freeze and Cherry 1979). Minipiezometers were also used to sample interstitial water for field analyses of specific conductance (electric conductivity; type Merck, CM 85T), dissolved oxygen (OXY 85T), and pH (pH 85).

The data were treated statistically by using (*i*) Pearson product moment correlations to test the relationships between spatial distribution of heavy metals and grain-size characteristics (after log (x+1) transformation), and (*ii*) analysis of variance to highlight temporal (one-way ANOVA) and spatial (three-way ANOVA) distributions of interstitial fauna and heavy metals in the three stations (A, B, C), three substations (R, S, SL), and three depths (0 to −20, −50, −100 cm in the sediments). Prior to analyses, the data were tested for normality.

Results

Hydraulics and sediment characteristics

Average VHG between minipiezometers and the level of the Rhône River (Table 1) clearly differed among the three stations, with the highest (most negative) gradients at station A, negative gradients of intermediate magnitude at station B, and gradients close to zero at station C. Under some circumstances (cessation of pumping in the nearest production wells, sudden drop of water level in the river), the negative gradients temporarily became positive at stations B and C, thus indicating the discharge of groundwater into the river (or, rather, previously infiltrated river water, forming a part of so-called bank storage (Freeze and Cherry 1979). During 25 surveys in January 1993 – May 1994, this occurred 3 and 7 times at stations B and C, respectively. At station A, vertical gradients were always negative, indicating groundwater recharge. VHG measured between 0 and 20 cm sediment depth were always steeper (more negative) than those of 0–100 cm depth. The difference was most striking at the substations A-S and A-SL where 20-cm VHGs sometimes exceeded −100%. A significant increase in VHG from substation R to S (from less to more negative ones) was only observed at 20 cm sediment depth at stations A and B, and at ca. 100 cm sediment depth at station C.

Hydraulic conductivity at ca. 100 cm sediment depth (Table 1) showed small variations among the stations, with values ranging between 1 and 2×10^{-3} m·s^{-1}. Values were highest at substations B-S and C-S. Near the sediment surface (20 cm), variability in hydraulic conductivity increased. Four substations (A-R, A-S, C-SL, and C-S) had low hydraulic conductivity values, about two to four times lower than the 100 cm values. In contrast, all three B substations as well as C-R showed high hydraulic conductivity values ranging from 4.3 to 7.7×10^{-3} m·s^{-1} at 20 cm depth.

Grain-size analyses of the fine sediments indicated increasing particle size (i.e., a decreasing proportion of sediments <63 μm) with increasing depth in six of the nine substations (A-R, A-SL, B-R, B-S, B-SL, and C-S)

Fig. 3. Distribution of the heavy metal contamination factors (*F*) at different depths (20, 50, and 100 cm) for substations river (R; ■), Shoreline (SL; ○), and shore (S; ◆) and at different stations (A, B, and C) of the riverbank of the Rhône River (Grand Gravier site).

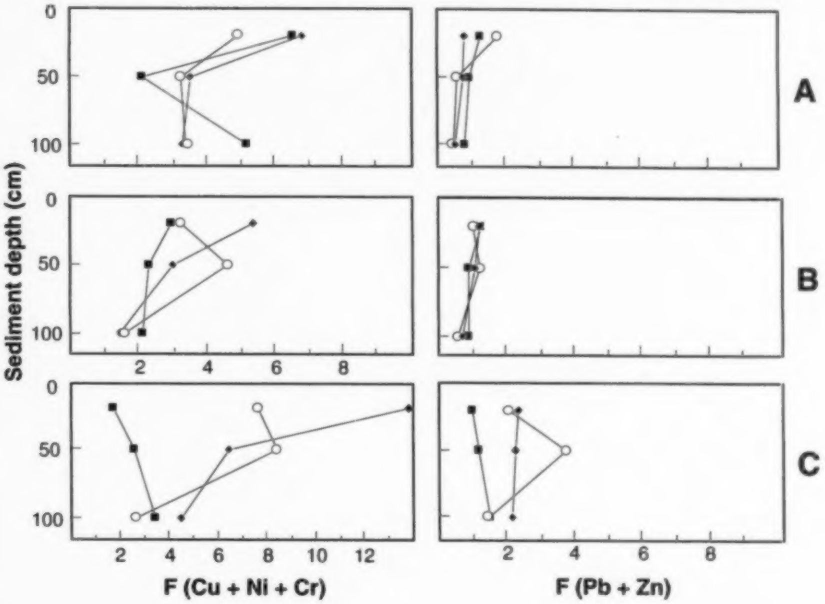

(Fig. 2). A similar pattern was also observed for the sorting coefficient, which decreased with depth at seven substations.

Pore-water chemistry

The specific conductance of pore water at 20 cm depth (Table 1) was, on average, slightly higher than that of river water at most stations (by 0–4%), with the exception of the substations B-S, C-R, and C-S, where the average values were 9–12% higher. At 100 cm depth, the pattern of pore-water specific conductances was similar to that of shallow samples, but the values were generally higher than in surface water and sometimes higher than at 20 cm depth. The highest specific conductances were associated with substation C-R (+21% compared with the river), and the lowest values with A-S (+2%).

Oxygen concentrations were typically below 3 mg·L^{-1} at 20 cm depth (Table 1). Exceptions were substations A-S, B-R, and B-SL, where DOC ranged from 3.8 to 5.3 mg·L^{-1}. These values were still about 40–60% lower than in river water. At 100 cm depth, mean oxygen concentrations were below 1 mg·L^{-1} at most substations. Only at A-S, B-S, and B-SL were DOC values somewhat higher, around 2 mg·L^{-1}.

The mean values of pH were highest in the river (7.62) and decreased slightly with increasing sediment depth (Table 1). The lowest mean pH values (7.3) were associated with substation A-R and all three C substations.

Heavy metal distribution

Heavy metal contents of fine sediments were highest near the sediment surface and decreased with increasing sediment depth, except at station C-R where metal concentrations increased with depth (Table 2). The average *F* value calculated for all five metals together was 3.0 for all samples at 20 cm, 2.3 at 50 cm, and 1.7 at 100 cm sediment depths. According to Agence de l'eau Rhône–Méditerranée–Corse (1993), sediment contamination was

Table 2. Average (n = 2) heavy metal concentration in the fine sediment (<200 μm) fraction (grams per gram dry weight of sediment) at stations A, B, C, substations river (R), shoreline (SL), and shore (S), in three different sediments depths (20, 50, and 100 cm).

	Depth (cm)	A			B			C		
		R	SL	S	R	SL	S	R	SL	S
Cr	20	212	142	202	68	95	153	47	161	350
	50	60	97	99	170	125	83	173	151	186
	100	159	113	107	62	47	44	98	75	127
Cu	20	98	83	111	61	49	91	34	268	378
	50	38	49	42	32	77	57	45	342	124
	100	70	24	35	26	27	22	56	55	92
Ni	20	125	104	140	69	72	113	35	106	226
	50	44	71	91	51	103	62	56	105	122
	100	112	83	74	50	32	32	74	51	83
Zn	20	138	212	109	153	118	146	102	262	318
	50	103	67	98	103	142	134	123	542	258
	100	83	51	50	113	59	80	173	171	227
Pb	20	53	68	24	46	41	45	44	63	61
	50	40	22	23	35	49	37	50	84	86
	100	38	22	25	30	25	28	57	52	90

Table 3. An overview of significant correlations (†, $P < 0.10$, *, $P < 0.05$, **, $P < 0.01$, ***, $P < 0.001$) between heavy metal concentrations, and sediment grain size (D_5, D_{25}, D_{50}, D_{75}, D_{95}, 63 μm, 100 μm, sort (sorting coefficient), K (average hydraulic conductivity)), average vertical hydraulic gradient (VHG), average values of oxygen concentration (no correlation at $P < 0.10$ level), specific conductivity, and pH in the pore water of stations A, B, and C.

	A					B					C				
	Cr	Cu	Ni	Zn	Pb	Cr	Cu	Ni	Zn	Pb	Cr	Cu	Ni	Zn	Pb
Substation					0.48*						−0.58*		−0.55*		−0.48*
Depth		−0.46*		−0.70***	−0.44†	−0.73**	−0.67**	−0.73**	−0.69**	−0.64**					
VHG		0.68*		0.59†		0.86**	0.88**	0.88**	0.81**	0.87**					
Conductivity															
O_2															
pH				0.61†						0.65†	0.59†		0.59†		
D_5					−0.45*	−0.60*	−0.45†	−0.55*			−0.49*	−0.48*	−0.46†		
D_{25}					−0.38†	−0.78***	−0.60*	−0.75***	−0.47†	−0.43†	−0.40†	−0.43†			
D_{50}						−0.75***	−0.55*	−0.73**	−0.47†						
D_{75}						−0.70**	−0.50*	−0.67**							
D_{95}						−0.47†									
<63 μm					0.43†	0.82***	0.68**	0.81***	0.55*	0.50*	0.49*	0.49*	0.45†		
<100 μm						0.80***	0.87***	0.77***	0.54*	0.49†		0.40†			
Sort					0.55*						0.67**	0.65**	0.66**	0.45†	
K											−0.61†	−0.74*	−0.62†	−0.64†	
TOM						—[a]	—	—	—	—	—	—	—	—	—
DOC	0.46†	0.83**	0.41†	0.65**	0.53*	—	—	—	—	—	—	—	—	—	—

Note: The number of observations ranged between 16 and 20, with the exception of the average values where $n = 9$. Before analysis, data were log $(x + 1)$ transformed. Total organic matter (TOM) and dissolved organic carbon (DOC) values were obtained for a different study on the same dates (Marmonier et al. 1995).

[a] —, no data.

Table 4. Spatial and temporal variations of total numbers of individuals (N), taxa (S), and some taxonomic groups.

	Oligochaeta	Nematoda	Cyclopoida	Gastropoda	Chironomidae	N	S
Total one-way ANOVA							
Date of survey			4.09**		8.3***		
Total three-way ANOVA							
Station (St)							
Substation (SbSt)	5.43**	4.11*				4.81*	11.7***
Depth	12.13***	12.56***	3.87*			14.51***	27.76***
St × SbSt							
St × depth							
SbSt × depth	4.38**					2.74*	
St × SbSt × depth							

Note: Values are results of analysis of variance ($n = 4$). Levels of significance are as follows: *, $P < 0.05$; **, $P < 0.01$; ***, $P < 0.001$.

generally weak ($F < 6$) except at station C (20 cm) where contamination was definite ($6 < F < 18$) (Fig. 3). On the basis of vertical distribution, two groups of heavy metals can be distinguished (Fig. 3). Depth contamination profiles for Cu, Ni, and Cr decreased consistently with depth at the S substation. At the SL substation, contamination factors were lower at 100 cm than at 20 cm depth, whereas at the R substation depth contamination profiles were variable in the three stations. Depth contamination profiles for Pb and Zn were poorly developed. Patterns of Pb + Zn concentrations were similar in stations A and B (Fig. 3). By contrast, the profiles differed at station C, where all metal concentrations varied greatly among substations and were generally high near the surface of substations S and SL (Table 2, Fig. 3).

Correlation analyses (Table 3) showed strong differences among the three stations. In stations A and B, most of the metals were significantly negatively correlated with depth in the sediments. In contrast, there were no significant correlations with depth in station C because of the high lateral heterogeneity of the three substations. All of the metals displayed significant negative correlations with diameter size quartiles and positive correlations with the <63-μm and <100-μm sediment fractions at station B (Table 3). At station C, Cr, Cu, and Ni were significantly negatively correlated with diameter size quartiles (D_5 and D_{25}) and hydraulic conductivity and positively correlated with the <63-μm sediment fraction and the sorting coefficient. At station A, only Pb was significantly positively or negatively correlated with sediment grain-size characteristics (Table 3).

There was no correlation between sediment metal concentrations, interstitial DOC, and specific conductance and only a weak correlation with pH (Zn in station A, Pb in station B, and Cr and Ni in station C) (Table 3). At station A (where organic matter data were available; Marmonier et al. 1995), all the heavy metals were positively correlated with the DOC but not with the total organic matter content of the sediment.

Faunal structure

The most abundant groups in this section of the Rhône River were the oligochaetes (48%), nematodes (20%), cyclopoids (15%), gastropods (5%), lamellibranchs (5%), cladocerans (3%), and chironomids (2%). There was a significant interaction between total numbers of individuals and depth × substation (Table 4). This total number decreased with depth in all three stations but different degrees of changes were observed among the three stations (Fig. 4). The total number of individuals in the R and SL substations did not differ significantly, but S substation was less populated ($P < 0.01$), particularly at depths below 20 cm. At station B, the sediment was well colonized even at 50 cm depth. The mean densities of organisms at 50 cm depth at substation SL (106 individuals per 10 L) and at 20 cm at the substation S (114 individuals per 10 L) were higher than at the two other stations (60 and 61 individuals per 10 L, respectively, for A-SL and C-SL; 52 and 18 individuals per 10 L, respectively, for A-S and C-S).

The number of taxa decreased with depth across all stations (number vs. depth $P < 0.0001$; Fig. 5, Table 4). However, in contrast to station C, station B displayed a well-diversified fauna to 50 cm depth in all three substations, with oligochaetes and microcrustaceans as dominant groups. Samples from the S substation contained lower taxa ($P < 0.0001$).

The spatial distribution of the most abundant groups differed between substations and depths. Oligochaetes and nematodes decreased significantly with depth and distance from the R to the S substations (Table 4). Cyclopoids also decreased with depth, while gastropods and chironomid larvae did not show any significant differences in spatial distribution ($P > 0.05$).

Temporal variations were only significant for cyclopoids and chironomids (Table 4) that were less abundant during winter and spring (data not shown).

The species composition of crustaceans differed between stations (Fig. 6). The number of species at stations A and C was 13 and 12 species, respectively, and dominated by epigean (living in surface environment) crustaceans. In contrast, the crustacean assemblage at station B was composed of 20 species including 6 typical hypogean (living in the subsurface environment extending below the soil) species belonging to the ostracods, isopods, and amphipods. The only hypogean species found outside station B was the isopod *Proasellus* sp., recorded at station C.

If we consider the spatial distribution of the eight most abundant crustacean species (four epigean and four

Fig. 4. Average numbers of individuals ($n = 4$) per 10-L sample at different depths (20, 50, and 100 cm) for substations river, shoreline, and shore and at different stations (A, B, and C) of the riverbank of the Rhône River (Grand Gravier site).

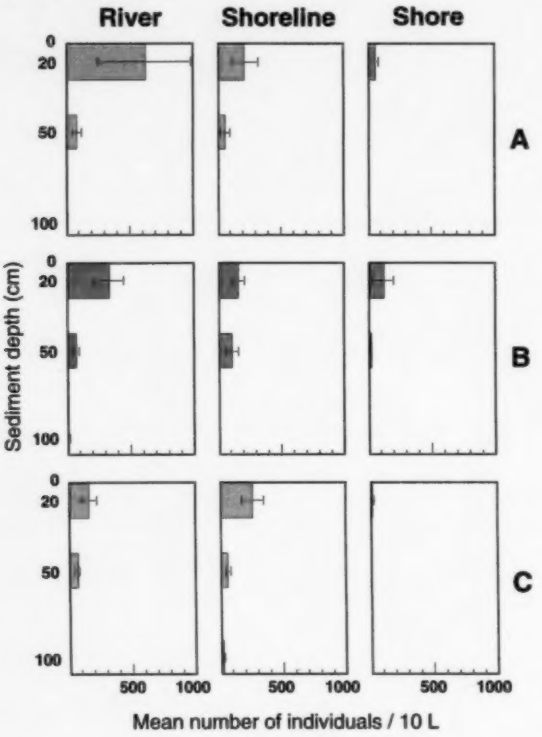

Fig. 5. Average numbers of taxa ($n = 4$) per 10-L sample at different depths (20, 50, and 100 cm) for substations river, shoreline, and shore and at different stations (A, B, and C) of the riverbank of the Rhône River (Grand Gravier site).

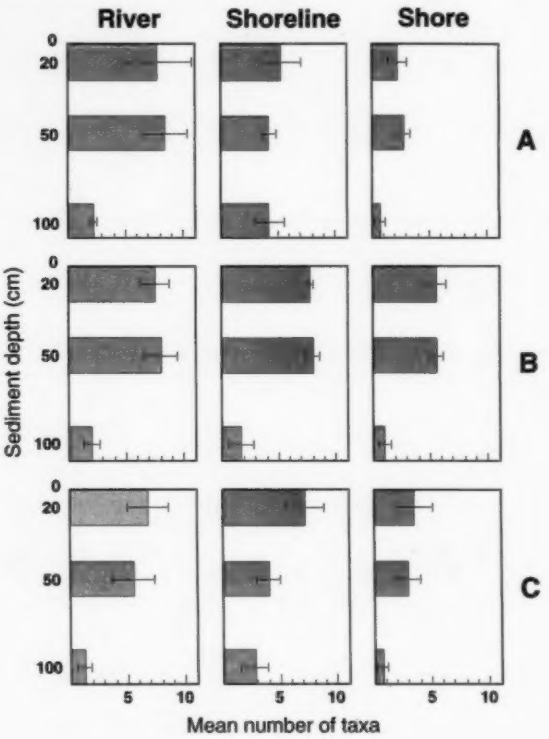

hypogean species; Fig. 7), two distinct patterns were observed. (*i*) The epigean species were most abundant in the R substation (*Darwinula stevensoni*) or in the SL substation (*Daphnia cuculata*) (Fig. 7). Only a few epigean species, such as *Bosmina longirostris*, also colonized S substation sediments. (*ii*) The hypogean species were most abundant at the S (*Pseudocandona zschokkei*) or SL substations (*Pseudocandona belgica*), and numbers decreased toward the R substation. The abundance of both epigean and hypogean species decreased with depth and became very low at 100 cm depth. This result is frequently found for epigean species but is particularly surprising for the hypogean species, which were generally found deeper in the sediments of the unpolluted sectors of the Rhône River (i.e., below 50 cm depth for *Niphargopsis casparyi* and *Pseudocandona zschokkei* in Miribel canal; Dole-Olivier and Marmonier 1992*a*, 1992*b*). In this study, all of the hypogean species disappeared at 100 cm depth.

Discussion

Rivers and their associated aquifers comprise complex three-dimensional ecosystems (Danielopol 1980; Hynes 1983; Ward 1989; Gibert et al. 1990). This study of bank filtration illustrates the importance of hydrologic flow paths and alluvial grain-size characteristics in generating longitudinal (among stations), lateral (from river to bank), and vertical (with interstitial depth) gradients in pore-water chemistry, heavy metal concentrations, and invertebrate community composition within the surface water – groundwater ecotone.

Vertical hydraulic gradients were always steepest (most negative) near station A, intermediate near station B, and close to zero near station C (Table 5). Undoubtedly, this pattern is primarily driven by the average distance to pumping wells, which is shortest at station A, intermediate at station B, and longest at station C. At all stations, the VHGs were steepest near the sediment surface and decreased with increasing depth. This pattern is most probably caused by the presence of shallow sediment layers of lower hydraulic conductivity. Estimated hydraulic conductivities indicate that the thickness of this layer is variable. At station B, this low permeable surficial layer is probably only a few centimetres thick and locally may be missing. At the remaining stations, however, this layer seems to reach, or perhaps exceed, the shallowest sampling depth of 20 cm (Table 1). The low-permeability layers near the sediment surface, even if not yet described in detail, seem to have a

Fig. 6. Total number of epigean and hypogean crustaceans per 10-L sample at stations A, B, and C, Grand Gravier site. I, Isopoda; A, Amphipoda.

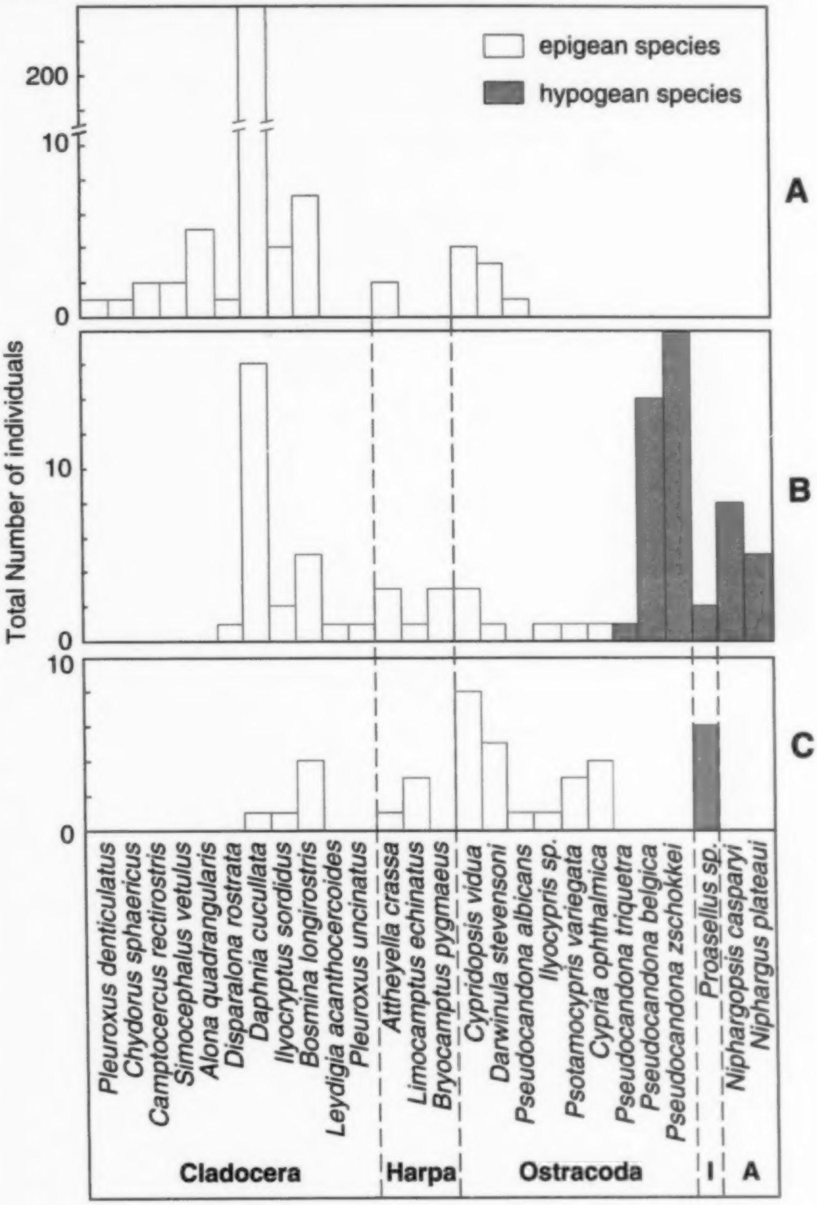

profound effect not only on the vertical hydraulic gradients and seepage velocities, but also on (*i*) the fate of fine sediment particles inside the sediment (internal clogging; V. Vanek, unpublished data) and (*ii*) the chemical composition of the infiltrating river water (Bourg and Bertin 1993; Bourg and Richard-Raymond 1994).

The lowest oxygen concentrations at 20 cm depths were observed in station C where low hydraulic conductivity and weak hydraulic gradients generate long residence times. Longer contact of river water with the sediments promotes more extensive biological oxygen utilization. Accordingly, the highest oxygen values were measured in substations B-R and B-SL) as a result of the high hydraulic conductivity of the shallow sediments and strong VHGs (Table 5). The local differences in pore-water specific conductance are typically due to the in situ dissolution of various minerals. In our case, evaporation and concentrations of salts in soil only occasionally modified the specific conductance of

Fig. 7. Distributions of eight epigean and hypogean crustaceans at different depths (20, 50, and 100 cm) for substations river (R), shoreline (SL), and shore (S) at all three stations, Grand Gravier site. The scale is comparable between the various species except for *Daphnia cuculata*, which was present in high numbers.

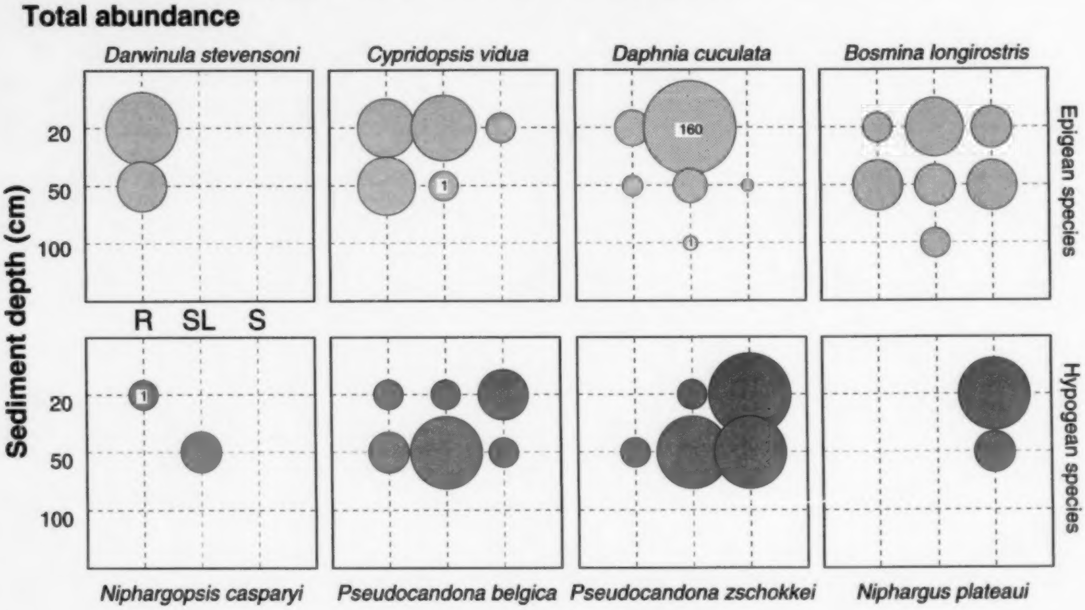

the S substations at 20 cm depth. High pore-water specific conductances associated with station C may be interpreted as a result of the slowest transport velocities in these points, while the low, more riverlike pore-water specific conductances associated with stations A and B are due to the high transport velocities (Table 5). Pore-water specific conductance measurements by Vanek (1994) indicated that most seepage near the Grand Gravier was concentrated within a narrow nearshore strip, which at station A reached, at most, some 5–6 m offshore, while its width near station B was about 3–5 m and near station C only about 1–2 m.

According to the Agence de l'eau Rhône–Méditerranée–Corse (1993), the *F* values calculated (Fig. 3) suggest that the area studied is possibly polluted by heavy metals. It is well known that heavy metals in shallow river sediments are often closely associated with the fine sediment fraction (e.g., Müller 1979; Förstner and Salomons 1980; de Groot et al 1982; Hakanson 1984). In our samples, the correlation between heavy metals and grain-size characterstics was rather weak (within the <200-μm sediment fraction) except at station B, where strong correlations occurred between fine sediment fraction (25% and median), faunal abundance, and metal concentrations (Table 3). At station B, there was also a strong negative correlation between metals and sediment depth, and metal levels were significantly correlated with most of the other grain-size characteristics. Sediment hydraulic conductivity was high at site B, and at the same time, vertical hydraulic gradients were medium to low. This combination may result in retention of some fine particles laden with heavy metals in the shallowest sediment layer where the hydraulic conductivity is somewhat lower. Those fine particles that penetrate through this layer and enter the highly permeable gravel below it are then flushed away by groundwater flow. Some of the fine sediment particles trapped near the surface may then be back-flushed during short periods of reversed hydraulic gradients.

In station A, average seepage velocities are higher because of the high hydraulic gradients but there is no similar layer of sediment with high hydraulic conductivity at 80–100 cm sediment depth as is present at station B. Therefore, the metal-laden fine particles that are brought in from the surface with infiltrating river water are trapped within the whole sediment column. Also, at this station there is no back-flushing of fine sediment particles because the hydraulic gradients always remain negative. The lack of significant correlation between heavy metals and the total organic matter content of the sediment at site A shows clearly that metals are not associated with particulate organic matter in this sector of the river. The correlation with DOC could be explained by a similar relation to depth of both DOC and heavy metals (i.e., less DOC with increasing depth; Marmonier et al. 1995). Thus, metals and DOC may not be causally linked.

Finally, at station C, low interstitial velocities do not cause any significant movement of fine sediments. Most fine particles laden with heavy metals in this station probably were deposited with sediment, and their spatial distribution may have been modified only during floods of sufficient magnitude to mobilize river-bottom sediments. This explains the correlation between heavy metal concentrations and sediment sorting. The sorting coefficient

Table 5. Summary of the hydrological, chemical, granulometric, and biological characteristics of the three stations.

	A	B	C
Hydraulic head	High Downwelling	Medium Possible direction changes	Low Few water exchanges
Highest hydraulic head	Shore −20 cm	Shore −20 cm	Shoreline −20 cm
Permeability	Low at all depths	High at −20 cm, heterogeneous at −100 cm	Low to medium at all depths
Sediment granulometry (% of fine sediment)	Decrease with depth in river and shoreline	Decrease with depth	Increase with depth in river and shoreline
Conductivity	Increase with depth	Increase with depth	Increase with depth
Lowest conductivity	Shoreline −20 cm	River and shoreline −20 cm	Shoreline −20 cm
Oxygen content	Low to medium	Medium to high at −20 cm	Low
Highest oxygen content	Shore −20 cm	River and shoreline −20 cm	Shoreline −20 cm
Heavy metal concentration			
Correlation with depth	Cu, Zn, Pb	All metals	ns[a]
Correlation with fine sediment	Pb	All metals	Cr, Cu, Ni
Correlation with sorting coefficient	Pb	ns[a]	Cr, Cu, Ni, Zn
Faunal composition	Only epigean animals	Both epigean and hypogean animals	Mostly epigean animals with hypogean species
Vertical distribution of the abundances	Rapid decrease with depth	Still well populated until −50 cm depth	Rapid decrease with depth
Vertical distribution of the biodiversity	Low diversity with rapid decrease with depth	High diversity, still well diversified until −50 cm	Low diversity with rapid decrease with depth

[a] ns, not significant.

is a sediment characteristic that probably is more closely related to the water velocity during deposition and creation of the sediment layer than other grain-size parameters.

No significant correlation was found between the concentrations of oxygen in the pore water and heavy metals in the fine sediment fraction (Table 3). This indicates that most heavy metals are not present in redox-sensitive forms. An important factor may be that oxygen concentrations in our samples seldom reach very low values below 0.2 $mg \cdot L^{-1}$, which means that the redox is still too high to allow, for example, precipitation of metal sulfides of Fe, Ni, Zn, or Pb (Di Toro and Rosa 1994).

These physical characteristics of interstitial water and sediment act together with the influence of chronic river pollution to govern the biological properties of the shallow interstitial spaces. Compared with two other Rhône River sectors (Miribel Canal and Donzère sector; Fig. 1) sampled with the same methods as the Grand Gravier sector (Creuzé des Châtelliers 1991; Schmidt et al. 1991), the interstitial assemblages of the Grand Gravier sector are characterized by a lack of epigean amphipods (such as *Gammarus* sp.) and of most insect larvae (Ephemeroptera, Coleoptera, Trichoptera, Plecoptera). In contrast, groups with pollution resistant species (such as chironomids, oligochaetes) show a high diversity (33 oligochaete species, for example; M. Lafont, CEMAGREF, Division des systèmes aquatiques, Lyon, France, personal communication) and abundance in this sector. These characteristics of the interstitial community reflect the chronic pollution of the Rhône River downstream from Lyon. However, animals with short life cycles (such as Ostracoda or Cladocera) were abundant and diverse (9 and 12 species, respectively; Schmidt et al. 1991). The occurrence of these organisms capable of rapidly developing abundant populations in the interstitial habitat suggests that pollutants are generally soluble and can be flushed from the system, causing temporally varying pollution levels in this sector. This fraction of the interstitial assemblage is still poorly studied but may represent an essential source of information for understanding both human-influenced and natural systems.

Hydrologic features and sediment characteristics explained the faunal differences observed among the three stations (Table 5). Station B was characterized by high hydraulic conductivity (with medium to high oxygen content in pore water until 50 cm depth) and temporal changes in water flux direction. Diversified and abundant interstitial fauna was sampled in this station to 50 cm depth, with a consistent fraction of hypogean organisms. In contrast, stations A and C are characterized by low-permeability layers near the sediment surface (that induces low oxygen contents) and a poorly developed interstitial assemblage. The lack of directional changes in water fluxes and the high seepage velocity measured in station A may explain the lack of hypogean fauna, which is highly sensitive to environmental characteristics. An intermediate situation is observed in station C, where the scarcity of hypogean organisms (limited to one species) can be explained by the low hydraulic conductivity, reduced pumping influence that induces low flow velocity, and only rare changes in water flux direction.

Hypogean organisms were absent at 100 cm depth in the sediments, even at station B where they occurred at 20 and 50 cm depths. These animals are generally abundant at 100 cm depth in the Rhône River sediments (Dole-Olivier and Marmonier 1992*a*, 1992*b*). In the Grand Gravier sector, the oxygen concentrations measured at 100 cm depth (often as low as 0.9 $mg \cdot L^{-1}$) are much lower than at similar depths in other sectors (DO ≈2–5 ppm) (H.M. Valett, personal communication), which may explain this unique vertical distribution. This result disagrees with that of Rouch (1988) who found a specific crustacean assemblage (characterized by a bathynellid and a hypogean harpacticoid) in the hypoxic area of the Lapchein River. The differences between the two systems can be explained by the generally higher interstitial oxygen concentration in the Rhône system.

The importance of water flux direction on the composition of interstitial assemblages has been well documented during the last 10 years (Marmonier and Dole 1986; Dole-Olivier and Marmonier 1992*a*, 1992*b*; Stanley and Boulton 1993; Hakenkamp et al. 1993). This study is the first to use quantitative hydrologic measures to assess flow and its influences on biota and to demonstrate that hypogean organisms can integrate long-term parameters (such as grain-size characteristics) and short-term conditions (such as water flux direction).

In conclusion, the first metre of riverbed sediments functions as a filter for river sediment load, particle-associated heavy metals, and epigean organisms. The efficiency of this filter depends mainly on the natural or human-influenced velocity of river water infiltration and the grain sizes of the sediment. These physical constraints influence flow rates and residence times, which, in turn, govern porewater oxygen levels, metal distribution, and faunal structure. Low oxygen content and low biodiversity appear to accompany clogging of the shallow sediment layer.

Acknowledgements

This study was supported by the Program for Interdisciplinary Research on the Environment Écologie et dynamique biogéochimique des écosystèmes souterrains within the Unité de recherche associée n° 1451 du Centre national de la recherche scientifique Écologie des eaux douces et des grands fleuves. We thank everyone who helped us in the field, especially D. Martin and R. Laurent (University of Lyon 1), and M. Valett (University of New Mexico, Albequerque, N.M.) for criticisms and editing the English manuscript.

References

Agence de l'eau Rhône–Méditerranée–Corse. 1993. La pollution des cours d'eau par les métaux. Carte. Agence de l'eau Rhône–Méditerranée–Corse, Lyon, France.

Asano, T. (*Editor*). 1985. Artificial recharge of groundwater. Butterworth Publishers, Boston, Mass.

Bou, C., and R. Rouch. 1967. Un nouveau champ de recherches sur la faune aquatique souterraine. C. R. Acad. Hebd. Seances Sci. 265: 369–370.

Boulton, A.J., C.G. Peterson, N.B. Grimm, and S.G. Fisher. 1992. Stability of an aquatic macoinvertebrate community in a multiyear hydrologic disturbance regime. Ecology, 73: 2192–2207.

Bourg, A.C.M., and C. Bertin. 1993. Biogeochemical processes during the infiltration of river water into an alluvial aquifer. Environ. Sci. Technol. 27: 661–666.

Bourg, A.C.M., and F. Richard-Raymond. 1994. Spatial and temporal variability in the water redox chemistry of the M27 experimental site in the Drac River calcareous alluvial aquifer (Grenoble, France). J. Control Hydrol. 15: 93–105.

Bravard, J.P. 1987. Le Rhône: du Léman à Lyon. Collection l'homme et la nature. La Manufacture, Lyon, France.

Carbiener, R., and M. Tremolières. 1990. The Rhine rift valley groundwater–river interactions: evolution of their susceptibility to pollution. Regul. Rivers Res. Manage. 5: 375–389.

Comité de Bassin Rhône–Méditerranée–Corse. 1993. Rapport de synthèse, mars 1993. Groupe de travail Qualité des eaux du Rhône, Sous-Groupe Micropollution Toxique, Agence de l'eau Rhône–Méditerranée–Corse, Lyon, France.

Creuzé des Châtelliers, M. 1991. Dynamique de repartition des biocénoses interstitielles du Rhône en relation avec des caractéristiques géomorphologiques. Ph.D. thesis, University Claude Bernard Lyon I, Lyon, France.

Dahlblom, P., and G. Lindh. (*Editors*). 1988. Interaction between groundwater and surface water. *In* Proceedings of the International IAHR–AIRH Symposium, Ystad, Sweden, May 30 – June 3, 1988.

Danielopol, D.L. 1980. The role of the limnologist in ground water studies. Int. Rev. Gesamten Hydrobiol. 65: 777–791.

Danielopol, D.L. 1984. Ecological investigations on the alluvial sediments of the Danube in the Vienna area. A phreatobiological project. Verh. Int. Ver. Theor. Angew. Limnol. 22: 1755–1761.

de Groot, A.J., K.H. Zschuppe, and W. Salomons. 1982. Standardization of methods of analysis for heavy metals in sediments. Hydrobiologia, 92: 689–695.

Di Toro, D.M., and L.D. de Rosa. 1994. Sediment toxicity and equilibrium partitioning. *In* Proceedings of the IIASA: Remediation and Management of Degraded River Basins with Emphasis on Central and Eastern Europe, Laxenburg, Austria, June 13–16, 1994. pp. 1–41.

Dole-Olivier, M.J., and P. Marmonier. 1992*a*. Patch distribution of interstitial communities: prevailing factors. Freshwater Biol. 27: 177–191.

Dole-Olivier, M.J., and P. Marmonier.1992*b*. Effects of spates on interstitial assemblages structure. Disturbance–perturbation relationship, rate of recovery. Hydrobiologia, 230: 49–61.

Durbec, A., and C. Leduc. 1989. The alluvial aquifer of the Grand Gravier (Rhône Valley, France) modelling and protection. *In* Groundwater management: quantity and quality. IAHS Publ. No. 188. pp. 581–593.

Fetter, C.W. 1988. Applied hydrogeology. 2nd ed. Merrill Publishing, Columbus, Ohio.

Förstner, U., and W. Salomons. 1980. Trace metal analysis on polluted sediment. I. Assessment of sources and intensities. Environ. Technol. Lett. 1: 494–505.

Freeze, R.A., and J.A. Cherry. 1979. Groundwater. Prentice-Hall, Englewood Cliffs, N.J.

Gaillard, B., D. Getto, P. Mouyon, and D. Marion. 1990. Étude du pouvoir de filtration des berges et de la vulnérabilité des captages de L'Île de Grand Gravier (Rhône) face à la pollution du fleuve. Compte-rendu des opérations de traceurs effectuées en 1989. Centre d'études nucléaires de Grenoble, Grenoble, France.

Gaillard, B., D. Getto, and D. Marion. 1991. Étude du pouvoir de filtration des berges et de la vulnérabilité des captages de L'Île de Grand Gravier (69) face à la pollution du Rhône.

Compte-rendu des opérations de traçages effectuées en 1990. Centre d'études nucléaires de Grenoble, Grenoble, France.

Gibert, J. 1990. Behavior of aquifers concerning contaminants: differential hydraulic conductivity and importance of the different purification processes. Water Sci. Technol. 212: 101–108.

Gibert, J. 1992. CNRS – Programme environnement Écologie et dynamique biogéochimique des systèmes souterrains. Rapport d'activités 1992. Université Lyon 1, Lyon, France.

Gibert, J. 1994. CNRS – Programme environnement Écologie et dynamique biogéochimique des systèmes souterrains. Rapport d'activités 1994. Université Lyon 1, Lyon, France

Gibert, J., M.J. Dole, P. Marmonier, and P. Vervier. 1990. Surface water – groundwater ecotones. *In* The ecology and management of aquatic–terrestrial ecotones. *Edited by* R.J. Naiman and H. Décamps. Parthenon Publishing Group, Carnforth, U.K. pp. 199–225.

Häkanson, L. 1984. Sediment sampling in different aquatic environments. Statistical aspects. Water Resour. Res. 20: 41–46.

Häkanson, L., and M. Jansson. 1983. Principles of lake sedimentology. Springer-Verlag, Berlin.

Hakenkamp, C.C., H.M. Valett, and A.J. Boulton. 1993. Perspectives on the hyporheic zone: integrating hydrology and biology. J. North Am. Benthol. Soc. 12: 94–99.

Holland, M.M., P. Risser, and R.J. Naiman. 1991. Ecotones: the role of landscape boundaries in the management and restoration of changing environments. Chapman & Hall, London.

Hynes, H.B.N. 1983. Groundwater and stream ecology. Hydrobiologia, 100: 93–99.

Ille, C. 1992. Interface rivière–nappe : caractérisation physique et chimique; rôle protecteur de l'aquifère. Cas de L'île du Grand Gravier (69). Ph.D. thesis, University J. Fourier Grenoble 1, Grenoble, France.

Ille, C., M.F. Suais, A. Durbec, B. Gaillard, and M. Lafont. 1991. Caractérisation du pouvoir épurateur des berges d'un fleuve. Application à l'Ile du Grand Gravier (Rhône). Hydrogeologie, 4: 283–289.

Lafont, M., and A. Durbec. 1990. Essai de description biologique des interactions entre eau de surface et eau souterraine : vulnérabilité d'un aquifère à la pollution d'un fleuve. Ann. Limnol. 26: 119–129.

Lafont, M., A. Durbec, and C. Ille. 1992. Oligochaete worms as biological describers of the interactions betweeen surface and groundwaters: a first synthesis. Regul. Rivers Res. Manage. 7: 65–73.

Lee, D.R., and J.A. Cherry. 1978. A field exercise on groundwater flow using seepage meters and mini-piezometers. J. Geol. Educ. 27: 6–10.

Marmonier, P., and M.J. Dole. 1986. Les amphipodes des sédiments d'un bras court-circuité du Rhône : logique de répartition et réaction aux crues. Sci. Eau, 5: 461–486.

Marmonier, P., D. Fontvieille, J. Gibert, and V. Vanek. 1995. Distribution of disolved organic carbon and bacteria at the interface between the Rhône River and its alluvial aquifer. J. North Am. Benthol. Soc. 14: 382–392.

Müller, G. 1979. Schwermetalle in den Sedimenten des Rheins – Veränderungen seit 1971. Umschau, 79: 778–783.

Naiman, R.J., and H. Décamps. 1990. Ecology and management of aquatic–terrestrial ecotones. Man and the biosphere series. Parthenon Publishing Group, Carnforth, U.K.

Plénet, S. 1995. Freshwater amphipods as biomonitors of trace-metal pollution in surface and interstitial aquatic systems. Freshwater Biol. 33: 127–137.

Poinsart, D. 1992. Effets des aménagements fluviaux sur les débits liquides et solides. L'exemple du Rhône dans les plaines de miribel-Jonage et de Donzère-Mondragon. Ph.D. thesis, Université Lyon 1, Lyon, France.

Rouch, R. 1988. Sur la répartition spatiale des Crustacés dans le sous-écoulement d'un ruisseau des Pyrénées. Ann. Limnol. 24: 213–234.

Schmidt, C.M., P. Marmonier, S. Plénet, M. Creuzé des Châtelliers, and J. Gibert. 1991. Bank filtration and interstitial communities. Example of the Rhône River in a polluted sector (downstream of Lyon, Grand-Gravier, France). Hydrogeologie, 3: 217–223.

Stanley, E.H., and A.J. Boulton. 1993. Hydrology and the distribution of hyporheos: perspectives from a mesic river and a desert stream. J. North Am. Benthol. Soc. 12: 79–83.

Stuyfzand, P.J. 1989. Hydrology and water quality aspects of Rhine bank groundwater in the Netherlands. J. Hydrol. (Amsterdam), 106: 341–363.

UNESCO-ICGW Working Group. 1992. Hydrological basis of ecologically sound management of soil and groundwater. IHP-IV Project M-3-1. Report of the UNESCO-ICGW working group. UNESCO, Paris.

U.S. Environmental Protection Agency. 1992. Framework for ecological risk assessment. Risk assessment forum EPA/630/R92/001. U.S. Environmental Protection Agency, Washington, D.C.

Valett, H.M., C.C. Hakenkamp, and A.J. Boulton. 1993. Perspectives on the hyporheic zone; integrating hydrology and biology. Introduction. J. North Am. Benthol. Soc. 12: 40–43.

Vanek, V. 1993. Groundwater regime of a tidally influenced coastal pond. J. Hydrol. 151: 317–342.

Vanek, V. 1994. Water flows through the River Rhône sediments near Lyon, their effect on groundwater chemistry and biology. Folia Fac. Sci. Nat. Univ. Masarykianae Brun. Biol. 91: 149–157.

Vanek, V. 1995. Heterogeneity of groundwater – surface water ecotones. *In* Groundwater/surface water ecotones. *Edited by* J. Gibert, J. Mathieu, and F. Fournier. Cambridge University Press, Cambridge, U.K. In press.

Ward, J.V. 1989. The four-dimensional nature of lotic ecosystems. J. North Am. Benthol. Soc. 8: 2–8.

Wright, C.E. 1980. Surface water and groundwater interaction. *In* Studies and reports in hydrology. No. 29. UNESCO, Paris.

Fecundity of the ocean shrimp (*Pandalus jordani*)

Robert W. Hannah, Stephen A. Jones, and Michele R. Long

Abstract: Fecundity of the ocean shrimp *Pandalus jordani* was analyzed from eight samples from the years 1989–1993 and compared with historical fecundity data for this species. Linear regressions of $\log_e$ fecundity on $\log_e$ carapace length from the 1989–1993 samples had significantly different slopes. Interannual variation in fecundity exceeded that found between areas within the same year, making it difficult to determine if the observed variation in fecundity resulted from geographic location or interannual variation. No consistent differences between the length–fecundity relationships of the recent and historical samples were demonstrated. A graphical comparison of fecundity with sea level height data provided preliminary evidence that sea bottom temperature may be influencing shrimp fecundity. Egg production, estimated from the length–fecundity relationships and from size and sex composition data from the commercial catch, showed wide variation between years and areas. Variation in sex composition explained roughly 62% of the variation in egg production. Egg production estimates, derived from a pooled length–fecundity relationship, deviated from estimates based on the individual samples by ±13–18%. These deviations were considered to be a minor source of added variance when compared with other sources of variation in the total egg production of ocean shrimp.

Résumé : La fécondité de la crevette océanique *Pandalus jordani* a été analysée à partir de huit échantillons prélevés de 1989 à 1993 et comparée à des données antérieures sur la fécondité de cette espèce. Les régressions linéaires du $\log_e$ de la fécondité par rapport au $\log_e$ de la longueur de la carapace dans les échantillons de 1989 à 1993 présentent des pentes qui diffèrent considérablement. La variation annuelle de la fécondité est plus grande que celle que l'on observe entre les diverses régions au cours de la même année; par conséquent, il est difficile de déterminer si la variation dans la fécondité est liée à l'emplacement géographique ou à la variation annuelle. Aucune différence systématique n'a été démontrée dans le rapport longueur–fécondité entre les échantillons récents et les échantillons plus anciens. Un graphique de la fécondité en fonction de la profondeur par rapport à la surface semble montrer que la température de l'eau au fond pourrait avoir une incidence sur la fécondité de ces crevettes. La production d'oeufs, estimée à partir de la relation longueur–fécondité et des données sur la composition par taille et par sexe dans les prises commerciales, varie beaucoup selon les années et les régions. La variation dans la composition par sexe explique environ 62% de la variation dans la production d'oeufs. Les estimations de la production d'oeufs, dérivées de la relation longueur–fécondité pour l'ensemble des échantillons, diverge des estimations fondées sur l'analyse des échantillons individuels par un facteur de ±13–18%. Ces écarts sont considérés comme étant une source mineure de variation supplémentaire par rapport à d'autres sources de variation dans la production totale d'oeufs de la crevette océanique.

[Traduit par la Rédaction]

Introduction

Maintaining spawning stocks at adequate levels to ensure future recruitment is an important goal of fishery management. Rothschild and Fogarty (1989) and others have pointed out that stock-recruitment theory actually concerns the relationship between recruitment and egg production. Accordingly, to measure the effects of fishing on recruitment, managers need to know to what extent fishing reduces the egg production of a stock. In practice, this requires estimates of the adult spawning stock, the size and sex composition of the population, and average fecundity.

Several attempts have been made to evaluate the influence of changes in parent stock levels on subsequent recruitment in ocean shrimp (*Pandalus jordani*), without success (Abrahamson and Tomlinson 1972; Gotshall 1972; Hannah 1993). In these studies, parent stock was measured as the estimated number or biomass of female shrimp, or even more crudely, via a simple index of catch per unit effort (CPUE) in the fall just prior to spawning. These studies may have been unsuccessful because the stock indices used did not accurately reflect changes in total egg production. The principal objective of this study was to investigate the possibility of developing an index of annual egg

Received September 28, 1994. Accepted April 28, 1995.
J12595

R.W. Hannah, S.A. Jones, and M.R. Long. Oregon Department of Fish and Wildlife, Marine Region,
2040 Southeast Marine Science Drive, Newport,
OR 97365, U.S.A.

production for ocean shrimp by examining the variation found in ocean shrimp fecundity.

Dahlstrom (1970) described the fecundity of ocean shrimp from the Pacific States Marine Fisheries Commission (PSMFC) areas 92 and 94, for the year 1964 (Fig. 1). J.G. Robinson (1971, Oregon Department of Fish and Wildlife (ODFW), Newport, Oreg., unpublished data) also collected some data on the length–fecundity relationship for areas 86 and 82 for the years 1965 and 1967, respectively. However, these early data may not be suitable for estimating the fecundity of the present-day shrimp population. First, overall sample sizes were small, the largest single sample comprising only 62 shrimp, with other samples being much smaller. Second, the early samples were almost exclusively age-2 and older shrimp, while the modern day spawning population is generally composed of a large percentage of age-1 females (Hannah and Jones 1991). A third problem is that age-specific mean lengths are quite variable for ocean shrimp and have increased since the early years of the fishery (Hannah and Jones 1991). Two additional objectives of this study were to compare recent fecundity data with data from the 1960s, and to gather data to more accurately describe the average fecundity of ocean shrimp, given that age-1 females are now prevalent.

Methods

Shrimp samples were obtained opportunistically during ride-along trips on commercial shrimp trawlers. Each sample was collected on a single fishing trip, during 1 day of fishing, whenever possible. Gravid females were selected directly from each vessel's picking table or from a sample collected from the hopper. The shrimp were collected at sea, rather than from processing plants, to minimize the possibility of egg loss. Each shrimp was measured (carapace length) to the nearest 0.1 mm using vernier callipers. Shrimp were assigned to 0.5-mm length intervals by rounding downwards. For example, shrimp from 22.0 to 22.4 mm were grouped into the 22.0-mm interval. This approach was used to maintain consistency between fecundity samples and the monthly samples of fishery catch that have been collected by the ODFW since 1966. Shrimp for fecundity analysis were preserved in individual vials with 70% ethanol. Sampling of shrimp continued in this manner until a set number of shrimp from each 0.5-mm length interval had been collected. This approach was used, rather than simple random sampling, to minimize the total sample size needed to accurately depict the length–fecundity relationship of each sample. The number of shrimp collected from each size interval varied from year to year. In 1989, we collected the first five shrimp from each interval represented in the catch. In 1990 we collected the first 10 shrimp from each interval. After analyzing the 1989 and 1990 collections, we determined that collecting eight shrimp per interval should accurately depict the length–fecundity relationship, while minimizing the time spent analyzing samples. In subsequent years, eight shrimp were collected per interval. Shrimp were fixed for 24 h in 10% Formalin and then returned to 70% ethanol for storage. All eggs were carefully removed from the pleopods and counted using a dissecting scope or illuminated magnifying lens. The preservative was also strained to recover loose eggs, which were included in the total count for each specimen.

Fig. 1. Location of commercial concentrations of ocean shrimp along the U.S. Pacific coast (shaded areas) in PSMFC statistical areas 72–94.

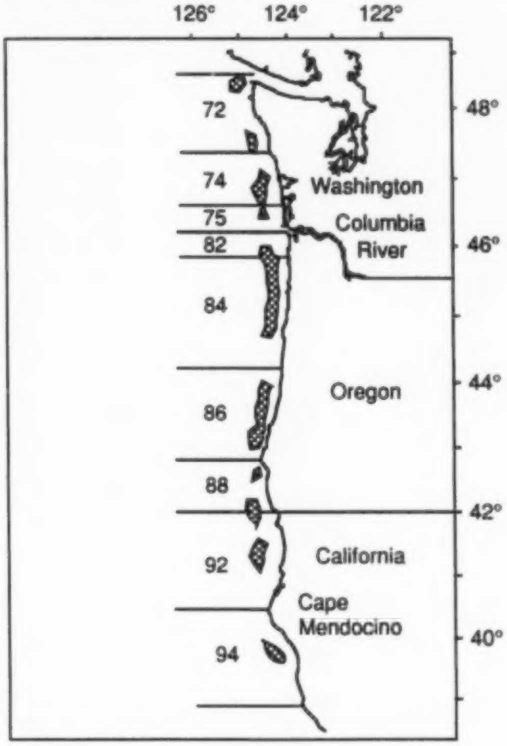

In most years, sampling was completed during late October. However, in 1991 the fishery had slowed dramatically by October and samples were not obtained. In March 1992, prior to larval release, an opportunity to obtain fecundity samples arose during other trawl survey work and three fecundity samples were collected representing the 1991 spawning population. Data from two samples described in previous studies have also been included here for comparative purposes. The earliest sample consists of egg counts from 51 gravid shrimp collected in November, 1964, from PSMFC statistical area 92, as previously described by Dahlstrom (1970). The individual data points were digitized from Dahlstrom's (1970) Fig. 5. Dahlstrom (1970) also reported on a fecundity sample from PSMFC area 94, which was not included in this study because it is geographically distant from the collections we made off Oregon and Washington. The second sample included here consists of counts from 62 gravid shrimp collected using pots in November 1967 from PSMFC area 82. These two samples, along with fecundity data for the southern California populations of ocean shrimp, have been analyzed previously by J.G. Robinson (1971, ODFW, unpublished data).

A stepwise process was used to assess the relationship between carapace length and fecundity. First, the

Table 1. Summary of ocean shrimp fecundity samples, 1989–1993.

Year	Month	PSMFC area	Sample size	Carapace length range (mm)
1989	October	84	115	17.0–25.0
1990	October	84	101	20.5–26.5
1992	March	84	109	17.5–25.0
1992	March	72	70	16.5–24.0
1992	March	74	105	17.0–26.0
1992	October	74	49	16.0–25.0
1992	October	88	129	18.0–28.0
1993	October	88	74	19.5–28.0
1964[a]	November	92	51	18.9–24.0
1967[b]	November	82	62	17.3–25.0

Note: Carapace length range is for gravid females only.

[a] Dahlstrom (1970).

[b] J.G. Robinson (1971, ODFW, unpublished data).

length–fecundity samples, including previous collections, were analyzed graphically to determine the approximate form of the underlying relationship and to determine if a transformation was needed to stabilize the variance. Most of the scattergrams showed some evidence of increasing variance with carapace length; consequently, a $\log_e - \log_e$ transformation was applied to all samples. A standard analysis of covariance, employing least-squares regression, was then performed to test for homogeneity of slopes. Geometric mean regression techniques were also used to fit lines to the transformed variates. Geometric mean regression corrects the slope estimates for the effect of different ranges in the independent variable (Ricker 1973). The slopes obtained via geometric mean regression were then compared graphically using Gabriel's approximation of the GT2 method (Sokal and Rohlf 1981, pp. 507–508).

The impact of variation in the length–fecundity relationship and of other sources of variation, such as variation in sex composition, on egg production of ocean shrimp was of principal interest in this study. Since it is difficult to directly interpret the regression equations from log-transformed data, the back-transformed values for each length–fecundity relationship were compared graphically. Back-transformed values were calculated using the geometric mean regression equations. In this and all other uses of back-transformed estimates, the correction factor used by Pope et al. (1961) and Raitt (1968), as reported in Bagenal and Braum (1978), was employed to correct for transformation bias.

A graphical approach was used to determine if sea bottom temperatures might be responsible for any observed variation in fecundity. On the basis of inspection of the back-transformed length–fecundity values, samples were grouped by year of collection and classified as either high or low fecundity. The two categories were then compared graphically with an index of sea bottom temperatures. We used April–August mean sea level at Crescent City, California, as an index of bottom temperature. Sea level height data were obtained from the National Oceanic and Atmospheric Administration archives, through the Sea and Lake Levels Branch. We used sea level to index sea bottom temperatures because Kruse (1981) found inverse-barometer corrected sea level at Newport, Oregon, and Neah Bay, Washington, to be highly correlated with sea bottom shelf temperatures. Chelton and Davis (1982) and others have also demonstrated that sea level variation along the west coast of North America is coherent over very large spatial scales.

Estimates of egg production were also calculated for each fecundity sample and compared. To estimate egg production, information was needed on the length–fecundity relationship, the sex ratio, and the length frequency of females in the population. Since we used quota sampling and collected only gravid female shrimp, the fecundity samples could not be used to estimate egg production of the shrimp population. However, market samples obtained from fishery landings, from the same areas and time periods, were available for this purpose. Market samples were collected at the docks, prior to processing of the shrimp. The collection of each sample involved a number of steps. First, the vessel logbook was inspected to determine the areas fished. A delivery was not sampled unless at least a full day of fishing occurred in one statistical area, and the correct portion of the delivery to sample could be identified. A sample of 1–2 kg of shrimp was collected throughout that portion of the load, whenever possible. Each sample was mixed and 100 shrimp were randomly selected for sexing and measuring. Shrimp were measured (carapace length, millimetres) and classified as male, transitional, or female following the methods of Tegelberg and Smith (1957). Whenever possible, 4–12 samples of 100 shrimp were obtained for each area and month, with more samples collected in the larger statistical areas (Fig. 1). The individual samples from each area and month were combined and nadirs in the length–frequency histogram were used to assign ages to individual shrimp. We assumed that market samples were representative of the shrimp population in the areas from which the samples were taken. The available data on shrimp growth and mesh selectivity suggest that, by October, age-1 shrimp are fully recruited to the trawl gear presently in use in this fishery (Hannah and Jones 1991; Hannah 1993; S.A. Jones and R.W. Hannah, ODFW, Newport, Oreg., unpublished data).

As mentioned above, some of the fecundity samples were collected in the early spring, prior to egg release. To calculate egg production from the spring fecundity samples, market samples from the prior fall were used. This was necessary because spring market samples probably do not provide accurate information on the sex composition of the spawning population, because of sex change of males over the winter. The fecundity of each female shrimp in the market sample was estimated from carapace length, using the least-squares $\log_e - \log_e$ regression of fecundity on carapace length for that area and year. The estimated fecundity of all of the female shrimp in the market sample was then summed. To standardize between market samples of different size, the sum was then divided by the sample weight (kilograms), to estimate egg production as a number of eggs per kilogram. Egg production was not calculated for the samples from 1964 (Dahlstrom 1970) and 1967 (J.G. Robinson, 1971; ODFW, unpublished data) because market sample data from the early years of the fishery were probably not representative of the population. In the

Fig. 2. Scattergrams of carapace length (mm) versus fecundity for ocean shrimp collected from PSMFC statistical areas 72 and 84, 1989–1992.

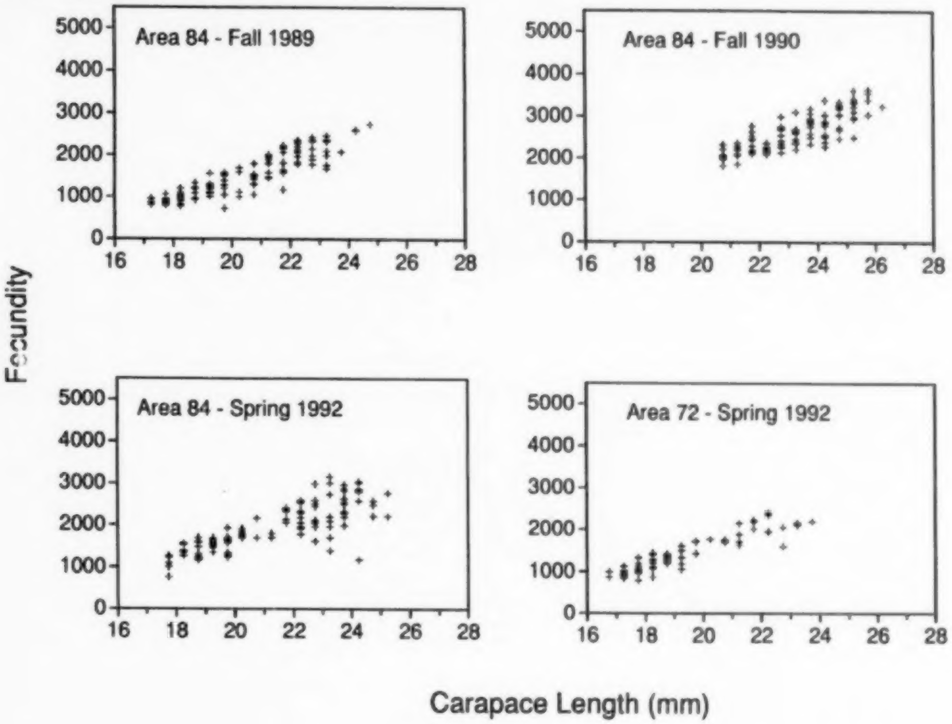

early years of the fishery for ocean shrimp, when larger mesh trawls were fished, age-1 shrimp were probably not fully recruited to the gear (Hannah and Jones 1991; Hannah 1993). Accordingly, market sample data could only be used to calculate egg production for the recent samples.

Collecting fecundity samples from each area every year to produce a time series of egg-production estimates represents a large commitment of sampling effort and laboratory time. Accordingly, we wanted to compare egg production estimates calculated from an average length–fecundity relationship with estimates calculated from the individual samples. We first estimated egg production from market sample length and sex data for the specific years and areas sampled, but using a pooled length–fecundity relationship from the 1989–1993 samples. These were then compared with similar estimates derived from the length–fecundity relationships from the individual samples. The deviations between the two methods are a measure of the added variance that could be expected if an average length–fecundity relationship was used to generate estimates of egg production from historical market sample data.

Results and discussion

Length variation

Eight samples of gravid female ocean shrimp were analyzed, spanning the years 1989–1993 and PSMFC areas 72, 74, 84, and 88 (Table 1, Fig. 1). The carapace length ranges sampled reflected the highly variable age and sex composition of ocean shrimp and geographic variation in the growth of ocean shrimp (Charnov et al. 1978; Hannah and Jones 1991). For example, in the area 84 sample from the fall of 1990, gravid shrimp below 20.5 mm carapace length were absent. This reflected the response of the shrimp population to the failure of the 1989 year-class (year of spring larval release, unless noted; Hannah 1993). In 1990, with age-1 shrimp at very low levels, very few age-1 shrimp changed into females (Charnov et al. 1978). Sampling in the same area in fall 1989, however, produced gravid females ranging from 17.0 to 25.0 mm carapace length, including many age-1 females. The widest size range of gravid shrimp resulted from samples taken in area 88. Growth was most rapid in area 88, and shrimp generally attained a larger maximum size, possibly accounting for the wide range in sizes encountered (Hannah and Jones 1991; Zirges et al. 1982).

Length–fecundity relationships

Scattergrams of carapace length versus fecundity for all 10 samples (Figs. 2–4) showed only slight evidence of upward curvature. More importantly, several of them showed increasing variance, necessitating the logarithmic transformation of both variates. All of the regressions were highly significant (Table 2; $p < 0.0001$). Both least-squares and geometric mean regression produced a wide range of slope estimates. Using analysis of covariance, the least-squares

Fig. 3. Scattergrams of carapace length (mm) versus fecundity for ocean shrimp collected from PSMFC statistical areas 74 and 88, 1989–1992.

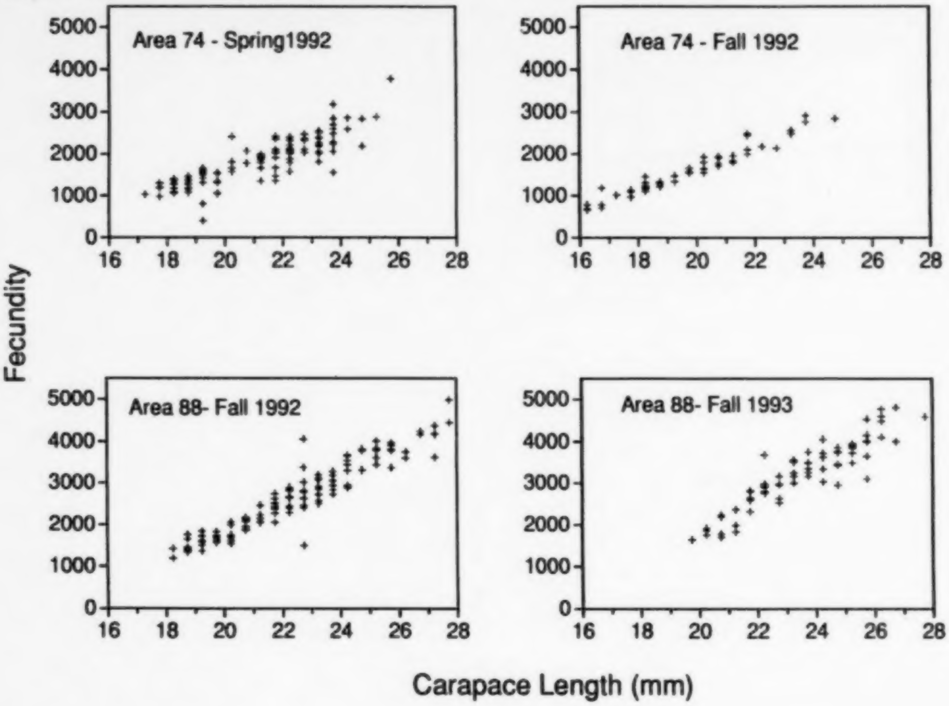

slope estimates were found to be significantly different ($p < 0.0001$). Slope estimates based on geometric mean regression were higher than the least-squares estimates and were more homogeneous. A comparison of all 10 regression slopes obtained via geometric mean regression, using the GT2 test, indicated that the slopes were significantly different ($p < 0.05$; Fig. 5). However, no consistent differences in slope by either year or area sampled were demonstrated. The regression slope of the 1989 sample from area 84 was greater than that of the 1990 sample from the same area, as was the slope of the 1992 sample from area 74. The 1993 sample from area 88 also had a marginally higher slope coefficient than the 1990 sample from area 84. The other slope coefficients were not significantly different ($p > 0.05$).

The use of a power curve to fit the length–fecundity relationship for ocean shrimp in this study contrasts with the use of simple linear regression by J.G. Robinson (1971, ODFW, unpublished data) and by Apollonio et al. (1986) for the northern shrimp, *Pandalus borealis*. Some researchers have used the power curve approach for northern shrimp, citing an a priori belief that the underlying relationship was probably curvilinear (Parsons and Tucker 1986; Teigsmark 1983). The confusion about which approach to use has probably stemmed from the lack of visible curvature in the length–fecundity scattergrams for pandalid shrimp (Figs. 2–4). Pandalid shrimp are short lived in comparison with many species of fish, and are protandric hermaphrodites that exhibit flexible rates of sex change (Charnov et al. 1978; Dahlstrom 1970). Accordingly, the length range of females in any single fecundity sample is likely to be limited, and with high variability in fecundity at a given length, curvature is not easily detected by inspection.

Variation in fecundity

An examination of the fitted, back-transformed values for each length–fecundity relationship (Fig. 6) suggests that the fecundity of ocean shrimp can vary substantially between years and areas. Across most of the length ranges sampled, fecundity was elevated in both samples from area 88, and also at the larger carapace lengths in the 1992 sample from area 84. The other length–fecundity relationships, including the two samples from the 1960s, showed a large degree of overlap. A careful comparison of the curves suggests that the magnitude of interannual variation in fecundity may exceed that seen between areas within the same year. For example, the two curves from fall 1992 collections are in close agreement, as are the three curves for the spring 1992 collections (Fig. 6), despite the fact that the areas sampled are quite far apart (Fig. 1). Conversely, the three sets of curves from areas 74, 88, and 84 that cover several years, are more disparate (Fig. 6). The curves displayed in Fig. 6 could be interpreted as evidence for higher fecundity in southern populations or as evidence for a general increase in fecundity in 1992 and 1993.

Fig. 4. Scattergrams of carapace length (mm) versus fecundity for ocean shrimp collected from PSMFC statistical areas 92 (from Dahlstrom 1970) and 82 (from J.G. Robinson 1971, ODFW, unpublished data) in 1964 and 1967, respectively.

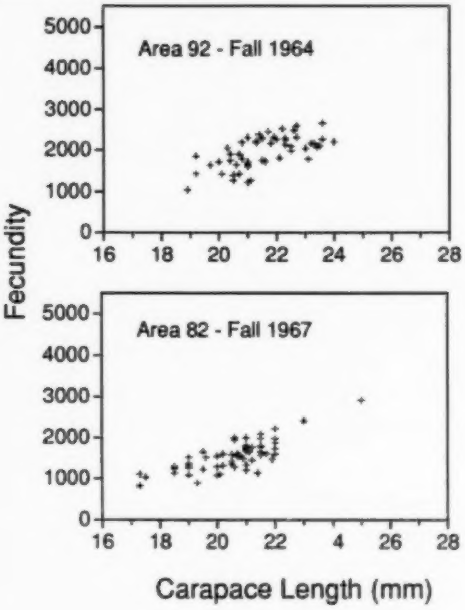

Fig. 5. Comparison of slopes from geometric mean regression of $\log_e$ fecundity on $\log_e$ carapace length for samples of ocean shrimp from PSMFC areas 72–92 (1964–1993). Error bars indicate 95% confidence intervals by the GT2 method. Slope estimates with bars that do not overlap are significantly different ($p < 0.05$). Samples are identified by statistical area followed by an S or F denoting spring or fall collection, followed by the year of collection (84 F89 denotes a sample collected from area 84 in the fall of 1989).

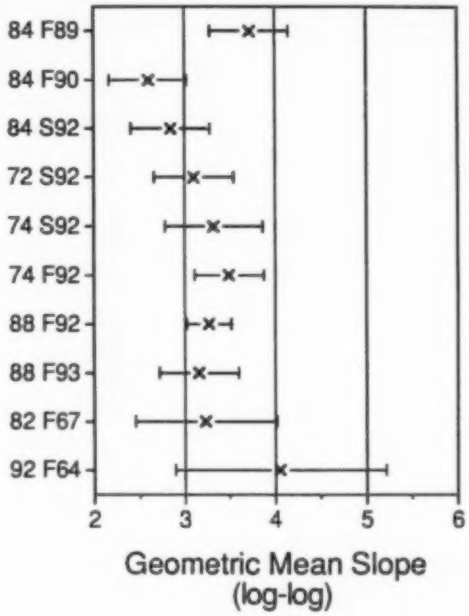

A comparison of the recent samples with those from the 1960s (Fig. 6) suggests that fecundity has not changed in any consistent fashion since the early days of the shrimp fishery. A comparison of the length–fecundity relationships from area 88, with the 1964 sample from area 92, does suggest higher fecundity in recent years, in the southern areas. However, given the large degree of interannual variation observed in the samples, it is impossible to make any conclusion about how fecundity may have changed since the early years of the fishery.

A graphical comparison of the high- and low-fecundity years with mean sea level at Crescent City (Fig. 7) provides some preliminary evidence that increased sea bottom temperatures could be responsible for the elevated fecundity observed in 1992 and 1993. J.G. Robinson (1971, ODFW, unpublished data) speculated that the higher fecundity he observed in the southern populations of ocean shrimp was probably caused by higher sea bottom temperatures, although his study did not address interannual variation. Nunes (1984) demonstrated that the fecundity of northern shrimp, under laboratory conditions, was influenced by changes in water temperature, increasing from 3 to 6°C, and decreasing from 6 to 9°C. Parsons and Tucker (1986) found no clear relationship between temperature and fecundity for the northern shrimp in the Northwest Atlantic, while Teigsmark (1983) attributed the variation in fecundity of northern shrimp to differences in food availability, possibly related to shrimp density. Teigsmark (1983) also suggested that, for northern shrimp, density-independent changes in fecundity may have obscured an underlying relationship between density and fecundity. Analysis of samples spanning more years and areas is needed to determine how geographic location and interannual variation interact to influence ocean shrimp fecundity.

The substantial variation in fecundity observed in this study agrees generally with other research on pandalid shrimp. The only other comparable study of ocean shrimp fecundity is one by J.G. Robinson (1971, ODFW, unpublished data) in which he analyzed two small fecundity samples from Oregon and compared them with Dahlstrom's (1970) samples from California. J.G. Robinson (1971, ODFW, unpublished data) found significant differences in mean fecundity between several samples, with increasing fecundity to the south. As in this study, J.G. Robinson's (1971, ODFW, unpublished data) samples covered a number of years, and the variability he attributed to geographic location may have simply been interannual variation. The variability in fecundity we observed between years suggests that simultaneous collection of samples from many areas is needed to determine if southern populations of ocean shrimp are consistently more fecund. Teigsmark (1983) found substantial geographic and interannual variation in fecundity for northern shrimp in the Barents Sea, with the

Table 2. Results of linear regression analysis of $\log_e$ fecundity on $\log_e$ carapace length for samples of ocean shrimp from PSMFC areas 72–88, in the years 1989–1993, and from area 82 in 1967 (J.G. Robinson, 1971, ODFW, unpublished data) and from area 92 in 1964 (Dahlstrom 1970).

Sample	Intercept	Slope of standard regression	Intercept of GM regression	Slope of GM regression	Half width of 95% confidence interval for slope	R^2	*p* value
Present study							
Area 84, fall 1989	−2.879	3.365	−3.954	3.721	0.297	0.817	0.0001
Area 84, fall 1990	1.158	2.131	−0.306	2.597	0.296	0.672	0.0001
Area 84, spring 1992	0.282	2.374	−1.157	2.846	0.301	0.695	0.0001
Area 72, spring 1992	−1.146	2.830	−1.950	3.102	0.308	0.832	0.0001
Area 74, spring 1992	−0.805	2.714	−2.656	3.322	0.373	0.669	0.0001
Area 74, fall 1992	−2.721	3.370	−3.089	3.494	0.268	0.931	0.0001
Area 88, fall 1992	−1.051	3.002	−2.347	3.274	0.170	0.905	0.0001
Area 88, fall 1993	−1.419	3.000	−1.912	3.157	0.307	0.840	0.0001
All samples combined	−2.413	3.263	−3.493	3.616	0.109	0.821	0.0001
Prior data							
Area 82, fall 1967	−0.034	2.438	−2.447	3.235	0.545	0.568	0.0001
Area 92, fall 1964	0.213	2.393	−4.880	4.053	0.811	0.418	0.0001

Note: Slope estimates for the standard predictive and geometric mean regressions are shown along with the estimated half width of the 95% confidence interval for the slope estimates. Model is $\log_e$ (fecundity) = $a + b(\log_e$ (carapace length)). Values of R^2 and *p* refer to standard regressions only.

Fig. 6. Graphical comparison of back-transformed, fitted values (corrected for transformation bias) from geometric mean regression of $\log_e$ fecundity on $\log_e$ carapace length for samples of ocean shrimp from PSMFC areas 72–92, 1964–1993.

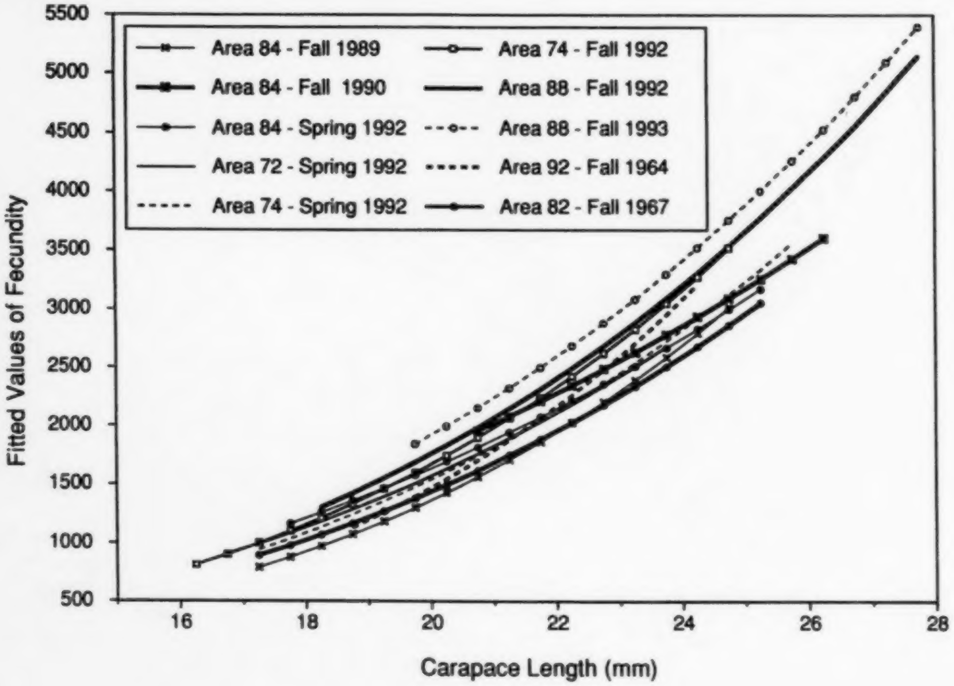

Table 3. Summary of ocean shrimp market samples used to estimate population fecundity.

Fecundity sample	Market sample	Sample size	Percent females	Percent transitionals	Age composition (%)			
					Age 0	Age 1	Age 2	Age 3+
Area 84, fall 1989	Area 84, Oct. 1989	499	25.7	0.0	0.0	80.0	19.8	0.2
Area 84, fall 1990	Area 84, Oct. 1990	301	38.9	2.0	0.0	19.6	79.4	1.0
Area 84, spring 1992	Area 84, Sept. 1991	716	30.5	7.3	0.1	85.9	8.8	5.2
Area 72, spring 1992	Area 72, Oct. 1991	263	31.2	0.8	0.3	75.6	14.4	9.7
Area 74, spring 1992	Area 74, Oct. 1991	605	40.5	0.2	1.0	88.5	3.1	7.4
Area 74, fall 1992	Area 74, Oct. 1992	202	45.0	0.0	0.0	91.1	7.9	1.0
Area 88, fall 1992	Area 88, Oct. 1992	747	57.4	6.3	0.8	94.5	4.6	0.1
Area 88, fall 1993	Area 88, Oct. 1993	436	37.8	6.2	15.8	37.2	44.2	2.8

Fig. 7. Comparison of high and low fecundity years with April–August mean sea level height at Crescent City, California. Numbers denote the year samples were collected. See Fig. 6 for high and low fecundities.

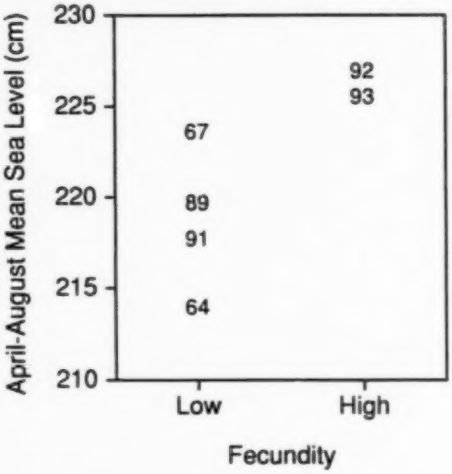

Fig. 8. Estimated ocean shrimp egg production (thousands/kg), derived from market samples (Table 3), using the length–fecundity relationships shown in Table 2. Samples are identified by statistical area followed by an S or F denoting spring or fall collection, followed by the year of collection (84 F92 denotes a sample collected from area 84 in the fall of 1992).

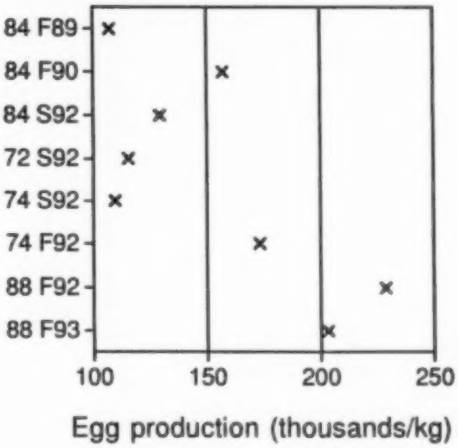

southernmost population showing the highest fecundity. In Teigsmark's (1983) study, the interannual variation in fecundity within an area was as great as the variation between areas in a single year, making it difficult to come to a conclusion about differences in fecundity between populations. The results of this study of ocean shrimp are consistent with Teigsmark's observations for northern shrimp. Parsons and Tucker (1986) also found significant variation in fecundity between years and areas for northern shrimp in the Northwest Atlantic; however, Apollonio et al. (1986) did not.

Egg production

The egg production estimates (Fig. 8) varied substantially, on a unit weight basis, among areas and years. The largest estimate was roughly 2.1 times the minimum estimate. High egg production was generally associated with an elevated length–fecundity curve (Fig. 6), but variation in sex composition also had a strong influence on total egg production. In a simple linear regression, the percentage of female shrimp in the market samples explained roughly 62% of the variation in egg production ($p < 0.05$), with higher percentages of females associated with increased egg production. The estimated egg production for the fall 1992 sample from area 74 was based on a market sample with 45% females (Table 3). The increased egg production for this sample resulted, in part, from higher levels of female shrimp than in most of the other samples.

The egg production estimates derived from individual samples deviated markedly from similar estimates calculated from a pooled length–fecundity relationship (Table 4). The purpose of this comparison was to measure the approximate magnitude of added variance that would be introduced by calculating historical estimates of egg production from the data collected in this study. The deviations ranged from an overestimate of 17.6% to an underestimate of 13.2%. Clearly, without a substantial annual effort to measure fecundity for ocean shrimp, it seems that the most accurate

Table 4. Comparison of estimates of population fecundity derived from ocean shrimp market sample data using two methods.

Sample	Population fecundity using method 1 (eggs/kg)	Population fecundity using method 2 (eggs/kg)	Percent difference
Area 84, fall 1989	107 270	126 201	17.6
Area 84, fall 1990	157 121	160 969	2.4
Area 84, spring 1992	129 317	133 216	3.0
Area 72, spring 1992	115 275	123 325	7.0
Area 74, spring 1992	109 517	113 312	3.5
Area 74, fall 1992	173 270	176 503	1.9
Area 88, fall 1992	228 648	206 949	−9.5
Area 88, fall 1993	203 209	176 322	−13.2

Note: Method 1 uses the length–fecundity relationship from the individual samples, while method 2 uses a length–fecundity relationship from all eight samples combined.

index of egg production that can be developed would still routinely under- or over-estimate reproductive output by 13–18%.

Deviations of this magnitude, while of some concern, may still be small in relation to other sources of variation in estimates of total annual egg production of ocean shrimp. This analysis has shown that much of the variation in egg production can be accounted for by using age-composition and sex-composition data for specific years and areas, even when using an average length–fecundity relationship. The parent stock index used by Hannah (1993), which was based on a simple average of ocean shrimp CPUE at the end of the trawl season, varied from under 50 to over 450 kg/h, a ninefold variation in density. Hannah (1995) showed that the geographic area populated by ocean shrimp in PSMFC areas 82–88 (Fig. 1) varies from roughly 81 000 to over 550 000 ha. This is roughly a sevenfold variation in stock area. Moreover, the same study linked low stock abundance with reduced geographic range and high stock abundance with expanded geographic range. In comparison, the maximum estimate of egg production from this study was roughly 2.1 times as large as the minimum estimate. Accordingly, if an index of reproductive output incorporated density (from CPUE), stock area data, and fecundity estimates based on area-specific age- and sex-composition data, it would be expected to vary broadly, with maximum values well over 10 times as large as the minimum values. With such a broad range, this type of index might still give correct information about changes in reproductive output, despite the added variance resulting from using an average length–fecundity relationship to estimate egg production. Put another way, the largest improvement in an index of reproductive output for ocean shrimp based on CPUE would likely come from incorporating the effect of changes in geographic stock area, followed by the effect of age- and sex-composition on average fecundity, followed by the effect of shifts in the length–fecundity relationship. Constructing such an index and revisiting the relationship between stock, recruitment, and the ocean environment is the next logical step in investigating the population dynamics of ocean shrimp.

Acknowledgments

This project was financed in part with Federal Interjurisdictional Fisheries Act funds through the U.S. National Marine Fisheries Service. The Oregon shrimp industry was crucial to the success of this project, particularly the owners and operators of the following fishing vessels: *Prospector, Lady Kaye, Ginger B,* and *Panda.* Bruce Miller and Rick Starr helped with some of the at-sea sampling.

References

Abramson, N.T., and P.K. Tomlinson. 1972. An application of yield models to a California ocean shrimp population. Fish. Bull. 70: 1021–1041.

Apollonio, S., D.K. Stevenson, and E.E. Dunton. 1986. Effects of temperature on the biology of the northern shrimp, *Pandalus borealis*, in the Gulf of Maine. NOAA Tech. Rep. NMFS No. 42.

Bagenal, T.B., and E. Braum. 1978. Eggs and early life history. *In* Methods for assessment of fish production in fresh waters. *Edited by* T.B. Bagenal. IBP Handb. 3. Blackwell Scientific Publications Ltd., Oxford, U.K. pp. 165–202.

Charnov, E.L., D.W. Gotshall, and J.G. Robinson. 1978. Sex ratio: adaptive response to population fluctuations in pandalid shrimp. Science (Washington, D.C.), 200: 204–206.

Chelton, D.B., and R.E. Davis. 1982. Monthly mean sea-level variability along the west coast of North America. J. Phys. Oceanogr. 12: 757–784.

Dahlstrom, W.A. 1970. Synopsis of biological data on the ocean shrimp *Pandalus jordani*, Rathbun, 1902. FAO Fish. Rep. 57: 1377–1416.

Gotshall, D.W. 1972. Population size, mortality rates, and growth rates of northern California ocean shrimp *Pandalus jordani*, 1965 through 1968. Calif. Dep. Fish Game Fish. Bull. 155: 1–47.

Hannah, R.W. 1993. Influence of environmental variation and spawning stock levels on recruitment of ocean shrimp (*Pandalus jordani*). Can. J. Fish. Aquat. Sci. 50: 612–622.

Hannah, R.W. 1995. Variation in geographic stock area, catchability, and natural mortality of ocean shrimp (*Pandalus jordani*): some new evidence for a trophic interaction with Pacific hake (*Merluccius productus*). Can. J. Fish. Aquat. Sci. 52: 1018–1029.

Hannah, R.W., and S.A. Jones. 1991. Fishery induced changes in the population structure of pink shrimp (*Pandalus jordani*). Fish. Bull. 89: 41–51.

Kruse, G.H. 1981. Relationship between shelf temperatures, coastal sea level, the coastal upwelling index, and English sole (*Parophrys vetulus*) spawning activity off Oregon. M.S. thesis, Oregon State University, Corvallis, Oreg.

Nunes, P. 1984. Reproductive and larval biology of northern shrimp *Pandalus borealis* Krøyer, in relation to temperature. Ph.D. dissertation, University of Alaska, Fairbanks, Alaska.

Parsons, D.G., and G.E. Tucker. 1986. Fecundity of northern shrimp, *Pandalus borealis*, (Crustacea, Decapoda) in areas of the northwest Atlantic. Fish. Bull. 84: 549–558.

Pope, I.A., D.H. Mills, and W.M. Shearer. 1961. The fecundity of the Atlantic salmon (*Salmo salar* Linn.). Freshwater Salmon Fish. Res. No. 26.

Raitt, D.F.S. 1968. The population dynamics of the Norway pout in the North Sea. Mar. Res. Vol. 68. No. 5.

Ricker, W.E. 1973. Linear regressions in fishery research. J. Fish. Res. Board Can. 30: 409–434.

Rothschild, B.J., and M.J. Fogarty. 1989. Spawning-stock biomass: a source of error in recruitment/stock relationships and management advice. J. Cons. Cons. Int. Explor. Mer, 45: 131–135.

Sokal, R.R., and F.J. Rohlf. 1981. Biometry. W.H. Freeman & Co., New York.

Tegelberg, H.C., and J.M. Smith. 1957. Observations on the distribution and biology of the pink shrimp (*Pandalus jordani*) off the Washington coast. Wash. Dep. Fish. Res. Pap. 2: 25–34.

Teigsmark, G. 1983. Populations of the deep-sea shrimp (*Pandalus borealis* Krøyer) in the Barents Sea. Fiskeridir. Skr. Ser. Havunders. 17: 377–430.

Zirges, M.H., M.R. Saelens, and J.E. McCrae. 1982. Total catch and effort tables, and summary biological statistics for pink shrimp caught in Oregon statistical areas 18–28 by month and area 1966–1981; catch numbers expanded by age and sex, effort in hours by vessel type. Inf. Rep. Ser. Fish. No. 82-4. Oregon Department of Fish and Wildlife, Newport, Oreg.

Limits to tolerance of temperature and salinity in the quagga mussel (*Dreissena bugensis*) and the zebra mussel (*Dreissena polymorpha*)[1]

Adrian P. Spidle, Edward L. Mills, and Bernie May

Abstract: The quagga mussel (*Dreissena bugensis*) and the zebra mussel (*Dreissena polymorpha*) were exposed to varied levels of salinity and temperature in the laboratory to compare the tolerance of each species to environmental stress. The zebra mussel could tolerate 30°C for extended periods and higher temperatures (<39°C) for a period of hours depending on the acclimation temperature and the rate of temperature change. The upper thermal limit of the quagga mussel may be as low as 25°C. Mussels of both species acclimated to 5°C were less able to survive at high temperatures (30–39°C) than mussels acclimated to 15 or 20°C. The reduced upper temperature limit of the quagga mussel implies that it will not be able to expand as far south in North America as has the zebra mussel. Both *D. bugensis* and *D. polymorpha* were exposed to three concentrations of NaCl (5, 10, and 20‰) to test salinity tolerance. No individuals of either species survived beyond 18 days in salinities of 5‰ or higher. No interspecific difference occurred in salinity-induced mortality rate.

Résumé : La moule couagga (*Dreissena bugensis*) et la moule zébrée (*Dreissena polymorpha*) ont été exposées à divers niveaux de salinité et de température en laboratoire dans le but de comparer la tolérance des deux espèces à un stress environnemental. La moule zébrée peut tolérer une température de 30°C pendant de longues périodes et même des températures supérieures (<39°C) pendant quelques heures, selon la température d'acclimatement et la vitesse de variation de la température. La limite supérieure de température tolérée par la moule couagga ne semble pas dépasser 25°C. Les moules des deux espèces acclimatées à 5°C sont moins aptes à survivre à de hautes températures (de 30 à 39°C) que les moules acclimatées à des températures de 15 ou 20°C. Étant donné le bas niveau de la limite supérieure de température tolérée par la moule couagga, celle-ci ne peut pas, en Amérique du Nord, se répandre aussi loin vers le sud que la moule zébrée. *Dreissena bugensis* et *D. polymorpha* ont été exposées à trois concentrations de NaCl (5, 10 et 20‰) afin d'évaluer leur tolérance à la salinité. Aucun spécimen des deux espèces n'a survécu plus de 18 jours à des salinités de 5‰ et plus. Aucune différence interspécifique n'a été observée dans le taux de mortalité imputable à la salinité.

[Traduit par la Rédaction]

Introduction

The first public response to the invasion of an exotic species such as the quagga mussel (*Dreissena bugensis*) or the zebra mussel (*Dreissena polymorpha*) is to predict its potential distribution in the new habitat. Research to determine the effect of the introduced species on its new habitat and to find control mechanisms can then follow. Tolerance to salinity and temperature needs to be assessed experimentally for both species of *Dreissena* to determine if their environmental limits overlap, and what their final distributions in North America might be. *Dreissena bugensis* has been observed to displace *D. polymorpha* in many parts of their overlapping habitat in Ukraine (Pligin 1984). Whether this pattern will be repeated in North America is unclear.

Substantial genetic differentiation has been documented between *D. bugensis* and *D. polymorpha* (May and Marsden 1992; Rosenberg and Ludyanskiy 1994; Spidle et al. 1994). The large genetic distance between the quagga and zebra mussels suggests that these two species will not respond identically to their new habitat. Ecological evidence suggests that the two North American species of *Dreissena* behave differently in lakes Erie and Ontario, where the quagga

Received August 16, 1994. Accepted May 12, 1995.
J12543

A.P. Spidle[2] **and B. May.**[3] Department of Natural Resources, Cornell University, Ithaca, NY 14853, U.S.A.
E.L. Mills. Cornell Biological Field Station,
900 Shackelton Point Road, Bridgeport, NY 13030, U.S.A.

---

[1] Contribution No. 167 of the Cornell Biological Field Station, Bridgeport, N.Y.

[2] Present address: Marine Molecular Biotechnology Laboratory, School of Fisheries, University of Washington, 3707 Brooklyn Avenue, Seattle, WA 98105, U.S.A.

[3] Present address: Department of Animal Science, University of California, Davis, CA 95616, U.S.A.

Can. J. Fish. Aquat. Sci. **52**: 2108–2119 (1995). Printed in Canada / Imprimé au Canada

mussel occurs disproportionately or exclusively in deeper areas where temperatures seldom exceed 5–10°C (Dermott and Munawar 1993; Mills et al. 1993). Models in the current literature may not be able to predict the distribution of the quagga mussel with the same accuracy they do for the zebra mussel (McMahon 1990; Strayer 1991; Ramcharan et al. 1992*a*, 1992*b*; Schneider 1992).

If the quagga mussel's tolerance to high temperatures is less than that of the zebra mussel, as suggested by previous research (Dermott and Munawar 1993; Mills et al. 1993), then *D. bugensis* may not be able to colonize the southern United States, where *D. polymorpha* currently infests areas in which midsummer water temperatures regularly reach 30°C. Additionally, the temperature of the hot water used to back-flush intake pipes, an important control mechanism for industrial facilities drawing cooling water from *Dreissena*-infested waterways, must be chosen on the basis of the temperature tolerance of the species involved. If the quagga mussel's thermal maximum is the same as or lower than that of the zebra mussel, *D. bugensis* may not pose an additional threat to commercial enterprises.

To date, three studies using three different techniques have tested the tolerance of *D. polymorpha* to temperature increase. McMahon et al. (1993) tested animals by gradually increasing the temperature from acclimation temperature to test temperature, after methods previously used to evaluate the vertical distribution of littoral gastropods (Broekhuysen 1940; Stirling 1982). Iwanyzki and McCauley (1993) exposed animals to lethal temperature without gradual change from acclimation temperature, to avoid the confounding factor of time spent in changing temperatures, after methods developed by Fraenkel (1960, 1968) for testing the vertical distribution of intertidal snails. A temperature of 30°C was estimated to be 100% fatal to zebra mussels across acclimation temperatures ranging from 2.5 to 25°C by one research group (Iwanyzki and McCauley 1993), while other reports suggest that zebra mussels are capable of tolerating 30°C indefinitely, with temperatures of 31°C or higher being lethal (McMahon et al. 1993, 1994). This result is perhaps anomalous, as Stirling (1982) demonstrated that the method used by McMahon et al. (1993) would, if anything, overestimate the lethal temperature for a given species of gastropod mollusc relative to the method of Iwanyzki and McCauley (1993). An additional study using the method of Iwanyzki and McCauley (1993) comparing the responses of quagga and zebra mussels to lethal temperatures indicated that the quagga mussel dies sooner at temperatures lethal to both species (Domm et al. 1993).

The range of salinity levels inferred to limit *D. polymorpha* in Eurasia is quite wide, from 2 to 12‰ in inland seas, but only 0.5‰ in estuaries on the Atlantic coast of the Netherlands (for review see Strayer and Smith 1993). However, the composition of the salinity in these areas is variable. The salinity of the inland seas is more rich in minor divalent ions (Ca^{+2}, Mg^{+2}, and SO_4^{-2}) than marine salinity (Strayer and Smith 1993). The presence of minor ions may reduce the effect of Cl^-, which is suggested to be the ion most limiting to the distribution of *D. polymorpha* (Strayer and Smith 1993; see also Zhadin 1952). Mg^{+2} in particular is essential for osmoregulation in *D. polymorpha* (Dietz et al. 1994).

As an alternative to the ion ratio model of salinity tolerance, Strayer and Smith (1993) also pointed out that the Caspian and Aral seas, with *D. polymorpha* populations found at 8 and 12‰, respectively, do not undergo such wide swings in salinity as the coastal areas do. Thus, the zebra mussel may exhibit tolerance to moderate salinity when it is constant (8–12‰), but to lower salinities (0.5‰) if the salinity undergoes frequent changes, as in tidal estuaries. Exposure to 1.6‰ NaCl for a week was fatal to zebra mussels in one set of laboratory experiments (Horohov et al. 1992), while other tests showed perturbations in respiration, but no mortality, resulting from increasing salinity from 0 to 10‰ over a period of 10 days (Karpevich 1947).

We report the results of tests to experimentally determine the relative susceptibility to mortality from salinity and (or) temperature of *D. bugensis* and *D. polymorpha* under the following conditions: (*i*) chronic temperature stress such as may occur during range expansion (immersion in 30°C water for up to 14 days); (*ii*) acute temperature stress caused by increasing the temperature at varying rates and then returning to ambient levels, as would occur during the use of thermal mitigation techniques in industrial cooling systems, following the methods of McMahon et al. (1993); and (*iii*) different constant levels of salinity in combination with different constant (sublethal) levels of temperature.

Methods

Sample collection and maintenance

Quagga and zebra mussels were collected by bottom trawling in Lake Ontario offshore from Olcott, New York, in April 1993 and in Lake Erie near Dunkirk, New York, in July 1993, at depths of 25–30 m. The mussels were immediately transported to the Cornell Biological Field Station in Bridgeport, New York, where they were divided into three groups that were acclimated to temperatures of 5, 15, and 20°C. Temperatures were changed from ambient at a rate of 1°C/h. Animals were considered acclimated after being left undisturbed at a constant temperature (±0.5°C) for a minimum of 14 days, at which point most of the animals had bysally attached to each other and (or) surfaces in their containers. The process was intended to allow recovery from the stress of collection and transport and to simulate seasonal variation in response to environmental stress. Mussels acclimated to 5°C were held in 800-L fiberglass tanks with temperatures maintained by circulating chillers. Mussels acclimated to 15 and 20°C were held in 75-L glass tanks insulated by 5 cm of Styrofoam with temperatures maintained by circulating heaters. Two attempts to acclimate zebra and quagga mussels to 25°C failed because sufficient numbers of quagga mussels could not be kept alive at that temperature to complete the experimental designs. Zebra mussels in the same aquarium suffered no mortality. Filtered and aerated Oneida Lake (New York) water was used in all holding tanks and all test baths.

The mussels were not fed and were used within 4 weeks if held at elevated temperatures and within 8 weeks if held at 5°C (after Horohov et al. 1992; McMahon et al. 1993). The mussels collected at Olcott were maintained at 5°C for 14 days and then adjusted to their final acclimation temperatures. The mussels collected at Dunkirk were immediately divided into acclimation groups. The Olcott mussels were used in temperature experiments while the Dunkirk mussels were used in salinity experiments.

All treatments called for either 10 or 12 mussels per experimental unit. When possible, mussels that were bysally attached to each other were used, attachment being used as evidence of lack of stress. When extra mussels could not be removed from a clump without disrupting the remainder of mussels, they were included in the test, and when there were not enough small clumps to sum to the total required in a treatment, then available attached mussels were used. Each experimental unit was always within two mussels of the designated size, with preference given to exceeding rather than falling short of the designed sample size. Individual mussels greater than 20 or less than 10 mm in length were not used unless they were inextricably attached to a test clump of mussels.

Response to chronic temperature stress

To test the differential response of the *Dreissena* species to a constant elevated temperature, 50 animals of each species from each of the three temperature acclimation groups (5, 15, and 20°C; 300 animals total) were maintained at temperatures of 30 and 35°C (increase to test temperature from acclimation temperature was at a rate of 1°C/h) for a maximum of 14 days. These temperatures were chosen because they are among the highest temperatures that these mussels might encounter in the northeast United States but that may or may not cause rapid mortality in zebra mussels (Iwanyzki and McCauley 1993; McMahon et al. 1993). Mussels of each species from each acclimation group were divided and placed into five labeled glass dishes (50 mm high × 80 mm in diameter) covered with a 1-mm nylon mesh to prevent migration. The daily mortality of the zebra and quagga mussels was recorded for each dish. Gaping individuals that did not respond to stimulus with a soft-bristle brush were tested with a dissecting probe. If this elicited no response, the animal was considered dead. Dead animals were measured for length and discarded. This definition of death was used in all three experiments discussed in this paper. At the conclusion of the experiment the length of all survivors was measured. This experiment was run twice at 30°C and once at 35°C.

Response to acute temperature stress

Experiments were designed to test the tolerance of each species of *Dreissena* to different regimes of acute temperature change ranging from a quick pulse of heat to prolonged exposure. The response to acute temperature stress was examined using a fully factorial design of quagga and zebra mussels from each of three acclimation temperatures (5, 15, and 20°C) at four different rates of temperature increase (1°C per 5, 15, 30, or 60 min), for a total of 24 treatments (2 species × 3 acclimation temperatures × 4 rates of temperature increase). One hundred mussels were used in each treatment, for a total of 2400 animals. Each treatment was tested once. Our procedure follows that of McMahon et al. (1993).

The two species were tested simultaneously in the same water bath for a given combination of acclimation temperature and rate of temperature increase. For each treatment the mussels were divided into groups of approximately 10 animals that were placed into glass dishes (10 dishes for each species in a given trial) covered with a 1-mm nylon mesh to prevent escape as in the chronic temperature stress experiment. Each dish was an experimental unit for analytical purposes. No treatments were replicated. The 20 dishes were placed into an insulated water bath (60-L cooler) held at the appropriate acclimation temperature for those treatments. After a 2-h waiting period to minimize additional stress from transfer to the test bath, the temperature was raised from the initial acclimation temperature at the test rate of increase: 1°C every 5, 15, 30, or 60 min. One dish of each species was removed from the heated bath when the temperature reached 30°C, well before mortality. The nylon mesh was removed and the warm water in the dish was allowed to equilibrate to room temperature (13–18°C). A new pair of dishes was removed from the bath as each temperature degree was reached (from 30 to 39°C) and allowed to equilibrate to room temperature until all dishes had been removed.

The mussels were surveyed for mortality 1 and 12 h after removal from the test bath. The number of dead mussels out of the total number in a dish was determined for the 10 dishes of each species of mussel in a trial. Because some recovery was observed between 1- and 12-h observations, only the latter were used in the analysis. The temperature at which 100% sample mortality was observed to occur (SM_{100}) was recorded. At the conclusion of each experiment the length of all animals was measured.

A logistic regression model was used (logit analysis) to describe the effect of species, acclimation temperature, rate of temperature increase, instantaneous test temperature of observation (30–39°C), degree-minutes (a measure of the combined effect of temperature and time), and all interactions on survival of temperature stress by *Dreissena*. Length was used as a covariate. Length and instantaneous test temperature were coded continuously, but the other predictors were coded categorically because there were not enough levels of observation to justify continuous coding of acclimation temperature or rate of temperature increase. Nonsignificant terms were omitted from the final model ($\alpha = 0.05$). The experimental unit for analysis was the group of mussels within a given dish, coded as number dead out of total number. Logit models were also used to predict the LT_{50} and LT_{100} (temperature causing 50 or 99.9% mortality) for each species in each treatment. This analysis was carried out using SYSTAT LOGIT (Steinberg and Colla 1991).

Regression coefficients in the multivariate logit model represent the natural logarithm of the odds of response (death) given a particular level of a predictor (probability of death for each level of predictor divided by probability of death at a baseline level of predictor). The baseline model against which all predictors in this study were compared is a zebra mussel acclimated to 5°C with temperature increased by 1°C per 60 min. If a coefficient is negative, the interpretation is that the given level of the predictor is less likely than the baseline level to cause a mussel to die. Positive coefficients indicate that a given level of the predictor is more likely to cause mortality. The coefficients were exponentiated (antilog of the regression coefficient) to give an odds ratio for survival at each level of each predictor relative to the baseline (regression coefficients were generated for species = quagga, acclimation temperature = 15 or 20°C, and rate of temperature change = 1°C per 5, 15, or 30 min). See Hosmer and Lemeshow (1989) for further discussion of logistic regression.

Response to salinity

Salinity experiments were designed to include the effect of temperature on the mussels' ability to tolerate different concentrations of Na^+ and Cl^-, the principal ions in seawater. Mussels were maintained at four constant concentrations of NaCl for a maximum of 18 days (0, 5, 10, and 20‰). Samples of about 24 mussels of each species from each acclimation temperature (5, 15, and 20°C) were tested in a fully factorial design at each of three test temperatures (5, 15, and 20°C). Each sample was divided into two replicates of 12 mussels each. As in the temperature tolerance experiments, mussels from each species – acclimation temperature combination were divided and placed into individually labeled glass dishes covered with 1-mm nylon mesh. Each treatment was replicated once (two dishes per treatment).

All mussels began in fresh water (0‰). Jars of mussels were randomly assigned to treatments before being exposed to salinity. On day 1 of the test, 24 h after temperatures had been adjusted from acclimation to test temperature (at a rate of 1°C/h) all test mussels were moved into water with 5‰ NaCl. Control mussels (temperature manipulation only) remained in fresh water. After a further 24 h mussels to be tested at elevated salinities were moved from the 5‰ baths into water with 10‰ NaCl. After a final 24 h, mussels to be tested at 20‰ were moved into baths of that salinity from the 10‰ baths. The daily mortality of zebra and quagga mussels was recorded for each dish and dead animals were measured and removed from that dish. At the end of the experiment the length of all survivors was measured.

The results were examined using analysis of variance. The experimental unit was the glass dish containing approximately 12 mussels. There were, therefore, two observations for each treatment (combination of species, test temperature, acclimation temperature, and salinity). The response variable, mean survival time of the mussels in each glass dish, was transformed by taking the natural logarithm to stabilize variance in the model. Mussels that died before reaching the designated test salinity (mussels acclimated at 20‰ that died in the 5‰ bath, for instance) were coded as having died on day 0. All other mussels were coded as having died on day *X*, where *X* is the number of 24-h periods (from 1 to 18) after each mussel reached its designated test salinity until death occurred.

Candidate predictors included temperature of prior acclimation, level of salinity, test temperature (temperature at which the animals were exposed to salinity), and all interactions. Length was used as a covariate. All predictors but the length covariate were coded categorically. Nonsignificant terms were omitted from the final model ($\alpha = 0.05$). Post-ANOVA comparisons to determine significant differences in mean survival time of all treatments were calculated using Fisher's least significant difference procedure (LSD) to correct for multiple simultaneous tests (overall $\alpha = 0.05$; Fisher 1966; see also Ott 1988). This analysis was carried out using SYSTAT for Windows 5.02 (Wilkinson 1992).

Table 1. Percent survival through time of *D. bugensis*, acclimated to three different temperatures (5, 15, and 20°C) and exposed to 30°C.

	5°C		15°C		20°C	
Day	*a*	*b*	*a*	*b*	*a*	*b*
1	18.37	48.98	100.00	98.00	83.33	92.00
2	0.00	2.04	75.51	92.00	81.25	88.00
3	—	2.04	59.18	88.00	58.33	84.00
4	—	2.04	24.49	72.00	37.50	74.00
5	—	0.00	12.24	60.00	25.00	64.00
6	—	—	4.08	60.00	20.83	56.00
7	—	—	2.04	58.00	4.17	48.00
8	—	—	0.00	54.00	2.08	44.00
9	—	—	—	48.00	2.08	42.00
10	—	—	—	48.00	2.08	38.00
11	—	—	—	+42.00	2.08	+36.00
12	—	—	—	—	2.08	—
13	—	—	—	—	2.08	—
14	—	—	—	—	0.00	—

Note: The experiment was replicated once. Trial *a* lasted 14 days. Trial *b* ended after day 11 because of mechanical failure; + indicates the percent surviving mussels in the last assay before failure occurred. *Dreissena polymorpha* was tested in the same aquarium as *D. bugensis* for each trial, in different sample dishes, and experienced no mortality.

Results

Response to chronic temperature stress

Experiments designed to test the response of quagga and zebra mussels to chronic temperature stress indicate that the zebra mussel is much more tolerant of elevated temperatures than the quagga mussel. In the first of two replicates, only one quagga mussel survived longer than 7 days at 30°C, and it died on the 14th day. No zebra mussel mortality occurred in 14 days of observation. The second replicate was disrupted after day 11 when the thermostat malfunctioned and the temperature was raised to 37°C, killing all remaining mussels of both species. In this second trial, the mortality rates for the quagga mussel appeared to be different from those in the first trial (Table 1). The gross result, of extreme quagga mortality and no zebra mussel mortality at 30°C, was the same, however.

When tested at 35°C, all animals of both species (n = 300) had died by the first observation period, 24 h after the test temperature was reached. No mortality occurred in the control treatments in which quagga and zebra mussels from each acclimation temperature were adjusted to sublethal temperatures (5, 15, and 20°C).

Response to acute temperature stress

When a logistic regression model was fit to the data, each of the main effects except degree-minutes and the covariate

Table 2. Response of zebra and quagga mussels to increasing temperature.

	Regression coefficient			Odds ratio		
Predictor	Estimate	SE	p	95% CI lower bound	Estimate	95% CI upper bound
Constant	−45.578	2.017	<0.001	—	—	—
Rate = 30	−0.445	0.210	0.034	0.425	0.641	0.967
Rate = 15	−1.204	0.218	<0.001	0.196	0.300	0.460
Rate = 5	−2.483	0.235	<0.001	0.053	0.083	0.132
Acclimation = 15	−1.838	0.199	<0.001	0.108	0.159	0.235
Acclimation = 20	−2.660	0.215	<0.001	0.046	0.070	0.107
Temperature	1.317	0.058	<0.001	3.332	3.733	4.183
Species = quagga	2.602	0.184	<0.001	9.410	13.496	19.358

Note: The baseline model is a zebra mussel acclimated to 5°C in a bath with the temperature increased by 1°C each 60 min. The odds ratio indicates the change in risk for an individual mussel at each level of the predictor relative to the baseline. If the odds ratio is greater than one, that predictor is a positive risk, and increasing it increases the risk to the individual: if the odds ratio is less than one, the predictor is a negative risk and increasing it reduces the risk to the individual.

Fig. 1. Percent survival of quagga (●) and zebra (○) mussels, combined across four rates of temperature increase, for each of three acclimation temperatures (5, 15, and 20°C) and 10 test temperatures from 30 to 39°C.

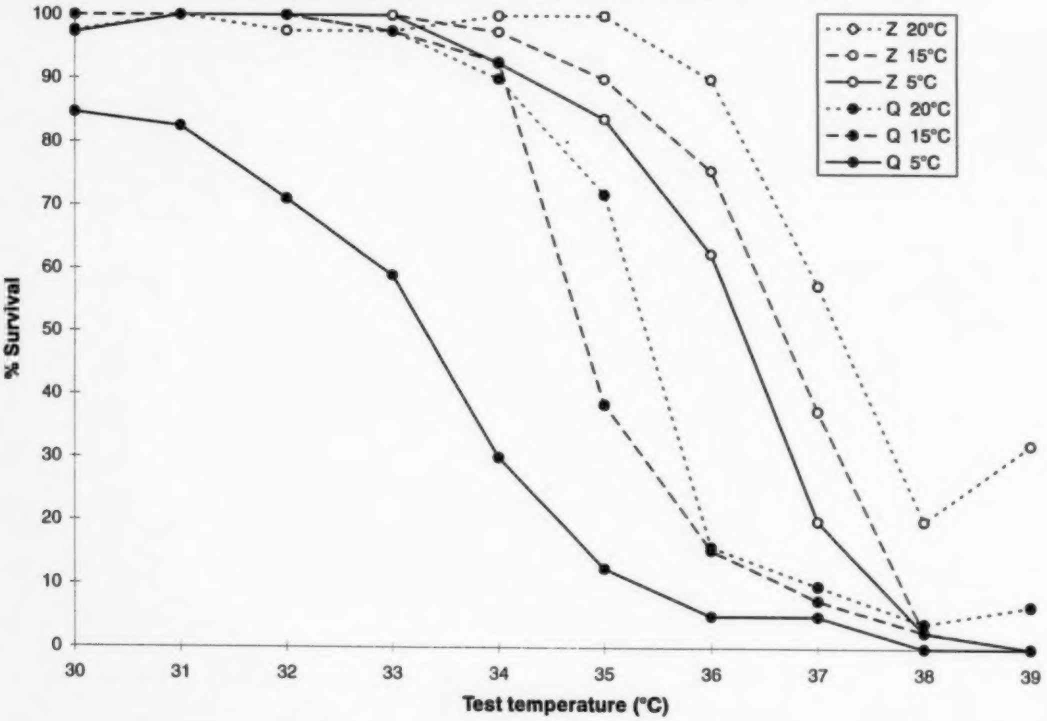

of length was significant ($p < 0.05$) and retained in the final model (Table 2). No interaction term was found to have a significant effect ($p < 0.05$) on the likelihood of survival for a given mussel and all were dropped from the final model. Species was the predictor found to have the greatest effect on survival. In any treatment the quagga mussel had a 10- to 20-fold greater chance of dying than the zebra mussel at a given instantaneous temperature of observation. Instantaneous temperature level followed species as a significant positive risk. Each degree of temperature increase, within the range of observation, was found to raise the risk of death by 3–4 times (Table 2).

Fig. 2. Percent survival of quagga (●) and zebra (○) mussels, combined across three acclimation temperatures, for each of four rates of temperature increase and 10 test temperatures from 30 to 39°C. Rate is given as minutes per degree Celcius.

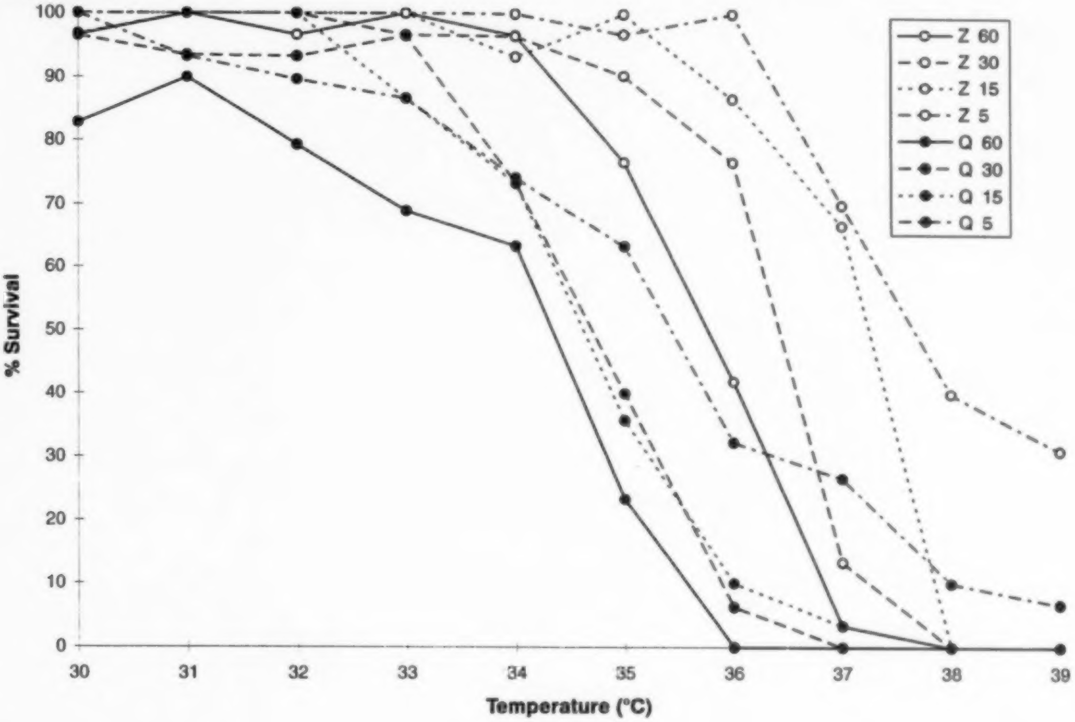

Increasing acclimation temperature improved the mussels' likelihood of survival relative to be baseline model (zebra mussel acclimated to 5°C with temperature raised 1°C per 60 min; see Fig. 1). Mussels of each species acclimated to 15 or 20°C were less likely to die from acute stress due to increased temperature than those acclimated to 5°C ($p < 0.01$). The two higher acclimation temperatures were slightly different from each other ($p = 0.05$; see Table 2 for confidence intervals around the predicted odds ratios).

The rate of temperature increase was also a negative risk to survival (Fig. 2). The effects of the two intermediate rates (1°C increase per 30 or 15 min) increased the likelihood of survival relative to the baseline (1°C increase per 60 min) by 2–5 times but were not significantly different from each other ($p > 0.05$). The fastest rate of temperature increase (1°C per 5 min) significantly increased the likelihood of survival for each species relative to the two intermediate rates ($p < 0.05$) by 2–10 times and by 10–20 times over the baseline rate of 1°C per 60 min. This result suggests a correlation between survival and time exposed to an elevated temperature, since mussels exposed to slower rates of temperature increase spent more time in temperature baths regardless of the final temperature reached.

The LT_{50} of the quagga mussel ranged from 1 to 5°C below that of the zebra mussel in every treatment but one (20°C acclimation: temperature increased by 1°C per 30 min; $p > 0.05$; see Table 3). The LT_{100} values for each species were significantly different in only one treatment (20°C acclimation; temperature increased by 1°C per 30 min; $p < 0.05$; see Table 3). Predicted LT_{100} values were substantially different from the observed SM_{100} values. However, LT_{100} and SM_{100} values did follow trends similar to those of LT_{50} as determined by treatment levels. Complete mortality did not occur in the trials for either species acclimated to 20°C when the temperature was raised by 1°C per 5 min. The quagga mussels experienced 80% mortality at 38 and 39°C, while the zebra mussels experienced no mortality at all in this trial.

Response to salinity

Quagga and zebra mussels exposed to salinity (≥5‰) exhibited 100% mortality within 18 days (Table 4). No significant mortality occurred in the control treatments, where temperatures were varied but no salt was added ($p < 0.001$). Analysis of variance (response variable was mean survival time for each experimental unit (approximately 10 mussels in each glass dish) from the salinity >0‰ treatments) indicates that test temperature, salinity, and an interaction between test temperature and salinity were significant predictors of mortality rate (which was transformed by taking the natural logarithm to stabilize variance). Species, prior acclimation, and the covariate of length did not affect mortality rate of *Dreissena* spp. exposed to salinity ($p > 0.05$); therefore, these predictors were dropped from the final

Table 3. LT_{50} and LT_{100} estimated from logit models, and SM_{100} observed for each treatment in the acute temperature stress experiment for quagga (QM) and zebra (ZM) mussels.

Rate (min/°C increase)	Acclimation temperature	LT_{50}		SM_{100}		LT_{100}	
		QM	ZM	QM	ZM	ZM	ZM
60	5	30.869	35.003	35	37	39.166	39.822
60	15	34.056	35.669	35	37	34.335	38.755
60	20	35.063	36.201	36	38	35.332	40.276
30	5	33.057	36.014	36	38	39.451	39.717
30	15	34.815	36.099	37	37	36.931	38.940
30	20	35.479[a]	36.444[a]	37	38	36.961[b]	42.276[b]
30	5	34.099	36.306	37	38	38.869	41.005
15	15	34.949	37.192	39	39	39.410	39.348
15	20	34.634	37.085	37	38	39.793	37.652
5	5	33.491	37.001	38	39	42.767	39.261
5	15	36.102	37.203	39	39	40.223	40.489
5	20	36.442	—[c]	na[d]	na	45.195	—[c]

[a] These LT_{50} values were not significantly different. All other values of LT_{50} were significantly different between quagga and zebra mussels at $p < 0.05$.

[b] These LT_{100} values were significantly different. No other values of LT_{100} were significantly different between quagga and zebra mussels at $p < 0.05$.

[c] No mortality occurred during the period of observation.

[d] na, 100% mortality was not reached.

model describing the response of the zebra and quagga mussels to salinity (Table 5). The mean survival time for each of the nine test treatments in the final model was compared (corrected by Fisher's LSD procedure to maintain an overall error rate of $\alpha = 0.05$; Table 6).

Increasing the test temperature from 5 to 15 to 20°C greatly increased the mortality rate of the quagga and zebra mussels in the presence of salinity ($p < 0.001$; Fig. 3; note natural logarithm transformation of survival time). Averaged over each test temperature, the two lower salinity levels were statistically equivalent in their effect on survival of *Dreissena* spp. ($p < 0.05$); when tested at 20‰, however, there was a marked increase in mortality rate ($p < 0.05$; Fig. 4; note natural logarithm transformation of survival time). There was a significant interaction between test temperature and salinity level ($p < 0.001$). This was due to a deviation from the linear temperature response at low temperatures. The mean survival time of mussels tested at 5°C did not vary with salinity, although the mussels tested at 5°C and 10‰ salinity did survive longer than those tested at 5°C and 20‰ or 15°C and 5‰ (Table 6).

Discussion

The current distribution of the quagga mussel in North America is much more limited than that of the zebra mussel. The quagga mussel is found in large numbers only in the St. Lawrence River and lakes Erie and Ontario (Dermott and Munawar 1993; Mills et al. 1993), while the zebra mussel occurs in all of the Great Lakes and many waterways east of the Mississippi River (Nalepa and Schloesser 1993). Where the two species coexist in lakes Erie and Ontario, their populations exhibit marked stratification by depth. The correlation between water temperature and the proportion of quagga mussels suggests that the quagga mussel may be more tolerant of the cold temperatures (<10°C) in the deeper waters of lakes Erie and Ontario than of the warmer temperatures found in shallower waters (Mills et al. 1993). The current study does not shed light on the relative performance of the two North American species of *Dreissena* at low temperature, but it does indicate that the quagga mussel was at a marked disadvantage to the zebra mussel when the temperature was raised past 20°C in these experiments.

Tests of the tolerance to elevated temperatures of both North American species of *Dreissena* showed that the quagga mussel could not survive in warm water (30°C), as opposed to the zebra mussel, which suffered no mortality at all in our experiments. These results correspond with those of McMahon et al. (1994) who reported that zebra mussels can be maintained indefinitely at 30°C. Our results showing 100% mortality of each species when kept at 35°C also correspond with those of McMahon et al. (1994) who demonstrated that zebra mussels cannot survive temperatures above 31°C for more than a week. These results correspond with observations of the zebra mussel's distribution through the southern Mississippi River, into areas where summer surface temperatures approach 30°C (McMahon et al. 1994). Subsurface temperatures experienced by the mussels are presumably lower.

Laboratory measurements of LT_{50} from exposure to acute increases in temperature support the results of Domm et al. (1993) indicating that the quagga mussel is more vulnerable than the zebra mussel under most combinations of acclimation temperature and rate of temperature increase (Table 3). The predicted LT_{100} values are much higher than the observed SM_{100} values because of the use of multiplicative rather than additive variance in logistic regression,

Table 4. Mean survival time (maximum survival time in parentheses) for both species of *Dreissena* in each combination of salinity and test and acclimation temperatures.

Test temperature (°C)	Salinity (‰)	Acclimation temperature (°C)	Mean survival time (days)	
			Quagga mussel	Zebra mussel
5	5	5	4.8 (13)	4.9 (18)
5	5	15	7.4 (13)	5.3 (18)
5	5	20	6.8 (12)	3.7 (16)
5	10	5	6.1 (10)	8.0 (12)
5	10	15	6.4 (10)	6.8 (12)
5	10	20	5.9 (10)	3.8 (11)
5	20	5	3.4 (7)	6.0 (9)
5	20	15	4.5 (7)	5.3 (9)
5	20	20	4.7 (8)	3.1 (9)
15	5	5	4.4 (9)	4.2 (9)
15	5	15	4.4 (8)	4.7 (9)
15	5	20	4.9 (9)	4.7 (9)
15	10	5	3.4 (5)	2.9 (6)
15	10	15	3.5 (6)	4.1 (7)
15	10	20	4.2 (6)	3.6 (7)
15	20	5	2.1 (4)	2.6 (6)
15	20	15	2.6 (4)	3.2 (5)
15	20	20	2.7 (4)	3.4 (6)
20	5	5	3.1 (5)	2.2 (6)
20	5	15	3.4 (5)	2.7 (6)
20	5	20	3.2 (5)	3.2 (6)
20	10	5	2.0 (3)	1.5 (4)
20	10	15	1.8 (3)	2.3 (4)
20	10	20	2.8 (4)	2.9 (4)
20	20	5	0.9 (2)	1.1 (3)
20	20	15	1.3 (2)	1.5 (3)
20	20	20	1.2 (2)	1.6 (3)

Table 5. ANOVA model to describe the mortality rate (natural log transformed) of *Dreissena* species in salinity.

Source	Sum of squares	df	Mean square	*F*	*p*
Test temperature	10.845	2	5.422	100.543	<0.001
Salinity	4.440	2	2.220	41.168	<0.001
Test temperature × salinity	1.761	4	0.440	8.161	<0.001
Error	5.339	99	0.054		

Note: Acclimation temperature and species were not significant predictors ($p > 0.05$) and were not included in this final model.

suggesting that the effect of extreme temperatures cannot be predicted reliably from these models. SM_{100}, which reflects observed mortality, seems to be preferable to the predicted LT_{100} value, which underestimates the mortality rate of *Dreissena* species in temperatures that will cause rapid mortality (Table 3).

In three treatments (quagga mussels acclimated to 15°C with temperature increased by 1°C each 60 min, quagga mussels acclimated to 20°C with temperature increased by 1°C each 60 min, and zebra mussels acclimated to 20°C with temperature increased by 1°C each 15 min) the SM_{100} is very close to the predicted LT_{100} (Table 3). This is because there was no gradual transition between 100% survival and 100% mortality at two observation points (no mortality observed at 34°C and complete mortality observed at 35°C, for instance). This phenomenon, termed complete or quasicomplete sample separation, occurs when the predictors perfectly fit the data (temperature of observation exactly predicts when 100% mortality will occur in these three cases). Quasicomplete sample separation resulted from the small sample size (10 mussels in each observation) and lack of replication (Bryson and Johnson 1981; see

Table 6. Matrix of differences between mean survival times of *D. bugensis* and *D. polymorpha* (corrected by Fisher's LSD to maintain overall α = 0.05) of each salinity treatment.

Treatment (°C–‰)	Mean survival time (days)	Treatment (°C–‰)							
		5–5	5–10	5–20	15–5	15–10	15–20	20–5	20–10
5–5	5.3	x	—	—	—	—	—	—	—
5–10	5.9	ns	x	—	—	—	—	—	—
5–20	4.7	ns	*	x	—	—	—	—	—
15–5	4.4	ns	**	ns	x	—	—	—	—
15–10	3.6	**	**	**	*	x	—	—	—
15–20	2.7	**	**	**	**	**	x	—	—
20–5	2.8	**	**	**	**	**	ns	x	—
20–10	2.1	**	**	**	**	**	**	**	x
20–20	1.2	**	**	**	**	**	**	**	**

Note: Because there was no significant difference between species, both species have been pooled within temperature × salinity treatments here. ns, no significant difference in survival times ($p > 0.05$); *, significant difference between treatments ($0.01 < p < 0.05$); **, highly significant difference between treatments ($p < 0.01$).

Fig. 3. Effect of test temperature on natural log transformed mean survival time per treatment of both *Dreissena* species (pooled because there is not significant difference in response between the species; $p > 0.05$) in salinity. Error bars are ±1 SE.

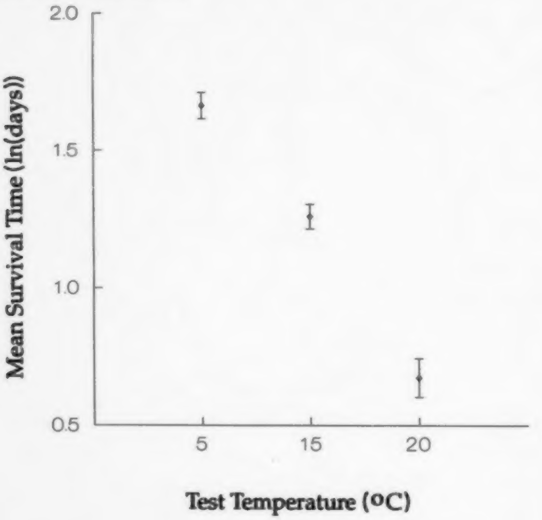

also Hosmer and Lemeshow 1989). Because the predicted LT_{50} values for those cases follow the trend observed in the other 21 cases (quagga mussels reasonably lower than zebra mussels), these estimates still seem reasonable.

Zebra mussel LT_{50} values predicted using the current model (Table 2) are within a degree of that predicted from the models of McMahon et al. (1993) in all cases but two. First, the predicted LT_{50} values of zebra mussels acclimated to 5°C were as much as 2°C higher in the current model than in that of McMahon et al. (see Table 3). This result is still well within the range of variation one might expect from comparisons across laboratories of animals collected in different places at different times. Second, no mortality was observed in this study for zebra mussels acclimated to 20°C tested with the temperature increasing 1°C every 5 min in the range 30–39°C, while McMahon et al. (1993) reported complete mortality within that temperature range. The quagga mussels tested under these conditions also followed the observed trend, never reaching 100% mortality (Table 3). Our two other tests of zebra mussels at temperature increases of 1°C every 5 min produced very similar results to those of McMahon et al. (1993), as did our three other tests of zebra mussels acclimated to 20°C.

The response of the zebra mussel to acute temperature change reported here follows similar trends to those reported previously, with increasing acclimation temperature resulting in increased survival time at lethal temperature levels (Iwanyzki and McCauley 1993). The sole exception to this trend occurred when Iwanyzki and McCauley (1993) found that mussels acclimated to 2.5°C and exposed to 30°C water had the longest mean survival time. This exception suggests that acclimation temperature does not have a linear effect on tolerance to thermal stress in *Dreissena* spp. Our results differ from those of Iwanyzki and McCauley (1993) in that they observed complete mortality in zebra mussels previously acclimated to 5, 15, and 20°C maintained at 30°C for 14 days and we observed none at all. A possible explanation for this difference is that in our experiments the temperature was raised gradually (1°C/h) to the test temperature whereas Iwanyzki and McCauley (1993) transferred the mussels directly from the acclimation to the test baths, resulting in instantaneous temperature change. The current results do correspond with those of McMahon et al. (1994) who also found that zebra mussels could be indefinitely maintained at 30°C regardless of acclimation temperature.

The quagga mussel was found to have lower LT_{50} values than the zebra mussel throughout the range from 30 to 39°C. However, both species can tolerate short-term exposure (a few hours) to temperatures that would be lethal if experienced for an entire day. While the quagga mussel is in general more likely to die from pulses of warm water than the zebra mussel (Table 2), both species are more tolerant of temperature stress if acclimated to higher temperatures (15 or 20°C). Quagga mussels acclimated to 5°C were particularly vulnerable to thermal stress (see Fig. 1). These results suggest that thermal back-flushing treatments which successfully control zebra mussel infestation of water intakes will be equally effective in controlling the quagga mussel.

A brief discussion of the relative merits of different methods of testing upper thermal tolerance in molluscs is appropriate. Stirling (1982) demonstrated that gradually raising the temperature from acclimation levels to lethal levels will overestimate the acute lethal temperature relative to that determined by exposing a mollusc directly to a lethal temperature. Part of this effect could be due to temperature acclimation during temperature increase, as pointed out by Domm et al. (1993), and the remainder is due to the confounding factor of time, as pointed out by Fraenkel (1960, 1968). Our analysis did not discriminate fully between the effect of acute lethal temperature and the cumulative effect of time spent at elevated sublethal but potentially stressful temperatures until the final lethal temperature was reached. Nonetheless, our experimental design does match what mussels would experience in intake pipes or in smaller bodies of water that may change temperature rapidly.

Temperature stress may explain the failure of the quagga mussel to colonize the inland waterways of New York State. The initial discovery of the quagga mussel was based on a single individual from the Eric Canal near Palmyra, New York (May and Marsden 1992). Individual quagga mussels were found in the midst of large zebra mussel populations from several sites in the Erie Canal and the outlet from Onondaga Lake (New York) in 1991 (Mills et al. 1993). However, no quagga mussels have been found outside lakes Erie and Ontario since the fall 1991 field season. While the quagga mussel may be able to hitchhike toward inland waters on boats, it will not survive there unless it finds a thermal refuge that will not reach 30°C. Our inability to maintain quagga mussels at 25°C for further testing (see Methods) suggests that the thermal maximum of the quagga mussel is even lower than could be tested during the experiments reported here.

No significant differences were found between the two species of *Dreissena* in terms of mortality rate in the presence of salinity. Zebra and quagga mussels could not tolerate NaCl alone in concentrations of 5‰ or greater. Prior acclimation to low levels of salinity (<2‰) has been suggested to mitigate the effect of sudden salinity changes, as were implemented in the first 3 days of the current salinity experiment, on respiration in *D. polymorpha* (Karpevich 1947). Karpevich's results also showed that mussels acclimated to fresh water and plunged into a salinity of 5‰, as in the current experiments, experienced no change in respiration. All of the freshwater mussels we plunged into salinities of 5‰ or greater died, a much more extreme response than cutting hourly respiration by 66% as Karpevich observed when plunging the mussels into salinities as high as 20‰ (see Fig. 4 in Strayer and Smith 1993). The extent of difference between the response observed here (complete mortality) and that reported by Karpevich (depressed respiration) suggests a drastically different conditioning regime for the animals that were tested, Karpevich's Caspian populations and ours from Lake Erie.

Fig. 4. Effect of salinity (‰) on natural log transformed mean survival time per treatment of both *Dreissena* species (pooled because there is no significant difference in response between the species; $p > 0.05$). Error bars are ±1 SE.

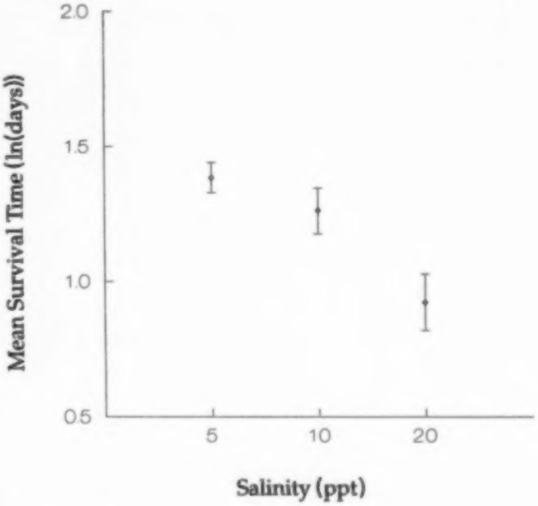

Whether an increase in the amount of divalent ions would have enabled the mussels to tolerate salinity levels of 5, 10, or 20‰ needs to be examined further (see Strayer and Smith 1993; Dietz et al. 1994). The data reported here do not provide a basis to evaluate the hypothesis that constant salinity is more bearable than variable salinity to the zebra mussel (suggested by Strayer and Smith 1993). The mussels tested here experienced salinity changes of 5‰/day for 1 or 2 days, followed by a further 10‰ if tested at 20‰ (see Methods). Mussels treated with the least variation in salinity (5‰) survived the longest but still experienced complete mortality in spite of evidence that they shouldn't even have experienced respiratory distress (Karpevich 1947). One recent study did show 100% mortality of *D. polymorpha* in <2‰ NaCl (Horohov et al. 1992). Predictions of the range expansion of *D. polymorpha* through tidal estuaries on the basis of a limit of 2‰ salinity appear reasonable (Strayer and Smith 1993). The current results suggest that zebra and quagga mussels certainly cannot be expected to survive in tidal areas with salinity greater than 5‰.

Expansion of the quagga mussel into water bodies beyond the Great Lakes is unlikely where summer temperatures exceed its upper thermal limit, which is <30°C according to our results. If attempts to acclimate *D. bugensis* to different temperatures are a guide, the upper thermal limit of the quagga mussel may be 25°C. A reasonable prediction is that *D. bugensis* will have a difficult time expanding its range toward inland waters in the absence of thermal refugia. The current results suggest that these two related bivalves are distinct in terms of physiological response to temperature if not salinity. These differences should be taken into account when formulating control mechanisms or predicting the spread of these aquatic nuisances through North America. However, it is important to retain the distinction between upper lethal temperature and predictors of success in the natural environment. Definitive predictions of the final range of *D. bugensis* and *D. polymorpha* await studies of the relative abilities of each species to successfully reproduce and grow through the range of environments they may encounter throughout the Great Lakes basin and the rest of North America. The relative performance (growth and spawning ability), not just mortality, of *D. bugensis* and *D. polymorpha* at low temperatures will be of particular interest.

Acknowledgments

E.F. Roseman, the crew of the R/V *Kahoe*, and the Lake Ontario Biological Station of the National Biological Service collected mussels in Lake Ontario, and R. Zimar, the crew of the R/V *Argos*, and the Dunkirk office of the New York Department of Environmental Conservation collected mussels in Lake Erie. L. Alexander provided laboratory assistance while supported by a Cornell Field Station summer internship. G. Churchill and S. Schwager provided statistical advice. C.C. Krueger and two anonymous reviewers provided helpful comments on an earlier draft of the manuscript. This research was funded in part by Central Hudson Gas and Electric, Consolidated Edison, the Monroe County Water Authority, the New York Sea Grant Institute, New York State Electric and Gas, and Rochester Gas and Electric.

References

Broekhuysen, G.J. 1940. A preliminary investigation of the importance of dessication, temperature and salinity as factors controlling the vertical distribution of certain intertidal marine gastropods in False Bay, South Africa. Trans. R. Soc. S. Afr. 28: 255–292.

Bryson, M.C., and M.E. Johnson. 1981. The incidence of monotone likelihood in the Cox model. Technometrics, 23: 381–384.

Dermott, R.M., and M. Munawar. 1993. The invasion of Lake Erie offshore sediments by *Dreissena*, and its ecological implications. Can. J. Fish. Aquat. Sci. 50: 2298–2304.

Dietz, T.H., D. Lessard, H. Silverman, and J.W. Lynn. 1994. Osmoregulation in *Dreissena polymorpha*: the importance of Na, Cl, K, and particularly Mg. Biol. Bull. (Woods Hole), 187: 76–83.

Domm, S., R.W. McCauley, E. Cott, and J.D. Ackerman. 1993. Physiological and taxonomic separation of two dreissenid mussels in the Laurentian Great Lakes. Can. J. Fish. Aquat. Sci. 50: 2294–2297.

Fisher, R.A. 1966. The design of experiments. 8th ed. Hafner Publishing Co., New York.

Fraenkel, G. 1960. Lethal high temperatures for three marine invertebrates: *Limulus polyphemus*, *Littorina littorea* and *Pagurus longicarpus*. Oikos, 11: 171–182.

Fraenkel, G. 1968. The heat resistance of intertidal snails at Bimini, Bahamas; Ocean Springs, Mississippi; and Woods Hole, Massachusetts. Physiol. Zool. 41: 1–13.

Horohov, J., H. Silverman, J.W. Lynn, and T.H. Dietz. 1992. Ion transport in the freshwater zebra mussel, *Dreissena polymorpha*. Biol. Bull. (Woods Hole), 183: 297–393.

Hosmer, D.W., and S. Lemeshow. 1989. Applied logistic regression. John Wiley & Sons, New York.

Iwanyzki, S., and R.W. McCauley. 1993. Upper lethal temperatures of adult zebra mussels (*Dreissena polymorpha*). *In* Zebra mussels: biology, impacts, and control. *Edited by* T.F. Nalepa and D.W. Schloesser. Lewis Press, Boca Raton, Fla. pp. 667–673.

Karpevich, A.F. 1947. The adaptability of metabolism in north Caspian mussels (genus *Dreissena*) to variations in salinity regime. (*In Russian*.) Zool. Zh. 26: 331–338. (Cited in Strayer and Smith 1993.)

May, B., and J.E. Marsden. 1992. Genetic identification and implications of another invasive species of dreissenid mussel in the Great Lakes. Can. J. Fish. Aquat. Sci. 49: 1501–1506.

McMahon, R.F. 1990. The zebra mussel: U.S. utility implications. Electric Power Research Institute, Palo Alto, Calif.

McMahon, R.F., T.A. Ussery, A.C. Miller, and B.S. Payne. 1993. Thermal tolerance in zebra mussels (*Dreissena polymorpha*) relative to rate of temperature increase and acclimation temperature. *In* Proceedings of the 3rd International Zebra Mussel Conference, Toronto, Ont., February 1993. *Edited by* J.L. Tsou and Y.G. Mussalli. EPRI TR-102077. Electric Power Research Institute, Palo Alto, Calif. pp. 4-96 – 4-118.

McMahon, R.F., M.A. Matthews, T.A. Ussery, R. Chase, M. Clarke, and T.H. Dietz. 1994. Further studies of heat tolerance in zebra mussels: effect of temperature acclimation and chronic exposure to lethal temperatures. *In* Proceedings of the 4th International Zebra Mussel Conference, Madison, Wis., March 7–10, 1994. *Edited by* A.H. Miller and C. Kraft. University of Wisconsin Sea Grant Institute, Madison, Wis. pp. 251–272.

Mills, E.L., R.M. Dermott, E.F. Roseman, D. Dustin, E. Mellina, D.B. Conn, and A.P. Spidle. 1993. Colonization, ecology, and population structure of the quagga mussel (Bivalvia: Dreissenidae) in the lower Great Lakes. Can. J. Fish. Aquat. Sci. 50: 2305–2314.

Nalepa, T.F., and D.W. Schloesser. (*Editors*). 1993. Zebra mussels: biology, impacts, and control. Lewis Press, Boca Raton, Fla.

Ott, L. 1988. An introduction to statistical methods and data analysis. 3rd ed. PWS-Kent Publishing Co., Boston, Mass.

Pligin, Y.V. 1984. Extension of the distribution of *Dreissena bugensis*. Malacol. Rev. 17: 143–144. (Abstr.)

Ramcharan, C.W., D.K. Padilla, and S.I. Dodson. 1992*a*. A multivariate model for predicting population fluctuations of *Dreissena polymorpha* in North American lakes. Can. J. Fish. Aquat. Sci. 49: 150–158.

Ramcharan, C.W., D.K. Padilla, and S.I. Dodson. 1992*b*. Models to predict potential occurrence and density of the zebra mussel, *Dreissena polymorpha*. Can. J. Fish. Aquat. Sci. 49: 2611–2620.

Rosenberg, G., and M.L. Ludyanskiy. 1994. A review of Russian species concepts of *Dreissena*, with identification of the quagga mussel as *Dreissena bugensis* (Bivalvia: Dreissenidae). Can. J. Fish. Aquat. Sci. 51: 1474–1484.

Schneider, D. 1992. A bioenergetics model of zebra mussel growth in the Great Lakes. Can. J. Fish. Aquat. Sci. 49: 1406–1416.

Spidle, A.P., J.E. Marsden, and B. May. 1994. Identification of the Great Lakes quagga mussel as *Dreissena bugensis* from the Dnieper River, Ukraine, on the basis of allozyme variation. Can. J. Fish. Aquat. Sci. 51: 1485–1489.

Steinberg, D., and P. Colla. 1991. LOGIT: a supplementary module for SYSTAT. SYSTAT, Inc., Evanston, Ill.

Stirling, H.P. 1982. The upper temperature tolerance of prosobranch gastropods of rocky shores at Hong Kong and Dar Es Salaam, Tanzania. J. Exp. Mar. Biol. Ecol. 63: 133–144.

Strayer, D.L. 1991. Projected distribution of the zebra mussel, *Dreissena polymorpha*, in North America. Can. J. Fish. Aquat. Sci. 48: 1389–1395.

Strayer, D.L., and L.C. Smith. 1993. Distribution of the zebra mussel (*Dreissena polymorpha*) in estuaries and brackish water. *In* Zebra mussels: biology, impacts, and control. *Edited by* T.F. Nalepa and D.W. Schloesser. Lewis Press, Boca Raton, Fla. pp. 715–728.

Wilkinson, L. 1992. SYSTAT for Windows: statistics, version 5 edition. SYSTAT, Inc., Evanston, Ill.

Zhadin, V.I. 1952. Molluscs of fresh and brackish waters of the U.S.S.R. Academy of Sciences of the U.S.S.R., Moscow. (Translated from Russian by Israel Program for Scientific Translations, Jerusalem. 1965.)

Influence of log additions on physical and biotic characteristics of a mountain stream

J. Bruce Wallace, Jackson R. Webster, and Judith L. Meyer

Abstract: Three pairs of cobble riffle study sites were established in a second-order stream in North Carolina and logs added to the downstream riffle at each site. At log addition transects, stream depth increased, current velocity decreased, cobble substratum was covered by sand and silt, and both coarse and fine particulate organic matter increased dramatically. Log additions had less dramatic effects on uptake lengths of ammonium, nitrate, and phosphate, but they had immediate and significant impacts on invertebrate community structure: abundances and biomass of scrapers and filterers decreased; collectors and predators increased; overall shredder biomass did not change, but biomass of trichopteran and dipteran shredders increased, while that of most plecopteran shredders decreased; and plecopteran predators also decreased despite greater abundances of potential prey. These observations suggest that physiological and morpho-behavioral constraints preclude many animals from tracking resources among patches when patches display very different abiotic conditions. Secondary production of scrapers and filterers decreased, whereas that of collectors and predators increased. The shifts in functional group abundances, biomass, and production between reference and debris-dam transects, which differed considerably from those previously reported for low-gradient, sandy-bottom streams, accentuate the importance of localized abiotic factors in structuring invertebrate communities within patches.

Résumé : Trois paires de sites d'étude constitués par des radiers de cailloux ont été établies dans un ruisseau de second ordre en Caroline du Nord, et des billots ont été placés dans le radier d'aval à chaque site. Aux transects où étaient installés les billots, la profondeur du ruisseau a augmenté, la vitesse du courant a diminué, et le substrat de cailloux s'est recouvert de sable et de limon; en outre, la quantité de particules de matières organiques fines et grossières a augmenté de façon spectaculaire. La mise en place de billots a eu des effets moins importants sur la durée d'absorption de l'ammonium, des nitrates et des phosphates, mais une incidence immédiate majeure sur la structure de la communauté d'invertébrés : l'abondance et la biomasse des organismes racleurs et filtreurs ont diminué, tandis que la quantité d'organismes collecteurs et prédateurs a augmenté; la biomasse totale des organismes broyeurs n'a pas changé, mais celle des organismes broyeurs de l'ordre des trichoptères et des diptères a augmenté alors que celle de la plupart des organismes broyeurs de l'ordre des plécoptères a diminué; le nombre de prédateurs de l'ordre des plécoptères a diminué également malgré une abondance accrue de proies éventuelles. Ces observations laissent supposer que des contraintes sur le plan physiologique et morpho-comportemental empêchent de nombreux animaux de suivre les ressources d'une parcelle à l'autre lorsque les conditions abiotiques qui y prévalent sont très différentes. La production secondaire des organismes racleurs et filtreurs a diminué, alors que celle des organismes collecteurs et prédateurs a augmenté. Les changements dans l'abondance, la biomasse et la production des groupes fonctionnels entre les transects témoins et les transects où l'on a installé un barrage de revenue de débris, qui diffèrent considérablement de ceux qui ont été signalés pour des cours d'eau de faible pente à fond sableux, mettent en relief l'importance de facteurs abiotiques localisés dans la composition des communautés d'invertébrés à l'intérieur des parcelles.

[Traduit par la Rédaction]

Received February 3, 1995. Accepted April 28, 1995.
J12753

J.B. Wallace.[1] Departments of Entomology and Ecology, University of Georgia, Athens, GA 30602, U.S.A.
J.R. Webster. Department of Biology, Virginia Polytechnic Institute and State University, Blacksburg, VA 24061, U.S.A.
J.L. Meyer. Department of Ecology, University of Georgia, Athens, GA 30602, U.S.A.

[1] Author to whom all correspondence should be addressed.

Can. J. Fish. Aquat. Sci. **52**: 2120–2137 (1995). Printed in Canada / Imprimé au Canada

Introduction

In streams, large woody debris influences a wide array of abiotic features as well as biotic community structure and function (Harmon et al. 1986). The diverse effects of woody debris in streams include the following: formation of stair-step profiles that result in rapid dissipation of stream energy in high gradient systems (Heede 1972; Bilby and Likens 1980; Smith et al. 1993*b*); increased stream depth and lower current velocities, which increase transit time through a reach (Trotter 1990; Gregory 1992); and increased retention of particulate inorganic and organic matter (e.g., Bilby and Likens 1980; Mosley 1981; Speaker et al. 1984; Smock et al. 1989; Trotter 1990; Smith et al. 1993*a*). All of these factors may influence both trophic and nutrient dynamics of stream ecosystems (e.g., Bilby 1981; Molles 1982; Newbold et al. 1982; Melillo et al. 1983; Webster and Swank 1985).

Especially in mountain streams, large woody debris may be the principal factor determining characteristics of aquatic habitats (Swanson and Lienkaemper 1978). Woody debris influences biotic structure by providing habitat for fish (Triska and Cromack 1980; Sedell et al. 1982; Angermeier and Karr 1984) and substrate for invertebrates (Nilson and Larimore 1973; Anderson et al. 1978; Keller and Swanson 1979; Cudney and Wallace 1980; Benke et al. 1984; Wallace and Benke 1984; Smock et al. 1985). Molles (1982) observed differences in functional structure of trichopteran communities and organic matter storage among streams draining climax and successional forest. He attributed these differences to the greater abundance of debris dams in streams draining mature forests. In Buzzards Branch, a low-gradient headwater stream of the southeastern Coastal Plain, Smock et al. (1989) found much greater organic matter storage at debris dams than in other areas. Also, abundances, biomass, and secondary production of most invertebrates were much higher at debris dams in these low-gradient streams (Smock et al. 1989; Roeding and Smock 1989; Smock et al. 1992).

In small, high-gradient streams of the southern Appalachians, abundances (Gurtz and Wallace 1984) and production and biomass (Huryn and Wallace 1987*a*; Lugthart and Wallace 1992) of various taxa and functional feeding groups of invertebrates vary greatly between erosional and depositional habitats. For example, pools have lower current velocity, smaller substrate particle sizes, and greater storage of particulate organic matter (POM) than cobble riffle habitats (Huryn and Wallace 1987*a*). Biomass and production of a number of invertebrates, including most shredders, collector–gatherers, and predators were greater in pools, whereas riffles supported greater biomass and production of filterers and scrapers (Huryn and Wallace 1987*a*). Since depositional or pool habitats in these streams are primarily found upstream of large woody debris (Huryn and Wallace 1987*a*), inputs of large woody debris can apparently induce major changes in biotic communities in southern Appalachian streams. To experimentally test some of our previous descriptive results relating to different community structure at debris-dam pools compared with cobble riffles, we performed an experimental manipulation by adding logs to cobble riffles.

The overall objectives of this study were to examine changes in physical characteristics and the biotic community of a southern Appalachian stream induced by a series of log additions to cobble riffles. Specifically, we address the following questions: (*i*) What physical changes occur in cobble riffle habitats following log additions? (*ii*) How comparable is POM storage in manipulated and unmanipulated riffles? (*iii*) How comparable are uptake rates of ammonium, nitrate and phosphate in reaches with and without added logs? and (*iv*) How comparable is invertebrate community structure in terms of abundances, biomass, and production, in manipulated and unmanipulated riffles?

Study site

This study was conducted at the United States Forest Service's Coweeta Hydrologic Laboratory in the Blue Ridge Province of the southern Appalachians in Macon County, North Carolina, U.S.A. Forest vegetation is characterized as mixed hardwoods, with riparian vegetation consisting of occasional hemlocks (*Tsuga caroliniana* Englemann) and a dense understory of rosebay rhododendron (*Rhododendron maximum* L.), which results in heavy year-round shading of the stream. The stream channel consists primarily of cobble-sized substratum with localized areas of boulder and bedrock outcrop as well as a few depositional areas.

Three stations, draining areas of ca. 46 (station I) to ca. 90 ha (station III), were established along a 0.8 km reach of Cunningham Creek. Successive stations were separated from others by a distance of ca. 400 m. Elevations range from 914 (station I) to 865 m a.s.l. (station III) and the stream has an average gradient of ca. 0.06 m/m, though the gradients at the three stations are 0.03, 0.03, and 0.04 m/m. The uppermost station is ca. 75 m downstream of catchment 32, a 42-ha long-term reference catchment. Catchment 32 has remained undisturbed since 1927, as has the remainder of the drainage of the three stations. Over the 4-year study period, annual temperature averaged 11.1°C (4052 annual degree days) with a range of 0.2–17.5°C. The average diel temperature flux was 1.1°C (range = 0.2–4.5°C; data from a recording thermistor).

Maximum daily discharge measurements at the weir of catchment 32 averaged 23.5 $L \cdot s^{-1}$ (Fig. 1). During the study, maximum daily discharge ranged from 4.1 (30 October 1988) to 294 $L \cdot s^{-1}$ (16 February 1990). Annual discharge ranged from 319 550 m^3 in 1988 (the second lowest year of 59-year record) to 714 355 m^3 in 1990. During the pretreatment period, discharge at the time of sampling averaged 9.7 $L \cdot s^{-1}$ compared with 25.2 $L \cdot s^{-1}$ during the treatment period.

Similar to other streams draining the Blue Ridge or crystalline Appalachians, Cunningham Creek has low ionic concentrations of biologically important elements: K, 0.30; Ca, 0.48; Mg, 0.28; nitrate-N, 0.002; ammonium-N, 0.002; and phosphate-P, 0.001 $mg \cdot L^{-1}$ (Swank and Waide 1988).

Methods

Log additions

Permanent stakes (1/2-in. rebar) were placed at 2-m intervals for 18–20 m along the banks of the stream at each station. In July 1986, prior to log addition, we used these

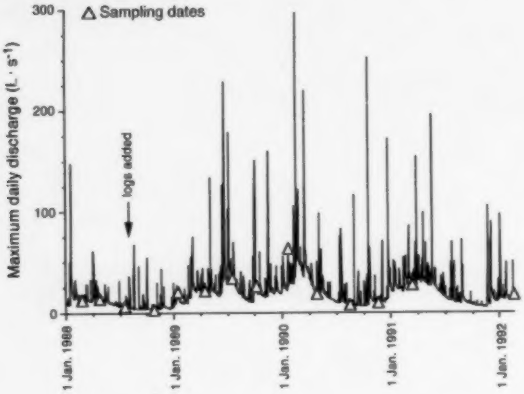

Fig. 1. Maximum daily discharge for Cunningham Creek during the study period as measured at Coweeta watershed 32 about 75 m upstream of station I. The open triangles denote the benthic sampling dates. Note the extremely low discharges during 1988 compared with later periods (data from Coweeta Data Files of the U.S. Forest Service).

stakes to establish 10 permanent cross sections at stations I and II and 11 cross sections at station III. The exact location of each cross section was determined with a transit, and elevations were measured with a stadia rod and Dumpy level at 20-cm intervals along each cross section. After addition of logs, elevations along each cross section were remeasured in July 1988, July 1991, and June 1992. Additionally, in June 1994 we measured elevation every 20 cm along the thalweg. The thalweg was determined from the lowest point on each cross section from the 1986 measurements.

In late July 1988, a log of tulip poplar, *Liriodendron tulipifera*, ranging from 20 to 32 cm in diameter, was placed in approximately the center of each of three stations. These logs spanned the stream from bank to bank and were oriented perpendicular to flow. They were anchored with stakes, rocks, or existing tree trunks.

Measuring nutrient uptake

Nutrient uptake lengths were measured at reference and treatment sites before and after log addition using previously established field procedures (Munn and Meyer 1990) and calculations (Stream Solute Workshop 1990). We measured ammonium uptake on three dates (June 1988; July 1989; and August 1993), nitrate uptake on four dates (July and August 1987; July 1989; and August 1993), and phosphate uptake on five dates (July and August 1987; June 1988; July 1989; and August 1993).

Concentrated solutions of ammonium chloride, sodium nitrate, sodium phosphate, and sodium chloride were dripped into the stream in each reference section and about 15 m above each log addition site. Chloride concentrations were elevated to 5–15 $mg \cdot L^{-1}$, ammonium concentrations to 10–20 $\mu g\ N \cdot L^{-1}$, nitrate concentrations to 10–15 $\mu g\ N \cdot L^{-1}$, and phosphate concentrations to 5–12 $\mu g\ P \cdot L^{-1}$. We began addition experiments at the reach furthest downstream and progressed to upstream reaches. After allowing concentrations to stabilize for 40 min, samples were taken at 10-min intervals for 40 min from sites 0, 5, 10, 15, and 20 m downstream from a point 1 m below the dripper. Samples were filtered immediately, kept cold, and returned to the laboratory for analysis.

Ammonium nitrogen was analyzed using a Technicon Autoanalyzer II from 1987 to 1989 and an Alpchem Analyzer in 1993 using standard methods (American Public Health Association 1985). Chloride was analyzed with a Technicon Autoanalyzer II from 1987 to 1989 using standard methods (American Public Health Association 1985); in 1993 chloride was measured continuously during the release with an ion-specific electrode (Orion model 290A). Phosphate was determined spectrophotometrically using the ammonium molybdate reaction (Murphy and Riley 1962).

After correcting measured concentrations for dilution using chloride concentrations and subtracting pre-addition nutrient concentrations, the negative log of the ratio of concentration at each point – initial concentration was plotted versus distance downstream. The inverse of the slope of the line fitted to those points is the uptake length, which is the distance travelled by the average molecule before it is removed from the water column (Stream Solute Workshop 1990). Changes in nutrient uptake length with treatment were examined using ANOVA on log-transformed pretreatment and posttreatment data from reference reaches and those to which logs had been added. Scheffé analyses were considered significant at $P < 0.05$.

Invertebrate sampling

At each station, we established two invertebrate sampling transects, a reference transect in a riffle at the upstream end of the station and a debris-dam transect 0.5–1.0 m upstream of the log addition site. Water depths at 15–20 cm intervals and wetted-width measurements were made prior to sampling at each transect. Current velocity was measured at three to four locations across each transect using a Gessner bag meter (Gessner 1950). For each benthic sample, a visual estimate of the percent substrate composition by particle size was made using a modified Wentworth scale (Cummins 1962).

On 14 April 1994, a series of bottom shear stress measurements were made at debris-dam ($N = 15$) and reference transects ($N = 17$) using FST hemispheres (Statzner and Müller 1989) (KC maskin og laboratorieudstyr, Holmbladsvej 17, DK-8600 Silkeborg, Denmark) and expressed as $dyn \cdot cm^{-2}$ (1 dyn = 10 μN) using data provided by Statzner et al. (1991). These bottom shear stress measurements were made during a period of relatively high flows (48.8 $L \cdot s^{-1}$).

Three Surber samples (0.24-mm mesh) were taken on each transect in February, April, July (before log addition), and October 1988 (after log addition). During sampling, substrates were disturbed to a depth of ca. 10 cm. In January 1989, increased water depth and reduced velocities at the debris-dam transects resulted in conditions that were unsuitable for Surber sampling. Instead, three 400-cm^2 core samples were taken for subsequent samples (January, April, July, and October 1989; January, April, August, and

November 1990; March 1991; and February 1992) at debris-dam transects. At the reference riffles, Surber samples were taken throughout the study duration on the same dates.

For core samples, materials within the sampler were excavated to a depth of ca. 10 cm and placed in a large pail. Contents of the pail were elutriated (6–8×) by pouring the stirred contents through a 0.24-mm mesh net to standardize mesh sizes between the Surber and core samples. Elutriated material, which included organic and fine inorganic material and invertebrates, was preserved in a 6–8% formalin solution containing Phloxine B dye to facilitate sorting. Surber samples were preserved in an identical manner.

In the laboratory, organic matter, invertebrates, and remaining inorganic matter were washed through a series of nested 1-mm and 0.25-mm sieves. After animals were removed from the 1-mm sieve, coarse particulate organic matter (CPOM, ≥1 mm diameter) was separated into leaf, wood, and miscellaneous (e.g., seeds, cones, flowers, moss) categories, dried (60°C, 5 days), weighed, ashed (490°C, 12 h), and reweighed to obtain ash free dry mass (AFDM). Fine particulate organic matter (FPOM, <1 mm >0.25 mm), the material remaining on the 0.25-mm sieve, was placed in a graduated bucket with a known volume of water, stirred, and subsampled (ca. 1% of volume removed with a graduated syringe). The remainder of the sample was concentrated on a 0.25-mm sieve and preserved for later sorting of small invertebrates. The FPOM subsamples were filtered through pre-ashed and pre-weighed glass fiber filters (Gelman A/E), oven dried (60°C for 5 days), weighed, ashed (490°C for 2–4 h), and reweighed to obtain AFDM. This procedure does not account for FPOM <0.25 mm in diameter; therefore, our estimates of FPOM standing crops are conservative. This is especially true for core samplers at debris-dam transects, as very turbid water was observed passing through the net during field elutriation.

All invertebrates on the 1-mm sieve were removed by hand sorting using a stereo microscope at 15× magnification. Small invertebrates in the <1-mm >0.25-mm size fraction were subsampled (1/8th to 1/64th of whole sample) using a sample splitter (Waters 1969) and hand sorted using a stereo microscope at 15× magnification. Identifications of most insect taxa were to genus or species. Throughout the study Chironomidae were identified as either Tanypodinae (predators) or non-Tanypodinae (collectors). Chironomids from station II (both debris-dam and reference transects) were identified to generic or specific levels during pretreatment (February, April, and July 1988) and initial stages of treatment (October 1988; January, April, and July 1989) to ascertain any large-scale changes in taxa occuring as a result of debris-dam additions. Non-insect invertebrates were identified to the ordinal level or higher. The body lengths of all specimens were measured to the nearest millimetre using 10–15× magnification and a graduated stage or ocular micrometer. For *Cambarus* (crayfish) carapace lengths were measured. Biomass of Nematoda, Hydracarina, Copepoda, Cladocera, and Ostracoda were based on average weights of >50 individuals obtained from nearby streams (Huryn 1986; Lugthart 1991). For other taxa, biomass was obtained from length–weight regressions derived from various studies in Coweeta streams (Huryn 1986, and A.D. Huryn, unpublished data; G.J. Lugthart and J.B. Wallace, unpublished data), or from the study by Smock (1980) using a 0.85× factor for dry mass to AFDM conversion. Production of most taxa at each site was estimated using mean biomass of each taxon × known production/biomass (P/B) ratios that have been published for nearby streams at Coweeta (Huryn and Wallace 1987*a*; Huryn and Wallace 1987*b*; Lugthart and Wallace 1992) or other Coweeta data (L. Houston and J.B. Wallace, unpublished data). Production of collector chironomid taxa was measured using the community-level method of Huryn (1990).

Invertebrates were assigned to functional feeding groups, i.e., scrapers, shredders, collector–gatherers (collectors), collector–filterers (filterers), and predators. Most follow the designation of Merritt and Cummins (1984) or our own observations based on Coweeta fauna. Although crayfish (*Cambarus bartonii*) abundances are low, the crayfish contribute significantly to invertebrate biomass because of their large size, and these omnivores may perform several functional roles (Momot et al. 1978) including predators, collectors, and shredders (Huryn and Wallace 1987*b*). Furthermore, Surber and core sample sizes are probably inadequate to sample these large omnivores. Crayfish biomass was analyzed separately; however, for production and P/B estimates of various functional feeding groups, *Cambarus* biomass was included and equally apportioned among shredder, collector, and predator functional groups.

Organic matter, invertebrate abundances, and biomass of the three samples at each transect on each date were pooled for all statistical analyses. The relationships between the means and variances of untransformed abundances and biomass of common taxa of invertebrates was highly significant ($P < 0.001$); therefore, a $\log_{10}(x + 1)$ transformation was applied to all invertebrate data prior to statistical analyses. Analyses of variance followed by a Sheffé multiple range test was applied to functional feeding group abundances and biomass. Groups in ANOVA and discussions that follow are identified as follows: R-P, reference transects before log addition; DD-P, debris-dam transects prior to log additions; R-T, reference transects following log additions; and DD-T, debris-dam transects after log addition. Comparisons of biomass for various taxa between reference and debris-dam transects were made with a two-tailed, paired *t* test. Sheffé and *t*-test analyses were considered significant at $P < 0.05$. Substrate percent composition was arcsine–square root transformed prior to statistical analyses (Zar 1984).

Results

The data we have provided here are the elevations of the streambed along the thalweg from 1986 and 1994 measurements (Fig. 2).

Immediately after putting logs in the stream, small pools formed upstream. Over the next few months, these pools deepened as leaves and sediment accumulated and prevented water from going under the logs. Over several years, there was significant accumulation of fine sediments upstream of each log, though we noticed that much of the

Fig. 2. Elevation profiles along the thalweg of the stream at each station. Measurements were made before (1986) and after (1994) log addition.

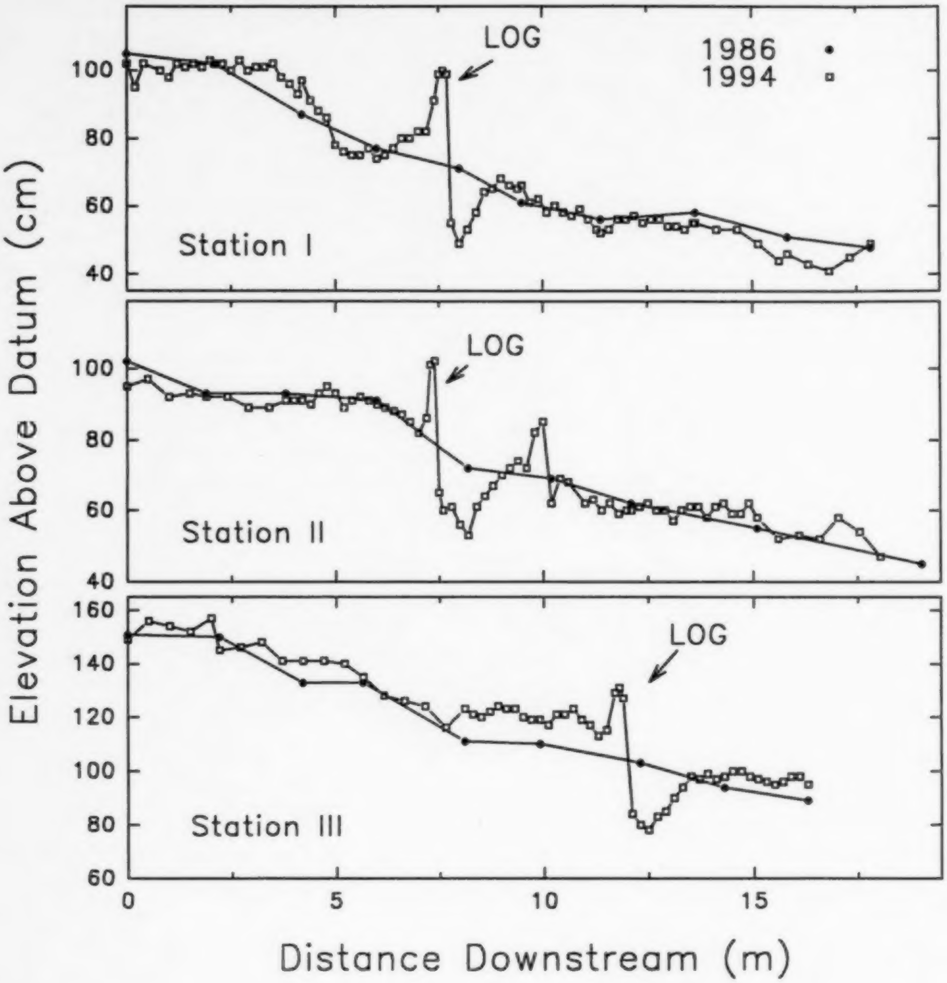

surficial fine sediments were washed out during storms. At station I and especially at station III, there was also slow accumulation of larger bed material in the pools (Fig. 2). However, this was not evident at station II where the stream was constrained between two large trees opposite each other, which we had used to anchor the added log. Downstream plunge pool formation was very evident below each log (Fig. 2). At each station there was a 20- to 30-cm deepening of the streambed immediately below the log and an accumulation of bed material 1–2 m downstream.

Average velocity ($cm \cdot s^{-1}$) did not differ significantly among stations before log additions (Table 1). After log additions, discharge was much greater than during the pretreatment period and average velocities at reference transects were significantly greater; however, velocities at debris-dam transects were significantly lower, as depth and wetted width increased significantly following log additions (Table 1, Fig. 3). The proportion of surface substratum composed of cobble-, pebble-, and gravel-sized particles decreased significantly at debris-dam transects after log addition, and sand and silt increased sharply as the habitat shifted from erosional to depositional substratum.

Bottom shear stress measurements at debris-dam transects ranged from 0.828 to 2.72 $dyn \cdot cm^{-2}$ during April 1994 (mean = 1.666 ± 0.218 (95% CI)). On the same date, shear stress of reference transects ranged from 5.29 to 44.8 $dyn \cdot cm^{-2}$ (mean = 14.086 ± 5.449 $dyn \cdot cm^{-2}$).

Enhanced retention upstream from debris dams resulted in large increases of standing crop for all types of POM compared with pretreatment and reference transects after log addition (Table 2 and Fig. 4). There were no significant differences in organic matter standing crop between debris-dam and reference transects prior to log additions or between reference sites prior to and following log additions, whereas

Table 1. Average current velocity, mean depth, wetted width, and percent surface substratum consisting of cobble, pebble, gravel, sand, and silt measured at each sampling site on each date.

	N	Velocity (cm·s^{-1})	Depth (cm)	Wetted width (m)	% cobble	% pebble	% gravel	% sand and silt
R-P	9	37±10*a*	5±1*a*	2.3±0.6*ab*	54±14*a*	18±6*a*	15±4*a*	13±4*a*
DD-P	9	32±7*a*	5±2*a*	2.2±0.7*a*	56±8*a*	16±5*a*	13±6*a*	15±5*a*
R-T	33	54±16*b*	6±2*a*	2.6±0.9*ab*	69±8*b*	15±4*a*	9±3*a*	7±3*a*
DD-T	33	14±4*c*	13±5*b*	3.0±0.8*b*	3±9*c*	2±4*b*	4±6*b*	91±12*b*
*P**		0.0001	0.0001	0.02	0.0001	0.0001	0.0001	0.0001

Note: Values represent means ± 1 SD at reference (R) and debris-dam transects (DD) before (−P) and after log additions (−T) to DD. Differences among mean values are indicated by different letters (Sheffé multiple range test, $P \le 0.05$), *N*, number of samples. Substratum percentages were arcsine transformed for analyses.

*From one-way analysis of variance.

Fig. 3. Average stream velocity, depth, percent cobble, and percent sand and silt at reference and debris-dam sites on each sampling date. Arrows indicate the time of log additions to debris-dam sites.

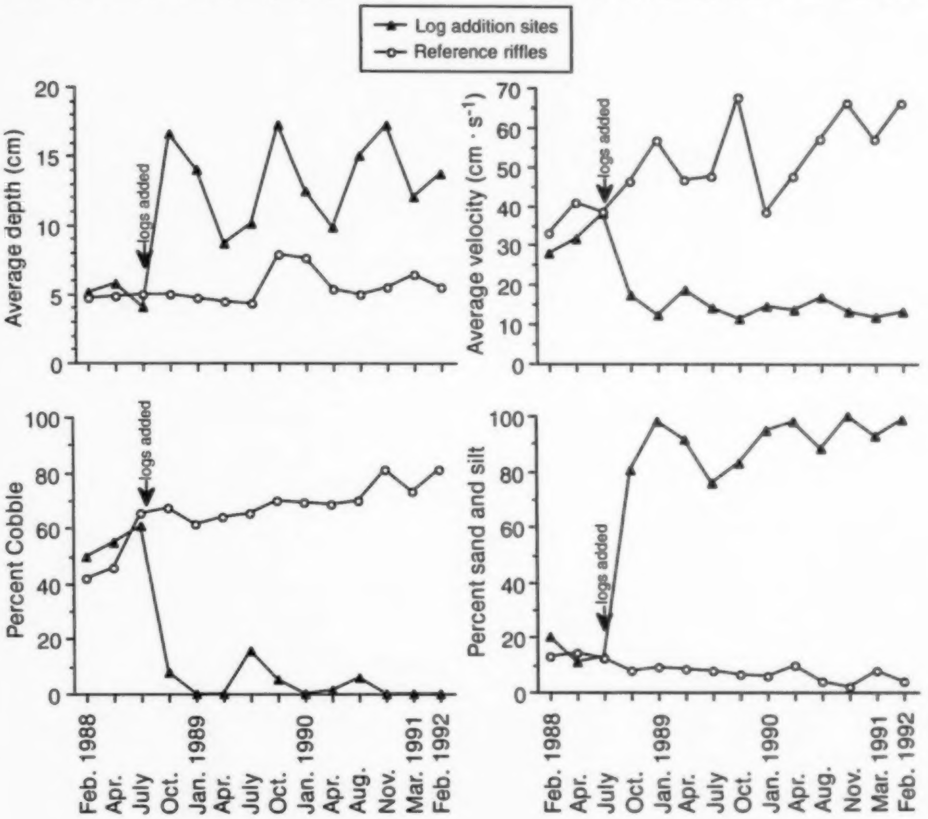

leaf detritus, small woody litter, miscellaneous organic matter, and FPOM increased greatly ($P < 0.0001$, ANOVA) at debris-dam transects following log additions. The increase in POM occurred during the first 3–6 months following log additions (Fig. 4), and all classes of POM remained higher at debris-dam transects throughout the remainder of the study.

In late February 1990, Cunningham Creek experienced the greatest discharge recorded during the 5-year period (297 L·s^{-1}). The summer of 1989 was the wettest on record

Table 2. Organic matter standing crop (g $AFDM \cdot m^{-2}$) (mean ± 1 SD) at reference transects (R) and debris-dam transects (DD) before (−P) and after (−T) log addition to DD.

	N	Leaf standing crop	Small woody debris	Miscellaneous organic matter	FPOM	Total organic matter
R-P	9	46±49*a*	65±54*a*	35±39*a*	20±16*a*	166±103*a*
DD-P	9	19±7*a*	28±16*a*	27±17*a*	15±7*a*	88±23*a*
R-T	33	71±67*a*	54±49*a*	31±22*a*	16±16*a*	171±122*a*
DD-T	33	332±309*b*	315±226*b*	494±411*b*	427±332*b*	1568±952*b*
*P**		0.0001	0.0001	0.0001	0.0001	0.0001

Note: Differences among mean values are indicated by different letters (Sheffé multiple range test, $P \leq 0.05$); *N*, number of samples. Miscellaneous organic matter consisted of flowers, seeds, cones, and materials of unknown origin >1 mm diameter; FPOM, fine particulate organic matter <1 mm diameter.

*From one-way analysis of variance.

Table 3. Uptake lengths (m) for ammonium, nitrate, and phosphate at reference riffles (R) and log addition sites (DD) before (−P) and after (−T) log addition in 20-m reaches of stream that included the reference or log-added sections.

	Ammonium	Nitrate	Phosphate
R-P	3.7±1.2 (3)*a*	137±38 (6)*ab*	81±21 (9)*a*
DD-P	3.3±1.4 (3)*a*	874±760 (6)*a*	128±60 (9)*a*
R-T	20.5±6.8 (6)*a*	24±11 (6)*bd*	67±35 (6)*a*
DD-T	24.7±5.8 (6)*b*	16±3 (6)*cd*	27±7 (7)*a*

Note: Values reported are means ± standard error (*N*). Differences among mean values are indicated by different letters (Sheffé test on log-transformed data).

at Coweeta, and two storms (228 and 178 $L \cdot s^{-1}$, peak discharge) occurred 29 and 12 days prior to benthic sampling in July 1989 (Fig. 1). The sharp depressions in POM standing crop in the summer of 1989 and spring of 1990 were probably due to scouring during these extreme discharges prior to sampling.

Nutrient uptake

Measured uptake lengths were highly variable for all nutrients (Table 3). Uptake lengths for ammonium were significantly longer after log addition in the reaches to which logs were added (Table 3). Longer uptake length indicates slower nutrient uptake rates. Uptake lengths for nitrate were significantly shorter after log addition. Shorter nutrient uptake length indicates more rapid nutrient uptake rates. Mean phosphate uptake length after log addition was not statistically different. Although the direction of change was the same in reference and debris-dam reaches for all three nutrients, uptake lengths were not significantly different pre- and post-treatment in the reference section. Hence the log addition increased the uptake length for ammonium, decreased it for nitrate, and did not change it for phosphate.

Invertebrates

Total invertebrate abundances did not differ significantly among transects before log additions (Table 4). Abundances in reference transects after log addition were significantly greater (2.4×) than those of reference and debris-dam transects prior to treatment (Table 4). Invertebrate abundances were significantly greater at debris-dam transects after log addition than those of other sites and periods. Abundances at log-addition transects were 24× those prior to log addition and, following log addition, exceeded those of reference riffles by >8×.

Invertebrate biomass in the reference transects was 1.8× greater during the log addition period than prior to log addition; however, the difference in biomass among reference transects before and after log addition were not significant. Following log additions, biomass at debris-dam transects was significantly greater than before log addition (Table 4). Although biomass of several functional feeding groups exhibited dramatic changes at debris-dam transects following log additions, total biomass was not significantly different.

Among noninsect taxa, excluding crayfish, biomass was significantly higher at debris-dam transects (Table 5). Although biomass of Odonata was >4× greater at debris dams than any other site, differences were not significant. Dipterans were the only group of insects that displayed a significant increase at log-addition transects. In contrast, biomass of Ephemeroptera, Plecoptera, Coleoptera, and Trichoptera was significantly lower at debris dams than at reference transects following log addition. However, many taxa within these orders displayed distinctly different responses to the manipulation (see below).

Functional feeding groups

Abundances of scrapers decreased significantly at debris-dam transects following log addition (Table 4 and Fig. 5), whereas they increased by ca. 2× above pretreatment levels at reference transects. Following log addition, scraper

Fig. 4. Average particulate organic matter (POM) standing crop for leaf detritus, small woody debris, miscellaneous (flowers, seeds, cones, and materials of unknown origin) coarse particulate organic matter (CPOM, ≥1 mm diameter), total CPOM (leaf detritus + small woody debris + miscellaneous organic matter), fine particulate organic matter (FPOM, ≤1 mm diameter), and total POM (CPOM + FPOM) at reference sites and debris-dam sites on each sampling date. Arrows indicate the time of log additions to debris-dam sites.

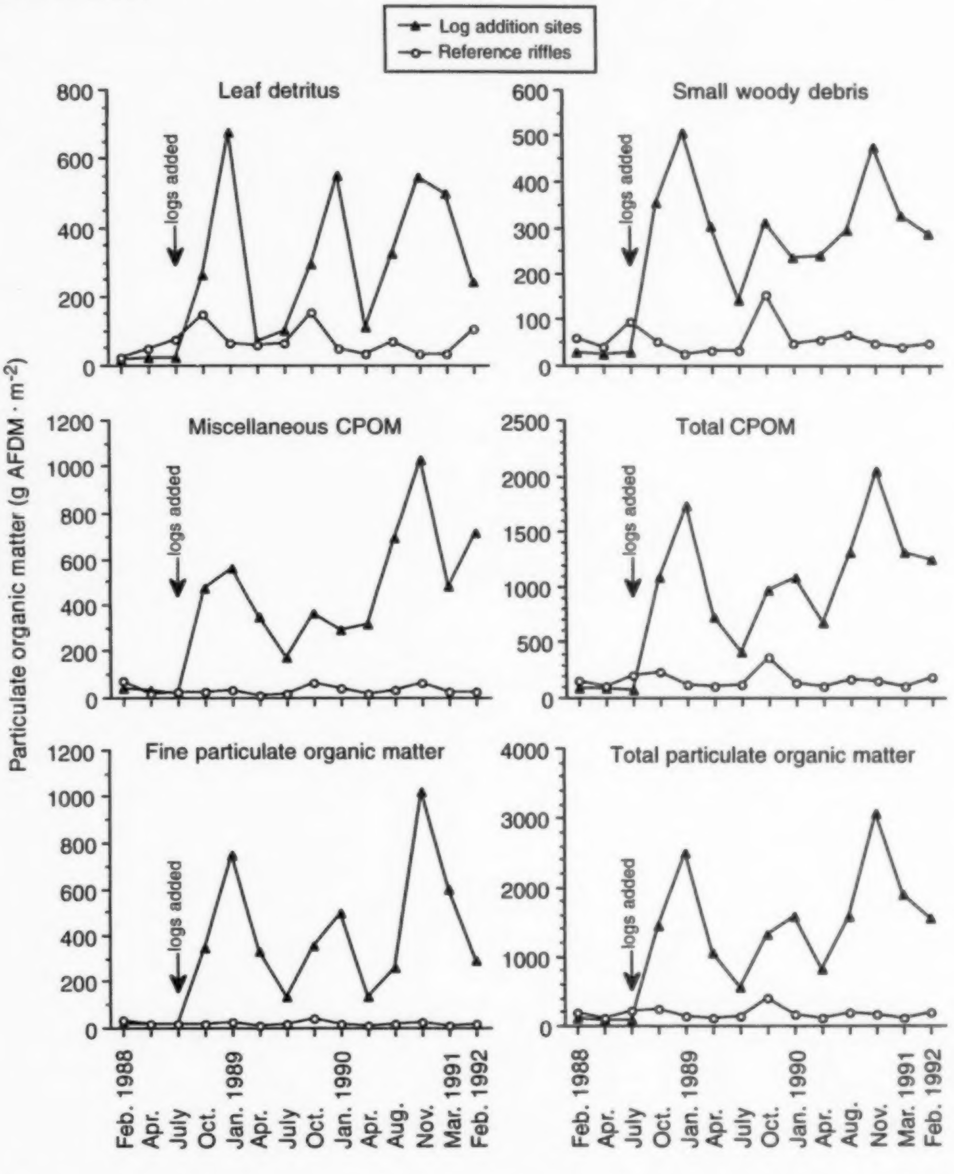

abundances were significantly greater (Table 4) in reference transects where they exceeded those of debris-dam transects by 3.4×. Biomass of scrapers did not differ among untreated riffle transects (DD-P, R-P, and R-T); however, scraper biomass at log-addition transects was lower (Table 4 and Fig. 6). Nine taxa of scrapers exhibited significantly lower biomass at debris-dam transects than reference transects following log addition, and no scraper taxon exhibited increased biomass at debris-dam transects (Table 6). Scraper biomass at debris-dam transects declined sharply by the January 1989 sampling date and remained low throughout the study (Fig. 6).

Total shredder abundances did not differ significantly between debris-dam and reference transects following log

Table 4 . Functional group standing stock abundances (individuals·m^{-2}) and biomass (mg AFDM·m^{-2}) (mean ± 1 SD) at reference (R) and debris-dam transects (DD) before (−P) and after (−T) log addition to DD.

	N	Scrapers	Shredders	Collectors	Filterers	Predators	Total animals
				Abundance			
R-P	9	448±248*ab*	1272±802*ab*	3149±2405*a*	406±203*a*	823±362*a*	6098±3810*a*
DD-P	9	442±191*ab*	835±373*a*	2641±1094*a*	382±399*a*	697±323*a*	4998±1986*a*
R-T	33	922±394*b*	2076±1401*ab*	8400±4422*b*	772±429*a*	2370±1332*b*	14541±6179*b*
DD-T	33	272±349*c*	3951±5067*b*	110296±67538*c*	112±175*b*	5858±2982*c*	120496±70875*c*
*P**		0.0001	0.02	0.0001	0.0001	0.0001	0.0001
				Biomass			
R-P	9	112±29*a*	230±228*a*	165±268*ab*	148±95*a*	177±217*ab*	832±607*ab*
DD-P	9	126±47*a*	454±1043*a*	68±43*a*	82±53*a*	69±48*b*	798±1093*a*
R-T	33	209±88*a*	594±897*a*	210±277*b*	257±178*a*	304±399*ac*	1573±1299*bc*
DD-T	33	38±52*b*	513±719*a*	591±325*c*	20±54*b*	516±385*c*	1678±1023*c*
*P**		0.0001	0.03	0.0001	0.0001	0.0001	0.0002

Note: Differences among mean values are based on log transformed values and indicated by different letters (Sheffé multiple range test, $P \le 0.05$); *N*, number of samples.

*From one-way analysis of variance.

Table 5. Standing stock biomass (mg AFDM·m^{-2}) (mean ± 1 SD) of major insect groups and noninsects (w/o crayfish) at reference transects (R) and debris-dam transects (DD) before (−P) and after (−T) log addition to DD.

	N	Non-insects	Odonata	Ephemeroptera	Plecoptera	Coleoptera	Trichoptera	Diptera
R-P	9	110±244*ab*	11±17*a*	122±45*a*	371±357*ac*	103±64*ab*	132±118*ab*	51±34*a*
DD-P	9	15±14*a*	7±11*a*	111±46*a*	479±1081*ab*	103±54*ab*	75±46*ab*	50±30*ab*
R-T	33	196±479*b*	28±38*a*	217±91*a*	701±918*c*	167±122*a*	244±217*a*	116±103*b*
DD-T	33	343±227*c*	117±181*a*	94±168*b*	97±64*b*	71±141*b*	225±666*b*	771±492*c*
*P**		0.0001	0.04	0.0001	0.0001	0.0001	0.004	0.0001

Note: Differences among mean values are based on log transformed values and indicated by different letters (Sheffé multiple range test, $P \le 0.05$); *N*, number of samples.

*From one-way analysis of variance.

addition, and biomass did not differ among transects or treatment periods (Table 4). Although abundances of shredders increased 1.6× at reference transects after log addition and over 4.7× at debris dams following log addition, only the debris-dam increase was significantly different from pretreatment (Table 4). Abundances of shredders exhibited greater fluctuations at debris dams than reference transects following log additions (Fig. 5). The large variations in shredder biomass during the first year after log additions are primarily attributed to *Pteronarcys* spp. at reference transects and trichopteran and dipteran shredders at debris-dam transects (Fig. 6).

Despite little difference in total shredder biomass, individual taxa of shredders exhibited many changes (Table 6). Biomass of trichopteran and dipteran shredders increased sharply at debris-dam transects following log additions. However, with the exception of *Leuctra* spp., biomass of plecopteran shredders decreased at debris-dam transects

Fig. 5. Average abundances of invertebrate functional feeding groups (scrapers, shredders, collectors, filterers, predators, and total abundances) at reference and debris-dam sites on each sampling date. Arrows indicate the time of log additions to debris-dam sites.

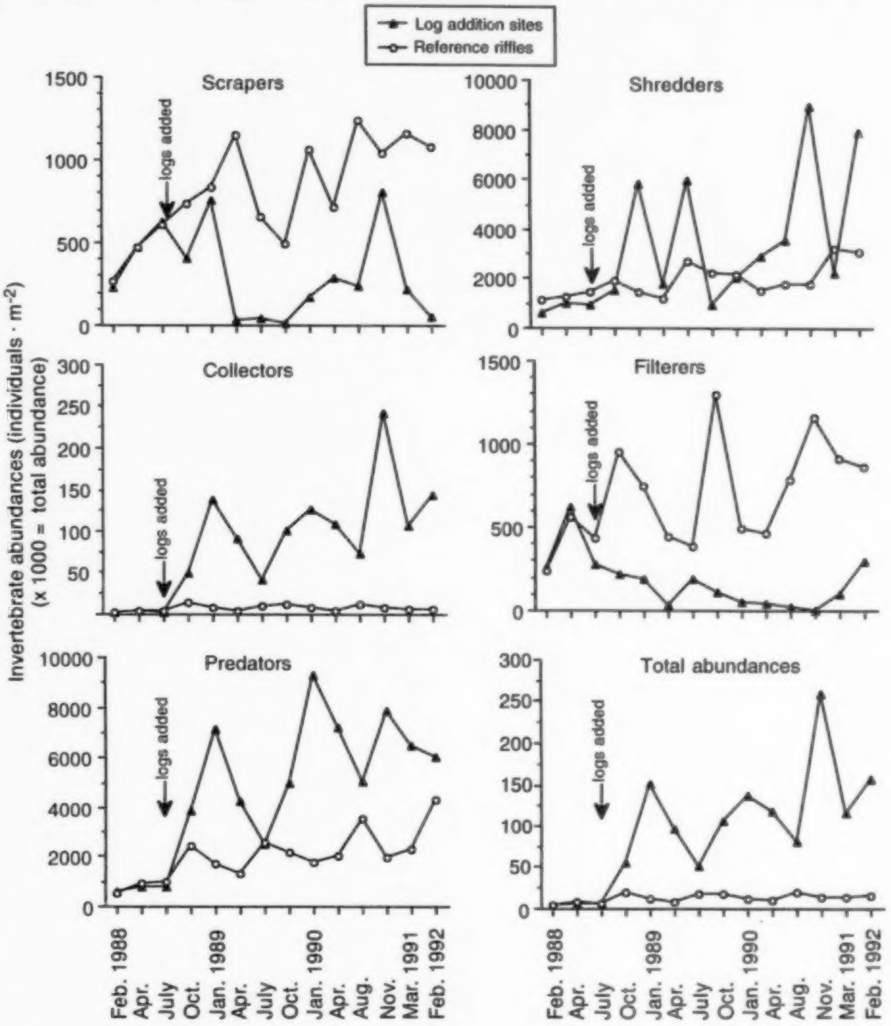

despite increased resource availability (Fig. 7). Plecopteran shredder biomass (y) decreased at debris-dam sites despite the presence of greater CPOM resources ($y = 3.555 - 0.552X$, $r^2 = 0.187$, $n = 66$, $P = 0.0003$), whereas trichopteran and dipteran shredder biomass displayed a stong positive association with CPOM resources ($y = -3.524 + 2.01X$, $r^2 = 0.774$, $n = 66$, $P < 0.0001$) and increased at debris dams (Fig. 7).

Collector abundance and biomass was much greater at debris-dam than reference transects following log addition ($P < 0.05$, Table 4). Although abundance of collectors increased significantly at both reference and debris-dam transects after log addition, the magnitude of increase was greater for debris-dam (>41×) than reference transects (2.7×). The change in collector biomass was much lower than that for abundance (Table 4). The increase in collector biomass at all sites during the last four collection dates (Fig. 6) is primarily attributable to large oligochaetes.

As observed for other functional groups, individual taxa of collectors exhibited diverse changes following log additions. Some mayfly collectors declined at debris-dam transects, e.g., members of the genera *Serratella* and *Paraleptophlebia*, while others, e.g., members of the genera *Ephemera* and *Habrophlebia*, increased (Table 6). Noninsects (e.g., Nematoda, Oligochaeta, Cladocera, Copepoda) and some dipteran collectors, e.g., collector chironomids, exhibited large increases in biomass at debris dams (Table 6).

Filterer abundance and biomass declined significantly at debris-dam transects following log addition (Table 4;

Fig. 6. Average standing stock biomass of invertebrate functional feeding groups and total invertebrate biomass at reference and debris-dam sites on each sampling date. Note crayfish biomass is not included in these data (see text). Arrows indicate the time of log additions to debris-dam sites.

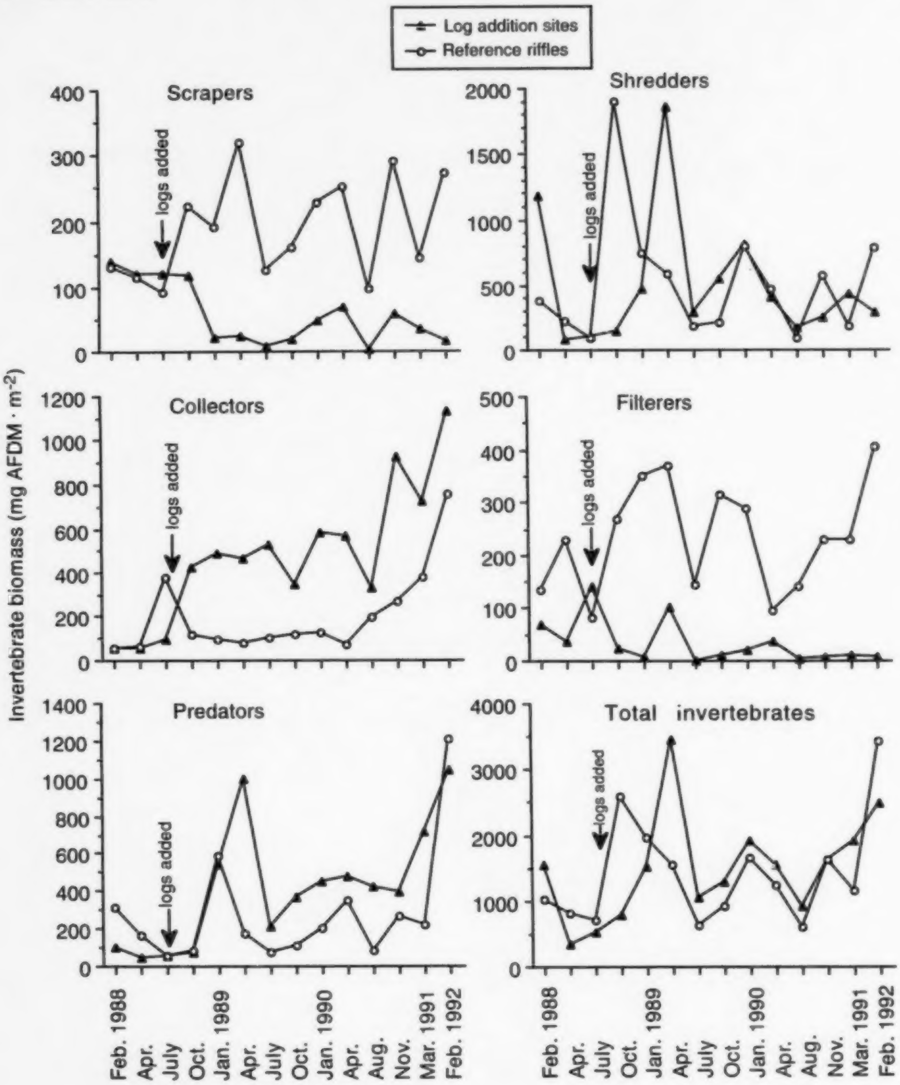

Figs. 5 and 6). Total filterer biomass was less than 10% of that of reference transects (Fig. 6 and Table 4). Unlike other functional groups, no filterer taxon exhibited increased biomass at debris dams relative to reference transects. In contrast, six of eight filterer taxa exhibited strong decreases in biomass at debris dams relative to reference transects ($P < 0.001$, Table 6).

Predator abundance was significantly greater following log addition at reference (2.9×) and debris-dam transects (8.6×) than before log additions ($P < 0.05$, Table 4 and Fig. 5). Additionally, predator abundance in debris-dam transects was significantly greater than in reference transects after log addition (Table 4 and Fig. 5). Despite greater abundances at debris dams, total predator biomass did not differ significantly from that of reference transects (Table 4 and Fig. 6). Predator biomass did not differ significantly before and after log additions at reference transects; however, debris-dam predator biomass was significantly greater than before log additions (Table 4).

Predator taxa exhibiting significantly lower biomass at debris dams after log addition compared with reference transects included Turbellaria, several plecopterans, and

Table 6. Taxa that showed significant decreases or increases, ($P < 0.05$) or no significant changes ($P > 0.05$), in standing stock biomass at debris-dam transects relative to reference transects following log addition at debris-dam transects on the basis of a paired t test of log (x + 1) standing stock biomass (N = 33).

	Scrapers	Shredders	Collectors	Filterers	Predators
Decreasing taxa	*Epeorus* (E)* *Stenonema* (E)* *Baetis* (E)* *Drunella* (E) *Ectopria* (C)* Elmidae (adults) (C)* *Optioservus* (larvae) (C)* *Oulimnius* (larvae) (C) *Neophylax* (T)	*Pteronarcys* (P) Peltoperlidae (P)* *Taeniopteryx* (P)	*Serratella* (E)* *Paraleptophlebia* (E) *Nemoura* (P)* *Amphinemura* (P)*	*Isonychia* (E) *Dolophilodes* (T)* *Wormaldia* (T)* *Diplectrona* (T)* *Parapsyche* (T)* *Simulium* (D)*	Turbellaria *Malerikus* (P)* *Isoperla* (P)* *Beloneuria* (P)* *Rhyacophila* (T)*
Increasing taxa	None	*Leuctra* (P) *Lepidostoma* (T)* *Pycnopsyche* (T)* *Fattigia* (T)* *Molophilus* (D)* *Tipula* (D)*	Nematoda* Oligochaeta* Cladocera* Copepoda* *Ephemera* (E) *Habrophlebia* (E)* C-G Chironomidae (D)* Sciaridae (D)	None	Ceratopogonidae (D)* Chironomidae (Tanypodinae)* *Pseudolimnophila* (D)* *Rhabdomastix* (D) *Hexatoma* (D)* Empididae (D)
No significant change	*Glossosoma* (T)	*Anchytarsus* (C)	*Ameletus* (E) *Lype* (T)	*Polycentropus* (T) *Dixa* (D)	Hydracarina *Cordulegaster* (O) *Lanthus* (O) *Alloperla* (P) *Sweltsa* (P) *Molanna* (T) *Dicranota* (D)

Note: Taxa with an * displayed highly significant ($P < 0.001$) differences in biomass among treatment and reference transects. None of the taxa listed displayed significant differences in standing stock biomass between treatment and reference riffles prior to log addition ($P > 0.05$, N = 9). Insect orders are as follows: (C), Coleoptera; (D), Diptera; (E), Ephemeroptera; (O), Odonata; (P), Plecoptera; and (T), Trichoptera.

Rhyacophila spp. (Trichoptera) (Table 6). In contrast, many dipteran predators displayed much greater biomass at debris-dam than at reference transects ($P < 0.001$, Table 6). Dipteran predators, especially Ceratopogonidae and Tanypodinae, were primarily responsible for the rapid increase in predator abundance following log additions (Fig. 5). Odonata and chloroperlid stoneflies, as well as some trichopteran and dipteran predators, exhibited no significant changes in biomass at debris dams (Table 6).

Because of their overwhelming abundance, collectors dictated total invertebrate abundances at all sites (Fig. 5). Sharp increases in abundances at debris-dam sites occurred within 6 months of log addition (winter 1989), when dams were first sealed with organic and inorganic debris. In contrast, total biomass of invertebrates during the first three seasons following log additions was erratic (Fig. 6), reflecting that of large shredders (primarily *Pteronarcys* spp. at reference transects and *Pycnopsyche* and *Tipula* at debris dams).

Crayfish, *Cambarus bartonii*, constituted an important component of the biomass at all sites, comprising from 24% (542 mg AFDM·m^{-2} at DD-T) to 64% (1492 mg AFDM·m^{-2} at R-P) of total invertebrate biomass. Despite the large differences between reference and debris-dam transects, the variance associated with sampling was very high and the difference was not significant.

Secondary production

Secondary production, including crayfish, at reference and debris-dam transects ranged from 4.5 to 11.9 g AFDM·m^{-2}·yr^{-1}, which is within the range found for other Coweeta streams. Both reference and debris-dam transects had lower total production before log addition, coinciding with a period of relative drought (Table 7). At reference transects, production of all functional groups was greater after log addition. This increase coincided with a period of higher flow (Fig. 1 and Table 7). Following log addition, increase in production was greater at debris-dam transects (2.7×) than reference transects (1.8×).

The proportional distribution of production in reference transects was fairly even both before (from 11.9% for scrapers to 27.2% for collectors) and after (from 13.5% scrapers to 31.8% collectors) log addition. In contrast, that of debris-dam transects fluctuated widely between before (from 9.8% predators to 48.4% shredders) and after (from 1% filterers to 53% collectors) log additions. After log

Table 7. Secondary production and P/B ratios of functional feeding groups at reference (R) and debris-dam transects (DD) before (−P) and after (−T) log addition to DD.

Functional group	R-P	R-T	DD-P	DD-T
	Production (mg AFDM $m^{-2} \cdot yr^{-1}$)			
Scrapers	619 (11.9)	1244 (13.5)	649 (14.6)	172 (1.4)
Shredders	1349 (25.9)	2939 (31.8)	2105 (47.3)	3088 (25.9)
Collectors	1416 (27.2)	1843 (20.0)	709 (15.9)	6265 (52.6)
Filterers	986 (18.9)	1703 (18.4)	552 (12.4)	130 (1.1)
Predators	840 (16.1)	1503 (16.3)	438 (9.8)	2262 (19.0)
Total	5210	9233	4453	11918
	Production/biomass (P/B ratio)			
Scrapers	5.5	5.9	5.2	4.6
Shredders	1.9	2.7	2.8	4.5
Collectors	2.1	2.6	2.0	8.1
Filterers	6.6	6.6	6.8	6.6
Predators	1.2	1.9	1.2	3.2
Average (total)	2.2	3.0	2.7	5.4

Note: Percent of total secondary production at each site shown in parentheses. These data include crayfish, which were apportioned equally to shredder, collector, and predator groups.

Fig. 7. Plecopteran shredder biomass versus CPOM standing crop in individual samples and same for trichopteran and dipteran shredder biomass during the treatment period (October 1988 to February 1992).

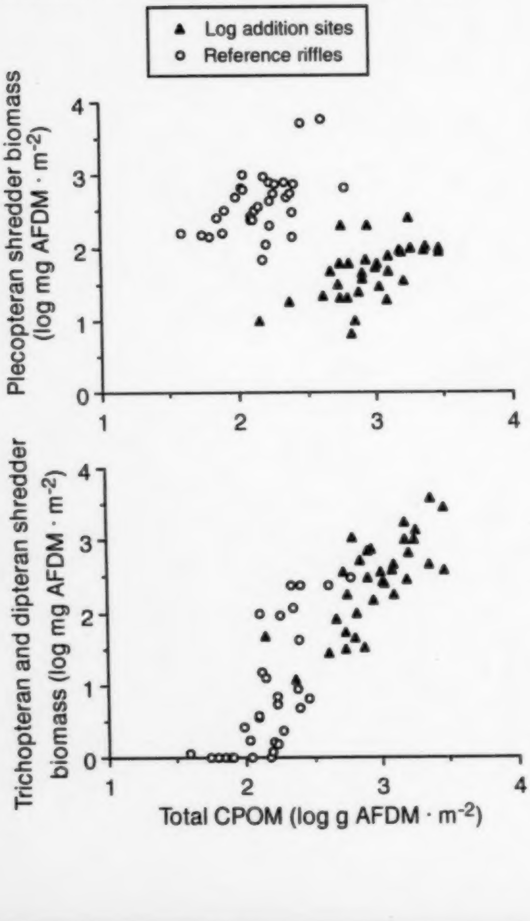

addition, scrapers and filterers exhibited strong declines in production at debris-dam transects (Table 7), whereas production of shredders increased (1.5×), as did that of predators (5.1×) and collectors (10.5×). Although crayfish contributed substantially to total invertebrate biomass at debris-dam and reference transects, their contribution to total production ranged from 2.6% (DD-T) to 16.6% (R-P). Following log addition, percent change in production of most functional groups at debris-dam transects was much greater than that of reference transects (Fig. 8).

Community P/B ratios displayed little change at reference transects before (2.2) and after (3.0) log addition, while those of debris dams increased from 2.7 to 5.4 during the corresponding period (Table 7). The greatest differences at the debris-dam transects were attributable to increases in P/B ratios for collector, predator, and shredder taxa. These changes in P/B reflect the altered community structure at debris addition sites.

Number of taxa

Prior to log addition, the average number of nonchironomid taxa collected on each date at log-addition sites (mean ($\bar{X}$) = 48) and reference riffles ($\bar{X}$ = 50) did not differ. However, following log addition, the average number of taxa collected at reference riffles increased, whereas that at debris-addition sites decreased. The reference riffles had significantly more taxa ($\bar{X}$ = 57) than log-addition sites ($\bar{X}$ = 42) when analyzed by sampling date (P = 0.03, paired (by date), two-tailed, t test).

A total of 35 chironomid taxa were found at station II reference and debris-dam transects between February 1988 and July 1989. The average number of chironomid taxa at debris-dam sites increased from 13 to 24 following log addition. Collector chironomids displaying the strongest increases in abundances at debris-dam transects were members of the genera *Corynoneura*, *Heleniella*, *Rheosmittia*, *Constempellina*, and *Stempellinella*. The only taxa displaying

Fig. 8. Percent change in annual secondary production for each functional group and total production from pretreatment to treatment (log additions to debris-dam riffles) for reference and debris-dam sites ((pretreatment − treatment) pretreatment × 100). Scr, scrapers; Shr, shredders; C-G, collector-gatherer (collectors); Filt, filterers; and Pred, predators. These data include crayfish whose production was assigned equally to shredder, collector, and predator functional groups.

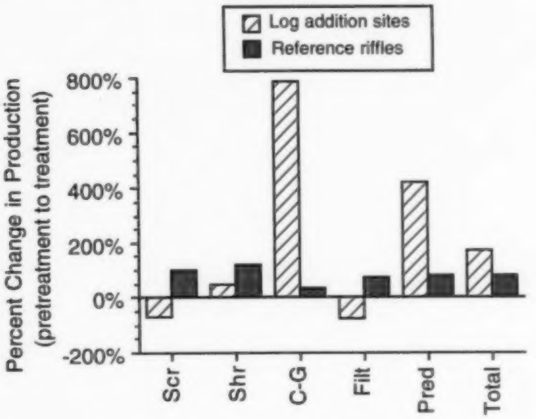

decreased abundances following log addition were members of the genera *Eukiefferiella*, *Microspectra*, *Microtendipes*, and *Rheotanytarsus*. Among the Tanypodinae, members of the genera *Brundiniella*, *Larsia*, and *Meropelopia* increased following log addition and no tanypodines exhibited decreased abundances at the debris-dam transects.

On the basis of only the presence or absence of nonchironomid taxa, the total number of taxa present at combined (log-addition + reference) sites increased from an average of 56 before treatment to 60 after treatment (t test, $P < 0.03$). In contrast, the number of nonchironomid taxa shared between reference and log-addition sites decreased from an average of 31 shared taxa before treatment to 23 after treatment (t test, $P < 0.002$) (Fig. 9). The nonshared taxa among sites before treatment were primarily attributed to relatively rare taxa that constituted a small proportion of total abundances. Furthermore, the percent shared taxa was negatively related to time after log addition, i.e., elapsed day (x) versus arcsine square root percent shared taxa (y), with the following equation: $y = 48.05 - 0.17x$, $r^2 = 0.70$, $P < 0.001$.

Functional groups and organic matter standing crops

Both abundances and biomass of scrapers and filterers were inversely related to POM standing crop (Table 8). Although shredder abundances showed a positive and significant relationship with both FPOM and total CPOM (including leaves, wood, and miscellaneous organic matter), organic matter standing crop explained a very small proportion of the shredder abundance, and no significant relationship existed between shredder biomass and FPOM or total CPOM. However, log-transformed shredder biomass was positively related to log-transformed leaf detritus ($r^2 = 0.18$, $N = 84$, $P = 0.0001$). The strongest relationships between functional groups and organic detritus were displayed by abundances of collectors and total invertebrates, which were dominated by collectors. Regressions of biomass of collectors and total invertebrates with particulate organic matter were significant but had consistently smaller coefficients of determination than for abundances (Table 8).

Fig. 9. Average number of nonchironomid taxa collected at combined sites (log-addition + reference sites = total taxa), the number of taxa common to both sites (shared taxa), and the percent shared to total taxa during pretreatment and first 2 years of treatment (log addition).

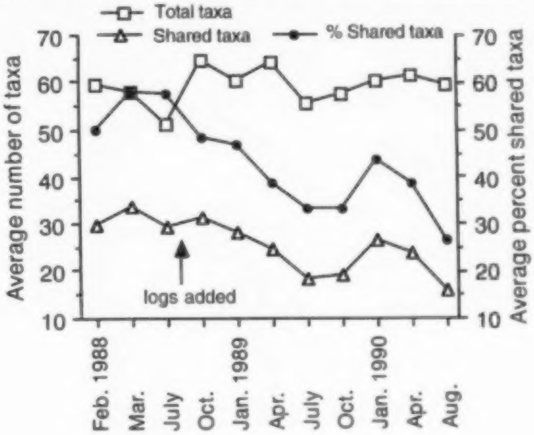

Discussion

Pringle et al. (1988) defined a patch as a spatial unit that is determined by the organism(s) and problem(s) in question. These authors noted that in streams many interacting factors (i.e., substratum conditions, topography, current velocity, organisms, and disturbance) influence patch formation. On the basis of all physical parameters measured in this study, as well as POM storage (Fig. 4), it is obvious that the addition of logs to riffle areas of Cunningham Creek changed riffles to depositional zones in a region upstream of the logs. Though bottom shear stress was measured only on one date during a period of relatively high flow following the study, average shear stress at riffle transects was ca. 9× greater than that of debris dams. Decreased current velocity, smaller substrate particle size, and enhanced storage of POM are all characteristic of depositional areas.

Webster et al. (1994) pointed out that the efficiency with which organic matter is used in a stream results from the balance between two antagonistic forces: biological conversion of organic carbon to CO_2 and physical downstream transport. The presence of woody debris dams clearly increases efficiency by decreasing transport. However, in this study the morphological characteristics of the stream associated with the logs also had important effects on the stream community, underscoring the strong influence of the physical template on biotic structure and function. For

Table 8. Coefficient of determination (r^2), probability values (P), and form (linear, logarithmic, and power regressions) obtained by regressing invertebrate functional group abundance and biomass (dependent variable) with grams of AFDM per square metre of fine particulate organic matter (FPOM) and coarse particulate organic matter (CPOM) standing crops (independent variable) in all samples (N = 84 for each).

	FPOM standing crop			CPOM standing crop		
Functional group	r^2	P	Form	r^2	P	Form
			Abundance			
Shredders	0.12	0.0015	Linear	0.14	0.004	Logarithmic
Collectors	0.76	0.0001	Linear	0.76	0.0001	Linear
Scrapers	0.28	0.0001	Power (−)	0.212	0.0001	Power (−)
Filterers	0.51	0.0001	Power (−)	0.37	0.0001	Power (−)
Predators	0.45	0.0001	Power	0.55	0.0001	Power
Total invertebrates	0.73	0.0001	Power	0.77	0.0001	Power
			Biomass			
Shredders	0.005	0.52	Linear	0.006	0.477	Logarithmic
Collectors	0.27	0.0001	Power	0.281	0.0001	Power
Scrapers	0.44	0.0001	Power (−)	0.43	0.0001	Power (−)
Filterers	0.53	0.0001	Power (−)	0.46	0.0001	Power (−)
Predators	0.11	0.003	Power	0.22	0.0001	Power
Total invertebrates	0.07	0.02	Power	0.16	0.0002	Power

Note: A (−) following form of regression indicates negative relationships or slopes.

example, the decline in scraper biomass at log-addition sites may be directly associated with the loss of suitable substrate as deposition associated with reduced current velocities obliterated cobble substrata.

Although shredder biomass exhibited no significant changes between reference transects and debris dams, there were massive changes of individual taxa of shredders (see below). Collectors, especially noninsects, some mayflies, and chironomids (Table 6), exhibited strong increases at debris dams, as did their FPOM food resources (Fig. 4). Filterers in Cunningham Creek are primarily passive and rely on sufficient current to support delivery of suspended food. As expected, filterer taxa displayed strong decreases in abundances at the lower current velocities that were associated with debris-dam transects. The only filterers that did not display a significant decrease were the trichopteran *Polycentropus* sp. and the dipteran *Dixa* sp. *Polycentropus* sp. is somewhat unusual in that it is known to inhabit lentic as well as lotic habitats by changing the form of their catchnet between these two extremes (Wiggins 1977). *Dixa* sp. uses mandibular brushes to generate currents for feeding at the surface film (Nowell 1951).

The changes in physical structure and organic matter storage associated with the addition of a debris dam had less of an impact on nutrient uptake rates than it did on the stream biota. Webster et al. (1991) also found few differences in nutrient uptake in streams draining Coweeta catchments with different disturbance histories, yet those streams differ in both organic matter storage and insect community composition. In our study, the absence of a dramatic effect is partly because of the way nutrient uptake was determined. We measured nutrient uptake over a 20-m reach of stream, yet the added log caused changes in channel structure and organic matter storage over only a 2–3 m section of that reach; hence log addition altered the characteristics of only 10–15% of the reach. Had the proportion of reach altered been greater, we would expect more dramatic effects. There is some observational evidence to support this: in Coweeta stream reaches where at least half of the reach is influenced by natural debris dams, uptake lengths for phosphate were consistently shorter than in reaches dominated by gravel substrate, although those differences were not observed for nitrate uptake length (Munn 1989).

Our results provide direct experimental evidence for some observational differences among cobble riffle and depositional substratum in a study of upper Ball Creek on catchment 27 at Coweeta (Huryn and Wallace 1987*a*). In catchment 27, cobble riffles had greater biomass of scrapers and filterers than depositional areas, whereas depositional areas had greater biomass of shredders, collectors, and predators. With the exception of shredders, these same patterns emerged as a result of log addition (Table 4). The failure of shredders to increase at debris-dam transects is primarily due to the presence of *Pteronarcys* spp., and their preference for riffle rather than debris-dam transects in Cunningham Creek. *Pteronarcys* spp. are absent in higher elevation streams such as upper Ball Creek (catchment 27). When the biomass of *Pteronarcys* spp. is excluded, insect shredder biomass at log-addition transects averaged 669 mg/m^2 compared with 415 mg/m^2 at reference transects following log addition. The only plecopteran shredders that did not decrease in debris-dam transects were *Leuctra* spp. (Table 6), and early instars of this stonefly have been designated as collectors rather than shredders (Dobson and Hildrew 1992). Huryn and Wallace (1987*a*) also found the biomass of *Leuctra* spp. was higher in depositional than riffle areas. Crayfish were another important factor in the failure of debris-dam transects to display increased shredder production. Although only one third of their biomass was assigned to the shredder functional group, their biomass was 2.7× greater at reference than debris-dam transects following log addition.

Our results for total shredders also differ considerably from that observed for debris dams in the low-gradient stream, Buzzards Branch, in the coastal plain of Virginia (Roeding and Smock 1989; Smock et al. 1992). These authors found a much higher shredder abundance, biomass, and production at debris dams than at sandy-stream sediments. However, plecopteran shredders were extremely rare in the sandy-bottom stream studied by Smock and his colleagues compared with the cobble-dominated substratum of Cunningham Creek. Most shredders that increased at debris dams in Buzzards Branch were trichopterans and dipterans, whose abundances and biomass also increased at debris dams in our study. The contrast in our results with those of Smock et al. (1992) underscores differences among ecoregions as well as local geomorphic setting and the need to explore invertebrate structure and function at debris dams in different geographical and geomorphic settings before predicting effects of environmental change. Even within the confines of the Coweeta Basin, differences would probably exist among elevational and stream-size gradients. In larger (4th-order and greater) lower elevation streams at Coweeta, *Pteronarcys* spp. dominate shredder biomass and production (L. Houston, J.W. Grubaugh, and J.B. Wallace, unpublished data). The addition of debris dams to these larger, lower-elevation sites might result in a community structure that differs considerably from that observed in Cunningham Creek, where *Pteronarcys* spp. are relatively uncommon.

Even within individual functional feeding groups, all organisms do not respond similarly to the rather distinct patch formed at debris dams. As a group, plecopteran shredders did not track the increased abundances of leaf litter at debris dams during treatment, as observed for trichopteran and dipteran shredders (Fig. 7). This may be related to differences in respiratory requirements of most Plecoptera, which require current velocities higher than those found at debris dams. In contrast, larval cases of trichopteran shredders are known to enhance respiration (Wiggins 1977), and dipteran shredders with posterior spiracles are known to migrate to the air–water interface to obtain oxygen. Most plecopterans belonging to other functional groups also declined in number at debris dams, despite greater abundances of food resources (FPOM and potential prey) at these sites. These include collectors (*Nemoura* spp. and *Amphinemura* spp.) and predators (*Malerikus* spp., *Isoperla* spp., *Acroneuria* spp., and *Beloneuria* spp.). These observations suggest that physiological and morpho-behavioral constraints of individual organisms preclude many taxa from tracking resources among patches when patches display very different abiotic conditions.

The addition of logs resulted in patches that displayed large changes in functional group production compared with reference sites (Fig. 8 and Table 7). Only shredder production failed to show large differences from that of reference sites following log additions; however, there were large shifts in production of various taxa within the shredder functional group. The shifts in functional group production between reference and debris-dam transects accentuate the importance of localized abiotic factors (e.g., current velocity, substratum particle size and composition, and organic matter retention) in structuring invertebrate communities within patches.

Patch formation also influenced overall growth (P/B) of invertebrates by changing the resident invertebrate community structure. The rather low community P/B ratios at reference and debris-dam transects prior to log additions (range from 2.2 to 3.0, Table 7) are attributable to a large portion of the biomass in either crayfish or several semivoltine plecopterans, especially *Pteronarcys* spp. and Peltoperlidae. The shift to higher P/B (5.4, Table 7) after log addition is attributable to several factors, including: (*i*) shifts in collector populations to greater biomass in small, multivoltine taxa (e.g., chironomids and copepods) rather than long-lived collectors with lower P/Bs, such as crayfish and some stonefly taxa; (*ii*) shifts in the proportion of biomass of longer-lived shredders (e.g., crayfish and the plecopterans, Peltoperlidae and *Pteronarcys* spp.) to those with shorter, univoltine life-cycles (e.g., trichopteran and dipteran shredders); and (*iii*) shifts in predator biomass from fewer semivoltine taxa (e.g., perlid stoneflies, *Acroneuria* spp., and *Beloneuria* spp.) to greater biomass in univoltine dipteran taxa (e.g., Tanypodinae, and some tipulid predators).

Decomposition of large woody debris is extremely slow in freshwater environments (e.g., Harmon et al. 1986). Over a long period of time (i.e., >20 years), we anticipate that areas immediately upstream of debris dams will gradually fill with larger and coarser inorganic sediments, i.e., gravel, pebble, and cobble, that are less amenable to movement, even during high flows. Hence, as debris dams fill with coarser sediments over several decades, we anticipate that with reduced retention of POM and increased current velocities, invertebrate community structure will gradually shift back toward that of original cobble riffles.

The changes induced by log additions in our study have considerable similarity with those reported for beaver ponds. For example, beaver ponds exhibit much greater storage of FPOM and CPOM than upstream riffle habitats (Naiman et al. 1986; McDowell and Naiman 1986). During most seasons in northeastern Quebec, scrapers exhibited lower densities in beaver ponds than in upstream riffles, and collectors and predators exhibited greater densities in ponds than in upstream riffles, whereas shredders and filterers exhibited no significant differences between ponds and riffles (McDowell and Naiman 1986). Although filterers as a group did not show any differences between beaver ponds and riffles, McDowell and Naiman (1986) found riffle-inhabiting Simuliidae and net-spinning caddisflies were replaced at pond sites by sphaeriid clams (*Pisidium* spp.). Although there is considerable similarity in physical features and functional structure between pools created by log addition and beaver ponds, there are major differences including: (*i*) addition of woody debris to high-gradient streams such as Coweeta results in depositional patches that influence a much smaller portion of the stream bed than ponds formed by beavers; (*ii*) there is no extensive flooding of adjacent riparian areas, nor beaver activity to open the forest canopy; and, (*iii*) other than small gaps formed by individual trees, there is little opening of the canopy, and any increase in solar radiation is minor because of the dense riparian understory of rhododendron.

One deficiency in this study is the absence of benthic data immediately downstream of debris-addition sites. We did not sample benthos in the plunge pools and areas farther downstream of debris dams where extensive redistribution of streambed substratum occurred. Visual observations of such features as little POM storage immediately downstream of debris dams compared with the extensive POM storage upstream of debris dams, would suggest that substantial changes in benthic community structure occurred in these downstream areas. Conceivably, reduced input of FPOM and CPOM from upstream reaches, as well as scouring and absence of deposition on cobble below debris dams, may enhance populations of filterers and scrapers while reducing those of collectors and shredders. Thus, the downstream effects on benthic community structure may be extensive and counteract to some extent those changes that occur upstream of debris dams.

In the larger picture, log-created debris dams increase the retention of POM and the efficiency with which organic matter is used within a stream reach. Additionally, dams greatly increase morphological diversity of the stream, creating patches of suitable habitat for many benthic invertebrates, as total number of nonchironomid taxa exhibited a small, but significant increase following log addition. In contrast, the number of taxa common to both log-addition and reference sites declined with time as community structure became more distinct among treatment and reference sites. Without debris dams, community structure would be much more uniform throughout long reaches of streams. Thus, enhancement of abiotic diversity by debris dams increases biotic diversity in these headwater streams.

Acknowledgments

We thank Dr. Alex Huryn, Dr. Matt Whiles, Dr. Jack Grubaugh, Lisa Houston, Gretchen Schurr, Sue Eggert, Dr. Kuen Chung, Debra Wohl, Sara Baer, John Hutchens, Dr. Nancy Munn, Mary Schaeffer, Terry Ehrman, Dr. Greg Peters, Jennifer Tank, Dr. D.J. D'Angelo, Dr. Francesc Sabater, Dr. Ben Stout, Peter Vila, Michael Paul, and Robert Webster for assistance with various phases of the field and laboratory work. Jim Buchanan, Bryant Cunningham, Dr. Wayne Swank, and other personnel of the Coweeta Hydrologic Laboratory assisted with various aspects of the project. We thank Dr. R.E. Bilby and an anonymous referee for constructive reviews on the manuscript. This work was supported by grants from the National Science Foundation, LTER program.

References

American Public Health Association. 1985. Standard methods for the examination of water and wastewater. 16th ed. *Edited by* A.E. Greenberg, R.R. Trussel, and L.S. Clesceri. American Public Health Association, Washington, D.C.

Anderson, N.H., J.R. Sedell, L.M. Roberts, and F.J. Triska. 1978. The role of invertebrates in processing wood debris in coniferous forest streams. Am. Midl. Nat. 100: 64–82.

Angermeier, P.L., and J.R. Karr. 1984. Relationships between woody debris and fish habitat in a small warm-water stream. Trans. Am. Fish. Soc. 113: 716–726.

Benke, A.C., T.C. Van Arsdall, Jr., D.M. Gillespie, and F.K. Parrish. 1984. Invertebrate productivity in a subtropical blackwater river: the importance of habitat and life history. Ecol. Monogr. 54: 25–63.

Bilby, R.E. 1981. Role of organic debris dams in regulating the export of dissolved and particulate matter from a forested watershed. Ecology, 62: 1234–1243.

Bilby, R.E., and G.E. Likens. 1980. Importance of organic debris dams in the structure and function of stream ecosystems. Ecology, 61: 1107–1113.

Cudney, M.D., and J.B. Wallace. 1980. Life cycles, microdistribution, and production dynamics of six species of net-spinning caddisflies (Trichoptera) in a large southeastern (U.S.A.) river. Holarct. Ecol. 3: 169–182.

Cummins, K.W. 1962. An evaluation of some techniques for the collection and analysis of benthic samples with special emphasis on lotic waters. Am. Midl. Nat. 67: 477–504.

Dobson, M., and A.G. Hildrew. 1992. A test of resource limitation among shredding detritivores in low order streams in England. J. Anim. Ecol. 61: 69–77.

Gessner, F. 1950. Die okologische Bedeutung der Stromungsgeschwindigkeit fliessender Gewasser und ihre Mesung auf kleinstem Raum. Arch. Hydrobiol. 43: 159–165.

Gregory, K.J. 1992. Vegetation and river channel process interactions *In* River conservation and management. *Edited by* P.J. Boon, P. Calow, and G.E. Petts. John Wiley & Sons, Chichester. pp. 255–269.

Gurtz, M.E., and J.B. Wallace. 1984. Substrate mediated response of stream invertebrates to disturbance. Ecology, 65: 1556–1569.

Harmon, M.E., J.F. Franklin, F.J. Swanson, P. Sollins, S.V. Gregory, J.D. Lattin, N.H. Anderson, S.P. Cline, N.G. Aumen, J.R. Sedell, G.W. Lienkaemper, K. Cromack, Jr., and K.W. Cummins. 1986. Ecology of coarse woody debris in temperate ecosystems. Adv. Ecol. Res. 15: 133–302.

Heede, B.H. 1972. Influence of a forest on the hydraulic geometry of two mountain streams. Water Resour. Bull. 8: 523–530.

Huryn, A.D. 1986. Secondary production of the macroinvertebrate community of a high-elevation stream in the southern Appalachian Mountains. Ph.D. dissertation, University of Georgia, Athens, Ga.

Huryn, A.D. 1990. Growth and voltinism of midge larvae: spatial patterns across an Appalachian Mountain landscape. Limnol. Oceanogr. 35: 339–351.

Huryn, A.D., and J.B. Wallace. 1987*a*. Local geomorphology as a determinant of macrofaunal production in a mountain stream. Ecology, 68: 1932–1942.

Huryn, A.D., and J.B. Wallace. 1987*b*. Production and litter processing by crayfish in an Appalachian Mountain stream. Freshwater Biol. 18: 277–286.

Keller, E.A., and F.J. Swanson. 1979. Effects of large organic material on channel form and fluvial processes. Earth Surf. Processes Landforms, 4: 361–380.

Lugthart, G.J. 1991. Macrofaunal community structure and production in disturbed and undisturbed headwater streams. Ph.D. dissertation, University of Georgia, Athens, Ga.

Lugthart, G.J., and J.B. Wallace. 1992. Effects of disturbance on benthic functional structure and production in mountain streams. J. North Am. Benthol. Soc. 11: 138–164.

McDowell, D.M., and R.J. Naiman. 1986. Structure and function of a benthic invertebrate stream community as influenced by beaver (*Castor canadensis*). Oecologia (Berl.), 68: 481–489.

Melillo, J.M., R.J. Naiman, J.D. Aber, and K.N. Eshleman. 1983. The influence of substrate quality and stream size on wood decomposition dynamics. Oecologia (Berl.), 58: 281–285.

Merritt, R.W., and K.W. Cummins (*Editors*). 1984. An introduction to the aquatic insects of North America. 2nd ed. Kendall/Hunt Publishing Company, Dubuque, Iowa.

Molles, M.C., Jr. 1982. Trichopteran communities of streams associated with aspen and conifer forests: long-term structural change. Ecology, 63: 1–6.

Momot, W.T., H. Gowing, and P.D. Jones. 1978. The dynamics of crayfish and their role in ecosystems. Am. Midl. Nat. 99: 10–35.

Mosley, M.P. 1981. The influence of organic debris on channel morphology and bedload transport in a New Zealand forest stream. Earth Surf. Processes Landforms, 6: 571–579.

Munn, N.L. 1989. The role of stream substrate and local geomorphology in the retention of nutrients in headwater streams. Ph.D. dissertation, University of Georgia, Athens, Ga.

Munn, N.L., and J.L. Meyer. 1990. Habitat-specific solute retention in two small streams: an intersite comparison. Ecology, 71: 2069–2082.

Murphy, J., and J.P. Riley. 1962. A modified single solution method for the determination of phosphate in natural waters. Anal. Chim. Acta, 27: 31–36.

Naiman, R.J., J.M. Melillo, and J.E. Hobbie. 1986. Ecosystem alteration of boreal forest streams by beaver (*Castor canadensis*). Ecology, 67: 1254–1269.

Newbold, J.D., R.V. O'Neill, J.W. Elwood, and W. VanWinkle. 1982. Nutrient spiralling in streams: implications for nutrient limitation and invertebrate activity. Am. Nat. 120: 628–652.

Nilson, H.C., and R.W. Larimore. 1973. Establishment of invertebrate communities on log substrates in the Kaskaskia River, Illinois. Ecology, 54: 366–374.

Nowell, W.R. 1951. The dipterous family Dixidae in western North America. Microentomology, 16: 187–270.

Pringle, C.M., R.J. Naiman, G. Bretschko, J.R. Karr, M.W. Oswood, J.R. Webster, R.L. Vannote, and M.J. Winterbourn. 1988. Patch dynamics in lotic systems: the stream as a mosaic. J. North Am. Benthol. Soc. 7: 503–524.

Roeding, C.E., and L.A. Smock. 1989. Ecology of macroinvertebrate shredders in a low-gradient sandy-bottomed stream. J. North Am. Benthol. Soc. 8: 149–161.

Sedell, J.R., F.H. Everest, and F.J. Swanson. 1982. Fish habitat and streamside management: past and present. *In* Proceedings of the Society of American Foresters Annual Meeting, September 27–30, 1981. Society of the American Foresters, Bethesda, MD. pp. 244–255.

Smith, R.D., R.C. Sidle, and P.E. Porter. 1993*a*. Effects on bedload transport of experimental removal of woody debris from a forest gravel-bed stream. Earth Surf. Processes Landforms, 18: 455–468.

Smith, R.D., R.C. Sidle, P.E. Porter, and J.R. Noel. 1993*b*. Effects of experimental removal of woody debris on the channel morphology of a forest gravel-bed stream. J. Hydrol. (Amsterdam), 152: 153–178.

Smock, L.A. 1980. Relationships between body size and biomass of aquatic insects. Freshwater Biol. 10: 375–383.

Smock, L.A., E. Gilinsky, and D.L. Stoneburner. 1985. Macroinvertebrate production in a southeastern United States blackwater stream. Ecology, 66: 1491–1503.

Smock, L.A., G.M. Metzler, and J.E. Gladden. 1989. The role of organic debris dams in the structuring and functioning of low-gradient headwater streams. Ecology, 70: 764–775.

Smock, L.A., J.E. Gladden, J.L. Riekenberg, L.C. Smith, and C.R. Black. 1992. Lotic macroinvertebrate production in three dimensions: channel surface, hyporheic, and floodplain environments. Ecology, 73: 876–888.

Speaker, R.W., K.W. Moore, and S.V. Gregory. 1984. Analysis of the process of retention of organic matter in stream ecosystems. Verh. Int. Ver. Theor. Angew. Limnol. 22: 1835–1841.

Statzner, B., and R. Müller. 1989. Standard hemispheres as indicators of flow characteristics in lotic benthos research. Freshwater Biol. 21: 445–459.

Statzner, B., F. Kohmann, and A.G. Hildrew. 1991. Calibration of FST-hemispheres against bottom shear stress in laboratory flume. Freshwater Biol. 26: 227–231.

Stream Solute Workshop. 1990. Concepts and methods for assessing solute dynamics in stream ecosystems. J. North Am. Benthol. Soc. 9: 95–119.

Swank, W.T., and J.B. Waide. 1988. Characterization of baseline precipitation and stream chemistry and nutrient budgets for control watersheds. *In* Forest hydrology and ecology at Coweeta. *Edited by* W.T. Swank and D.A. Crossley. Ecol. Stud. Ser. No. 66. Springer-Verlag, New York, N.Y. pp. 57–76.

Swanson, F.J., and G.W. Lienkaemper. 1978. Physical consequences of large organic debris in Pacific Northwest streams. U.S. Dept. Agr. For. Serv. Tech. Rep. PNW-69. Portland, Oreg.

Triska, F.J., and K. Cromack, Jr. 1980. The role of wood debris in forest and streams. *In* Forests: fresh perspectives from ecosystem analysis. *Edited by* R.H. Waring. Oregon State University Press, Corvallis, Oreg. pp. 171–190.

Trotter, E.H. 1990. Woody debris, forest–stream succession, and catchment geomorphology. J. North Am. Benthol. Soc. 9: 142–156.

Wallace, J.B., and A.C. Benke. 1984. Quantification of wood habitat in subtropical Coastal Plain streams. Can. J. Fish. Aquat. Sci. 41: 1643–1652.

Waters, T.F. 1969. Subsampler for dividing large samples of stream invertebrate drift. Limnol. Oceanogr. 14: 813–815.

Webster, J.R. and W.T. Swank. 1985. Within-stream factors affecting nutrient transport from forested and logged watersheds. *In* Proceedings of forestry and water quality: a mid-south symposium, Little Rock, Ark., May 8–9, 1985. *Edited by* B.G. Blackmon. Cooperative Extension Services, University of Arkansas, Fayetteville, Ark. pp. 18–41.

Webster, J.R., D.J. D'Angelo, and G.T. Peters. 1991. Nitrate and phosphate uptake in streams at Coweeta Hydrologic Laboratory. Verh. Int. Ver. Theor. Angew. Limnol. 24: 1681–1686.

Webster, J.R., A.P. Covich, J.L. Tank, and T.V. Crockett. 1994. Large organic particle retention in streams in the southern Appalachian Mountains. J. North Am. Benthol. Soc. 13: 140–150.

Wiggins, G.B. 1977. Larvae of the North American caddisfly genera (Trichoptera). University of Toronto Press, Toronto, Ont.

Zar, J.H. 1984. Biostatistical analysis. 2nd ed. Prentice-Hall, Inc., Englewood Cliffs, N.J.

Relationship between respiration rate of juvenile brook trout (*Salvelinus fontinalis*), water temperature, and swimming characteristics

Ming Tang and Daniel Boisclair

Abstract: We estimated the cost of spontaneous swimming and the swimming characteristics of juvenile brook trout for 21 combinations of water temperature (3.5, 6, 9, 12, 15, 18, and 20.7°C) and respirometer volume (27, 54, and 108 L). Spontaneous swimming costs were estimated as the oxygen depletion in the respirometers corrected for biological oxygen demand of the water and standard metabolism of the fish. Spontaneous swimming costs varied 9-fold among our experiments. Swimming characteristics, such as the average and the variance of speed, acceleration, and turning rates, were determined using a pair of video cameras. Swimming characteristics varied 2- to 10-fold among experiments. Speed and turning rate tended to increase with water temperature up to 18°C and decreased at 20.7°C. Water temperature ($r^2 = 0.44$) was the only variable that could explain a significant portion of the variations of spontaneous swimming costs between 3.7 and 20.7°C. Variance of speed (partial $R^2 = 0.32$) and the average turning rate (partial $R^2 = 0.34$) explained 53% of the variation between 3.7 and 18°C. Average speed never explained more than 35% of spontaneous swimming cost variation.

Résumé : Nous avons estimé les coûts de nage spontanée et les caractéristiques de nage d'ombles de fontaine juvéniles pour 21 combinaisons de température de l'eau (3,5, 6, 9, 12, 15, 18 et 20,7°C) et de volume de respiromètre (27, 54 et 108 L). Les coûts de nage spontanée ont été estimés par la diminution d'oxygène dans les respiromètres corrigée pour la demande biologique en oxygène de l'eau et le métabolisme standard des poissons. Les coûts de nage spontanée ont varié par un facteur de 9 entre nos expériences. Les caractéristiques de nage comme la moyenne et la variance de la vitesse, des taux d'accélération et de virage ont été estimés à l'aide d'une paire de vidéo caméras. Les caractéristiques de nage ont varié par un facteur de 2 à 10 entre les expériences. La vitesse et le taux de virage ont augmenté avec la température de l'eau jusqu'à 18°C et ont diminué à 20,7°C. La température de l'eau ($r^2 = 0{,}44$) a été la variable indépendante la plus puissante pour expliquer les variations de coûts de nage spontanée entre 3,7 et 20,7°C. La variance de la vitesse (R^2 partiel = 0,32) et le taux moyen de virage (R^2 partiel = 0,34) ont expliqué un total de 53% des variations de coûts de nage spontanée entre 3,7 et 18°C. La vitesse moyenne n'a jamais expliqué plus de 35% des variations des coûts de nage spontanée.

Introduction

Bioenergetic models have been used to predict fish growth under given sets of environmental conditions (Brandt et al. 1992), to estimate the effects of fish on their prey community (Rice et al. 1983), to evaluate the importance of fish on nutrient cycles in lakes (Kraft 1992; Carpenter et al. 1992; He et al. 1993), and to improve management strategies (Johnson et al. 1988). The precision of the output from these models depends on accurate estimation of consumption, growth, and respiration rates. Activity is the least-understood component of fish respiration. This situation is compounded by the possibility that inappropriate assumptions regarding activity rates may cause a 2- to 3-fold deviation of the predictions made by bioenergetics models (Boisclair and Leggett 1989; Lucas et al. 1991; Hansen et al. 1993; Madon and Culver 1993; Ney 1993). Estimation of activity rates is the first step towards adequately representing the activity component of fish bioenergetic models.

One approach to evaluate fish activity rates requires the estimation of water temperature and fish swimming speed. The most common models used to estimate fish respiration from these variables are based on laboratory experiments in which respiration was measured at specific water temperatures while fish were forced to swim against a current of constant speed and direction (Brett 1964; Beamish 1978; Stewart et al. 1983). Such relationships, however, may

Received August 2, 1994. Accepted May 9, 1995.
J12511

M. Tang and D. Boisclair. Université de Montréal, Département de sciences biologiques, C.P. 6128, succursale Centre-Ville, Montréal, QC H3C 3J7, Canada.

underestimate true activity costs by a factor ranging from 3 to 8 presumably because of the inability of forced swimming experiments to adequately represent the costs associated with the execution of spontaneous movements that imply changes in speed and direction (Webb 1991; Boisclair and Tang 1993; Krohn and Boisclair 1994). Despite the potential influence of spontaneous movements there are currently no models available to estimate fish swimming costs using a complete set of swimming characteristics.

Our objectives were (*i*) to quantify the influence of water temperature and swimming characteristics (speed, acceleration, and turning rates) on the respiration rate of juvenile brook trout (*Salvelinus fontinalis*) and (*ii*) to develop a model to estimate the costs of spontaneous movements using water temperature and swimming characteristics as independent variables.

Methods

Experimental design

Assessment of the influence of water temperature and fish swimming characteristics on spontaneous swimming costs requires the estimation of oxygen consumption of fish kept at different temperatures and under conditions that induce them to display different swimming characteristics. These requirements were met by executing a series of 21 respirometry experiments at 3.5, 6, 9, 12, 15, 18, and 20.7°C using respirometers of 27, 54, and 108 L. This approach was adopted because the volume available for swimming has a significant influence on fish swimming characteristics (Tang and Boisclair 1993; Krohn and Boisclair 1994). Each experiment was one combination of a water temperature and respirometer size. Fish swimming characteristics (speed, acceleration, and turning rates) were estimated using the stereocinematographic method (Ménard 1991; Boisclair 1992*a*, 1992*b*). Young-of-the-year (YOY) brook trout were selected as the subject of our work because individuals of a standard size and a homogenous genotype could be easily obtained from a fish farm (Réserve La Petite Nation, Quebec).

Experimental procedure

Estimation of spontaneous swimming cost

Fish were acclimatized to a given water temperature in a 500-L Living Stream aquarium (LSW 700). During this acclimatization period, water temperature was increased 1°C/day until it reached the expected level. Fish were maintained at that temperature for 7–14 days prior to an experiment. For experiments performed at temperatures below 6°C, fish were not fed for 4 days prior to an experiment to avoid confounding effects of respiration associated with digestion processes (Brett 1964; Beamish 1978). The starvation period was set at 3 days for temperatures between 9 and 15°C, and at 2 days for temperatures above 18°C.

The respirometers consisted of Plexiglas boxes with lids. Three sides of the respirometers were covered with black tape to reduce disturbance from outside and improve fish visibility. The respirometers were placed in a second LSW 700 to insure better control of water temperature during the experiments. Two water pumps were installed inside the respirometers: pump A was used for mixing and maintaining a homogenous oxygen concentration within the respirometer during the experimental period, and pump B allowed a connection to be made between the inside and outside of the respirometers.

Four YOY brook trout (total length 5 ± 0.2 cm (mean ± SD); wet weight 1.21 ± 0.15 g; Table 1) were transferred from the acclimatization tank to the respirometer 24 h before the start of an experiment to allow them to adapt to their new environment (referred to as the stabilization period). The respirometer was then sealed without residual air bubbles. During the stabilization period, pump B generated a small exchange between the respirometer and the holding tank. This circulation of water maintained 75–80% oxygen saturation inside the respirometer. At the beginning of an experiment, pump B was connected to the oxygen meter (inTab 565; ±0.005 ppm), thereby preventing new water from entering the respirometer from the holding tank. The initial oxygen concentration was measured after two steps. First, pump A was turned on for 1 min. Second, pump B transferred water from the respirometer to the probe of the oxygen meter and back to the respirometer. Water from the respirometer never contacted air during this process. Additional measurements of oxygen concentration were taken every hour without turning on pump A to reduce disturbance to fish (excitement, stress, and the energetic cost to overcome the current).

An experiment was terminated when fish had consumed more than 0.5 ppm of oxygen or after 12 h of observation. No observations were made below oxygen concentrations of 7.6 ppm. This limit was imposed to minimize the influence of low oxygen concentrations on fish behaviour. The water temperature never varied by more than 0.5°C during an experiment. At the end of an experiment fish were immediately removed from the respirometer and killed by an overdose of 2-phenoxyethanol (1 mg/L). Their weight (±0.005 g wet weight) and total length (±0.05 cm) were measured individually. Biological oxygen demand (BOD) was determined within 24 h of an experiment by using the same procedure as described above but without fish in the tank.

Estimation of swimming characteristics

Fish swimming characteristics were estimated from the temporal variation of fish positions in an x, y, z Cartesian coordinate system. The movements executed by fish during each experiment were filmed, and then analyzed by computer.

Fish movements in the respirometers were filmed by a pair of video cameras (Panasonic WV-BL602) through a glass window (0.3 × 1.5 m) located on the side of the LSW 700. Two fluorescent lights were placed above the respirometers to improve the quality of the images. The cameras were parallel and separated by 10 cm. Images obtained by the two cameras were synchronized and combined side by side in a single image by a videoprocessor (Panasonic Quad WJ-450). The time of recording was printed by a time and date camera titler (Panasonic WJ-810) accurate to ±0.005 s. The final images were sent to a video-cassette recorder (Sony EV-C3). Fish were filmed 10–20 min/h depending on the duration of the

Table 1. Experimental conditions.

Experiment	Water temperature (°C)	Aquarium dimensions (cm)	Aquarium volume (L)	Mean fish weight (g)	Mean fish total length (cm)
1	3.5	30×30×30	27	1.21	4.95
2	3.5	60×30×30	54	1.18	4.98
3	3.8	120×30×30	108	1.16	4.88
4	5.6	30×30×30	27	1.22	4.93
5	5.8	60×30×30	54	1.25	5.05
6	6.0	120×30×30	108	1.25	5.05
7	9.0	30×30×30	27	1.19	5.05
8	8.9	60×30×30	54	1.27	5.03
9	9.1	120×30×30	108	1.27	5.13
10	11.9	30×30×30	27	1.24	5.08
11	11.9	60×30×30	54	1.14	4.95
12	12.0	120×30×30	108	1.33	5.13
13	15.2	30×30×30	27	1.18	4.98
14	15.0	60×30×30	54	1.21	4.95
15	15.0	120×30×30	108	1.29	5.03
16	18.0	30×30×30	27	1.28	5.05
17	17.9	60×30×30	54	1.23	5.13
18	18.0	120×30×30	108	1.12	5.00
19	20.7	30×30×30	27	1.17	4.95
20	20.7	60×30×30	54	1.10	4.90
21	20.5	120×30×30	108	1.12	4.88

experiment (6–12 h). We recorded 120 min of film per experiment.

Images recorded were analyzed using the Jandel video analysis software. The calibrations necessary to convert the images filmed into fish x, y, z positions were performed using the method described by Boisclair (1992*a*, 1992*b*) and Krohn and Boisclair (1994). The position of a fish was quantified by four pairs of coordinates, the x and y coordinates of the head and tail of the fish. Fish coordinates were estimated at 1-s intervals. We randomly selected 5–10 fish observed during each recording session (10–20 min) and estimated 10 successive positions of each fish selected. This procedure allowed us to estimate 600 fish positions for each experiment. Individual fish inside the respirometer were classified as swimming or resting. The resting mode was assigned to fish moving less than 0.5 cm/s for 3 consecutive s.

Computation

Estimation of spontaneous swimming cost

Spontaneous metabolism (C_R; milligrams O_2 per fish) of an average fish during a specific experiment was calculated as

$$[1] \quad C_R = \frac{(\Delta[O_2] - \text{BOD})V}{4}$$

where $\Delta[O_2]$ is oxygen depletion during an experiment, (milligrams O_2 per litre), BOD is the biological oxygen demand of the water (milligrams O_2 per litre), V is the volume of the respirometer (litres), and 4 is the number of fish inside the respirometer. Spontaneous swimming cost (C_S; milligrams O_2 per hour) was estimated as

$$[2] \quad C_S = \frac{C_R - (\text{SMR} \cdot t)}{t \cdot P_t}$$

where SMR is the standard metabolic rate of a fish (milligrams O_2 per hour), t is the duration of the experiment (hours), and P_t is the proportion of time fish were swimming.

SMR was determined by the following model developed using data on standard metabolism of brook trout (0.19–54.1 mL O_2/h) weighing 5–1000 g held at water temperatures ranging from 5 to 20°C (Job 1955):

$$[3] \quad \log_{10}(\text{SMR}) = 1.041 \cdot \log_{10}(T) - 1.975 \qquad r^2 = 0.99, \ p < 0.0001$$

where T is the water temperature (degrees Celcius). This equation was developed in three steps: (*i*) we estimated a series of relationships between SMR and body mass of fish at four temperatures (5, 10, 15, and 20°C) using regression analysis; (*ii*) we determined the SMR for the mean weight of our fish (1.2 g) at each temperature by extrapolation from these relationships; and (*iii*) we derived the final equation by regressing the SMR of a 1.2-g fish against water temperature. We assessed the influence of extrapolation to a weight of 1.2 g by comparing eq. 3 with an equation developed following the same procedure but using fish weighing only 5–135 g (a 7.4-fold reduction of the maximum fish weight in the analysis). The two models were identical, suggesting that the range of fish sizes used to derive eq. 3 had a relatively small influence on the value of the parameters in the model. In the experiments performed by Job (1955), the

Fig. 1. Spontaneous swimming costs for the 21 combinations of water temperature and aquarium size.

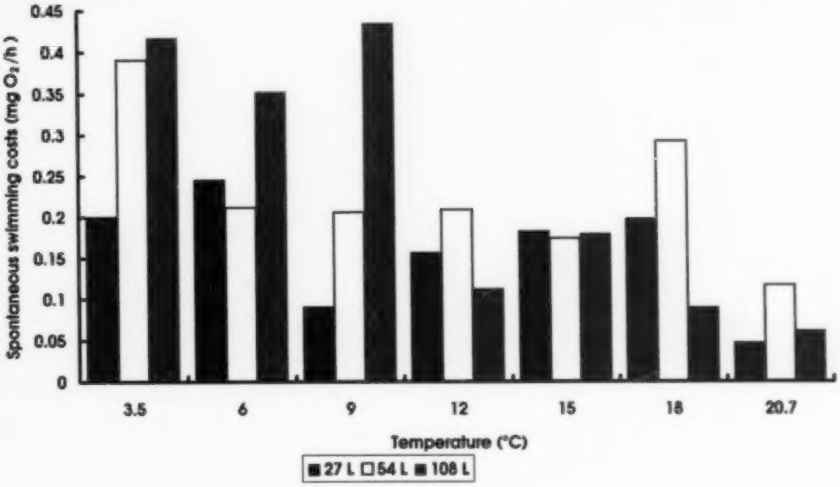

fish were starved for sometimes as little as 12 h. This protocol may not be sufficient to eliminate the oxygen consumption associated with digestion processes. Furthermore, SMR were defined as the lowest rate of oxygen consumption of fish during any 2-h interval in a 24-h period. The setup used by Job (described by Fry and Hart 1948) allowed fish to swim freely. This situation implies that the SMR estimates produced by eq. 3 may represent maximum values (including costs of digestion and spontaneous activity), and consequently that our measures of activity costs should be interpreted as minimum values.

P_t was estimated as

$$[4] \quad P_t = \frac{\left(\sum_{k=1}^{K} P_k\right)}{K \cdot 240}$$

where P_k is the total number of seconds that fish were in the swimming mode during 1 min sampled at random from within every 5 min of filming, K is the number of times P_k was estimated during an experiment (K = 120 min of filming per experiment, i.e., there were 24 5-min intervals), and 240 is the maximum number of seconds fish can be active per minute (4 fish per respirometer × 60 s). Time available for swimming is here defined as $K \cdot 240$ (5760 s). When more than 1 fish was in the swimming mode during a given second, the number of seconds added to P_k was equal to the number of fish swimming.

Swimming characteristics

Fish movements were described using three characteristics: speed, acceleration, and turning rates. Swimming characteristics were estimated from the displacements of a fish in an *x*, *y*, *z* coordinate system during a given time period (generally 1–2 s). A complete description of the geometric formulae used to estimate fish swimming characteristics from successive *x*, *y*, *z* positions of the tail and of the head of a fish was presented by Tang and Boisclair (1993).

Data analysis

Spontaneous swimming costs

Spontaneous swimming costs were compared among experiments by using a permutation procedure consisting of four steps. (*i*) A total of 10 500 pseudovalues (PV) of spontaneous swimming cost were created for the 21 experiments (further referred to as nominal sets of PV). Each set of 500 PV was generated by adding 500 error values to the respiration rate estimated during a specific experiment. Error values were randomly chosen from a normal distribution having a mean of 0 and a standard deviation of 0.007. The standard deviation was estimated using the instrumental error (0.005 mg O_2/L) of the respirometer, the number of O_2 readings necessary to estimate fish respiration (four; two readings for total respiration and two readings for BOD), and the property that over 99% of observations from a normal distribution are within ±3 SD of the mean ($0.005 \cdot 4/3 = 0.007$). (*ii*) Variations in respiration rates among the 21 sets of PV were tested using a parametric two-way ANOVA. *F* values were calculated for water temperature, aquarium size, and the interaction term (aquarium × water temperature). (*iii*) An additional series of 999 two-way ANOVAs were executed. Each ANOVA was done using 21 reconstructed sets of swimming cost PV (500 PV per set). Reconstruction was performed by redistributing 10 500 swimming cost PV at random into 21 groups. (*iv*) Among-experiment variations were declared significant when the *F* value of the ANOVA performed using the nominal swimming cost PV was greater than 95% of the 999 *F* values obtained using the reconstructed sets. Similarly, the statistical significance of the influence of aquarium size, water temperature, and the interaction term was determined by comparing their *F* values obtained using the nominal swimming cost PV with respective sets of 999 *F* values calculated using reconstructed sets.

Table 2. Fish swimming characteristics during the 21 experiments.

	Speed			Turning rate	
Experiment	Average (cm/s)	Variance	Acceleration variance	Average (degrees/s)	Variance
1	4.80	10.97	25.53	43.1	1436
2	4.43	6.80	18.69	33.8	1505
3	6.63	19.05	26.78	30.9	1387
4	6.48	14.99	26.48	48.3	1752
5	5.13	15.78	26.34	36.3	1705
6	6.10	17.73	31.44	32.7	1426
7	7.63	21.43	31.56	58.9	2423
8	8.69	14.40	22.37	58.6	2349
9	5.72	8.02	7.17	32.0	1678
10	6.21	12.04	16.56	45.0	1425
11	6.87	13.14	14.38	47.7	1903
12	7.52	27.70	40.64	38.1	1897
13	7.69	20.01	23.33	63.5	2350
14	7.82	16.97	21.86	50.7	2077
15	8.00	28.92	28.64	40.1	2029
16	7.08	41.86	60.37	59.5	2608
17	7.57	21.72	25.93	49.4	2073
18	9.66	66.46	66.34	38.9	1797
19	3.98	7.46	7.23	44.2	1658
20	5.11	14.16	15.77	38.7	1978
21	7.28	35.44	30.92	33.6	1514

Swimming characteristics

Among-experiment variations in swimming characteristics were tested using a permutation procedure similar to that used for spontaneous swimming costs but with two differences. (*i*) We did not have to use PV to perform the tests; the sets of swimming characteristics estimated from fish coordinates were used directly. (*ii*) The nominal data set for each experiment contained 200 swimming characteristics instead of 500 spontaneous swimming cost values. Homogeneity of the variance of the swimming characteristics among experiments was assessed using Bartlett's test performed following a permutation procedure (Sirois and Boisclair 1995).

Variations in the proportion of time that fish spent in the swimming mode were assessed using a two-way ANOVA without replicates.

Models

The relationships among spontaneous swimming costs, water temperature, and swimming characteristics were developed using multiple regression analysis (stepwise analysis). The average and the variance of each swimming characteristic were used as independent variables. One exception to this rule was acceleration rates, which are always expected to average 0.

Results

Spontaneous swimming cost

Spontaneous swimming costs ranged from 0.047 (experiment 19) to 0.435 mg O_2/h (experiment 9; Fig. 1). These values corresponded to 0.17–7.6 times the SMR (0.054–0.28 mg O_2/h). Spontaneous swimming costs varied with aquarium volume ($p < 0.01$) and water temperature ($p < 0.01$). The interaction was also significant ($p < 0.01$). Activity costs tended to decrease with water temperature but no clear trend was observed with respirometer size.

Swimming characteristics

Speed

Average swimming speed ranged from 3.98 (experiment 19) to 9.66 cm/s (experiment 18; Table 2) and tended to increase with water temperature up to 18°C. The average speed of fish observed above that limit tended to decrease. We interpret this to mean that the behaviour of brook trout may be negatively affected by temperatures above 18°C. Respirometer size ($p < 0.01$) and water temperature ($p < 0.01$) both influenced fish swimming speed (interaction; $p < 0.01$). The variance of speed ranged from 6.8 (experiment 2) to 66.5 (experiment 18; Table 2) and varied among experiments ($p < 0.01$).

Acceleration

Average acceleration rates were always close to 0 cm/s^2 and were not analyzed any further. Variances of acceleration varied from 7.2 (experiment 9) to 66.3 (experiment 18; Table 2) and differed among experiments ($p < 0.01$).

Turning rate

The average turning rates ranged from 30.9 degrees/s (experiment 3) to 63.5 degree/s (experiment 13; Table 2) and tended to decrease with respirometer size. Average turning rates varied among respirometer size ($p < 0.01$) and water temperature ($p < 0.01$). The interaction term was also significant ($p < 0.01$). Variance of turning rates varied 2-fold among experiments (from 1387 for experiment 3 to 2608 for experiment 16; Table 2), a significant difference.

The proportion of time spent swimming

Fish were in the swimming mode between 30.2% (experiment 16) and 84.2% (experiment 10) of the time available for swimming (Table 3). The proportion of time spent on swimming was negatively related to water temperature ($F_{[6,20]} = 12.03$; $p < 0.01$) but was independent of respirometer size ($F_{[2,20]} = 2.85$; $p = 0.10$).

Models

Multiple regression analysis (stepwise) was performed including and excluding experiments conducted at water temperatures >18°C because of the potential negative influence of water temperature above that level. When all experiments were included in the analysis, 44% of the variation in spontaneous swimming cost was explained by water temperature. Exclusion of experiments performed at temperatures >18°C allowed the development of two regressions (Table 4). The average speed alone could explain 35% of the variation and the combination of variance of speed (partial $R^2 = 0.32$) and average turning rate (partial $R^2 = 0.34$) could improve prediction up to 53%. The correlation between these two variables was relatively weak ($r = 0.24$).

Table 3. Percentage of the time that available fish were in the swimming mode.

Experiment	%
1	66.3
2	79.7
3	69.7
4	81.6
5	70.6
6	80.0
7	76.5
8	74.5
9	61.1
10	84.2
11	82.8
12	63.4
13	72.3
14	80.2
15	67.3
16	30.2
17	44.9
18	39.3
19	65.6
20	61.4
21	52.9

Discussion

Our results indicate that water temperature and swimming characteristics such as the average and the variance of speed and the average of turning rate can explain up to 53% of the 9-fold variation in spontaneous swimming costs observed among our experiments. Our results further suggest that it is possible to estimate the cost of spontaneous swimming for fish observed under natural conditions using an underwater video-camera system similar to that used in our study. The relative importance of water temperature and swimming characteristics in explaining swimming cost variation tended to vary with the range of temperatures considered. Water temperature ($r^2 = 0.44$) was the only variable to explain a significant proportion of the variability of spontaneous swimming costs for our complete data set (3.5–20.7°C). Below 18°C, water temperature was no longer significant. Instead, the variance of speed and the average turning rate explained up to 53% of the variation in swimming costs. This situation should be taken into account during the selection of a model to estimate swimming costs in the field.

Many models have been developed to estimate fish swimming costs using speed as an independent variable (Brett 1964; Beamish 1978; Stewart et al. 1983). Our work contrasts with these studies because it suggests that speed may not be the most important variable to explain spontaneous swimming costs. Speed explained a significant fraction of swimming cost variation in only one of the models we found and the r^2 value associated with this variable was 0.35.

Two hypotheses can be proposed to explain the moderate performance of swimming speed in the models developed. First, the range of average speeds observed among our experiments may not represent a realistic fraction of the range of speeds utilized by fish in the field. As showed by Tang and Boisclair (1993), the size of the enclosure can have a significant influence on fish swimming characteristics. The average speed of brook trout observed in 1- to 27-m^3 enclosures (9–1000 times larger than the aquaria we used in this study) ranged from 6.4 to 11.1 cm/s. Trudel and Boisclair (1995) used a video-camera system to determine that the average swimming speed of a dace (*Phoxinus eos* × *Phoxinus neogaeus*) in the field ranged from 6.7 to 12.3 cm/s during the day. Corresponding values observed in our aquaria were 3.98 to 9.66 cm/s. While trout and dace are different species, the size and body shape of the YOY trouts we used are very similar to those of dace. Moreover, they have the same locomotion pattern (subcarangiform) and feeding behaviour (zooplanktivores; Trudel and Boisclair 1995; Boisclair and Sirois 1993; Sirois and Boisclair 1995). The maximum average speed we observed was therefore 78.5% of that found under field situations or in large in situ enclosures. Furthermore, the range of the average speeds we estimated (5.7 cm/s) was comparable to that in other studies (4.7–5.6 cm/s). We therefore suggest that the range of speeds observed within our aquaria may not be responsible for the relative importance of this variable in the models we developed.

The second hypothesis is that the cost of spontaneous swimming at a given average speed cannot be adequately represented by fish swimming in a flume at that speed. Other studies (Webb 1991; Boisclair and Tang 1993; Krohn and Boisclair 1994) have shown that spontaneous swimming at a given average speed can be 2–15 times more

Table 4. Models developed to estimate spontaneous swimming costs using water temperature and swimming characteristics as independent variables.

Model	r^2	p
Models including experiments conducted above 18°C		
$\log_{10}(C_s) = -0.290 \cdot T - 0.401$	0.44	<0.01
Models excluding experiments conducted above 18°C		
$\log_{10}(C_s) = -0.087 \cdot \mathrm{MS} - 0.070$	0.35	<0.05
$C_s = -0.200 \cdot \log_{10}(\mathrm{VarS}) - 0.508 \cdot \log_{10}(\mathrm{MAng}) + 1.314$	0.53	<0.01

Note: C_s is the cost of swimming (mg O_2/h), T is the water temperature (°C), MS represents the average speed, VarS is the variance of speed, and MAng is the average turning rate.

expensive than forced swimming at that speed. This difference has been attributed to the costs of changing speed and direction. Our present work supports this interpretation. We estimated the cost of forced swimming at the mean speed observed during each of our 21 experiments with the model developed by Boisclair and Tang (1993). The cost of spontaneous swimming at a given mean speed was, on average, 5.3 times higher than that of forced swimming at the same speed (range 1.4–15.3).

Fish respiration has generally been described as a positive function of water temperature (Brett 1964; Beamish 1978). Similarly, the cost of swimming has been hypothesized to increase with the frequency and intensity of changes in speed and direction (i.e., variance of speed and angle of turn; Webb 1991; Boisclair and Tang 1993). Our results do not fully support traditional expectations or more recent hypotheses. We did find that spontaneous swimming costs were higher than forced swimming costs at a same speed. However, we also found a relatively strong negative relationship between the net cost of swimming and the water temperature over the complete range of temperatures. Furthermore, the experiments performed between 3.5 and 18°C suggest that swimming costs decrease with the complexity of fish movements. Our work illustrates that swimming pattern may explain the difference between the costs of forced and spontaneous swimming in accordance with the current hypothesis (i.e., costs increase from forced to spontaneous swimming because of swimming complexity). However, our study may also indicate that different mechanisms may have to be invoked to explain the variability within a series of spontaneous swimming cost values. We believe that the negative relationships we found between swimming costs and water temperature or swimming characteristics illustrate the possibility that as temperature and the speed of the movements increase, fish gradually switch the strategy used to create a movement to minimize energy expenditures. This hypothesis is supported by the observations of Stevens (1979) who found that the tail beat frequency of rainbow trout swimming at a constant speed was negatively related to water temperature. This work suggests that the energy expenditure associated with swimming at a given speed may decrease with water temperature. Stevens argued that this situation may arise because higher temperature might improve muscle efficiency (the force developed per contraction) and reduce water resistance (decrease in viscosity). Interestingly, Stevens observed the opposite trend for largemouth bass (*Micropterus salmoides*). Finally, Magnuson and Prescott (1966) also found that for the Pacific bonito (*Sarda chiliensis*), similar tail beat frequencies can be associated with different swimming speeds. Taken together, these two studies suggest that different fish species may have different strategies (patterns of muscle recruitment, succession of gliding and cruising, burst–coast) to create a given swimming characteristic (e.g., speed) and that the strategies and their energetic consequences may vary with water temperature. While our results do not allow us to describe the different strategies used by fish to create the movements we observed, they are compatible with the hypothesis that fish may increase their propulsive efficiency as temperature increases and swimming characteristics become more complex.

Acknowledgments

We thank the Natural Sciences and Engineering Research Council of Canada (NSERC) and the Fonds pour la formation de chercheurs et l'aide la recherche (FCAR) for their financial support through grants to D.B. (FCAR Nouveau chercheur; NSERC research grant) and to the Freshwater Ecology Group of the Université de Montréal (FCAR équipe). We are also grateful to the Université de Montréal for providing funds through the Comité d'attribution des fonds internes de la recherche, research development funds, and NSERC (internal funds). M.T. was supported by a postgraduate fellowship from NSERC, Fonds spécial de la Faculté des études supérieures from Université de Montréal, and a scholarship obtained through the Groupe de recherche interuniversitaire en limnologie (GRIL; FCAR centre).

References

Beamish, F.W.H. 1978. Swimming capacity. *In* Fish physiology. Vol. 7. *Edited by* W.S. Hoar and D.J. Randall. Academic Press, New York. pp. 101–187.

Boisclair, D. 1992*a*. An evaluation of the stereocinematographic method to estimate fish swimming speed. Can. J. Fish. Aquat. Sci. 49: 523–531.

Boisclair, D. 1992*b*. Relationship between feeding and activity rates for actively foraging juvenile brook trout (*Salvelinus fontinalis*). Can. J. Fish. Aquat. Sci. 49: 2566–2573.

Boisclair, D., and W.C. Leggett. 1989. The importance of activity in bioenergetics models applied to actively foraging fishes. Can. J. Fish. Aquat. Sci. 46: 1859–1867.

Boisclair, D., and P. Sirois. 1993. Testing assumptions of fish bioenergetics models by direct estimation of growth, consumption, and activity rates. Trans. Am. Fish. Soc. 122: 784–796.

Boisclair, D., and M. Tang. 1993. Empirical analysis of the influence of swimming pattern on the net cost of swimming in fishes. J. Fish Biol. 42: 169–183.

Brandt, S.B., D.M. Mason, and E.V. Patrick. 1992. Spatially-explicit models of fish growth rate. Fisheries, 17: 23–33.

Brett, J.R. 1964. The respiratory metabolism and swimming performance of young sockeye salmon. J. Fish. Res. Board Can. 21: 1183–1226.

Carpenter, S.R., C.E. Kraft, R.A. Wright, X. He, P.A. Soranno, and J.R. Hodgson. 1992. Resilience and resistance of a lake phosphorus cycle before and after food web manipulation. Am. Nat. 140: 781–798.

Fry, F.E.J., and J.S. Hart. 1948. The relation of temperature to oxygen consumption in the goldfish. Biol. Bull. (Woods Hole), 94: 66–77.

Hansen, M.J., D. Boisclair, S.B. Brandt, S.W. Hewett, J.F. Kitchell, M.C. Lucas, and J.J. Ney. 1993. Applications of bioenergetic models to fish ecology and management: where do we go from here? Trans. Am. Fish. Soc. 122: 1019–1030.

He, X., J.F. Kitchell, S.R. Carpenter, J.R. Hodgson, D.E. Schindler, and K.L. Cottingham. 1993. Food web structure and long-term phosphorus recycling: a simulation model evaluation. Trans. Am. Fish. Soc. 122: 773–783.

Job, S.V. 1955. The oxygen consumption of *Salvelinus fontinalis*. Univ. Toronto Stud. Biol. Ser. No. 61. Publ. Ont. Fish. Res. Lab. No. 73. pp. 1–39.

Johnson, B.M., R.A. Stein, and R.F. Carline. 1988. Use of a quadrat rotenone technique and bioenergetics modelling to evaluate prey availability to stocked piscivores. Trans. Am. Fish. Soc. 117: 127–141.

Kraft, C.E. 1992. Estimates of phosphorus and nitrogen cycling by fish using a bioenergetics approach. Can. J. Fish. Aquat. Sci. 49: 2596–2604.

Krohn, M., and D. Boisclair. 1994. The use of stereo–video system to estimate the energy expenditure of free-swimming fish. Can. J. Fish. Aquat. Sci. 51: 1119–1127.

Lucas, M.C., I.G. Priede, J.D. Armstrong, A.N.Z. Gindy, and L. De Vera. 1991. Direct measurements of metabolism, activity and feeding behaviour of pike, *Esox lucius* L., in the wild, by the use of heart rate telemetry. J. Fish Biol. 39: 325–345.

Madon, S.P., and D.A. Culver. 1993. Bioenergetics model for larval and juvenile walleyes: an in situ approach with experimental ponds. Trans. Am. Fish. Soc. 122: 797–813.

Magnuson, J.J., and J.H. Prescott. 1966. Courtship, locomotion, feeding, and miscellaneous behavior of Pacific bonito. Anim. Behav. 14: 54–67.

Ménard, C. 1991. Utilisation de la vidéo pour mesurer les poissons in situ. M.Sc. thesis, Université de Montréal, Montréal, Que.

Ney, J.J. 1993. Bioenergetics modelling today: growing pains on the cutting edge. Trans. Am. Fish. Soc. 122: 736–748.

Post, J.R. 1990. Metabolic allometry of larval and juvenile yellow perch (*Perca flavescens*): in situ estimates and bioenergetic models. Can. J. Fish. Aquat. Sci. 47: 554–560.

Rice, J.A., J.E. Breck, S.M. Bartell, and J.F. Kitchell. 1983. Evaluating the constraints of temperature, activity and consumption on growth of largemouth bass. Environ. Biol. Fishes, 9: 263–275.

Sirois, P., and D. Boisclair. 1995. The influence of prey biomass on activity and consumption rates of brook trout (*Salvelinus fontinalis* Mitchill). J. Fish Biol. 46: 787–805.

Stevens, E.D. 1979. The effect of temperature on tail beat frequency of fish swimming at constant velocity. Can. J. Zool. 57: 1628–1635.

Stewart, D.J., D. Weininger, D.V. Rottiers, and T.A. Edsall. 1983. An energetics model for lake trout, *Salvelinus namaycush*: application to the Lake Michigan population. Can. J. Fish. Aquat. Sci. 40: 681–698.

Tang, M., and D. Boisclair. 1993. Influence of the size of enclosures on the swimming characteristics of juvenile brook trout (*Salvelinus fontinalis*). Can. J. Fish. Aquat. Sci. 50: 1786–1793.

Trudel, M., and D. Boisclair. 1994. Seasonal consumption by dace (*Phoxinus eos* × *P. neogaeus*): a comparison between field and bioenergetic model estimates. Can. J. Fish. Aquat. Sci. 51: 2558–2567.

Trudel, M., and D. Boisclair. 1995. Estimation of fish activity costs using underwater video cameras. J. Fish Biol. In press.

Webb, P.W. 1991. Composition and mechanics of routine swimming of rainbow trout (*Oncorhynchus mykiss*). Can. J. Fish. Aquat. Sci. 48: 583–590.

Optimal allocation of sampling effort in lake sediment studies

David J. Rowan, Joseph B. Rasmussen, and Jacob Kalff

Abstract: A sampling algorithm requiring only bathymetric and catchment parameters has been derived from several recent empirical developments and should drastically reduce the number of sites and replicates necessary to characterize the distribution, trace element concentrations, and sediment accumulation rates of lake sediments. A test of this algorithm with sediments from 96 sites in three basins of morphometrically complex Jack Lake, Ontario, demonstrates the utility of this approach. A priori application of the algorithm would have reduced the number of sample sites on our sampling grid from 96 to 22 (a reduction of 77%), without losing precision. This reduction in sample sites (and in time and money expended) would allow for sampling additional lakes or sites of local significance (e.g., river or creek mouths, pollution point sources), or measuring additional parameters. The relationships between lake morphometry, sediment distribution, and sediment texture, along with the relationships between sediment texture and inter- and intra-site variability, can also be used to extrapolate sediment characteristics from a few samples to the whole lake or to predict the zone to which sediment is focused.

Résumé : Plusieurs découvertes empiriques récentes ont permis l'établissement d'un algorithme d'échantillonnage ne nécessitant que des paramètres bathymétriques et les caractéristiques des bassins versants; cet algorithme devrait réduire considérablement le nombre de sites d'expériences en parallèle nécessaires à la caractérisation de la répartition des sédiments dans les lacs, de leurs concentrations d'éléments traces et de leurs vitesses d'accumulation. Un essai de cet algorithme avec les sédiments de 96 sites dans trois bassins du lac Jack (Ontario), de morphométrie complexe, démontre l'utilité de cette approche. L'application préalable de cet algorithme aurait permis de réduire le nombre de sites de notre grille d'échantillonnage de 96 à 22, soit une diminution de 77%, sans perte de précision. Cette réduction dans le nombre de sites d'échantillonnage (en plus des économies de temps et d'argent) permettrait l'échantillonnage d'autres lacs et de sites ayant une importance à l'échelle locale (p. ex., embouchures de rivière et de ruisseaux, sources ponctuelles de pollution), ou la mesure d'autres paramètres. La relation existant entre la morphométrie des lacs, la répartition et la texture des sédiments, de même que la relation entre la texture des sédiments et la variabilité observée dans un même site ou entre les sites peut également servir à l'extrapolation des caractéristiques des sédiments pour l'ensemble du lac à partir de quelques échantillons, ou encore à prédire la zone où les sédiments vont se déposer.

[Traduit par la Rédaction]

Introduction

Because sediment properties, such as water content, organic content, trace element concentrations, and sediment accumulation rates, are highly variable in lakes, the questions of the number of sites that should be sampled and the number of replicates needed at each site are critical to any sediment investigation. Some authors have sampled lakes on an extensive grid system (Thomas 1988; Thomas and Dell 1978; Cahill 1981; Kelderman et al. 1984; Hakanson and Ahl 1976), usually with only one core or grab at each site and without any formal basis for deciding a priori the spacing of the grid points or the number of replicates required for a specified precision at each point. Other authors have attempted to characterize lake sediments with only one or a few sites (Brenner and Binford 1988; Johnson 1987; Brunskill and Schindler 1971), thereby essentially ignoring spatial variation. Because most surveys suffer severe constraints of both time and money, the question of how to optimize sampling effort is a major one.

Hakanson (1984) and Downing and Rath (1988) outlined statistical guidelines for estimating the intrasite sampling effort required for a specified level of precision, while Hakanson (1992), Hakanson and Jansson (1983), and Dillon and Evans (1982) developed crude algorithms for determining the number of sites to sample on the basis of lake depth and other morphometric features. However, no statistically rigorous system for optimal allocation of intra- and inter-site sampling effort has been proposed to

Received July 14, 1994. Accepted May 11, 1995.
J12480

D.J. Rowan. Environmental Research, Atomic Energy of Canada Ltd., Chalk River Laboratories, Chalk River, ON K0J 1J0, Canada.
J.B. Rasmussen and J. Kalff. Department of Biology, McGill University, 1205 Dr. Penfield Avenue, Montreal, QC H3A 1B1, Canada.

date. Such a system would stimulate more benthic research and promote a systemic approach to the comparative analysis of sediment survey data.

Recent advances in lake sedimentology (Rowan et al. 1992*a*, 1992*b*) have identified some fundamental patterns in the distribution of lake sediments that can serve as the basis for an optimal sampling strategy. These include the prediction of the mud deposition boundary depth from site exposure and slope (Rowan et al. 1992*a*) and the prediction of sediment water content in the depositional zone from exposure and inorganic sedimentation rate (Rowan et al. 1992*b*). In the present paper, we present relationships between sediment water content and inter- and intra-site variability and demonstrate how these can be used for a priori decisions regarding the number of sites and replicates required for a specified level of precision. On the basis of these empirical developments, we first derive an algorithm that predicts the most likely patterns of sediment variation in a given lake from bathymetric and watershed parameters. We then test the algorithm with sediments from 96 sites in three distinct basins of Jack Lake, a morphometrically complex Ontario lake (Fig. 1).

Methods

To determine intra- and inter-site sediment variability, 161 sites in 31 Quebec and Ontario lakes were sampled, with 5–10 replicate cores or grabs per site for a total of 1268 cores and grabs. To test the predictive power of the sampling algorithm, regularly spaced sites in Brooks Bay (21 sites, 53 cores and grabs), Sharpe Bay (55 sites, 132 cores and grabs), and Williams Bay (20 sites, 51 cores and grabs) of Jack Lake, Ontario, were sampled along transects (Figs. 2*a*, 3*a*, and 4*a*). Sediment was sampled with a lightweight gravity corer fitted with 25-cm^2 Plexiglas core tubes at all but the coarsest sites, where penetration was impossible. At the latter sites, an Ekman grab was used. Two replicate cores were collected at cored sites, while at the other sites, three replicate grabs were taken. The surficial 2 cm of sediment was extruded from the core tubes or removed from the central portion of grab samples. Only sediment from undisturbed cores or grabs was retained. Sediment water content (as a percentage of the wet weight of the sample) was determined by drying at 60°C (Hakanson and Jansson 1983).

Exposure, or the circular integral of fetch (Rasmussen 1988), describes the lake area exposed or visible from a site and was determined from maps. Percent slope was determined from high-resolution echo-sounder transects oriented perpendicular to contours. The depth and location of each sampling site on a transect were determined from echo-sounder records.

Inorganic sedimentation rates (ISR; $g \cdot m^{-2} \cdot yr^{-1}$), important in the estimation of profundal sediment texture, were predicted from catchment inorganic sediment loads (Rowan et al. 1992*b*):

$$[1] \quad \log \mathrm{ISR} = 0.460 \log ((\mathrm{CISL} \times \mathrm{SRC})/(\mathrm{SA} \times \mathrm{DZ})) + 1.337$$

where CISL is the estimated inorganic sediment load ($g \cdot yr^{-1}$), SRC is the sediment retention coefficient (O'Connor 1988); SA is the lake surface area (m^2), and DZ is the depositional zone, or the fraction of the lake below the mud deposition boundary depth (Rowan et al. 1992*a*).

Fig. 1. Map of Jack Lake showing basins sampled.

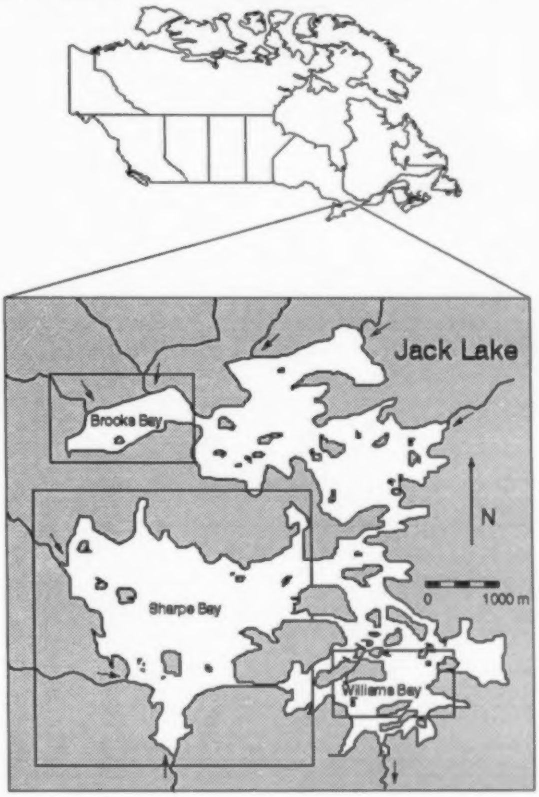

The catchment inorganic sediment load was estimated as (Rowan et al. 1991)

$$[2] \quad \mathrm{CISL} = [\mathrm{SED}] \times \mathrm{RO} \times \mathrm{DCA}$$

where [SED] is the mean suspended sediment concentration ($g \cdot m^{-3}$) of local stream water obtained from water-quality reports (Ontario Ministry of the Environment 1978, 1979), RO is the annual run-off ($m \cdot yr^{-1}$), and DCA is the direct catchment area (m^2), which excludes upstream lakes and their catchments.

Results

Applicability of the sampling algorithm

The first step in the sampling algorithm is to predict the mud deposition boundary depth (mud DBD, m) and compare it with lake maximum depth (h_{max}, m) (Fig. 5, step 1). The mud DBD represents the depth at which near-bottom wave velocity equals threshold velocity for 23-μm particles. Sediments with mean particle sizes of 23 μm (5.5 phi, phi = $-\log_2$ (particle size, mm)) or 60% water content mark the boundary between high-energy environments with coarse-grained, noncohesive sediments and lower energy transitional and depositional environments with fine-grained,

Fig. 2. (*a*) Bathymetric map of Brooks Bay showing transects and sites sampled. (*b*) Sediment distribution as predicted by mud DBD theory (■, correctly classified; ▲, misclassified).

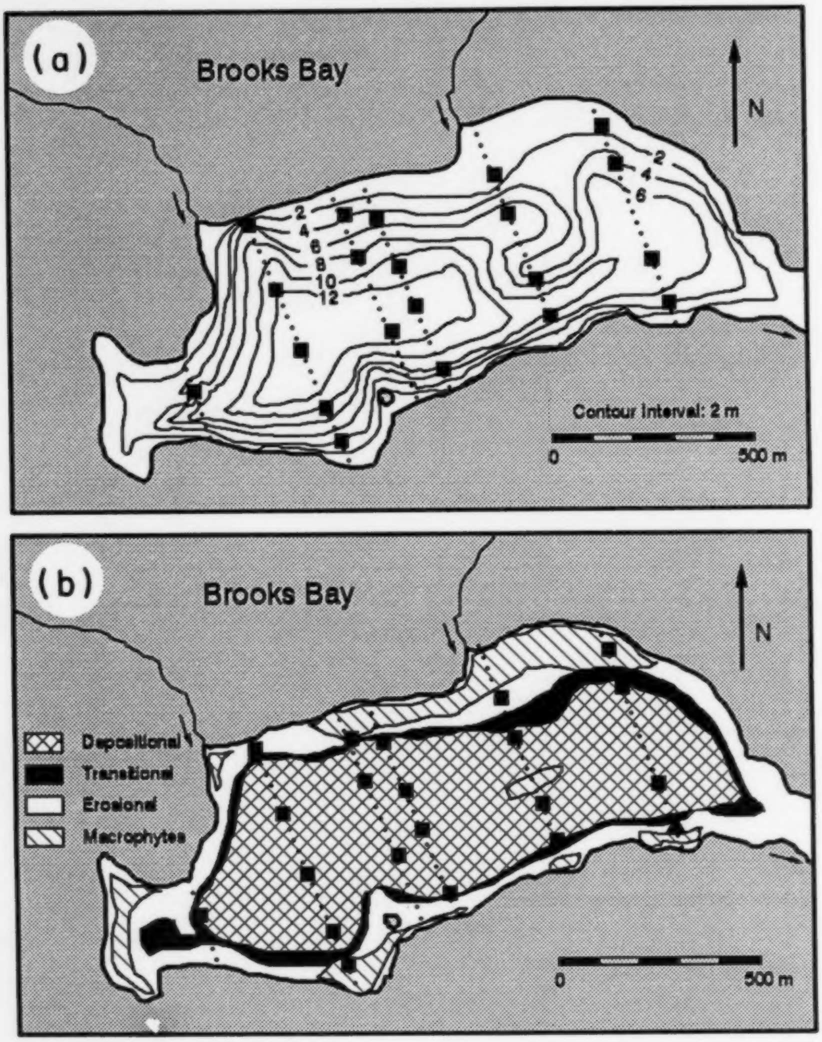

cohesive sediments (Rowan et al. 1992*a*). At maximum depth (or any site where slope is low), the mud DBD is predictable from the theory of waves and sediment thresholds (Rowan et al. 1992*a*):

$$\text{[3]} \qquad \text{mud DBD} = 2.685\ E^{0.305}$$

where E is exposure (km^2).

If the mud DBD estimated from midlake or basin exposure is less than the maximum depth, then the algorithm is applicable. If the mud DBD is greater than the maximum depth, then sediment resuspension is possible over the entire lake bottom. In such lakes, sediment distribution is not controlled by waves, and the sampling algorithm is not applicable unless outflow is sufficient to remove all resuspended fine particles. Other lakes where the algorithm does not apply include lakes dominated by macrophytes that baffle wave energy or lakes with such an extremely high sediment supply that it overwhelms wave energy (McCave 1971; Stanley et al. 1983), because in these situations, wave energy does not directly control sediment distribution.

Predicting sediment distribution

Once the applicability of the algorithm to the lake or basin has been determined, the next step is to predict the distribution of sediments in these lakes or basins from bathymetric maps (Fig. 5, step 3). The erosional zone is found at depths shallower than the mud DBD, i.e., at depths

Fig. 3. (*a*) Bathymetric map of Sharpe Bay showing transects and sites sampled. (*b*) Sediment distribution as predicted by mud DBD theory (■, correctly classified; ▲, misclassified).

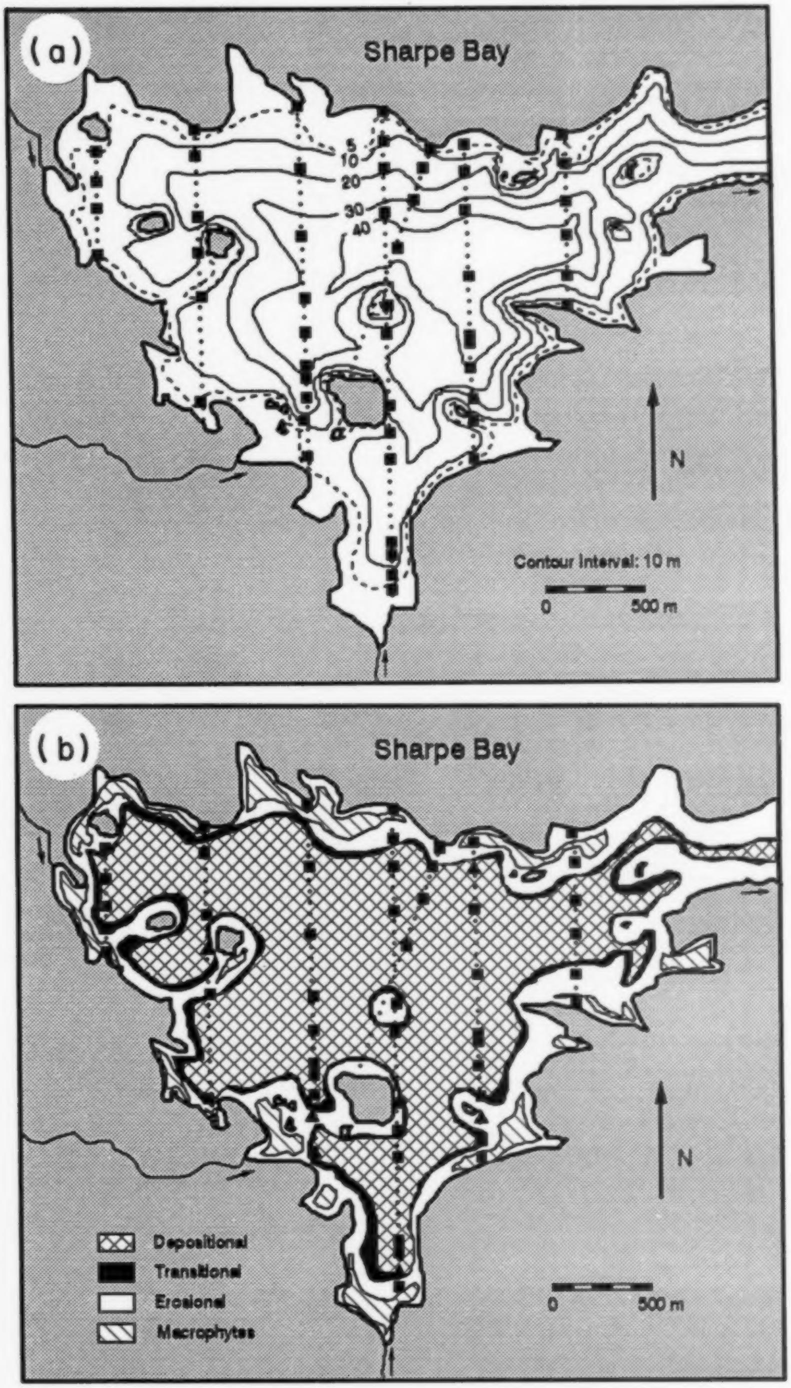
(a)
Sharpe Bay
5
10
20
30
40
N
Contour Interval: 10 m
0
500 m
(b)
Sharpe Bay
Depositional
Transitional
Erosional
Macrophytes
N
0
500 m

Fig. 4. (*a*) Bathymetric map of Williams Bay showing transects and sites sampled. (*b*) Sediment distribution as predicted by mud DBD theory (■, correctly classified; ▲, misclassified).

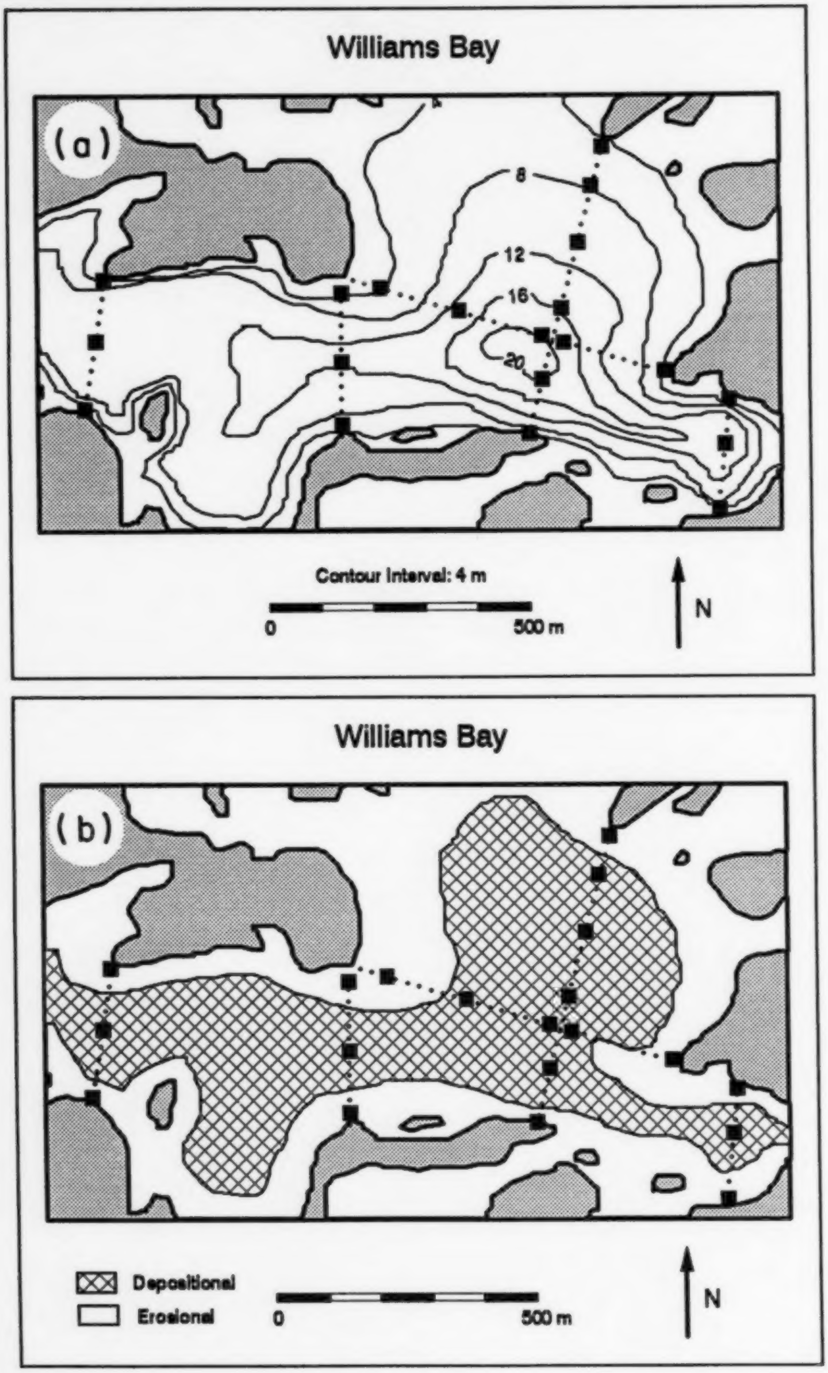
Williams Bay
(a)
8
12
16
20
Contour Interval: 4 m
0
500 m
N
Williams Bay
(b)
Depositional
Erosional
0
500 m
N

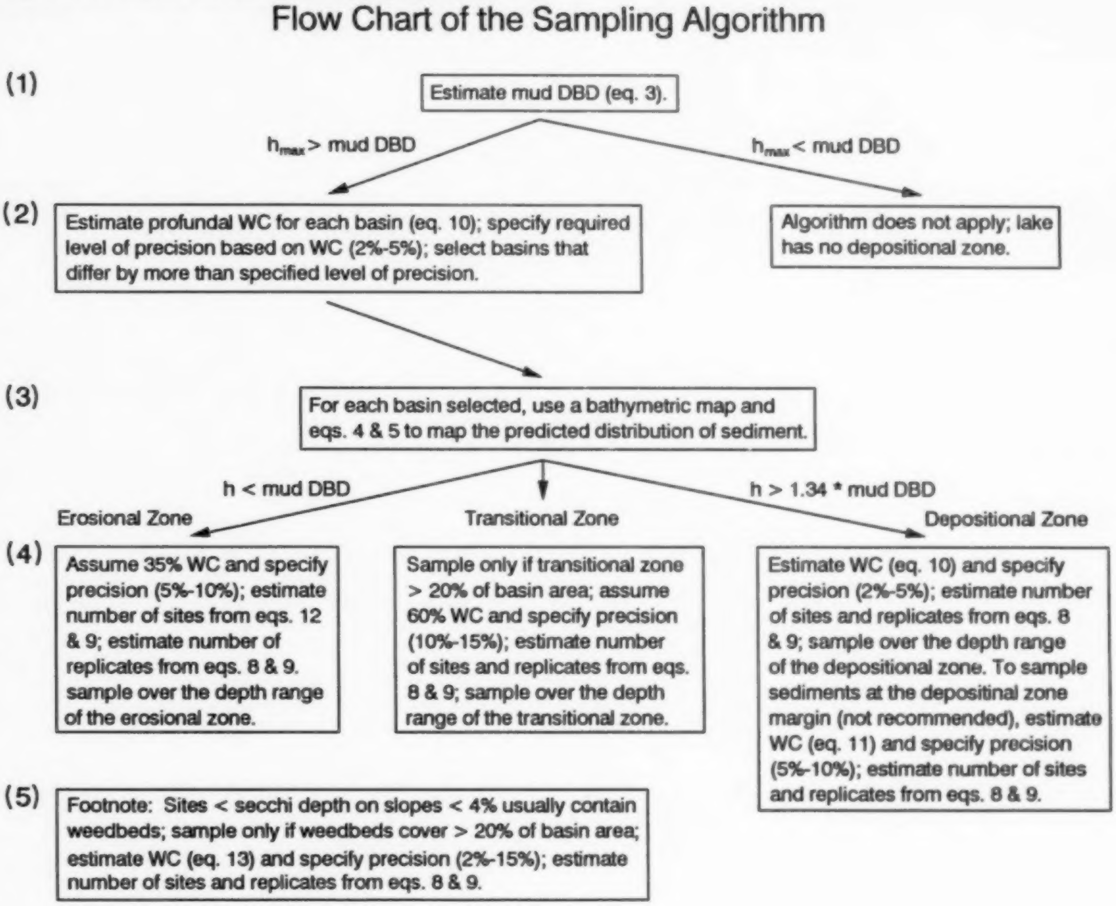

Fig. 5. Flow chart of the sediment sampling algorithm.

Flow Chart of the Sampling Algorithm
(1)
Estimate mud DBD (eq. 3).
h_{max} > mud DBD
h_{max} < mud DBD
(2)
Estimate profundal WC for each basin (eq. 10); specify required level of precision based on WC (2%-5%); select basins that differ by more than specified level of precision.
Algorithm does not apply; lake has no depositional zone.
(3)
For each basin selected, use a bathymetric map and eqs. 4 & 5 to map the predicted distribution of sediment.
h < mud DBD
h > 1.34 * mud DBD
Erosional Zone
Transitional Zone
Depositional Zone
(4)
Assume 35% WC and specify precision (5%-10%); estimate number of sites from eqs. 12 & 9; estimate number of replicates from eqs. 8 & 9. sample over the depth range of the erosional zone.
Sample only if transitional zone > 20% of basin area; assume 60% WC and specify precision (10%-15%); estimate number of sites and replicates from eqs. 8 & 9; sample over the depth range of the transitional zone.
Estimate WC (eq. 10) and specify precision (2%-5%); estimate number of sites and replicates from eqs. 8 & 9; sample over the depth range of the depositional zone. To sample sediments at the depositinal zone margin (not recommended), estimate WC (eq. 11) and specify precision (5%-10%); estimate number of sites and replicates from eqs. 8 & 9.
(5)
Footnote: Sites < secchi depth on slopes < 4% usually contain weedbeds; sample only if weedbeds cover > 20% of basin area; estimate WC (eq. 13) and specify precision (2%-15%); estimate number of sites and replicates from eqs. 8 & 9.

where the largest annual storm is capable of transporting fine-grained particles (Rowan et al. 1992*a*). The transitional zone is intermittently affected by less frequent storms (up to 1.34 times more severe than annual storms), and the depositional zone lies at depths beyond the effects of waves (Rowan et al. 1992*a*). The mud DBD can be predicted as the greater of

[4] $\log \text{mud DBD} = 0.429 + 0.305 \log E$

which includes no slope effect, or

[5] $\log \text{mud DBD} = 0.123 + 0.370 \log E + 0.0526S$

which includes a slope effect, where S is the percent slope (Rowan et al. 1992*a*). Erosional sites are found at depths shallower than the mud DBD, depositional sites are found at depths greater than 1.34 times the mud DBD, and transitional sites are intermediate.

A comparison of the mud DBD and site depth allows for the classification of sites as erosional (water content less than 60%), transitional (water content more than 60% but less than in depositional sites), or depositional (water content more than 60%). In this manner, the predicted distribution of sediments within a lake can be mapped prior to sampling.

Number of sites and replicates required

Now that the distribution of sediments has been mapped, the next step is to select the sample sites and the number of replicates required at each site (Fig. 5, step 4). First, however, we will develop inter- and intra-site mean–variance relationships for sediment water content, show how these can be used to predict sample size for a given sediment water content and precision, and then provide models that predict sediment water content within the various sedimentary environments along with guidelines for sampling effort.

We chose water content (percentage of wet weight) as a measure of sediment texture, because we can predict it (Rowan et al. 1992*b*). Lake sedimentary environments are largely depositional and water content provides an integrative measure of many properties of cohesive sediments (Hakanson 1977; Fukada and Lick 1980; McCave 1984). Water content is also highly correlated with sediment metal concentrations and organic matter (Rowan and Kalff 1993).

Table 1. The number of sites required for a specified level of intersite precision as a function of sediment water content (WC) (estimated from eq. 9).

WC	Precision (%)					
(% wet wt)	1	2	3	5	10	15
95	8	4	3	3	2	1
90	18	5	4	3	2	2
85	41	12	7	4	3	3
80	90	25	12	6	3	3
75	173	46	22	9	4	3
70	298	77	35	14	6	4
65	450	115	52	20	7	4
60	593	149	68	26	8	5

Table 2. The number of replicates required for a specified level of intrasite precision as a function of sediment water content (WC) (estimated from eq. 9).

WC	Precision (%)					
(% wet wt)	1	2	3	5	10	15
95	5	3	3	2	1	1
90	9	4	3	3	2	1
85	19	7	4	3	3	2
80	40	12	7	4	3	3
75	76	21	11	5	3	3
70	128	34	17	8	4	3
65	193	51	24	10	5	3
60	254	66	30	12	5	4
35	136	37	18	8	4	3

Inter- and intra-site variance in sediment WC

Plots of the logarithms of inter- and intra-site variance in sediment water content versus mean sediment water content have parabolic shapes (Figs. 6*a* and 6*b*), with low variance within the low water content (<60% wet weight) and high water content (>60% wet weight) zones, and with maximum variance in the transitional zone (around the mud DBD). We regressed these data using a polynomial of sediment water content (WC) and obtained the following:

$$[6] \quad \log \text{intersite variance} = -1.282(1.115) + 0.125(0.040)\text{WC} - 0.001\,23\,(0.000\,32)\,\text{WC}^2$$
$$r^2 = 0.490,\ \text{SE}_{\text{est}} = 0.868,\ n = 53$$

and

$$[7] \quad \log \text{intrasite variance} = -1.992(0.429) + 0.124(0.014)\text{WC} - 0.001\,17\,(0.000\,11)\,\text{WC}^2$$
$$r^2 = 0.653,\ \text{SE}_{\text{est}} = 0.509,\ n = 161$$

The coefficients of these regressions do not differ significantly, so we combined the two data sets and added a categorical variable (intersite) equal to 1 for intersite variance and 0 for intrasite variance and obtained the following:

$$[8] \quad \log \text{inter- or intra-site variance} = -1.793(0.433) + 0.368(0.098)\text{intersite} + 0.121(0.015)\text{WC} - 0.001\,16\,(0.000\,12)\,\text{WC}^2$$
$$r^2 = 0.599,\ \text{SE}_{\text{est}} = 0.616,\ n = 214$$

These regressions can be used to predict inter- or intrasite variance as a function of sediment water content and suggest that intersite variance is about twice as great as intrasite variance.

Estimating sample size from water content and inter- and intra-site variance

The sample size (n) required for a specified level of precision in sediment water content (δ; percentage of wet weight) can be estimated as a function of variance (eqs. 6 and 7, or 8) in sediment water content (s^2, percentage of wet weight):

$$[9] \quad n = \frac{s^2}{\delta^2}(t_{\alpha,\nu} + t_{\beta,\nu})^2$$

We performed two-tailed tests, accounting for both type 1 and type 2 errors, and conservatively set $\alpha = \beta = 0.05$ (Peterman 1990). Few authors have accounted for type 2 errors or maintained high power ($1 - \beta$), even though this is critical to many investigations, especially sampling design (Peterman 1990). Equation 9 is summarized for various levels of precision in Tables 1 and 2 to illustrate the relationship.

Predicting sediment water content and sampling effort

Depositional zone

In a previous study (Rowan et al. 1992*b*), we demonstrated that the water content of lake sediments within the depositional zone is determined by *E* and ISR. Lakes or basins with low *E* and low ISR have sediments with the greatest water content. Thus, if exposure and ISR are variable among basins within a lake, sediment texture within the depositional zone should also be variable. With midlake or basin *E* (or lake area if morphometry is simple) and ISR (as estimated by eq. 1), depositional sediment water content (percentage of wet weight) can be estimated as (Rowan et al. 1992*b*):

$$[10] \quad \text{WC} = 102.657 - 5.326 \log \text{ISR} - 2.314 \log E$$

Using the depositional-zone water contents predicted by eq. 10, and the relationships between inter- and intra-site variability (eqs. 6 and 7, or 8), it is possible to estimate the number of sites and replicates required for a specified level of precision (eq. 9; Tables 1 and 2). With four sites and three replicates, the sediment water content of shield lakes (depositional water contents near 95%) can generally be characterized with a precision of 2%. Lakes with catchments of sedimentary rocks (depositional water contents near 90%) require five sites and four replicates for a precision of 2%. Seven to nine sites and four or five replicates are required for precisions of 3–5% in lakes with high *E* or ISR (depositional water contents near 80%). Although we recommend no more than 10 sites with five replicates in the depositional zone to optimize sampling effort, precision can be modestly increased with additional replicates and sites. In our data set, a few lakes (Brome, Orford, and Memphremagog) showed variation in sediment water content within the depositional zone related to depth; therefore, we recommend sampling over the range in depths found within the depositional zone.

Depositional zone margins

At the margin of the depositional zone, usually at the base of steep slopes, and within 2 m of the depth of the slope break, sediment water contents are often intermediate between depositional and transitional zones. If these sediments are of interest, sediment water content can be estimated from the following regression derived from the mean marginal and depositional water contents (percentage of wet weight) of 10 lakes:

[11] $$\text{marginal WC} = -15.892(26.388) + 1.088\ (0.293)\ \text{depositional WC}$$
$$r^2 = 0.633,\ \mathrm{SE}_{\mathrm{est}} = 2.913,\ n = 10$$

With water contents of these marginal sites generally ranging from 70 to 80%, precisions of 10% can be achieved with four sites and three replicates (eqs. 10, 11, 6 and 7 or 8, and 9; Tables 1 and 2) (Fig. 5, step 4). Although more effort could be expended on these sediments, they are generally spatially restricted and highly variable because of slope transport processes, and sampling effort could be used more effectively elsewhere.

Transitional zone

The transitional zone (sediment water content of about 60%) should be sampled only if substantial areas of the basin are transitional (>20%). Because of extremely high variability within this zone, precise characterization of sediments is difficult if not impossible (Tables 1 and 2). Therefore, if this zone is sampled, assume a water content of 60%, estimate variance (eqs. 6 and 7, or 8), specify precision, and estimate the number of samples and replicates required. We recommend no more than five sites with four replicates for a precision of 15% (Fig. 5, step 4).

Erosional zone

Erosional zone sediments (sand) vary little in water content among lakes (mean 35.0%, SD = 5.1, n = 17), and this variation is not predictable. Obviously, if we used this mean value in eqs. 6 or 8 to estimate intersite variance, we would obtain the same value for all lakes. However, we hypothesized that erosional zone intersite variance should be a function of the complexity of this environment. One means of quantifying this complexity is through the mean mud DBD. If the mean mud DBD is shallow, then the lake is small and has a restricted depth range for its erosional environments. If the mean mud DBD for a lake is deep, then either the lake is large or it has steep slopes and is deep for its size. In either of the latter cases, there is a greater range in depth of the erosional zone and a greater probability of complexity and increased variance. We tested this hypothesis by regressing the intersite variance of erosional zone sediment water contents versus the mean mud DBD and obtained the following:

[12] $$\log \text{intersite variance} = -1.401(0.658) + 1.975\ (0.432) \log \text{mean mud DBD}$$
$$r^2 = 0.617,\ \mathrm{SE}_{\mathrm{est}} = 0.530,\ n = 15$$

The number of erosional sites to sample can now be estimated from the mean mud DBD and a suggested precision of 10% (eqs. 12 and 9). The number of replicates can be estimated from the intrasite variance for a water content of 35% and a suggested precision of 10% (eqs. 7 or 8, and 9). A precision of 10% requires four replicates per site (Table 2).

Weed beds

Although mud DBD theory does not apply to weed beds, sites less than the Secchi depth with slopes less than 4% usually contain weed beds (Duarte and Kalff 1986). Thus, predictions of weed bed distribution can be added to the sediment distribution map. A regression of the mean water content of weed bed sediment versus the mean water content of the depositional zone for eight lakes yields the following:

[13] $$\text{weed bed WC} = -260.579(68.204) + 3.682(0.740)\ \text{depositional zone WC}$$
$$r^2 = 0.805,\ \mathrm{SE}_{\mathrm{est}} = 8.587,\ n = 8$$

Using the predicted depositional zone water content (eq. 10), weed bed water contents can be predicted (eq. 13), inter- and intra-site variance can be estimated (eqs. 6 and 7, or 8), precision can be specified, and finally the number of sample sites and replicates can be calculated (eq. 9). Unless weed beds cover more than 20% of the lake area, we do not recommend sampling their sediments.

Multibasin or multilake surveys

If a sediment study involves a number of lakes within a region or a multibasin lake, a decision regarding which of the lakes or basins to sample must inevitably be made. We propose the use of predicted depositional zone sediment water contents (Rowan et al. 1992*b*) and mean–variance relationships to estimate sample size for a specified precision, with basins or lakes that differ in predicted depositional sediment water content by more than the specified level of precision selected for sampling (Fig. 5, step 2).

Predictions of the sampling algorithm: Jack Lake

With the algorithm (summarized in Fig. 5), a priori decisions can be made regarding precision, replication, and number of sample sites from only lake morphometry and catchment characteristics. We next provide a test of the algorithm with sediments from a multibasin lake.

Jack Lake, an oligo-mesotrophic Canadian Shield lake, typical of many in eastern Canada, has complex morphometry and bathymetry, and consists of several distinct basins (Figs. 1, 2*a*, 3*a*, and 4*a*). Its complexity makes it a suitable candidate for examining the predictive power of the sampling algorithm. The three basins selected to test the sampling algorithm include the largest and deepest (Sharpe Bay); one of the smaller, shallower basins (Brooks Bay), which receives the major sediment input via rivers; and the terminal basin (Williams Bay) (Figs. 1, 2*a*, 3*a*, and 4*a*, Table 3).

The first step in the sampling algorithm (Fig. 5) requires exposures to estimate the midlake mud DBD (eq. 3). Exposures determined from maps for midlake sites (Figs. 2*a*, 3*a*, and 4*a*) were used to estimate mud DBDs for each basin (Table 3). A comparison of mud DBDs (eq. 3) and

Table 3. Morphometry and catchment characteristics of the three basins of Jack Lake sampled for this study.

Basin	Sites	SA (km^2)	E (km^2)	Mud DBD (m)	h_{mean} (m)	h_{max} (m)	CA (km^2)	WRES (yr)	ISR (g·m^{-2}·yr^{-1})
Brooks Bay	21	0.93	0.82	2.5	6.0	13.6	24.7	0.58	59
Sharpe Bay	55	5.13	3.13	3.8	16.9	46.1	13.0	14.75	18
Williams Bay	20	2.10	0.86	2.6	12.2	21.9	79.5	0.84	10

Note: SA is surface area, E is midlake exposure, mud DBD is from eq. 3, h_{mean} is mean depth, h_{max} is maximum depth, CA is catchment area, WRES is water residence time, and ISR is predicted inorganic sedimentation rate (eq. 1).

Table 4. Classifications of mud DBD theory (eqs. 4 and 5) compared with the observed distribution of sediments in Jack Lake.

Basin	Erosional	Transitional	Marginal	Depositional
Brooks Bay	67% (2/3)	100% (3/3)	100% (5/5)	100% (7/7)
Sharpe Bay	90% (18/20)	— (0/0)	100% (5/5)	88% (24/28)
Williams Bay	100% (11/11)	— (0/0)	— (0/0)	100% (9/9)
Total	91% (31/34)	100% (3/3)	100% (10/10)	91% (40/44)

Note: Five sites classified as erosional by mud DBD theory contained weed beds (see Fig. 5).

maximum depths (Table 3) shows that these basins are considerably deeper than their mud DBDs and therefore the algorithm is appropriate.

The next step is to predict depositional zone sediment-water content, specify precision, and determine which basins to sample (Fig. 5, step 2). However, to test the algorithm, we had already decided to sample all three basins and went straight to the third step: predicting sediment distribution. Mud DBDs were determined from exposure and slope (eqs. 4 and 5) for each basin by using the bathymetric maps (Figs. 2*a*, 3*a*, and 4*a*). In this manner, predicted sediment distribution was mapped for the three basins (Figs. 2*b*, 3*b*, and 4*b*). Mean mud DBDs for these Jack Lake basins are 6.6 m in Brooks Bay, 17.6 m in Sharpe Bay, and 10.3 m in Williams Bay.

The fourth step of the sampling algorithm (Fig. 5) involves predicting sediment water contents, specifying precision, and estimating the number of sites and replicates required. Predicted water contents are summarized in Table 5. If we had wanted to optimize our sampling effort by using the algorithm, we would have specified a precision of 2% for depositional zone sediments and 10% for erosional zone sediments. This would have resulted in four depositional zone sites with three replicates for each basin, three erosional zone sites with four replicates at Brooks and Williams bays, and four sites with four replicates at Sharpe Bay. No marginal, transitional, or weed bed sites would have been selected, because each of these regions occupies 12% or less of the sedimentary environments in these basins.

However, to evaluate the performance of the algorithm relative to sampling a complete grid, it was necessary to sample more extensively. Because of the large number of grid points to sample (96), we decided to sacrifice some intrasite precision by reducing the number of intrasite replicates to two at depositional zone sites and to three at erosional zone sites, for a total of 236 cores and grabs. The result is an estimated intrasite precision of 6.6% for depositional sites at Brooks Bay, 5.6% at Sharpe Bay, and 4.1% at Williams Bay. For erosional zone sites, the three replicates result in an estimated intrasite precision of 13.5%. As it makes no sense to have higher intersite than intrasite precision, the number of sites would have been reduced to two depositional zone sites per basin, two erosional zone sites in Brooks Bay, and three erosional zone sites in Sharpe and Williams bays. With this sampling effort, depositional zone intersite precisions were estimated at 10.1% for Brooks Bay, 8.5% for Sharpe Bay, and 6.3% for Williams Bay. Erosional zone intersite precisions would be reduced to 17.1% for Brooks Bay, 14.0% for Sharpe Bay, and 8.4% for Williams Bay.

Performance of the sampling algorithm: Jack Lake

It is now possible to evaluate the predictive performance of the sampling algorithm. A fair test of the ability of the algorithm to predict sediment distribution (Fig. 5, step 3) would be to suppose that we had randomly sampled sites in the erosional, transitional, marginal, and depositional zones, and compare the observed with predicted sediment distribution. If we had sampled any of the grid points above the mud DBD (excluding weed beds), we would have encountered erosional zone sediments at 91% of the sites (Table 4, Figs. 2*b*, 3*b*, and 4*b*). All of the transitional and marginal sites were correctly classified. Sampling below the mud DBD in the depositional zone would have resulted in low-energy sediments at 91% of the sites (Table 4, Figs. 2*b*, 3*b*, and 4*b*). Thus, the algorithm correctly predicts the sediment distribution of Jack Lake at 91% of the grid points.

The prediction of sediment water content is critical to the algorithm, because the prediction of inter- and intra-site variance depends on it. The observed water contents of

Table 5. Observed and predicted mean sediment water content (percentage of wet weight) for the weed bed (eq. 13), erosional, transitional, marginal (eq. 11), and depositional (eq. 10) zones.

	Weedbed		Erosional		Transitional		Marginal		Depositional	
Basin	Obs.	Pred.	Obs.	Pred.	Obs.	Pred.	Obs.	Pred.	Obs.	Pred.
Brooks Bay	79.5	83.3	37.0	35.0	65.4	60.0	78.8	85.7	93.4	93.4
Sharpe Bay	78.5	88.8	31.7	35.0	—	60.0	86.4	87.4	95.4	94.9
Williams Bay	—	98.4	35.3	35.0	—	60.0	—	90.2	97.3	97.5

Note: None of the differences between observed and predicted values are statistically significant.

Table 6. A comparison of observed and predicted intra- and inter-site precision in sediment water content (percentage of wet weight) for sites selected according to the algorithm.

	Erosional zone precision				Depositional zone precision			
	Intrasite		Intersite		Intrasite		Intersite	
Basin	Obs.	Pred.	Obs.	Pred.	Obs.	Pred.	Obs.	Pred.
Brooks Bay	18.8	13.5	14.0	17.1	14.6	6.6	5.4	10.1
Sharpe Bay	17.2	13.5	51.9	14.0	5.6	5.6	0.0	8.5
Williams Bay	33.1	13.5	—	—	2.4	4.1	9.3	6.3

Note: None of the observed values are significantly different from the predictions.

Jack Lake sediments are compared with the predictions in Table 5. None of the predictions differ significantly from the observed means.

Thus, if the inter- and intra-site variances observed for Jack Lake are within the confidence bands of the variance regressions (eqs. 6 and 7, or 8), then the algorithm will have performed properly, i.e., within its statistical limitations. Plots of inter- and intra-site variance versus water content with the 95% confidence interval of eq. 8 are presented in Fig. 7. As we used eq. 12 to predict intersite variance for the erosional zone, the predictions of eq. 12 (±2 SE_{est}) are shown in Fig. 7*a* for Brooks and Sharpe bays (in Williams Bay, sediments were found at only 1 of 11 erosional zone sites; the remaining sites had bedrock or cobble bottoms that could not be sampled with an Ekman grab). These plots show that inter- and intra-site sediment variances at Jack Lake are in excellent agreement with the model predictions. In fact, a regression of these data is not significantly different from that obtained from the multilake data set, except that the categorical variable is marginally insignificant:

$$[14]\quad \log \text{inter- or intra-site variance} = -1.803(0.698) + 0.500(0.315)\text{intersite} + 0.133(0.026)\text{WC} - 0.001\,31\,(0.000\,21)\,\text{WC}^2$$

$$r^2 = 0.571,\ SE_{est} = 0.929,\ n = 87$$

The final tests of the algorithm are whether the predicted inter- and intra-site precisions, and mean basin water contents would have been obtained by sampling the range in depths found within the depositional and erosional zones. For this aspect of the algorithm performance, we selected the deepest and shallowest of the depositional zone sites, the two erosional zone sites in Brooks Bay and the shallowest, mean, and deepest erosional zone sites in Sharpe Bay. The observed and predicted intra- and inter-site precisions for this sampling effort are given in Table 6. Although some of the observed precisions are higher than the predictions, none of these differences are statistically significant.

Brooks Bay is shallow (mean depth of 6 m), and only seven of the grid sites have true depositional sediments, all more than 1 m below the depositional zone margin (Fig. 8, Table 4). At these sites, there are significant intersite differences in water content ($p < 0.001$) uncorrelated with depth (Fig. 8). Sampling at maximum depth and at the shallowest depositional site would have yielded a mean water content (93.0%) that is not significantly different from the grid mean (93.4%). As only two erosional sites were sampled on the grid, we cannot compare the algorithm's performance on erosional zone water content.

Sharpe Bay, with much greater depth, has a higher proportion of depositional sites, all more than 1 m below the depositional zone margin. Intersite variation for depositional sites is significant ($p < 0.0001$), and is weakly positively correlated with depth below 1.34 times the mud DBD ($r^2 = 0.26$; Fig. 8). The mean water content at maximum depth and the shallowest depositional site (95.4%) is identical to the grid mean (95.4%). The mean water content (28.6%) at the three erosional zone sites (shallowest, deepest, and intermediate) is not significantly different from the grid mean (31.7%).

There are significant intersite differences in the water content of Williams Bay depositional zone sediments ($p < 0.025$) that are positively correlated with depth below

Fig. 6. Plots of intersite (*a*) and intrasite (*b*) variance in sediment water content versus site mean sediment water content. Variance maxima occur within the transitional zone (water contents near 60%). The lines are from eqs. 6 (*a*) and 7 (*b*).

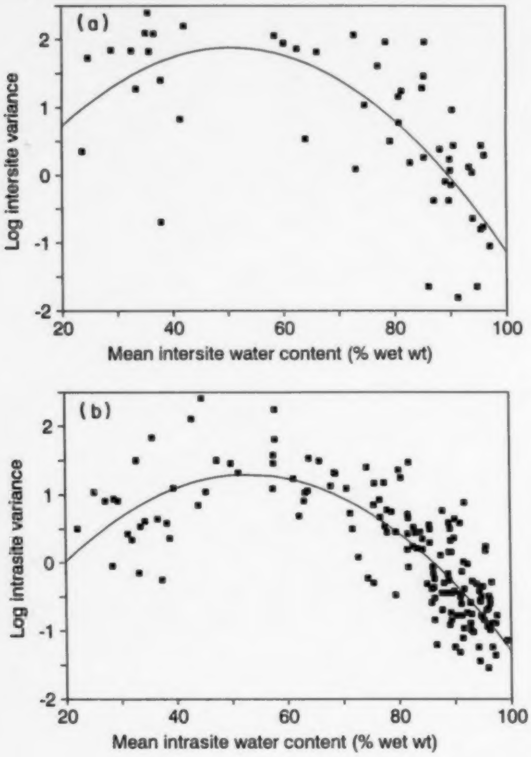

Fig. 7. Observed intersite (*a*) and intrasite (*b*) variance of Jack Lake sediments plotted versus mean sediment water content. In *a*, the predictions of eq. 12 (±2 SE_{est}) are plotted for erosional sites in Sharpe and Brooks bays. The curves are the 95% confidence bounds of eq. 8. The observed variances are in excellent agreement with the predictions of eqs. 8 and 12.

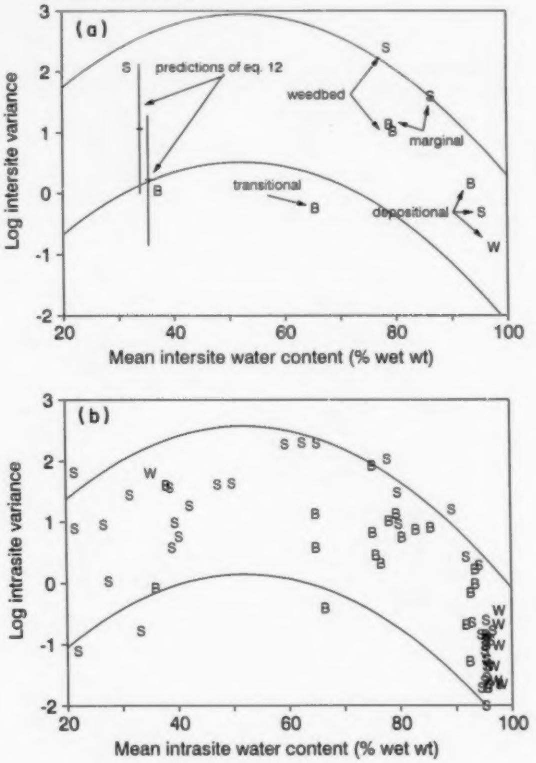

1.34 times the mud DBD ($r^2 = 0.80$; Fig. 8). However, sampling at maximum depth and the shallowest depositional zone site would have resulted in an observed water content (97.3%) identical to the grid mean (97.3%).

The decision to avoid sampling weed bed, transitional, and marginal sites is also supported by the results of this study. Even though we can predict the spatial distribution of these sediments (Table 4), estimate sediment water content fairly well (Table 5), and estimate inter- and intrasite variance within the limitations of the regressions (Fig. 7), the variability within these environments precludes precise determinations of sediment water content. This is particularly true for Sharpe Bay (Fig. 6), where weed bed and marginal inter- and intra-site variance lies near the upper bound of the regression (eq. 8).

High variance in environments marginal to the depositional zone is expected because slope transport processes lead to mixtures of coarse and fine particles dependent on upslope deposits and their stability. These sediments, along with transitional sediments, form a very narrow zone, often only several metres wide, between true depositional and erosional sediments (Fig. 8). Weed beds can be exceedingly complex sedimentary environments, dependent on the density and growth forms of plants and their resultant effect on wave energy. It is possible within a single weed bed to have bottoms composed of patches of sand, mud, and organic debris. Characterization of these environments with any degree of precision involves a substantial effort, unwarranted unless these environments predominate or are of particular significance to an investigation.

Thus, the algorithm provides an accurate sampling guide for Jack Lake sediments. The models upon which it is based accurately describe the distribution, water content, and variance of the sediments of Jack Lake.

Discussion

We have developed and tested an algorithm requiring only bathymetric and catchment parameters that can be used to optimize sampling effort in lake sediment surveys. We could have avoided sampling 77% of the sites on our Jack Lake grid without losing any precision. The savings in time and money would have allowed for the sampling of additional lakes or measurement of additional parameters.

The models on which this algorithm is based are likely applicable to most lakes, having been derived from large, multilake data sets that in many cases cover the spectrum from very small Canadian Shield lakes to the Laurentian Great Lakes (eqs. 1, 3–5, 10, and 12) or from very small Canadian Shield lakes to Lake Memphremagog (90 km^2) (eqs. 6–8, 11, and 13).

It is highly likely that similar reductions in site numbers could have been obtained by others had they applied this type of rationale prior to sampling their lakes on grids. For example, Lake Superior was sampled on a grid with 379 sites (Cook 1975). Mud DBD theory classifies 85 sites as erosional, 31 as transitional, and 263 as depositional. The lake has nine distinct depositional basins (Thomas and Dell 1978) and according to the sampling algorithm, a precision of 2% could be obtained by sampling six depositional sites with four replicates in each basin. No transitional sites would have been selected, as the transitional zone occupies less than 10% of the lake area. With a mean mud DBD of 131 m, 79 erosional sites with four replicates per site (10% precision) would have been selected. Consequently, the total number of sites selected with the algorithm would be approximately 133 (54 depositional and 79 erosional sites) for a reduction of 65%. The reduction is greatest for depositional sites (79%), with a modest decrease for erosional sites (7%). Even if local questions had been at issue (e.g., point source inputs of contaminants), sampling on the grid was far from cost effective. The dramatic reductions in the number of redundant depositional sites could have been used to more intensively sample areas proximal to known pollution point sources or other inshore areas of greater local significance (e.g., river and creek mouths) that, despite the heavy grid sampling regime, were completely neglected in the Great Lakes surveys.

In addition, Robbins (1980) collected sediments from 62 sites in southern Lake Huron and analyzed them for a variety of trace elements. Mud DBD theory classifies 8 of the sites as depositional, 15 as transitional, and 39 as erosional. If the sampling algorithm (Fig. 5) had been followed prior to sampling, 23 erosional sites with four replicates (10% precision), 5 transitional sites with four replicates (15% precision), and 6 depositional sites with four replicates (10% precision) would have been sampled. This represents a significant reduction (45%) in the number of sites sampled. For the elements Cu, Fe, Pb, and Zn, variation is less than 15% about the mean at the depositional sites defined by mud DBD, whereas the transitional and erosional zones are much more variable, with over an order of magnitude variation in the concentration of these elements. Thus, once the depositional zone is defined by mud DBD theory, there is little variation in sediment elemental composition.

At the opposite extreme, many authors have sampled at only one site (often with no replicates) per basin, usually near the maximum depth. Although this may be useful in comparative studies, within-lake variation is completely ignored, and even within the depositional zone, precision will be low. In addition to poor precision, extrapolations from a single depositional zone core in mass balances of nutrients, contaminants, or particulate matter will be further compromised without accurate estimates of the areal extent of the depositional zone.

Fig. 8. Site depth relative to the mud DBD versus sediment water content for depositional, marginal depositional, and transitional sites. Marginal depositional sites, all less than 1 m below the mud DBD, are highly variable, with much less variation at sites from greater depths. Depositional sediments from both Sharpe and Williams bays show slight, but statistically significant, increases in sediment water content with site depth.

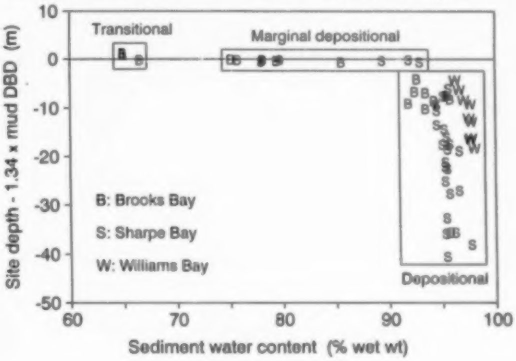

In a recent study, Rowan et al. (1995) found undisturbed ^{210}Pb profiles in cores from the depositional zone below the mud DBD, with disturbed ^{210}Pb profiles in cores from the transitional and erosional zones. Although variation in sediment accumulation rates within the depositional zone are small and unrelated to depth, 5–10 cores are still necessary for reasonable precision. In another study, Stephenson et al. (1995) found that ^{14}C accumulation in lakes in the Experimental Lakes Area could also be explained in terms of mud DBD theory. These results suggest that mud DBD theory can account for the effects of sediment focusing, i.e., the depositional zone defined by mud DBD theory is the zone to which fine-grained sediments are focused. Thus, in addition to optimizing sampling effort, prediction of the depositional zone from the sampling algorithm may greatly simplify extrapolations and interpretations from sediment cores.

Acknowledgements

We thank D.R.S. Lean for use of the Jack Lake field station during sampling and P.A. White and S. Lamontagne for field assistance.

References

Brenner, M., and M.W. Binford. 1988. Relationships between concentrations of sedimentary variables and trophic state in Florida lakes. Can. J. Fish. Aquat. Sci. 45: 294–300.

Brunskill, G.J., and D.W. Schindler. 1971. Geography and bathymetry of selected lake basins, Experimental Lakes Area, northwestern Ontario. J. Fish. Res. Board Can. 28: 139–155.

Cahill, R.A. 1981. Geochemistry of recent Lake Michigan sediments. Ill. State Geol. Surv. Circ. No. 517.

Cook, D.G. 1975. A preliminary report on the benthic macroinvertebrates of Lake Superior. Fish. Res. Board Can. Tech. Rep. No. 572.

Dillon, P.J., and R.D. Evans. 1982. Whole-lake lead burdens in sediments of lakes in southern Ontario, Canada. Hydrobiologia, 91: 121–130.

Downing, J.A., and L.C. Rath. 1988. Spatial patchiness in the lacustrine sedimentary environment. Limnol. Oceanogr. 33: 447–458.

Duarte, C.M., and J. Kalff. 1986. Littoral slope as a predictor of the maximum biomass of submerged macrophyte communities. Limnol. Oceanogr. 31: 1072–1080.

Fukada, M.K., and W.J. Lick. 1980. The entrainment of cohesive sediments in freshwater. J. Geophys. Res. 85: 2813–2824.

Hakanson, L. 1977. The influence of wind, fetch, and water depth on the distribution of sediments in Lake Vanern, Sweden. Can. J. Earth Sci. 14: 397–412.

Hakanson, L. 1984. Sediment sampling in different aquatic environments: statistical aspects. Water Resour. Res. 20: 41–46.

Hakanson, L. 1992. Sediment variability. *In* Sediment toxicity assessment. *Edited by* G.A. Burton, Jr. Lewis Publishers, Ann Arbor, Mich. pp. 19–35.

Hakanson, L., and T. Ahl. 1976. Lake Vattern, recent sedimentary deposits and sediment chemistry. SNV PM 740. National Swedish Environmental Protection Board, Uppsala.

Hakanson, L., and M. Jansson. 1983. Principles of lake sedimentology. Springer-Verlag, Berlin.

Johnson, M.G. 1987. Trace element loadings to sediments of fourteen Ontario lakes and correlations in fish. Can. J. Fish. Aquat. Sci. 44: 3–13.

Kelderman, P., J. Niewenhuize, A.M. Meerman-Van De Repe, and J.M. Van Liere. 1984. Changes of sediment distribution patterns in lake Grevelingen, an enclosed estuary in the SW Netherlands. Neth. J. Sea Res. 18: 273–285.

McCave, I.N. 1984. Erosion, transport and deposition of fine-grained marine sediments. *In* Fine-grained sediments. *Edited by* D.A.V. Stow and D.J.W. Piper. Blackwell Scientific Publications, London. pp. 35–69.

O'Connor, D.J. 1988. Models of sorptive toxic substances in freshwater systems. II. Lakes and reservoirs. J. Environ. Eng. (N.Y.), 114: 533–551.

Ontario Ministry of the Environment. 1978. Water quality data: Ontario lakes and streams 1977. Vol. 13. Ontario Ministry of the Environment, Toronto, Ont.

Ontario Ministry of the Environment. 1979. Water quality data: Ontario lakes and streams 1978. Vol. 14. Ontario Ministry of the Environment, Toronto, Ont.

Peterman, R.M. 1990. Statistical power analysis can improve fisheries research and management. Can. J. Fish. Aquat. Sci. 47: 2–15.

Rasmussen, J.B. 1988. Littoral zoobenthic biomass in lakes, and its relationship to physical, chemical, and trophic factors. Can. J. Fish. Aquat. Sci. 45: 1436–1447.

Robbins, J.A. 1980. Sediments of southern Lake Huron: elemental composition and accumulation rates. EPA-600/3-80-080. U.S. Environmental Protection Agency, Washington, D.C.

Rowan, D.J., and J. Kalff. 1993. Predicting sediment metal concentrations in lakes without point sources. Water Air Soil Pollut. 66: 145–161.

Rowan, D.J., J. Kalff, and J.B. Rasmussen. 1991. The limnological implications of catchment sediment load. Verh. Int. Ver. Theor. Angew. Limnol. 24: 2980–2984.

Rowan, D.J., J. Kalff, and J.B. Rasmussen. 1992*a*. Estimating the mud deposition boundary depth in lakes from wave theory. Can. J. Fish. Aquat. Sci. 49: 2490–2497.

Rowan, D.J., J. Kalff, and J.B. Rasmussen. 1992*b*. Profundal sediment organic content, and physical character do not reflect lake trophic status, but rather reflect inorganic sedimentation and exposure. Can. J. Fish. Aquat. Sci. 49: 1431–1438.

Rowan, D.J., J. Cornett, K. King, and B. Risto. 1995. Sediment focusing and ^{210}Pb dating: a new approach. J. Paleolimnol. 13: 107–118.

Stanley, D.J., S.K. Addy, and E.W. Behrens. 1983. The mudline: variability of its position relative to shelfbreak. *In* The shelfbreak: critical interface on continental margins. *Edited by* D.J. Stanley and G.T. Moore. SEPM Spec. Publ. No. 30. pp. 279–298.

Stephenson, M., D.J. Rowan, C. Kelly, W.J. Schwartz, M.F. Motycka, and R.D. Roshon. 1995. Fate and distribution in sediments of carbon-14 added to Canadian Shield lakes of differing trophic state. Limnol. Oceanogr. 40: 779–790.

Thomas, R.L. 1988. Distribution and composition of the surficial sediments of Georgian Bay and North Channel. Hydrobiologia, 163: 35–45.

Thomas, R.L., and C.K. Dell. 1978. Sediments of Lake Superior. J. Great Lakes Res. 43: 264–275.

Differences in habitat utilization among native, native stocked, and non-native stocked brown trout (*Salmo trutta*) in a hydroelectric reservoir

T. Hesthagen, O. Hegge, J. Skurdal, and B.K. Dervo

Abstract: Native and native-stocked brown trout (*Salmo trutta*) in Lake Tesse, a regulated hydroelectric reservoir (southern Norway), were spatially segregated according to size: small individuals occurred mainly in the epibenthic habitat and larger individuals mainly in the pelagic habitat. In contrast, all size groups of non-native stocked brown trout were mostly restricted to the epibenthic habitat. Age-specific lengths were generally larger for non-native than for native stocked trout, which were larger than native fish. However, growth rate between age 3 and 4 was significantly lower for non-native stocked fish than for native and native stocked fish. Differences in body length were mainly due to strain but also to some extent to habitat. Native fish had significantly fuller stomachs in the pelagic than in the epibenthic habitat in summer. Epibenthic non-native fish had significantly fuller stomachs than native and native stocked fish in August but not in July. Native and native stocked fish fed mainly on surface insects and planktonic crustaceans in both habitats. We hypothesize that the non-native brown trout stocked in Lake Tesse do not use the pelagic habitat in the home lake and are therefore less adapted to utilize such habitat than populations originating from lakes where pelagic habitat is available.

Résumé : On a déterminé la répartition spatiale, en fonction de la taille, des truites brunes (*Salmo trutta*) indigènes sauvages et ensemencées dans le lac Tesse, un réservoir hydroélectrique régularisé du Sud de la Norvège : les individus de petite taille se trouvaient principalement dans l'habitat épibenthique, les autres fréquentant surtout l'habitat pélagique. En revanche, tous les groupes de taille de truites brunes non indigènes ensemencées se retrouvaient en majorité dans l'habitat épibenthique. En général, la longueur selon l'âge des truites non indigènes était plus grande que celle des truites indigènes ensemencées, qui étaient elle-mêmes de plus grande taille que les truites sauvages. Cependant, le taux de croissance entre 3 et 4 ans était beaucoup plus faible chez les truites non indigènes ensemencées que chez les poissons indigènes sauvages et ensemencés. La différence de longueur des individus était due principalement à la souche en cause, mais aussi, dans une certaine mesure, à l'habitat. Les poissons indigènes avaient l'estomac beaucoup plus rempli dans l'habitat pélagique que dans l'habitat épibenthique en été. Chez les individus non indigènes de l'habitat épibenthique, au mois d'août, l'estomac était beaucoup plus plein que chez les truites indigènes sauvages et ensemencées, mais ce n'était pas le cas au mois de juillet. Les truites indigènes sauvages et ensemencées se nourrissaient principalement d'insectes de surface et de crustacés planctoniques dans les deux habitats. Nous sommes d'avis que les truites brunes non indigènes ensemencées dans le lac Tesse n'utilisaient pas l'habitat pélagique dans leur lac d'origine, et sont donc moins adaptées à l'utilisation de cet habitat comparativement aux populations provenant de lacs où existe un habitat pélagique.

[Traduit par la Rédaction]

Received February 26, 1991. Resubmitted February 17, 1995. Accepted April 28, 1995.
J10917

T. Hesthagen. Norwegian Institute for Nature Research, Tungasletta 2, N-7005 Trondheim, Norway.
O. Hegge. Oppland County, Environmental Administration, Statsetatenes hus, N-2600 Lillehammer, Norway.
J. Skurdal. Eastern Research Institute, Skurva, P.O. Box 1006, N-2601 Lillehammer, Norway.
B.K. Dervo. Norwegian Association of Hunters and Anglers, P.O. Box 96, N-1364 Hvalstad, Norway.

Can. J. Fish. Aquat. Sci. **52**: 2159–2167 (1995). Printed in Canada / Imprimé au Canada

Introduction

Habitat use has important implications for fish production, and there is now considerable interest regarding behavior and ecological traits of newly or supplementarily stocked fish (O'Hara 1986; Wydoski 1986). Little is known about whether habitat utilization by fish from different stocks will be identical when they are offered identical environmental conditions. There are several examples of differences in food and habitat use between sympatric morphs within salmonid species (e.g., Svärdson 1979; Hindar and Jonsson 1982; Ferguson 1986; Sandlund et al. 1987). In contrast, lake plantings of domestic, hybrid, and wild strains of brook trout (*Salvelinus fontinalis*) and brown trout (*Salmo trutta*) showed use of space and food resources similar to that of native trout (Fraser 1981; Lachance and Magnan 1990; L'Abée-Lund and Sægrov 1991; L'Abée-Lund et al. 1992). Studies of resource utilization also indicate that an intrinsic preference for space and food exists in several salmonid species (Olson et al. 1988).

Stocking of brown trout is widely carried out to compensate for reduced natural propagation in Norwegian hydroelectric reservoirs. Most supplementary stocking involves fry of non-native stocks raised in large central hatcheries. This species usually occupies shallow littoral areas (Nilsson 1963; Thorpe 1974; Svärdson 1976; Langeland et al. 1991). However, in large deep lakes with small littoral zones, brown trout also exploit pelagic habitats, where they feed on surface insects and crustacean zooplankton (e.g., Klemetsen 1968; Haraldstad and Jonsson 1983; Hegge et al. 1989; Schei and Jonsson 1989; Langeland et al. 1991). Such resource utilization is especially important in hydroelectric reservoirs where the prey fauna in littoral areas is reduced by water level fluctuations (Grimås 1962). In brown trout, there are marked differences in habitat utilization according to size; small and large individuals generally occupy benthic and pelagic habitats, respectively (Haraldstad and Jonsson 1983; Hegge et al. 1989; Jonsson 1989).

The purpose of this study was to test the null hypotheses that there are no significant differences in feeding habits and use of space between native and non-native brown trout. Lake Tesse, a Norwegian hydroelectric reservoir where allopatric brown trout exploit both epibenthic and pelagic habitat, was chosen for our experiments. Two of the most frequently used hatchery strains in Norway, Tunhovdfjord and Bjornesfjord, were used for the experiment. As a reference we also stocked the lake with offspring from native brown trout stock.

Study area

Lake Tesse is located in southern Norway at an altitude of 853.9 m above sea level. Lake Tesse was first regulated in 1943, and until 1963 the mean annual water level fluctuation was 7.3 m (range 3.7–11.8 m). In 1963, the glacier-fed River Veo was transferred into Lake Tesse through the River Smådøla (Hesthagen and Fjellheim 1987). The annual water level fluctuation increased to 12.4 m, of which 0.9 m is dammed. The reservoir covers an area of 937 and 1426 ha at the lowest and highest water levels, respectively. The catchment area of 430 km^2 mainly consists of basic deep rocks such as anortsite and Valdres sparagmite. Lake Tesse was originally a clear-water lake, but is now heavily influenced by glacier-fed water from the River Veo. The Secchi disc transparency was 4.0 m during the study period in 1989, as opposed to 8–10 m prior to regulation (Huitfeldt-Kaas 1906). The dominant proportion of the basin is between 5 and 30 m deep, and the deepest area is 64 m. The pH is near neutral (6.7) and the calcium concentration is 1.4 mg/L.

The spawning grounds for brown trout in the outlet of Lake Tesse were lost because of the construction of a dam. Further, channelization and transfer of glacier-fed water strongly reduced recruitment in the inlet River Smådøla, which was the main spawning river. Brown trout spawn in the lake along the shore at depths of 3–5 m (S. Bjørgen, 2685 Garmo, personal communication), and these areas now dry out at low water levels during winter. Brown trout also still spawn in several smaller tributaries that drain into the reservoir.

Methods

Juvenile (age 0+) brown trout, originating from both native and non-native stocks (Bjornesfjord and Tunhovdfjord strains), were marked and released in Lake Tesse in the autumn. Non-native fish were raised in circular tanks at Reinsvoll Hatchery about 250 km south of Tesse and fed artificial food. The Bjornesfjord strain has been domesticated since 1966, whereas the Tunhovdfjord strain originated from wild parents (Stabell et al. 1988). The fertilized eggs of native brown trout from Lake Tesse were placed in a hatchery at Lemonsjøen shortly after fertilization. The unfed fry were released in an earthen pond about 10 km from Lake Tesse in early June, where they fed on natural food items.

During the period from 1980 to 1987, a total of 88 000 non-native and 72 800 native fish were released in the lake. In addition, 14 000 native stocked fish were released in four tributaries. Of the non-native fish in the present study, individuals of age 3+ originated from the Tunhovdfjord strain while those of age 4+ to 6+ were offspring of the Bjornesfjord strain. Mean length at release for non-native fish was 47–60 mm compared with 42–55 mm for native stocked fish. Juvenile (age 0+) native fish caught in the tributaries usually range between 35 and 45 mm in length.

The fish were marked by removing the adipose and either left or right pelvic fins of native and non-native individuals, respectively. Fish released in the tributaries were marked by removing the adipose fin only. All non-native brown trout and those native stocked fish released in 1984–1987 (age 2+ to 5+ at recapture in 1989) were marked. Only 48% of the 5200 native stocked fish released in the reservoir during the period 1980–1983 were marked. Non-native fish were marked prior to transportation from the hatchery.

The number of circuli in the scales can be used to separate naturally produced and stocked brown trout (L'Abée-Lund and Sægrov 1991). We counted the number of first-year circuli on scales from fish of known origin, i.e., those of age 2+ to 5+. On the basis of the number of first-year

Fig. 1. Length–frequency distributions of non-native stocked (NNA-S), native stocked (NA-S), and native (NA) brown trout caught in the epibenthic (black area) and pelagic (open area) habitat in Lake Tesse in July and August 1989. *D*, Kolmogorov–Smirnov two-sample test statistic for difference in length distribution between epibenthic and pelagic catches. n_1 and n_2, number of fish caught in epibenthic and pelagic nets, respectively.

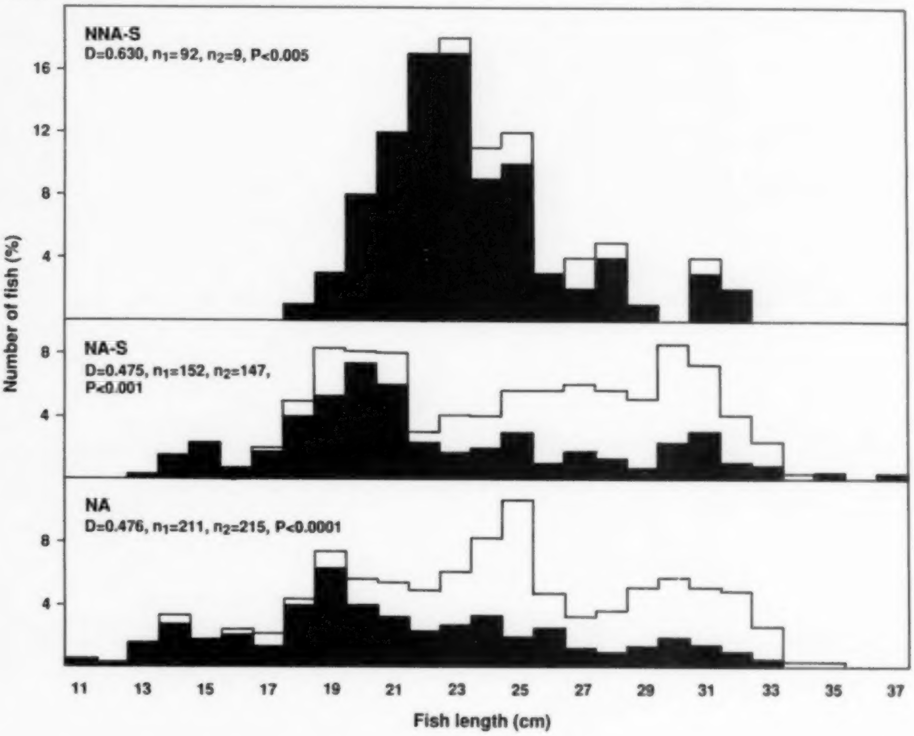

circuli (C) of classified stocked and native fish, we performed an unstandardized canonical discriminant function (CDF): CDF = −3.003 + 0.580*C*, which grouped 79.7% of native brown trout as native and 72.0% of stocked brown trout as stocked. We used this function to classify fish of age 6+ to 8+ as either native or native stocked.

Prior to stocking in late August to early September, fish from both groups were mixed and placed overnight in a net cage in the reservoir. The fish were released along the shore throughout most of the reservoir except for the northern and southern parts where the littoral bed consists of fine gravel.

The fish were caught with 25 m long benthic and pelagic monofilament nets that were 1.5 and 6.0 m in vertical dimension, respectively. Eight nets consisted of panels with the following bar mesh sizes: 16.6, 21.0, 21.0, 26.0, 29.0, 35.0, 39.0, and 45 mm. Mesh sizes between 21.0 and 45.0 mm caught 20- to 38-cm brown trout with equal efficiency (Jensen 1977). Benthic nets were set perpendicular to the shore at depths ranging from 0 to 27 m, while pelagic nets were set at a station about 500 m offshore at depths of 45–55 m. Benthic nets were used during three 24-h periods in July covering depth zones 0–10 m. In August, benthic nets were used during two 24-h periods. Pelagic nets were used during three 24-h periods in July and one 24-h period in August, and these nets were set at depths of 0–6 and 6–12 m. The catch per unit effort (CPUE) is presented as the number of fish caught per 100 m^2 net area during 24 h of fishing. Tests for the goodness of fit by means of chi-square analyses were done with actual frequencies.

Table 1. Catch per unit effort for native (NA) native stocked (NA-S), and non-native stocked (NNA-S) brown trout expressed as catches per 100 m^2 net area during 24 h of fishing in the epibenthic (C_B) and pelagic zone (C_P) in Lake Tesse in July and August 1989.

Month	Strain	C_B	*N*	C_P	*N*
July	NA	3.48	94	1.32	143
	NA-S	2.52	68	0.84	91
	NNA-S	2.48	67	0.07	8
August	NA	9.75	117	6.00	72
	NA-S	7.00	84	4.67	56
	NNA-S	2.08	25	0.08	1

Note: *N*, total number of fish caught.

Table 2. Back-calculated growth in length (L2–L7; mm) for native (NA), native stocked (NA-S), and non-native stocked (NNA-S)

		Age 2		Age 3			Age 4				Age 5				
Habitat	Strain	L2	*N*	L2	L3	*N*	L2	L3	L4	*N*	L2	L3	L4	L5	*N*
B	NA	117±16*x*	31	103±12*x*	155±18*x*	72	106±12*x*	148±17*x*	205±26*x*	68	99±18*x*	143±28*x*	192±35*x*	246±26*x*	14
B	NA-S	133±15*y*	20	111±10*y*	166±16*y*	72	115±15*y*	159±19*y*	219±22*y*	29	124±13*y*	176±23*y*	228±28*y*	272±22*y*	11
B	NNA-S			130±11*z*	195±18*z*	70	136±10*z*	183±13*z*	233±20*y*	15	143±10*y*	195±15*y*	231±15*y*	277±9*y*	3
P	NA	121±1*x*	2	111±9*x*	172±18*x*	16	109±12*x*	153±16*x*	218±20*x*	102	109±15*x*	161±23*x*	214±34*x*	261±29*x*	29
P	NA-S	152±9*y*	2	117±9*xy*	178±18*x*	28	122±10*y*	169±16*y*	238±21*y*	45	123±12*y*	176±19*y*	235±22*y*	277±19*y*	42
P	NNA-S			142±13*z*	219±8*y*	4	140±16*z*	201±29*z*	242±9*y*	4					

Note: Values are given as the mean ± standard deviation. *N*, number of fish. Data for one NNA-S fish of age 7 are omitted. Within age groups and same letter are not significantly different ($P > 0.05$). In cases were NNA-S and NA fish are significantly different, but neither group is different

Fig. 2. Instantaneous growth rate (*G*) for native (NA), native stocked (NA-S), and non-native stocked (NNA-S) brown trout of different ages in Lake Tesse.

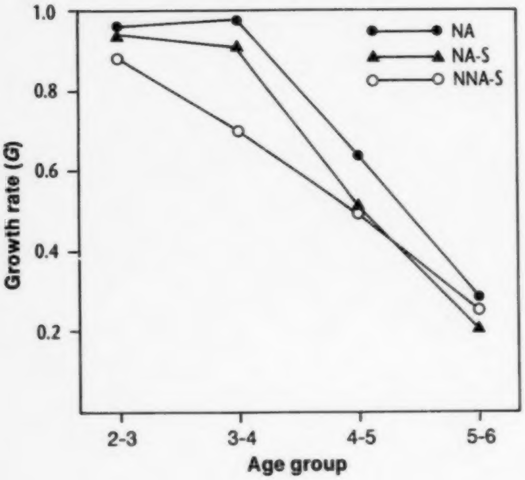

Each fish was examined for marks, and total length (millimetres) and weight (grams) were measured. The fish were aged from scales and otoliths (Jonsson 1976). The scale sample was taken from the left side of the fish just below the lateral line (below the adipose fin). Back-calculated lengths were used to pool the material obtained in both July and August. Impressions of four to six scales were made in celluloid and read using a microfiche projector. Distances from the focus of the scale to each annulus and to the outer scale margin were measured. Body length at age x (SL_x) was back-calculated according to the Fraser-Lee method (Ricker 1975; Francis 1990):

$$SL_x = \frac{(SL_c - SL_0)R_x}{R_c} + SL_0$$

where SL_c is length at capture, SL_0 is the fish length when scales first appear, R_x is the distance from the focus of the scale to annulus x, and R_c is scale radii at capture. SL_0 can be derived from the intercept of the regression of fish length on scale radius. The relationship between fish length (SL_c, millimetres) and scale length (R_c, millimetres) is given by the equation $R_c = 0.38\ SL_c - 3.42$, $R^2 = 0.67$, $p < 0.000\ 01$. In the present study, any estimate of SL_0 is biased because of the lack of individuals smaller than 10 cm in length in the sample. Therefore, we used data from the literature. SL_0 for brown trout in Norwegian waters ranges between 35 and 41 mm (Gunnerød 1966; Jonsson 1976; Jensen and Johnsen 1982). We chose the value 35 mm in our model. The back-calculated length at age 1 is not presented because this value may be biased (cf. Francis 1990).

The back-calculated lengths were further converted to weights from the weight–length relationships by logarithmic transformation of weights (W, grams) and total lengths (L, millimetres) at capture. The relationship between weights and lengths is given by the equation $\ln W = 2.93 \ln L - 4.40$, $R^2 = 0.97$, $p < 0.000\ 01$. Growth rates for individual fish were then expressed as the instantaneous growth coefficient (G), which was estimated from the formula $G = \ln W_{t+1} - \ln W_t$, where W_{t+1} and W_t are the weights at ages $t + 1$ and t, respectively. The initial size of non-native fish was larger than that of native stocked and native fish. This may affect the growth rate between age 1 and 2. Therefore, we omitted G values for these two age groups in our analysis.

Fish stomachs were preserved in 70% ethanol for later examination with a binocular microscope. The mean percent composition of each taxonomic category in each stomach was determined from dry weights, which were calculated from body lengths according to formulas for different taxonomic categories (Bottrell et al. 1976; Langeland 1982; Hindar et al. 1988; Langeland et al. 1991). The number of different prey items in each stomach was counted except for samples containing a high number of zooplankton, in which case a 10 or 25% subsample was counted.

We used the Schoener (1968) index to measure diet overlap (DOI) between different trout strains and fish caught in different habitats:

$$DOI = 1 - 0.5\sum_{i=1}^{n}(p_i - q_i)$$

where p_i is the weight proportion of food item i in the diet of trout strain 1, and q_i is the weight proportion of food item i in the diet of trout strain 2.

brown trout of ages 2–7 caught in epibenthic (B) and pelagic (P) habitat in Lake Tesse in 1989.

Age 6						Age 7						
L2	L3	L4	L5	L6	*N*	L2	L3	L4	L5	L6	L7	*N*
110±13*x*	159±22*x*	218±33*x*	265±31*x*	291±22*x*	18	103±20*x*	151±38*x*	205±54*x*	256±46*x*	278±40*x*	297±26*x*	7
130±19*y*	195±37*y*	245±37*x*	284±26*x*	304±23*x*	11	131±8*x*	188±18*y*	251±26*y*	289±19*x*	305±20*x*	316±23*x*	9
152±22*y*	206±23*y*	254±21*x*	289±19*x*	315±12*x*	4							
113±14*x*	163±20*x*	222±27*x*	268±26*x*	294±20*x*	41	109±11*x*	166±18*x*	239±25*x*	279±22*x*	299±17*x*	311±14*x*	17
124±12*y*	183±26*y*	241±28*y*	278±21*x*	299±18*x*	22	133±12*y*	203±22*y*	272±15*y*	303±16*y*	317±16*y*	325±15*y*	7

habitat, mean lengths followed by different letters (*x*,*y*,*z*) are significantly different ($P < 0.05$) and mean lengths followed by the compared with NA-S fish, this latter group is labelled by both *x* and *y*.

Results

Spatial distribution

There were no significant differences between frequencies of native and native stocked brown trout caught in the epibenthic and pelagic zones of Lake Tesse in either July ($\chi^2 = 0.26$, $p > 0.05$) or August ($\chi^2 = 0.12$, $p > 0.05$). The data were therefore pooled (Table 1). There was a significant difference in habitat use among native, native stocked brown trout, and non-native brown trout (both the Tunhovd and Bjornesfjord strains). Non-native brown trout were strongly underrepresented in the pelagic habitat (July $\chi^2 = 59.6$, $p < 0.0001$ and August $\chi^2 = 12.9$, $p < 0.01$).

Size and age distribution

All size groups of non-native brown trout were mainly restricted to epibenthic habitat (Fig. 1). On the other hand, native and native stocked fish were spatially segregated according to size. About 58% of both naturally recruited and native individuals <220 mm occupied epibenthic habitat, while 86–87% of individuals >220 mm occupied the pelagic habitat. A Kolmogorov–Smirnov two-sample test showed that the length frequency distributions of fish caught in the epibenthic and pelagic habitats were significantly different (Fig. 1).

Back-calculated lengths of individuals caught in epibenthic and pelagic zones showed that non-native fish were generally significantly larger than individuals of corresponding age of native stocked fish, which in turn were significantly larger than native fish (ANOVA, $p < 0.05$; Table 2). The *G* values between ages 2 and 3 did not differ significantly between different groups (ANOVA, $p > 0.05$; Fig. 2). However, between ages 3 and 4, the *G* values for both native and native stocked fish were significantly higher than for non-native individuals ($F_{[2,259]} = 14.28$, $p < 0.000\,01$). Between ages 4 and 5 and between ages 5 and 6, the *G* value for native fish was significantly higher than for native stocked individuals, $F_{[2,95]} = 4.45$, $p < 0.05$ and $F_{[2,93]} = 3.53$, $p < 0.05$, respectively. It was not possible to compare the growth rates of non-native fish of ages >5 because of low numbers ($n = 4$).

Fish obtained in the pelagic zone were usually significantly larger than individuals of corresponding age obtained in the epibenthic zone (Table 2). Analysis of covariance showed that the differences in back-calculated lengths were mainly due to strain but also to some extent to habitat, after the effect of age was removed (Table 3).

Table 3. Analysis of covariance (back-calculated length at ages 2–7) of different strains of brown trout caught in epibenthic and pelagic habitat in Lake Tesse in July and August 1989.

	MS	df	*F*	*p*	r^2
L2					
Age	50.043	1	0.275	0.6000	0.302
Habitat	1 692.095	1	9.284	0.0020	
Strain	32 349.390	2	177.484	<0.0001	
Residual	182.266	818			
L3					
Age	25.021	1	0.062	0.8030	0.338
Habitat	5 397.086	1	13.399	<0.0001	
Strain	78 708.225	2	195.404	<0.0001	
Residual	402.798	763			
L4					
Age	16 179.158	1	22.686	<0.0001	0.202
Habitat	15 997.488	1	22.431	<0.0001	
Strain	31 442.666	2	44.088	<0.0001	
Residual	713.184	501			
L5					
Age	2 322.478	1	3.598	0.0590	0.136
Habitat	1 851.031	1	2.868	0.0920	
Strain	10 412.642	2	16.131	<0.0001	
Residual	645.503	236			
L6					
Age	50.142	1	0.113	0.7370	0.083
Habitat	466.889	1	1.056	0.3060	
Strain	2 773.102	2	6.275	0.0020	
Residual	441.946	139			
L7					
Age	66.477	1	0.181	0.6730	0.143
Habitat	1 229.404	1	3.348	0.0740	
Strain	2 056.983	1	5.602	0.0220	
Residual	367.184	44			

Feeding habits

There were small differences in diet between native and non-native fish and between native stocked and non-native

Fig. 3. Percent composition (dry weight) of major prey items for native (NA), native stocked (NA-S), and non-native stocked (NNA-S) brown trout caught in epibenthic and pelagic habitat in Lake Tesse in July and August 1989. Number of stomachs examined is given above each column.

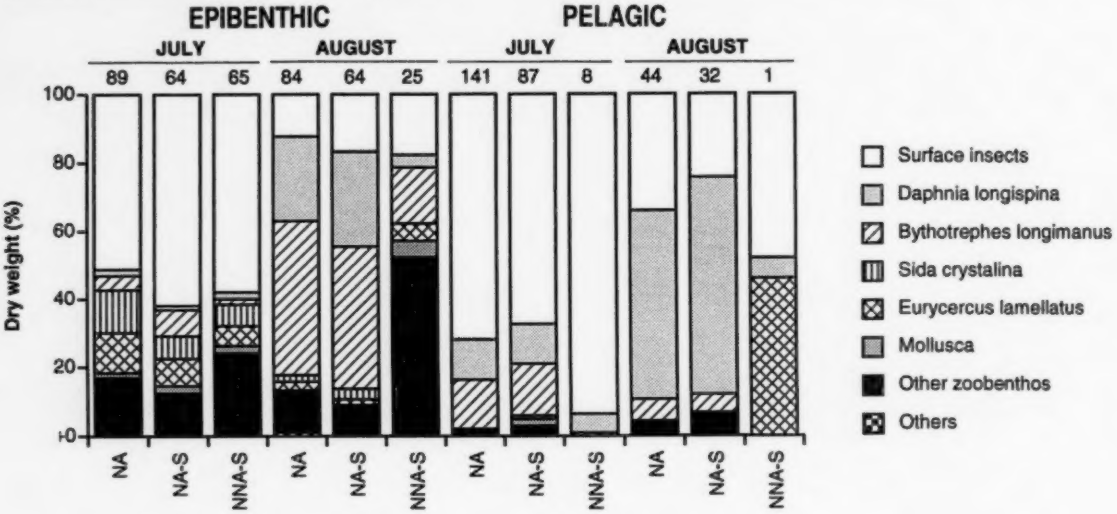

fish in July as indicated by the high diet overlap (DOI = 0.85 and 0.87, respectively). The diets of all three types of brown trout in epibenthic habitat consisted mostly of terrestrial insects and the benthic crustaceans *Eurycercus lamellatus* and *Sida crystalina* (Fig. 3). Mollusca and other zoobenthos represented only 15–26% of the dry weight of food items regardless of fish type.

Surface insects were less important as food for fish caught in the epibenthic zone in August. At that time, zoobenthos were the dominant food for non-native fish, while *Bythotrephes longimanus* and *Daphnia longispina* dominated the diet of native and native stocked trout. The difference in diet between native and non-native fish and between native stocked and non-native fish is illustrated by the relatively low diet overlap (DOI = 0.47 for both categories).

Native and native-stocked fish caught in pelagic nets in July fed mainly on surface insects (70%). The planktonic crustaceans *B. longimanus* and *D. longispina* made up the main part of the rest of the diet. In August, surface insects were of less importance as food for trout in offshore regions, and *D. longispina* was the predominant food item. The diet overlap indices of native and native stocked trout caught in the pelagic zone were 0.95 in July and 0.89 in August.

In epibenthic and pelagic habitats, the stomach fullness (100 × (dry weight/body weight)) of both native and native stocked fish was significantly higher in July than in August (ANOVA, $p < 0.005$; Fig. 4). The difference in stomach fullness between July and August for non-native fish was not significant (test for epibenthic habitat only; $p > 0.05$). Native fish exhibited a significantly higher stomach fullness in pelagic than in epibenthic habitat in July ($p < 0.01$) but not in August ($p > 0.05$). For non-native fish, a difference was found in August only ($p < 0.01$). Non-native fish had a significantly higher stomach fullness than both native fish and native stocked fish in epibenthic habitat in August ($p < 0.000\,01$) but not in July ($p > 0.05$). Native fish in pelagic habitat had a significant higher stomach fullness in both July ($p < 0.0001$) and August ($p < 0.05$).

Discussion

The habitat use of native and native stocked brown trout differed significantly from that of non-native brown trout in Lake Tesse. Naturally recruited and native stocked trout were both spatially segregated according to size. Small individuals occurred mainly in the epibenthic habitat while larger individuals dominated in the pelagic habitat. In contrast, the habitat use of all size groups of non-native brown trout was restricted mainly to the epibenthic habitat.

The diet of brown trout in the epibenthic habitat mainly consisted of terrestrial insects and zooplankton. Benthic foods were of little importance. Brown trout caught in the pelagic habitat fed almost exclusively on surface insects and the two planktonic crustaceans *B. longimanus* and *D. longispina*. Pelagic trout utilized a broad part of the water column when foraging. Observations in summer of higher stomach fullness of pelagic brown trout compared with those caught in epibenthic habitat, indicate that food access was temporally better in the pelagic habitat. This finding is in accordance with data on the resource base in Lake Tesse, which show low densities of zoobenthos, whereas the biomass of zooplankton was relatively high compared with other Norwegian lakes (Jensen 1988; T. Hesthagen, unpublished data).

Non-native fish exhibited a significantly lower growth rate than either native or native stocked fish between ages 3 and 4. At this age, there was an increase in the number of pelagically caught fish; hence, the habitat switch of native and native stocked fish was manifested in better growth. Differences in growth rate and longevity are not related to the maturity pattern as very few non-native fish were sexually mature compared with native and native stocked brown trout (T. Hesthagen, unpublished data). The disappearance of older non-native fish is probably only to a small extent related to size-selective fishery as brown trout in Lake Tesse is harvested with gill nets of 35-mm mesh size.

Several authors (e.g., Haraldstad and Jonsson 1983; Jonsson and Gravem 1985; Hegge et al. 1989; Jonsson 1989) reported that small individuals of brown trout prefer epibenthic habitat despite better food access in pelagic habitats. This is interpreted as a strong need of small individuals for shelter to avoid predation and agonistic encounters with larger individuals (Haraldstad and Jonsson 1983; Hegge et al. 1989). This behavior may cause reduced food intake and growth depression (cf. Brown 1946; Fenderson et al. 1968; Jobling and Reinsnes 1986). Another study conducted in Lake Tesse demonstrated that smaller brown trout were more strongly associated with the bottom than larger fish (Hegge et al. 1993). Accordingly, the most profitable habitat for smaller brown trout seems to be the epibenthic habitat where fish have access to shelter among stones. We suggest that the most profitable habitat for larger individuals in Lake Tesse may be the pelagic zone where food resources are best.

Spatial segregation within population according to size appears to represent an ontogenetic niche shift (cf. Werner and Gilliam 1984). Jonsson et al. (1988) hypothesized that such a habitat shift is brought about by size-related differences in competitive abilities. However, in spite of a greater initial length and larger size in all age groups of non-native fish than in native and native stocked fish, the non-natives remained in the epibenthic zone without exhibiting any apparent niche shift. It is unlikely that non-native brown trout are forced to remain in epibenthic habitat by social interactions with native brown trout because the outcome of agonistic encounters is primarily a function of size (Bachman 1984). Another explanation would be that non-native trout are inherently less aggressive than natives (cf. Rosenau and McPhail 1987). In addition, exploitative competition may exclude non-native trout from the pelagic area; in the presence of natives, pelagic resources are depleted and non-natives find this habitat unprofitable, but if natives were absent they would move. Size-based territory defence and dominance hierarchies are important mechanisms for limiting access to food in streams (Hartman 1965; Chapman 1966). In lakes, trout seem to have home ranges (Shepherd 1973), and competition may be more exploitative.

Differences in habitat use between native and non-native fish in Lake Tesse could be due to a delayed phenotypic response to new environmental conditions. However, size-related differences between native stocked and non-native stocked fish were small. Behavioral changes (e.g., habitat shift) related to experience during development cannot be overlooked (Huntingford 1986). Our experimental fish differed in rearing background; non-native fish were hatchery reared whereas native stocked fish were pond reared. However, the fact that the diet of hatchery-reared brown trout released in natural waters differs from that of native fish shortly after release (Johnsen and Ugedal 1989) may indicate that any habitat shift several years later is not related to rearing background.

Fig. 4. Stomach fullness expressed as 100 × dry weight/body weight of native (NA), native stocked (NA-S), and non-native stocked (NNA-S) brown trout in epibenthic (E) and pelagic (P) gill nets in Lake Tesse in July and August 1989. For number of stomachs examined in each category, see Fig. 3.

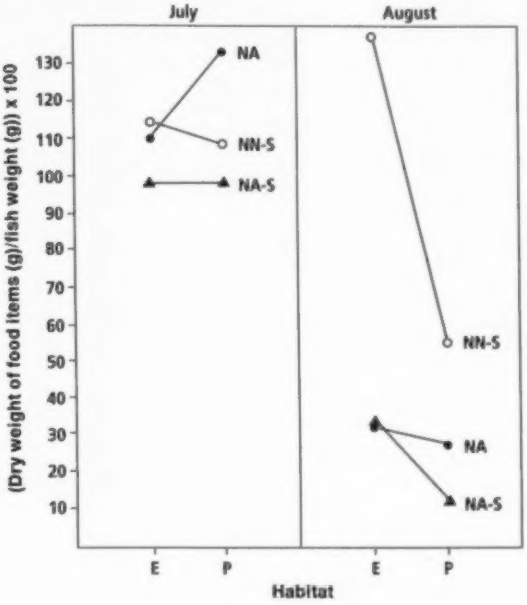

Segregation in resource utilization has been found in phenotypically and ecologically different sympatric populations of salmonids elsewhere (e.g., Svärdson 1979; Hindar and Jonsson 1982; Ferguson 1986; Sandlund et al. 1987). Ferguson (1986) found differences in the feeding preference and habitat use of the three sympatric populations of brown trout in Lough Melvin (Ireland), and stated that these differences appear to be genetically controlled. Similarly, native and native stocked Bjornesfjord and Tunhovdfjord brown trout mostly utilized the same habitat and were mainly caught in the epibenthic zone (L'Abée-Lund and Sægrov 1991; L'Abée-Lund et al. 1992).

The existence of genetically determined differences between stocks in characteristics such as behavior, morphology, and physiology is well documented in various fish species (e.g., Svärdson 1979; Rosseland and Skogheim 1987; Skúlason et al. 1989; Magurran 1990). These differences may result from adaptations to local environmental conditions (Magurran 1990). Such characteristics may influence feeding efficiency (e.g., Kliewer 1970; Schulz and Northcote 1972; Henderson and Northcote 1985; Townsend and Winfield 1985; Lavin and McPhail 1986) and thus feeding habits and habitat choice. Variation in habitat choice as a result of species differences in feeding efficiency is well documented (e.g., Werner and Hall 1979;

Persson 1987; Ehlinger and Wilson 1988; Hindar et al. 1988). Differences in food choice also seem to exist among populations within a single species, e.g., for brown trout in Lough Melvin, which differ in morphometric and meristic characteristics (Cawdery and Ferguson 1988). In addition, differences in head morphology of coexisting Arctic char (*Salvelinus alpinus*) in Thingvallavatn (Iceland) appear to be related to differences in feeding habits (Skúlason et al. 1989). Olsson et al. (1988) suggested that resource utilization by stocked fish in Lake Ontario is due to previously evolved morphological and physiological traits.

We hypothesized that the rigid use of space by nonnative fish stocked in Lake Tesse may be related to a lack of adaptation to pelagic habitat utilization in their home lakes. Lake Bjornesfjorden has a maximum depth of 6 m and consequently a limited pelagic zone (Tysse and Garnås 1990; L'Abée-Lund and Sægrov 1991). In the regulated Lake Tunhovdfjord, the pelagic zone is mainly occupied by Arctic char, which were introduced about 70 years ago (L'Abée-Lund et al. 1992). Thus, it seems reasonable to hypothesize that brown trout from these two lakes are adapted to exploit epibenthic habitats and are less adapted to utilizing pelagic habitat when stocked in Lake Tesse in the same manner as native brown trout. As there were only small differences in habitat use between native and stocked brown trout of native origin, we suggest that the observed variation between native and non-native brown trout were influenced by genetic differences.

Acknowledgments

Financial support was received from the research programme Dynamics and Enhancement of Freshwater Fish Populations of the Norwegian Research Council for Science and the Humanities (NAVF), Glommens og Laagens Brukseierforening, Foreningen til Bægnavassdragets Regulering, and Oppland Energiverk. We thank Bror Jonsson, Jan Hennig L'Abée-Lund, Dr. Magnan, and two anonymous reviewers for valuable comments on this paper; Amy Lightfoot for linguistic assistance; and Leidulf Fløystad for the age analysis.

References

Bachman, R.A. 1984. Foraging behavior of free-ranging wild and hatchery brown trout in a stream. Trans. Am. Fish. Soc. 113: 1–32.

Bottrell, H.H., A. Duncan, Z.M. Gliwicz, E. Grygierek, A. Herzig, A. Hillbricht-Ilkowska, H. Kurasawa, R. Larsson, and T. Weglenska. 1976. Review of some problems in zooplankton production studies. Norw. J. Zool. 24: 419–456.

Brown, M.E. 1946. The growth of brown trout (*Salmo trutta* Linn.). I. Factors influencing growth of trout fry. J. Exp. Biol. 22: 118–129.

Cawdery, S.A.H., and A. Ferguson. 1988. Origins and differentiation of three sympatric species of trout (*Salmo trutta* L.) in Lough Melvin. Pol. Arch. Hydrobiol. 35: 267–277.

Chapman, D.W. 1966. Food and space as regulators of salmonid populations in streams. Am. Nat. 100: 345–357.

Ehlinger, T.J., and D.S. Wilson. 1988. A complex foraging polymorphism in bluegill sunfish. Proc. Natl. Acad. Sci. U.S.A. 85: 1878–1882.

Fenderson, O.C., W.H. Everhart, and L.M. Muth. 1968. Comparative agonistic and feeding behaviour of hatchery-reared and wild salmon in aquaria. J. Fish. Res. Board Can. 25: 1–14.

Ferguson, A. 1986. Lough Melvin, a unique fish community. R. Dublin Soc. Occas. Pap. Ir. Sci. Technol. 1: 1–17.

Francis, R.I.C.C. 1990. Back-calculation of fish length: a critical review. J. Fish Biol. 36: 883–902.

Fraser, J.M. 1981. Comparative survival and growth of planted wild, hybrid, and domestic strains of brook trout (*Salvelinus fontinalis*) in Ontario lakes. Can. J. Fish. Aquat. Sci. 38: 1672–1684.

Grimås, U. 1962. The effect of increased water level fluctuation upon the bottom fauna in Lake Blåsjön, northern Sweden. Rep. Inst. Freshwater Res. Drottningholm, 44: 14–41.

Gunnerød, T.B. 1966. Dannelse av annuli i skjellene og tilvekst hos ørret (*Salmo trutta* L.) i et overbefolket myrvann i det sørlige Norge. (*In Norwegian.*) Cand.real thesis, University of Oslo, Oslo, Norway.

Haraldstad, Ø., and B. Jonsson. 1983. Age and sex segregation in habitat utilization by brown trout in a Norwegian lake. Trans. Am. Fish. Soc. 112: 27–37.

Hartman, G.F. 1965. The role and interaction of underyearling coho salmon (*Oncorhynchus kisutch*) and steelhead trout (*Salmo gairdneri*). J. Fish. Res. Board Can. 22: 1035–1081.

Hegge, O., B.K. Dervo, J. Skurdal, and D.O. Hessen. 1989. Habitat utilization by sympatric arctic charr (*Salvelinus alpinus* (L.)) and brown trout (*Salmo trutta* L.) in Lake Atnsjø, south-east Norway. Freshwater Biol. 22: 143–152.

Hegge, O., T. Hesthagen, and J. Skurdal. 1993. Vertical distribution and substrate preference of brown trout in a littoral zone. Environ. Biol. Fishes, 36: 17–24.

Henderson, M.A., and T.G. Northcote. 1985. Visual prey detection and foraging in sympatric cutthroat trout (*Salmo clarki clarki*) and Dolly Varden (*Salvelinus malma*). Can. J. Fish. Aquat. Sci. 42: 785–790.

Hesthagen, T., and A. Fjellheim. 1987. Effects of transferring glacier-fed water to a clear-water mountain river on the production and food organisms of brown trout (*Salmo trutta* L.) in southern Norway. Regul. Rivers Res. Manage. 1: 161–170.

Hindar, K., and B. Jonsson. 1982. Habitat and food segregation of dwarf and normal Artic charr (*Salvelinus alpinus*) from Vangsvatnet Lake, western Norway. Can. J. Fish. Aquat. Sci. 39: 1030–1045.

Hindar, K., B. Jonsson, J.H. Andrew, and T.G. Northcote. 1988. Resource utilization of sympatric and experimentally allopatric cutthroat trout and Dolly Varden charr. Oecologia, 74: 481–491.

Huitfeldt-Kaas, H. 1906. Planktonundersøkelser i norske vande. (*In Norwegian, German summary.*) Nationaltrykkeriet, Christiania.

Huntingford, F.A. 1986. Development of behaviour in fish. *In* The behaviour of teleost fishes. *Edited by* T.J. Pitcher. Croom Helm, London, Sydney. pp. 47–68.

Jensen, A.J., and B.O. Johnson. 1982. Difficulties in aging Atlantic salmon (*Salmo salar*) and brown trout (*Salmo trutta*) from cold rivers due to lack of scales as yearlings. Can. J. Fish. Aquat. Sci. 39: 321–325.

Jensen, J.W. 1988. Crustacean plankton and fish during the first decade of a subalpine, man-made reservoir. Nord. J. Freshwater Res. 64: 5–53.

Jensen, K.W. 1977. On the dynamics and exploitation of the population of brown trout, *Salmo trutta* L., in Lake Øvre Heimdalsvatn, Southern Norway. Rep. Inst. Freshwater Res. Drottningholm, 56: 18–69.

Jobling, M., and T.-G. Reinsnes. 1986. Physiological and social constraints on growth of Arctic charr, *Salvelinus alpinus*

L.: an investigation of factors leading to stunting. J. Fish Biol. 28: 379–384.

Johnsen, B.O., and O. Ugedal. 1989. Feeding by hatchery-reared brown trout, *Salmo trutta* L. released in lakes. Aquacult. Fish. Manage. 28: 97–104.

Jonsson, B. 1976. Comparison of scales and otoliths for age determination in brown trout, *Salmo trutta* L. Norw. J. Zool. 24: 295–301.

Jonsson, B. 1989. Life history and habitat use of Norwegian brown trout (*Salmo trutta*). Freshwater Biol. 21: 71–86.

Jonsson, B., and F.R. Gravem. 1985. Use of space and food by resident and migrant brown trout, *Salmo trutta*. Environ. Biol. Fishes, 14: 281–293.

Jonsson, B., S. Skúlason, S.S. Snorrason, O.T. Sandlund, H.J. Malmquist, P.M. Jónasson, R. Gydemo, and T. Lindem. 1988. Life history variation of polymorphic Arctic charr (*Salvelinus alpinus*) in Thingvallavatn, Iceland. Can. J. Fish. Aquat. Sci. 45: 1537–1547.

Klemetsen, A. 1968. On the feeding habits of the population of brown trout (*Salmo trutta* L.) in Jølstervann, West Norway, with special reference to the utilization of planktonic crustaceans. Nytt Mag. Zool. (Oslo), 15: 50–67.

Kliewer, E.V. 1970. Gillraker variation and diet in lake whitefish (*Coregonus clupeaformis*) in northern Manitoba. *In* Biology of coregnid fishes. *Edited by* C.C. Lindsey and S. Woods. University of Manitoba Press, Winnipeg, Man. pp. 147–165.

L'Abée-Lund, J.H., and H. Sægrov. 1991. Resource use, growth and effects of stocking in alpine brown trout, *Salmo trutta* L. Aquacult. Fish. Manage. 22: 519–526.

L'Abée-Lund, J.H., H. Sægrov, and H. Lura. 1992. Resource partitioning and spatial segregation in native and stocked brown trout, *Salmo trutta* L., and Arctic charr, *Salvelinus alpinus* (L.), in a hydroelectric reservoir. Aquacult. Fish. Manage. 23: 623–632.

Lachance, S., and P. Magnan. 1990. Comparative ecology and behavoir of domestic, hybrid, and wild strains of brook trout, *Salvelinus fontinalis*, after stocking. Can. J. Fish. Aquat. Sci. 47: 2285–2292.

Langeland, A. 1982. Interactions between zooplankton and fish in a fertilized lake. Holarct. Ecol. 5: 273–310.

Langeland, A., J.H. L'Abée-Lund, B. Jonsson, and N. Jonsson. 1991. Resource partitioning and niche shift in Arctic charr *Salvelinus alpinus* and brown trout *Salmo trutta*. J. Anim. Ecol. 60: 895–912.

Lavin, P.A., and J.D. McPhail. 1986. Adaptive divergence of trophic phenotype among freshwater population of the threespine stickleback (*Gasterosteus aculeatus*). Can. J. Fish. Aquat. Sci. 43: 2455–2463.

Magurran, A.E. 1990. The inheritance and delevopment of anti-predator behaviour. Anim. Behav. 39: 834–842.

Nilsson, N.-A. 1963. Interaction between trout and char in Scandinavia. Trans. Am. Fish. Soc. 92: 276–285.

O'Hara, K. 1986. Fish behaviour and the management of freshwater fisheries. *In* The behaviour of teleost fishes. *Edited by* T.J. Pitcher. Croom Helm, London. pp. 496–521.

Olson, R.A., J.D. Winter, D.C. Nettles, and J.M. Haynes. 1988. Resource partitioning in summer by salmonids in south-central Lake Ontario. Trans. Am. Fish. Soc. 117: 552–559.

Persson, L. 1987. Effects of habitat and season on competitive interactions between roach (*Rutilus rutilus*) and perch (*Perca fluviatilis*). Oecologia, 73: 170–177.

Ricker, W.E. 1975. Computation and interpretation of biological statistics of fish populations. Bull. Fish. Res. Board Can. No. 191.

Rosenau, M.L., and J.D. McPhail. 1987. Inherited differences in agonistic behavior between two populations of coho salmon. Trans. Am. Fish. Soc. 116: 646–654.

Rosseland, B.O., and O.K. Skogheim. 1987. Difference in sensitivity to acidic soft water among strains of brown trout (*Salmo trutta* L.). Ann. Soc. R. Zool. Belg. 117(Suppl. 1): 255–264.

Sandlund, O.T., B. Jonsson, H.J. Malmquist, R. Gydemo, T. Linden, S. Skúlason, S.S. Snorrason, and P.M. Jónasson. 1987. Habitat use of Arctic charr *Salvelinus alpinus* in Thingvallavatn, Iceland. Environ. Biol. Fishes, 20: 263–274.

Schei, T.A., and B. Jonsson. 1989. Habitat use of lake-feeding, allopatric brown trout in Lake Oppheimsvatnet, Norway. *In* Proceedings of the 2nd International Salmonid Migration and Distribution Symposium, Trondheim, 23–25 June, 1987. *Edited by* E. Brannon and B. Jonsson. School of Fisheries, University of Washington, Seattle, Wash., and Norwegian Institute of Nature Research, Trondheim, Norway. pp. 156–168.

Schoener, T. 1968. The Anolis lizards of Bimini: resource partitioning in a complex fauna. Ecology, 49: 704–726.

Schutz, D.C., and T.G. Northcote. 1972. An experimental study of feeding behaviour and interaction of coastal cutthroat trout (*Salmo clarki clarki*) and Dolly Varden (*Salvelinus malma*). J. Fish. Res. Board Can. 29: 555–565.

Shepherd, B.G. 1973. Activity location in coastal cutthroat (*Salmo clarki clarki*) in a small bog lake. J. Fish. Res. Board Can. 31: 1246–1249.

Skúlason, S., D.L.G. Noakes, and S.S. Snorrason. 1989. Ontogeny of trophic morphology in four sympatric morphs of Arctic charr *Salvelinus alpinus* in Thingvallavatn, Iceland. Biol. J. Linn. Soc. 38: 281–301.

Stabell, F.R., F. Hafsund, and J. Skurdal. 1988. Rognstørrelse og rognantall for stamfisk av ørret *Salmo trutta* (L.) med ulik alder og avstamning. (*In Norwegian.*) Rapp. 1-1988. A/L Settefisk, Reinsvoll.

Svärdson, G. 1976. Interspecific population dominance in fish communities of Scandinavian lakes. Rep. Inst. Freshwater Res. Drottningholm, 55: 144–171.

Svärdson, G. 1979. Speciation of Scandinavian *Coregonus*. Rep. Inst. Freshwater Res. Drottningholm, 57: 834–842.

Thorpe, J.E. 1974. The movements of brown trout *Salmo trutta* L. in Loch Leven, Kinross. J. Fish Biol. 6: 153–180.

Townsend, C.R., and I.J. Winfield. 1985. The application of optimal foraging theory to feeding behaviour in fish. *In* Fish energetics, new perspectives. *Edited by* P. Tytler and P. Calow. Croom & Helm, London. pp. 67–98.

Tysse, Å., and E. Garnas. 1990. Fiskeribiologisk undersøkjing i Langesjøen og Bjornesfjorden, Nore og Uvdal kommune 1989. (*In Norwegian.*) Rapp. 11-1990. Fylkesmannen i Buskerud, Miljøvernavd.

Werner, E.E., and J. Gilliam. 1984. The ontogenetic niche and species interactions in size-structured populations. Annu. Rev. Ecol. Syst. 15: 393–425.

Werner, E.E., and D.J. Hall. 1979. Foraging efficiency and habitat switching in competing sunfishes. Ecology, 60: 256–264.

Wydoski, R.S. 1986. Informational needs to improve stocking as a cold-water fisheries management tool. *In* Fish Culture in Fisheries Management: Proceedings of a Symposium on the Role of Fish Culture and Fisheries Management, Lake Ozark, Mo., March 31 – April 3, 1985. *Edited by* R.H. Stroud. American Fisheries Society, Bethesda, Md. pp. 41–57.

Swimming performance and predator avoidance by mummichog (*Fundulus heteroclitus*) larvae after embryonic or larval exposure to methylmercury

Judith S. Weis and Peddrick Weis

Abstract: Embryos of the mummichog, *Fundulus heteroclitus*, were exposed to 5 and 10 μg/L methylmercury throughout development; these are concentrations below those that cause teratological effects. Larvae were maintained in clean seawater or in water with methylmercury, and tested for swimming performance by chasing them with a glass rod. Swimming performance improved with larval age. Larvae that had been exposed to methylmercury as embryos swam greater distances than controls, while those that were exposed only as larvae swam less than controls. The effects of the embryonic exposure diminished over time, and the larval environmental conditions took precedence. Larvae were also tested with two predators, the grass shrimp, *Palaemonetes pugio*, and 1-year-old mummichogs. Those that had been exposed to mercury as embryos (which swam more than controls) or as larvae (which swam less than controls) were more susceptible to predation than controls. The increased swimming of those exposed as embryos may have reflected greater activity, making them more likely to attract the predator's attention, while the slower swimming of those exposed as larvae could make them easier to capture.

Résumé : Des embryons de choquemort, *Fundulus heteroclitus*, ont été exposés pendant toute la durée de leur développement à des concentrations de 5 à 10 $\mu g \cdot L^{-1}$ de méthylmercure, ce qui est inférieur au seuil de tératogénicité. Les larves ont été maintenues dans de l'eau de mer propre ou contenant du méthylmercure, et l'on a étudié leur aptitude à la nage en les stimulant à l'aide d'une baguette de verre. L'aptitude à la nage augmente en fonction de l'âge. Les larves qui ont été exposées au méthylmercure au stade embryonnaire nagent sur de plus grandes distances que les individus témoins, alors que celles qui n'y ont été exposées que pendant le stade larvaire ont une performance inférieure à celle des témoins. Les effets de l'exposition pendant le stade embryonnaire diminuent avec le temps, et les conditions environnementales prévalant pendant le stade larvaire ont un effet prédominant. On a également examiné les larves en présence de deux prédateurs, la crevette *Palaemonetes pugio*, et des choquemorts âgés d'un an. Les larves exposées au méthylmercure pendant le stade embryonnaire (qui nagent davantage que les témoins) ou le stade larvaire (qui nagent moins que les témoins) sont plus vulnérables à la prédation que les témoins. Le fait que les larves exposées au méthylmercure pendant le stade embryonnaire nagent plus que les autres pourrait correspondre à une activité plus intense, ayant pour effet d'attirer sur elles l'attention des prédateurs, alors que celles qui sont exposées au stade larvaire sont plus faciles à capturer en raison de la lenteur de leur nage.

[Traduit par la Rédaction]

Introduction

Behavior, including feeding and predator avoidance, can be adversely affected by exposure to toxicants. For larval fish, a small contaminant-induced reduction in predator avoidance might result in a large reduction in survivorship. Larvae are especially sensitive to environmental contaminants, since the chorion, which protects the embryo, is no longer present. A number of studies have demonstrated impaired predator avoidance by organisms exposed to contaminants (Little et al. 1990; Farr 1977; Sullivan et al. 1978; Kraus and Kraus 1986). It is clear that toxicants can affect swimming performance and compromise the ability to escape from predators.

Larval stages are particularly sensitive to contaminants, but only recently has work on larval behavioral toxicology become a focus of study (Little et al. 1993). In some cases, exposure to contaminants during embryological stages can alter subsequent behavioral patterns. In mammalian teratology, it has become clear that functional impairment is

Received November 29, 1994. Accepted May 17, 1995.
J12651

J.S. Weis. Department of Biological Sciences, Rutgers University, Newark, NJ 07102, U.S.A.
P. Weis. Department of Anatomy, Cell Biology and Injury Science, New Jersey Medical School, Newark, NJ 07103, U.S.A.

Can. J. Fish. Aquat. Sci. **52**: 2168–2173 (1995). Printed in Canada / Imprimé au Canada

more subtle than the production of gross anatomical abnormalities. The field of behavioral teratology is the study of behavioral abnormalities after embryonic exposure to toxicants. Although there has been considerable work on effects of contaminants on morphological development of fish (reviewed by Weis and Weis 1989), there has been little attention paid to behavioral responses following embryonic exposures to pollutants. Ostrander et al. (1990) found that rainbow trout (*Oncorhynchus mykiss*) embryos, exposed during late organogenesis to benzo[*a*]pyrene, subsequently exhibited a decreased tendency to orient themselves upstream, a response critical for salmonid survival. A recent study (Weis and Weis 1995) showed that larvae of the mummichog (*Fundulus heteroclitus*) exposed as embryos to 5 or 10 ppb methylmercury (concentrations below those that cause structural malformations; Weis and Weis 1977) were less effective in capturing prey than were controls. The differences between experimental and control larvae decreased over time until they were no longer significant.

Antipredator behavior in fish larvae undergoes normal development in association with the development of the sensory and locomotor systems that gradually refine the animal's capabilities to detect predators and time an appropriate response. The normal development of evasive capabilities of fish larvae has been reviewed recently by Fuiman and Magurran (1994), who emphasize the difference between predator avoidance, defined as behaviors that reduce the likelihood of a predator's attack (e.g., reduced conspicuousness), as contrasted with predator evasion, defined as behaviors that reduce capture success after an attack has begun. Developments in the acousticolateralis and visual sensory systems, accompanied by growth in the skeletal and muscular tissues, result in improvements in the timing, magnitude, and direction of the escape response, increasing the probability of successful escape. Evolutionary history and experience can also play a major role. Fuiman (1993) found that as herring (*Clupea harengus*) larvae developed, swimming speed in escapes increased. Escape success was dependent on rapid acceleration when the predator was near, rather than a more prolonged flight initiated earlier. Defense behaviors by prey species, such as freezing, predator inspection, and escape, can be modified by learning (Csanyi and Doka 1993).

The following studies were undertaken (*i*) to ascertain whether embryonic exposure to methylmercury (at concentrations lower than those that cause morphological abnormalities) would affect swimming performance and predator avoidance of mummichog larvae and (*ii*) to ascertain whether larval exposure to methylmercury would affect swimming performance and predator avoidance.

Materials and methods

The mummichog is a very abundant fish that plays an intermediate role in the trophic structure of east-coast marshes of North America. Adults consume primarily crustaceans and annelids and feed on the marsh surface at high tide (Kneib and Stiven 1978). They are significant predators of the grass shrimp, *Palaemonetes* sp. (Knieb 1987), and are in turn eaten by predators such as white perch (*Morone americana*), striped bass (*Morone saxatilis*), and blue crab (*Callinectes sapidus*) (Kneib 1986). Young mummichogs eat primarily meiofauna and small macrofauna (Kneib 1986). Adult grass shrimp, which are important food of large mummichogs, can consume larval mummichogs (Kneib 1987).

Adult mummichogs were collected with minnow traps from East Hampton, New York, during June–July. Eggs and sperm were obtained by stripping the fish. Fertilized eggs from numerous females and males were pooled and placed in glass finger bowls with 50 mL filtered seawater (27‰). Any eggs that did not cleave (a small number) were removed. Methylmercuric chloride (ICN Pharmaceuticals, Plainview, N.Y.) was added from a 0.1 mg/mL stock solution to expose groups of embryos to nominal concentrations of 0, 5, or 10 μg/L methylmercury in 50 mL seawater during development.

Three replicate dishes, each with about 100 eggs, were used for each exposure. Solutions were changed daily until hatching, which occurred 2 weeks after fertilization. Embryos were kept in an incubator at 22°C and a 14 h light : 10 h dark cycle. After hatching, larvae were maintained in filtered seawater in finger bowls in the same incubator, and were fed *Artemia salina* nauplii daily. They were tested starting on the day of hatching and at regular intervals thereafter for swimming performance and predator avoidance.

The test of swimming performance was described by Heath et al. (1993). Larvae were placed, one at a time, in a 9 cm diameter Petri dish with radiating lines on the bottom and a 5 cm diameter Petri dish was placed upside down in the middle, thus creating a "race track" on the outside. Larvae were chased around the track with a glass rod, and the number of lines crossed in 1 min was recorded. To maintain consistency, the same person administered a given group of tests, and tests were done "blind." Heath et al. (1993) thought that this test reliably indicated maximum swimming ability, which is important in evading predation. Our modification of the test involved using 16 radiating lines rather than 8 and recording the number of lines crossed at 30 s as well as at 60 s. In some cases we recorded the number of reversals of direction (180° turns) made during the test. Twenty larvae from each group (about 7 selected randomly from each replicate dish) were tested in all experiments. Before testing, larvae were given 2 min to acclimate to the Petri dish, and after testing they were returned to the finger bowls. Since the number of larvae for each exposure far exceeded the numbers actually tested, it is unlikely (but possible) that some of the same larvae were retested as they grew older.

The normal development of swimming performance in untreated larvae was observed in preliminary tests conducted on larvae hatched from eggs fertilized in June. In July, four experiments (trials) were performed to investigate the effects of methylmercury exposure on subsequent swimming performance. The first experiment used embryonic exposure only, and larvae were tested at 1 day and at 3 or 4 days after hatching. The second experiment was a repeat of this with another batch of eggs, but in these tests we also recorded the number of turns, as well as the lines crossed. The third experiment used larvae that had not been previously exposed as embryos. At 3 weeks of age, one group was placed in 10 μg/L methylmercury for

Table 1. Experiment 1: swimming performance measured as number of lines crossed in 30 and 60 s by 1-day-old and 3- to 4-day old mummichog larvae after embryonic exposure to methylmercury.

	1-day-old larvae		3- to 4-day-old larvae	
	30 s	60 s	30 s	60 s
Treatment				
Control	27.7±2.14	48.45±3.61	43.7±2.8	69.3±4.9
5 μg/L	28.85±1.67	50.4±3.56	43.8±2.4	72.3±4.4
10 μg/L	36.9±1.67	63.70±3.13	50.2±1.4	76.8±2.5
ANOVA				
F	7.65	6.12	2.76	0.90
P	0.0001	0.0039	<0.05	>0.05
Bonferroni	10 > 5, C	10 > 5, C	10 > 5, C	

Note: Values are given as the mean ± SE.

Fig. 1. Swimming performance of mummichog larvae of different ages. The bars show the mean and standard error of the number of lines crossed. $N = 20$.

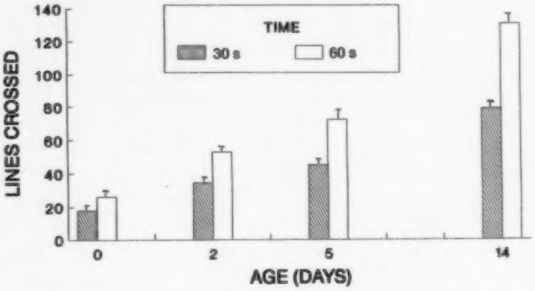

1 week, after which time 20 experimental and 20 control larvae were tested. Then the experimental larvae were returned to clean water for a week of depuration, after which 20 controls and 20 experimentals were again tested (at 5 weeks of age). The fourth experiment combined embryonic and larval exposures. One group was in clean water throughout (C-C), the second group was in clean water as embryos and in 10 μg/L methylmercury as larvae (C-10), the third group was in 10 μg/L methylmercury as embryos and clean water as larvae (10-C), and the fourth group was in 10 μg/L methylmercury throughout (10-10). These larvae were tested at 1 and 2 weeks after hatching.

For tests that included three or more exposure groups (e.g., controls, 5, and 10 μg/L) data were tested by one-way ANOVA followed by Bonferroni multiple comparison tests in cases where the *F* value was significant to the 0.05 level. In trials with only two groups, *t* tests were employed.

A second series of experiments utilized real predators. Larvae up to 2 weeks old were placed in groups of 10 in 5-L plastic containers (17 × 28 cm) filled to a depth of 5.5 cm with 27‰ seawater. Each container had three unfed adult grass shrimp (*Palaemonetes pugio*), which had been collected from Southampton, New York, acclimated to laboratory conditions for at least 1 week, and then given 1 h of acclimation time in the test container. The containers were in an isolated part of the room, where they would not be disturbed. While the larvae were being introduced at one end of the tank, the predators were held at the other end with a net. We used as many replicates as possible depending on the number of available larvae. The number of larvae remaining after 24 h was recorded. Since the room had natural light, about 14 h were daytime and 10 h nighttime. Data were analyzed by ANOVA and chi-square tests.

By about 2 weeks of age, larvae could not be captured by *P. pugio*, and so were tested using three 1-year-old mummichogs as predators. The predators had been acclimated to the laboratory for at least 2 weeks, and to the test tank for 1 h. A large rock placed in the center of the tank served as a refuge. The number of larvae remaining after 10 min was recorded. Data were analyzed by *t* tests and chi-square tests.

Results

Swimming performance

Preliminary data on untreated larvae indicated rapid improvement of swimming performance with age and growth (Fig. 1). The 30-s distance was more than half of the 60-s distance, indicating that fish were tiring during the second half of the test. However, the ratio of the 60 s / 30 s distance increased steadily from 1.4 for newly hatched to 1.7 for 2-week-old larvae, indicating increased stamina.

A number of different response patterns were noted: (*a*) rapid swimming, seldom changing direction; over time the distance covered decreases (most common in younger larvae), suggesting fatigue; (*b*) much changing of direction, seldom exceeding one fourth of the way around the track before changing direction, often passing only one or two lines before turning; (*c*) refractory or (presumedly exhausted) no response, seen only in very young larvae; (*d*) a combination of *a* and *b*, rapid swimming and rapid direction changes, evasive behavior (seen most in oldest larvae). During the 1-min test, most fish started with *a* and switched to *b*, though some started with *b* and switched to *a*. A few fish exhibited an *a-b-a* or *b-a-b* pattern. Very young fish often exhibited an *a-c*, *a-c-a*, or *a-c-b* pattern over the 60 s.

The first larvae that had been exposed to methylmercury as embryos were tested in early July ($N = 20$ for each group). Treatment with 5 μg/L had no effect, but larvae that had been exposed to 10 μg/L showed increased swimming performance (Table 1). Bonferroni pairwise comparisons of means for 1-day-old larvae showed that the fish treated at 10 μg/L methylmercury swam significantly further than the other two groups at both 30 and 60 s. When 3- to 4-day-old larvae were tested, a similar pattern was seen. Bonferroni pairwise comparisons of means showed that the fish treated with 10 μg/L methylmercury swam significantly more than the other two groups at 30 s but not at 60 s. Again there was a substantial improvement in performance between the 1-day-old and 3- to 4-day old larvae. Since 5 μg/L methylmercury had no effect, this dose was not used in later experiments.

Table 2. Experiment 2: number of turns made by 1-day-old larvae after embryonic exposure to methylmercury.

	No. of turns	
	30 s	60 s
Treatment		
Control	0.92±0.20	2.17±0.40
10 μg/L	4.33±1.36	7.25±2.20
t	2.49	2.27
P	<0.05	<0.05

Note: Values are given as the mean ± SE.

Table 3. Experiment 3: swimming performance and turns made by 4-week-old larvae after 1 week of larval exposure to methylmercury, followed by tests after 1 week of depuration (5 weeks old).

	Lines crossed		Turns	
	30 s	60 s	30 s	60 s
	4-week-old larvae			
Control	68.7±2.96	108.1±5.0	14.4±1.2	24.6±1.9
10 μg/L	49.0±3.06	84.8±4.4	7.8±1.5	14.4±2.1
t	4.63	3.50	3.44	3.60
P	<0.005	<0.005	<0.005	<0.005
	5-week-old larvae			
Control	71.25±2.2	129.2±4.0		
Depurated	68.4±2.3	126.4±4.7		

Note: Values are given as the mean ± SE. The differences between values for 5-week-old larvae in the control and depuration groups were not statistically significant.

When this experiment was repeated with another group of larvae (experiment 2) the data were similar (not shown). However, the number of turns was monitored and the 10 μg/L methylmercury group was observed to change direction more often than controls (Table 2).

In experiment 3, effects of larval exposure were examined on 3-week-old larvae that had not been exposed previously. The data indicated that exposure to methylmercury significantly reduced swimming performance (Table 3). It was also noted that the methylmercury-exposed fish changed direction significantly less often than the controls. After 1 week of depuration, however, there were no longer any significant differences in swimming performance, indicating recovery from the effects of the larval exposure. The number of turns was not monitored on this occasion.

The fourth experiment examined the effects of combined or separate embryonic and larval exposures to 10 μg/L methylmercury. Larvae were tested for swimming performance 1 week after hatching. Bonferroni analysis for the 30- and 60-s trials revealed three groups that differed significantly (Table 4): (*i*) C-10 (which swam the least), (*ii*) C-C and 10-10 (which were intermediate and not significantly different from each other), and (*iii*) 10-C (which swam the most). These results indicate that the C-10 group had lower swimming performance than controls resulting from larval exposure, that the 10-C group had greater swimming performance resulting from the effects of embryonic exposure, and that the 10-10 group was comparable with controls, perhaps because the embryonic and larval exposures, with opposite effects, had cancelled each other out. Two weeks after hatching, larvae were tested again. Bonferroni analysis for 30- and 60-s trials revealed two groups: C-10 and 10-10 (reduced swimming), and C-C and 10-C (unaffected). Thus, by this time, those exposed only as embryos were no longer swimming more than controls, but all those exposed as larvae were swimming less than controls. This indicates that the effect of the embryonic exposure was fading, but that continuous larval exposure still resulted in reduced swimming performance.

Grass shrimp predation

Larvae from many of the above experiments were tested for predator avoidance with the grass shrimp. Since the shrimp were rather ineffective predators, the predator and prey were kept together for 24 h. The fish reacted to the shrimp by dashing away, and the shrimp did not pursue them. Often, accidental contact with the shrimp's antennae provoked the fish's escape response. Roughly half of the fish in each container apparently found that the surface of the water provided a refuge, and remained there, something never seen in fish in containers without shrimp. Fish that were not at the surface were not preyed upon heavily either. When a shrimp did capture a fish, it was not by pursuit but by ambush; the shrimp made a quick lunge and caught a passing larva in its chela.

There was a consistent trend toward increased predation on larvae that had been exposed as embryos or larvae to methylmercury, although for any given trial, the variability was high and the number of replicates fairly low (about five each time) because of the limited number of larvae available, so that the data were not statistically significant. However, if data from three different trials were pooled to provide 15 replicates, statistical significance was achieved (Fig. 2; ANOVA, $F = 3.74$, $P = 0.032$). Bonferroni pairwise comparisons of means showed two groups: the controls and 5 μg/L, and the 5 and 10 μg/L. The control and 10 μg/L data were significantly different ($\chi^2 = 10.44$, $P < 0.01$). This indicates that, despite the increased swimming seen in the Petri dish tests, larvae that had been exposed to 10 μg/L methylmercury as embryos were more susceptible to grass shrimp predation than controls.

Tests on the C-C, C-10, 10-C, and 10-10 groups from the last experiment also indicated a trend toward less capture of the C-C group than the other three, but because of variability and limited numbers of replicates, data did not reach statistical significance.

Mummichog predation

One-year-old mummichogs were allowed to prey on 1-month-old larvae exposed for 1 week to methylmercury. Once mummichogs noticed the larvae, they aggressively chased and captured them. The only larvae that survived were

Table 4. Experiment 4: swimming performance measured by number of lines crossed at 30 and 60 s, of 1- and 2-week-old larvae after embryonic and (or) larval exposure to 0 µg/L (control, C) or 10 µg/L methylmercury (10).

	1-week-old larvae		2-week-old larvae	
	30 s	60 s	30 s	60 s
Treatment[a]				
C-C	48.45±1.96	78.3±3.58	57.4±3.74	103.65±4.27
C-10	41.05±1.28	67.85±2.52	40.65±2.83	76.5±4.32
10-C	58.5±2.60	95.45±3.30	65.25±2.25	110.6±4.74
10-10	51.35±2.27	81.85±3.82	49.95±2.76	88.20±4.84
ANOVA				
F	12.14	12.11	17.48	11.95
P	<0.0005	<0.0005	<0.0005	<0.0005
Bonferroni	C-10 < C-C = 10-10 < 10-C	C-10 < C-C = 10-10 < 10-C	C-10 = 10-10 < C-C = 10-C	C-10 = 10-10 < C-C = 10-C

Note: Values are given as the mean ± SE.

[a] C-C, control (embryos and larvae not exposed to methylmercury); C-10, control embryos, larvae exposed to 10 µg/L methylmercury; 10-C, embryos exposed to 10 µg/L methylmercury, control larvae; 10-10, embryos and larvae exposed to 10 µg/L methylmercury.

Fig. 2. Predation on control and methylmercury-exposed mummichog larvae by grass shrimp or 1-year-old mummichogs, shown as the mean number of survivors (+SE). The first three bars represent predation in 24 h by grass shrimp on groups of ten 4-day-old larvae after embryonic exposure. The last two bars represent predation in 10 min by 1-year-old mummichogs on groups of ten 4-week-old larvae after 1 week of larval exposure.

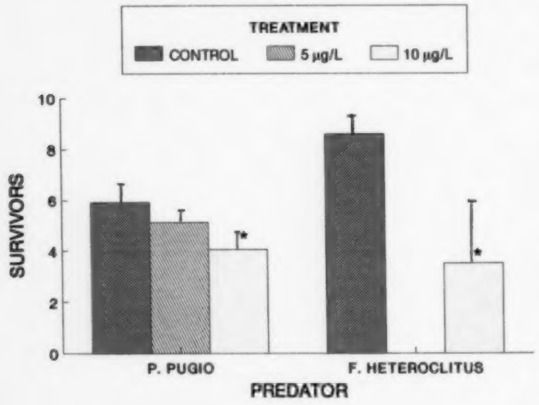

those that hid under the rock. After 10 min, the number of controls surviving was significantly higher than the number of exposed larvae (Fig. 2; $t = 2.26$, $P < 0.05$; $\chi^2 = 24.8$, $P < 0.001$). Because of heavy predation on the methylmercury-exposed larvae, too few remained to repeat the experiment after the week of depuration.

Mummichog predation was also tested on the C-C, C-10, 10-C, and 10-10 groups from the fourth experiment when they were 3 weeks old. Because of variability and numbers of replicates, there were no significant differences, but there was a trend in which those exposed to methylmercury as embryos or as embryos and larvae were more susceptible to predation than the controls.

Discussion

The test of swimming performance indicated that embryonic exposure to 10 µg/L methylmercury increased swimming performance (and, when measured, turns), while larval exposure decreased it. Increased swimming performance and number of turns could be evasive techniques to escape predators but might also reflect general hyperactivity. In mammalian behavioral teratology, there have been many instances of prenatal exposures causing hyperactivity, not necessarily seen in later exposures. Rats exposed to DDT (1,1-bis(*p*-chlorophenyl)-2,2,2-trichloroethane) during gestation ran a maze faster than controls, while those exposed during both gestation and lactation were slower than controls (Craig and Ogilvie 1974). Gray et al. (1981) found increased activity in 16- and 20-day-old rat pups prenatally exposed to endrin, but this increase was no longer seen at 90 days of age. Studies have shown hyperactivity in rats after prenatal lead exposure (Hastings et al. 1977; Zenick et al. 1979). However, many children with elevated lead concentrations exhibit muscle weakness, and lead-treated monkeys developed anorexia, lethargy, and muscle weakness (Van Gelder 1978). McCarren and Eccles (1983) found that exposure of rats to lead from birth to weaning produced hyperactivity in the young animals, but as adults these animals were hypoactive. Some natural neuronal substances can also have different effects on developing versus older nervous systems. Myelin-associated glycoprotein, which stimulates neurite outgrowth from developing neurons, was recently found to inhibit neurite outgrowth of adult central nervous system cells in culture (Mukhopadhyay et al. 1994).

In our experiments on mummichogs, the embryonic effects of methylmercury in stimulating swimming performance decreased over time. The temporary effects of embryonic exposure are similar to that which was noted in the prey capture ability of mummichogs after embryonic exposure to methylmercury (Weis and Weis 1995). The concentrations used here are higher than would be found in polluted waters; however, fish embryos from polluted environments could get additional Hg burden via the yolk.

By using the Heath et al. (1993) test as well as real predators, we could investigate whether altered swimming performance was comparable with avoiding a predator. In the latter situation, additional factors, such as quick reaction and the ability to be inconspicuous (e.g., hiding or remaining motionless), are important. The increased swimming performance following embryonic exposure to 10 ppb methylmercury was not associated with improved avoidance of grass shrimp predation, but rather with greater predation. Since the shrimp did not chase the larvae, swimming performance as measured here is irrelevant. Inconspicuousness and quick response are probably more important. Swimming performance might be more important in avoiding some other predator, however. The most important behavior needed to avoid predation by 1-year-old mummichogs was hiding under the rock. While greater swimming performance might prolong a larva's life by a few seconds, the larvae cannot outswim their larger conspecifics. Thus, this test is useful in evaluating swimming performance, but swimming performance is only relevant in certain predator–prey situations, and not in the ones studied here.

Possibly the improved swimming performance after embryonic methylmercury exposure reflected increased overall activity, which might have increased the conspicuousness of the fish, causing them to be attacked more than controls. Increased activity of parathion-exposed grass shrimp made them more conspicuous, resulting in increased capture (Farr 1977). Thus, predator avoidance, in the sense of limiting encounters (Fuiman and Magurran 1994), appears to be more important than predator evasion after an attack has begun in cases where the prey species has limited swimming abilities. As Fuiman and Magurran (1994) stated, "their best ploy might be to remain motionless."

Acknowledgments

We appreciate the hospitality of the Marine Science Center of Southampton College, especially Drs. Thomas Haresign, Sandra Shumway, and Howard Reisman. We also appreciate the technical assistance of Laura Glenn and Jason Campbell, and the critical review of an earlier draft of this paper by Lee Fuiman.

References

Craig, G.R., and D.M. Ogilvie. 1974. Alteration of T-maze performance in mice exposed to DDT during pregnancy and lactation. Environ. Physiol. Biochem. 4: 189–199.

Csanyi, V., and A. Doka. 1993. Learning interactions between prey and predator fish. Mar. Behav. Physiol. 23: 63–78.

Farr, J.A. 1977. Impairment of antipredator behavior in *Palaemonetes pugio* by exposure to sublethal doses of parathion. Trans. Am. Fish. Soc. 106: 287–290.

Fuiman, L.A. 1993. Development of predator evasion in the Atlantic herring, *Clupea harengus* L. Anim. Behav. 45: 1101–1116.

Fuiman, L.A., and A. Magurran. 1994. Development of predator defences in fishes. Rev. Fish Biol. Fish. 4: 145–183.

Gray, L.E., Jr., R.L. Kavlock, N. Chernoff, J.A. Gray, and J. McLamb. 1981. Perinatal toxicity of endrin in rodents. III. Alteration of behavioral ontogeny. Toxicology, 21: 187–202.

Hastings, L., G.P. Cooper, R.L. Bornschein, and I.A. Michaelson. 1977. Behavioral effects of low level neonatal lead exposure. Pharmacol. Biochem. Behav. 7: 37–42.

Heath, A.G., J. Cech, J. Zinkl, B. Finlayson, and R. Fujimora. 1993. Sublethal effects of methyl parathion, carbofuran, and molinate on larval striped bass. *In* Water quality and the early life history of fishes. *Edited by* L. Fuiman. Am. Fish. Soc. Symp. 14: 17–28.

Kneib, R.T. 1986. The role of *Fundulus heteroclitus* in salt marsh trophic dynamics. Am. Zool. 26: 259–269.

Kneib, R.T. 1987. Predation risk and use of intertidal habitats by young fishes and shrimp. Ecology, 68: 379–386.

Kneib, R.T., and A. Stiven. 1978. Growth, reproduction and feeding of *Fundulus heteroclitus* (L) on a North Carolina salt marsh. J. Exp. Mar. Biol. Ecol. 31: 121–140.

Kraus, M.L., and D.B. Kraus. 1986. Differences in effects of mercury on predator avoidance in two populations of grass shrimp, *Palaemonetes pugio*. Mar. Environ. Res. 18: 277–289.

Little, E.E., R.D. Archeski, B. Flerov, and V. Kozlovskaya. 1990. Behavioral indicators of sublethal toxicity in rainbow trout. Arch. Environ. Contam. Toxicol. 19: 380–385.

Little, E.E., J.F. Fairchild, and A.J. DeLonay. 1993. Behavioral methods for assessing impacts of contaminants on early life stages of fishes. *In* Water quality and the early life history of fishes. *Edited by* L. Fuiman. Am. Fish. Soc. Symp. 14: 67–76.

McCarren, M., and C.U. Eccles. 1983. Neonatal lead exposure in rats. 1. Effects on activity and brain metals. Neurobehav. Toxicol. Teratol. 5: 527–531.

Mukhopadhyay, G., P. Doherty, F. Walsh, P. Crocker, and M.T. Filbin. 1994. A novel role for myelin-associated glycoprotein as an inhibitor of axonal regeneration. Neuron, 13: 757–767.

Ostrander, G., J.J. Anderson, J.P. Fisher, M.L. Landolt, and R.M. Kocan. 1990. Decreased performance of rainbow trout, *Oncorhynchus mykiss* emergence behaviors following embryonic exposure to benzo[*a*]pyrene. Fish. Bull. 88: 551–555.

Sullivan, J.F., G.J. Atchison, D.J. Kolar, and A.W. MacIntosh. 1978. Changes in predator–prey behavior of fathead minnow (*Pimephales promelas*) and largemouth bass (*Micropterus salmoides*) caused by cadmium. J. Fish. Res. Board Can. 35: 446–451.

Van Gelder, G.A. 1978. Lead and the nervous system. *In* Toxicity of heavy metals in the environment. *Edited by* F.W. Oehme. Marcel Dekker Inc., New York. pp. 101–121.

Weis, J.S., and P. Weis. 1989. Effects of environmental pollutants on early fish development. Rev. Aquat. Sci. 1: 45–73.

Weis, J.S., and P. Weis. 1995. Effects of embryonic exposure to methylmercury on larval prey capture ability in the mummichog, *Fundulus heteroclitus*. Environ. Toxicol. Chem. 14: 153–156.

Weis, P., and J.S. Weis. 1977. Methylmercury teratogenesis in the killifish, *Fundulus heteroclitus*. Teratology, 16: 317–326.

Zenick, H., J. Ward, W. Rodriguez, P. Aragon, and R. Scrivseth. 1979. Offspring open field performance following maternal lead exposure: a question of dosage and nutritional status. Pharmacol. Biochem. Behav. 11: 35–38.

Empirical and theoretical analyses of correction of time-series bias in stock-recruitment relationships of sockeye salmon (*Oncorhynchus nerka*)

Josh Korman, Randall M. Peterman, and Carl J. Walters

Abstract: Using data from 30 sockeye salmon (*Oncorhynchus nerka*) stocks and Monte Carlo simulations, we examined the importance of time-series bias on estimates of optimal harvest rate, optimal escapement, and sustainable yield. We compared the performance of the least-squares procedure for fitting a Ricker curve with an existing bias-correction method. Simulations showed that the effect of time-series bias is greatest for low-productivity stocks that exhibit a high degree of autocorrelation among residuals of the stock-recruitment relationship. A strong inverse empirical relationship between autocorrelation and stock productivity among the 30 stocks suggests that time-series bias is a more important concern for low-productivity northern stocks than for more productive southern stocks. The corrected method reduced bias in optimal escapement estimates under a limited set of conditions but at the price of increased variance in the estimates. For a constant escapement goal policy, using the bias correction thus resulted in sustainable yields slightly lower than or equal to expected values for 28 of the 30 stocks compared with yields obtained using the standard least-squares estimation method. We demonstrate the value of using a decision theoretic approach to evaluate the performance of estimation methods.

Résumé : À partir de données provenant de 30 stocks de saumon rouge (*Oncorhynchus nerka*) et en utilisant des simulations de Monte Carlo, nous avons étudié l'effet du biais des séries chronologiques sur les estimations du taux de capture optimal, de l'échappée optimale et de la production équilibrée. Nous avons comparé la performance de la méthode des moindres carrés pour ajuster une courbe de Ricker avec une méthode existante de correction de justesse. Les simulations montrent que l'effet du biais des séries chronologiques est au plus haut dans le cas de stocks à faible productivité, pour lesquels on note un degré élevé d'autocorrélation dans la variance résiduelle de la relation stock-recrutement. L'importante relation empirique inverse observée dans les 30 stocks entre l'autocorrélation et la productivité du stock semble indiquer que le biais des séries chronologiques est plus inquiétant chez les stocks nordiques peu productifs que chez les stocks méridionaux plus productifs. La méthode corrigée diminue les biais dans les estimations de l'échappée optimale dans des conditions précises, mais il en résulte une variance accrue dans les estimations. Si l'on vise une échappée constante, le recours à la correction de justesse aboutit donc à une production légèrement inférieure ou égale à la production équilibrée escomptée pour 28 des 30 stocks par rapport aux résultats obtenus à l'aide de la méthode d'estimation des moindres carrés. Nous avons démontré la valeur de l'approche fondée sur une méthode de décision théorique pour l'évaluation de la performance des méthodes d'estimation.

[Traduit par la Rédaction]

Introduction

The relationship between stock and recruitment is fundamental to setting harvest rates and target escapements for Pacific salmon (*Oncorhynchus* spp.) stocks. There has been much research concerning biases and estimation problems that occur when fitting these relationships to stock-recruit observations (Walters and Ludwig 1981; Ludwig and Walters 1981; Walters 1985, 1990; Armstrong and Shelton 1988; Caputi 1988; Walters and Collie 1988). Bias means that the average value of the parameter based on a sample would not equal the true parameter value (Hilborn and Walters 1992). An important bias first pointed out by Walters (1985) arises from the fact that stock-recruitment (SR) relationships are generally estimated from time-series data where stock sizes are not controlled perfectly but vary over time because of environmental effects and deviations from target escapements. As a result of these effects, successive stock-recruit observations are not independent and

Received November 15, 1994. Accepted April 28, 1995.
J12630

J. Korman[1] **and R.M. Peterman.** School of Resource and Environmental Management, Simon Fraser University, Burnaby, BC V5A 1S6, Canada.
C.J. Walters. Fisheries Centre, University of British Columbia, Vancouver, BC V6T 1W5, Canada.

[1] Author to whom all correspondence should be addressed. Present address: 3320 West 5th Avenue, Vancouver, BC V6R 1R7, Canada.

Can. J. Fish. Aquat. Sci. **52**: 2174–2189 (1995). Printed in Canada / Imprimé au Canada

can generate parameter estimates of maximum recruits per spawner that are too high and estimates of unfished equilibrium stock size that are too low (Walters 1985, 1990). Walters termed this time-series bias. If these biased Ricker parameters are used to set management policies, optimal escapements will be underestimated and optimal harvest rates will be overestimated.

Time-series bias also results in an underestimate of the temporal correlation among residuals (Kendall et al. 1983) from the SR relationship (hereafter referred to as autocorrelation) and therefore affects both the estimation of the average SR relationship and our ability to understand what drives the interannual variability around this relationship. Potential causes for such patterns in residuals include changes over time in stock structure, the physical and biological environment altering natural mortality rates, and the proportion of catch misallocated to different stocks owing to interception fisheries. Autocorrelation attributed to stock structure or the physical or biological environment has been referred to as nonstationarity in SR parameters (see Hilborn and Walters 1992).

Other simulation studies have defined the factors controlling the degree of time-series bias in α and β (parameters of the Ricker model) as estimated using the standard least-squares method ($\log_e (R/S)$ vs. S (Ricker 1975), where R = recruits and S = spawners). Cass (1989) found that the bias was profoundly affected by variation in stock size within his simulated data sets and that bias increased with decreasing sample size (i.e., shorter SR time series). Myers and Barrowman (1995) used a multispecies data set of 27 Pacific salmon stocks from B.C. and Alaska to set bounds for plausible ranges of α, harvest rates, residual SR variation, and autocorrelation of residuals used in their simulations. Their results were similar to Cass' (1989), but also showed that the bias in Ricker parameters increased with residual SR variation and autocorrelated recruitment. Walters (1990) developed a procedure to correct time-series bias and tested its performance using Monte Carlo simulations. The performance of this correction was found to be dependent on the amount of interannual variability in spawning stock size and the extent of autocorrelation in residuals. For example, the correction did not improve the estimate of β when the stock-recruit data were generated under conditions simulating severe recruitment overfishing.

Comparison of estimates of optimal escapement or optimal harvest rates and the resulting yields from applying these two estimation procedures are considerably more relevant to fisheries managers than Ricker α and β parameters and yet little work has been done on this to date. Cass (1989) and Myers and Barrowman (1995) provided a detailed characterization of time-series bias, but their studies focused solely on the bias in α and β, and they did not translate these biases into their effect on estimates of optimal escapement or harvest rates. Estimates of bias in α and β, which are based on the average value of a large number of simulations, cannot be directly translated to biases in optimal management strategies because the relationship between optimal harvest rate or optimal escapement and α and β is not linear. Walters (1985) computed the bias in uncorrected optimal escapement and optimal harvest rate estimates, but the range of his simulations describing different stock characteristics was very narrow. Walters' (1990) evaluation of the correction method was also done over a narrow range of stock characteristics, and the performance of the estimator was only evaluated in terms of bias in α and β values.

In our study we translate parameter bias into its effects on estimates of optimal harvest rates or optimal escapement targets, and we do this over a broad range of simulated stock characteristics. We take our analysis one step further than previous research by examining the extent to which yield is reduced by applying biased, and therefore nonoptimal, estimates of constant harvest rate or target escapement. This approach is used to compare the performance of the standard least-squares estimation method (hereafter referred to as the uncorrected method) with the bias-correction method.

We used both empirical and simulation analyses. We compared the least-squares method with Walters' time-series bias-correction method using SR data from 30 sockeye salmon (*Oncorhynchus nerka*) stocks in B.C. and Alaska to quantify the difference in optimal harvest rate and optimal escapement estimates using real, rather than simulated, data. This empirical analysis identified stocks for which the bias correction makes a large difference in management strategies compared with estimates made using the uncorrected method of fitting Ricker SR models. However, based on these empirical results, we could not determine if the bias correction results in more accurate parameter estimates than the uncorrected ones because the true parameter values are not known. To address this issue, we used Monte Carlo simulations where we assumed some "true" parameter values. These simulations captured features of data from the 30 sockeye salmon stocks: the range in α, variance of residuals from the fitted SR relationships, temporal correlation structure of residuals, and the historical exploitation rates. By assuming some "true" value for these attributes, we compared the optimal escapement, optimal harvest rate, and maximum sustainable yield (MSY) with those estimated using the uncorrected and corrected procedures.

There were three main objectives to our study. The first was to examine the extent of time-series bias in optimal management strategies (rather than just Ricker α and β values) over a broad range of stock characteristics and the effect of the bias on yield. Our second objective was to define the conditions under which it is better to use the corrected method rather than the standard uncorrected one by comparing the performance of both estimators in terms of yield. Our final objective was to highlight the need to use a decision theoretic approach, rather than just point estimates of bias, to evaluate the performance of estimation methods used in fisheries management.

Methods

Empirical analyses

All the B.C. and Alaskan sockeye stock and recruitment data used in this analysis were from the International Pacific Salmon Commission (IPSC) (J. Woodey, IPSC, Vancouver, B.C., personal communication), the Canadian Department of Fisheries and Oceans (DFO) (L. Jantz, DFO, Prince Rupert, B.C., personal communication), and the

Table 1. Summary statistics of historical data and stock-recruitment relationships for 30 sockeye salmon stocks.

Stock name	Stock number	Region	Period covered (brood year)	Years of data	Mean age-at-return (years)	Mean recruits	Average harvest rate (%)	Uncorrected				Corrected			
								α	β	ρ	σ	α^*	β^*	ρ	σ
Adams	1	BC	1949–1984	36	4.0	2 080 467	77	2.47	7.26×10^{-7}	0.21	1.01	2.38	3.70×10^{-7}	0.21	1.02
Birkenhead	2	BC	1949–1984	36	4.1	394 903	84	2.96	9.97×10^{-6}	0.20	0.59	2.78	2.77×10^{-6}	0.23	0.60
Bowron	3	BC	1949–1984	36	4.1	51 592	81	2.69	6.98×10^{-5}	0.23	0.66	2.54	4.15×10^{-5}	0.27	0.68
Branch	4	AK	1957–1982	26	4.7	373 842	60	1.73	3.29×10^{-6}	0.84	0.83	1.49	1.56×10^{-6}	0.79	0.89
Chilko	5	BC	1948–1984	37	4.0	1 161 584	77	2.59	2.42×10^{-6}	0.16	0.63	2.42	1.05×10^{-6}	0.29	0.64
Cultus	6	BC	1949–1984	36	4.0	83 731	77	2.17	1.68×10^{-5}	0.27	0.80	1.94	-8.65×10^{-6}	0.21	0.82
Egegik	7	AK	1957–1982	26	5.3	3 513 569	57	2.43	1.13×10^{-6}	0.56	0.68	2.03	2.65×10^{-7}	0.58	0.70
Early Stuart	8	BC	1949–1984	36	4.1	296 844	77	2.44	4.85×10^{-6}	0.26	0.66	2.32	1.28×10^{-6}	0.35	0.68
Fennel	9	BC	1949–1984	36	4.2	11 347	76	3.57	3.36×10^{-6}	−0.14	0.92	3.52	3.05×10^{-6}	−0.13	0.92
Gates	10	BC	1952–1984	33	3.9	30 687	82	3.26	1.25×10^{-6}	0.11	1.00	3.16	7.63×10^{-7}	0.15	1.01
Harrison	11	BC	1950–1985	36	3.5	44 433	69	3.00	1.50×10^{-4}	0.17	0.86	2.86	1.31×10^{-4}	0.17	0.87
Horsefly	12	BC	1949–1984	36	4.0	580 811	77	2.80	-8.74×10^{-7}	−0.23	0.94	2.81	-5.20×10^{-7}	−0.23	0.94
Igugik	13	AK	1957–1982	26	4.9	795 842	49	2.30	4.02×10^{-6}	0.68	0.91	2.04	2.73×10^{-6}	0.68	0.95
Kvichak	14	AK	1957–1982	26	4.9	11 523 400	34	1.38	3.89×10^{-8}	0.53	0.92	1.25	-3.05×10^{-9}	0.51	0.93
Lower Shuswap	15	BC	1949–1984	36	4.0	169 385	80	3.16	4.83×10^{-7}	−0.29	1.48	3.19	6.79×10^{-7}	−0.32	1.48
Late Stuart	16	BC	1949–1984	36	4.1	363 651	79	2.71	4.25×10^{-7}	0.13	1.29	2.64	2.14×10^{-7}	0.13	1.30
Mitchell	17	BC	1949–1984	36	4.1	64 683	67	2.71	-2.84×10^{-6}	−0.07	1.63	2.65	-4.55×10^{-6}	−0.05	1.64
Nadina	18	BC	1950–1984	35	4.1	56 770	80	3.17	7.67×10^{-7}	0.08	0.87	3.07	5.58×10^{-7}	0.15	0.88
Naknek	19	AK	1957–1982	26	5.1	2 920 104	52	2.22	9.52×10^{-7}	0.24	0.49	2.21	9.23×10^{-7}	0.23	0.49
Nuyakuk	20	AK	1957–1982	26	4.8	1 004 846	50	2.02	1.45×10^{-6}	0.43	0.79	1.99	1.30×10^{-6}	0.42	0.79
Portage	21	BC	1949–1984	36	3.9	26 036	79	3.37	1.73×10^{-6}	0.19	1.14	3.19	9.89×10^{-7}	0.31	1.17
Raft	22	BC	1949–1984	36	4.2	28 619	78	2.69	1.44×10^{-6}	0.07	0.75	2.48	6.72×10^{-7}	0.11	0.76
Scotch	23	BC	1949–1984	36	4.0	11 843	78	3.21	2.00×10^{-6}	−0.41	1.51	3.11	1.27×10^{-6}	−0.47	1.52
Seymour	24	BC	1949–1984	36	4.0	125 161	79	2.67	2.41×10^{-5}	−0.01	0.79	2.61	1.84×10^{-5}	0.02	0.79
Skeena	25	BC	1948–1985	38	4.4	1 825 845	51	1.95	1.10×10^{-6}	−0.14	0.60	1.81	6.99×10^{-7}	−0.20	0.60
Stellako	26	BC	1949–1984	36	4.1	463 297	81	2.66	5.86×10^{-6}	−0.09	0.57	2.61	4.62×10^{-6}	−0.09	0.57
Togiak	27	AK	1957–1982	26	4.8	459 196	66	2.59	9.28×10^{-6}	0.54	0.55	2.49	8.00×10^{-6}	0.54	0.56
Ugashik	28	AK	1957–1982	26	5.0	1 915 019	34	1.61	3.57×10^{-7}	0.79	1.27	1.58	2.82×10^{-7}	0.79	1.27
Weaver	29	BC	1949–1984	36	4.1	236 183	73	2.43	3.58×10^{-6}	0.23	1.13	2.27	-5.36×10^{-6}	0.21	1.15
Wood	30	AK	1957–1982	26	4.6	2 300 442	44	1.92	8.93×10^{-7}	0.65	0.51	1.89	8.31×10^{-7}	0.63	0.51
			Min	26	3.5	11 347	34	1.38	-2.84×10^{-6}	−0.41	0.49	1.25	-8.65×10^{-6}	−0.47	0.49
			Mean	33	4.3	1 097 138	68	2.56	1.06×10^{-5}	0.21	0.89	2.44	6.90×10^{-6}	0.22	0.90
			Max	38	5.3	11 523 400	84	3.57	1.50×10^{-4}	0.84	1.63	3.52	1.31×10^{-4}	0.79	1.64

Note: Parameter estimates for the stock-recruitment relationships are shown as uncorrected (standard least-squares estimates) or corrected (using Walters' (1990) time-series bias correction). BC, British Columbian stocks; AK, Alaskan stocks; ρ, lag-1-year autocorrelation coefficient; σ, standard deviation of residuals from stock-recruitment curve. α and β values are in effective female spawner units.

Alaska Department of Fish and Game (ADFG) (Yuen and Nelson 1987; and H. Yuen, ADFG, Anchorage, Alaska, personal communication). All the Alaskan stocks spawn in rivers that empty into Bristol Bay in the Bering Sea. With the exception of the Skeena River stock, all the B.C. stocks used in this analysis originate in tributaries of the Fraser River, entering the ocean through the Strait of Georgia. The number of years of stock-recruit data for each stock varied from a minimum of 26 to a maximum of 38 (Table 1).

With the exception of the Skeena River stock, effective female spawners (*S*, number of females weighted by the proportion of their eggs that were laid) was used in place of total spawners as an index of stock size to reduce the effect of between-stock variability in sex ratios and egg retention on Ricker parameter estimates. For the Skeena River stock, data on effective female spawners were not available, so we assumed that half of the total spawners were effective female spawners. Recruits (catch + escapement) for a given brood year included all adult returns between ages 3 and 6 years that originated from one or two smolt age-classes, depending on the stock.

What we refer to here as the uncorrected Ricker SR parameters were estimated by the usual (Ricker 1975) regression of $\log_e(R/S)$ on S using the following model form:

$$[1] \quad R_t = S_t \cdot e^{\alpha + \beta \cdot S_t + v_t}$$

where R_t represents the number of recruits from effective female spawners in year t, S_t represents the number of effective female spawners in year t, e^{α} is the maximum number of recruits per effective female spawner, β is the parameter of density-dependence (α/β = unfished equilibrium stock size), and v_t is the normally distributed error term ($\bar{v} = 0$ and standard deviation = σ).

The corrected Ricker SR parameters were estimated by Walters' (1990) partial bias correction formula,

$$[2] \quad \beta^* = \beta + \sigma^2 \cdot \bar{S} \cdot (0.5 + \rho) \frac{\left(\frac{n}{k} - 1\right)}{\Sigma(S - \bar{S})^2}$$

to correct for time-series bias in the β parameter, where n denotes the number of years of data and k the mean age-at-recruitment, σ^2 is the variance of the residuals from the uncorrected stock-recruit relationship, $\bar{S}$ is the average of S across years, and ρ is the lag-1 autocorrelation coefficient of residuals of the SR relationship. The corrected estimate of α (α^*) was calculated using the standard equation for computing the intercept of a linear regression,

$$[3] \quad \alpha^* = \overline{\log_e \frac{R}{S}} - \beta^* \cdot \bar{S}$$

Simulation analyses

To assess the performance of the uncorrected and corrected estimators, we used Monte Carlo simulations that captured important features of our 30 stocks: the range in values of the Ricker productivity parameter (α), the standard deviation (σ) and temporal correlation structure of the residuals (ρ) from the fitted SR relationships, and the average historical harvest rates. A Ricker model assuming a lognormal error structure (Allen 1973; Ricker 1975) was used to generate simulated SR data sets with known α and β. For each Monte Carlo simulation, residuals were generated with a lag-1 autocorrelation using the following equation:

$$[4] \quad w_t = \rho \cdot w_{t-1} + v_t$$

where w_t represents the autocorrelated residual substituted for v_t in eq. 1. All simulations were 33 years long (the average number of SR data-years across all stocks) with a mean age-at-return of 4 years. Fixed proportional harvest rates (H) were used to calculate escapements that were then translated to effective female spawners using a 0.5 conversion factor so that the parameter estimates based on the simulated data would be in the same units as the estimates for the 30 stocks. Fixed harvest rates used to generate the SR data will maximize the time-series bias (Walters 1985, 1990) and will thus provide the strongest test of the utility of Walters' bias correction method. Initial stock sizes for each simulation were set at the fished equilibrium (dependent on α, β, and H) to minimize the effect of initial conditions on our evaluation procedure (Kope 1988).

Following each simulation, we calculated corrected and uncorrected estimates of α and β using the 33 years of simulated data. Optimal escapement and optimal harvest rate estimates (corrected and uncorrected) were calculated using an iterative search procedure on the average expected recruitment curve, rather than the most probable (i.e., modal) one estimated by the fitting procedures. The term $\sigma^2/2$ was added to the exponent of eq. 1 (Hilborn 1985) to convert the modal recruitment curve to the average one. Uncorrected and corrected sustainable yield (SY) estimates were computed by substituting the estimates of optimal escapement or optimal harvest rate into the "true" SR relationship; thus, suboptimal estimates led to sustainable yields less than MSY. What we refer to as loss in yield was simply the difference between annual SY and MSY for a given simulation and represents the cost (in terms of annual yield) of inaccurate estimates of optimal escapement or optimal harvest rate. Thus, large losses reflect relatively small sustainable yields. The expected loss in yield was the average loss in yield over a set of n simulations.

For simulations where negative values for α or β were estimated, or where e^{α} is less than replacement, the optimal management strategy is not to harvest any fish. In the event of such parameter estimates (hereafter referred to as estimation failures), managers will probably set a minimal harvest rate or default escapement target given (*i*) their uncertainty in the unusual parameter estimates and (*ii*) social and economic constraints of the fishery. To simulate this process, we assumed that in the event of an estimation failure, a minimal harvest rate (MH) of 0.2 would be applied for both the simulated constant harvest rate and fixed escapement policies. We later examined the sensitivity of our results to different values of MH. We calculated expected yield under both policies because the calculation of the optimal harvest rate requires valid estimates of α only, whereas estimating the optimal fixed escapement requires valid estimates of both α and β.

To evaluate the extent of the bias problem and the performance of the bias-correction method across a range of conditions, we performed 1000 simulations for each

Fig. 1. The ratio of (*a*) corrected to uncorrected (corr/uncorr) estimates of optimal escapement and (*b*) optimal harvest rate for 30 sockeye stocks in B.C. and Alaska (stock numbers in Table 1).

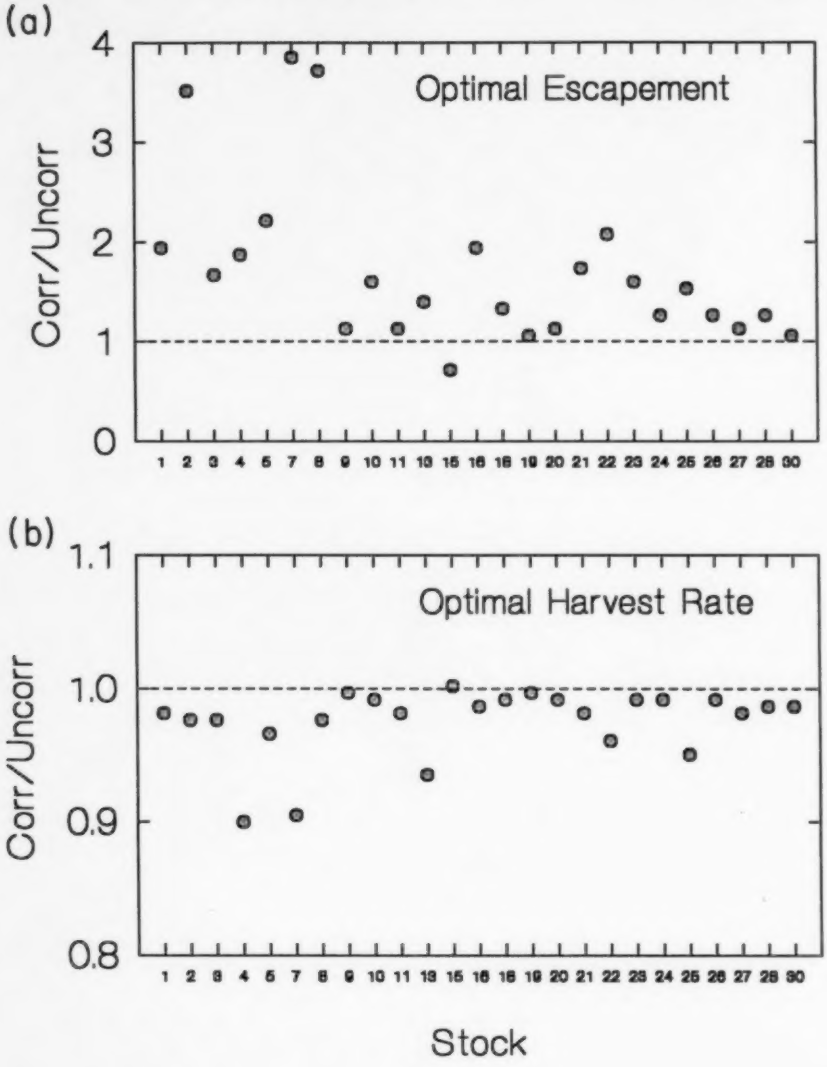

combination of α (1 to 4 at 0.5 increments), σ (0.5 to 1.5 at 0.5 increments), ρ (−0.6 to 0.8 at 0.2 increments), *H* (0.1 to 0.9 at 0.1 increments), and MH (0.2 to 0.8 at 0.2 increments). The ranges for these parameters were chosen to bound the uncorrected or historic average values of the 30 stocks (see Table 1).

Uncorrected and corrected values of α, β, optimal escapement, optimal harvest rate, and resulting yields (by substituting the optimal harvest rate or escapement estimates in the "true" SR relationship) were calculated for each simulation. Bias in α, β, optimal harvest rate, and optimal escapement estimates were calculated using the following equation,

$$[5] \quad \% \text{ bias} = 100 \cdot \frac{\sum_{i=1}^{n} \frac{P_{\text{est}} - P_{\text{true}}}{P_{\text{true}}}}{n}$$

where P_{est} and P_{true} denote the estimated and "true" values for a parameter, and *n* denotes the number of simulations (1000). An identical equation was used to compute the expected annual loss in yield as a percentage of the true MSY by replacing P_{est} and P_{true} in eq. 5 with SY and MSY, respectively. The coefficient of variation (CV) of optimal escapement or optimal harvest rate estimates (calculated over 1000 simulations) was used to compare the precision of uncorrected and corrected estimation methods.

To examine graphically how the biases and losses in yield associated with the uncorrected and corrected estimators varied as a function of harvest rate and autocorrelation (used to simulate the SR data for the estimation), we used a distance-weighted least-squares smoothing procedure (Wilkinson 1990) to plot isopleths of percentage bias or percentage loss as a function of harvest rate and autocorrelation. We then examined these plots at different stock productivity levels.

Results and discussion

Empirical analyses

The effect of correcting for time-series bias in Ricker α and β values and the subsequent effect on optimal harvest rate and escapement estimates was highly variable among stocks. With the exception of the lower Shuswap and Horsefly stocks, uncorrected estimates of α and β were higher than the corrected estimates (Table 1). Translating these differences into optimal escapement values, corrected estimates were on average 1.7 times greater than uncorrected ones (Fig. 1*a*). The ratio of corrected to uncorrected optimal escapements was extremely high for the Birkenhead (3.5), early Stuart (3.9), and Egegik stocks (3.7), indicating an extreme effect of applying the bias-correction method in these systems. In contrast with optimal escapement estimates, the effect of the bias-correction on optimal harvest rates was relatively small; corrected estimates were on average 0.97 of the uncorrected values (Fig. 1*b*). Consistent with Walters' (1990) findings, the bias correction generally did not increase the estimate of autocorrelation of residuals except for the Chilko, early Stuart, Nadina, and Portage stocks, where autocorrelation coefficients were roughly doubled (Table 1).

Increased autocorrelation among residuals in SR parameters has been shown to increase time-series bias (Walters 1990; Myers and Barrowman 1995) and the lag-1 autocorrelation in residuals (ρ) from the 30 SR curves (used here as an index of autocorrelation) was inversely related to the uncorrected α value (Fig. 2*a*; $r^2 = 0.46$, $p = 0.001$). Alaskan stocks had lower productivities (as indexed by α) than B.C. stocks, and exhibited much stronger autocorrelation among residuals of their SR relationships. Total recruitment of western Alaska sockeye salmon has been shown to be strongly correlated with interdecadal shifts in northeast Pacific Ocean conditions (Francis and Hare 1994; Hare and Francis 1995). The high autocorrelation in SR residuals of Alaskan stocks in this analysis is perhaps a different measure (i.e., residuals from the SR relationship rather than total recruitment) of the same relationship between climate and salmon. Further to this point, the correlation between ρ and α (Fig. 2*a*) may indicate that (*i*) the environmental forcing variable(s) causing the nonstationarity in SR relationships may have more effect in regions occupied by Alaskan sockeye than those where B.C. stocks are uniquely distributed; (*ii*) less productive stocks are more sensitive to factors such as changes in ocean climate that alter survival rates or carrying capacities over time (resulting in higher ρ estimates); and (or) (*iii*) northern stocks, having more smolt age-classes per brood than southern stocks, will have more overlap among adjacent broods in freshwater and marine environments, resulting in higher autocorrelation.

Fig. 2. Relationships between (*a*) the lag-1 autocorrelation coefficients of residuals from the fitted SR curves and the Ricker α parameters (not corrected for time-series bias) for 30 sockeye stocks, and (*b*) the historical average harvest rates and α. The solid line in (*b*) shows the optimal harvest rate predicted based on α.

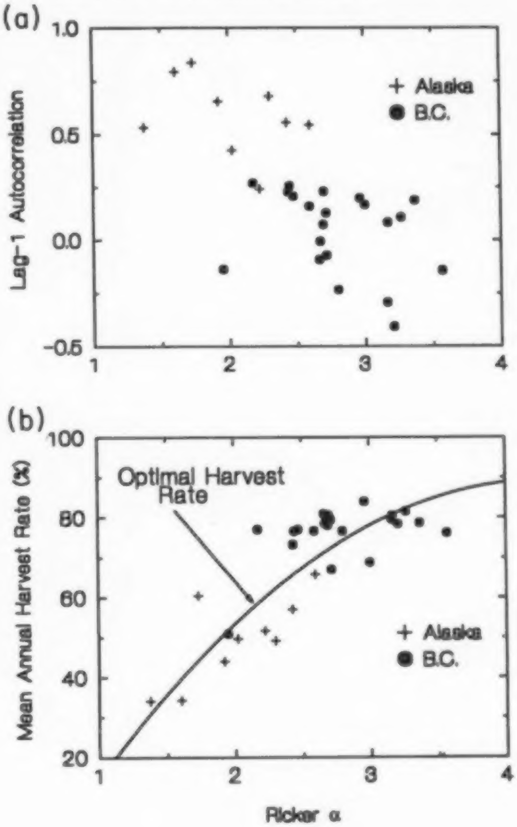

Average historical harvest rates of the 30 stocks were strongly related to stock productivity, as indexed by the uncorrected α value (Fig. 2*b*; $r^2 = 0.64$, $p = 0.001$). Because high harvest rates have been shown to increase time-series bias in SR parameters (Walters 1985; Cass 1989; Myers and Barrowman 1995), variation in historical harvest rates among stocks (determined in part by stock productivity and its influence on management policy) could lead to differences in the potential extent of time-series bias in the observed SR relationships. We calculated harvest rates that maximized MSY for a given α value using an iterative search procedure that was based on eq. 1. This produced a function relating optimal harvest rate to α (solid line, Fig. 2*b*). In comparison to these optimal rates, the Branch River and Cultus Lake stocks appear to be the most overexploited ones in the group examined here (see Table 1 for stock-specific α and harvest rate values to identify stocks in Fig. 2*b*). Management of Alaskan stocks is

Table 2. Summary of percentage bias in uncorrected and corrected α and β estimates based on 1000 simulations.

					% bias			
					α		β	
Uncorrected α group	Number of stocks	Mean harvest rate	Mean ρ	Assumed true α	Uncorrected	Corrected	Uncorrected	Corrected
α ≤ 1.75	3	0.42	0.72	1.5	3.3	−7.3	51.8	−28.2
1.75 < α ≤ 2.25	5	0.55	0.29	2.0	4.0	−4.0	15.2	−14.6
2.25 < α ≤ 2.75	13	0.72	0.22	2.5	2.8	−2.8	10.8	−14.0
2.75 < α ≤ 3.25	6	0.78	−0.08	3.0	0.3	−1.3	3.8	−2.2
α > 3.25	3	0.79	0.05	3.5	0.3	−2.0	0.6	−6.2

Note: Thirty sockeye salmon stocks were categorized into five groups based on their uncorrected α estimates. Stocks in those groups were used to calculate mean harvest rates and lag-1 autocorrelation (ρ) values. These means were used in conjunction with midrange α values (denoted as Assumed true α) for the simulations to estimate the bias in α and β parameters. Estimated parameters below the true value are shown by % bias values <0.

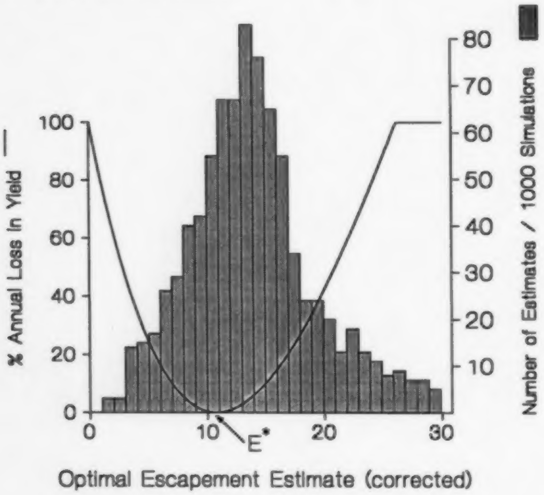

Fig. 3. An example illustrating the factors included in evaluation of the performance of the different methods of parameter estimation. Frequency distribution of corrected optimal escapement targets estimated from 1000 data sets (generated with $\alpha = 1.5$, $H = 0.4$, $\rho = 0.4$, $\sigma = 1.0$) shown in relation to the loss function. The true optimal escapement (10.8 in this case) is denoted by E*. The expected loss (28%) is the average loss across all estimates of optimal escapement, weighted by their frequency of occurrence.

% Annual Loss in Yield —
100
80
60
40
20
0
Number of Estimates / 1000 Simulations ▮
80
70
60
50
40
30
20
10
0
10
20
30
E*
Optimal Escapement Estimate (corrected)

possibly less aggressive than management of B.C. stocks: only 2 of 9 (22%) Alaskan stocks had average harvest rates above the optimal rate in comparison with 12 of 21 (57%) B.C. stocks. The correspondence between historical average annual harvest rates and the optimal ones predicted as a function of α for each stock suggests that (*i*) in spite of social and economic pressures to the contrary, many stocks are harvested on average close to the optimal rates; or (*ii*) excessive harvest rates prior to the beginning of a SR data series could have eliminated unproductive substocks and artificially raised the average α value for each stock complex. This would give the misleading impression that harvest rates have been at near optimal levels for each stock's average α value when in fact they may have been too high. We hope that further analyses of historical catch and escapement data in conjunction with a review of historical policies will allow us to distinguish between these two hypotheses.

Simulation analyses

Many evaluations of estimation methods have used average accuracy (i.e., bias) as the only measure of performance (e.g., Uhler 1980; Mohn 1980; Cass 1989; Myers and Barrowman 1995). Our evaluation took into account both the bias and variance of parameter estimates. It is well known that there is a tradeoff between the bias of an estimator and its variance such that estimators with smaller bias often have larger variance (i.e., reduced precision) than those with larger bias (Staudte and Sheather 1990). We calculated expected losses in yield that would result from managing using estimates of optimal escapement or optimal harvest rate rather than managing using the true values for these parameters. The approach of translating statistical properties of an estimator (e.g., bias, variance) into meaningful management terms has been applied previously. For instance, Ludwig and Walters (1989) evaluated different methods for determining optimal effort levels from surplus production models. In our study, losses in yield depended on the combined influence of four factors (Fig. 3): (*i*) the accuracy (i.e., bias) in α and (or) β and the resulting influence on management strategies (i.e., optimal escapement target or optimal harvest rate); (*ii*) the precision of the management parameter estimates (i.e., variability in estimates across 1000 simulations); (*iii*) the loss function, which is the relationship between loss in yield and the amount of deviation from the parameter estimate that maximizes yield (i.e., the true optimal escapement target or optimal harvest rate); and (*iv*) the failure rate of the estimation procedure (the proportion of cases that an arbitrary minimal harvest rate must be applied because of invalid estimates of α or β). For a given set of Monte Carlo simulations (e.g., 1000 trials), the expected loss in yield was the average of losses associated with individual optimal

Table 3. Coefficients of variation (CV) for uncorrected (uncorr) and corrected (corr) estimates of optimal escapement and optimal harvest rate for 1000 simulations at different α levels and harvest rates.

		Optimal escapement			Optimal harvest rate		
α	Harvest rate	Uncorr	Corr	Uncorr/Corr	Uncorr	Corr	Uncorr/Corr
1.5	0.2	0.21	0.40	0.53	0.14	0.16	0.89
1.5	0.4	0.71	1.40	0.50	0.14	0.15	0.92
1.5	0.6	11.25	6.59	1.71	0.13	0.14	0.95
1.5	0.8	5.75	10.56	0.54	0.14	0.15	0.97
2.5	0.2	0.07	0.52	0.14	0.06	0.07	0.87
2.5	0.4	0.09	0.43	0.22	0.06	0.07	0.86
2.5	0.6	0.15	0.29	0.51	0.06	0.07	0.86
2.5	0.8	0.64	13.20	0.05	0.05	0.06	0.92
3.5	0.2	0.04	0.69	0.05	0.02	0.03	0.91
3.5	0.4	0.05	0.66	0.07	0.02	0.03	0.90
3.5	0.6	0.06	0.51	0.12	0.02	0.03	0.88
3.5	0.8	0.12	0.36	0.32	0.02	0.03	0.85
			Mean	0.40			0.90

Note: Simulations were performed using $\sigma = 1.0$ and $\rho = 0$. Uncorr/Corr denotes the ratio of uncorrected/corrected CV values for optimal escapement or optimal harvest rate.

escapement or optimal harvest rate estimates, weighted by their frequency of occurrence.

Our simulation results are reported in six parts as follows: (*i*) bias in α and β; (*ii*) bias in optimal escapement and optimal harvest rate; (*iii*) precision of the estimates; (*iv*) failure rates of the parameter estimation methods; (*v*) expected losses in sustainable yield; and (*vi*) the sensitivity of our conclusions to values of σ and mean age-at-return used to generate the data, and to different values of the minimal harvest rate applied to simulations where estimation failures have occurred. Although we calculated expected losses in yield under both constant escapement and harvest rate policies, we mainly present results for the constant escapement policy because this is the most common current management policy for Pacific salmon. We discuss the results of the constant harvest rate policy in the general conclusions section of the paper.

Bias in estimates of α and β

On the basis of simulations that reflect the mean harvest rates and autocorrelations of the 30 stocks categorized into different levels of stock productivity, our results show that the standard uncorrected estimation method overestimates both α and β (positive bias in Table 2). This result is consistent with previous findings and emphasizes that the bias in uncorrected β estimates is much greater than the bias in uncorrected α estimates (Walters 1985, 1990; Cass 1989; Myers and Barrowman 1995). Less productive stocks generally show the greatest bias in α and β. These stocks tend to have lower harvest rates and higher autocorrelation compared with more productive stock groupings (Fig. 2).

Over our simulation conditions, Walters' (1990) bias correction consistently underestimated α (for all five sets of simulation conditions shown in Table 2). Although the bias correction also underestimated β values (i.e., decreased the degree of density dependence in the SR curve by too much), for three of five simulation conditions the absolute values of corrected estimates were slightly closer to the true values than the uncorrected ones. The corrected method resulted in a substantial improvement in the accuracy of the β estimate at the lowest true simulated α (α_{sim}) level of 1.5.

Bias in estimated optimal escapement and optimal harvest rate

Biases in estimated optimal escapement and optimal harvest rate depended mostly on stock productivity, but were also affected by simulated harvest rates and autocorrelation. Figure 4*a* shows the percentage difference between the uncorrected estimates of the optimal harvest rate and the true optimal ones across a range of H and ρ values for different levels of α. Figure 4*b* shows the same analysis but for uncorrected optimal escapement estimates. For both harvest rate and escapement, the percentage bias decreases as stock productivity increases. Over combinations of H and ρ reflecting data for real stocks (identified by black dots in Fig. 4) and at a high stock productivity ($\alpha = 2.5$), the potential overestimation in optimal harvest rate estimates (shown by positive contour lines in Fig. 4) was much smaller than the underestimations in optimal escapement. On the basis of the shape of the surfaces of the contour plots, bias in optimal harvest rate (requiring only α) is driven mostly by autocorrelation (i.e., bias increases as ρ increases or decreases relative to $\rho = 0$) while bias in optimal escapement (requiring estimates of α and β) is mostly controlled by simulated harvest rates that reduced variation in stock size in the simulated data sets.

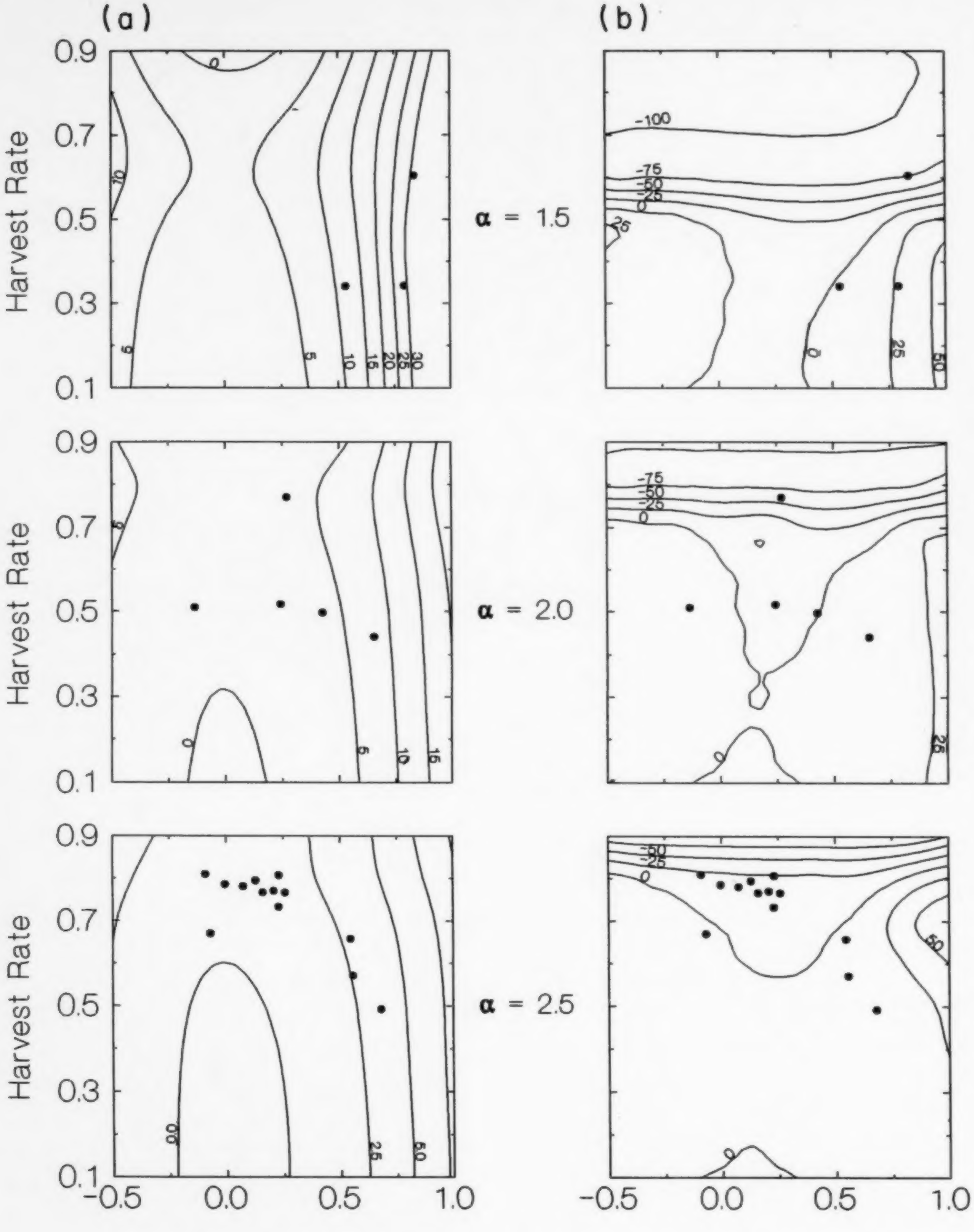
(a)
(b)
Harvest Rate
0.9
0.7
0.5
0.3
0.1
α = 1.5
α = 2.0
α = 2.5
0
5
10
15
20
25
30
-100
-75
-50
-25
0
25
50
0.0
2.5
5.0
-0.5
0.0
0.5
1.0
Lag-1 Autocorrelation

Fig. 4. Contour plots showing the percentage bias in (*a*) optimal harvest rates and (*b*) optimal escapements estimated from Ricker parameters not corrected for time-series bias. For each combination of harvest rate (H), lag-1 autocorrelation (ρ), and α, we simulated 1000 data sets with $\sigma = 1.0$ to estimate the bias under a range of conditions. The black dots are the average historical harvest rates and uncorrected ρ values for the 30 sockeye stocks; these identify realistic portions of parameter space. The dots are assigned to the different simulated α levels (α_{sim}) shown beside the graphs according to their uncorrected estimates of α (α_{emp}) based on the following categorization: $\alpha_{sim} = 1.5$ refers to $1.25 \le \alpha_{emp} < 1.75$; $\alpha_{sim} = 2.0$ refers to $1.75 \le \alpha_{emp} < 2.25$; $\alpha_{sim} = 2.5$ refers to $2.25 \le \alpha_{emp} < 2.75$.

Precision of estimated optimal escapement and optimal harvest rate

In most cases, corrected estimates of optimal escapement were considerably less precise (had higher CV's) than uncorrected ones (Table 3). Uncorrected estimates had on average a CV that was 40% of the CV for corrected estimates (Table 3). In contrast, precision of estimates of corrected and uncorrected optimal harvest rates were very similar. Within lowest stock productivity category (α_{sim} = 1.5), higher harvest rates used to simulate SR data sets generally led to greater uncertainty in estimates of optimal escapement but did not affect the precision in estimates of optimal harvest rates. This was because high simulated harvest rates reduced variation in spawning stock size, which increased the variability in the estimates of β but not α. For both optimal escapement and optimal harvest rate, precision increased with increasing α values because of increased contrast in spawning stock size and a reduction in the effect of autocorrelation on α estimates as simulated α values were increased.

Failure rate in estimation of optimal escapement and harvest rate

Both uncorrected and corrected methods failed more frequently when estimating optimal escapement than estimating optimal harvest rate (Fig. 5), because estimation of optimal escapement requires valid estimates of α (i.e., $\alpha > 0$ and e^{α} > replacement) and β ($\beta > 0$), while optimal harvest rate estimation requires only valid values of α. The failure rate of the procedure for estimating optimal escapements or optimal harvest rates is a potentially important component of its performance, because in the absence of valid parameter estimates, managers must use an alternative method or arbitrary rule to set harvest levels.

Rates of estimation failure decreased as stock productivity increased and were slightly higher for the corrected method than for the uncorrected one for optimal harvest rate estimates, but differences were small across realistic stock conditions (black dots in Fig. 5). Failure rates for optimal escapement estimates using the corrected method were considerably higher than the rates based on the uncorrected method for low-productivity stocks. For example, α, ρ, and H conditions reflecting the Branch River stock resulted in a 25% failure rate for uncorrected estimates of optimal escapement, but a 70% failure rate for corrected estimates. Under conditions simulating 13 of the 30 stocks within the α_{sim} category of 2.5, rates of failure for uncorrected and corrected optimal escapements were very similar and ranged from 0% to less than 20%.

Expected loss in equilibrium yield

The expected loss in yield (relative to the true MSY) is the average loss across 1000 simulations for a given set of stock characteristics. It represents the loss that would be anticipated due to bias, imprecision, and estimation failure of a management parameter such as optimal escapement or optimal harvest rate. Response surfaces of the percentage expected loss from using uncorrected estimates of escapement (Fig. 6) are similar but not identical to surfaces of biases in optimal escapement (Fig. 4) and show that expected losses (*i*) decrease as stock productivity, α, increases, and (*ii*) increase with increasing simulated harvest rates within an α category. Simulation conditions reflecting two stocks resulted in large expected losses in yield (65, 79%). Conditions reflecting 13 other stocks had smaller annual expected losses in SY (between 10 and 30%) while the conditions simulating the remaining 50% of the stocks showed annual expected losses in SY less than 10%. Response surfaces of the percentage expected loss in yield from using Walters' (1990) bias correction method showed a similar pattern, but losses were reduced for simulations reflecting low-productivity stocks with high harvest rates or autocorrelation.

To facilitate comparison of the performance of the corrected and uncorrected methods of parameter estimation, we plotted the ratio of the actual expected sustainable yields for the corrected method to the expected sustainable yields for the uncorrected method (SY_c/SY_u) based on a constant escapement policy. Ratios of $SY_c/SY_u > 1$ indicate that the corrected method generates higher expected sustainable yields than the uncorrected one. Figure 7 shows that the corrected estimator produces substantially higher yields than the uncorrected one when harvest rates used to generate the SR data are high relative to simulated stock productivity (α). This is because high harvest rates (relative to stock productivity) reduce variation in stock size and increase time-series bias in the uncorrected estimates of optimal escapement. Under these conditions the corrected estimator outperforms the uncorrected one even though the variance of the estimates (Table 3) and the estimation failure rates (Fig. 5) of the corrected estimator increases. However, as stock productivity increases, the region where the corrected method outperforms the uncorrected one shrinks because it takes a greater harvest rate to reduce variation in stock size sufficiently to create bias in the uncorrected estimates of Ricker curve parameters. As simulated stock productivity increased, differences in the performance of the two estimation methods became smaller. Most important, though, while there was a substantial region of parameter space in Fig. 7 where the corrected method outperformed the uncorrected one, for regions of space occupied by most of the stocks (28 of the 30 black dots in Fig. 7), the two methods perform about equally as well ($0.8 < SY_c/SY_u < 1.2$). Furthermore, the corrected method did not perform consistently better. Sometimes it produced lower yields than the uncorrected procedure and

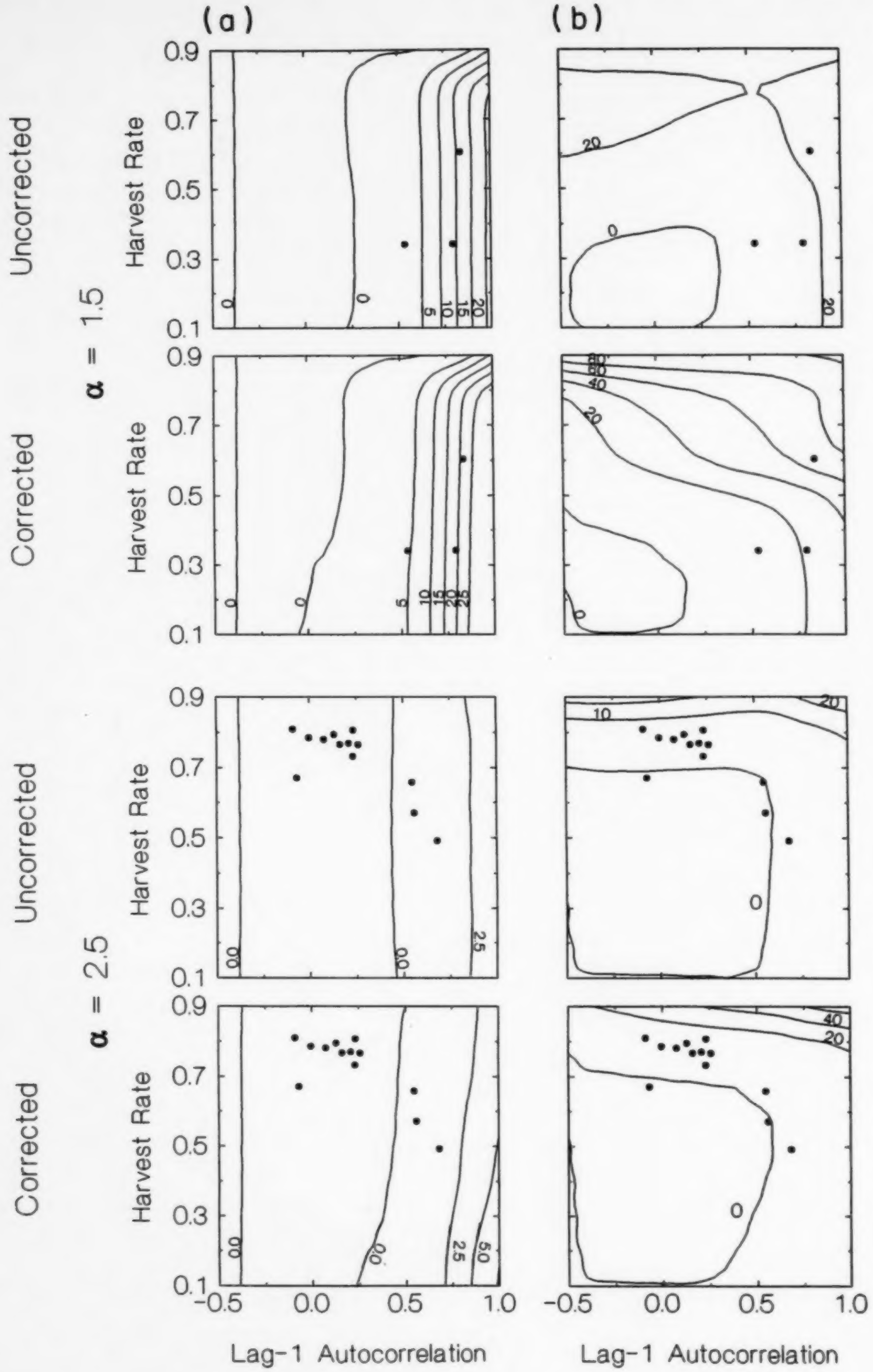
(a)
(b)
Uncorrected
Corrected
α = 1.5
α = 2.5
Harvest Rate
0.9
0.7
0.5
0.3
0.1
0
5
10
15
20
25
40
60
80
0.0
2.5
5.0
−0.5
0.0
0.5
1.0
Lag-1 Autocorrelation

Fig. 5. Contour plots showing the percentage of failures in estimation for (*a*) optimal harvest rates and (*b*) optimal escapements that occurred during 1000 simulations at each combination of harvest rate and lag-1 autocorrelation. Failures occurred in the estimation of optimal harvest rates when α was negative or e^{α} was below replacement. In the estimation of optimal escapements, failures occurred when α was negative, e^{α} was below replacement, or when β was negative. Black dots as in Fig. 4.

Fig. 6. Contour plots showing the expected losses in yield from using the uncorrected parameter estimates under a constant escapement policy (relative to the yield if the true optimal escapement was used). Black dots as in Fig. 4 and $\alpha_{sim} = 3.0$ refers to $\alpha_{emp} \geq 2.75$.

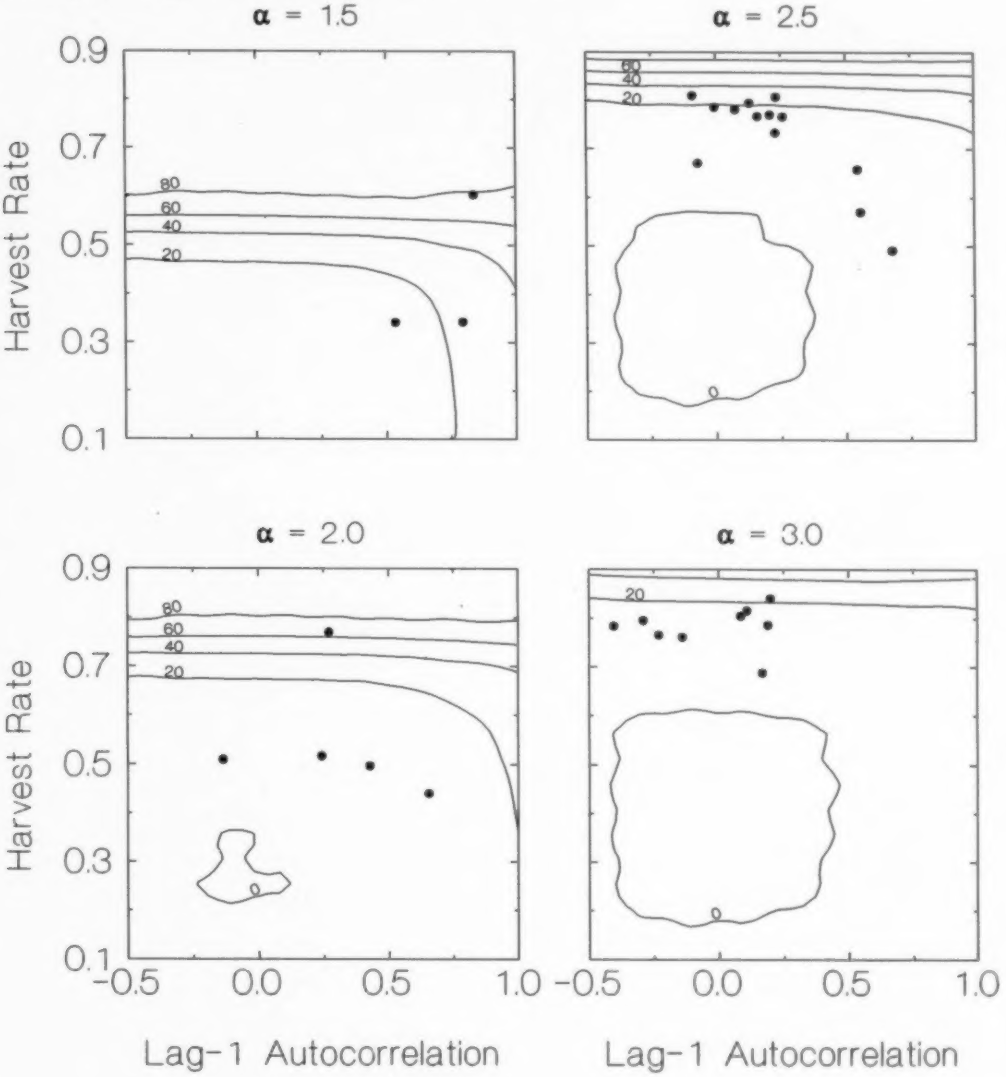

sometimes greater yields. However, the corrected method did substantially improve yields for the Branch River and Cultus Lake stocks.

Sensitivity analyses

We used this ratio of the actual expected sustainable yields for the corrected method to the expected sustainable yields for the uncorrected method to determine the conditions under which the corrected estimation method outperforms the uncorrected one. The following sensitivity analysis therefore focuses solely on the sensitivity of this ratio of yields to variation of residuals around the SR curve, mean age-at-return, and the minimal harvest rate used in the event of estimation failures. The sensitivity of biases in

Fig. 7. Contour plots showing the ratio of corrected to uncorrected expected sustainable annual yields (SY_c/SY_u) under a constant escapement policy. Black dots as in Fig. 6.

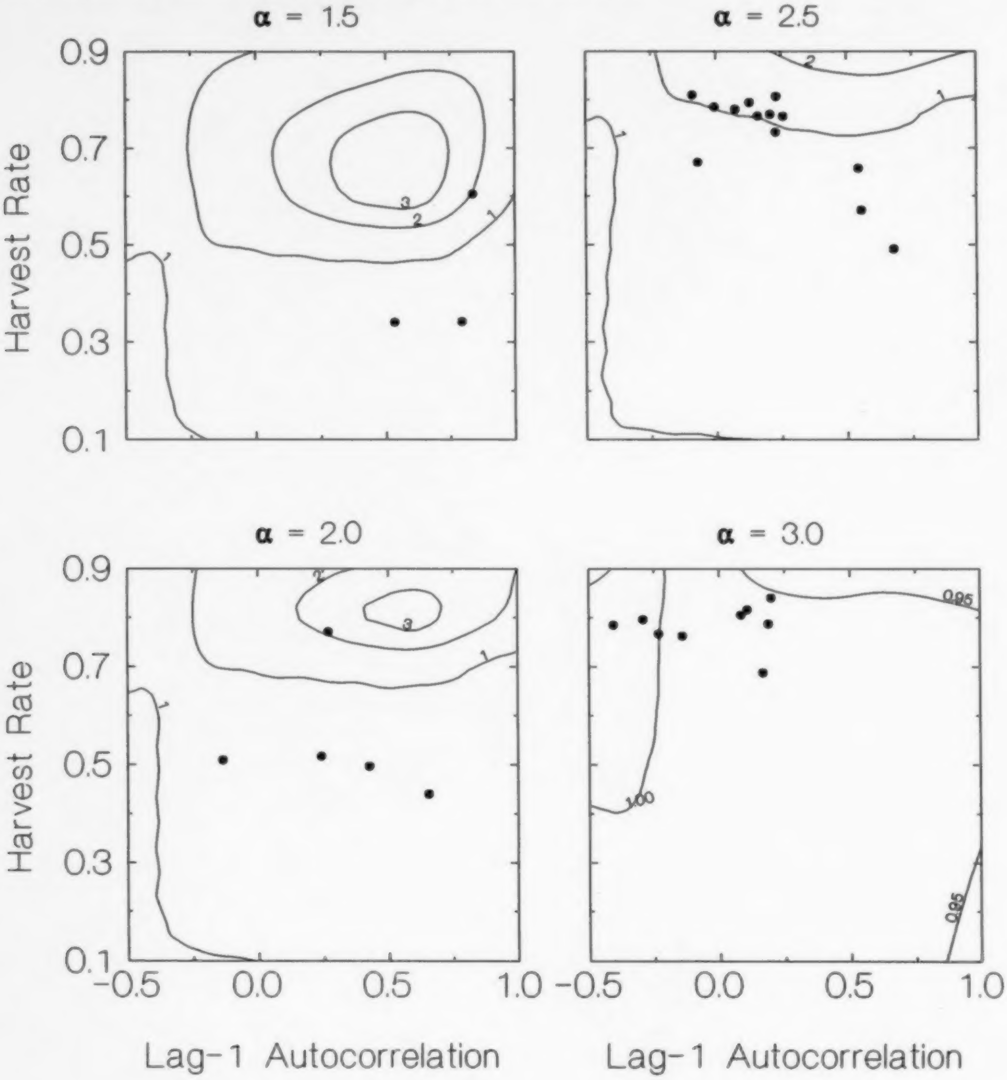

Ricker α and β estimates to residual variance (Walters 1985; Myers and Barrowman 1995) and sample size (Cass 1989; Myers and Barrowman 1995) have been thoroughly examined in previous studies.

First, to this point, our simulation results were based on a constant amount of residual variation around mean SR relationships ($\sigma = 1.0$), yet this quantity varies considerably across stocks (from 0.49 to 1.63, Table 1). When we varied σ, the ratio of corrected to uncorrected yields generally did not change at either low ($\sigma = 0.5$) or high ($\sigma = 1.5$) values. Under both these variance levels, applying the corrected method generated substantially higher yields than the uncorrected one for the Branch River and Cultus Lake stocks, but the ratio of SY_c/SY_u was close to 1.0 for the remaining 28 stocks. Thus, although the amount of residual variation has been shown to influence the bias in uncorrected estimates of α and β by other authors, our basic conclusions about the performance of Walters' (1990) correction method in comparison with the uncorrected method and in the context of the 30 stocks were not changed at different levels of σ; the bias-correction method generally appears to generate sustainable yields equal to or slightly smaller than those generated by the standard least-squares method.

The use of a mean age-at-return of 4 years in simulations reflecting Alaskan stocks potentially introduces error into estimates of expected yields because the average mean age-at-return for Alaskan stocks is 4.9 years (see Table 1). We therefore examined the sensitivity of our results to mean age-at-return by repeating the simulations with a mean age-at-return of 5 years and compared these results with those generated using a 4-year mean age-at-return. Over realistic portions of parameter space, the ratio of corrected to uncorrected yields was very insensitive to mean age-at-maturity. Increasing mean age-at-maturity from 4 to 5 years in our simulations did not change the ratio of yields from >1 to <1 or vice versa for any of the 30 stocks.

The use of a fixed MH in the event of estimation failures (when optimal escapement or optimal harvest rate values cannot be estimated) potentially introduced error into estimates of expected yield to the extent that managers use MH values different than our default value of 0.2. As a worst case scenario, we repeated the simulations using a minimal harvest rate of 0.8, a value approximating the upper limit of the average historical harvest rates for the 30 stocks (Table 1). As expected, the ratio of corrected to uncorrected yields decreased at this higher MH value because of the generally higher rate of estimation failure for the corrected method (Fig. 5). The sensitivity of the ratio of yields to MH was greatest when harvest rates used to generate the simulated data were high relative to the simulated stock productivity level, conditions which produced the highest rates of estimation failures (Fig. 5). For conditions simulating the 30 stocks, 29 stocks had SY_c/SY_u values ≤ 1 at an MH of 0.8, compared with 28 stocks at an MH of 0.2. Thus, although our choice of MH values of 0.2 for our simulations was somewhat arbitrary, our conclusion about the performance of the two estimators remains basically unchanged even for a very high MH value. This is because estimation failure rates were very low for most of the conditions reflecting real stocks that we simulated.

General conclusions

On the basis of our analyses of historical data, application of Walters' (1990) method for correcting time-series bias can cause large increases in optimal escapement estimates for some stocks compared with the traditional method of estimation, but the bias correction has little influence on optimal harvest rate estimates (Fig. 1). Simulation results showed that variation in stock size, as controlled by stock productivity and harvest rate, was the largest factor that determined the extent of time-series bias in management parameters, regardless of the estimation method (Fig. 4). The empirical analyses showed that there is a strong inverse relationship between lag-1 autocorrelation and stock productivity (Fig 2*a*). Autocorrelation and stock productivity are not independent but are correlated in a direction that magnifies the potential effect of time-series bias for less productive stocks and considerably reduces it for others. The potential for time-series bias in management parameters is therefore greatest for Alaskan stocks, which are generally less productive and show a higher degree of autocorrelation in residuals around their fitted SR curves than B.C. stocks.

Is it worth applying the bias-correction method when fitting sockeye SR relationships? For the sockeye salmon stocks we examined, the answer appears to be no. With the exception of the conditions approximating the Branch River and Cultus Lake stocks, the correction method did not consistently increase expected annual yields compared with the standard uncorrected method (Fig. 7). In fact, yields were often lower from using the bias-correction method. Why then did Walters (1990) recommend using this bias-correction method? First, it was because Walters simulated only a low-productivity stock (α_{sim} = 1.7 in effective female spawner units) where bias in uncorrected α and β estimates is large. At a similar simulated stock productivity level (α_{sim} =1.5), our results showed that the corrected method outperforms the uncorrected one, but this conclusion only holds for 2 of the 30 real stock conditions we simulated. Second, Walters evaluated the performance of the correction method using the bias in α and β as the only measure. Our analysis incorporated the reduced precision in management parameter estimates (Table 3) and increased estimation failure rate (Fig. 5) caused by using Walters' bias-correction method. Reduced precision increased the proportion of parameter estimates that occurred at the far ends of the loss function where losses in yield are higher (e.g., Fig. 3). Increased estimation failure rates increased the proportion of times that an arbitrary and nonoptimal harvest rate was applied, thereby reducing yield compared with yields that would have occurred with perfect information. Our analysis has therefore provided a more stringent test of the correction method than Walters (1990) since it incorporates the effect of parameter estimation failure, precision, and the loss function into the performance measure.

We used the uncorrected empirical estimates of α and ρ (Table 1) to find relevant portions of simulated parameter space but these estimates are, to some extent, biased. Stock-specific α values may be too high and ρ values too low compared to the true values for these parameters (Walters 1985, 1990). For the constant escapement policy, isopleths of bias (Fig. 4*b*) and expected loss in yield (Fig. 6) are generally parallel to the autocorrelation axis. Thus, shifting the stock-specific data points to the right to account for potential underestimations in ρ will not change our conclusions. However, the lower the simulated α and harvest rates, the more the isopleths begin to bend and become perpendicular to the autocorrelation axis, potentially increasing estimates of bias and loss resulting from underestimations of ρ. Overestimations of empirical α could potentially cause us to misclassify some stocks into simulated α categories that are too high where bias, variability, estimation failure rates, and expected loss in yield are generally lower. This misclassification would be most likely for stocks that have low variation in spawning stock size as a result of overfishing. Although uncertainty in the true α value for the 30 stocks could result in underestimations of the loss in yield, especially for the uncorrected estimator, it has little effect on our conclusions about the relative performance of the corrected and uncorrected methods (Fig. 7). Shifting more stocks to lower α categories would not appreciably increase the proportion of stocks where the bias-correction method outperforms the uncorrected one.

We did not incorporate another known source of bias into our analysis, which is the effect of measurement error in abundance estimates of recruits or spawners on SR parameters (Walters and Ludwig 1981). Caputi (1988) showed that biases resulting from autocorrelation of residuals (i.e., times-series bias) and measurement error were not additive and recommended that these two forms of bias be investigated simultaneously. We did not follow Caputi's recommendation because adding another variable to our analysis would complicate the interpretation of results and limit the generality of our conclusions, and it would not be possible to quantify the amount of measurement error for most of the stocks examined here. Caputi showed that including measurement error in the simulations reduced the magnitude of the overall bias in parameters, so if we had included this factor, we suspect that the degree of time-series bias would be smaller than presented here.

The accuracy of estimated optimal harvest rates was generally better than the accuracy of optimal escapement estimates generated under the same simulation conditions (Fig. 4). For brevity, we did not show contour plots of the expected losses in yield based on an uncorrected constant harvest rate policy. However, losses generated under these conditions were generally less than the expected losses in yield calculated using uncorrected optimal escapement estimates. Twenty-two of the thirty stocks had lower expected losses under a constant harvest rate policy than under a constant escapement policy. The differences in bias and expected losses between policies occurred because (*i*) optimal harvest rate estimates are only dependent on α, while optimal escapement estimates require both α and β; and (*ii*) the bias in α estimates is considerably less than the bias in β (Table 2). Estimates of carrying capacity required to calculate optimal escapement targets are much more uncertain than estimates of maximal stock productivity (at low stock sizes) for most SR datasets, especially for stocks that have been overfished (where variation in stock size is low). These are also the conditions where bias in β is greatest. Within our equilibrium framework, the constant harvest rate policy outperforms the constant escapement one. Deriso (1985) reached a similar conclusion using an analytical approach. Comparisons of constant escapement and constant harvest rate policies can also be made within a dynamic framework (e.g., Eggers 1993; Hall et al. 1988) where other factors related to parameter estimation and fisheries performance can be incorporated. We are currently doing such an extension to this work.

There is a need to incorporate decision theoretic approaches into the evaluation of estimation methods used in fisheries management. A comparison of the bias in uncorrected estimates of optimal escapement (Fig. 4) with expected losses (Fig. 6) shows that the surfaces are not identical, highlighting the need to incorporate uncertainty into the evaluation procedure rather than just using point estimates of bias. However, while these surfaces are not identical, they are similar because both the loss function and the probability distributions of optimal escapement estimates are relatively symmetric (e.g., Fig. 3). Estimation methods that generate highly asymmetric probability distributions or analyses that involve more asymmetric loss functions will often generate results that diverge significantly from ones based on point estimates (Morgan and Henrion 1990).

Acknowledgments

We thank Milo Adkison, Michael Bradford, and Shane Frederick for useful comments on earlier drafts of this paper. We thank Michael Lapointe for compiling the stock-recruitment data used in this analysis. Funding was provided by grants to R.M.P. and C.J.W. from the Natural Sciences and Engineering Research Council of Canada and the Ocean Production Enhancement Network, one of Canada's Networks of Centres of Excellence.

References

Allen, K.R. 1973. The influence of random fluctuations in the stock-recruitment relationship on the economic return from salmon fisheries. Rapp. P.-V. Cons. Cons. Int. Explor. Mer, 164: 350–359.

Armstrong, M.J., and P.A. Shelton. 1988. Bias in estimation of stock-recruit function parameters caused by nonrandom environmental variability. Can. J. Fish. Aquat. Sci. 45: 554–557.

Caputi, N. 1988. Factors affecting the time series bias in stock-recruitment relationships and the interaction between time series and measurement error bias. Can. J. Fish. Aquat. Sci. 45: 178–184.

Cass, A.J. 1989. Stock status of Fraser River sockeye. Can. Tech. Rep. Fish. Aquat. Sci. No. 1674.

Deriso, R.B. 1985. Risk adverse harvesting strategies. *In* Resource management. *Edited by* M. Mangel. Proceedings of the Second Ralf Yourque Workshop. Lecture Notes in Biomathematics No. 61. Springer-Verlag, Berlin. pp. 65–73.

Eggers, D.M. 1993. Robust harvest policies for Pacific salmon fisheries. In Proceedings of the International Symposium on Management Strategies for Exploited Fish Populations. Alaska Sea Grant College Program Report No. 93-02. *Edited by* G. Kruse, D.M. Eggers, R.J. Marasco, C. Pautzke, and T.J. Quinn. University of Alaska, Fairbanks. pp. 85–106.

Francis, R.C., and S.R. Hare. 1994. Decadal-scale regime shifts in the large marine ecosystems of the northeast Pacific: a case for historical science. Fish. Oceanogr. 3: 279–291.

Hall, D.L., R. Hilborn, M. Stocker, and C.J. Walters. 1988. Alternative harvest strategies for Pacific herring (*Clupea harengus pallasi*). Can. J. Fish. Aquat. Sci. 45: 888–897.

Hare, S.R., and R.C. Francis. 1995. Climate change and salmon production in the Northeast Pacific Ocean. *In* Climate change and northern fish populations. *Edited by* R.J. Beamish. Can. Spec. Publ. Fish. Aquat. Sci. No. 121. pp. 357–372.

Hilborn, R. 1985. Simplified calculation of optimum spawning stock size from Ricker's stock recruitment curve. Can. J. Fish. Aquat. Sci. 42: 1833–1834.

Hilborn, R., and C.J. Walters. 1992. Quantitative fisheries stock assessment: choice, dynamics, and uncertainty. Routledge, Chapman & Hall, Inc., New York.

Kendall, M.G., A. Stuart, and J.K. Ord. 1983. The advanced theory of statistics. Vol. 3. Charles Griffin and Company Ltd., London.

Kope, R.G. 1988. Effects of initial conditions on Monte Carlo estimates of bias in estimating functional relationships. Can. J. Fish. Aquat. Sci. 45: 185–187.

Ludwig, D., and C.J. Walters. 1981. Measurement errors and uncertainty in parameter estimates for stock and recruitment. Can. J. Fish. Aquat. Sci. 38: 711–720.

Ludwig, D., and C.J. Walters. 1989. A robust method for parameter estimation from catch and effort data. Can. J. Fish. Aquat. Sci. 46: 137–144.

Mohn, R.K. 1980. Bias and error propagation in logistic models. Can. J. Fish. Aquat. Sci. 37: 1276–1283.

Morgan, M.G., and M. Henrion. 1990. Uncertainty: a guide to dealing with uncertainty in quantitative risk and policy analysis. Cambridge University Press, Cambridge.

Myers, R.A., and N.J. Barrowman. 1995. Time series bias in the estimation of density-dependent mortality in stock-recruitment models. Can. J. Fish. Aquat. Sci. 52: 223–232.

Ricker, W.E. 1975. Computation and interpretation of biological statistics of fish populations. Bull. Res. Board Can. No. 191.

Staudte, R.G., and S.J. Sheather. 1990. Robust estimation and testing. John Wiley & Sons Ltd., New York.

Uhler, R. 1980. Least square regression estimates of the Schaefer production model: some Monte Carlo simulation results. Can. J. Fish. Aquat. Sci. 37: 1284–1294.

Walters, C.J. 1985. Bias in the estimation of functional relationships from time–series data. Can. J. Fish. Aquat. Sci. 42: 147–149.

Walters, C.J. 1990. A partial bias correction factor for stock-recruitment parameter estimation in the presence of autocorrelated environmental effects. Can. J. Fish. Aquat. Sci. 47: 516–519.

Walters, C.J., and J.S. Collie. 1988. Is research on environmental factors useful to fisheries management? Can. J. Fish. Aquat. Sci. 45: 1848–1854.

Walters, C.J., and D. Ludwig. 1981. Effects of measurement errors on the assessment of stock-recruitment relationships. Can. J. Fish. Aquat. Sci. 38: 704–710.

Wilkinson, L. 1990. SYSTAT: the system for statistics. SYSTAT, Inc., Evanston, Ill.

Yuen, H.J., and M.L. Nelson. 1987. 1983 Bristol Bay salmon (*Oncorhynchus* sp.): a compilation of catch, escapement, and biological data. Alaska Department of Fish and Game Tech. Data Rep. No. 191.

Spring flood: a primary cue for hatching of river spawning Coregoninae

Tor Næsje, Bror Jonsson, and Jostein Skurdal

Abstract: Increased water discharge during spring floods gives the primary cue for the start of hatching and drift of European vendace (*Coregonus albula*) and whitefish (*Coregonus lavaretus*) in the Norwegian River Lågen. The drift increased with water flow for discharges between 50 and 850 $m^3 \cdot s^{-1}$ (vendace: $R^2 = 0.91$; whitefish: $R^2 = 0.77$). The length of hatching period, as judged from the drift, was negatively correlated with the increase in water discharge (vendace: $R^2 = 0.73$; whitefish: $R^2 = 0.68$). The length of the egg incubation period and time of hatching were not significantly correlated with the ambient water temperature. Two artificial floods (220 $m^3 \cdot s^{-1}$), released before normal spring flooding, increased the total number of drifting Coregoninae larvae in the river. The first flood increased the number of vendace and whitefish larvae per second from 2.1 and 0.0 to 86.1 and 4.5, respectively, before returning to preflood levels. The second flood gave 18.9 and 1.8 individuals/s.

Résumé : L'accroissement du débit pendant les crues printanières donnerait le signal de l'éclosion et de la dérive de la marène (*Coregonus albula*) et du lavaret (*Coregonus lavaretus*) dans la rivière Lågen, en Norvège. La dérive augmente proportionnellement au débit pour des écoulements se situant entre 50 et 850 $m^3 \cdot s^{-1}$ (marène : $R^2 = 0{,}91$; lavaret : $R^2 = 0{,}77$). La durée de la période d'éclosion, estimée d'après la dérive, est inversement proportionnelle à l'augmentation de l'écoulement d'eau (marène : $R^2 = 0{,}73$; lavaret : $R^2 = 0{,}68$). Il n'y a pas de corrélation significative entre la durée de la période d'incubation des oeufs et le moment de l'éclosion, d'une part, la température ambiante de l'eau, d'autre part. Avant les crues printanières normales, on a provoqué deux crues artificielles (220 $m^3 \cdot s^{-1}$) qui ont eu pour effet d'augmenter le nombre total de larves de Coregoninae à la dérive dans la rivière. La première crue a fait passer le nombre par seconde de larves de marène de 2,1 à 86,1 et celui des larves de lavaret de 0,0 à 4,5, puis les chiffres sont revenus aux niveaux antérieurs. La seconde crue a donné lieu à des dénombrements de 18,9 et 1,8 larves/s, respectivement.

[Traduit par la Rédaction]

Introduction

The start of external feeding may be the most important bottleneck in the survival of juvenile fishes (Wootton 1990). To survive, larvae have to start feeding within a short period after hatching. In subfamily Coregoninae survival depends heavily upon environmental conditions during this critical period of about 2 weeks (Kokova 1979). In a preliminary study in the River Lågen, Næsje et al. (1986*a*) found that *Coregonus albula* L. (vendace) and *Coregonus lavaretus* L. (whitefish) hatched and drifted out during spring flooding. They hypothesized that the spring flood gave the cue for the start of hatching of river-spawned eggs of vendace and whitefish. In laboratory experiments, Næsje and Jonsson (1988) showed that, at the same temperature regime and at oxygen saturation, lake-spawning whitefish eggs agitated by water movements hatched earlier than those lying still. Mechanically disturbed eggs could hatch as much as 133 degree-days or 26% earlier than the unagitated controls.

The effects of temperature and oxygen concentration on the incubation period of fish eggs are recognized by a number of authors (e.g., Alderdice et al. 1958; Brooke 1975; DiMichele and Taylor 1980; Crisp 1981; Luczynski 1984). Few studies, however, give information on the importance of water flow. Hamor and Garside (1976) stressed the importance of flow as a means to increase the ambient oxygen level around eggs of Atlantic salmon (*Salmo salar*), thereby inducing early hatching. In whitefish, Næsje and Jonsson (1988) showed that agitation by water alone induced hatching in the laboratory.

Here, we tested if early spring floods cause early hatching of river spawned Coregoninae (vendace and whitefish) eggs. Relationships between drift of Coregoninae larvae and the abiotic factors, water discharge, and water temperature were investigated in a 5-year field study. Moreover, we performed a large-scale field experiment where two artificial spring floods were released prior to the natural spring flood.

Received October 20, 1994. Accepted May 17, 1995.
J12611

T. Næsje and B. Jonsson. Norwegian Institute for Nature Research, Tungasletta 2, N-7005 Trondheim, Norway.
J. Skurdal. County Governor in Oppland, Environmental Protection Department, Gudbrandsdalsveien 170, N-2600 Lillehammer, Norway.

Can. J. Fish. Aquat. Sci. **52**: 2190–2196 (1995). Printed in Canada / Imprimé au Canada

Materials and methods

Study area

The River Lågen (mean annual water discharge of 249 $m^3 \cdot s^{-1}$) is the main inlet of Lake Mjøsa (61°30′N, 10°25′E, surface area 365 km^2), the largest lake in Norway. During spring floods, the water discharge increases to more than 1000 $m^3 \cdot s^{-1}$. Spawning vendace and whitefish ascend the river from the lake in October at water temperatures between 4.5 and 8.5°C. In the period 1980–1990, the first spawning vendace in River Lågen were registered between 2 and 20 October, and the spawning ended between 13 and 31 October. In most years spawning lasted for 1–2 weeks. Whitefish spawn in the same period as vendace. The eggs hatch in April and May. Because of their small yolk sac, Coregoninae larvae have to start external feeding within a few days after hatching (John and Hasler 1956; Kokova 1979). From our study area, the newly hatched larvae are carried 7–8 km downstream into Lake Mjøsa where they aggregate and start external feeding in backwaters along the shore (Næsje et al. 1986*b*). The sampling area for drifting Coregoninae larvae was situated at the end of a 200-m long rapid immediately downstream of the main spawning area. The water current in the sampling area was turbulent, and velocities varied between 0.4 and 1.0 $m^3 \cdot s^{-1}$.

Sampling

Newly hatched vendace and whitefish larvae were sampled with three parallel drift nets in 1981, 1982, 1983, and 1988, and one drift net in 1986 and 1987. The drift nets had square openings of 0.3 m × 0.3 m and 1-mm stretched mesh and were placed 1–2 m from the river bank at depths of 0.4–0.6 m. Fifteen- to sixty-minute samples were taken during the potential hatching period in April and May. Water velocities through the nets were measured with a current meter. In the river, total outdrift of fish larvae (Y, s^{-1}) was calculated on the basis of number of larvae caught in the drift net (N), total water discharge in the river (D, $m^3 \cdot s^{-1}$), sampling time (T, s), area of opening of drift nets (A, m^2), and water velocity through the drift nets (V, $m \cdot s^{-1}$), where

$$[1] \quad Y = \frac{ND}{AVT}$$

The abundance of vendace and whitefish in Lake Mjøsa varies among years (Sandlund et al. 1981; Sandlund et al. 1991). The general drift of larvae (1981–1983, and 1986–1987) is therefore also variable and here presented as percentage of total drift.

Field experiment

In the spring of 1988 (26 April and 2 May), immediately after ice break-up in the river, two artificial floods of about 220 $m^3 \cdot s^{-1}$ were released at 09:00 (Norwegian standard time) from a hydroelectric power plant 2 km upstream of the spawning area (Fig. 1). At the time of release the water temperatures were 0.5 and 1.1°C, respectively. The floods lasted for 1 h. Normal water discharge in the period was about 90 $m^3 \cdot s^{-1}$, and the artificial floods were approximately 20% of the peak of the natural spring flood. The water took 15 to 20 min to travel from the hydroelectric dam to the sampling area. Water discharges and surface water temperatures were continuously measured at the power plant. The outdrift of larvae after the artificial floodings were compared with the mean outdrift of larvae at the same water discharge in spring during 5 previous years (1981–1983, 1986, and 1987).

Fig. 1. Water discharge and artificial floods (indicated by arrows) in the River Lågen in April and May 1988.

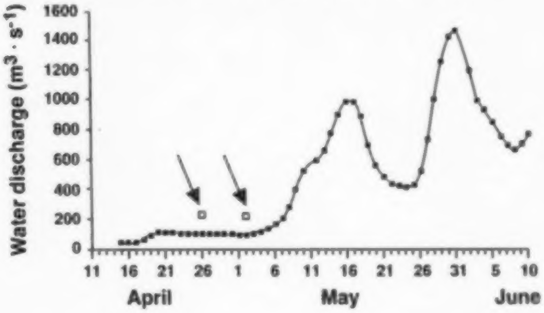

Outdrift of larvae as indicator of hatching activity

Vendace and whitefish deposit their eggs upon the substratum, and the slowly sinking, sticky eggs are transported with the water current until caught in holes and crevices between pebbles and gravel (Fabricius and Lindroth 1954; Lindroth 1957). The behaviour of Coregoninae yolk sac larvae differs from those of river-spawning Salmoninae species. Salmoninae larvae stay in the river substratum between hatching and swim-up stage. Larvae of *Coregonus* spp. have only a very small yolk sac and start to swim immediately after hatching (Fabricius and Lindroth 1954; Lindroth 1957; Braum 1964). They are positive photo- and rheo-tactic and unable to withstand current velocities higher than 0.07–0.08 $m \cdot s^{-1}$ (Lindroth 1957; Braum 1964; Bogdanov 1992). Immediately after hatching, the larvae are caught in the water currents and flush downstream (Lindroth 1957; Bogdanov 1992). This behaviour of Coregoninae larvae was confirmed by Næsje and Jonsson's (1988) laboratory experiments. In their study, whitefish eggs hatched at equal rates during light and dark periods. The yolk sac larvae began to swim immediately after hatching, and when incubated in running water they drifted with the water currents into collecting baskets.

In River Lågen, water velocities in the surface layers over the spawning ground varied between 0.2 and 0.8 $m \cdot s^{-1}$. There are few large stones or boulders for shelter, and larvae are likely to be swept away with the water as soon as they leave the bottom after hatching. Thus we conclude that the outdrift pattern of Coregoninae larvae immediately downstream from the spawning area is a good indicator of the hatching activity of vendace and whitefish in River Lågen.

Treatment of material

Newly hatched vendace and whitefish larvae can be distinguished by their body sizes; in the River Lågen they are 9–11 and 14–17 mm, respectively.

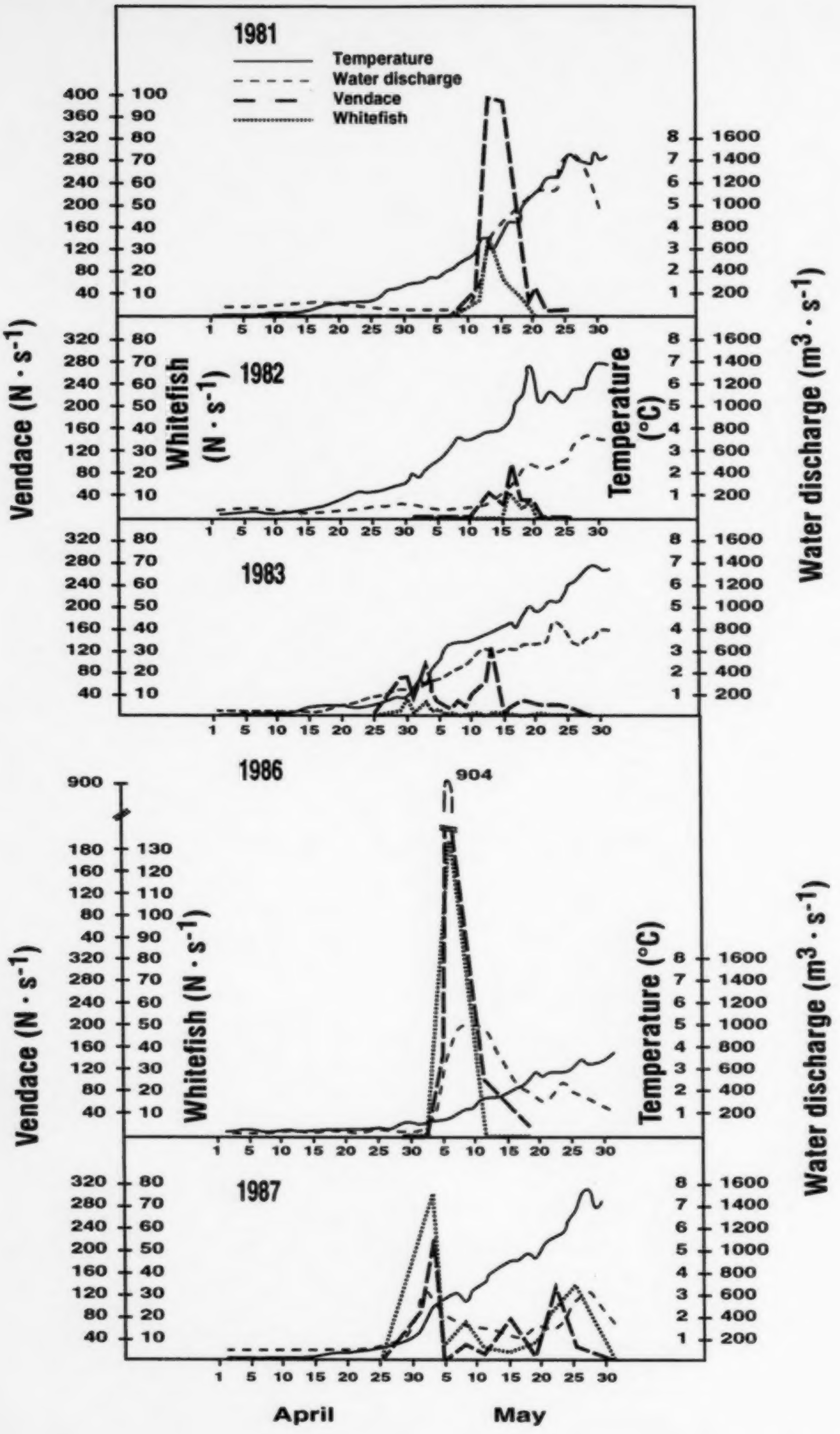
1981
Temperature
Water discharge
Vendace
Whitefish
1982
1983
1986
904
1987
Vendace (N · s-1)
Whitefish (N · s-1)
Temperature (°C)
Water discharge (m3 · s-1)
400
360
320
280
240
200
160
120
80
40
100
90
80
70
60
50
40
30
20
10
900
180
130
120
110
8
7
6
5
4
3
2
1
1600
1400
1200
1000
800
600
400
200
1
5
10
15
20
25
30
April
May

Fig. 2. Total drift of vendace and whitefish larvae (numbers (*N*) per second), water temperature, and water discharge in River Lågen in April and May in the years 1981–1983, 1986, and 1987. Note the broken axis of total outdrift of vendace in 1986.

Fig. 3. Total drift of vendace and whitefish larvae (numbers (*N*) per second), at different water discharges in River Lågen in the years 1981–1983, 1986, and 1987.

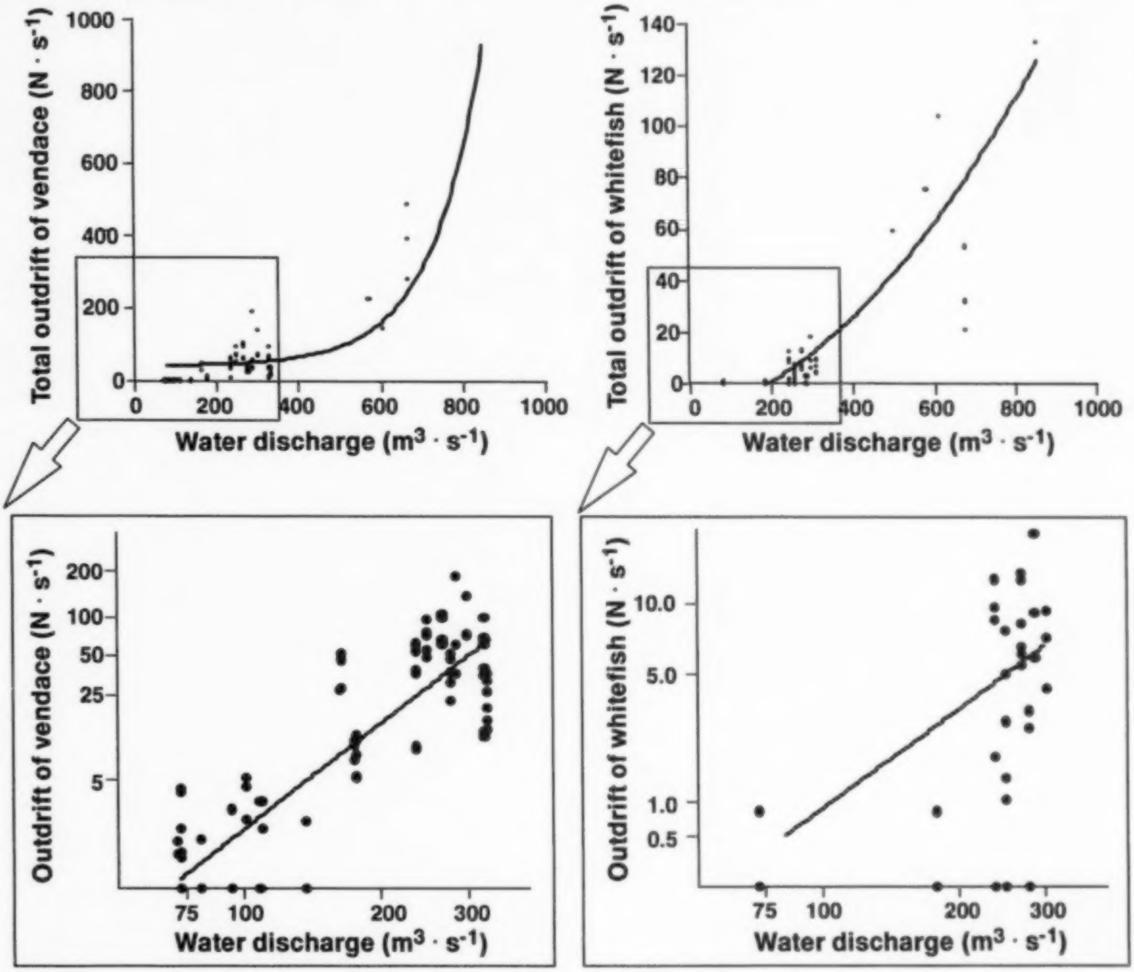

Relationships between the hatching activity as shown by the drift of Coregoninae larvae, water discharge, and water temperature were described by different regression models. The goodness of fit of the various models was tested by comparing the sum of squared residuals, and here we present the models giving the best fit. As input data, we only used the drift until 50% of total annual drift was reached.

Results

Natural hatching

Drift of vendace and whitefish larvae peaked during late April and May (Fig. 2), and hatching and drift of larvae started councurrently with the beginning of the spring flood. The length of the hatching period (number of days between 5 and 95% hatching) was significantly negatively correlated with the daily rate of increase in spring flood as shown by the slope of the water discharge curve during the hatching period in corresponding years (vendace: R^2 = 0.73, $P < 0.05$, df = 4; whitefish: R^2 = 0.68, $P < 0.05$, df = 4). Thus, the more quickly the discharge increased, the shorter the hatching period.

The total drift of Coregoninae larvae increased with water discharge (x, $m^3 \cdot s^{-1}$). In April–May 1981–1983, 1986, and 1987, the total numbers of drifting larvae (± SE) of vendace (Y_c) and whitefish (Y_w) in the river just downstream from the main spawning area, at water discharges between 50 and 850 $m^3 \cdot s^{-1}$, were (Fig. 3, nonlinear least squares error regression) as follows:

Fig. 4. Total drift of (*a*) vendace and (*b*) whitefish larvae in the River Lågen in 1988. The responses to the two artificial floods are marked with arrows.

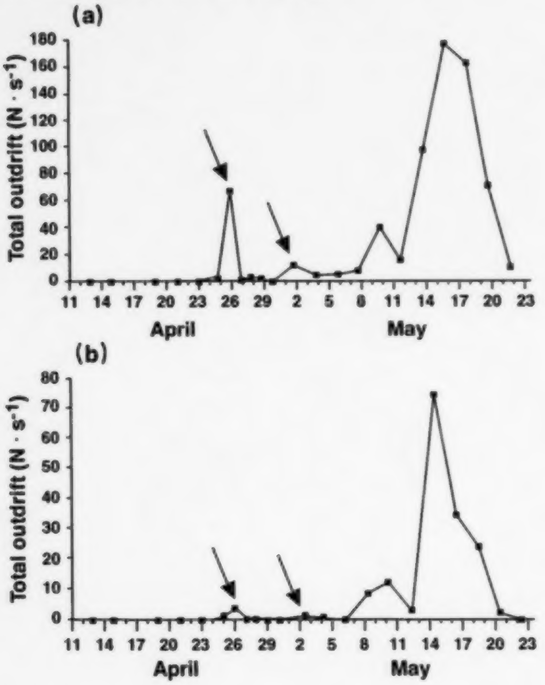

$$[2] \quad Y_c = 42.95\ (\pm\ 13.43) + e^{0.008\ (\pm\ 0.00008)x}\ (R^2 = 0.91)$$

$$[3] \quad Y_w = -12.56\ (\pm\ 26.58) + 0.045\ (\pm\ 0.14)x + 0.00014\ (\pm\ 0.00015)x^2\ (R^2 = 0.77)$$

Using water temperature (cumulative or absolute) as a second independent variable in multiple regressions did not add significantly to the models when water discharge was introduced as the first independent variable.

Most of the data were from water discharges between 50 and 350 $m^3 \cdot s^{-1}$, and the two artificially released floods were 220 $m^3 \cdot s^{-1}$. To make the best prediction of outdrift of larvae at this water discharge we limited the curve fit to data from water discharges between 50 and 350 $m^3 \cdot s^{-1}$. The best regressions were as follows:

$$[4] \quad \log_e Y_c = -11.26\ (\pm\ 1.98) + 2.67\ (\pm\ 0.39)\log_e x \quad (R^2 = 0.73)$$

$$[5] \quad \log_e Y_w = -5.56\ (\pm\ 3.35) + 1.26\ (\pm\ 0.62)\log_e x \quad (R^2 = 0.41)$$

The River Lågen drains large, snow covered, mountainous areas, and the water discharge in the spawning area during hatching (5–95% hatching for vendace and whitefish) was not correlated with water temperature ($R^2 = 0.01$, $P > 0.05$, df = 74 and 72, respectively). Moreover, we found no significant correlation between start, peak, or maximum numbers of drifting larvae and water temperature. The main hatching (50% hatched) occurred at different temperatures in different years, varying between 1.7 and 4.3°C for both vendace and whitefish. The number of degree-days for vendace, calculated from the first date of spawning to the first date of larvae observed in the river in 1981–83 and 1986–87, varied between 134 and 282 degree-days. Corresponding figures from last day of spawning until the first day of observed larvae were 52 and 206 degree-days. Degree-days from mid-spawning until peak hatching varied by more than 100, with a minimum of 142 degree-days and a maximum of 243 degree-days. For whitefish, the number of degree-days in the incubation period cannot be given because the exact time of spawning is unknown. The degree-days in the spring (temperature >0.1°C) for the same years varied between 15.7 and 71.1 degree-days for both species.

Field experiment

We used discharges of approximately 220 $m^3 \cdot s^{-1}$ in the two artificial floods. For this discharge, models in eqs. 4 and 5 predicted drifts of 23.1 and 3.4 individuals/s of vendace and whitefish, respectively.

The first artificial flood was released at the very beginning of the hatching period (Fig. 4). Three to four hours after the flood had passed the hatching and sampling area, the number of drifting larvae of vendace and whitefish increased from 2.1 and 0.0 individuals/s to peaks of 86.1 and 4.5 individuals/s, respectively (Fig. 5). The increased drift of larvae lasted for 2 to 3 h before decreasing to preflood levels. The same patterns of hatching and drift were observed after the second artificial flood. However, the responses were smaller and the peak drifts were 18.9 and 1.8 individuals/s for vendace and whitefish, respectively. The mean observed drifts in the two artificial floods were 45.7 ± 10.1 and 2.2 ± 0.7 individuals/s, respectively.

Discussion

Increased water flow during spring induced hatching of vendace and whitefish eggs and outdrift of the newly hatched larvae. This is shown through 6 years of field study and in a large-scale field experiment. This may be general for river-spawning Coregoninae, and even in lake-spawning whitefish, water movement of the eggs induced early hatching in a laboratory test (Næsje and Jonsson 1988). Similarly to this study in River Lågen, Bogdanov et al. (1992) related the downstream migration of river-spawned Coregoninae larvae to increased water flow when the embryos were ready to hatch.

The rate of embryonic development of fishes depends on water temperature (e.g., John and Hasler 1956; Crisp 1981), and according to Luczynski and Kirklewska (1984) eggs must pass a certain developmental stage before embryos can survive hatching. However, towards the end of the incubation period several factors other than temperature may terminate the larval development within the egg shell. In the River Lågen, the number of degree-days between spawning and hatching varied considerably among years, and there, water temperature alone is not giving the cue to start hatching.

In the River Lågen, the length of the hatching period depended on the rise in water discharge during the spring flood. A fast increase in water discharge and high water

Fig. 5. Total drift of vendace (solid line) and whitefish larvae (broken line) (numbers (*N*) per second, ± SE), water temperature, and water discharge during the first artificial flood in River Lågen, 26 April 1988.

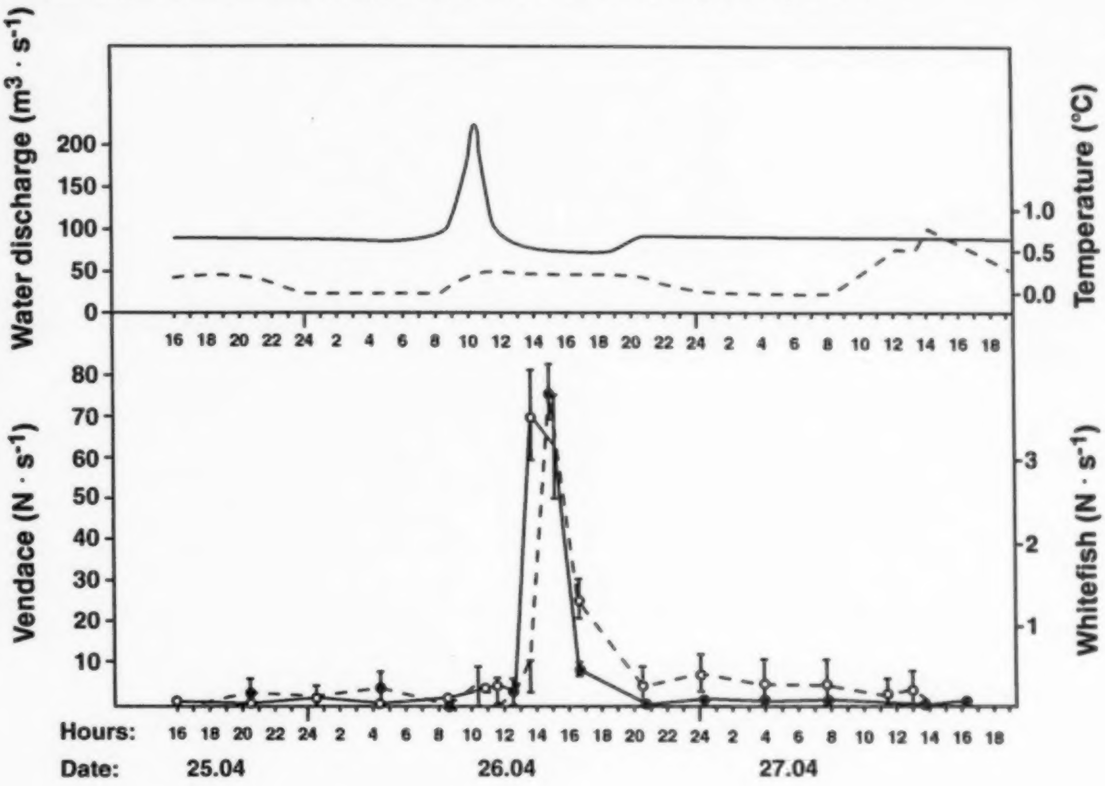

flow led to synchronous hatching. A small or varying flood gave longer hatching periods. This is in accordance with Næsje and Jonsson (1988) who found that eggs agitated by water hatched in narrower synchrony than controls lying still. There may be two reasons for this. First, increased water discharge may increase the agitation of the eggs on the bottom and induce hatching. Second, as a result of the shape of the hatching grounds and flow dynamics, larger areas are influenced by the flowing water, and more and more eggs are agitated and start to hatch.

Hatching of Coregoninae eggs is induced by a combination of movements of the embryo within the egg shells and the action of hatching enzymes, chorionases (Price 1940; Smith 1957). The secretion of the chorionases and the choriolysis itself are temperature dependent (Luczynski 1984, 1985). The enzymes have been found to be active at temperatures above approximately 3°C. In River Lågen, however, 50% of the annual hatching was reached at a temperature as low as 1.7°C in one of the years studied, which may indicate that the presence of active chorionases is not a requisite for hatching. Alternatively, the lower threshold temperature for chorionase activity may vary among populations.

In the field experiment, the increase in drift occurred 3 to 4 h after the flood had passed the hatching and sampling area. Yolk sac larvae of Coregoninae are positive phototactic and start to swim immediately after hatching (Fabricius and Lindroth 1954; Braum 1964; Næsje and Jonsson 1988). This indicates that the increased drift is due to increased hatching activity and not merely that already-hatched larvae were flushed out by the increased water flow.

The effect of mechanical stress upon Coregoninae eggs is also substantiated by in situ observations. With the use of dip nets in April 1987, we collected eggs from the spawning grounds before natural hatching. Also, these eggs hatched just after removal, if we slightly shook the glass jars with the eggs.

Coregoninae eggs incubate among surface gravel, and thus the eggs are exposed to mechanical stress caused by increasing water current. Other river-spawning Salmonidae, like salmon and trout, bury their eggs in gravel and may therefore be less affected by increases in flow. But increased flow may influence hatching of eggs of Atlantic salmon (*Salmo salar* L.) (Hamor and Garside 1976; Crisp 1990).

Coregoninae have small eggs compared with many other salmonids and must start feeding shortly after hatching. Furthermore, they exploit lakes and rivers at high altitudes and latitudes where weather is variable and the temperature and food conditions change rapidly during spring. In northern temperate areas, most lakes are ice covered until spring, and the ice breaks up partly as a result of the spring freshet. Most larvae that hatch before the ice break-up probably die from starvation. Coregoninae are visual predators, and poor light conditions under the ice handicap the larvae in their search for food. Shortly after ice-break, *Cyclops* spp. and *Bosmina* spp. increase rapidly in numbers, and these two groups are the most important initial food for whitefish and vendace in Lake Mjøsa (Næsje et al. 1986*b*). Under such climatic conditions there has probably been strong selection for using the spring flood as a cue to start hatching.

By using the spring flood as a cue for the start of hatching, Coregoninae become vulnerable to artificial changes in river flow. Early flooding, e.g., caused by a regulation for hydropower purposes, may induce hatching at an early date, when food is scarce. However, retention of water in spring, e.g., for irrigation or flood control, may also negatively influence the survival of the fish. The dependence of river-spawning Coregoninae on spring flooding should be taken into consideration when regulating the discharge of rivers.

Acknowledgements

We thank O.T. Sandlund, S. Gorseth, A.H. Eriksen, L. Klyve, S. Havdahl, H. Meland, B. Stene, T. Taugbøl, and R. Saksgård for helpful assistance during field work, in the laboratory, and with preparation of the paper. T. Forseth and I. Fleming assisted in making the mathematical models. Without the cooperation of Opplandskraft Power Company this work could not have been performed. Financial support was given by the Norwegian Institute for Nature Research and Water System Management Association.

References

Alderdice, D.F., W.P. Wickett, and J.R. Brett. 1958. Some effects of temporary exposure to low dissolved oxygen levels on Pacific salmon eggs. Can. J. Fish. Aquat. Sci. 15: 229–249.

Bogdanov, V.D., S.M. Melnichenko, and I.P. Melnichenko. 1992. Descent of larval whitefish from the spawning region in the Manya River (lower Ob basin). Vopr. Ikhtiol. 31: 776–782.

Braum, E. 1964. Experimentelle Untersuchungen zur ersten Nahrungsaufnahme und Biologie an Jungfischen von Blaufelchen (*Coregonus wartmanni* Bloch), Weissfelchen (*Coregonus fera* Jurine) und Hechten (*Esox lucius* L.). Arch. Hydrobiol. Suppl. 28: 183–244.

Brooke, L.T. 1975. Effect of different constant incubation temperatures on egg survival and embryonic development in lake whitefish (*Coregonus clupeaformis*). Trans. Am. Fish. Soc. 104: 555–559.

Crisp, D.T. 1981. A desk study of the relationship between temperature and hatching time for eggs of five species of salmonid fishes. Freshwater Biol. 11: 361–368.

Crisp, D.T. 1990. Some effects of application of mechanical shock at varying stages of development upon the survival and hatching time of British salmonid eggs. Hydrobiologia, 194: 57–65.

DiMichele, L., and M.H. Taylor. 1980. The environmental control of hatching in *Fundulus heteroclitus*. J. Exp. Zool. 214: 181–187.

Fabricius, E., and A. Lindroth. 1954. Experimental observations on the spawning of whitefish, *Coregonus lavaretus* L., in the stream aquarium of the Hölle Laboratory at River Indalsälven. Inst. Freshwat. Res. Drottningholm Rep. No. 35. pp. 105–112.

Hamor, T., and E.T. Garside. 1976. Developmental rates of embryos of Atlantic salmon, *Salmo salar* L., in response to various levels of temperature, dissolved oxygen, and water exchange. Can. J. Zool. 54: 1912–1917.

John, K.R., and A.D. Hasler. 1956. Observations on some factors affecting the hatching of eggs and the survival of young shallow-water vendace, *Leucichthys artedi* LeSueur, in Lake Mendota, Wisconsin. Limnol. Oceanogr. 1: 176–194.

Kokova, V. Ye. 1979. Feeding of larvae of the whitefish, *Coregonus lavaretus ladoga*, the Baikal omul, *Coregonus autumnalis migratorius*, and the 'peled,' *Coregonus peled*. J. Ichthyol. (Engl. Transl.), 18: 953–960.

Lindroth, A. 1957. A study of the whitefish (*Coregonus*) of the Sundsvall Bay district. Inst. Freshwat. Res. Drottningholm Rep. No. 38. pp. 70–108.

Luczynski, M. 1984. Temperature and electric shock control the secretion of chorionase in *Coregoninae* embryos. Comp. Biochem. Physiol. A Physiol. 78: 371–374.

Luczynski, M. 1985. Survival of *Coregonus albula* (L.) (Teleostei) embryos incubated at different thermal conditions. Hydrobiologia, 121: 51–58.

Luczynski, M., and A. Kirklewska. 1984. Dependence of *Coregonus albula* embryogenesis rate on the incubation temperature. Aquaculture, 42: 43–55.

Næsje, T.F., and B. Jonsson. 1988. Impacted stress: a causal agent of reduced whitefish (*Coregonus lavaretus*) egg incubation time. Can. J. Fish. Aquat. Sci. 45: 27–31.

Næsje, T.F., B. Jonsson, and O.T. Sandlund. 1986*a*. Drift of vendace and whitefish larvae in a Norwegian river. Trans. Am. Fish. Soc. 115: 89–93.

Næsje, T.F., O.T. Sandlund, and B. Jonsson. 1986*b*. Habitat use and growth of age-0 whitefish, *Coregonus lavaretus*, and vendace, *C. albula*. Environ. Biol. Fishes, 15: 309–314.

Price, J.W. 1940. Time–temperature relations in the incubation of the whitefish, *Coregonus clupeaformis* (Mitchill). J. Gen. Physiol. 23: 449–468.

Sandlund, O.T., T.F. Næsje, L. Klyve, and H. Hagen. 1981. The whitefish (*Coregonus lavaretus*) in Mjøsa. Age composition, growth, and food habits. DVF-Mjøsundersøkelsen, Rep. No. 5. pp. 1–54. (In Norwegian with English summary.)

Sandlund, O.T., B. Jonsson, T.F. Næsje, and P. Aass. 1991. Year-class fluctuations in vendace, *Coregonus albula* (Linnaeus): who's got the upper hand in intraspecific competition? J. Fish Biol. 38: 873–885.

Smith, S. 1957. Early development and hatching. *In* The physiology of fishes. *Edited by* M.E. Brown. Academic Press, New York. pp. 323–359.

Wootton, R.J. 1990. Ecology of teleost fishes. Chapman and Hall, London.

Pleistocene refuge areas and postglacial dispersal of copepods of the northeastern United States

Richard S. Stemberger

Abstract: The distribution of common freshwater copepods of the northeastern United States has a marked association with major meltwater drainage systems and coastal marine submergence zones formed during the retreat of the Wisconsinan ice sheet. Postglacial dispersal routes inferred from the deglaciation chronology indicate that zooplankton could have come from several major Pleistocene refuges in the Mississippi Valley, Appalachian Plateaus, and mid-Atlantic Coastal Plain, and from northern locations on the Atlantic Coastal Plain. Contemporary distribution patterns suggest that some species of copepods dispersed primarily in surface waters during advances and retreats of continental glaciers. These include species of the calanoid *Skistodiaptomus* and the cyclopoid *Diacyclops thomasi* that occur in coastal lowlands and in lower elevation lakes in mountainous areas that could be flooded by retreating ice-front lakes. There is little evidence, except for inadvertent introductions through human activities, that these species have expanded beyond their original postglacial dispersal boundaries. In contrast, other calanoid and cyclopoid species were widely distributed and are dominant in high-elevation lakes and lowland lakes behind mountain barriers unreachable by species dependent on water transport. These species commonly occur in permanent and temporary ponds and may produce dormant stages that are readily dispersed.

Résumé : La répartition des copépodes d'eaux douces communs dans le nord-est des États-Unis est nettement liée aux principaux systèmes de drainage des eaux de fonte et aux zones côtières marines de submersion formées pendant le retrait de la nappe glaciaire wisconsinienne. Les routes de dispersion post-glaciaires déduites de la chronologie de la déglaciation indiquent que le zooplancton pourrait provenir de plusieurs refuges importants du Pléistocène dans la vallée du Mississippi, les plateaux appalachiens et la région centrale de la plaine côtière atlantique, ainsi que d'endroits situés dans le nord de cette plaine côtière. D'après des schèmes contemporains de répartition, certaines espèces de copépodes se seraient dispersées principalement dans les eaux de surface pendant les avances et les retraits des glaciers continentaux. Parmi ces espèces, mentionnons le calanoïde *Skistodiaptomus* et le cyclopoïde *Diacyclops thomasi* que l'on trouve dans les basses terres côtières et dans les lacs de faible altitude des régions montagneuses qui ont pu être inondés par les lacs du front glaciaire lors du retrait. Il y a peu de preuves, sauf dans le cas d'introductions accidentelles liées aux activités humaines, que ces espèces aient dépassé les limites de leur aire originale de répartition post-glaciaire. Par contre, d'autres espèces de calanoïdes et de cyclopoïdes sont très répandues et dominantes dans les lacs de haute altitude et dans les lacs de basses terres situés derrière des montagnes formant une barrière infranchissable pour des espèces qui ne peuvent être transportées que par voie aquatique. Ces espèces se rencontrent fréquemment dans des étangs permanents et temporaires et peuvent connaître des stades de dormance pendant lesquels elles sont facilement dispersées.

[Traduit par la Rédaction]

Introduction

The lakes and drainage systems that formed at the end of the Pleistocene account for much of the present-day distribution of North American fishes (Hocutt and Wiley 1986). Recent evidence from genetic studies of fish populations in the northeast indicate that fishes arrived in the region from at least two Pleistocene refuge areas located in the Mississippi Valley and Atlantic Coastal Plain (Billington and Hebert 1988; Bernatchez and Dodson 1990, 1991; Todd and Hatcher 1993). These studies corroborate and extend our understanding of the biogeography of fishes in the northeast (Hocutt and Wiley 1986) and provide a hydrogeological framework for interpreting the present-day distribution of zooplankton.

Received November 16, 1994. Accepted May 11, 1995.
J12633

R.S. Stemberger. Department of Biological Sciences, Dartmouth College, Hanover, NH 03755, U.S.A.

Distributions of North American zooplankton species are generally known but are poorly delimited on regional scales (Wilson and Yeatman 1959; Yeatman 1959; Brooks 1957). Two studies in northeastern North America provide evidence suggesting that some species of zooplankton, particularly some cold-water calanoid copepods and the opposum shrimp (*Mysis relicta*), have distributions that follow late Pleistocene and early Holocene proglacial lake basins and their drainage systems (Dadswell 1974; Carter et al. 1980). Studies in Arctic regions indicate that some zooplankton have not colonized interior areas of Canada from their presumed Beringian refuge area (Hebert and Hann 1986; Boileau and Hebert 1991). These studies suggest that some species of copepods have low dispersal rates and very limited geographic distributions. This contrasts with the notion that zooplankton are ubiquitous and widely distributed because of dispersal of resting stages by wind, insects, birds, and mammals (Maguire 1963; Proctor 1964).

Unlike fish, which could swim against the outflow of proglacial lakes and meltwater channels, zooplankton, such as the glacial marine relict taxa, advanced northward in the retreating ice-front lakes and in the anastomosing lake systems that formed behind them (Segerstrale 1976). Such passive northward dispersal was possible because bedrock at the ice front was depressed by the weight of glacial ice. Hence, drainage from adjacent areas to the south could have flowed northward towards the retreating ice-front lakes. This process would have facilitated the northward dispersal of zooplankton and other aquatic organisms from their southern refuge locations adjacent to the ice front at its maximum advance. Zooplankton could also move passively within the flow of proglacial lake drainage systems through interconnecting waterways that traversed much of the continent (Prest 1970). Species having life-history characteristics that limit dispersal by animal carriers would likely be dispersed by surface water. Such species should be useful in reconstructing postglacial dispersal routes from Pleistocene refuge areas because they are likely to be confined to the lake drainage systems that they initially colonized. These species contrast with those using resting stages transported by animals as their primary mode of dispersal. A broad regional survey of the zooplankton can identify species that are likely dependent on passive dispersal in surface water and those that depend on animal dispersal of resting stages. For example, surface-water dispersants should not be present where geography prevented flooding by ice-front lakes, as in high-elevation lakes in mountain regions.

Knowledge of the geographic boundaries of species has other benefits as well. Expansions or contractions from a baseline record of the known ranges of species or departures from the expected range on the basis of historical reconstructions might reveal climatic change or regional anthropogenic disturbances. Disjunctions, for example, may indicate inadvertent introductions of species through cultural activities, such as fish stocking and transport by boaters and fishermen, or indicate historical geological events, such as stream capture and subsequent mixing of faunas between catchments. Biogeography can help establish historical drainage connections among glacial lakes where geology is not well understood. An understanding of species zoogeography aids species identification work and facilitates interpretation of suspicious historical species records. Finally, zooplankton zoogeography aids in the understanding of the biogeography of other groups that disperse in similar manner such as fish, mollusks, and aquatic plants.

In this study I present presence–absence data of prominent calanoid and cyclopoid copepods from over 300 lakes in the northeastern United States that were collected during the 1991–1994 pilot surveys for the Environmental Monitoring and Assessment Program – Surface Waters (EMAP-SW). The distributions of the copepods (*Skistodiaptomus*, *Leptodiaptomus*, *Aglaodiaptomus*, *Onychodiaptomus*, *Epischura*, *Acanthocyclops*, *Cyclops*, *Diacyclops*, *Mesocyclops*, *Orthocyclops*, and *Tropocyclops*) are interpreted with respect to the chronology and drainage connections of the Wisconsinan deglaciation in the northeast.

Methods

During the 1991–1993 EMAP-SW surveys of the U.S. Environmental Protection Agency 274 lakes were evaluated for their zooplankton species assemblages and other biological, physical, chemical, and land-use factors (Larsen and Christie 1993; Paulsen et al. 1991) (Fig. 1). Fifty-nine of these lakes were sampled a second time during the 8-week (July and August) sampling period. Revisit data were included if the presence of a species was not detected on the first visit. I also included 32 lakes from the 1994 EMAP-SW survey, 23 lakes and ponds from personal collections, and 4 lakes described in the regional literature to improve coverage in critical areas near drainage divides or where such data improved resolution in a species' range (Fig. 1).

Zooplankton samples were taken in the deepest portion of each lake with a single tow from 0.5 m off the bottom to the surface. Two nets were fitted to a single harness. A cone net (30-cm diameter, 202-μm mesh) was used for macrozooplankton and a Wisconsin net (48-μm mesh) with a 15-cm diameter and 25 cm long reducing collar was used for microzooplankton (Stemberger and Lazorchak 1994). Samples containing records of species in critical areas near physiographic boundaries or samples having species outside their expected ranges or elevations were routinely reexamined and validated for quality control on species identifications. Records were excluded from distribution plots if a single individual was reported during routine preparation of species lists, but could not be confirmed independently by another zooplankton taxonomist.

Results

The 1991–1994 EMAP-SW surveys in the northeastern United States reveal clear zoogeographic boundaries in some species of copepods that are associated with major physiographic discontinuities of the Mississippian and Atlantic postglacial drainage systems (Figs. 2–5). The Lake Champlain – Hudson River drainage divides the east–west boundaries of three major zoogeographic provinces delineated by *Skistodiaptomus* spp. but with notable disjunctions (Fig. 3). The Mohawk River Valley delineates the northern and southern discontinuity between Pleistocene

Fig. 1. Map of northeastern United States showing location of study lakes during the EMAP-SW 1991–1994 surveys. Open squares represent lakes for which the author has examined zooplankton or for which data are taken from reliable literature records. Shaded squares represent lakes that are referred to in the text. 1, Lake Champlain; 2, Lake Memphremagog; 3, Lake Willoughby; 4, Waterbury Reservoir; 5, lakes in the basin of glacial Lake Winooski; 6, Storres Pond (*Epischura nordenskioldi* present); 7, Lake St. Catherine (glacial marine relict species present); 8, Bullhead Pond (*Epischura nordenskioldi* present); 9, Green Lake; and 10, Mohawk Pool and Ringneck Marsh.

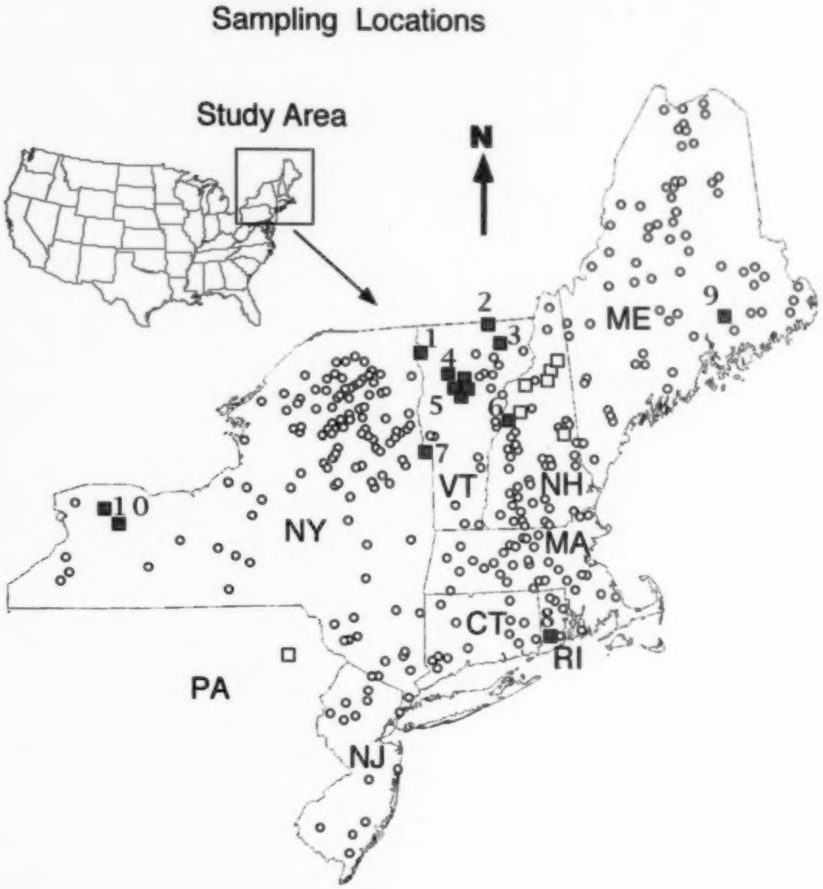

mid-Atlantic and Mississippian drainage systems east and west of the Hudson River, respectively (Fig. 2). *Skistodiaptomus pygmaeus* occupies the eastern portion of the Atlantic drainage as far west as the Connecticut River Valley of New Hampshire and north to the foothills of the White Mountains (Fig. 3). It was not found in lakes of northern Vermont and northern New Hampshire but it has been reported in recent collections from Lake Champlain where it may have been inadvertently introduced in the last 20 years (A. Ducovney, School of Natural Resources, Aiken Center, University of Vermont, Burlington, VT 05405, personal communication; R.S. Stemberger, personal observation). It extends south along the Connecticut River and to the west of the Hudson River Valley into southeastern New York and into New Jersey. The species dominates the northern Atlantic Coastal Plain and occurs in the lowlands and foothills along the northern Appalachian range of Maine and New Hampshire at elevations below 400 m. It extends eastward into the maritime provinces of Canada where it is common in Nova Scotia and coastal areas of New Brunswick and is likely bounded to the north by the St. Lawrence Great Lakes drainage divide in eastern Canada (Carter et al. 1980).

The western congener, *Skistodiaptomus oregonensis*, occupies the area north of the Mohawk River in the Great Lakes drainage and Adirondack region of New York in lakes below 600 m. It occurred in southern locations in the Hudson River Valley in lakes that occupied the former

Fig. 2. Elevation contours (500 m) of the northeastern United States and approximate locations of major glacial lakes, glacial drainage systems, and marine submergence zone. Arrows indicate presumed routes of recolonization from refuge areas. E, Lake Erie; O, Lake Ontario; Mo, Mohawk River drainage; A, Lake Albany; V, Lake Vermont and Champlain Valley; W, Lake Winooski; M, Lake Memphremagog; H, Lake Hitchcock; Wp, Lake Winnipesaukee; Cc, Lake Cape Cod; AdM, Adirondack Mountains; GM, Green Mountains; WM, White Mountains; PoM, Pocono Mountains. Thin wavy lines show the area of marine incursion. Thin broken line indicates the approximate contour of exposed Atlantic Coastal Plain during the late Wisconsinan. Thick wavy lines show the approximate area that was flooded or influenced by the St. Lawrence drainage during deglaciation. Dark areas represent major glacial lakes that were not influenced by the St. Lawrence drainage. Reconstructed from maps and sketches in Dineen et al. (1988), Stone and Peper (1980), Larson (1980), Thompson (1980), and Steward and MacClintock (1969).

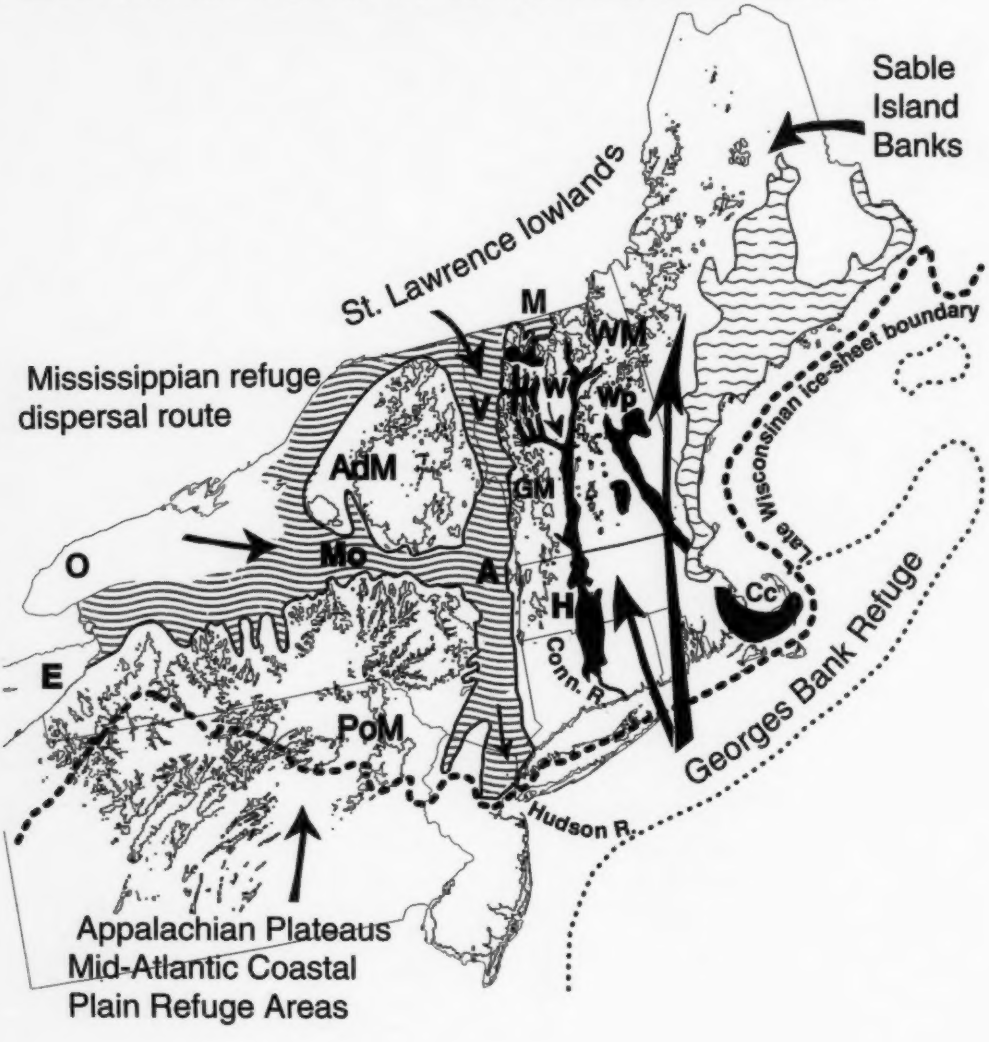
Sable Island Banks
St. Lawrence lowlands
M
WM
Mississippian refuge dispersal route
V
W
Wp
AdM
GM
Late Wisconsinan ice-sheet boundary
O
Mo
A
H
Cc
Georges Bank Refuge
E
Conn. R.
PoM
Hudson R.
Appalachian Plateaus Mid-Atlantic Coastal Plain Refuge Areas

basin of glacial Lake Albany (Fig. 2). *Skistodiaptomus oregonensis* is a dominant copepod of Lake Champlain and of the Laurentian Great Lakes and occurs in a few locations in northern Vermont east and south of present-day Lake Champlain in the former basin of glacial Lake Vermont. It occurs outside the Mississippian – Great Lakes drainage in a man-made impoundment near Cortland, New York, in the Susquehanna River drainage system but very near to the Great Lakes drainage divide. It is common in western Quebec and western Ontario (Carter et al. 1980) and occurs to the west coast of North America. It has been reported as far south as Colorado in the Rocky Mountains

Fig. 3. Distribution of *Skistodiaptomus* spp. in the northeastern United States. Open squares, *S. pallidus*; solid circles, *S. oregonensis*; solid triangles, *S. pygmaeus*; shaded circle, location of *S. oregonensis* and *S. pygmaeus* hybrids. Open circles indicate lakes where the species was not observed. Heavy line delineates northern margin of marine submergence zone.

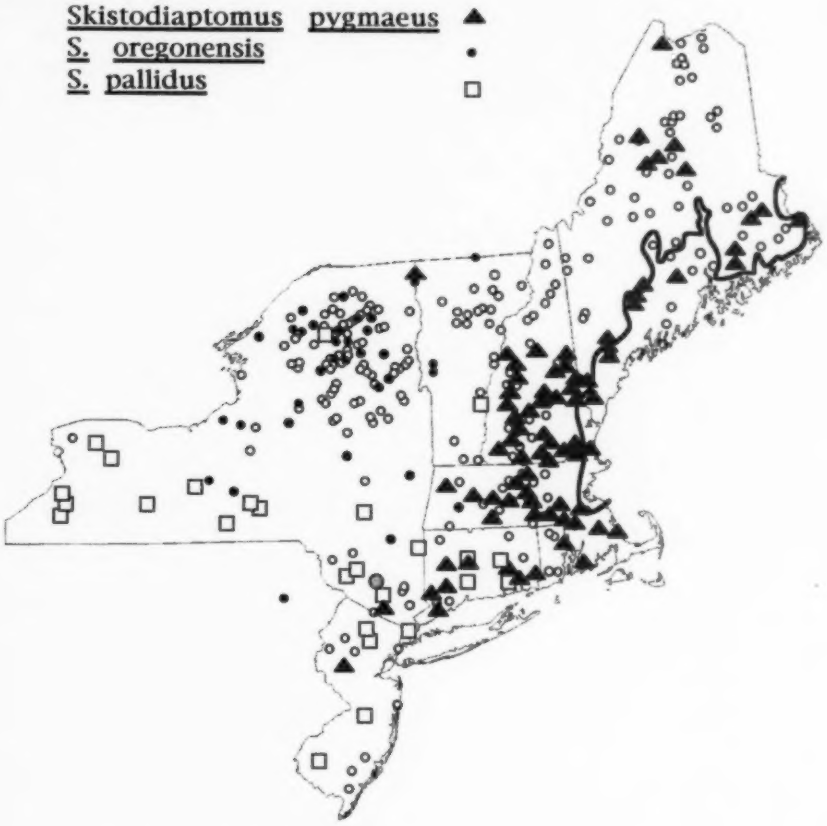

and north to the Northwest Territories (Wilson and Yeatman 1959).

Skistodiaptomus pallidus occupies the region of the Appalachian Plateaus south of the Mohawk River Valley and west of the Hudson River into southern New Jersey below 540 m elevation (Figs. 1–3). It occurs in two man-made impoundments (Mohawk Pool and Ringneck Marsh) in the Lake Ontario drainage of northwestern New York in the province of *S. oregonensis* and in the geographic province of *S. pygmaeus* in southeastern Connecticut (Fig. 1). A single adult male was observed in a sample from a flood control reservoir in east-central Vermont and in a pond in the central Adirondacks (Fig. 3). These records represent the furthest eastern and northern locations observed for the species.

Only rarely did more than one species of *Skistodiaptomus* occur in a lake. Recent samples from Lake Champlain, Vermont, had both *S. oregonensis* and *S. pygmaeus* present. In one southern New York lake near the physiographic discontinuity of the Mississippian and Appalachian plateaus (Fig. 3) there was clear evidence of hybridization between *S. oregonensis* and *S. pygmaeus*. The specimens could not be clearly identified as either species on the basis of the morphology of the fifth legs of the males. The presumptive hybrids had the smoothly arching curve in the claw of the fifth leg male characteristic of *S. oregonensis* but possessed the stout spearlike left endopod of *S. pygmaeus* (see Wilson and Yeatman 1959). Both *S. pallidus* and *S. pygmaeus* were present in a lake in central Connecticut (Fig. 3).

Other copepods showed similar distributions related to the major physiographic boundaries between the Mississippian and Atlantic drainages. *Diacyclops thomasi* occurs throughout the Laurentian Great Lakes basin including the Finger Lakes of New York and Lake Champlain and in lakes below 500 m in the Adirondack region (Fig. 4). Its range extends south along the Hudson River to the Atlantic Ocean and it has been recorded in the Pocono Mountains of Pennsylvania (Craig Williamson, Department of Earth and Environmental Sciences, Lehigh University, Bethlehem, PA 18015, personal communication). The latter record may represent dispersal from a former connection of the St. Lawrence drainage with the Susquehanna River basin

Fig. 4. Distribution of *Diacyclops thomasi* in the northeastern United States. Open circles indicate lakes where the species was not observed.

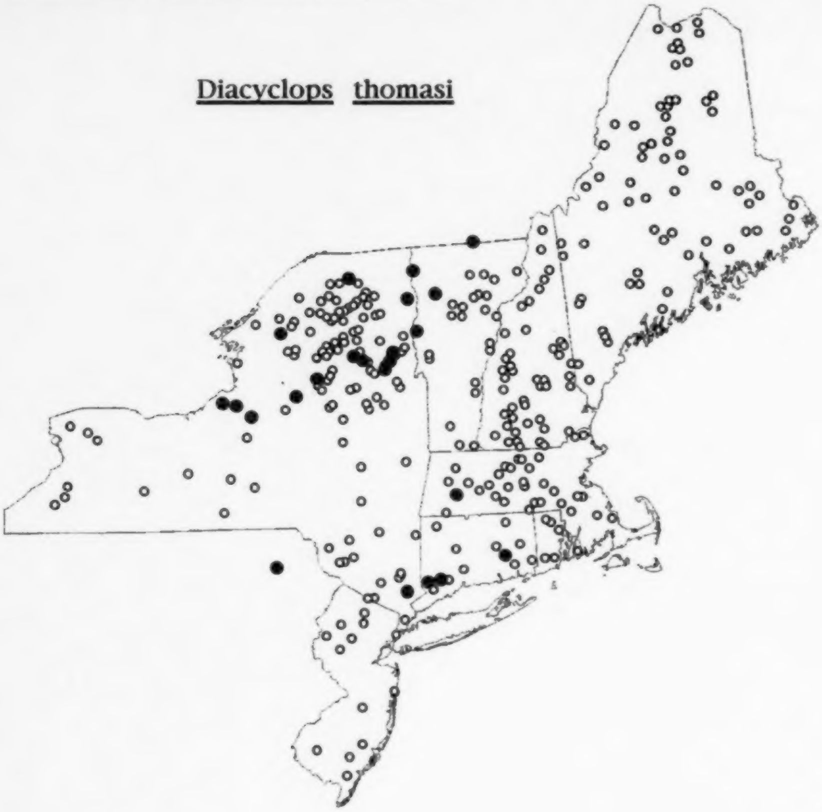

(Hocutt et al. 1986). The species extends to the east and south in the Connecticut River drainage of Massachusetts and Connecticut to the Atlantic Ocean (Figs. 1 and 4).

Epischura nordenskioldi occurs in two widely separated areas of the northeast. It is common in Nova Scotia (Carter et al. 1980) and is present in coastal lakes east of the Connecticut River in Massachusetts and Rhode Island (Fig. 5). We did not find it in lakes above 300 m. We have a record of the species in a man-made impoundment near Hanover, New Hampshire, near the Connecticut River where it cooccurs with *Epischura lacustris*.

Other common copepods such as *Epischura lacustris*, *Leptodiaptomus minutus*, and *Mesocyclops edax* (Figs. 5–7), and *Tropocyclops extensus* and to a lesser extent *Acanthocyclops robustus*, *Orthocyclops modestus*, and *Cyclops scutifer* are widely distributed and very common in the northeast, suggesting that they also have effective dispersal mechanisms that allow them to reach high-elevation lakes.

Less common species such as *Aglaodiaptomus spatulocrenatus*, *Aglaodiaptomus leptopus*, and *Onychodiaptomus sanguineus* infrequently cooccur in lakes having *Skistodiaptomus* spp. and are typically present in low- and high-elevation areas behind mountain ranges where ice-front lakes from the coast did not reach (Figs. 1 and 8, Table 1). These species are common in fishless temporary ponds and wetlands in the northeast (R.S. Stemberger and M.A. McPeek, personal observations). Hence, there appear to be three distinctive groups of copepods in the northeast that are defined by both their dispersal mechanisms (water dispersal vs. resting egg dispersal by animals) and by their ability to coexist with fish.

Discussion

The present-day distribution of freshwater copepods of the northeastern United States is intimately linked to the deglaciation history of the region. The distribution of some species clearly follows the physiographic discontinuity between the Atlantic and Mississippian drainages. These distributions suggested the locations of Pleistocene refuge areas as inferred from passive dispersal of species in the St. Lawrence drainage. The general direction of ice sheet retreat from southerly locations adjacent to the maximum advance of the ice-sheet also identified potential refuge locations on the Atlantic Coastal Plain and Appalachian Plateaus. A summary of the chronology of major events and features in the deglaciation of the northeast is as follows.

Fig. 5. Distribution of *Epischura* spp. in the northeastern United States. Solid circles, *E. lacustris*; shaded triangles, *E. nordenskioldi*. Open circles indicate lakes where the species were not observed.

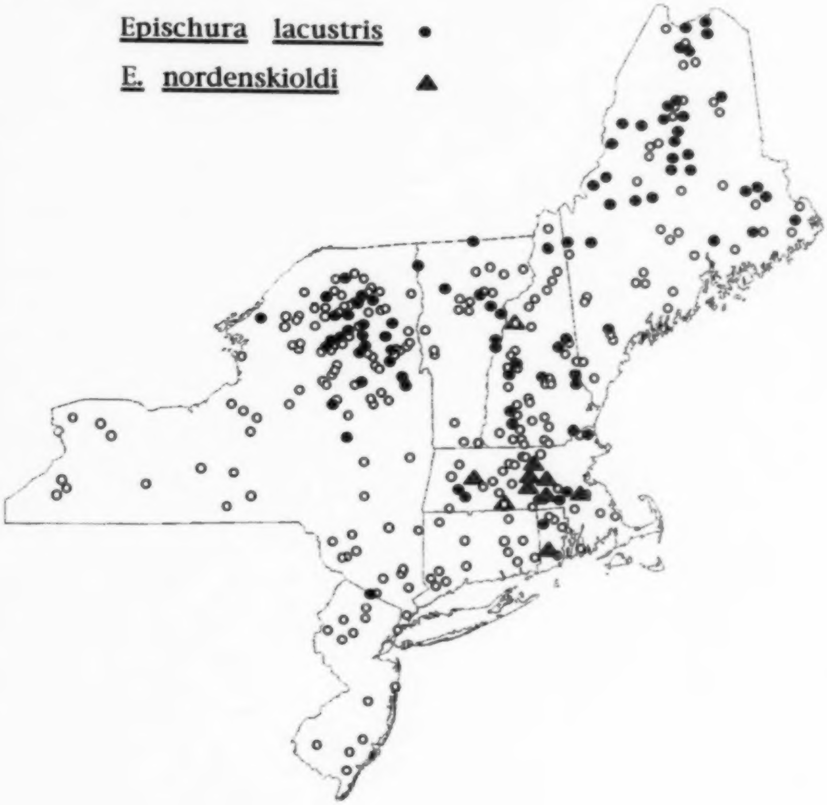

Dispersal from Atlantic Coastal Plain refuge areas

(*i*) Ice-sheet retreat began around 19 000 – 16 000 years ago (Muller and Calkin 1993; Davis and Jacobson 1985). Zooplankton began to disperse northward in ice-front lakes near their refuge areas in the Appalachian Plateaus and Georges Bank (Fig. 2).

(*ii*) Formation of early Lake Hitchcock began around 15 600 years ago (Ridge and Larsen 1990).

(*iii*) Eustatic rise in sea level and continued isostatic depression along the eastern Atlantic coast resulted in a major seawater inundation of coastal Maine. Seawater was in contact with the receding glacier margin across southern Maine from about 14 000 – 13 000 years ago (Davis and Jacobson 1985). Hence, copepod dispersal into interior Maine from the Georges Bank refuge area could not yet occur. However, at this time (13 000 years ago) Vermont and New Hampshire were largely ice free so that dispersal of copepods into the Appalachian foothills had probably already taken place.

(*iv*) The Maine coast reemerged by 11 000 years ago. Although ice remained in northeastern Maine it had melted from the rest of New England (Davis and Jacobson 1985). During the period from 13 000 – 12 000 years ago the ice sheet retreated in Maine in a northerly direction. The southern margin of the ice sheet now lay inland from the zone of marine incursion (Fig. 2). The retreat could have transported zooplankton into the lowland areas and lower elevations of the southern portions of the Appalachian Mountains in central and northern Maine from the Georges Bank refuge. Species from the Sable Island Banks refuge colonized Nova Scotia, New Brunswick, and perhaps parts of eastern Maine.

Dispersal from the Mississippian refuge area

(*i*) In western New York the St. Lawrence drainage emptied into the Mohawk River and glacial lakes of the Hudson River basin 13 600 – 12 000 years ago (Bailey and Smith 1981). This route provided the first opportunity for Mississippian refuge species to enter the region.

(*ii*) Lake Winooski in central Vermont drained into the Connecticut River Valley occupied by Lake Hitchcock 13 400 – 13 000 years ago (Larsen 1987*a*). However, there was no drainage connection between the St. Lawrence basin and Lake Hitchcock via Lake Vermont. Hence, Mississippian refuge species using surface water dispersal could not enter lakes of central Vermont and those of the Connecticut River basin.

Fig. 6. Distribution of *Leptodiaptomus minutus* in the northeastern United States. Solid circles indicate lakes where the species was observed and open circles indicate lakes where it was not observed.

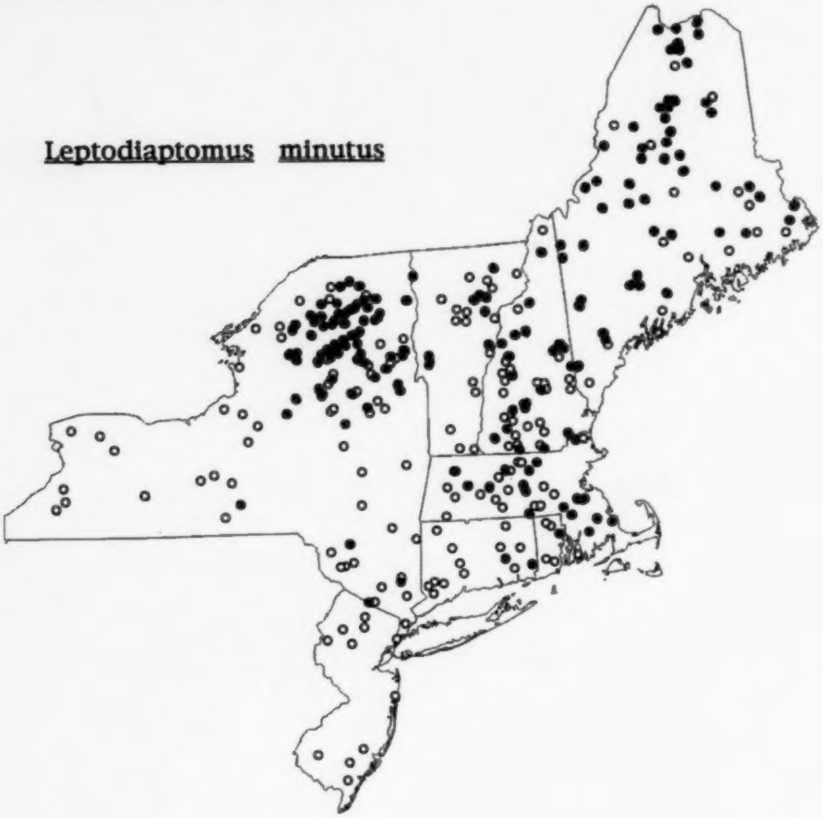

(*iii*) Lake Hitchcock drained from a breaching of the drift dam near New Britain, Connecticut, around 12 400 years ago (Ridge and Larsen 1990).

(*iv*) The Mohawk River outlet of glacial Lake Ontario ended and a northern connection with the St. Lawrence drainage (glacial Lake Iroquois) and Lake Vermont (glacial Lake Belleview – Fort Ann) was established around 12 000 years ago (Mandrak and Crossman 1992; Dadswell 1974). This connection probably resulted in the second major entry of Mississippian dispersants into the Lake Champlain – Hudson River drainage system of New York and Vermont.

(*v*) The collapse of the ice dam near Quebec City in the St. Lawrence lowlands resulted in a marine incursion that formed the Champlain Sea that extended into the Champlain Valley of former Lake Vermont from about 12 500 – 10 000 years ago (Larsen 1987*b*; Dadswell 1974). The event was probably catastrophic to most freshwater life.

(*vi*) Glacial Lake Champlain developed a new freshwater connection with the St. Lawrence River via Lampsilis Lake to the north by about 10 500 – 10 000 years ago (Underhill 1986). This connection probably provided the last major opportunity for dispersal of Mississippian fauna into the region during the late Pleistocene.

(*vii*) The modern configuration of the eastern St. Lawrence Great Lakes and the aquatic landscape of the northeast was established by 9000–3900 years ago (Bailey and Smith 1981; Davis and Jacobson 1985; Underhill 1986).

Dispersal routes from refuge areas

Arguments for a northern Atlantic Coastal Plain refuge have been proposed on the basis of the biogeography of fishes (Crossman and McAllister 1986; Underhill 1986). Genetic studies on yellow perch (*Perca flavescens*) and lake whitefish (*Coregonus clupeaformis*) provide additional evidence for coastal plain refugia during the Pleistocene (Bernatchez and Dodson 1990, 1991; Todd and Hatcher 1993). The largely nonoverlapping species distributions represented by *Skistodiaptomus* spp. are consistent with the major glacial drainage systems of the St. Lawrence basin, Appalachian Plateaus, and Georges Bank. The boundaries of these species' ranges provide evidence for the dispersal routes by which species entered the region from

Fig. 7. Distribution of *Mesocyclops edax* in the northeastern United States. Solid circles indicate lakes where the species was observed and open circles indicate lakes where it was not observed.

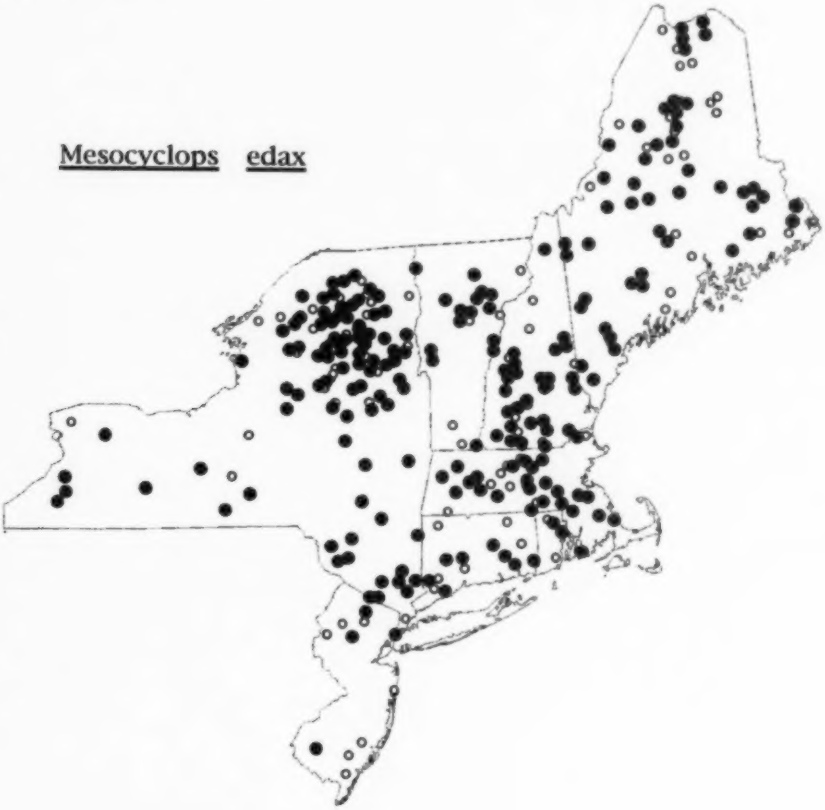

refuge areas. The eastern portion of the region was colonized by species such as *S. pygmaeus* and *Epischura nordenskioldi* that most likely originated in refugia in northerly locations on the Atlantic Coastal Plain of the Continental Shelf. A southern refuge, characterized by dispersal of *S. pallidus*, was probably located on the Appalachian Plateaus or on the coastal plain off southern Virginia or North Carolina as has been postulated for fishes of this region (Schmidt 1986). *Skistodiaptomus pallidus* may also have survived in a Mississippian refuge because it presently occurs in the Mississippi Valley and in plains states south to Texas and Louisiana and has been recently reported in the Laurentian Great Lakes (Mills et al. 1993). The species has not dispersed north of the Mohawk Valley into the Adirondack region, although we observed it in a lake in the Adirondack region and in wildlife impoundments in western New York in the Lake Ontario drainage and in eastern Vermont (Fig. 3).

Skistodiaptomus pallidus and *S. pygmaeus* must have colonized from their respective refuge areas by moving northward in retreating ice-front lakes that formed pools, ice-block lakes, and anastomosing lake systems behind them (Stone and Peper 1980). Isostatic rebound of the continental landmass would have helped to isolate ponds and lakes from further colonization by surface water dispersal.

Drainage connections of the Hudson River and Champlain valleys

Colonization by species from the Mississippian refuge area was fundamentally different from that by species arriving from the Appalachian Plateaus or Atlantic Coastal Plain. Here, aquatic species resident in the refuge areas of the Mississippi Valley were transported great distances eastward in the St. Lawrence basin (Prest 1970; Bailey and Smith 1981). Colonizing populations entered the region to the west in the Mohawk River outlet that drained the various glacial lake stages of present-day Lake Ontario (Bailey and Smith 1981) (Fig. 2). Later in the deglaciation these species could have also moved from the western regions of the continent into waterways that connected northern inlets of the St. Lawrence River to Lake Lampsilis (present-day Lake Champlain) to the Hudson River. Earlier in the deglaciation chronology, Mississippian zooplankton could have entered Lake Albany or Lake Vermont from the western Great Lakes through the Mohawk River outlet and then been transported south along the Hudson River Valley

Fig. 8. Distribution of species *Aglaodiaptomus* and *Onychodiatomus* in the northeastern United States. Solid circles, *A. spatulocrenatus*; shaded squares, O. *sanguineus*; solid triangles, *A. leptopus*. Open circles indicate lakes where the species were not observed.

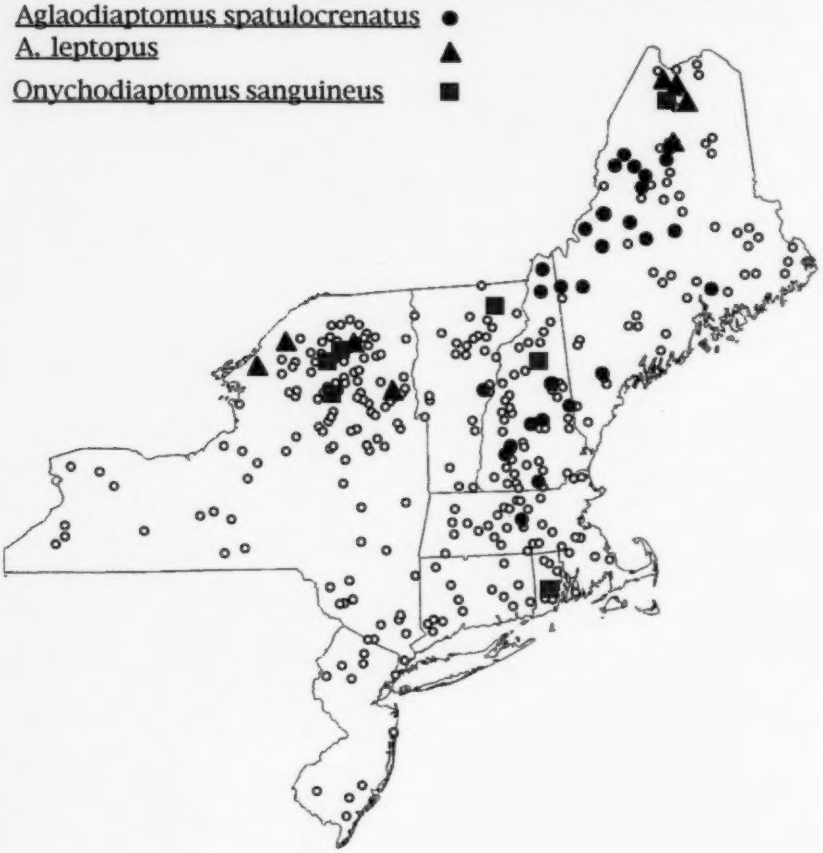
Aglaodiaptomus spatulocrenatus ●
A. leptopus ▲
Onychodiaptomus sanguineus ■

(Mandrak and Crossman 1992; Crossman and McAllister 1986; Underhill 1986).

Drainage connections east of the Hudson River and Champlain valleys

The dispersal route taken by *D. thomasi* and *S. oregonensis* into southern locations in the Connecticut River drainage is not established. The early postglacial Connecticut River drainage received the outflow from glacial Lake Winooski in north central Vermont through an early outlet near Williamstown, Vermont (Larsen 1987*a*, 1987*b*). This spillway fed into the impounded Connecticut River known as glacial Lake Hitchcock that extended into central Connecticut (Fig. 2). Glacial Lake Winooski (~13 000 years ago) may not have been confluent with Lake Vermont located just to the west in the Champlain Valley because the ice front would have prevented drainage to the east (Larsen 1987*a*). I sampled five lakes in the central and eastern portions of the Lake Winooski basin and did not find either *D. thomasi* or *S. oregonensis*. However, *D. thomasi* was present in Waterbury Reservoir near Waterbury, Vermont, marking the easternmost extension of Lake Vermont (Fig. 4) (Larsen 1987*b*). Although Lake Winooski may have received drainage from early stages of glacial Lake Memphremagog to the north there was no connection with the St. Lawrence basin because of the ice-sheet barrier to the west and north (Steward and MacClintock 1969). Support for this route is further diminished because I found no western refugial species in the Lake Winooski basin. Hence, another explanation for the presence of *D. thomasi* and *S. oregonensis* in the lower Connecticut River Valley is required (Figs. 3 and 4). Had these species resided in the Georges Bank refuge we would expect them to be more common in lakes of southern New England, unless they went extinct in most of the lakes over their former range. Alternatively, these records may indicate inadvertent introductions by humans across postglacial zoogeographic boundaries.

Copepod disjunctions

Carter et al. (1980) reported *D. thomasi* in Green Lake, Maine, east of the Penobscot River near the Atlantic coast. This record is not consistent with my interpretation of the

Table 1. The total number of lakes in the northeastern United States where copepod species were present and the number of lakes and percentages of cooccurrence (%) of these copepods in the geographic provinces of *Skistodiaptomus* spp.

Taxon	Total lakes	*S. pygmaeus* No.	*S. pygmaeus* %	*S. oregonensis* No.	*S. oregonensis* %	*S. pallidus* No.	*S. pallidus* %
Lakes having *Skistodiaptomus* spp.		62		32		23	
Aglaodiaptomus spatulocrenatus	25	8	12.9	0	0	0	0
Aglaodiaptomus leptopus	6	0	0	0	0	0	0
Onychodiaptomus sanguineus	8	4	6.5	1	3.3	0	0
Leptodiaptomus minutus	155	35	58.1	16	50.0	1	4.5
Epischura lacustris	62	16	27.4	8	25.0	0	0
Epischura nordenskioldi	13	7	11.3	0	0	0	0
Mesocyclops edax	207	61	98.4	25	78.1	19	82.6
Tropocyclops extensus	159	38	65.5	13	43.3	12	70.6
Acanthocyclops robustus	69	11	17.7	6	18.8	8	34.8
Cyclops scutifer	40	7	11.3	5	15.6	1	4.3
Orthocyclops modestus	50	11	17.7	10	31.2	3	13.0
Diacyclops thomasi	26	3	9.4	5	15.6	1	4.3

Note: Value under species column is the number of lakes where the two species cooccurred. Data are on 378 samples representing 319 lakes.

dispersal route and refuge area for the species. I examined 10 samples from various locations in Green Lake that were collected during the spring and summer of 1994. However, *D. thomasi* was not found. Carter et al. (1980) also reported *Eubosmina coregoni* from Green Lake, where I did not find it. This species occurred only in lakes with former or present-day connections with the Great Lakes drainage (R.S. Stemberger, unpublished data). I conclude that these records are probably in error and may represent mislabeled samples or contaminated nets from a lake in the Great Lakes drainage. These species also were absent from all lakes that were examined in Maine, further diminishing the likelihood of this record.

The disjunction of *Epischura nordenskioldi* in Nova Scotia and in southern New England is consistent with colonization from two northeastern refuge areas located on the Georges Bank and another on a more northerly location such as the Sable Island Banks or Grand Banks. This species produces a dormant egg bank in bottom sediments (De Stasio 1990). However, there is little indication that it has dispersed very widely in the region. This raises the possibility that its historical ice-age dispersers may no longer be present in the region. It has a distribution similar to that of some northern Appalachian fishes that are postulated to have come from these same upland coastal plain refugia (Fig. 5) (Schmidt 1986).

The presence of *S. oregonensis* and *D. thomasi* in higher elevation lakes of the Adirondack Mountains also suggests secondary introductions through human activities. The presence of *S. pallidus* in an Adirondack lake as well as in several impoundments outside of its zoogeographic province provides circumstantial evidence for inadvertent waterborne transfer of active stages or eggs through human activities. Alternatively, these species may have dispersal stages that are only marginally effective at being transported by animals and therefore have exceedingly low rates of dispersal.

Distributions at drainage boundaries

In the retreat of the ice sheet in southern Maine, eustatic rise in the sea level and continued isostatic depression resulted in a marine submergence of coastal lowlands (Figs. 2 and 3). Only after reemergence of the land through isostatic rebound was colonization possible by freshwater zooplankton. Colonization by surface-water dispersants would have come from drainages of lakes above the submergence zone. Of the 18 lakes that were sampled in and around this zone, only 1 lake having *S. pygmaeus* did not have a direct upstream connection to a source lake with the species (Fig. 3). Lakes in the submergence zone lacking *S. pygmaeus* had opportunist species like *Aglaodiaptomus spatulocrenatus* or *L. minutus* as the dominant calanoid copepods, a pattern repeated for upland areas where *S. pygmaeus* is absent (Figs. 2, 3, 6, and 8).

Some large deep lakes like Lake Willoughby (650 ha, 100 m deep) near the northern physiographic boundary of the Atlantic and Mississippian – St. Lawrence drainage in northern Vermont have the conditions to support the glacial marine relict fauna but lack the assemblage altogether (Dadswell 1974; R.S. Stemberger, unpublished data) (Figs. 1, 3, and 8). *Skistodiaptomus pygmaeus* apparently never reached this lake on the northeastern slopes of the Green Mountains just 40 km south of the Canadian border. The White Mountains to the southeast of Lake Willoughby presented a dispersal barrier for this species. Instead, *Onychodiaptomus sanguineus* is a dominant calanoid of this large, deep oligotrophic lake. The species frequently inhabits ponds and produces a dormant egg bank in sediments (De Stasio 1990; Hairston et al. 1990). Therefore, it may be effective at dispersing using animal carriers. Just 16 km north of Lake Willoughby in northern Vermont, Lake Memphremagog, situated on the St. Lawrence lowlands and hence influenced by the Great Lakes drainage, contains all the western refugial species including the glacial marine relict taxa (Dadswell 1974; Carter et al. 1980).

Implications for genetics of surface-water dispersants

That some species have apparently remained within their postglacial dispersal boundaries to the present day strongly supports their lack of ability to disperse. This limitation implies that founding populations have likely persisted in these lakes since their arrival 10 000 – 15 000 years ago and that local immigration in *Skistodiaptomus* spp. and *D. thomasi* is probably limited to contact between drainages. Disjunctions of *Skistodiaptomus* spp. seem to be associated with man-made impoundments and lakes affected by other cultural activities. Therefore, barring such exceptions, information on the genetic characteristics of populations might be used to map more precisely the location and, perhaps, the number of refuge sites during the maximum advance of the Wisconsinan ice sheet. If populations with restricted distributions like *S. pygmaeus* have experienced genetic drift or microevolution, then lake populations might be expected to show a high among-lake variance in genetic markers. *Skistodiaptomus pygmaeus* may be especially relevant in the identification of potential refuge locations along the Atlantic Coastal Plain. Evidence for these refuge areas might be found within the watersheds delineated by present-day rivers flowing into the Atlantic Ocean. If isolated refuge lakes occurred within such drainage boundaries, then the assemblages might have coalesced into the lake systems formed behind retreating ice-front lakes, and a minimum number of refuge locations might still be detectable. Genetic markers might also provide support for the influence of the Sable Island Banks refuge in eastern Maine and for a Grand Banks refuge off Newfoundland. A genetic comparison of populations of *Epischura nordenskioldi* from southern New England and Nova Scotia might provide further support for a Sable Island Banks refuge. Also, it should be possible to determine if widely distributed species such as *Epischura lacustris* have genetically distinct populations that correspond to several Pleistocene refuge areas.

Increasing human activities in lakes of the region may be responsible for the occurrences of species of *Skistodiaptomus* and *Diacyclops* outside their zoogeographical provinces. If humans are transporting zooplankton then genetic markers could help identify the geographic areas from which founding populations arrived. Finally, closely related taxa like *S. oregonensis* and *S. pygmaeus* probably diverged sometime during the last ice age. DNA studies of nucleotide substitutions could provide estimates of the time of isolation and divergence.

Copepod dispersal strategies

Dispersal mechanisms of copepods are poorly known but can be inferred from regional patterns in species distributions. Present-day distributions of *Skistodiaptomus* and *Diacyclops* species indicate that they were dispersed by retreating ice-front lakes and meltwater drainage systems. These species are largely absent from high-elevation lakes and lowland areas behind mountain barriers where cols and higher passes blocked the passage of retreating ice-front lakes. In contrast, other species of copepods are widely distributed and occur in high-elevation lakes, indicating that they have effective dispersal mechanisms that are not correlated with surface-water drainage connections. A major disadvantage for species using surface-water dispersal is their inability to colonize lakes at high elevations and those behind mountain ranges. They are also unlikely to recolonize lakes after local extinction. In this regard they share strong similarities with the dispersal limitations of glacial marine relict species (Stemberger 1995).

It seems likely that opportunistic species of calanoid copepods also arrived in lakes with *Skistodiaptomus* spp. and that they probably successfully immigrate regularly to lakes having *Skistodiaptomus* spp. However, they do not commonly cooccur, suggesting that members of genera such as *Aglaodiaptomus* and *Onychodiaptomus* may be inferior competitors or vulnerable to fish predation (Table 1). These species are common in small perennial and temporary ponds where insects may be their primary predators.

Transport of resting stages by animals may explain the wide distribution of some species. Resting stages of algae and crustaceans may survive ingestion and gut passage in waterfowl and shorebirds (Proctor 1959, 1964) and subitaneous eggs of copepods can survive gut passage in fish (Redden and Daborn 1991). The transport of dormant eggs on the fur, feathers, or legs of mammals and birds seems less probable because eggs in the bottom sediments may not easily come in contact with body surfaces. However, studies suggest that algae and protozoans may disperse in this way (Maguire 1963). Dispersal on animal surfaces might be effective when dormant stages float and become concentrated at lake margins as is sometimes observed for the ephippia of cladocerans. Even in species where resting stages have been documented, as in *Epischura nordenskioldi*, species may not be widely distributed. Such species may have coevolved with animal dispersers that no longer exist. For example, many mammals and birds that would have visited lakes and ponds during the Pleistocene have either disappeared from the region or are now extinct.

Conclusions

I draw a number of conclusions from this study of freshwater copepod biogeography. Previous studies have shown that the distribution of glacial marine relict species is limited to deep cold-water lakes in the former basins of proglacial lakes and their drainages (Dadswell 1974; Carter et al. 1980; Stemberger 1995). This study expands that pattern to include eurythermal copepods that are not limited to deep cold-water systems. Their present-day distribution indicates their likely postglacial dispersal routes from Pleistocene refuge areas. Some common species appear to disperse using surface-water transport and, therefore, as with the glacial marine relict species, are dependent on long-term climatic events that occur over geological time scales. Dispersal-limited species also appear either to be superior competitors or to have mechanisms that allow them to coexist with fish predators. They infrequently cooccur with opportunistic congeners that are often present in fishless systems. Hence, among the calanoid copepods in this study, there may be a trade-off between dispersal and competitive ability and the ability to persist with fish predation.

Populations of dispersal-limited species may be vulnerable to local extinction, and the monitoring of these species provides valuable information about long-term environmental changes. Inadvertent introductions of species requiring surface-water dispersal may be accelerating because of increasing human activities on lakes. Watercraft, bilges, live wells, motors, trailers, bait fisherman, and fish stocking programs may transport species to lakes they could not otherwise reach.

The absence of species in a large portion of lakes within their geographical provinces indicates that they either did not reach all the available habitats or have gone extinct from individual lakes. Elevation barriers and marine submergence of coastal lowlands account in part for the absence of species dependent on surface-water dispersal. Lakes in these areas are likely to have opportunistic species of copepods such as *L. minutus*, *O. sanguineus*, *Aglaodiaptomus spatulocrenatus* or *Aglaodiaptomus leptopus*, *M. edax*, and *Tropocyclops extensus*. *Aglaodiaptomus leptopus* sometimes achieves large body sizes (2.5 mm) and tends to occur in lowland ponds and lakes at high elevations without fish. High-elevation fishless habitats are shrinking because of fish stocking programs targeting remote mountain areas of the northeast.

Copepods from other regions of North America are also known to have low dispersal rates (Hebert and Hann 1986; Boileau and Hebert 1991). The present study provides a plausible explanation for why these species have restricted geographic distributions. The Arctic copepods that survived in the Beringian Refuge were never in direct contact with the ice-front lakes that formed along the southern margins of the ice sheet. Consequently, these species were unable to disperse from their Pleistocene refuge locations despite the disappearance of the ice sheet from the continent.

The absence of the glacial marine relict assemblage in eastern New England and in Nova Scotia and New Brunswick also suggests that this assemblage either did not have or did not survive in a Pleistocene refuge on the Atlantic Coastal Plain. The assemblage arrived in the region from the Mississippian refuge area and is present in Lake Champlain and in several small lakes in the Champlain Valley, in the Finger Lakes of New York, and throughout most of the St. Lawrence Great Lakes (Dadswell 1974) (Figs. 1 and 2). This assemblage probably occurred throughout the glacial lake systems in the Hudson River Valley during the early Holocene so the present-day distribution may represent a northward contraction in their ranges. The geographic fidelity that the water-dispersing species show with specific drainage systems should provide a useful tool for interpreting local drainage relationships that were established during deglaciation.

Finally, the varying dispersal abilities of copepods provide a dynamic framework for viewing the role of ponds and wetlands as sources of species that colonize larger lakes. Although small ponds (<1 ha) and wetlands are excluded from the EMAP-SW, these very common habitats occur in a mosaic within the landscape of larger lakes where dispersal-limited species occur. Their dispersal mechanisms allow them to invade new habitats that water-dispersing species cannot reach and allow them to colonize lakes where local extinctions of water-dispersing congenors or fish predators have created favorable conditions for their survival.

Acknowledgments

This study was supported by Environmental Protection Agency cooperative agreement CR 819689-01. I thank A.T. Packard and Marilyn Racine for their careful work on zooplankton identification and enumeration. A.T. Packard collected samples from Green Lake, Maine, and from high-elevation lakes in the Presidential Range of the White Mountains, New Hampshire. She assisted with verification and validation of species identifications and helped with the species distribution maps. Barb Rosenbaum produced the Geographical Information Systems elevation contour map. The comments of C.E. Williamson, M.A. McPeek, D.P. Larsen, R.M. Hughes, P.D.N Hebert, and those of an anonymous reviewer improved the manuscript. Woody Thompson of the Maine Geological Survey provided helpful comments and information on the deglaciation chronology. I thank Steve Paulsen, technical director of EMAP-SW, for his support of this project.

References

Bailey, R.M., and G.R. Smith. 1981. Origin and geography of the fish fauna of the Laurentian Great Lakes Basin. Can. J. Fish. Aquat. Sci. 38: 1539–1561.

Bernatchez, L., and J.J. Dodson. 1990. Allopatric origin of sympatric populations of lake whitefish (*Coregonus clupeaformis*) as revealed by mitochondrial-DNA restriction analysis. Evolution, 44: 1263–1271.

Bernatchez, L., and J.J. Dodson. 1991. Phylogeographic structure in mitichondrial DNA of lake whitefish (*Coregonus clupeaformis*) and its relation to Pleistocene glaciations. Evolution, 45: 1016–1035.

Billington, N., and P.D.N. Hebert. 1988. Mitochondrial DNA variation in Great Lakes walleye (*Stizostedion vitreum*) populations. Can. J. Fish. Aquat. Sci. 45: 643–654.

Boileau, M.C., and P.D.N. Hebert. 1991. Genetic consequences of passive dispersal in pond-dwelling copepods. Evolution, 45: 721–733.

Brooks, J.L. 1957. The systematics of North American *Daphnia*. Mem. Conn. Acad. Arts Sci. 13. pp. 1–180.

Carter, J.C.H., M.J. Dadswell, J.C. Roff, and W.G. Sprules. 1980. Distribution and zoogeography of planktonic crustaceans and dipterans in glaciated eastern North America. Can. J. Zool. 58: 1355–1387.

Crossman, E.J., and D.E. McAllister. 1986. Zoogeography of freshwater fishes of the Hudson Bay drainage, Ungava Bay and the Arctic Archipelago. *In* The zoogeography of North American freshwater fishes. *Edited by* C.H. Hocutt and E.O. Wiley. John Wiley & Sons, New York. pp. 53–104.

Dadswell, M.J. 1974. Distribution, ecology, and postglacial dispersal of certain crustaceans and fishes in eastern North America. *In* Publications in zoology. No. 11. National Museums of Canada, Ottawa, Ont.

Davis, R.B., and G.L. Jacobson, Jr. 1985. Late Glacial and early Holocene landscapes in northern New England and adjacent areas of Canada. Quat. Res. 23: 341–368.

De Stasio, B. 1990. The role of dormancy and emergence patterns in the dynamics of a freshwater zooplankton community. Limnol. Oceanogr. 35: 1079–1090.

Dineen, R.J., D.J. DeSimone, E.L. Hanson, R.E. Funk, D.W. Steadman, and E.H. Jokinen. 1988. Glacial Lake Albany and its successors in the Hudson lowlands. *In* Field trip guidebook AMQUA 1988. *Edited by* J. Brigham-Grette. Contrib. No. 63. Department of Geology and Geography, University of Massachusetts, Amherst, Mass. pp. 1–60.

Hairston, N.G., Jr., T.A. Dillon, and B.T. De Stasio, Jr. 1990. A field test of the cues of diapause in a freshwater copepod. Ecology, 71: 2218–2223.

Hebert, P.D.N., and B.J. Hann. 1986. Patterns in the composition of Arctic tundra pond microcrustacean communities. Can. J. Fish. Aquat. Sci. 43: 1416–1425.

Hocutt, C.H., and E.O. Wiley. (*Editors*). 1986. The zoogeography of North American freshwater fishes. John Wiley & Sons, New York.

Hocutt, C.H., R.E. Jenkins, and J.R. Stauffer, Jr. 1986. Zoogeography of the fishes of the central Appalachians and central Atlantic Coastal Plain. *In* The zoogeography of North American freshwater fishes. *Edited by* C.H. Hocutt and E.O. Wiley. John Wiley & Sons, New York. pp. 161–211.

Larsen, F.D. 1987*a*. History of glacial lakes in the Dog River Valley, central Vermont. *In* Guidebook for Field Trips in Vermont. Proceedings of the 79th New England Intercollegiate Geological Conference, Montpelier, Vt., October 16–18, 1987. Vol. 2. *Edited by* D.S. Westerman. pp. 213–236.

Larsen, F.D. 1987*b*. Glacial Lake Hitchcock in the valleys of the White and Ottauquechee Rivers, east-central Vermont. *In* Guidebook for Field Trips in Vermont. Proceedings of the 79th New England Intercollegiate Geological Conference, Montpelier, Vt., October 16–18, 1987. Vol. 2. *Edited by* D.S. Westerman. pp. 30–52.

Larsen, D.P., and S.J. Christie. 1993. Surface waters 1991 pilot report. EPA/620/R-93/003. U.S. Environmental Protection Agency, Cincinnati, Ohio.

Larson, G.J. 1980. Late Wisconsin glaciation of New England. *In* Late Wisconsinan glaciation of New England. *Edited by* G.J. Larson and B.D. Stone. Kendall/Hunt Publishing Co., Dubuque, Iowa. pp. 101–114.

Maguire, B., Jr. 1963. The passive dispersal of small aquatic organisms and their colonization of isolated water bodies. Ecol. Monogr. 33: 161–185.

Mandrak, N.E., and E.J. Crossman. 1992. Postglacial dispersal of freshwater fishes into Ontario. Can. J. Zool. 70: 2247–2259.

Mills, E.L., J.H. Leach, J.T. Carlton, and C.L. Secor. 1993. Exotic species in the Great Lakes: a history of biotic crises and anthropogenic introductions. J. Great Lakes Res. 19: 1–54.

Muller, E.H., and P.E. Calkin. 1993. Timing of Pleistocene glacial events in New York State. Can. J. Earth Sci. 30: 1829–1845.

Paulsen, S.G., D.P. Larsen, P. Kaufman, T.R. Whittier, J.R. Baker, D.V. Peck, J. McGue, R.M. Hughes, D. McMullen, D. Stevens, J.L. Stoddard, J.M. Lazorchak, W. Kinney, A.R. Selle, and R. Hjort. 1991. EMAP-surface waters monitoring and research strategy fiscal year 1991. EPA/600/3-91/022. U.S. Environmental Protection Agency, Corvallis, Oreg.

Prest, V.K. 1970. Quaternary geology of Canada. *In* Geology and economic minerals of Canada. *Edited by* R.J.W. Douglass. Econ. Geol. Rep. (Geol. Surv. Can.). No. 1. pp. 676–764.

Proctor, V.W. 1959. Dispersal of fresh-water algae by migratory water birds. Science (Washington, D.C.), 130: 623–624.

Proctor, V.W. 1964. Viability of crustacean eggs recovered from ducks. Ecology, 45: 656–658.

Redden, A.M., and G.R. Daborn. 1991. Viability of subitaneous copepod eggs following fish predation on egg-carrying calanoids. Mar. Ecol. Prog. Ser. 77: 307–310.

Ridge, J.C., and F.D. Larsen. 1990. Re-evaluation of Antev's New England varve chronology and new radiocarbon dates of sediments from glacial Lake Hitchcock. Geol. Soc. Am. Bull. 102: 889–899.

Schmidt, R.E. 1986. Zoogeography of the northern Appalachians. *In* The zoogeography of North American freshwater fishes. *Edited by* C.H. Hocutt and E.O. Wiley. John Wiley & Sons, New York. pp. 137–159.

Segerstrale, S.G. 1976. Proglacial lakes and the dispersal of glacial relicts. Commentat. Biol. 83.

Stemberger, R.S. 1995. The influence of mixing on rotifer assemblages of Michigan lakes. Hydrobiologia, 297: 149–161.

Stemberger, R.S., and J.M. Lazorchak. 1994. Zooplankton assemblage responses to disturbance gradients. Can. J. Fish. Aquat. Sci. 51: 2435–2447.

Steward, D.P., and P. MacClintock. 1969. The surficial geology and Pleistocene history of Vermont. Bull. Vt. Geol. Surv. No. 31.

Stone, B.D., and J.D. Peper. 1980. Topographic control of the late deglaciation of eastern Massachusetts: ice lobation and the marine incursion. *In* Late Wisconsinan glaciation of New England. *Edited by* G.J. Larson and B.D. Stone. Kendall/Hunt Publishing Co., Dubuque, Iowa. pp. 145–166.

Thompson, W.B. 1980. Recession of the late Wisconsinan ice sheet in coastal Maine. *In* Late Wisconsinan glaciation of New England. *Edited by* G.J. Larson and B.D. Stone. Kendall/Hunt Publishing Co., Dubuque, Iowa. pp. 211–228.

Todd, T.N., and C.O. Hatcher. 1993. Genetic variability and glacial origins of yellow perch (*Perca flavescens*) in North America. Can. J. Fish. Aquat. Sci. 50: 1828–1834.

Underhill, J.C. 1986. The fish fauna of the Laurentian Great Lakes, the St. Lawrence lowlands, Newfoundland and Laborador. *In* The zoogeography of North American freshwater fishes. *Edited by* C.H. Hocutt and E.O. Wiley. John Wiley & Sons, New York. pp. 105–160.

Wilson, M.S., and H.C. Yeatman. 1959. Free-living copepoda. *In* Fresh-water biology. 2nd ed. *Edited by* W.T. Edmondson. Wiley, New York. pp. 735–794.

Yeatman, H.C. 1959. Cyclopoida. *In* Fresh-water biology. 2nd ed. *Edited by* W.T. Edmondson. Wiley, New York. pp. 795–815.

Introduction to contaminants research at the Experimental Lakes Area

D.M. Rosenberg, R.E. Hecky, and P. Campbell

The previous two sets of papers honouring the 25th anniversary of the Experimental Lakes Area (ELA) dealt with studies of eutrophication (Hecky et al. 1994*a*) and natural processes (Hecky et al. 1994*b*). This final set of seven papers concerns contaminants research that has been ongoing at the ELA since the mid-1970s. Early studies at the ELA focussed on the ecological effects of acidification (e.g., Kennedy 1980; Malley 1980; Müller 1980; Schindler et al. 1980*b*; Kelly et al. 1982), metals (e.g., Brunskill et al. 1980; Furutani and Rudd 1980; Marshall et al. 1981), radionuclides as tracers for metals (see below), or combinations of these (e.g., Schindler et al. 1980*a*). These classes of contaminants continue to be studied, as exemplified by the papers in this series (see also Malley 1996 for details of the Lake 382 cadmium experiment).

The five papers devoted to acidification research in this series properly emphasize the strong tradition of acidification research at the ELA. Most of the past research was aimed at understanding the effects of acidification on the structure and function of the pelagic zone (e.g., Schindler et al. 1985). In this issue, Turner et al. (1995*a*, 1995*b*, 1995*c*) continue earlier studies of acidification effects on littoral communities (e.g., Müller 1980; Turner et al. 1987, 1991; Howell et al. 1990). Turner et al. (1995*c*) reveal substantial differences in responses to acidification between pelagic and littoral foodwebs; Turner et al. (1995*b*) demonstrate the importance of the ecosystem approach to understanding the complex and indirect effects of contaminants; and Turner et al. (1995*a*) provide knowledge that will be important in developing controls for nuisance filamentous green algae in the shallow waters of acidified lakes.

Recognition of the interconnections between the terrestrial and aquatic parts of catchments led to acidification research in wetland and upland areas of the ELA (e.g., Bayley et al. 1987; Rochefort et al. 1990). Two papers here further extend the research on the effects of terrestrial acidification. Allan (1995) describes responses to acidification and fertilization of soils and runoff in two ELA catchments. Rosenberg et al. (1995) examine responses of the Chironomidae (midge flies) to acidification of the Lake 239 fen, site of the original wetland acidification experiment (Bayley et al. 1987).

One paper in the set deals with metal toxicity. Bird et al.'s (1995*a*) biomonitoring study attempts to detect cadmium stress by examining the incidence of morphological deformities in the menta of chironomid larvae. Several past papers devoted to biomonitoring at various spatial and temporal scales have appeared under the ELA imprimatur (e.g., Schindler et al. 1985; Schindler 1987; Malley et al. 1993; Palace and Klaverkamp 1993), and the ELA is currently part of a national acidification monitoring network (Shaw et al. 1995). These past and present research efforts indicate the growing importance of biomonitoring in contaminants research at the ELA.

Finally, in this issue Bird et al. (1995*b*) examine the fate of metal radiotracers added to the hypolimnion of Lake 226 to simulate possible effects of nuclear fuel waste disposal on the aquatic environment. The experimental use of metal radiotracers at the ELA has become a valuable technique for following lake processes and metal dynamics in lakes (e.g., Emerson and Hesslein 1973; Hesslein et al. 1980; Klaverkamp et al. 1983; Santschi et al. 1986; Anderson et al. 1987; Playle 1987; Malley et al. 1989).

The seven papers in this set represent a bridge between past and future contaminants research at the ELA; some are clearly derivatives made possible by earlier ELA work. Practical applications of the results are considered to varying degrees in each paper. The ultimate goal of contaminants research at the ELA is to provide sufficient understanding of the effects of contaminants at the whole-ecosystem level to enable the design of mitigation programs and effective management of toxic pollutants in the environment.

Received August 8, 1995. Accepted August 17, 1995.
J13042

D.M. Rosenberg, R.E. Hecky, and P. Campbell.
Department of Fisheries and Oceans, Freshwater Institute,
501 University Crescent, Winnipeg, MB R3T 2N6,
Canada.

References

Allan, C.J. 1995. Hydrochemical response of upland Precambrian Shield catchments to additions of H_2SO_4 and NH_4NO_3 during snowmelt. Can. J. Fish. Aquat. Sci. 52: 2213–2228.

Anderson, R.F., P.H. Santschi, U.P. Nyffeler, and S.L. Schiff. 1987. Validating the use of radiotracers as analogs of stable metal behaviour in enclosed aquatic ecosystem experiments. Can. J. Fish. Aquat. Sci. 44(Suppl. 1): 251–259.

Bayley, S.E., D.H. Vitt, R.W. Newbury, K.G. Beaty, R. Behr, and C. Miller. 1987. Experimental acidification of a *Sphagnum*-dominated peatland: first year results. Can. J. Fish. Aquat. Sci. 44(Suppl. 1): 194–205.

Bird, G.A., M.J. Rosentreter, and W.J. Schwartz. 1995*a*. Deformities in the menta of chironomid larvae from the Experimental Lakes Area, Ontario. Can. J. Fish. Aquat. Sci. 52: 2290–2295.

Bird, G.A., M. Stephenson, R. Roshon, W.J. Schwartz, and M. Motycka. 1995*b*. Fate of ^{60}Co and ^{134}Cs added to the hypolimnion of a Canadian Shield lake. Can. J. Fish. Aquat. Sci. 52: 2276–2289.

Brunskill, G.J., B.W. Graham, and J.W.M. Rudd. 1980. Experimental studies on the effect of arsenic on microbial degradation of organic matter and algal growth. Can. J. Fish. Aquat. Sci. 37: 415–423.

Emerson, S., and R. Hesslein. 1973. Distribution and uptake of artificially introduced radium-226 in a small lake. J. Fish. Res. Board Can. 30: 1485–1490.

Furutani, A., and J.W.M. Rudd. 1980. Measurement of mercury methylation in lake water and sediment samples. Appl. Environ. Microbiol. 40: 770–776.

Hecky, R.E., D.M. Rosenberg, and P. Campbell. 1994*a*. The 25th anniversary of the Experimental Lakes Area and the history of Lake 227. Can. J. Fish. Aquat. Sci. 51: 2243–2246.

Hecky, R.E., P. Campbell, and D.M. Rosenberg. 1994*b*. Introduction to experimental lakes and natural processes: 25 years of observing natural ecosystems at the Experimental Lakes Area. Can. J. Fish. Aquat. Sci. 51: 2721–2722.

Hesslein, R.H., W.S. Broecker, and D.W. Schindler. 1980. Fates of metal radiotracers added to a whole lake: sediment–water interactions. Can. J. Fish. Aquat. Sci. 37: 378–386.

Howell, E.T., M.A. Turner, R.L. France, M.B. Jackson, and P.M. Stokes. 1990. Comparison of Zygnematacean (Chlorophyta) algae in the metaphyton of two acidic lakes. Can. J. Fish. Aquat. Sci. 47: 1085–1092.

Kelly, C.A., J.W.M. Rudd, R.B. Cook, and D.W. Schindler. 1982. The potential importance of bacterial processes in regulating rate of lake acidification. Limnol. Oceanogr. 27: 868–882.

Kennedy, L.A. 1980. Teratogenesis in lake trout (*Salvelinus namaycush*) in an experimentally acidified lake. Can. J. Fish. Aquat. Sci. 37: 2355–2358.

Klaverkamp, J.F., M.A. Turner, S.E. Harrison, and R.H. Hesslein. 1983. Fates of metal radiotracers added to a whole lake: accumulation in slimy sculpin (*Cottus cognatus*) and white sucker (*Catostomus commersoni*). Sci. Total Environ. 28: 119–128.

Malley, D.F. 1980. Decreased survival and calcium uptake by the crayfish *Orconectes virilis* in low pH. Can. J. Fish. Aquat. Sci. 37: 364–372.

Malley, D.F. 1996. Cadmium whole-lake experiment: an anachronism. Can. J. Fish. Aquat. Sci. 53. In press.

Malley, D.F., P.S.S. Chang, and R.H. Hesslein. 1989. Whole lake addition of cadmium-109: radiotracer accumulation in the mussel population in the first season. Sci. Total Environ. 87–88: 397–417.

Malley, D.F., J.F. Klaverkamp, S.B. Brown, and P.S.S. Chang. 1993. Increase in metallothionein in freshwater mussels *Anodonta grandis grandis* exposed to cadmium in the laboratory and the field. Water Pollut. Res. J. Can. 28: 253–273.

Marshall, J.S., J.I. Parker, D.L. Mellinger, and S.G. Lawrence. 1981. An in situ study of cadmium and mercury stress in the plankton community of Lake 382, Experimental Lakes Area, northwestern Ontario. Can. J. Fish. Aquat. Sci. 38: 1209–1214.

Müller, P. 1980. Effects of artificial acidification on the growth of periphyton. Can. J. Fish. Aquat. Sci. 37: 355–363.

Palace, V.P., and J.F. Klaverkamp. 1993. Variation of hepatic enzymes in three species of freshwater fish from Precambrian Shield lakes and the effect of cadmium exposure. Comp. Biochem. Physiol. C: Pharmacol. Toxicol. Endocrinol. 104: 147–154.

Playle, R.C. 1987. Methods and feasibility of using aluminum-26 as a biological tracer in low pH waters. Can. J. Fish. Aquat. Sci. 44(Suppl. 1): 260–263.

Rochefort, L., D.H. Vitt, and S.E. Bayley. 1990. Growth, production, and decomposition dynamics of *Sphagnum* under natural and experimentally acidified conditions. Ecology, 71: 1986–2000.

Rosenberg, D.M., A.P. Wiens, B. Bilyj, and L. Armstrong. 1995. Experimental acidification of a poor fen in northwestern Ontario: effects on emergence of Chironomidae (Diptera). Can. J. Fish. Aquat. Sci. 52: 2229–2237.

Santschi, P.H., U.P. Nyfeller, R.F. Anderson, S.L. Schiff, P. O'Hara, and R.H. Hesslein. 1986. Response of radioactive trace metals to acid–base titrations in controlled experimental ecosystems: evaluation of transport parameters for application to whole-lake radio-tracer experiments. Can. J. Fish. Aquat. Sci. 43: 60–77.

Schindler, D.W. 1987. Detecting ecosystem responses to anthropogenic stress. Can. J. Fish. Aquat. Sci. 44(Suppl. 1): 6–25.

Schindler, D.W., R.H. Hesslein, R. Wagemann, and W.S. Broecker. 1980*a*. Effects of acidification on mobilization of heavy metals and radionuclides from the sediments of a freshwater lake. Can. J. Fish. Aquat. Sci. 37: 373–377.

Schindler, D.W., R. Wagemann, R.B. Cook, T. Ruszczynski, and J. Prokopowich. 1980*b*. Experimental acidification of Lake 223, Experimental Lakes Area: background data and the first three years of acidification. Can. J. Fish. Aquat. Sci. 37: 342–354.

Schindler, D.W., K.H. Mills, D.F. Malley, D.L. Findlay, J.A. Shearer, I.J. Davies, M.A. Turner, G.A. Linsey, and D.R. Cruikshank. 1985. Long-term ecosystem stress: the effects of years of experimental acidification on a small lake. Science (Washington, D.C.), 228: 1395–1401.

Shaw, M.A., I.J. Davies, E.A. Hamilton, A. Kemp, R. Reid, P.M. Ryan, N. Watson, W. White, and K.M. Murphy. 1995. The DFO National LRTAP Biomonitoring Programme: baseline characterization, 1987–1989. Can. Tech. Rep. Fish. Aquat. Sci. No. 2032. pp. vi + 63.

Turner, M.A., M.B. Jackson, D.L. Findlay, R.W. Graham, E.R. DeBruyn, and E.M. Vandemeer. 1987. Early responses of periphyton to experimental lake acidification. Can. J. Fish. Aquat. Sci. 44(Suppl. 1): 135–149.

Turner, M.A., E.T. Howell, M. Summerby, R.H. Hesslein, D.L. Findlay, and M.B. Jackson. 1991. Changes in epilithon and epiphyton associated with experimental acidification of a lake to pH 5. Limnol. Oceanogr. 36: 1390–1405.

Turner, M.A., E.T. Howell, G.G.C. Robinson, J.F. Brewster, L.J. Sigurdson, and D.L. Findlay. 1995*a*. Growth characteristics of bloom-forming filamentous green algae in the littoral zone of an experimentally acidified lake. Can. J. Fish. Aquat. Sci. 52: 2251–2263.

Turner, M.A., G.G.C. Robinson, B.E. Townsend, B.J. Hann, and J.A. Amaral. 1995*b*. Ecological effects of blooms of filamentous green algae in the littoral zone of an acid lake. Can. J. Fish. Aquat. Sci. 52: 2264–2275.

Turner, M.A., D.W. Schindler, D.L. Findlay, M.B. Jackson, and G.G.C. Robinson. 1995*c*. Disruption of littoral algal associations by experimental lake acidification. Can. J. Fish. Aquat. Sci. 52: 2238–2250.

Hydrochemical response of upland Precambrian Shield catchments to additions of H_2SO_4 and NH_4NO_3 during snowmelt[1]

Craig J. Allan

Abstract: Two of three upland Precambrian Shield catchments received additions of H_2SO_4 and NH_4NO_3 prior to snowmelt in 1989 and 1990; loading levels were equivalent to 18 $kg \cdot ha^{-1} \cdot yr^{-1}$ as SO_4^{2-} and 2.62 $kg \cdot ha^{-1} \cdot yr^{-1}$ as N. The third catchment served as a reference. The manipulated catchments retained 96–98% of the added NH_4^+, 73–94% of the added NO_3^-, 31–48% of the added SO_4^{2-}, and 72–92% of the added H^+. Proton neutralization was attributed to increased cation export ($Ca^{2+} + Mg^{2+} + Na^+ + K^+ + Al^{n+} + Mn^{2+} + Fe^{2+}$: 26–53%) and SO_4^{2-} retention (48–67%). The protonation of weak organic acids accounted for a 13–34% decline in organic anions during snowmelt. No significant change in dissolved organic carbon export was observed. In manipulated catchments, inorganic monomeric Al export increased from 30 to 80% over reference levels, and the ratio of inorganic to organic monomeric Al changed from <1.0 to 2.7. Differences in response of the manipulated catchments were attributed to differences in soil thickness and the extent of forest cover. Interannual differences in responses were attributed to differences in snow accumulations, melt sequences, and hydrologic flushing of catchment soils.

Résumé : Dans deux bassins hydrographiques des hautes terres du bouclier précambrien, on a ajouté du H_2SO_4 et du NH_4NO_3 avant la fonte des neiges en 1989 et en 1990; les niveaux de charge étaient équivalents à 18 $kg \cdot ha^{-1} \cdot an^{-1}$ pour le SO_4^{2-}, et ceux de l'azote, de 2,62 $kg \cdot ha^{-1} \cdot an^{-1}$. Un troisième bassin versant a servi de témoin. La rétention des ions ajoutés dans les bassins hydrographiques modifiés était la suivante : 96–98% du NH_4^+, 73–94% du NO_3^-, 31–48% du SO_4^{2-} et 72–92% du H^+, tous des ions ajoutés. La neutralisation des protons a été attribuée à une exportation accrue des cations ($Ca^{2+} + Mg^{2+} + Na^+ + K^+ + Al^{n+} + Mn^{2+} + Fe^{2+}$: 26–53%) et à la rétention de SO_4^{2-} (48–67%). La diminution des anions organiques à la fonte des neiges est due en partie (13–34%) à la protonation des acides organiques faibles. On n'a observé aucune variation importante de l'exportation du carbone organique dissous. Dans les bassins hydrographiques modifiés, l'exportation d'Al sous forme de monomère inorganique a augmenté de 30 à 80% par rapport aux niveaux de référence, et le rapport de l'Al monomère inorganique sur l'Al monomère organique a passé de <1,0 à 2,7. Les différences dans les réponses des bassins hydrographiques modifiés sont attribuables à des différences dans l'épaisseur des sols et l'étendue de la couverture forestière; quant aux différences dans les réponses d'une année à l'autre, elles s'expliqueraient par les écarts dans les accumulations de neige, dans les séquences de fonte et dans le taux de lessivage des sols des bassins.

[Traduit par la Rédaction]

Introduction

Acid precipitation is known to cause the acidification of surface, soil, and ground waters (Schindler et al. 1980; Chew et al. 1988; Ulrich 1980). The sensitivity of terrestrial systems to increased deposition of S and N compounds is dependent upon geologic setting, deposition levels, hydrologic regime, vegetative cover, and land use (Langdon and Wilson 1992). Low-order, headwater catchments on silicious bedrock, such as occur at the Experimental Lakes Area (ELA), display the greatest sensitivity and the quickest response to increased acid deposition because of minimal buffering capacities of the soils and rapid water transit through the catchment (Johnson et al. 1981; Lawrence et al. 1988). In this paper, the results are presented of a 2-year acid and fertilizer addition to two pristine, acid-sensitive catchments on the Canadian Precambrian Shield.

The purpose of the experiment was to determine the effects of fixed inputs of SO_4^{2-}, NO_3^-, NH_4^+, and H^+ on soil and runoff waters from Precambrian Shield catchments.

Received January 24, 1994. Accepted April 28, 1995.
J12246

C.J. Allan.[2] Department of Geography, York University, 4700 Keele Street, North York, ON M3J 1P3, Canada.

---

[1] This paper is one of a series done in honor of the 25th anniversary of the Experimental Lakes Area.

[2] Present address: Department of Geography and Earth Science, University of North Carolina at Charlotte, Charlotte, NC 28223, U.S.A.

Can. J. Fish. Aquat. Sci. **52**: 2213–2228 (1995). Printed in Canada / Imprimé au Canada

Table 1. Physiographic features of the study catchments.

	Area (m^2)	Slope	Percent bedrock	Percent forest	Mean soil depth (cm)[a]
U1	5553	0.177	73	27	8
U3	4006	0.169	79	21	8
U4	1730	0.230	60	40	10

[a] Soil volume/catchment area (m^3/m^2).

Data from such catchment manipulations are necessary to calibrate stream chemistry models. To date, these models have been tested and validated mostly on systems already heavily affected by acid precipitation (Christophersen et al. 1982; Cosby et al. 1985). The following hypotheses were tested: (*i*) added H^+ would protonate weak organic acids, resulting in their precipitation and a decrease in dissolved organic carbon (DOC) export but no change in runoff pH; (*ii*) increases in proton levels would cause increased Al^{3+} concentrations as a result of ion-exchange reactions or the increased dissolution of $Al(OH)_3$ minerals; and (*iii*) NH_4NO_3 additions would increase inorganic N concentrations in runoff.

Site description and experimental design

Three headwater catchments located in the ELA, northwestern Ontario (49°40′N, 93°43′W) were studied (Table 1). Natural water and chemical budgets and catchment descriptions are presented in Allan et al. (1993). Catchment U1 served as a reference basin, whereas catchments U3 and U4 were treated with H_2SO_4 and NH_4NO_3 prior to snowmelt during 1989 and 1990. The first year of monitoring (1988) served as a background year for all three catchments.

Catchments U1 and U3 are underlain by leucocratic coarse-grained metagranites with smaller areas of microcline feldspar metagranites. Catchment U4 is underlain by a quartzo-feldspathic orthogneiss (Allan et al. 1993). Soil deposits (Table 2) within the catchments are patchy and thin and classified as truncated orthic humic regosols and sombric brunisols (Canadian Soil Survey Committee Subcommittee on Soil Classification 1978). A typical soil profile consists of a 5- to 15-cm organic LFH horizon underlain by one or more Ah horizons. A C or Cg horizon consisting of a relatively unweathered or gleyed lacustrine sediment underlies deeper soil deposits. However, the distribution of C horizon soils is patchy and isolated from the main hydrologic flowpaths operating in the catchments (Allan et al. 1993; Allan and Roulet 1994*a*). Bulk mineral soil chemistry for Ah horizons is comprised of, by weight, 75% SiO_2, 15% Al_2O_3, 4% Fe_2O_3, 2.4% K_2O, and 1.7% Na_2O. The clay fraction consists of a complex mixture of hydroxy-interlayered vermiculite, smectite, Fe-rich chlorite, and kaolinite. Catchment soils are texturally classed as silt loams, and the <2-μm clay fractions constitute 20–30% of the mineral soil mass.

Vegetation on the soil deposits consists of an overstorey of *Pinus banksiana* Lamb., *Picea mariana* (Mill.) BSP, and a few *Pinus strobus* L. The understorey of the forested areas consists of a shrub layer of *Acer rubrum* L., *Prunus pensylvanica* L., *Juniperus virginiana* L., and *Vaccinium angustifolium* Ait.; the herb *Pteridium aquilinum* (L.) Kuhn; and a ground cover of *Cladina mitis* (Sandst.) Hustich and *Pleurozium schreberi* (Brid.) Mitt. Areas of exposed bedrock are colonized by *Andreaea rupestris* Hedw., *Polytrichum piliferum* Hedw., *Polytrichum juniperinum* Hedw., *Cladina mitis*, *Rhizocarpon geographicum* (L.) DC, and *Racomitrium microcarpon* (Hedw.) Brid. (Vitt 1989). The study catchments have never been logged and the last forest fire occurred over 100 years ago.

Physiographic characteristics of the study catchments differ. Catchment U4 has approximately 50% more forest cover and deeper average soils than catchments U3 and U1 (Table 1). The occurrence of large areas of open, lichen-covered bedrock in each catchment (60–79% total area) results in the widespread occurrence of Horton overland flow in response to snowmelt and rainfall, once depression storage (4–6 mm) in open bedrock areas is satisfied (Allan and Roulet 1994*a*). Close to 100% of precipitation runs off during large rain events or high antecedent moisture levels.

Runoff is naturally acidic (volume-weighted pH is 4.21–4.51) because of high levels of organic acidity (56–61% of the anion charge total). Total Al concentration in runoff varies from 400 to 1600 $\mu g \cdot L^{-1}$ with organic monomeric (OAl), inorganic monomeric (IAl), and acid soluble aluminum (ASAl) constituting approximately 48, 28, and 24% of the aluminum total, respectively (Allan et al. 1993).

Mean monthly temperatures for the ELA range from −16.5 for January to 20.1°C for July. Mean annual total precipitation is 508 mm, 36% as snow (Beaty and Lyng 1989). Atmospheric deposition as measured by bulk collectors ranged from 6.8 to 9.0 $kg \cdot ha^{-1} \cdot yr^{-1}$ for SO_4^{2-} and from 4.7 to 9.0 $kg \cdot ha^{-1} \cdot yr^{-1}$ for total N during the study period (M. Stainton, Department of Fisheries and Oceans, Winnipeg, Man., unpublished data).

Methods

Bulk winter precipitation (Nipher shielded snow gauge) and precipitation chemistry (Plexiglas bulk collector) were measured at the ELA meteorological station located 4 km from the study catchments. Rainfall was recorded by standard Atmospheric Environment Service (AES) rainfall gauges located in catchment U1 and another catchment <500 m from the study area.

Discharge from the study catchments was calculated from continuous water-level measurements behind 60° V-notch weirs at each catchment outlet. Water samples were collected in clean polyethylene bottles and taken to the ELA analytical laboratory within a few hours for processing. Chemistry samples during snowmelt were collected once or twice a day depending upon runoff rate. Water samples during rainfall were collected on an event basis; 1–14 samples were collected during each event.

Water samples were filtered and analyzed for NO_3^-, NH_4^+, total dissolved nitrogen (TDN), total dissolved phosphorus (TDP), pH, specific conductance, and dissolved inorganic carbon (DIC) at the ELA analytical laboratory, usually within 24 h of collection. Analyses of IAl and OAl

Table 2. Chemical and physical characteristics of the Experimental Lakes Area upland soils.

Soil horizon	Forested soil island			Open bedrock soils	
	LFH	Ah	C	LFH	Ah
N (sample size)	8	18	2	3	2
Sand/silt/clay (%)	—/—/—[a]	12/57/30	7/77/22	—/—/—	47/28/25
Bulk density ($kg\cdot m^{-3}$)	142.0	650.0	—	—	—
Saturated hydraulic conductivity (K_{fs}; $m\cdot s^{-1}$)	0.052	0.015	0.00049	—	—
pH $CaCl_2$	3.33	3.67	4.06	3.44	3.26
Organic carbon (%)	31	7	1	36	19
CEC (mequiv·$(100\ g)^{-1}$)[b]	17	5	1	13	9
Base saturation (%)[c]	59	15	10	66	24
Al ($Na_2P_2O_7$ extractable; % dry wt)	0.4	0.9	0.3	0.4	0.5
Al ($(NH_4)C_2O_4$ extractable; % dry wt)	0	1.3	0.5	0.4	0.6
SO_4^{2-} (H_2O extractable; $\mu g\cdot g^{-1}$)	85.0	13.3	7.6	84.6	18.7
SO_4^{2-} (NaH_2PO_4 extractable; $\mu g\cdot g^{-1}$)	0	152.0	31	35.7	22.8

[a] —, not measured.

[b] Cation exchange capacity (CEC) calculated as the sum of exchangeable Ca + Mg + K + Al (mequiv·$(100\ g)^{-1}$). Soil extractions performed with 1 M NaCl followed by atomic absorption spectrometry (AAS) analysis of Ca, Mg, K, and Al.

[c] % base saturation calculated as:

$$\%\ \text{base sat.}^{d} = \frac{Ca + Mg + K}{Ca + Mg + K + Al} \times 100$$

[d] All cations are exchangeable as operationally defined by extraction with 1 M NaCl followed by AAS analysis of Ca, Mg, K, and Al.

were also performed at the ELA, usually within 3 d of collection. Analyses for particulate nitrogen (PN), particulate phosphorus (PP), and particulate carbon (PC), major ions, DOC, Fe, Mn, total Al (TAl), and soluble reactive silicon (SRSi) were performed at the Department of Fisheries and Oceans analytic laboratory in Winnipeg (Stainton et al. 1977). However, SO_4^{2-} and Cl^- analyses were performed by ion chromatography (Tabatabai and Dyck 1983). Total labile aluminum (TCVAl), and OAl concentrations were determined at the ELA using a manual ion-exchange procedure equivalent to the automated procedure reported by LaZerte et al. (1988). Inorganic labile aluminum was calculated as the difference between OAl and TCVAl. Inorganic aluminum speciation was estimated with the chemical speciation program ALCHEMI (Schecher and Driscoll 1987). Thermodynamic calculations were corrected for the effects of temperature and ionic strength. Organic anions ($RCOO^-$) were calculated as the charge difference between cations ($Ca^{2+} + Mg^{2+} + Na^+ + K^+ + H^+ + Al^{n+} + NH_4^+$) and anions ($SO_4^{2-} - Cl^- - NO_3^-$). Acid neutralizing capacity (ANC) was calculated as the equivalent sum of base cations minus the equivalent sum of strong acid anions. No correction was made for the marine fraction of ions because of the low concentrations of Cl^- and the midcontinental location of the ELA.

Catchment additions

A solution of 36 N H_2SO_4 diluted to approximately pH 2.0 was applied over the late-winter snowpack using a backpack sprayer. Care was taken to avoid directly spraying vegetation. Reagent grade NH_4NO_3 as a solid pellet was dispersed over the snowpack at the same time the H_2SO_4 was added. Applications in both years occurred 1–2 d prior to the commencement of spring runoff to ensure that none of the addition drifted across catchment boundaries. Target loadings to both experimental catchments were 18 $kg\cdot ha^{-1}$ as SO_4^{2-} and 2.62 $kg\cdot ha^{-1}$ as N; this corresponded to an annual loading of 50 $kg\cdot ha^{-1}\cdot yr^{-1}$ of SO_4^{2-} and 7.29 $kg\cdot ha^{-1}\cdot yr^{-1}$ of N (prorated to the 36% of ELA precipitation that falls as snow; Beaty and Lyng 1989). Loading levels did not include atmospheric SO_4^{2-} and N inputs currently received at the ELA. Experimental loading levels were based on actual SO_4^{2-} and N wet and dry deposition levels recorded at the Air and Precipitation Monitoring Network (APMN) Long Point station in Ontario in the early 1980s (Barrie and Sirois 1986).

The effects of the H_2SO_4 and NH_4NO_3 additions were assessed by first calculating a reference ratio (RR_{88}) of chemical export between the reference basin (U1) and the two experimental basins (U3, U4) for 1988, the preacidification year:

[1] $\text{U3 or U4 yield } (kg\cdot m^{-2})/\text{U1 yield } (kg\cdot m^{-2}) = RR_{88}$

Second, a ratio of change (RC) was calculated for each experimental year (*e*) and compared to the RR_{88}:

[2] $RR_e/RR_{88} = RC$

All RC values were adjusted to account for changes in the differences of hydrologic yield between the experimental and reference catchments. For example, U3 exported 9% more water than U1 in 1988 (Table 3). However, U3 exported 2% more water than catchment U1 in 1989. Therefore, the 1989 U3 RC values were increased by 7%. The significance of the RC value was assessed from

Table 3. Winter precipitation totals, snowmelt runoff, and runoff coefficients for U1, U3, and U4 catchments, 1988–1990.

	Winter precipitation totals (mm)[a]	Snowmelt runoff (mm)	Runoff coefficient[b]
1988			
U1	194	115	0.59 (45)
U3	194	131	0.68 (49)
U4	194	102	0.53 (56)
1989			
U1	219	173	0.80 (51)
U3	219	180	0.82 (54)
U4	219	141	0.64 (59)
1990			
U1	70	43	0.61 (22)
U3	70	59	0.84 (24)
U4	70	52	0.74 (30)

[a] Winter precipitation totals were used rather than snow water equivalence data from snow surveys because the snow survey data did not account for winter precipitation metamorphosed to ground ice (substantial in open lichen and bedrock areas) and snow melted and accumulated as soil water (important in forested areas). No runoff occurred from any of the catchments prior to the main snowmelt period.

[b] Values in parentheses are the percentages of annual runoff attributed to snowmelt.

estimated uncertainties (>2 SD) of the hydrologic and chemical budgets for the catchments. Hydrologic uncertainties were estimated from rating equation uncertainties and annual flow records, whereas chemical estimates included analytic and sampling uncertainties (Devito et al. 1989; Allan et al. 1993). Error estimates (2 SD) for elemental export averaged 12% for 1989 and 20% for 1990 (Allan et al. 1993). Ratio-of-change values exceeding these estimates were considered significant. The effects of the spring catchment manipulations (increased SO_4^{2-} and base cation export in particular) were still detectable after the snowmelt runoff period, so annual, rather than just snowmelt, yields were used in the above analyses.

Results

Hydrology

Snow comprised 33, 44, and 22% of the annual precipitation in 1988, 1989, and 1990, respectively; snowmelt contributed 22–59% of the annual runoff during the same period (Table 3). Patterns of snowmelt discharge differed substantially among study years but did not differ appreciably among basins in any given year (Fig. 1). The snow cover was patchy in 1990, and areas of bare ground were exposed before the thaw.

Snowmelt was continuous during 1988 and occurred mostly over 6 d (Fig. 1*a*). Four major melt periods occurred during 1989 and two occurred during 1990. Cold periods during both years interrupted and prolonged snowmelt runoff from 29 to 37 d. No significant rain events occurred during the melt periods, although the final runoff peak during both 1989 and 1990 was attributed to mixed rain and snow events.

Ammonium

Ammonium concentrations were similar among catchments in 1988 and 1989 (Figs. 2*a*, 3*a*). A significant increase in annual NH_4^+ export occurred in 1990 where U4 export was 1.6 times that from U1 (Table 4). Catchments U3 and U4 retained 96–98% of the added NH_4^+ in 1989 and 1990.

Peak spring NH_4^+ concentrations in 1989 (330 $\mu g \cdot L^{-1}$) and in 1990 (180 $\mu g \cdot L^{-1}$) were measured in the U3 catchment, generally in the first or second sample (Figs. 3*a*, 4*a*). Later in the melt period, little difference in NH_4^+ concentration was evident between catchments. A significant proportion of the ions accumulated in the winter snowpack together with the added chemicals caused the high runoff concentrations observed for NH_4^+ and other chemical constituents in the initial increment of snowmelt (Johannessen and Henriksen 1978). The most likely source of this material is the snowpack nearest the outlet weirs; thus, these initial meltwaters had minimal contact with organic and mineral surfaces.

Nitrate

Nitrate export increased significantly in 1989 and 1990 for U3 and U4 (Table 4), after NO_3^- export and runoff concentrations were similar among the three catchments during 1988. Nitrate retention was 91 (U3) and 93% (U4) of that added in 1989 and 73 (U3) and 95% (U4) in 1990. Elevated NO_3^- concentrations were associated with high-flow periods during 1988 and 1989 and the first high-flow period during 1990 (Figs. 2*b*, 3*b*, 4*b*).

Sulphate

Sulphate export increased significantly in U3 and U4 in 1989 and 1990 relative to U1 (Table 4). Sulphate retention was 48 (U3) and 57% (U4) of that added in 1989 and 49 (U3) and 67% (U4) in 1990.

The export pattern for U1, U3, and U4 indicates a rapid flushing of both background and added SO_4^{2-} over a relatively short period (Figs. 2*c*, 3*c*, 4*c*). Sulphate concentrations peaked with initial flows in all 3 years. However, unlike NO_3^-, subsequent SO_4^{2-} concentrations exhibited a regular nonlinear decline over time, independent of discharge. In both 1989 and 1990, 90% or more of the added SO_4^{2-} lost from the catchments was exported from both manipulated catchments during the spring snowmelt period. The remaining 5–10% of the excess SO_4^{2-} was exported during rain events in May and early June. No excess SO_4^{2-} export was detected later during the growing season.

Hydrogen ion

Proton export increased significantly from 1988 to 1989 in U3 and U4 but only U3 exhibited a significant increase in 1990 relative to U1 (Table 4). Hydrogen ion retention was 84 and 94% of that added in 1989 and 89 and 98% in 1990 for U3 and U4, respectively. As for SO_4^{2-}, H^+ concentrations displayed a nonlinear decrease with time, independent of discharge (Figs. 3*d*, 4*d*). Maximum pH depressions to 3.96 and 3.09 (U3) and 4.26 and 4.21 (U4) were measured for 1989 and 1990, respectively, compared with 4.49 and 4.51 recorded for U1.

Fig. 1. Temporal changes in snowmelt runoff for catchments U1, U3, and U4 in 1988 (*a*), 1989 (*b*), and 1990 (*c*).

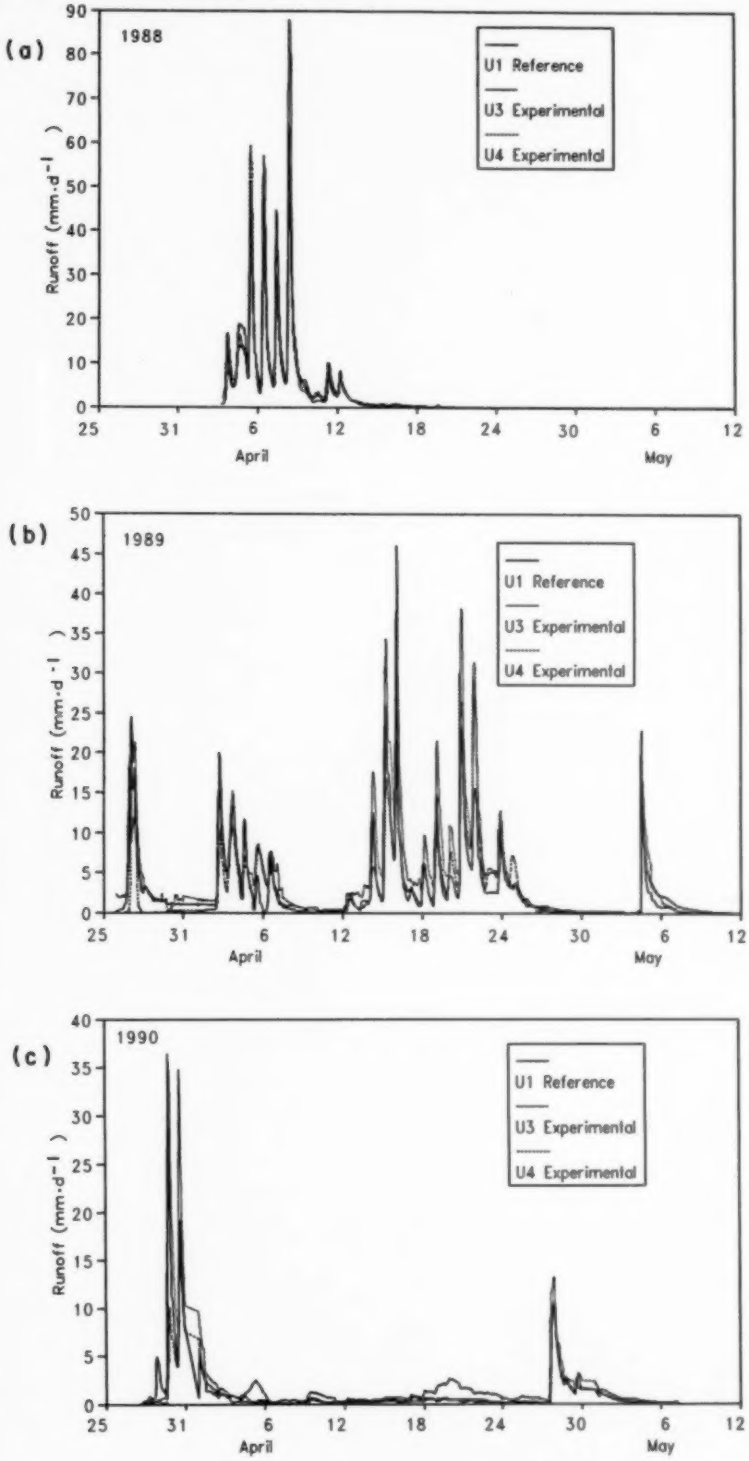

Fig. 2. Temporal changes in snowmelt runoff concentrations of NH_4^+ (*a*), NO_3^- (*b*), SO_4^{2-} (*c*), H^+ (*d*), Ca^{2+} (*e*), and Si (*f*) during the reference year (1988). Ref., reference; Ex., experimental. Note different scales.

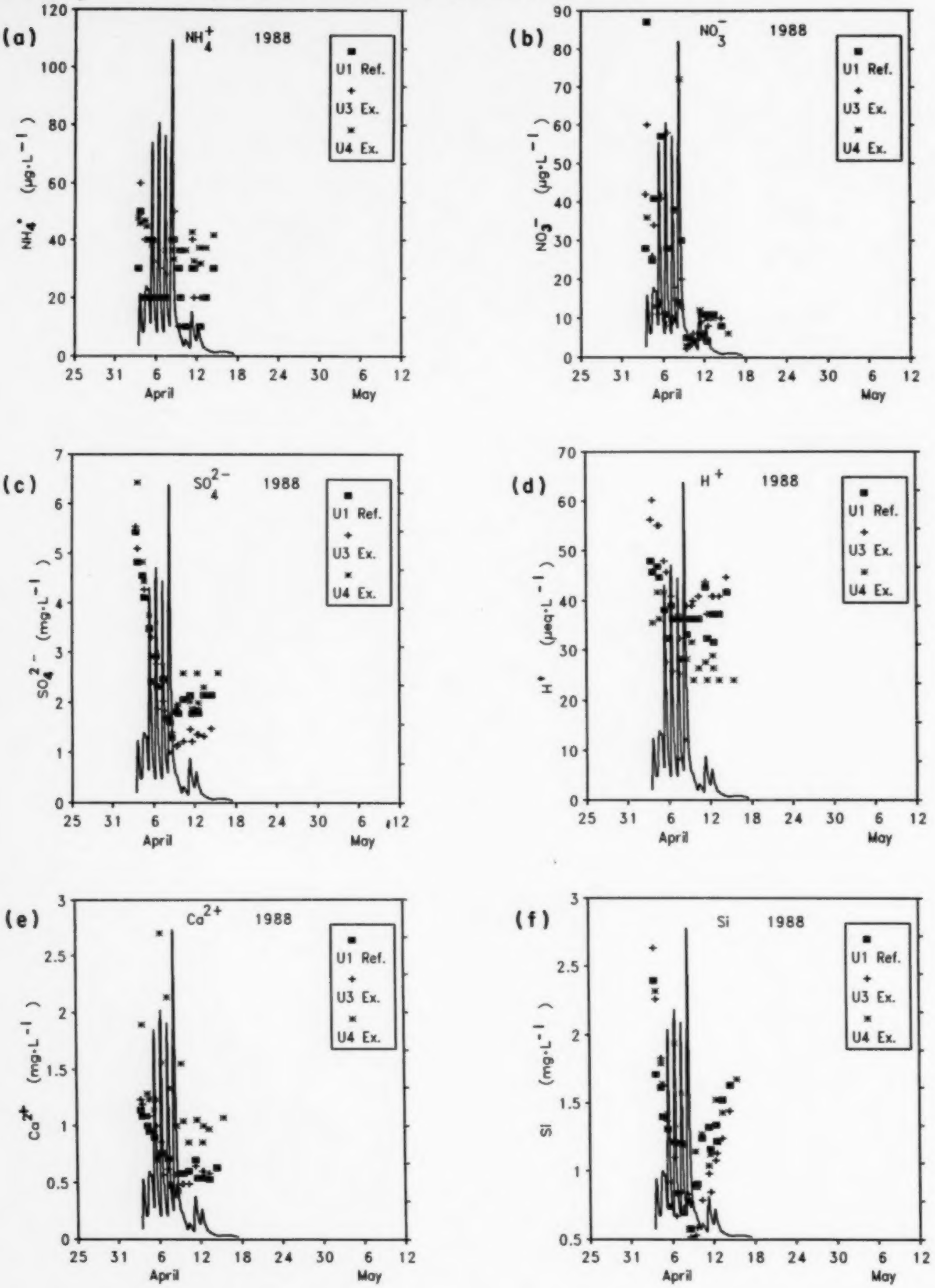

Fig. 3. Temporal changes in snowmelt runoff concentrations of NH_4^+ (*a*), NO_3^- (*b*), SO_4^{2-} (*c*), H^+ (*d*), Ca^{2+} (*e*), and Si (*f*) during the first manipulation year (1989). Ref., reference; Ex., experimental. Note different scales.

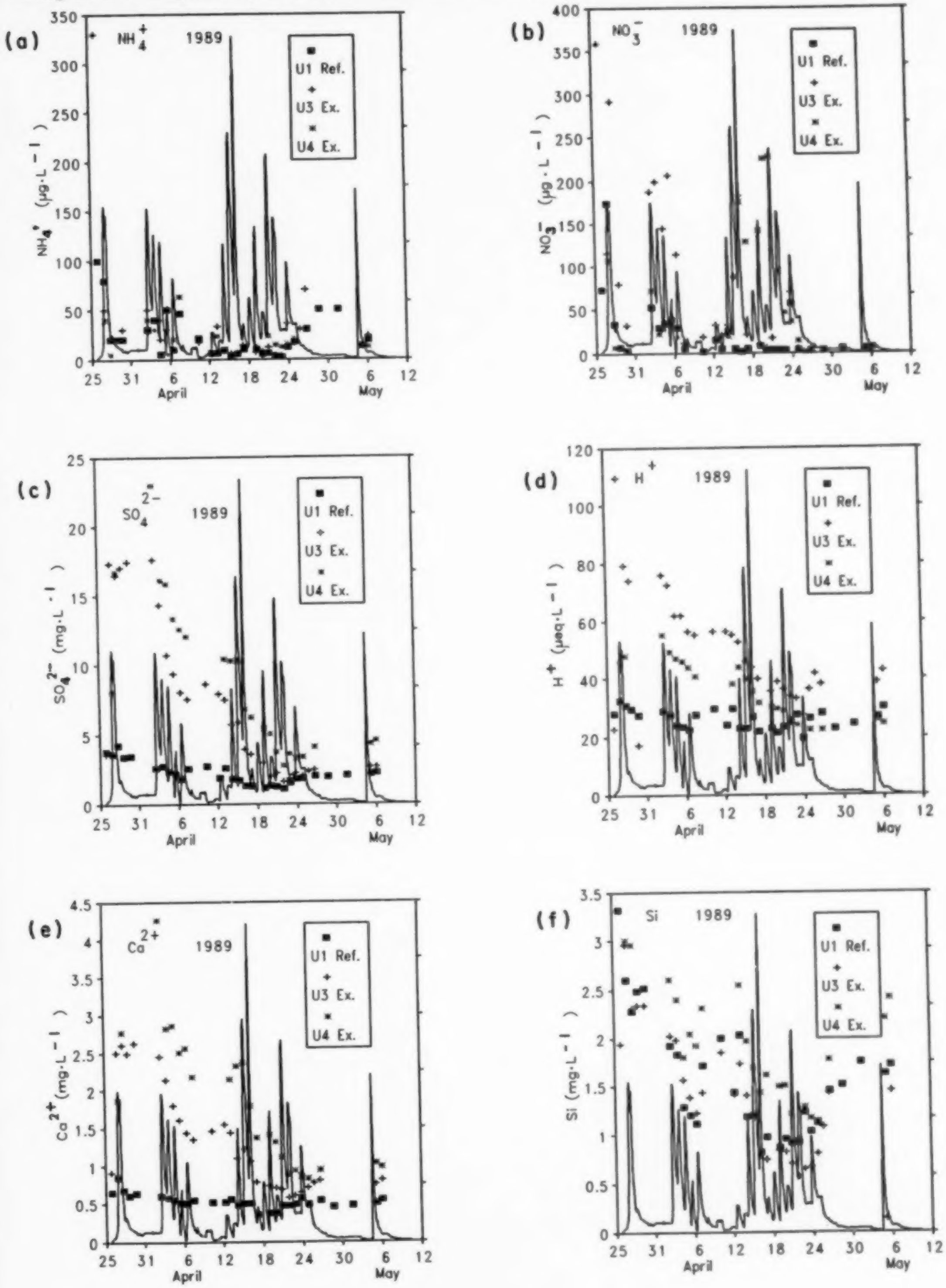

Table 4. Chemical export yields of spring snowmelt and ratio of change (RC) values for reference (U1) and experimental (U3, U4) catchments, 1988–1990.

Constituent[a]	Catchment	1988	1989	1990
NO_3^- (equiv·ha^{-1})	U1	2.3	3.2	0.4
	U3	2.3	11.3 (1.5)*	25.6 (16.2)*
	U4	2.7	8.7 (2.2)*	3.1 (6.6)*
NH_4^+ (equiv·ha^{-1})	U1	2.2	2.2	0.3
	U3	5.8	2.6 (0.8)	1.3 (1.2)
	U4	1.9	1.7 (0.9)	1.3 (1.6)*
TDN (g·ha^{-1})	U1	374	476	114
	U3	472	589 (0.9)	530 (1.4)*
	U4	446	444 (0.7)*	199 (0.9)
PN (g·ha^{-1})	U1	91	79	23
	U3	131	83 (0.7)*	40 (1.0)
	U4	146	64 (0.6)*	33 (1.7)*
TN (g·ha^{-1})	U1	464	555	137
	U3	603	671 (0.9)	568 (1.4)*
	U4	593	508 (0.7)*	232 (1.0)
TDP (g·ha^{-1})	U1	8.1	8.4	1.8
	U3	8.9	8.7 (0.9)	2.9 (1.1)*
	U4	10.4	7.2 (0.8)*	2.7 (1.6)*
PP (g·ha^{-1})	U1	10.1	8.8	3.6
	U3	14.6	9.4 (0.7)*	4.8 (0.8)*
	U4	17.4	8.7 (0.7)*	3.8 (1.6)*
TP (g·ha^{-1})	U1	18.2	17.2	5.4
	U3	23.5	18.0 (0.8)*	7.7 (0.9)
	U4	27.8	15.9 (0.7)*	6.5 (1.4)*
DIC (g·ha^{-1})	U1	1.13	1.86	—[b]
	U3	0.75	1.21 (1.1)	—
	U4	1.05	2.19 (1.4)*	—
DOC (g·ha^{-1})	U1	14.42	17.84	3.78
	U3	18.75	20.13 (0.9)	6.36 (1.2)
	U4	17.96	14.21 (0.9)	5.71 (0.9)
PC (g·ha^{-1})	U1	0.77	0.79	0.18
	U3	1.13	1.06 (0.8)	0.34 (0.9)
	U4	1.41	0.65 (0.7)*	0.27 (2.0)*
TC (g·ha^{-1})	U1	16.32	20.49	—
	U3	20.64	22.40 (0.9)	—
	U4	20.42	17.05 (0.9)	—
H^+ (μequiv·ha^{-1})	U1	41	44	7
	U3	51	91 (1.4)*	41 (1.7)*
	U4	56	45 (1.5)*	19 (1.3)
Ca^{2+} (μequiv·ha^{-1})	U1	37	46	9
	U3	44	115 (1.4)*	80 (2.1)*
	U4	66	110 (1.3)*	52 (1.6)*
Mg^{2+} (μequiv·ha^{-1})	U1	24	31	6
	U3	27	77 (1.6)*	51 (2.0)*
	U4	31	65 (1.6)*	32 (1.7)*
Na^+ (μequiv·ha^{-1})	U1	16	26	5
	U3	18	29 (1.5)*	13 (1.2)
	U4	16	26 (1.1)	15 (1.5)*

Table 4 (*concluded*).

Constituent[a]	Catchment	1988	1989	1990
K^+ (μequiv·ha^{-1})	U1	6	6	2
	U3	7	12 (1.0)	11 (2.1)*
	U4	9	9 (0.9)	6 (2.1)*
IAl (μequiv·ha^{-1})[c]	U1	—	22	4
	U3	—	32 (1.3)*	28 (1.8)*
	U4	—	10 (1.7)*	19 (1.7)*
OAl (g·ha^{-1})[c]	U1	—	386	61
	U3	—	313 (1.1)	102 (1.4)*
	U4	—	108 (1.1)	116 (1.1)
TAl (g·ha^{-1})	U1	368	778	139
	U3	476	751 (1.0)	403 (1.4)*
	U4	396	858 (1.3)*	355 (1.2)
Mn^{2+} (μequiv·ha^{-1})	U1	20	21	5
	U3	21	51 (1.5)*	51 (2.9)*
	U4	42	53 (1.8)*	31 (2.8)*
Fe^{2+} (μequiv·ha^{-1})	U1	122	266	43
	U3	207	366 (0.8)*	146 (1.3)*
	U4	95	235 (1.0)	74 (1.1)*
SO_4^{2-} (μequiv·ha^{-1})	U1	57	74	15
	U3	59	263 (2.5)*	177 (3.6)*
	U4	62	211 (2.5)*	109 (3.1)*
Cl^- (μequiv·ha^{-1})	U1	4	4	6
	U3	6	5 (0.7)*	3 (1.1)
	U4	4	4 (0.7)*	4 (1.5)*
$RCOO^-$ (μequiv·ha^{-1})	U1	74	97	12
	U3	98	79 (1.0)	11 (1.1)
	U4	123	42 (0.8)*	14 (0.9)
Si (g·ha^{-1})	U1	1.13	2.38	0.42
	U3	1.18	1.64 (1.0)	0.89 (1.3)*
	U4	1.26	2.13 (1.2)*	1.20 (1.5)*
ANC (μequiv·ha^{-1})	U1	21.5	19.9	22.5
	U3	27.3	−19.9 (0.45)*	−81.4 (0.32)*
	U4	59.4	−4.8 (0.25)*	−8.9 (0.42)*

Note: Results with an * denote a significant ($P < 0.05$) increase or decrease in annual chemical yield for an experimental catchment in relation to U1. Numbers in parentheses are annual RC values for the U3 and U4 catchments in 1989 and 1990. RC values represent annual differences and have been adjusted for changes in hydrologic yield between years.

[a] Abbreviations are explained in the text.

[b] —, not measured.

[c] IAl and OAl were not measured in 1988. Reference ratio (RR) values are given instead for 1989 and 1990.

Cations

The temporal runoff patterns of most cations closely followed those of SO_4^{2-}, displaying a constant decrease in concentration with time irrespective of changes in discharge (Figs. 3*e*, 4*e*). A similar pattern was displayed by Mg^{2+}, Na^+, K^+, Al^{n+}, and Mn^{2+}. Concentrations of Ca^{2+}, Mg^{2+}, and Mn^{2+} increased significantly in U3 and U4 during 1989 and 1990, relative to U1 (Table 4).

Significant increases in TAl export occurred from U4 in 1989 and U3 in 1990 (Table 4). Higher IAl concentrations accounted for 49 (U4, 1989), 79 (U3, 1990), and 100% (U4, 1990) of the increase in TAl export. OAl export remained relatively constant during the 2 manipulation years (U3, 1990 excepted). The IAl:OAl ratio for U1 during snowmelt averaged 0.6 for 1989 and 1990. The IAl:OAl ratios were 1.0 and 2.7 for U3 and 0.9 and 1.6 for

Fig. 4. Temporal changes in snowmelt runoff concentrations of NH_4^+ (*a*), NO_3^- (*b*), SO_4^{2-} (*c*), H^+ (*d*), Ca^{2+} (*e*), and Si (*f*) during the second manipulation year (1990). Ref., reference; Ex., experimental. Note different scales.

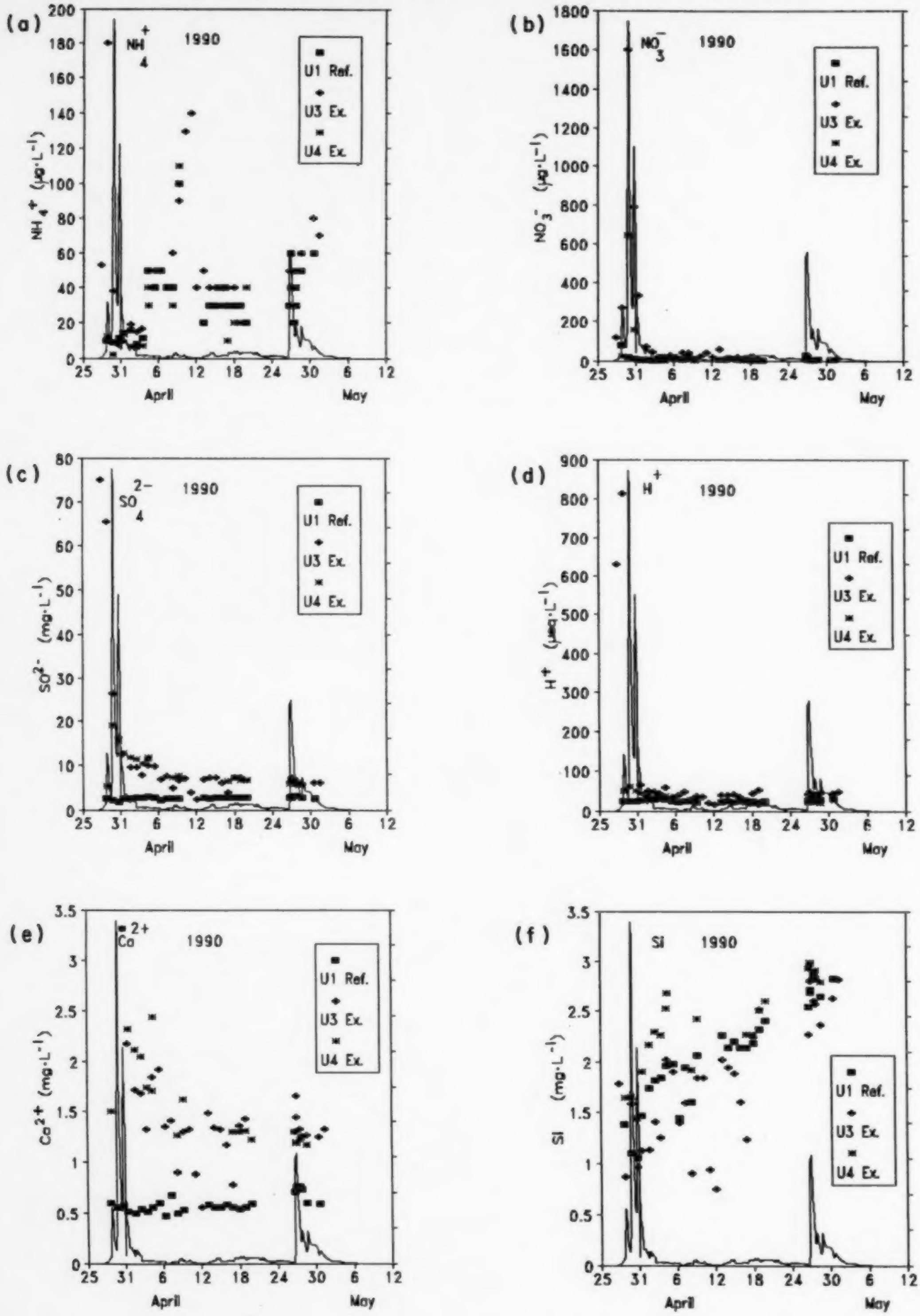

Table 5. Summary of strong acid buffering and export of added H^+ in experimental catchments (U3, U4).

	U3				U4			
	1989 (added 150 equiv H^+)		1990 (added 150 equiv H^+)		1989 (added 65 equiv H^+)		1990 (added 65 equiv H^+)	
	equiv H^+	%	equiv H^+	%	equiv H^+	%	equiv H^+	%
SO_4^{2-} adsorption	71.3	48	73.6	49	36.9	57	43.2	67
Increased cation export[a]	50.4	34	67.4	45	13.1	20	15.6	24
Increased IAl export	6.2	4	11.98	8	4.0	6	2.7	4
Protonation of $RCOO^-$	0	0	−9.73	−7	8.0	12	2.6	4.1
Increase in NO_3^- export	−2.0	−1	−9.74	−7	−0.9	−1	−0.7	−1
Total H^+ neutralization	125.9	84	133.5	89	61.1	94	63.4	98
Increased H^+ export	24.2	16	10.0	7	4.7	7	3.0	5
Total	150.1	100	143.5	96	65.8	101	66.4	103

[a] Ca + Mg + Na + K + Mn + Fe.

U4 in 1989 and 1990, respectively. Al^{3+} constituted ≥80% of the IAl total in both experimental and control catchments.

DOC and $RCOO^-$

No significant change in DOC export from any catchment was observed during this study. However, during snowmelt, $RCOO^-$ charge per unit DOC declined 13–34%, from approximately 5.6 to 3.6–5.2 μequiv·mg^{-1} DOC. The change in $RCOO^-$ was generally undetectable on an annual basis; the only significant decline in $RCOO^-$ occurred in U4 in 1989 (Table 4).

Silica

Silica export from U4 significantly increased in both manipulation years, but only in the second year for U3 (Table 4). However, the magnitude of change in Si fluxes was relatively small when compared with the changes in cation fluxes, and there was little difference in runoff Si concentrations between reference and treatment catchments after the chemical additions (Figs. 3*f*, 4*f*). Temporal trends in Si concentrations tended to follow those displayed by Ca^{2+} and other cations during 1988 and 1989 (Figs. 2*a*–*f*, 3*a*–*f*). However, during 1990 Si concentrations increased with time independent of discharge, opposite to the trend displayed by Ca^{2+} and other cations (Figs. 4*a*–*f*).

Discussion

Ammonium nitrate additions

The added NH_4NO_3 had little effect on runoff chemistry because of efficient abiotic (ion-exchange for NH_4^+) and biotic retention of NH_4^+ and NO_3^-. Watersheds in the ELA are N limited; they exhibit annual inorganic (NH_4^+ + NO_3^-) N-retention levels of ≥90% and total nitrogen (TN) retention levels of >80% (Allan et al. 1993). The efficient retention of N, applied either as NH_4NO_3 or HNO_3, by N-limited forested systems has been reported in other studies (Edwards et al. 1991; Wright et al. 1993).

The N added prior to snowmelt may have affected elemental export later during the growing season. During the 1989 growing season, the export of nutrients and trace elements important to plant growth, including NH_4^+ (0.75× for U3, 0.85× for U4), NO_3^- (0.62×, 0.42×), TDP (0.69×, 0.66×), K^+ (0.64×, 0.74×), Fe^{2+} (0.72×, 0.74×), and Mn^{2+} (0.74×, 0.5×), all declined relative to that of U1 (Allan 1993). Nitrogen added during spring may have stimulated plant growth, which increased biotic demand for these nutrients later in the growing season. Alternatively, the labile pool of K^+, Fe^{2+}, and Mn^{2+} may have been depleted by the acid additions during snowmelt runoff. A greater proportion of the added N and SO_4^{2-} was exported in 1990 than 1989 in the post-snowmelt period, and a decrease in only TDP export from the manipulated catchments (0.77×, U3 and 0.86×, U4) was detectable.

The slightly lower NO_3^- retention in relation to NH_4^+ reflects the preferential uptake of NH_4^+ by vegetation and microbial communities, resulting in a greater mobility in forested systems (Johnson and Cole 1980), and (or) cation exchange of NH_4^+. Higher NO_3^- export during 1990 than during 1989 resulted from extremely high NO_3^- concentrations during the initial runoff period (Figs. 3*b*, 4*b*). Different melt conditions between years probably affected the proportion of the added chemicals exported in initial meltwaters (Johannessen and Henriksen 1978). In addition, the widespread occurrence of ground ice on bedrock surfaces probably minimized meltwater and surface contact during the first runoff period in 1990.

Intercatchment differences in NO_3^- export observed in 1989 and 1990 (Table 4) reflected small-scale differences in catchment physiography. Catchment U3 has large areas of open, lichen-covered bedrock just above the outlet weir. Initially, when NO_3^- runoff concentrations were highest, the majority of melt occurred from open-bedrock surfaces (C.J. Allan, unpublished data). Highly concentrated runoff passed over largely ice-covered bedrock surfaces before exiting U3, presenting little opportunity for biotic retention. Runoff from both U1 and U4 had to pass through more extensive, treed soil deposits before exiting each catchment.

During 1989, the NO_3^- peaks for U3 and U4 catchments were offset: elevated NO_3^- concentrations for U3 occurred during the first two runoff periods, whereas the highest NO_3^- concentrations for U4 occurred during the third melt

Fig. 5. Changes in annual runoff chemistry export (equivalents) resulting from H_2SO_4 and NH_4NO_3 additions to catchments U3 and U4. Positive values represent increases in export; negative values indicate decreases.

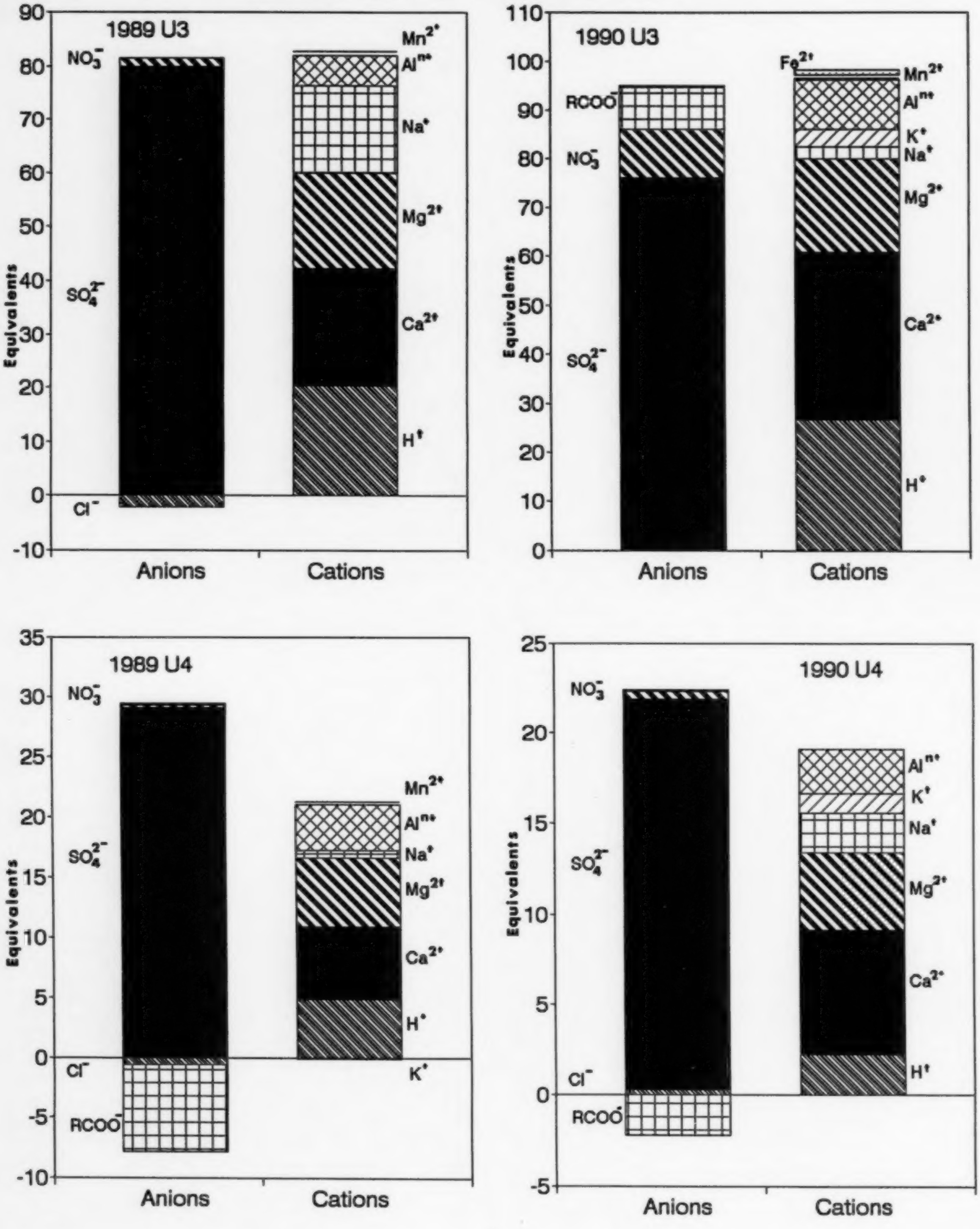

period (Fig. 3*b*). However, the SO_4^{2-} peaks coincided (Fig. 3*c*). The NH_4NO_3 and H_2SO_4 were added at the same time, so the differences in timing of NO_3^- peaks reflected different transport times through the soil covers of U3 and U4. Nitrate passed through and over the shallow soil cover of the U3 catchment quickly during initial high flows. A longer duration of high discharge appeared necessary to transport NO_3^- through the deeper and more areally extensive soil deposits of U4. The extended period of low discharges during 1990 would tend to conceal these inter-catchment differences.

Sulphuric acid additions

The primary effect of spring H_2SO_4 additions was to increase the acidity (1.7–2.8×) and dissolved ionic concentration (1.6–2.8×) of snowmelt runoff (Tables 4, 5).

Sulphate retention was the primary buffering mechanism for strong acids in U3 and U4 (Table 5). Neither catchment approached a steady state of SO_4^{2-} inputs and outputs after the two H_2SO_4 additions. A steady-state condition is commonly observed in acid-impacted systems with young soils (Rochelle et al. 1987). There was no evidence of increased sulphate leaching after mid-June in either manipulated catchment, which suggested that the SO_4^{2-} retained in both catchments was stored in organic soil pools, sequestered by vegetation (Strickland and Fitzgerald 1984) or stored as reduced S compounds (Bayley et al. 1987).

Increased SO_4^{2-} retention in U4 in 1990 compared with 1989 probably resulted from lower snowmelt runoff during 1990; catchment soils were flushed only approximately one-third as much in 1990 as in 1989. Long SO_4^{2-} residence time would allow for more incorporation of SO_4^{2-} into nonmobile, soil-complexed forms of S.

The added H^+ displaced cations from organic and mineral exchange sites. It also dissolved primary and secondary minerals in the soil matrix and on bedrock surfaces, releasing cations to solution. Sulphate behaved as a mobile counter-ion to the cations mobilized by H^+. Increases in cation export measured in runoff probably represent an underestimate of the total amount of cations released through increased weathering and ion-exchange reactions for the manipulated basins. Allan et al. (1993) reported that treed soil islands in the study catchments sequestered cations transported from open-bedrock surfaces, indicating that a steady-state vegetative uptake of cations could not be assumed.

Increases in the base cations Al^{n+} and Mn^{2+} in runoff was largely attributed to the 'salt-effect' resulting from either increased ionic-strength and ion-exchange reactions (Reuss and Johnson 1986), or the incongruent dissolution of aluminosilicate minerals, or both. If the congruent dissolution of primary and secondary aluminosilicate and mafic minerals was the primary source of the mobilized cations, then changes in the temporal runoff patterns of Si and Ca^{2+} should correspond in the manipulated catchments. Silicon concentrations were similar among manipulated and reference catchments in 1989 (Fig. 3*f*), but Ca^{2+} concentrations were different (Fig. 3*e*). In 1990, no correspondence between Si and Ca^{2+} and other cation concentrations was obvious (Figs. 4*e*, 4*f*). Laboratory leaching experiments indicated that base cations were primarily mobilized from organic LFH soil horizons by acidic solutions, whereas Ah mineral soils were an important source of Al (Allan and Roulet 1994*b*). The distribution of exchangeable base cations and Al within catchment soils supported these conclusions (Table 2).

Ca^{2+} and Mg^{2+} were the primary cations that balanced increased SO_4^{2-} in runoff (Fig. 5). Catchment U3 exhibited the following order of increase: $Ca^{2+} > H^+ > Mg^{2+} > Al^{n+}$, $Na^+ > K^+$, Mn^{2+}. The order of increase for U4 was $Ca^{2+} > Mg^{2+} > H^+$, $Al^{n+} > Na^+$, $K^+ > Mn^{2+}$. A greater proportion of the added SO_4^{2-} was retained in U4 than in U3; this greater retention reduced the number of mobile anions and protons in runoff. The increased proportion of proton neutralization attributable to increased cation export (14–21%) in U3 is proportional to the lesser importance (9–19%) of SO_4^{2-} retention when compared with catchment U4 (Table 5).

Increases in the export rates of Ca^{2+}, Mg^{2+}, Al^{n+} (U3 only), Fe^{2+}, Mn^{2+}, and Si for manipulated catchments compared with those of the reference catchment were higher in 1990 than 1989. This reflects the lower 1990 snow–water equivalent that would have intensified the salt effect and reduced dilution of the chemical additions. The higher acidity and increased surface–acid contact time for snowmelt waters in 1990 would increase the incongruent and congruent dissolution of primary and secondary aluminosilicate minerals. The behavior of Na^+ is problematic because concentrations decreased between 1989 and 1990 for U3, but increased for U4. The latter may be attributed to an increase in weathering of the underlying plagioclase feldspar, which could similarly explain the other cation increases. However, the decrease in Na^+ in 1990 for U3 is opposite to what should have occurred if this argument was true. It is possible that the initial acid addition in 1989 depleted a labile pool of Na^+ from bedrock surfaces and soils in U3; however, insufficient data are available to compare differences in soil and bedrock surface chemistry among catchments.

An increase in $Ca^{2+} + Mg^{2+}$ export rates of 7–14 mequiv·m^{-2}·yr^{-1} was observed for the ELA catchments that received an additional 37.5 mequiv H^+·m^{-2}·yr^{-1} over natural deposition rates. This export rate was higher than the approximately 5 mequiv·m^{-2}·yr^{-1} reported for the acidified SOG2 catchment in western Norway, which received an additional 77–102 mequiv H^+·m^{-2}·yr^{-1} as H_2SO_4 (Wright et al. 1988; Frogner 1990). The ELA catchments produced higher $Ca^{2+} + Mg^{2+}$ export rates than those in Norway despite lower H^+ additions and additions being confined to the snowmelt period when interactions between meltwater and catchment were minimal. Two explanations are possible: (*i*) the cation-exchange capacity of ELA upland soils, in particular the LFH horizon, are approximately 4× and the base saturation approximately 9× higher than those reported for the Sogndal catchments; and (*ii*) ELA treatments resulted in exposure to solutions 3.5× (1989) and 11.5× (1990) higher in ionic strength than those from natural snowmelt; this exposure is much higher than the Norwegian experiment where solutions were approximately 2.1× higher in ionic strength. Therefore, the salt effect in the ELA catchments would be greater.

Fig. 6. Natural gibbsite (May et al. 1979) saturation indices for 1989 and 1990 runoff waters (spring and early growing season) from catchments U1, U3, and U4. Positive values indicate a solution oversaturated with respect to natural gibbsite, whereas negative values indicate undersaturation. Values near zero indicate an equilibrium condition.

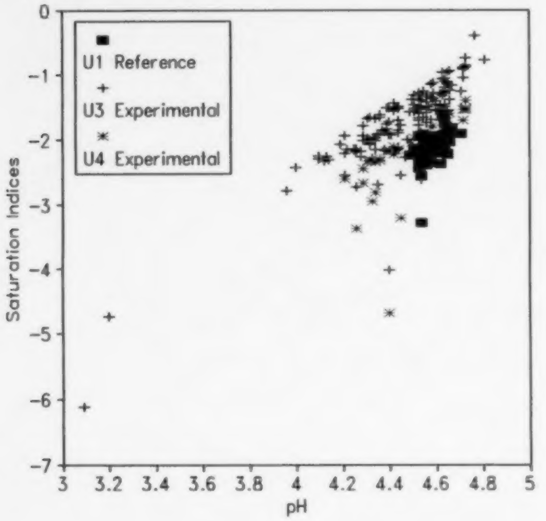

Aluminum solubility controls

Natural runoff waters from the study catchments were almost always undersaturated with respect to $Al(OH)_3$ mineral-solubility controls (Allan et al. 1993; Allan and Roulet 1994*b*). Runoff Al^{3+} concentrations measured from the manipulated catchments were also highly undersaturated with respect to $Al(OH)_3$ mineral-solubility controls (Fig. 6). Episodic and persistent $Al(OH)_3$ undersaturation has often been observed during snowmelt in large stream and lake systems in eastern Canada (Campbell et al. 1992), Scandinavia (Sullivan et al. 1986; Seip et al. 1989), and the northeastern U.S.A. (Driscoll and Schafran 1984; Hooper and Shoemaker 1985). Disequilibrium with $Al(OH)_3$ during snowmelt is caused by changes in hydrologic flow path that result in either runoff being routed through organic soils where humic-absorbent complexes control Al solubility, or the depletion of labile soil Al during high flow periods, or both. Allan and Roulet (1994*b*) found that dissolved Al^{3+} concentrations in runoff waters were controlled by both humic adsorption complexes and kinetic constraints resulting from the combination of short water-residence times and slow dissolution kinetics of aluminosilicate minerals on bedrock surfaces. Some degree of undersaturation during snowmelt may be expected because of the widespread occurrence of Horton and saturation overland flow resulting in minimal solution and surface contact during peak snowmelt periods. However, runoff waters from the manipulated catchments remained consistently undersaturated with respect to $Al(OH)_3$ minerals during the latter stages of snowmelt and the early post-snowmelt period when prolonged solution and surface contact had occurred. In addition, leachates from acid soil-leaching solutions and acid-leached natural bedrock surfaces were consistently undersaturated with respect to $Al(OH)_3$ solubility controls (Allan and Roulet 1994*b*). Clearly, the use of a mineral $Al(OH)_3$ solubility control to predict the response of dissolved Al concentrations to increased inputs of strong acids would lead to an overprediction of Al export from ELA upland catchments.

The increase of IAl from the ELA catchments was lower (30–80%) than that exhibited by the Sogndal catchments (100–300%; Frogner 1990). Aluminum solubility behavior also differed. During the first and fourth year of H_2SO_4 additions at Sogndal, IAl concentrations reflected an apparent $Al(OH)_3$ solubility control corresponding to natural gibbsite (Wright et al. 1988). Data from the second and third year of the H_2SO_4 additions at Sogndal are similar to the ELA results in that IAl concentrations were lower and undersaturated with respect to $Al(OH)_3$ minerals. Increased dissolution rates in 1984 and 1987 at Sogndal were attributed to the dissolution of $Al(OH)_3$ precipitates on streambed surfaces. These Al-rich deposits apparently are absent in upland drainage channels at the ELA, where organic acidity maintained low runoff pHs despite the degassing of oversaturated soil solutions (Allan et al. 1993).

Organic acid buffering

It has been suggested (Davis et al. 1985; Krug 1989) that, for aquatic and terrestrial systems acidified by mineral acids, a change in pH will be buffered by the protonation of weak organic acids and a concurrent loss of DOC through the flocculation of organic matter. Buffering of the added H^+ by the protonation of organic acids resulted in a measurable (11–34%) reduction in $RCOO^-$ during snowmelt. On an annual basis, the decline in $RCOO^-$ was only marginally significant for U4 during 1989 (Table 4). Mineral-acid buffering by the protonation of organic acids was less important than SO_4^{2-} retention or ion-exchange reactions in the ELA catchments. In addition, significant pH depressions occurred during snowmelt despite organic acid buffering.

The charge density of approximately 5.6 $\mu equiv \cdot mg^{-1} \cdot C^{-1}$ was similar to the range (3–5.5 $\mu equiv \cdot mg^{-1} \cdot C^{-1}$) of charge density values reported for several studies in northeastern North America and Scandinavia (summarized by Kahl et al. 1989, and Wright 1989). The buffering capacity of 0.4–2.0 $\mu equiv \cdot mg^{-1}$ DOC observed during snowmelt was similar to the 2.0 $\mu equiv \cdot mg^{-1}$ DOC reported for a brown-water stream in New Hampshire acidified with H_2SO_4 (Hedin et al. 1990) and slightly lower than the approximate 3.6 $\mu equiv \cdot mg^{-1}$ TOC reported by Wright (1989) and Wright et al. (1993) for the RAIN catchment in southern Norway.

Conclusions

In summary, ELA upland runoff water quickly and dramatically reflected springtime chemical additions. Additions of H_2SO_4 commonly resulted in levels of runoff IAl and acidity that have been identified as toxic to aquatic biota (Muniz and Leivestad 1980; Driscoll et al. 1980; Baker and Schofield 1982). Concentrations of Al^{3+} increased approximately 30–80% over pretreatment levels. Increases in Al^{n+} and other cations were attributed to ion-exchange reactions and (or) the incongruent dissolution of aluminosilicate minerals. Aluminum hydroxide minerals did not appear to control Al^{3+} concentrations in ELA runoff waters.

Sulphate adsorption was the primary acid-neutralization mechanism in the manipulated catchments, similar to the acidified Sogndal catchments, but its importance varied among years and catchments. Increased cation transport was the second most important mechanism for neutralizing strong acidic inputs. The magnitude of the increase in cation export differed by a factor of 1.7–1.9 between U3 and U4 and was inversely proportional to the importance of SO_4^{2-} retention. Allan et al. (1993) found that ELA catchments strongly sequestered cations and N in the individual forested soil islands. Increased cation losses from acid deposition combined with increased fertilization from enhanced N inputs may further exacerbate the cation deficiency. Alternatively, an increase in the supply of cations from increased weathering or ion-exchange reactions may also stimulate forest growth. This would result in more acidic runoff and higher Al export as cations are exchanged for protons by the aggrading vegetation.

The protonation of weak organic acids did not result in a significant decrease in DOC export. Despite some protonation of weak organic acids, SO_4^{2-} retention, and increased cation export, pH depressions on the order of 0.3–1.4 pH units occurred in runoff waters from treatment catchments. Ammonium nitrate additions were efficiently retained. However, significant NO_3^- losses occurred during periods of high discharge.

Acknowledgments

I thank A. Dufrense, S. Hardill, H. Ziervogel, D. Cruikshank, R. Geater, G. Holmes, and A. Bordeleau for field and laboratory assistance during this study. I also acknowledge the support and assistance of other staff of the Department of Fisheries and Oceans at the Experimental Lakes Area and the Freshwater Institute. Comments by N. Roulet, R. Hesslein, G. McCullough, B. LaZerte, D. Rosenberg, and an anonymous reviewer greatly improved earlier versions of the manuscript. Financial assistance for the project was provided by the Ontario Ministry of the Environment, the Department of Fisheries and Oceans, and the National Science and Engineering Research Council (grant to N.T. Roulet and York University).

References

Allan, C.J. 1993. The hydrology and biogeochemistry of low order Precambrian Shield catchments. Ph.D. thesis, York University, North York, Ont.

Allan, C.J., and N.T. Roulet. 1994*a*. Runoff generation in zero order Precambrian Shield catchments: the stormflow response of a heterogeneous landscape. Hydrol. Processes, 8: 369–388.

Allan, C.J., and N.T. Roulet. 1994*b*. Solid phase controls of dissolved aluminum within upland Precambrian Shield catchments. Biogeochemistry, 26: 85–114.

Allan, C.J., N.T. Roulet, and A.R. Hill. 1993. The biogeochemistry of pristine, upland Precambrian Shield catchments: an analysis of material cycling in a heterogeneous landscape. Biogeochemistry, 22: 37–79.

Baker, J.P., and C.L. Schofield. 1982. Aluminum toxicity to fish in acid waters. Water Air Soil Pollut. 18: 289–309.

Barrie, L.A., and A. Sirois. 1986. Wet and dry deposition of sulphates and nitrates in eastern Canada: 1979–1982. Water Air Soil Pollut. 30: 303–310.

Bayley, S.E., D.H. Vitt, R.W. Newbury, K.G. Beaty, R. Behr, and C. Miller. 1987. Experimental acidification of a *Sphagnum*-dominated peatland: first year results. Can. J. Fish. Aquat. Sci. 44(Suppl. 1): 194–205.

Beaty, K.J., and M.E. Lyng. 1989. Hydrometeorological data for the Experimental Lakes Area, northwestern Ontario, 1982 to 1987. Can. Data Rep. Fish. Aquat. Sci. No. 759.

Campbell, P.G.C., H.J. Hansen, B. Dubreuil, and W.O. Nelson. 1992. Geochemistry of Quebec North Shore salmon rivers during snowmelt: organic acid pulse and aluminum mobilization. Can. J. Fish. Aquat. Sci. 49: 1938–1952.

Canadian Soil Survey Committee Subcommittee on Soil Classification. 1978. The Canadian system of soil classification. Can. Dep. Agric. Publ. No. 1646. Supply and Services Canada, Ottawa.

Chew, H., L.M. Johnston, D. Craig, and K. Inch. 1988. Aluminum contamination of groundwater: spring melt in Chalk River and Turkey Lakes watersheds — preliminary results. Can. J. Fish. Aquat. Sci. 45(Suppl. 1): 66–71.

Christophersen, N., H.M. Seip, and R.F. Wright. 1982. A model for streamwater chemistry at Birkenes, Norway. Water Resour. Res. 18: 977–996.

Cosby, B.J., R.F. Wright, G.M. Hornberger, and J.N. Galloway. 1985. Modelling the effects of acid deposition: assessment of a lumped parameter model of soilwater and streamwater chemistry. Water Resour. Res. 21: 51–63.

Davis, R.B., D.S. Anderson, and F. Berge. 1985. Paleolimnological evidence that lake acidification is accompanied by loss of organic matter. Nature (London), 316: 436–438.

Devito, K.J., P.J. Dillon, and B.D. LaZerte. 1989. Phosphorus and nitrogen retention in five Precambrian Shield wetlands. Biogeochemistry, 8: 185–204.

Driscoll, C.T., and G.C. Schafran. 1984. Characterization of short-term changes in the base neutralizing capacity of an acidic Adirondack, N.Y., lake. Nature (London), 310: 308–310.

Driscoll, C.T., J.P. Baker, J.J. Bisogni, and C.L. Schofield. 1980. Effect of aluminum speciation on fish in dilute acid waters. Nature (London), 284: 161–164.

Edwards, P.J., J.N. Kochenderfer, and D.W. Seegrist. 1991. Effects of forest fertilization on stream water chemistry in the Appalachians. Water Resour. Bull. 27: 265–274.

Frogner, T. 1990. The effect of acid deposition on cation fluxes in artificially acidified catchments in western Norway. Geochim. Cosmochim. Acta, 54: 769–780.

Hedin, L.O., G.E. Likens, K.M. Postek, and C.T. Driscoll. 1990. A field experiment to test whether organic acids buffer acid deposition. Nature (London), 345: 798–800.

Hooper, R.P., and C.A. Shoemaker. 1985. Aluminum mobilization in an acidic headwater stream: temporal variation and mineral dissolution equilibria. Science (Washington, D.C.), 229: 463–465.

Johannessen, M., and A. Henriksen. 1978. Chemistry of snow meltwater: changes in concentration during melting. Water Resour. Res. 14: 615–619.

Johnson, D.W., and D.W. Cole. 1980. Anion mobility in soils: relevance to nutrient transport from forest ecosystems. Environ. Int. 3: 79–80.

Johnson, N.M., C.T. Driscoll, J.S. Eaton, G.E. Likens, and W.H. McDowel. 1981. 'Acid rain', dissolved aluminum and chemical weathering at the Hubbard Brook Experimental Forest, New Hampshire. Geochim. Cosmochim. Acta, 45: 1421–1437.

Kahl, J.S., S.A. Norton, R.K. MacRae, T.A. Haines, and

R.B. Davis. 1989. The influence of organic acidity on the acid–base chemistry of surface waters in Maine, USA. Water Air Soil Pollut. 46: 221–233.

Krug, E.C. 1989. Assessment of the theory and hypotheses of the acidification of watersheds. Ill. State Water Surv. Rep. Invest. No. 457.

Langdon, S., and M.J. Wilson. 1992. Predicting the regional occurrence of acid surface waters in Scotland using an approach based on geology, soils, and land use. J. Hydrol. (Amsterdam), 138: 515–528.

Lawrence, G.B., C.T. Driscoll, and R.D. Fuller. 1988. Hydrologic control of aluminum chemistry in an acidic headwater stream. Water Resour. Res. 24: 659–669.

LaZerte, B.D., C. Chun, D. Evans, and F. Tomassini. 1988. Measurement of aqueous aluminum species: comparison of dialysis and ion exchange techniques. Environ. Sci. Technol. 22: 1106–1108.

May, H.M., P.A. Helmke, and R. Jackson. 1979. Gibbsite solubility and thermodynamic properties of hydroxyaluminum ions in aqueous solutions at 25°C. Geochim. Cosmochim. Acta, 43: 861–868.

Muniz, I.P., and H. Leivestad. 1980. Toxic effects of aluminum on the brown trout, *Salmo trutta* L. *In* Ecological impact of acid precipitation. *Edited by* D. Drabløs, and A. Tollan. Proceedings of International Conference, Sandefjord, Norway, March 1980. SNSF Project, Oslo, Norway. pp. 320–321.

Reuss, J.O., and D.W. Johnson. 1986. Acid deposition and the acidification of soils and waters. Ecol. Stud. Anal. Synth. 59: 25–31. Springer-Verlag, New York.

Rochelle, B.P., M.R. Church, and M.B. David. 1987. Sulphur retention at intensively studied sites in the U.S. and Canada. Water Air Soil Pollut. 33: 73–83.

Schecher, W.D., and C.T. Driscoll. 1987. An evaluation of the uncertainty associated with Al equilibrium calculations. Water Resour. Res. 23: 525–534.

Schindler, D.W., R. Wagemann, R.B. Cook, T. Ruszczynski, and J. Prokopowich. 1980. Experimental acidification of Lake 223, Experimental Lakes Area: background data and the first three years of acidification. Can. J. Fish. Aquat. Sci. 37: 342–354.

Seip, H.M., D.O. Andersen, N. Christophersen, T.J. Sullivan, and R.D. Vogt. 1989. Variations in concentrations of aqueous aluminum and other chemical species during hydrological episodes at Birkenes, southernmost Norway. J. Hydrol. (Amsterdam), 108: 387–405.

Stainton, M.P., M.J. Capel, and F.A.J. Armstrong. 1977. The chemical analysis of fresh water. Can. Fish. Mar. Serv. Misc. Spec. Publ. No. 25.

Strickland, T.C., and J.W. Fitzgerald. 1984. Formation and mineralization of organic sulphur in forest soils. Biogeochemistry, 1: 79–95.

Sullivan, T.J., N. Christophersen, I.P. Muniz, H.M. Seip, and P.D. Sullivan. 1986. Aqueous aluminum chemistry: response to episodic increases in discharge at Birkenes, southern Norway. Nature (London), 323: 324–327.

Tabatabai, M.A., and W.A. Dick. 1983. Simultaneous determination of nitrate, chloride, sulphate, and phosphate in natural waters by ion chromatography. J. Environ. Qual. 12: 209–213.

Ulrich, B. 1980. Production and consumption of hydrogen ions in the ecosphere. *In* Proceedings from NATO Advanced Research Institute Conference on Effects of Acid Precipitation on Terrestrial Ecosystems. *Edited by* T.C. Hutchinson, and M. Havas. Plenum Press, New York. pp. 255–282.

Vitt, D.H. 1991. Patterns of growth of the drought tolerant moss, *Racomitrium microcarpon*, over a three year period. Lindbergia, 15: 181–187.

Wright, R.F. 1989. RAIN project: role of organic acids in moderating pH change following reduction in acid deposition. Water Air Soil Pollut. 46: 251–259.

Wright, R.F., E. Lotse, and A. Semb. 1988. Reversibility of acidification shown by whole-catchment experiments. Nature (London), 334: 670–675.

Wright, R.F., E. Lotse, and A. Semb. 1993. RAIN project: results after 8 years of experimentally reduced acid deposition to a whole catchment. Can. J. Fish. Aquat. Sci. 50: 258–268.

Experimental acidification of a poor fen in northwestern Ontario: effects on emergence of Chironomidae (Diptera)[1]

David M. Rosenberg, Allen P. Wiens, Bohdan Bilyj, and Llwellyn Armstrong

Abstract: The effects of experimental acidification and N fertilization on chironomid emergence from a poor fen in northwestern Ontario were studied from 1984 to 1989. Experimental treatments did not affect the numbers of chironomids emerging weekly, the timing of emergence, or species composition of emergence during the study period. Weekly emergence counts were higher ($P < 0.05$) from the periphery of the fen than the central part. Total seasonal emergence was higher from the area previously burned in a forest fire than the unburned part of the fen, although the difference was not statistically significant. Stability of species composition, despite experimental treatments and physiographic differences in the fen, may be a widespread characteristic of Canadian acidic peatlands.

Résumé : Entre 1984 et 1989, on a étudié les effets expérimentaux de l'acidification et de la fertilisation azotée sur l'émergence des chironomidés dans une tourbière minérotrophe pauvre en éléments nutritifs du nord-ouest de l'Ontario. Les traitements expérimentaux n'ont pas eu d'incidence sur le nombre de chironomidés émergés par semaine, le moment de l'émergence ni la composition spécifique des individus ayant émergé pendant la période de l'étude. Les dénombrements de chironomidés émergés par semaine étaient supérieurs ($P < 0{,}05$) en périphérie de la tourbière comparativement à la partie centrale. L'émergence saisonnière totale était supérieure dans la partie brûlée antérieurement au cours d'un incendie de forêt par rapport à la partie non touchée de la tourbière, bien que cette différence ne soit pas significative sur le plan statistique. La stabilité de la composition spécifique semble être une caractéristique répandue des tourbières acides du Canada, malgré les traitements expérimentaux et les différences géomorphologiques dans la tourbière.

[Traduit par la Rédaction]

Introduction

Peatlands cover more than 100 × 10^6 ha of Canada yet they are poorly known faunistically (Danks and Rosenberg 1987; Rosenberg et al. 1988; Zoltai 1988). Likewise, the effects of acid precipitation on the fauna of these habitats have been virtually ignored (Gorham et al. 1984; Bayley et al. 1987). The experimental acidification of a poor fen[3] in the Experimental Lakes Area (ELA) of northwestern Ontario, which was intended to determine the effects of known concentrations of sulphate, nitrate, and hydrogen ion on vegetation and water chemistry (Bayley et al. 1987), provided an opportunity to study the effects of acid precipitation on the emergence of Chironomidae from a peatland habitat.

Study site

The Lake 239 fen (49°40′N, 93°43′W), which covers 3.67 ha, is a typical peatland for this part of the Canadian Shield (Vitt and Bayley 1984). Its tree layer is predominantly *Picea mariana*; the shrub layer is *Chamaedaphne calyculata* and *Ledum groenlandicum*; the herb layer is *Smilacina trifolia* and *Carex trisperma*; and the ground

Received July 27, 1993. Accepted April 28, 1995.
J12022

D.M. Rosenberg, A.P. Wiens, and B. Bilyj.[2] Department of Fisheries and Oceans, Central and Arctic Region, Freshwater Institute, 501 University Crescent, Winnipeg, MB R3T 2N6, Canada.
L. Armstrong. Statistical Advisory Service, University of Manitoba, Winnipeg, MB R3T 2N2, Canada.

---

[1] This paper is one of a series done in honour of the 25th anniversary of the Experimental Lakes Area.

[2] Present address: BIOTAX, 12 Westroyal Road, Weston, ON M9P 2C3, Canada.

[3] Mitsch and Gosselink (1986, pp. 291–292) identify poor fens as transition peatlands that "...are intermediate between mineral-nourished (minerotrophic) and precipitation-dominated (ombrotrophic) peatlands." Minerotrophic peatlands are true fens that receive water that has passed through mineral soil, whereas ombrotrophic peatlands are true raised bogs that receive nutrients and other minerals exclusively by precipitation.

Can. J. Fish. Aquat. Sci. **52**: 2229–2237 (1995). Printed in Canada / Imprimé au Canada

Fig. 1. Schematic drawing of the Lake 239 fen showing salient physiographic and experimental features. Shaded area represents the minerotrophic zone as identified by Bayley et al. (1987); cross-hatching represents the area to which NH_4NO_3 was applied; A, acid-mixing site.

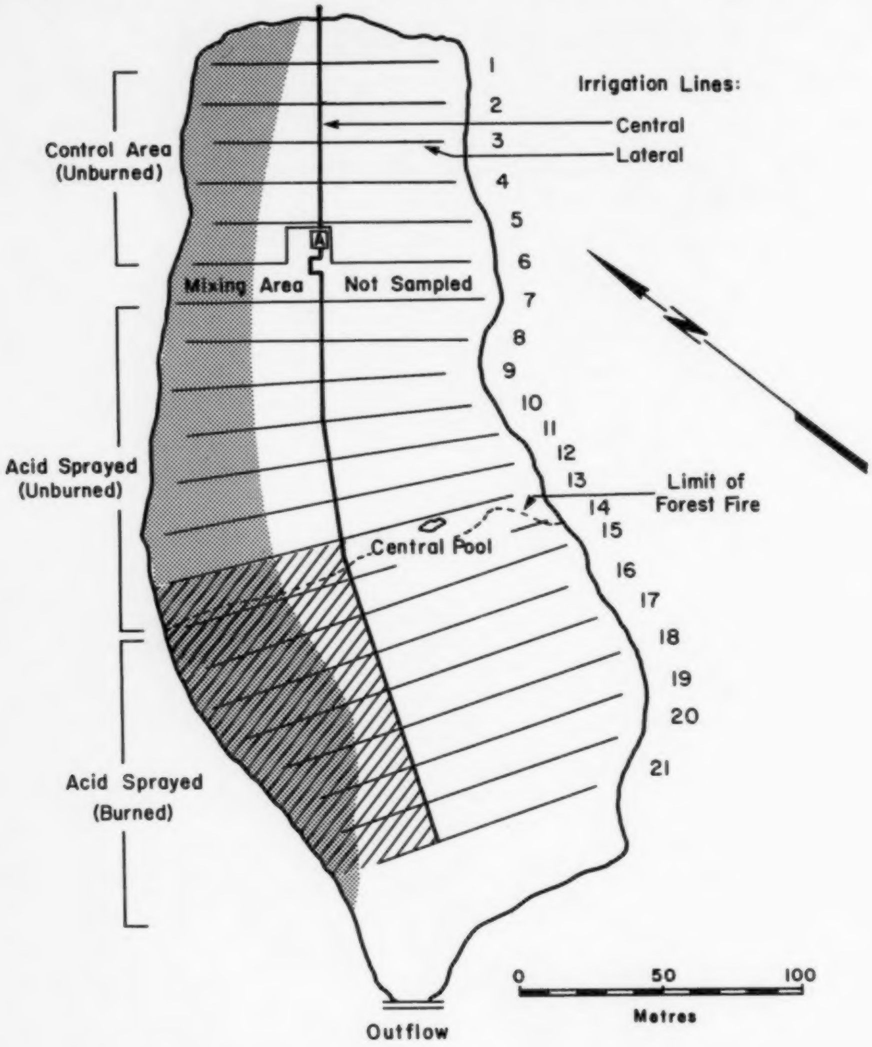
Irrigation Lines:
Central
Lateral
Control Area (Unburned)
A
Mixing Area
Not Sampled
Acid Sprayed (Unburned)
Acid Sprayed (Burned)
Central Pool
Limit of Forest Fire
N
1
2
3
4
5
6
7
8
9
10
11
12
13
14
15
16
17
18
19
20
21
0
50
100
Metres
Outflow

layer is *Sphagnum angustifolium* and *Sphagnum magellanicum* (Bayley et al. 1987). Bayley et al. (1987) described a minerotrophic zone (1.26 ha) along the western edge of the fen; the remaining 2.41 ha of the fen was considered to be oligotrophic but not ombrotrophic. pH averaged 4.45 and 4.09 in the surface water of the minerotrophic and oligotrophic zones, respectively (Rochefort et al. 1990). The southern 41% of the fen burned in 1974 (Fig. 1).

The upper third of the fen (0.85 ha) was kept as a control area, whereas the lower two thirds (2.66 ha) became the treatment area. Because of differences in vegetation between the burned and unburned parts of the treatment area (see Figs. 2 and 3 in Vitt and Bayley 1984) and differences in total seasonal emergences obtained in the first year of the study (see below), the treatment area was subsequently subdivided into approximately equal parts (Fig. 1).

Methods

Acidification

The intent of the experiment was to lower the pH of precipitation on the fen from the long-term natural average of 4.9 to 4.0, the level of most acid precipitation in the eastern United States and Canada (Bayley et al. 1987). The target pH was reached by using a mixture of equal amounts of concentrated H_2SO_4 and HNO_3. Treatment rates represented an annual supplement to atmospheric deposition of 0.5 $g{\cdot}m^{-2}{\cdot}yr^{-1}$ of NO_3^--N and 2.0 $g{\cdot}m^{-2}{\cdot}yr^{-1}$ of SO_4^{2-}.

Fig. 2. Schematic diagram of the changing design of emergence collections from the Lake 239 fen. See text for explanation of emergence trap allocations.

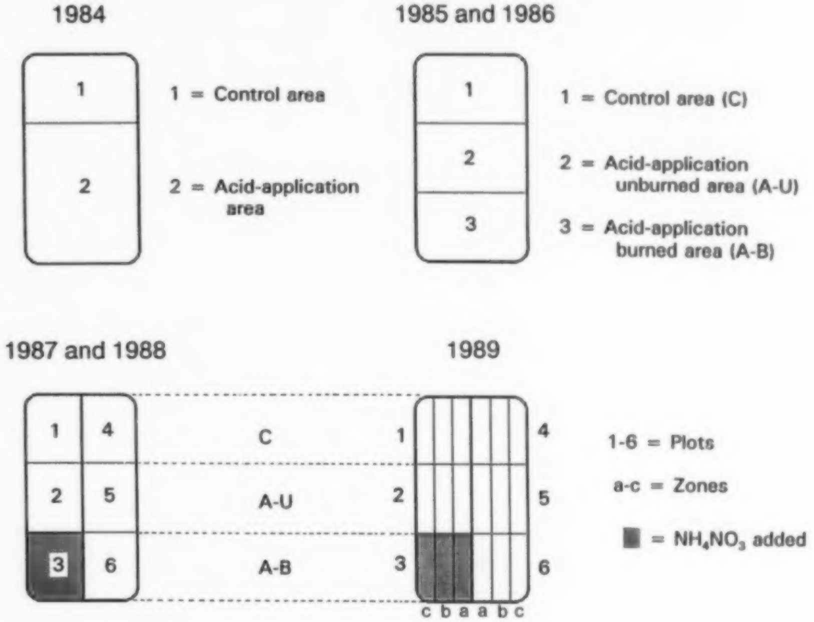

Natural atmospheric deposition and runoff from the adjacent upland watershed also provided N and S to the fen. The mean annual concentration applied experimentally was 6.8 $mg·L^{-1}$ of NO_3^--N and 26.9 $mg·L^{-1}$ of SO_4^{2-} (Rochefort et al. 1990).

A grid of irrigation pipes and sprinklers was used to create the acid rain events (Fig. 1). Plain lake water was applied to the control area, whereas the acid mixture was applied to the treatment part of the fen. Five-hour irrigations were carried out monthly from May to October for the duration of the study (1984–1989). From 1987 to 1989, additional N (1.5 g $N·m^{-2}·yr^{-1}$) was added in the form of NH_4NO_3 to the southwestern quarter of the treatment area (lateral irrigation lines 13W–21W). The frequency and duration of NH_4NO_3 irrigations matched those for the acids. Details of the applications can be found in Bayley et al. (1987) and Beaty (1987).

Emergence

Insect emergence from the sphagnum ground layer was sampled using a modified version of the model "week" trap of LeSage and Harrison (1979) (basal area: 0.5 m^2). Emerging insects fly up through the pyramidal base of the trap, enter the collecting head at the top, and fall into a jar containing preservative (ethylene glycol) attached to the collecting head. The traps capture a variety of semi-aquatic and terrestrial insects.

The trapping season lasted from the first week of May, when the fen thawed, to the first week of September, when emergence had virtually ceased. Traps were cleared weekly and were randomly moved to nearby locations every 2 wk to avoid shading effects on the sphagnum.

Design of the fen study changed as the habitat became better known and understood, and as additional chemical treatments were applied (Fig. 2). From 1984 to 1986, a total of 15 randomly placed traps was used: 5 in the control area (C) and 10 in the acid-application area in 1984; and 5 each in the control area, acid-application unburned area (A–U), and acid-application burned area (A–B) in 1985 and 1986. The 1984 emergence data from the treatment area were retroactively separated into A–U and A–B portions, to the extent possible, for all subsequent data treatments, except the statistical analyses (see below). The NH_4NO_3 additions that began in 1987 and continued through to 1989 required a further alteration in sampling design: six traps were placed in each of the C, A–U, and A–B areas but half were randomly assigned to the west of the centre line and half were randomly assigned to the east; this created six plots. Finally, identification of a minerotrophic zone along the western edge of the fen (Bayley et al. 1987) led to further subdivision in 1989 of the fen into six approximately equal north–south zones; traps were randomly assigned to each zone within each plot.

Weekly counts (no.$·m^{-2}$) from each trap were used in the statistical analyses (see below). Weekly counts from each trap were summed over the trapping season and averaged for C, A–U, and A–B areas of the fen to yield total emergence (TE; mean no.$·m^{-2}·yr^{-1}$). Species of adult chironomids were identified for all years of the study except 1989.

Data analysis

Examination of the weekly count data for significant treatment effects required an adaptive analysis of variance (ANOVA) approach (Table 1) that partitioned variance

Table 1. Analyses of variance done on the 1984–1989 weekly counts of chironomid emergence from the Lake 239 fen.

Date	SAS mixed model statement[a]
1984	lnbugs = trmt trap(trmt) week trmt×week
1985 and 1986	lnbugs = trmt year trmt×year trap(trmt×year) week trmt×week year×week trmt×year×week
1987 and 1988	lnbugs = plot year year×plot trap(year×plot) week plot×week year×week year×plot×week
1989	lnbugs = plot zone plot×zone week plot×week zone×week

Note: lnbugs, ln (weekly counts of chironomids + 1); trmt, treatments (control and acid-application areas) as shown in Fig. 2, 1984–1986. trmt becomes plot in 1987–1989 analyses (Fig. 2).

[a] Trap effects were considered as random; all other effects were considered as fixed.

Table 2. Total emergences (TEs) of Chironomidae from the Lake 239 fen.

	TEs (no.·m^{-2}·yr^{-1})		
Date	Control	Acid–Unburned	Acid–Burned
1984	1384.0±729.3	1534.4±484.4	1780.0±804.1
1985	860.6±407.8	859.8±412.3	1051.0±421.0
1986	492.8±248.3	402.4±162.1	695.8±711.6
1987	769.0±295.5	453.3±346.9	958.3±491.3[a]
1988	415.2±183.3	567.7±222.5	666.7±405.3
1989	656.7±495.8	556.7±161.3	641.0±279.1

Note: All values given in mean ± SD.

[a] Plot 6 corrected to exclude mass emergence of *Micropsectra tori* Säw. into one trap during week of June 1.

Table 3. Significant results ($P \leq 0.05$) from SAS mixed model ANOVAs done on weekly chironomid emergence data from the Lake 239 fen.

Date	Factors	$P > F$
1984	trap(trmt)	0.0001
	week	0.0001
1985 and 1986	year	0.0002
	trap(trmt×year)	0.0001
	week	0.0001
1987 and 1988	plot	0.0261
	trap(year×plot)	0.0065
	year×week	0.0001
1989	zone	0.0001
	plot×week	0.0244

Note: See Table 1 for explanation of trmt.

Table 4. Total emergence (no.·m^{-2}) of Chironomidae from zones *a*, *b*, and *c* of the Lake 239 fen in 1989.

	Zone		
Plot	*a*	*b*	*c*
1	568	296	1438
2	616	448	780
3	970	736	558
4	264	284	1090
5	472	348	676
6	300	368	914

Note: Counts are for single traps over a period of 18 wk. See Fig. 2 for a description of plots and zones.

according to the sampling and treatment changes implemented over the course of the study. Analyses were done using the SAS Institute Inc. (1989) General Linear Models (GLM) procedure on log-transformed ($\ln (x + 1)$) weekly counts (see above) and the data were examined for conformance with the assumptions required for ANOVA.

The experimental design of the parent study presented the chironomid emergence study with little option but to pseudoreplicate (sensu Hurlbert 1984). Therefore, although ANOVA was used in the data analysis, in a strict sense statistical differences between control and treatment areas cannot be attributed to treatment effects. Significant differences demonstrate only that the chironomid community did not show parallel trends in control and treatment areas, although departure from these parallel trends coincident with treatment would imply an effect resulting from acidification. Verification of this effect would require true replication.

Year-to-year changes in species composition of emergence were assessed using Kendall's tau (Siegel 1956; Ghent 1963; Wilkinson 1986). Only the species considered to be true peatland fauna by Rosenberg et al. (1988) were used in these comparisons.

Results

Total emergence

Total annual emergences (TEs) ranged from approximately 400 to 1800·m^{-2} over the 6-yr study period and were higher from A–B than from the other areas in all years except 1989 (Table 2).

Fig. 3. Seasonal curves of chironomid emergence from control, acid-application unburned, and acid-application burned areas of the Lake 239 fen for the duration of the study (1984–1989). Weekly data points are simple means of counts of traps in each area.

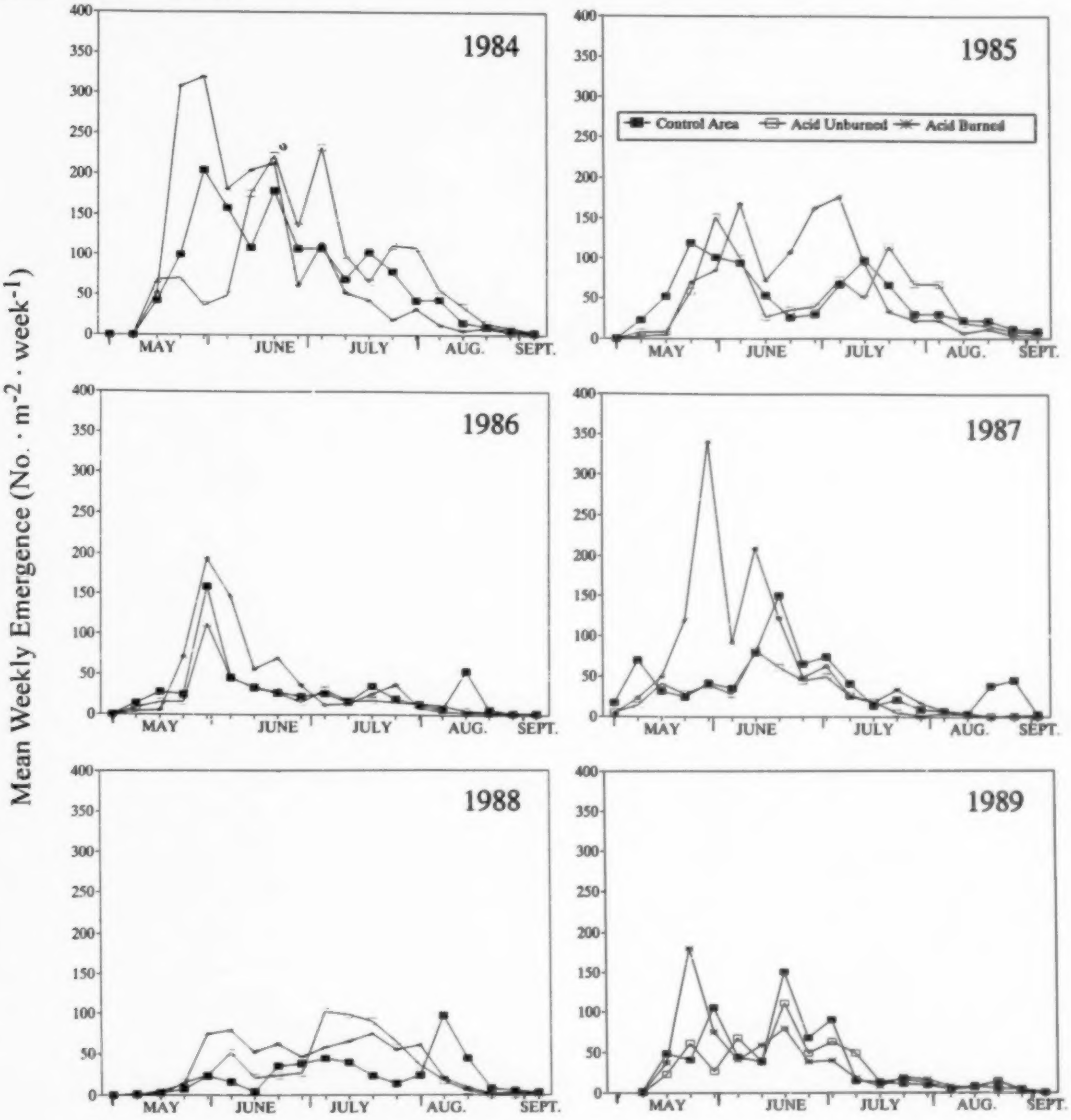

Statistical analyses of weekly counts

SAS Institute Inc. (1989) analyses of residuals indicated that variances were homogeneous and that data were normally distributed in each of the four ANOVAs done.

Most of the significant results of the ANOVAs, either main effects or interactions, appeared to be caused by trap-to-trap variability within year and treatment conditions and temporal differences in emergence rather than by treatment effects (Table 3). Differences among traps were significant in the 1984, 1985 and 1986, and 1987 and 1988 analyses (Table 3). Intertrap differences were not tested in 1989 because only one trap was available in each zone of each plot (Fig. 2, Table 1). Temporally, significant weekly differences in emergence occurred in all four ANOVAs and significant yearly differences occurred in the two multiyear analyses; 1985 had higher emergences than 1986, and 1987 had higher emergences than 1988 (Fig. 3). The significant year×week interaction term in the 1987 and 1988 data resulted from higher counts early and late in the 1987 season, but higher counts in midseason in 1988 (Fig. 3).

Significant treatment effects caused by either acid or NH_4NO_3 application were not evident. In the 1987 and

Table 5. Rankings of the 10 most abundant species of Chironomidae emerging from the Lake 239 fen, 1984–1988 (—, not ranked in top 10 species).

	Total emergences (TEs; mean no.·m^{-2}·yr^{-1}) and rank									
	1984		1985		1986		1987		1988	
	TE	Rank	TE	Rank	TE	Rank	TE	Rank	TE	Rank
Gymnometriocnemus (*R.*) *brumalis* (Edw.)[a]	643.7	1	265.7	1	232.4	1	153.4	2	127.8	2
Limnophyes minimus (Meig.)	413.2	2	202.0	2	88.3	2	128.7	4	41.9	5
Doithrix villosa Saeth. and Subl.	215.8	3	158.6	3	29.2	4	141.2	3	190.6	1
Pseudorthocladius (s.str.) *destitutus* Saeth. and Subl.	111.5	4	67.7	4	16.4	8	32.5	6	22.3	6
Corynoneura miniscula Brund.	76.8	5	—	—	—	—	—	—	—	—
Pseudorthocladius (s.str.) *curtistylus* (Goetgh.)	65.0	6	22.3	9	25.2	6	30.3	7	72.8	3
Pseudosmittia forcipata (Goetgh.)	60.8	7	45.2	5	22.7	7	24.0	9	10.7	8
Smittia nr. *nudipennis* Goetgh.	45.8	8	37.8	6	28.3	5	35.4	5	42.0	4
Paramerina nr. *smithae* Subl. (dark form)	21.8	9	24.3	8	30.1	3	—	—	—	—
Pseudorthocladius (s.str.) *uniserratus* Saeth. and Subl.	14.1	10	—	—	—	—	27.6	8	13.0	7
Limnophyes nr. *minimus* (Meig.)	—	—	16.4	10	—	—	—	—	—	—
Paraphaenocladius exagitans (Joh.)	—	—	—	—	—	—	9.6	10	7.2	9
Micropsectra tori Säw.[b]	—	—	30.6	7	13.3	9	156.2	1[c]	—	—
Micropsectra nr. *insignilobus* Kieff.	—	—	—	—	11.7	10	—	—	—	—
Gymnometriocnemus (s.str.) *subnudus* (Edw.)[d]	—	—	—	—	—	—	—	—	2.9	10

Note: 1989 material was not identified.

[a] As *G.* (*R.*) *acigus* Saeth. in Rosenberg et al. (1988).

[b] As *M.* nr. *xantha* (Rob.) in Rosenberg et al. (1988); new North American record.

[c] Caused by mass emergence into one trap during week of June 1.

[d] As *G.* (s.str.) *marionensis* Saeth. in Rosenberg et al. (1988).

1988 analysis, the significant plot effect (Table 3) was caused by plot 5 (Fig. 2), which had much lower numbers emerging in 1987 than from the other five plots. In 1989, the effect of plot depended on the week being examined (significant plot×week interaction). Effects caused by acid application would have been manifested in plots 2, 3, 5, and 6; effects caused by NH_4NO_3 application would have appeared in plot 3 (Fig. 2).

The analyses indicated somewhat unexpected physiographic similarities and differences in emergence from the fen. First, there were no significant differences in emergence from the burned and unburned areas of the fen. Second, the significant zone effect in 1989 was caused by higher emergences of chironomids from the periphery of the fen (both zones *c*) than from its centre (zones *a* and *b*; Table 4). These results indicated that any significant differences in emergence had a physiographic rather than treatment basis.

Patterns of emergence

The annual emergence curves (Fig. 3) generally verified the importance of physiographic as opposed to treatment differences in the fen. First, acidification neither delayed nor accelerated emergence; the curves had similar shapes for all three areas. Second, acidification did not appear to affect the magnitude of emergence. The curves for the C area generally fell between those for the A–U and A–B areas, but lay closer to A–U than A–B for most of the season; moreover, emergence from the A–B area usually was greater than that from the C and A–U areas. However, the 1988 and 1989 emergence curves did not fit all of these generalizations.

Air temperatures and precipitation were highly variable from year to year (Beaty and Lyng 1989; K. Beaty, Freshwater Institute, Winnipeg, Man., personal communication) and no simple relationship was apparent between annual weather patterns and the shape of the annual emergence curves.

Effects on species

The most abundant species in the 239 fen remained relatively stable from year to year (Table 5). With a few exceptions (e.g., *Corynoneura miniscula* in 1984, *Micropsectra tori* in 1987), ranks of the seven most abundant species were similar. These species accounted for approximately 85–95% of total numbers from 1984 to 1988. Although no new peatland species were collected in 1987 and 1988 (i.e., since Rosenberg et al. 1988, which dealt with emergence from 1984 to 1986), additional species were collected that are believed to be migrants from nearby ELA lakes (Table 6).

Given the apparent stability in species composition of the fen taken as a whole, does the species composition vary according to physiographic differences (unburned vs. burned, minerotrophic vs. oligotrophic) or treatments (control vs. acidified, NH_4NO_3 application)? To answer these questions, species compositions of the C, A–U, and A–B areas, and the western and eastern halves of these areas (plots 1–6, 1987 and 1988 data only) were compared using Kendall's tau. Table 7 indicates a remarkable homogeneity

Table 6. Species of Chironomidae collected from the Lake 239 fen in 1987 and 1988 that are believed to be migrants from nearby Experimental Lakes Area lakes (see Rosenberg et al. 1988, Appendix).

Subfamily	Tribe	Species
Tanypodinae		
		Djalmabatista pulchra (Joh.)
Orthocladiinae		
		Psectrocladius (s.str.) *oligosetus* Wülk.
		Synorthocladius semivirens (Kieff.)
Chironominae	Chironomini	
		Cryptochironomus scimitarsus Town.
		Tribelos jucundum (Walk.)
	Tanytarsini	
		Constempellina brevicosta (Edw.)
		Stempellina sp.
		Stempellinella leptocelloides (Webb)
		Tanytarsus bathophilus (Kieff.)[a]
		T. recurvatus Brund.
		Tanytarsus sp. C

Note: Discrimination between true peatland species and lake species is discussed in Rosenberg et al. (1988, pp. 21, 24).

[a] New Nearctic record.

between burned and unburned regions and no detectable effect as a result of experimental acidification. Comparisons between plots 1 through 6 also yielded highly significant and similar tau values (1987: 0.43–0.61, $P < 0.001$; 1988: 0.58–0.71, $P < 0.001$), indicating that species composition of oligotrophic and putative minerotrophic areas of the fen was similar and that NH_4NO_3 application did not alter species composition.

Discussion

Effects of chemical treatments

Experimental treatment of the 239 fen with a mixture of H_2SO_4 and HNO_3 and additional application of NH_4NO_3 to the southwestern quarter of the treatment area did not affect emergence counts or species composition of chironomid emergence over the duration of the study. The lack of response by the chironomid fauna is consistent with the limited chemical changes caused by the experimental treatment (Bayley et al. 1987, 1988) and the minor increase in growth of the sphagnum in response to treatment (Rochefort et al. 1990).

A number of processes may be responsible for maintaining natural pH levels in the fen and protecting the invertebrate fauna from the short-term bursts of noxious chemicals caused by the experimental treatments. Spraying with mineral acids did not change long-term acidity in the 239 fen (Rochefort et al. 1990), although short-term (1–2 d) changes were observed (S. Bayley, University of Alberta, Edmonton, Alta., personal communication). Apparently, acid deposited at the application rates used in this experiment was buffered by the high levels of dissolved organic carbon (DOC) and organic acids in the fen. In addition, NO_3^- was rapidly removed by the fen vegetation because of N deficiency (Bayley et al. 1987; Urban et al. 1988). SO_4^{2-} was taken up by the sphagnum through ion exchange, and this was followed by sulfate reduction (Bayley et al. 1986). In the end, these processes in the fen may be creating a protective effect for sphagnum-dwelling aquatic invertebrates analogous to that produced by bacteria at the mud–water interface of acidified lakes (Rudd et al. 1986), which has been postulated to protect some species of benthic invertebrates from the effects of acidification (e.g., Grapentine and Rosenberg 1992).

Table 7. Comparison of chironomid communities emerging from three areas of the Lake 239 fen.

	Kendall's tau				
Comparison	1984	1985	1986	1987	1988
C vs. A–U	0.61**	0.58**	0.66**	0.61**	0.64**
C vs. A–B	0.55**	0.39*	0.66**	0.52**	0.65**
A–U vs. A–B	0.58**	0.49**	0.69**	0.48**	0.63**

Note: C, control; A–U, acid-application unburned; A–B, acid-application burned. H_o for Kendall's tau is that the two communities are unrelated. A significant P-level for z therefore disproves the H_o and indicates that the communities are similar.

*$0.001 < P < 0.05$.

**$P < 0.001$.

Rochefort et al. (1990) reported that decomposition rates of sphagnum species did not change in response to acid treatment. Therefore, it appears that the energy base for the chironomid community was largely unaffected, a factor that would contribute to the stability of the chironomid community.

It is possible that the levels of NO_3^- and SO_4^{2-} applied were too low or that more years of experimental acidification were needed to detect cumulative, deleterious changes to the chironomid community. Obvious changes in

Fig. 4. Weekly differences in sphagnum temperature between burned and unburned parts of the Lake 239 fen, 1987. Temperatures were taken in the morning (08:00–10:00) using a field thermometer inserted into the sphagnum halfway up a hummock; direct sunlight was avoided.

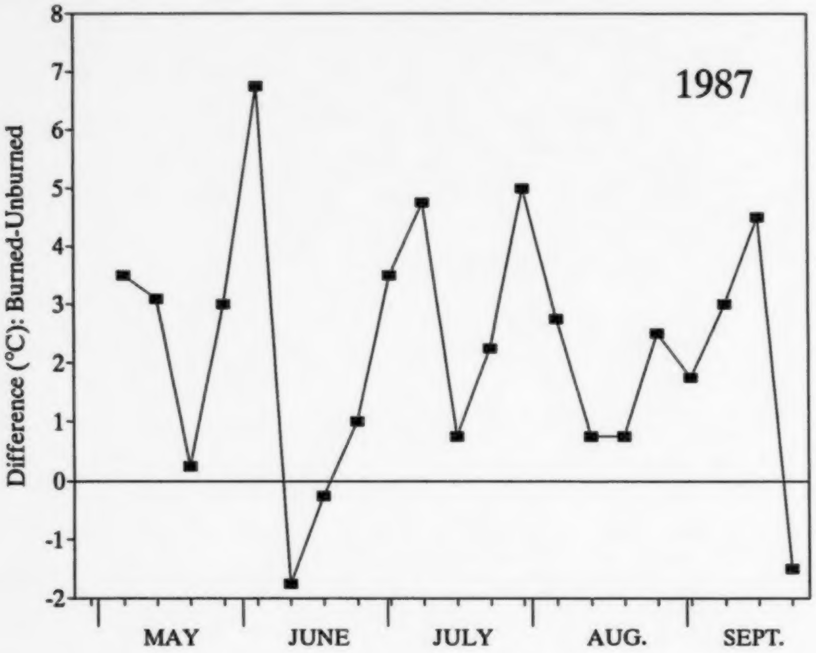

the chironomid community of experimentally acidified Lake 223 began to appear only after 6 yr of progressively greater acidification that reduced the pH from 6.5 to 5.02, although subtle community changes may have appeared just 3 yr after acidification began (Davies 1991). However, the lake and fen systems are not directly comparable because of naturally low pH in the fen and because it is difficult to alter pH when natural levels are at about 4.0. Higher dose rates resulting in a dramatic pH decline in the fen may have produced changes over the duration of this study; however, such dose rates, which would have been characteristic of Great Britain and Europe, would not have mimicked current acidic deposition rates in the United States and Canada.

Statistical variability and physiographic differences

Significant intertrap variability was probably caused by the patchy distribution of Chironomidae in the fen. For example, numbers and species richness of emerging chironomids were higher from sphagnum hollows than hummocks, perhaps because of higher moisture content in the hollows (D. Hutchison, Winnipeg, Man., unpublished data). Random placement of the traps may be reflecting the highly variable nature of the sphagnum with regard to its chironomid community. Rochefort et al. (1990) demonstrated a number of differences in ecological processes among the sphagnum species of hummocks and hollows, so differences in chironomid emergence between these two habitats is not surprising.

Strong temporal differences in emergence detected by the ANOVAs were expected. Weekly differences in emergence occur naturally over the course of a season, and year-to-year variability can be pronounced (Fig. 3).

Although TE was higher from the A–B area than from the A–U area (Table 2), this difference was not significant according to the ANOVAs done on weekly counts (Table 3). The lack of a statistically significant difference between burned and unburned parts of the fen was surprising because the fire removed much of the overstory vegetation and caused obvious differences in the appearance of the fen. A lack of mature trees resulted in greater insolation and higher summer mean temperatures in the sphagnum of the burned part of the fen than in the unburned part (Fig. 4) but this did not result in significantly higher emergence from the burned area.

Perhaps a more surprising physiographically based result was the higher emergence of Chironomidae from the periphery of the fen than from its centre (Table 4). Identification of a minerotrophic zone along the outer edge of the western half of the fen (Fig. 1), together with higher nutrient content and pH values than in the remaining oligotrophic part of the fen (Bayley et al. 1987), produced expectations of higher emergence along only the western periphery. Drainage occurs around the entire periphery of the fen but especially from the north and the southeast (see Fig. 2 in Beaty 1987). On the basis of a typical water table contour plan (see Fig. 13 in Beaty 1987), water would move preferentially from the upper to the lower part of the fen (northeast to southwest) and down the western and eastern edges rather than from the sides to the centre. High water events also could bring nutrients into the fen along the edges. These factors may be producing more favourable habitat for chironomids along the outside edge of the fen than in the centre. Whatever physiographic differences did exist in the fen, they did not affect species composition of the chironomids, which remained relatively stable from 1984 to 1988 (Tables 5 and 7).

In summary, the species composition of the chironomid community remained stable from 1984 to 1988 despite the experimental treatments applied, physiographic differences in the fen, and highly variable year-to-year differences in air temperatures and precipitation. A dearth of long-term studies of the Chironomidae in Canadian peatlands (Danks and Rosenberg 1987; Wrubleski 1987) makes it difficult to judge whether the stability in species composition of the 239 fen is a local phenomenon or if it is a widespread characteristic of acidic peatlands. Nevertheless, it is tempting to predict the latter because these peatland habitats may be inhospitable to any other than a highly specialized, acidophilic fauna.

Acknowledgments

We thank S. Bayley for her input through all stages of the study. K. Beaty provided useful data and advice, and several summer students collected samples in the field and sorted them in the laboratory. N. Anderson, S. Bayley, D. Cobb, I. Davies, S. Kasian, and D. Wrubleski reviewed drafts of the manuscript. D. Laroque did the word processing. Funding was provided by World Wildlife Toxicology Fund grants to S. Bayley and by the Department of Fisheries and Oceans.

References

Bayley, S.E., R.S. Behr, and C.A. Kelly. 1986. Retention and release of S from a freshwater wetland. Water Air Soil Pollut. 31: 101–114.

Bayley, S.E., D.H. Vitt, R.W. Newbury, K.G. Beaty, R. Behr, and C. Miller. 1987. Experimental acidification of a *Sphagnum*-dominated peatland: first year results. Can. J. Fish. Aquat. Sci. 44(Suppl. 1): 194–205.

Bayley, S., B. Parker, D. Vitt, and D. Rosenberg. 1988. Experimental acidification of a freshwater wetland. Final report. Wildlife Toxicology Fund, Winnipeg, Man.

Beaty, K.G. 1987. An irrigation system and hydrological network for a wetland acidification project. Can. Tech. Rep. Fish. Aquat. Sci. No. 1551.

Beaty, K.G., and M.E. Lyng. 1989. Hydrometeorological data for the Experimental Lakes Area, northwestern Ontario, 1982 to 1987. Can. Data Rep. Fish. Aquat. Sci. No. 759.

Danks, H.V., and D.M. Rosenberg. 1987. Aquatic insects of peatlands and marshes in Canada: synthesis of information and identification of needs for research. Mem. Entomol. Soc. Can. 140: 163–174.

Davies, I.J. 1991. Canadian freshwater biomonitoring: the programme of Fisheries and Oceans. *In* Problems of ecological monitoring and ecosystem modelling. Vol. XIII. *Edited by* Y.A. Izrael, S.M. Semenov, G.E. Insarov, V.A. Abakumov, and T.A. Golovina. USSR Academy of Sciences, Leningrad. pp. 75–78. (In Russian; English version issued as Can. Transl. Fish. Aquat. Sci. No. 5551, 1992. Freshwater Institute Reprint 1087*a*.)

Ghent, A.W. 1963. Kendall's "tau" coefficient as an index of similarity in comparisons of plant or animal communities. Can. Entomol. 95: 568–575.

Gorham, E., S.E. Bayley, and D.W. Schindler. 1984. Ecological effects of acid deposition upon peatlands: a neglected field in "acid-rain" research. Can. J. Fish. Aquat. Sci. 41: 1256–1268.

Grapentine, L.C., and D.M. Rosenberg. 1992. Responses of the freshwater amphipod *Hyalella azteca* to environmental acidification. Can. J. Fish. Aquat. Sci. 49: 52–64.

Hurlbert, S.H. 1984. Pseudoreplication and the design of ecological field experiments. Ecol. Monogr. 54: 187–211.

LeSage, L., and A.D. Harrison. 1979. Improved traps and techniques for the study of emerging insects. Entomol. News, 90: 65–78.

Mitsch, W.J., and J.G. Gosselink. 1986. Wetlands. Van Nostrand Reinhold, New York.

Rochefort, L., D.H. Vitt, and S.E. Bayley. 1990. Growth, production, and decomposition dynamics of *Sphagnum* under natural and experimentally acidified conditions. Ecology, 71: 1986–2000.

Rosenberg, D.M., A.P. Wiens, and B. Bilyj. 1988. Chironomidae (Diptera) of peatlands in northwestern Ontario, Canada. Holarct. Ecol. 11: 19–31.

Rudd, J.W.M., C.A. Kelly, V. St. Louis, R.H. Hesslein, A. Furutani, and M.H. Holoka. 1986. Microbial consumption of nitric and sulfuric acids in acidified north temperate lakes. Limnol. Oceanogr. 31: 1267–1280.

SAS Institute Inc. 1989. SAS/STAT® user's guide, version 6, 4th edition. Vol. 2. SAS Institute Inc., Cary, N.C.

Siegel, S. 1956. Nonparametric statistics for the behavioral sciences. McGraw-Hill, New York.

Urban, N.R., S.J. Eisenreich, and S.E. Bayley. 1988. The relative importance of denitrification and nitrate assimilation in midcontinental bogs. Limnol. Oceanogr. 33: 1611–1617.

Vitt, D.H., and S. Bayley. 1984. The vegetation and water chemistry of four oligotrophic basin mires in northwestern Ontario. Can. J. Bot. 62: 1485–1500.

Wilkinson, L. 1986. SYSTAT: The system for statistics. SYSTAT Inc., Evanston, Ill.

Wrubleski, D.A. 1987. Chironomidae (Diptera) of peatlands and marshes in Canada. Mem. Entomol. Soc. Can. 140: 141–161.

Zoltai, S.C. 1988. Wetland environments and classification. *In* Wetlands of Canada. Ecological Land Classification Series No. 24. National Wetlands Working Group, Environment Canada, Ottawa, Ont. pp. 1–26.

Disruption of littoral algal associations by Experimental Lake acidification[1]

Michael A. Turner, David W. Schindler, David L. Findlay, Michael B. Jackson, and Gordon G.C. Robinson

Abstract: The effects of lake acidification on algal associations in the littoral zone were examined at the Experimental Lakes Area, northwestern Ontario. Net photosynthesis of periphyton declined, partly because of increased carbon limitation, as Lake 302S was experimentally acidified with sulfuric acid from pH 6.7 to 4.5. The ratio of respiration to photosynthesis increased in epilithon (periphyton on rock surfaces) as pH declined, largely because respiration increased rapidly. Changes in Lake 302N, which was acidified with nitric acid, were similar to those in Lake 302S. Major changes also occurred in epilithic algal composition, especially as pH decreased below 5. Abundance of filamentous green algae increased as pH decreased below 6. The filamentous green algae became metaphyton (no longer attached to the substratum) and bloomed at pH 5.5 and below; *Zygogonium* dominated at pH 4.5. Metaphytic filamentous green algae sometimes covered nearly the entire littoral zone bottom during blooms. In contrast to epilithon, metaphytic filamentous green algae did not display an increasing respiration to photosynthesis ratio with declining pH. The functional changes seen in littoral algal associations resulting from acidification, among the most sensitive ones known in aquatic ecosystems, became more conspicuous as acidification proceeded.

Résumé : Dans la région des lacs expérimentaux, au nord-ouest de l'Ontario, on a examiné les effets de l'acidification des lacs sur les associations d'algues dans la zone littorale. La photosynthèse nette du périphyton a diminué, en partie à cause d'une plus grande limitation du carbone, dans le cadre d'une expérience d'acidification du lac 302S, auquel on a ajouté de l'acide sulfurique, faisant passer le pH de 6,7 à 4,5. Le rapport entre la respiration et la photosynthèse a augmenté dans l'épilithon (périphyton se trouvant sur des surfaces rocheuses) parallèlement à la diminution du pH, phénomène imputable surtout à l'acroissement rapide de la respiration. Les modifications survenues dans le lac 302N, qui a été acidifié au moyen d'acide nitrique, étaient analogues à celles du lac 302S. Des changements majeurs sont également survenus dans la composition des algues de l'épilithon, en particulier lorsque le pH est tombé à moins de 5. L'abondance de chlorophycées filamenteuses ou les algues vertes s'est accrue lorsque le pH est passé à moins de 6. Les algues vertes sont devenues du métaphyton (après leur détachement du substratum) et ont proliféré à un pH de 5,5 et moins, *Zygogonium* étant prédominant à un pH de 4,5. Les algues vertes filamenteuses du métaphyton couvraient parfois presque la totalité du fond de la zone littorale pendant les périodes de prolifération. Contrairement à l'épilithon, ces algues ne présentent pas une augmentation du rapport entre la respiration et la photosynthèse parallèlement à la baisse du pH. Les modifications fonctionnelles observées dans les associations algales du littoral, les plus sensibles qui soient connues dans les écosystèmes aquatiques, qui sont attribuables à l'acidification deviennent plus évidentes à mesure que l'acidification progresse. [Traduit par la Rédaction]

Received August 8, 1993. Accepted April 28, 1995.
J12034

M.A. Turner and D.L. Findlay. Department of Fisheries and Oceans, Central and Arctic Region, Freshwater Institute, Winnipeg, MB R3T 2N6, Canada.
D.W. Schindler. Departments of Zoology and Botany, University of Alberta, Edmonton, AB T6G 2E9, Canada.
M.B. Jackson. Water Resources Branch, Ontario Ministry of the Environment, P.O. Box 213, 125 Resources Road, Rexdale, ON M9W 5L1, Canada.
G.G.C. Robinson. Department of Botany, University of Manitoba, Winnipeg, MB R3T 2N2, Canada.

[1] This paper is one of a series done in honor of the 25th anniversary of the Experimental Lakes Area.

Can. J. Fish. Aquat. Sci. **52**: 2238–2250 (1995). Printed in Canada / Imprimé au Canada

Introduction

Conflicting information exists about the effects of acidification on the metabolism of littoral algal communities in lakes. Almer et al. (1978) inferred that the production of benthic algae in acid lakes was high because of the appearance of dense felts of *Mougeotia*. Lazarek (1982) reported high rates of photosynthesis by benthic cyanoprokaryotes[2] in an acidified oligotrophic lake in Sweden. Müller (1980) reported that photosynthesis of periphyton on artificial substrata was unchanged by experimental acidification of mesocosms located in oligotrophic Lake 223 at the Experimental Lakes Area (ELA). Both Müller's (1980) and Lazarek's (1982) conclusions about the effects of acidification on photosynthesis, however, were obscured by the methods they used to control or analyse concentrations of dissolved inorganic carbon (DIC; Turner et al. 1987). In contrast, net photosynthesis of naturally occurring epilithon (periphyton associated with rock surfaces) declined in parallel with the acid-induced decline in DIC (Turner et al. 1987), as did that of epiphyton (periphyton associated with plant surfaces; Turner et al. 1991), during the experimental acidification of oligotrophic Lake 302S at the ELA. The importance of DIC in controlling photosynthetic rates of acidified periphyton was corroborated in studies of communities on artificial substrata (Fairchild and Sherman 1990, 1992), and of naturally occurring communities (Turner et al. 1991, 1994).

Less dispute exists about the effects of lake acidification upon the taxonomic composition of littoral algal associations. Müller (1980) reported that acidification lowered species richness in periphyton on artificial substrata in experimental mesocosms. Filamentous cyanoprokaryotes began to decline in importance as the pH of Lake 302S was decreased experimentally to 5 (Turner et al. 1991), in contrast to the report that *Lyngbya*-dominated mats were well adapted to acidification (Lazarek 1982). Filamentous green algae (FGA), initially identified as fungal felts (Hendrey et al. 1976), bloomed frequently in the littoral zones of acidic lakes in Scandinavia (Almer et al. 1978; Hendrey 1982) and North America (Stokes 1986; Wei et al. 1989; Howell et al. 1990; France et al. 1992). Filamentous green algae also proliferated in experimentally acidified lakes in northwestern Ontario (Müller 1980; Schindler and Turner 1982; Schindler et al. 1985; Howell et al. 1990) and Wisconsin (Webster et al. 1992; Brezonik et al. 1993).

The growth characteristics of FGA changed during the experimental acidification of Lake 302S. The FGA appeared initially both as a shoreline band of epilithon and as epiphyton at pH values >6 (Turner et al. 1987), changing to metaphyton (no longer truly attached to the substratum) as the pH declined to 5.5 and below (Howell et al. 1990; Turner et al. 1995*a*, 1995*b*). These FGA were successful at obtaining DIC at low concentrations, allowing them to overcome (at least partly) the carbon (C) limitation found in other acidified benthic algal associations (Turner et al. 1991).

Table 1. Basic morphometric characteristics (Beaty and Lyng 1989) and experimental status of the study lakes during the investigation.

Lake	Surface area (ha)	Mean depth (m)	Experimental status	Years of epilithic study
226S	7.8	6.3	Reference	—[a]
239	54.3	10.5	Reference	1981–1991
302N	12.8	5.7	+ HNO_3	1981–1984, 1986
302S	10.9	5.1	+ H_2SO_4	1981–1991
382	36.9	5.8	Reference	1984, 1986

Note: The years are given during which epilithic photosynthesis was studied.

[a] No epilithic data; only metaphytic filamentous green algae studied.

This report concerns the effects of continued acidification on littoral algal communities (epilithon and metaphyton) in two lakes (302S and 302N) that are being studied in ongoing experiments (Turner et al. 1987, 1991; Howell et al. 1990). The changes in metabolism and algal composition of naturally occurring communities in the acidified lakes are compared with those in unperturbed circumneutral reference lakes. The decline of normally dominant epilithic species, the emergence of the acidification-induced FGA, and the accompanying consequences for food webs and biogeochemical cycles in the littoral zone are described.

Methods and materials

Study lakes

The studies were conducted in small oligotrophic lakes at the ELA, located in the boreal forest of the Canadian Shield in northwestern Ontario (Table 1). Morphometric and chemical features of the study lakes are described by Brunskill and Schindler (1971). The early experimental histories of lakes 302S and 302N are described by Turner et al. (1987, 1991), Rudd et al. (1990), and Schindler et al. (1991). The southern basin (302S) was separated from its northern downstream basin (302N) using a vinyl curtain. The techniques for adding sulfuric (H_2SO_4) and nitric (HNO_3) acids to the epilimnia were equivalent to those described for Lake 223 (Schindler et al. 1985). The pH was lowered (H_2SO_4 addition) in Lake 302S from 6.5–6.8 in 1980–1981 to approximately 4.5 by 1988, and remained at approximately 4.5 through 1991 (Fig. 1). Equivalent amounts of HNO_3 (in μequiv.$\cdot L^{-1}$) were added from 1981 to 1986 to the north basin to test the relative acidification efficiencies of the two acids (Rudd et al. 1990). The pH in Lake 302N declined less than in Lake 302S (Fig. 1) because lakes neutralize HNO_3 more efficiently than H_2SO_4 (Rudd et al. 1990). Nearby lakes 239 and 382 were used as circumneutral reference lakes for studies of epilithon and FGA. Circumneutral Lake 226S was used as another reference lake to study the distribution of metaphytic FGA.

Chemical conditions resulting from the acidification of lakes 302S and 302N were described by Turner et al. (1987), Rudd et al. (1990), and Schindler et al. (1991). Epilimnetic concentrations of nitrate (NO_3^-; Lake 302N

---

[2] We use the term cyanoprokaryote as proposed by Kling et al. (1994) in lieu of blue-green algae or cyanobacteria.

Fig. 1. Mean pH in the epilimnia of the acidified lakes (302S and 302N) and reference lakes (239 and 382) during the open-water periods of the study. Acidification of lakes 302S (sulfuric) and 302N (nitric) began in July of 1982.

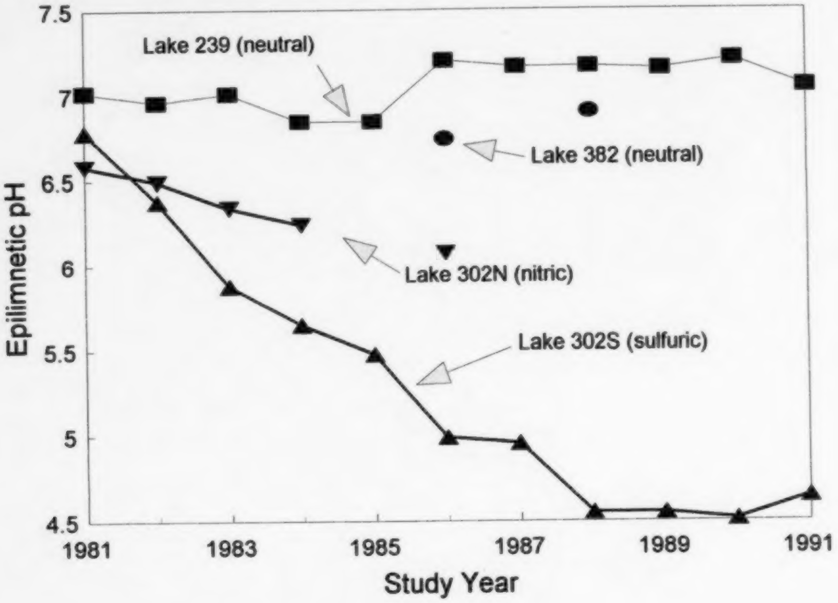

only), sulfate (SO_4^{2-}), ammonium (NH_4^+), calcium (Ca^{2+}), hydrogen ion (H^+), and total dissolved manganese (Mn) increased. Concentrations of dissolved organic C, DIC, and NO_3 (Lake 302S only) declined. Phosphorus (P) concentrations were unchanged. Metal concentrations (especially aluminum) may have been lower in these experimental lakes than in culturally acidified lakes because the Lake 302 watershed was not acidified.

Metabolism, biomass, and composition of epilithon

The bottom surface of the littoral zone of the study lakes is largely rock, so SCUBA-based techniques were developed (Turner et al. 1983, 1987) to measure the metabolism and composition of epilithon. Natural communities were studied because periphytic productivity is better examined using them than ones developed on artificial substrata (Aloi 1990). Epilithon was sampled on rock surfaces of low slope (<10°) at unshaded locations with southern exposures. Sampling was conducted in the middle littoral zone, typically between 1 and 2 m depth. Lakes were typically sampled every 4 wk during the ice-free season, except in 1981 when sampling started in late July, and in 1982 and 1983 when sampling was more frequent.

Rates of epilithic net photosynthesis were measured in situ by observing the changes in DIC that occurred in the water overlying samples of epilithon that were isolated by sealing chambers to rock surfaces (Turner et al. 1987, 1991). Concentrations of DIC were determined using an infrared gas analyzer (Turner et al. 1983). The rates measured thus reflected activities of the entire association rather than just the algal component. Usually each of four light conditions (including darkness) was sampled on each occasion at three different locations in each lake by using chambers that transmitted varying amounts of light. The maximum rate of net photosynthesis during each sampling period was estimated as the mean areal rate of DIC uptake measured in the three or more samples incubated at ambient DIC and exposed to 100% of in situ irradiance, usually for about 2 h. Such samples typically were light saturated (Turner et al. 1987) at in situ irradiances of $\geq 200\ \mu E \cdot m^{-2} \cdot s^{-1}$ ($1\ \mu E \cdot m^{-2} \cdot s^{-1} = 0.217\ W \cdot m^{-2}$) (Turner et al. 1983). Supplementary DIC was added to Lake 302 samples prior to incubation on several occasions in 1982 to test for C limitation; these estimates of photosynthesis have been excluded from the analysis of naturally occurring rates. Annual mean rates, computed as the simple average of the estimates derived from each sampling period, were equivalent to time-weighted means because of the regular sampling schedule.

The shift in seasonal patterns of epilithic photosynthesis was most clearly evident when the rate of net photosynthesis at each sampling period was calculated as a percentage of the annual maximum rate of photosynthesis. The average percentage for each month was then calculated for each year in which there were six or more sampling periods: 1982–1991 in lakes 239 and 302S; 1983, 1984, and 1986 in Lake 302N; 1984 and 1986 in Lake 382.

Respiration was measured in parallel with net photosynthesis as the mean areal rate of DIC released by the samples incubated in the dark. Values of respiration less than zero were probably caused by measurement error; in these cases, respiration was presumed to be $0.1\ \mu mol\ C \cdot m^{-2} \cdot h^{-1}$.

Gross photosynthesis was estimated by summing rates of net photosynthesis and the absolute value of dark respiration. This calculation overestimates actual gross photosynthesis because epilithic respiration in the light is less than in the dark (Graham and Turner 1987). The overestimation is usually unimportant, but it becomes important when the rate of dark respiration is as high as in acidified epilithon (see below). The effect of acidification on actual gross photosynthesis is unknown, but the calculated values are presented to demonstrate the potentially misleading conclusions that can result from their use.

The ratio of respiration to gross photosynthesis was calculated to examine whether the stress of acidification altered the balance between respiration and photosynthesis (Odum 1985). Although this value uses the calculated estimate of gross photosynthesis, the bias inherent in the estimate has less effect on the value because the bias is included in both the numerator and denominator.

Epilithon for taxonomic and C-content analyses was collected prior to 1986 by a diver using a nonquantitative syringe scraper (Stockner and Armstrong 1971). This collection method precluded estimation of areal concentrations. Subsequent modifications improved the collection method, and allowed estimation of areal concentrations of particulate C (Turner et al. 1991). Samples of epilithon (5 cm^2) were collected in duplicate at each of three sampling sites; two composite sample suspensions were then created in the laboratory by pooling one replicate from each site. Composite suspensions were then filtered (Turner et al. 1987), frozen, and analysed for particulate C (Stainton et al. 1977). Aliquots of these composite samples were also preserved for taxonomic analysis by adding equal quantities of acid Lugol's solution and FAA (formaldehyde, acetic acid, and alcohol) to achieve 4% final volume. The relative frequencies of algal taxa were determined using the methods described in Turner et al. (1987, 1991).

Metabolism, biomass, and composition of metaphytic FGA

The metabolism of FGA was assayed in the laboratory (Howell et al. 1990; Turner et al. 1995*a*) using samples collected from Lake 302S (1988–1991). Aliquots of these samples were incubated in gradients of light, algal density, and available DIC. Only the energy balance of the FGA, which was obtained by calculating the ratio of mean annual rates of dark respiration to estimated gross photosynthesis (computed as for the epilithon), is reported here.

In August or September of each year from 1982 to 1988, the entire perimeters of lakes 302S, 239, 226S (1988 only), and 382 (1983 and 1984 only) were surveyed for occurrences of metaphytic FGA. Thickness and percent shoreline coverage were determined visually (Turner et al. 1987). Stratified transect sampling (Howell et al. 1990; Turner 1993) was also used to measure FGA biomass in Lake 302S in 1988. Fifteen sampling plots (depths 0.25–4.0 m) were selected randomly along each of four transects, which were selected randomly from 91 equally spaced locations around the lake perimeter. A SCUBA diver measured the percentage of coverage by FGA of each plot area (0.5 × 0.5 m) and the median thickness of FGA growing there.

Taxonomic composition of the FGA was analysed until 1988 using collections made during the shoreline surveys (Turner et al. 1987). Thereafter, subsamples of collections made for metabolic measurements were analysed (Turner et al. 1995*a*).

Results

Metabolism of epilithon

Mean rates of net photosynthesis in epilithon during the open-water period declined as acidification progressed (Table 2, Fig. 2A). The rate of decline with acidification was similar in both the H_2SO_4 and HNO_3 lakes. Preacidification rates in epilithon of both basins of Lake 302 were lower than in the neutral lakes, probably reflecting the lower epilimnetic DIC in Lake 302 prior to manipulation (Turner et al. 1994). Much of the decline in the annual rates observed in Lake 302S occurred between pH values of approximately 7 and 5.5.

The pH-related change in the calculated estimates of gross photosynthesis (Fig. 2B) was very different from that of net photosynthesis (Fig. 2A). The calculated estimate of gross photosynthesis for Lake 302S epilithon appeared to increase at pH values ≤5, suggesting erroneously (see below) that the epilithon potentially existed in an improved metabolic state.

The seasonal pattern of epilithic net photosynthesis in acidified lakes was also very different from that in neutral lakes (Fig. 3). Epilithon in circumneutral lakes 239 and 382 displayed maximum rates of photosynthesis during July and August, whereas epilithon in acidified lakes 302S and 302N displayed spring and fall maxima, and minimum photosynthesis in July and August. Epilithon in highly acidic Lake 302S showed the most extreme deviation from normal. Seasonal patterns also appeared relatively more variable in the acidified communities than in the circumneutral communities. For example, the average standard error (SE) values of the monthly means were 7 and 4% in neutral lakes 239 and 382, respectively, whereas the corresponding values in acidified lakes 302S and 302N were 15 and 29%, respectively.

Epilithic respiration increased with acidification in both the HNO_3 and H_2SO_4 lakes (Fig. 4). The percentage of estimated gross photosynthesis used for respiration increased with acidification in both lakes 302S and 302N (Fig. 5). Respiration in Lake 302S averaged 90 ± 8% (mean ± SE, $n = 4$ yr) of estimated gross photosynthesis during the 4 yr that the lake was held at a pH of 4.5. In contrast, the ratio in epilithon of circumneutral lakes 239 and 382 was only 17 ± 2% ($n = 11$ yr) and 23 ± 3% ($n = 2$ yr), respectively.

Algal taxonomic composition and biomass of epilithon

The major algal taxonomic groups of the epilithon changed markedly with acidification (Fig. 6). Algal composition, which had been stable at pH values >5.6, became unstable at pH values ≤5. Filamentous cyanoprokaryotes (principally *Lyngbya* and *Anabaena*) remained the annually dominant taxa at pH values >5. Coccoidal cyanoprokaryotes (first *Merismopedia minutissima* Beck, Sched., and Krypt. and then *Chroococcus minutus* (Kuetz.) Naegeli) or diatoms

Table 2. Summaries of open-water epilithic metabolism in four lakes at the Experimental Lakes Area from 1981 to 1991.

Lake	Year	*N*	DIC (μM)	Dark respiration (μmol C·m^{-2}·h^{-1})	Net photosynthesis (μmol C·m^{-2}·h^{-1})	Areal carbon (mol C·m^{-2})
239	81	6	156	−105±34	315±33	
239	82	12	139	−111±22	346±18	
239	83	12	144	−126±31	396±39	
239	84	7	176	−76±34	488±77	
239	85	7	146	−57±26	358±16	
239	86	6	148	−54±8	378±48	1.82±0.17
239	87	7	143	−64±22	342±53	1.85±0.10
239	88	7	146	−138±43	343±45	2.12±0.26
239	89	6	153	−84±31	431±53	2.01±0.32
239	90	7	169	−80±27	459±36	1.88±0.20
239	91	7	173	−9±6	481±35	1.98±0.26
382	84	7	105	100±35	284±27	
382	86	6	86	72±18	316±25	2.03±0.16
302S	81	4	75	−74±26	231±26	
302S	82	12, 8	62	−121±17	221±33	
302S	83	9	32	−191±15	176±23	
302S	84	7	31	−181±38	98±42	
302S	85	7	29	−222±30	88±24	
302S	86	6	17	−366±46	58±11	1.63±0.27
302S	87	7	32	−371±72	133±25	2.08±0.29
302S	88	7	28	−333±61	46±26	1.60±0.25
302S	89	6	26	−403±70	45±47	1.16±0.10
302S	90	7	21	−444±76	−44±43	0.74±0.09
302S	91	7	27	−262±53	113±30	0.61±0.21
302N	81	3	80	62±35	256±51	
302N	82	7, 3	53	110±15	218±7	
302N	83	6	46	154±39	164±44	
302N	84	7	51	144±47	136±32	
302N	86	6	20	174±23	74±15	1.68[a]±0.09

Note: *N* is the number of sampling periods; two values are given when *N* differed for dark respiration and net photosynthesis. DIC is dissolved inorganic carbon. SE is standard error. Values are given as mean ± SE.

[a] 2.02 ± 0.35 including an outlier.

(e.g., *Eunotia pectinales* (Kuetz.) Rabenhorst and *Anomoeoneis serians* var. *brachysira* Breb.) dominated thereafter, but varied annually in importance. In contrast, diatoms and filamentous cyanoprokaryotes remained stable codominants in circumneutral Lake 239 throughout the study, annually representing 52 ± 3% and 39 ± 3% (n = 11 yr) of cells and filaments, respectively.

Areal concentrations of particulate C in Lake 302S epilithon declined as the pH decreased below 5 (Table 2). Mean open-water values of particulate C reached a minimum of 0.6 mol C·m^{-2} in 1991 at a pH value of 4.5. The decline in epilithic C in Lake 302S during 1991 mirrored that in photosynthesis, reaching an August low of 0.04 mol C·m^{-2}. Epilithic particulate C in Lake 239 was surprisingly stable during 1986–1991 by comparison, having a mean of 1.9 ± 0.1 mol C·m^{-2} (n = 6 yr). A similar value (2.0 mol C·m^{-2}) was observed in Lake 382 during 1986. More epilithon occurred in Lake 302S before acidification than in Lake 239 (M.A. Turner, unpublished observations), which makes even more dramatic the acidification-related decline in epilithon of Lake 302S. A possible decline of C at higher pH in Lake 302S is uncertain, however, because of nonquantitative sampling prior to 1986.

Metabolism of filamentous green algae

The mean annual ratio of respiration to estimated gross photosynthesis averaged 26 ± 3% in FGA during the four open-water periods that the pH of Lake 302S was approximately 4.5 (Fig. 5; cf. 15 ± 6% for Lake 239). This value differed sharply from the 90% ratio in the epilithon of Lake 302S during the corresponding period of time (see above).

Taxonomic composition and biomass of filamentous green algae

Taxonomic composition of the metaphytic FGA in Lake 302S, measured as the annual mean fraction of FGA biovolume, changed as acidification progressed (Fig. 7). *Spirogyra* dominated the metaphytic FGA at a pH value of about 5.5, but declined to low abundance at a pH value

Fig. 2. A: Annual means of the maximum areal rate of net photosynthesis (μmol·m^{-2}·h^{-1}) in epilithon during the open-water period. Each open-water value shown represents the mean of estimates from 3–12 seasonal samplings (typically 6 or 7), each of which involved at least three estimates of the maximum rate of net photosynthesis. B: Annual means of the maximum areal rate of calculated gross photosynthesis (μmol·m^{-2}·h^{-1}) in epilithon during the open-water period. The error inherent in the calculation of gross photosynthesis (see text) produced an inaccurate impression of the epilithic photosynthetic potential as acidification increased.

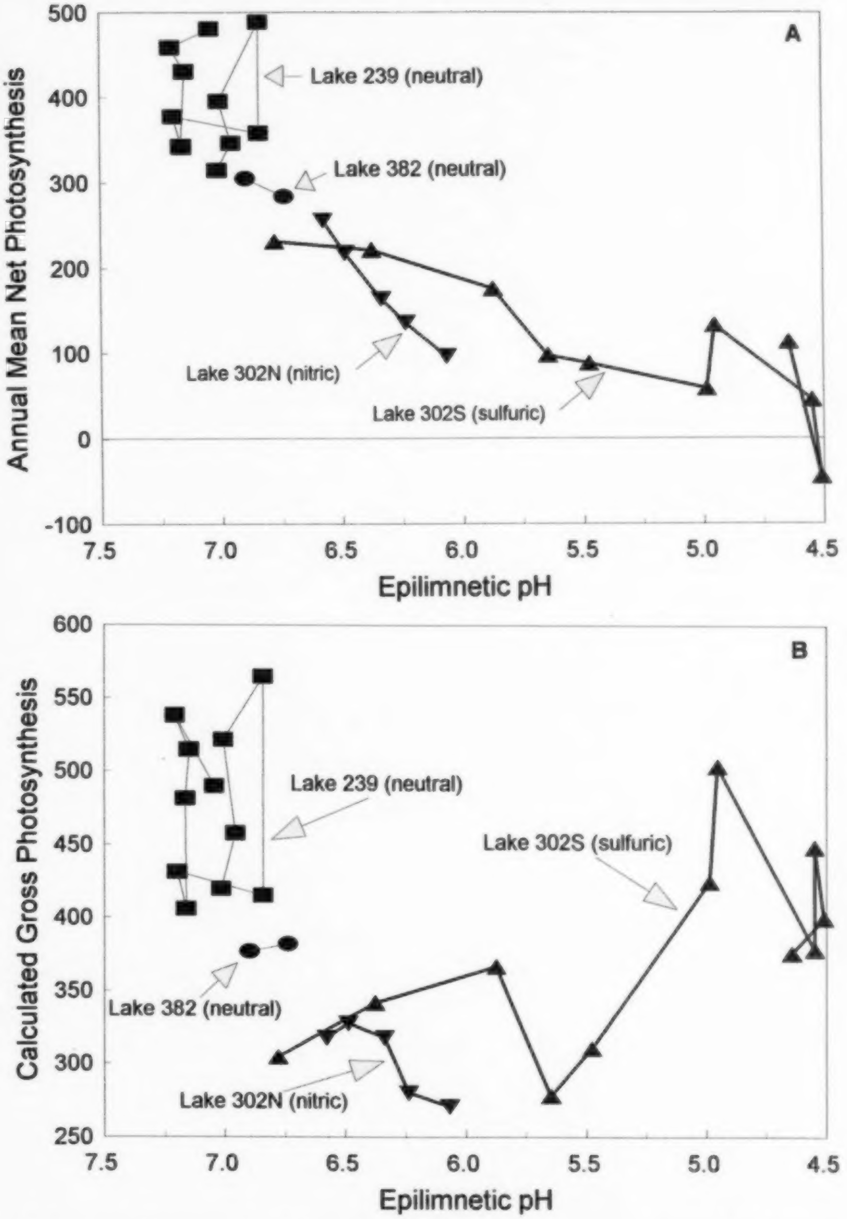

of about 5.0. *Mougeotia* dominated at a pH value of approximately 5.0, but declined in abundance as the pH decreased to 4.5. *Zygogonium* was consistently the most abundant metaphytic FGA at the lowest pH values.

Appreciable amounts of metaphytic FGA were first noted in Lake 302S during 1985 as the epilimnetic pH declined to approximately 5.5 (Fig. 8). Both the extent of metaphytic coverage and the thickness of growths increased

Fig. 3. The seasonal pattern of epilithic net photosynthesis in the acidified lakes (302S and 302N) compared monthly with that occurring in the reference lakes (239 and 382). Daily estimates of the maximum rate of net photosynthesis were standardized as a percentage of the corresponding annual maximum rate in each lake. Monthly mean percentages (shown) were then computed for the years described in the text.

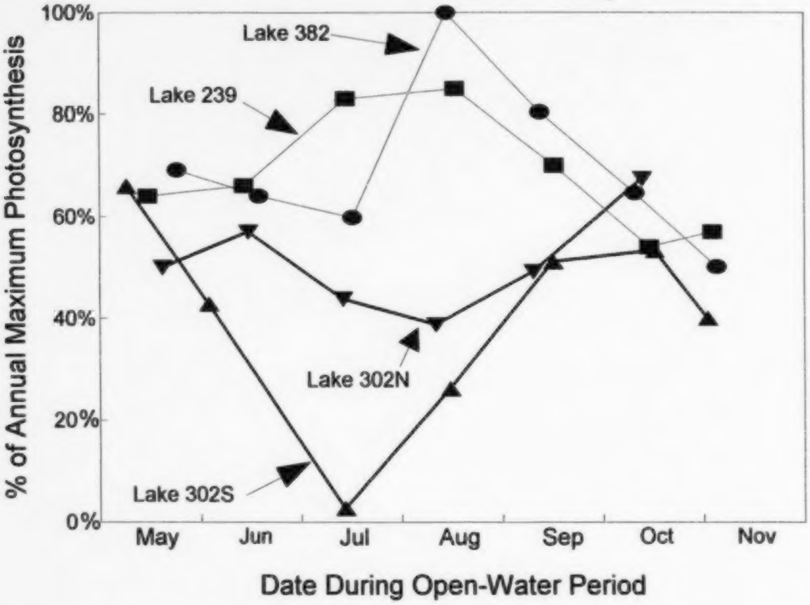

Fig. 4. Annual means of the areal rate of respiration ($\mu mol \cdot m^{-2} \cdot h^{-1}$) in epilithon during the open-water period. Sampling frequency paralleled that of net photosynthesis (Fig. 2*a*).

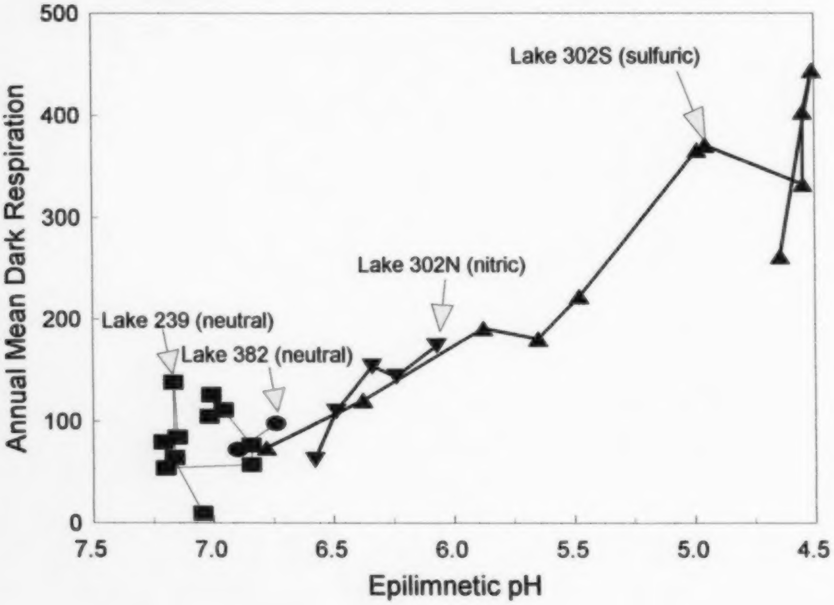

Fig. 5. Annual mean rates of respiration as a proportion of calculated overestimates of gross photosynthesis (see text) in epilithon of the study lakes and in filamentous green algae (FGA) of Lake 302S during the open-water period.

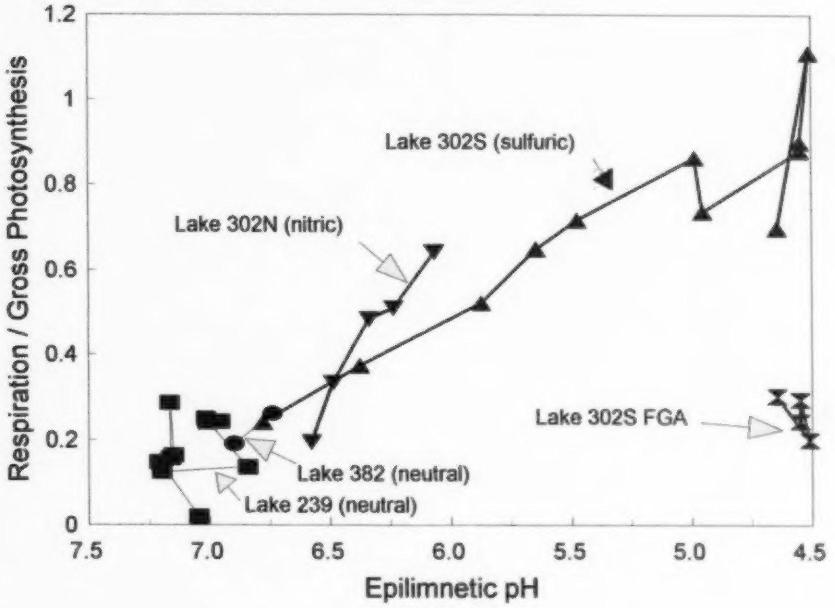

Fig. 6. Algal taxonomic composition of epilithon in Lake 302S. Values shown are the mean annual proportions that each major taxon contributed to the cell or filament frequency in the epilithon.

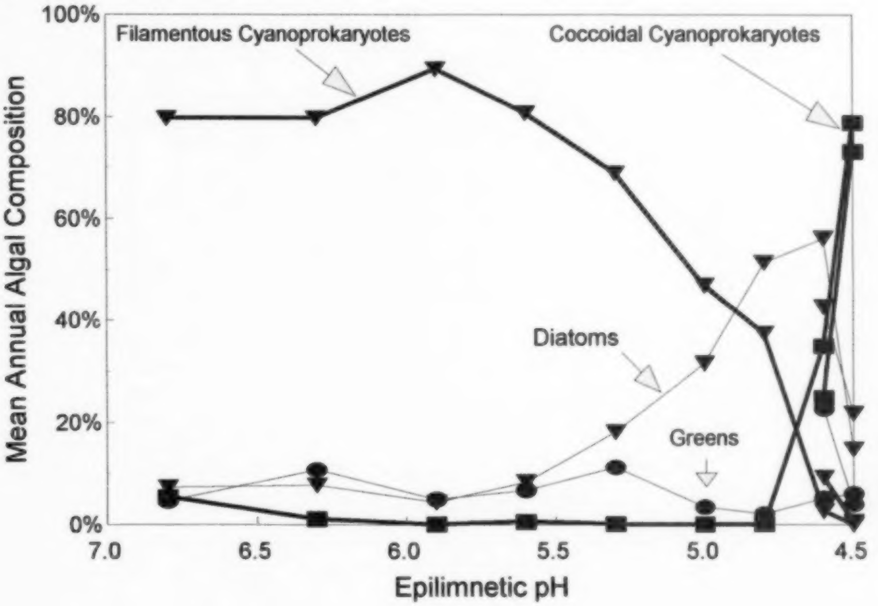

Fig. 7. Algal taxonomic composition of metaphytic blooms of filamentous green algae (FGA) during the acidification of Lake 302S. Values from 1989 to 1991 (at pH of approximately 4.5) were derived from Turner (1993).

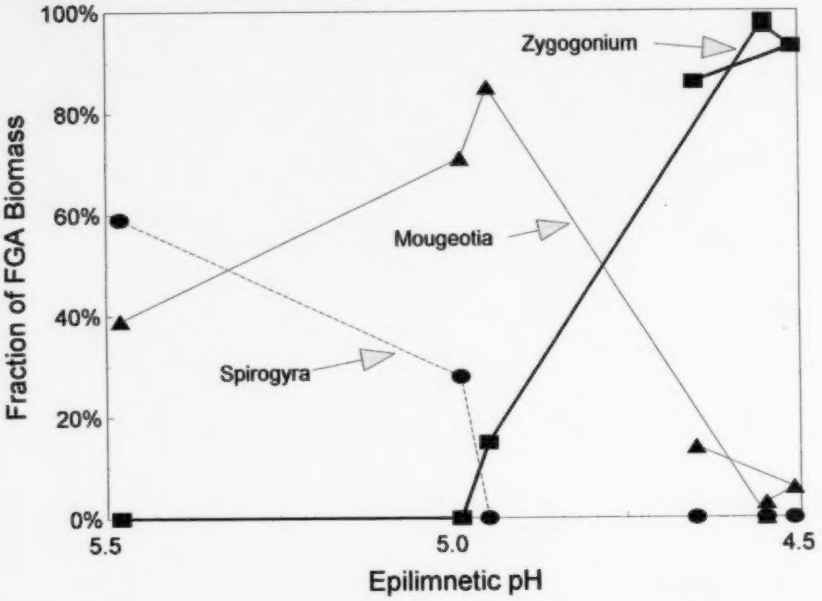

with further acidification. Most of the shoreline was affected by metaphyton of almost 30 cm median thickness in the first year of acidification to pH of 4.5. In this year, the transect survey corroborated the visual survey: 83% of the littoral bottom from 0 to 4 m was covered by FGA to a mean thickness of 22 cm (Turner et al. 1995*b*). In comparison, no detectable amounts of metaphytic FGA were found during annual surveys in circumneutral lakes 226S (1988), 239 (1982–1988), and 382 (1983 and 1984).

Discussion

Effects of acidification on the metabolism of littoral algal associations

A decline in net photosynthesis (Fig. 2A) was the first detected functional response of epilithon to acidification by either H_2SO_4 or HNO_3, even at a pH value >6 (Fig. 2A; Turner et al. 1987). This finding diverged from the expectation that photosynthesis of all benthic algal associations would increase with acidification, which was based upon reports of massive increases in benthic algal biomass resulting from acidification (e.g., Almer et al. 1978; Stokes 1986). The decrease in epilithic net photosynthesis, and increase in compensation irradiances (Turner et al. 1991), occurred partly because of C limitation as acidification depleted the DIC available for photosynthesis by eliminating the bicarbonate pool (Turner et al. 1987, 1994). A similar response to acidification was also seen in epiphyton on the common macrophyte *Eriocaulon septangulare* With (Turner et al. 1991). These findings are consistent with the conclusion that DIC would limit lentic epilithic growth where the water column ratio of DIC:DIN (dissolved inorganic nitrogen) was low, such as is found in acid lakes with low DIC and high NH_4^+ concentrations (Fairchild and Sherman 1992).

The seasonal pattern of the residual net photosynthesis of epilithon also changed with acidification, further altering the net epilithic contribution to the littoral food web. Maximum epilithic net photosynthesis occurred in midsummer in epilithon of circumneutral lakes (Fig. 3); the temperature enhancement of photosynthesis appeared to exceed the seasonal reduction in carbon dioxide (CO_2; Turner et al. 1987), probably because bicarbonate was available to counteract the reduced solubility of CO_2 in the warm water of summer. In comparison, maximum epilithic net photosynthesis in the acid lakes occurred in the spring and fall (Fig. 3), when water temperatures were low, solubility of CO_2 was high, and DIC concentrations were at their open-water maxima. Minimum net photosynthesis occurred during midsummer when water temperatures were high, solubility of CO_2 was low, and DIC concentrations were at their open-water minima.

The reduction of epilithic net photosynthesis by acidification contrasted with the lack of effect on phytoplankton photosynthesis, which was sustained or even increased as the lakes acidified (Shearer and DeBruyn 1986; Shearer et al. 1987; Schindler 1988, 1990). The diffusive boundary layer around phytoplankton may be thinner than that adjacent to many benthic algal associations in lakes because planktonic algae circulate within the epilimnion (Turner et al. 1991). The rate of nutrient uptake is inversely related to boundary layer thickness (Riber and Wetzel 1987) and to algal density (Stevenson and Glover 1993), so it is probable that phytoplankton are less limited than most lentic

Fig. 8. Percent coverage of the shoreline of Lake 302S by metaphytic (unattached) growths of filamentous green algae, and their median thickness (cm), as the pH declined.

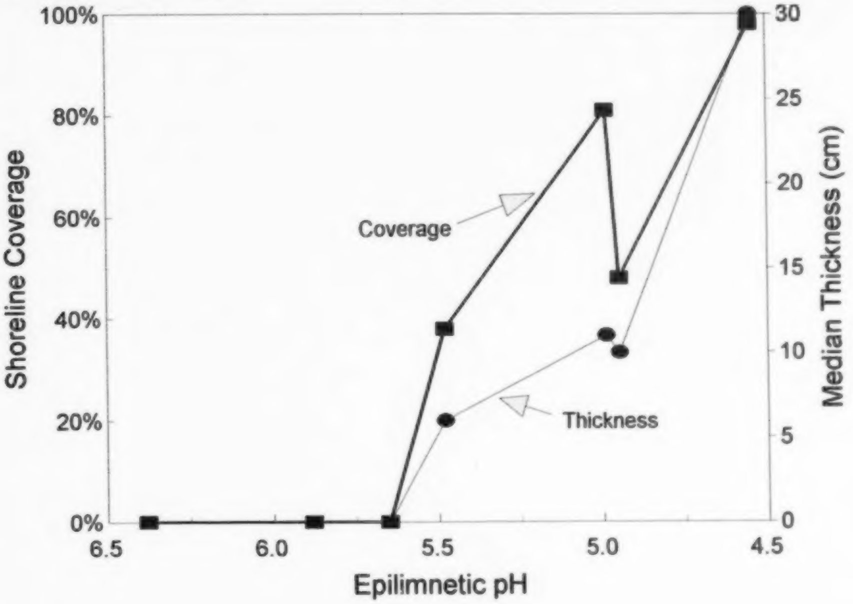

periphyton by the acidification-caused depletion of DIC. This hypothesis was verified in experimentally acidified Lake 223, where phytoplankton photosynthesis was never enhanced by DIC enrichment (Shearer et al. 1987).

Periphytic respiration was expected to decline with acidification, partly explaining the accumulation of organic detritus seen previously in littoral zones of acidified Scandinavian lakes (Hendrey et al. 1976; Almer et al. 1978; Traaen 1980). Instead, periphytic respiration increased as the lakes acidified (Fig. 4; Turner et al. 1991) in support of Odum's (1985) hypothesis that stress would increase community respiration. Epilithic respiration correlated with DIN in both acidified and unperturbed lakes, so that DIN may have accelerated epilithic respiration by enhancing the N:C ratio in decomposing materials (Turner et al. 1994). Other possible causes of increased respiration in acidified epilithon have been considered elsewhere (Turner et al. 1991; Turner 1993). Whether phytoplankton respiration changed is unknown because it was not measured by the ^{14}C technique.

Increased epilithic respiration, an open-water epilimnetic process, also appeared inconsistent with observations that summer hypolimnetic and under-ice whole-lake respiration were unaffected or slowed by acidification to pH values ≥5 (Kelly et al. 1984; Schindler 1990). Whole-lake or hypolimnetic respiration, however, may reflect decomposition of materials derived predominantly from planktonic and allochthonous sources rather than periphyton. The discrepancy may also be explained by a lowered availability of organic C for whole-lake or hypolimnetic decomposition if epilimnetic respiration was accelerated by acidification; i.e., the difference may reflect catabolism of 'new' C (epilithon during the open-water period) versus 'old' C (more refractory organics in sediments during winter) (Turner 1993).

The ratio of respiration to (gross) photosynthesis was considered by Odum (1971, 1985) to be, perhaps, the most important of all ecosystem functions. It can be deduced that acidified epilithon of Lake 302S would have become unable to support a typical littoral food web because respiration accounted for much of its estimated gross photosynthesis during the 4 yr that the lake was held at a pH of 4.5 (Fig. 5). This hypothesis is consistent with the decline seen in epilithic particulate C (Table 2), although other factors (e.g., herbivory) could also have been involved in the biomass decline. In contrast, the ratio of respiration to photosynthesis in the more successful metaphytic FGA was similar to the low values of circumneutral epilithon (Fig. 5), which is consistent with the ability of FGA to bloom under acid conditions (Howell et al. 1990; Turner et al. 1995*a*).

Calculated estimates of gross photosynthesis (Fig. 2B) yielded the wrong impression that epilithic photosynthetic potential had been increased by acidification. This error arose because of the inappropriate use of respiration rates measured in the dark (rather than in the light) for the estimate of gross photosynthesis (Graham and Turner 1987). The error inherent in this calculation procedure is usually not serious when respiration rates are low, but the error escalated as dark respiration increased strongly with acidification (Fig. 4) and represented an increasingly large fraction of calculated gross photosynthesis (Fig. 5).

Effects of acidification on species composition and community structure

Major structural changes in the algal composition of epilithon accompanied the decline in net photosynthesis resulting from acidification. A decrease in algal taxonomic richness marked by declining numbers of green and cyanoprokaryote taxa (M.A. Turner and D.L. Findlay, unpublished data) confirmed earlier experimental mesocosm observations (Müller 1980). Coccoidal cyanoprokaryotes and acidophilic diatoms replaced *Lyngbya*- and *Anabaena*-dominated filamentous cyanoprokaryotes as the pH declined below 5 (Fig. 6). Nitrogen-fixing capacity should also have been lost from the community as a result of the demise of heterocystous cyanoprokaryotes. This loss should have been relatively unimportant, however, as C became more limiting to periphyton (Turner et al. 1994), and as epilimnetic NH_4^+ concentrations increased (Rudd et al. 1988). Cyanoprokaryotes also disappeared from the plankton of Lake 302S (Findlay and Kasian 1990) and Little Rock Lake, Wisconsin (Brezonik et al. 1993), with acidification. Such declines are inconsistent with predictions that filamentous cyanoprokaryotes should be important in benthos of acidified lakes (Lazarek 1982).

Structural changes also included a dramatic decline in epilithic biomass (as inferred from concentrations of C) at a pH of 4.5 (Table 2). This was especially noticeable in Lake 302S during midsummer when rocks appeared almost bare; e.g., in the midsummer of 1991, organic C decreased to only 2% of values in the reference lakes. The character of sedimentary areas in the littoral zone changed similarly with acidification. The depth of sediment appeared to decrease over the several years of acidification, exposing previously buried ferromanganese encrustations in some regions (M.A. Turner, unpublished data). Such sediment consumption may cause relocation of the site of sedimentary oxidation–reduction reactions, followed by the potential reduction of internal alkalinity generation (Kelly et al. 1994) as organic supplies for bacterial decomposition decrease. An alternative explanation for the apparent decrease in littoral sediments is that the loss of filamentous cyanoprokaryotes, which may have helped stabilize the sediments in a manner analogous to that hypothesized to occur for hypolimnetic sediments (Schindler et al. 1987), caused littoral sediments to become destabilized and more subject to erosional forces.

Filamentous green algae proliferated with acidification of Lake 302S in contrast to the decline of the epilithon. Filamentous green algae first developed at pH values >6.0 both as epilithon attached to rocks in the wave zone and as epiphyton attached to macrophytes in the shallow depths (Turner et al. 1987). Filamentous green algae then developed annual blooms of unattached forms, or metaphyton, as the pH declined to values ≤5.5 (Fig. 8; Howell et al. 1990), spreading over additional bottom types and growing deeper. Extensive benthic growths of FGA were similarly first seen at a pH of 5.6 during the experimental acidification of Little Rock Lake (Webster et al. 1992).

The dominant taxa of the metaphytic FGA changed with progressive acidification: *Spirogyra* was replaced by *Mougeotia* and finally by *Zygogonium* at a pH of 4.5, the most common of the bloom-forming FGA in the littoral zone of acidic lakes in southcentral Ontario (Wei et al. 1989; France et al. 1992). These FGA proliferated partly because of their ability to adapt to low concentrations of DIC (Turner et al. 1991, 1995*a*) possibly because of a high affinity for CO_2 (G.G.C. Robinson, unpublished data). They also displayed the ability to use high light intensities (Howell et al. 1990; Turner et al. 1995*a*) in contrast with the epilithon (Turner et al. 1983), and tolerated high H^+ concentrations (Müller 1980). The loss of large potential grazers, such as *Hyalella* (Grapentine and Rosenberg 1992) and *Orconectes* (Davies 1989), may also have contributed to the buildup of FGA (Hendrey 1976), although this idea has been recently challenged in lotic experiments (Junger and Planas 1993).

Effects of changed littoral algal communities on other ecosystem processes

The fundamental character of energy flow within the littoral food web was altered by acidification. Net photosynthesis decreased in the normally dominant epilithon (Fig. 2*a*) and epiphyton (Turner et al. 1991) as the ratio respiration : (gross) photosynthesis increased (Fig. 5). The seasonality of the remaining epilithic net photosynthesis also became the opposite of that seen in reference communities (Fig. 3), thereby possibly forcing herbivores to adjust their feeding strategies if availability of food was limited. The edibility of the remaining epilithic algal taxa (dominated by mucilaginous coccoidal cyanoprokaryotes, Fig. 6) was probably diminished. Predictions for herbivores need to be verified.

It might be concluded that the blooms of FGA could compensate for the declining role of periphyton, given that FGA can be used as food by some invertebrates (Fulton 1988). Much of the FGA blooms remained ungrazed in early fall (Turner et al. 1995*a*), however, despite the associated abundance of several groups of littoral Cladocera (e.g., chydorids and macrothricids; M.A. Turner and B.J. Hann, University of Manitoba, Winnipeg, Man., unpublished data). With the decomposition of these blooms in late fall and in winter, the overall pattern of energy flow in the littoral zone would have been altered beyond that already resulting from dysfunction of periphytic metabolism. Furthermore, the seasonal pattern of FGA net photosynthesis was not fully complementary to that of the residual epilithic net photosynthesis (Turner et al. 1995*a*). If food was limiting the consumer community, FGA would also have been an unstable base for a food web because of particularly large intra- and inter-annual variations in biomass (Turner et al. 1995*b*). For example, FGA biomass varied by two orders of magnitude during the open-water period of 1991 (Turner et al. 1995*a*) and the maximum size of FGA blooms varied by more than one order of magnitude during the 4 yr Lake 302S was held at a pH of 4.5 (Turner et al. 1995*b*). Interannual variation in herbivory, which was unmeasured, could also have altered the size of the FGA blooms. Interannual variation in chronically acidified lakes may be lower than in Lake 302S, but this remains unknown.

The acid-induced blooms of FGA radically altered the littoral zone of Lake 302S in other ways. Wave energy and light reaching the lake bottom were reduced (Turner et al. 1995*b*), e.g., other phytobenthos were shaded (up to 90%) in proportion to the amount of FGA. The FGA also affected major nutrient cycles (C, N, and P), in part by the sequestering of nutrients (Turner et al. 1995*b*) as predicted by Hendrey (1982) and Stokes (1986). The FGA also affected internal alkalinity generation, but this effect was both seasonal and bidirectional (Turner et al. 1995*b*). Kelly et al. (1995) also concluded that FGA affected alkalinity generation via the sulfur (S) cycle by shifting the depth of sedimentary S reduction and permitting reoxidation of normally buried reduced products.

In summary, lake acidification disrupted the metabolism and structure of littoral algal associations, causing dramatic changes to the base of the typical circumneutral littoral food web. Changes in periphytic energy flow (net photosynthesis and respiration) in response to acidification supported Odum's (1985) hypotheses that as a community is stressed, its respiration would increase, and the ratio between photosynthesis and respiration would become unbalanced. Periphytic energy flow was thus one of the lake functions most sensitive to acidification; processes such as nitrification, nitrogen-fixation, and internal alkalinity generation were affected at much lower pH values (Schindler 1990; Schindler et al. 1991). Previous reviews, based largely on pelagic observations and done before consequences for the littoral zone were fully known, contained observations that ecosystem functions would be unaffected by acidification until relatively low pH values were reached (Schindler 1987). The importance of acid-induced shifts in the C cycle was similarly overlooked because the role of DIC in controlling growth of epilithon in low DIC lakes was incompletely understood (Turner et al. 1994).

The experimentally acidified lakes have been allowed to begin recovery, so it is unknown whether all the features thus far observed will pertain to chronically acidified lakes. Some of the observed effects might have occurred at higher pH (suggesting even greater sensitivity) had the experimental acidifications progressed more slowly. The general description provided here is likely to be accurate, however, on the basis of an earlier comparison of biota in experimentally and culturally acidified lakes (Schindler et al. 1991).

Acknowledgments

This research was supported by the Department of Fisheries and Oceans. We thank the following individuals: D. Cruikshank, R. Graham, K. Tyson-Shearer, M. Summerby, L. Sigurdson, N. Strange, B. Townsend, and S. Zettler for technical assistance; the ELA and Freshwater Institute chemistry staffs for analytical support; and an anonymous reviewer, P. Campbell, G.W. Fairchild, B. Hann, F.P. Healey, R. Hecky, N. Kenkel, and especially D. Rosenberg for critiquing earlier drafts. Some of this work was originally part of a Ph.D. thesis by M.A.T. at the University of Manitoba.

References

Almer, B., W. Dickson, C. Ekstrom, and E. Hornstrom. 1978. Sulfur pollution and the aquatic ecosystem. *In* Sulfur in the environment: part 2. Ecological impacts. *Edited by* J.O. Nriagu. John Wiley & Sons, New York. pp. 271–311.

Aloi, J.E. 1990. A critical review of recent freshwater periphyton field methods. Can. J. Fish. Aquat. Sci. 47: 656–670.

Beaty, K.G., and M.E. Lyng. 1989. Hydrometeorological data for the Experimental Lakes Area, northwestern Ontario, 1982 to 1987. Can. Data. Rep. Fish. Aquat. Sci. No. 759.

Brezonik, P.L, J.G. Eaton, T.M. Frost, P.J. Garrison, T.K. Kratz, C.E. Mach, J.H. McCormick, J.A. Perry, W.A. Rose, C.J. Sampson, B.C.L. Selley, W.A. Swenson, and K.E. Webster. 1993. Experimental acidification of Little Rock Lake, Wisconsin: chemical and biological changes over the pH range 6.1 to 4.7. Can. J. Fish. Aquat. Sci. 50: 1101–1121.

Brunskill, G.J., and D.W. Schindler. 1971. Geography and bathymetry of selected lake basins, Experimental Lakes Area, northwestern Ontario. J. Fish. Res. Board Can. 28: 139–155.

Davies, I.J. 1989. Population collapse of the crayfish *Orconectes virilis* in response to experimental whole-lake acidification. Can. J. Fish. Aquat. Sci. 46: 910–922.

Fairchild, G.W., and J.W. Sherman. 1990. Effects of liming on nutrient limitation of epilithic algae in an acid lake. Water Air Soil Pollut. 52: 133–147.

Fairchild, G.W., and J.W. Sherman. 1992. Linkage between epilithic algal growth and water column nutrients in softwater lakes. Can. J. Fish. Aquat. Sci. 49: 1641–1649.

Findlay, D.L., and S.E.M. Kasian. 1990. Phytoplankton communities of lakes experimentally acidified with sulfuric and nitric acids. Can. J. Fish. Aquat. Sci. 47: 1378–1386.

France, R.L., Y.-K. Yung, and P.M. Welbourn. 1992. Identification of metaphytic zygnematacean algae in acid-sensitive Canadian Shield lakes. Arch. Hydrobiol. Suppl. 66: 99–103.

Fulton, R.S., III. 1988. Grazing on filamentous algae by herbivorous zooplankton. Freshwater Biol. 20: 263–271.

Graham, R.W., and M.A. Turner. 1987. Photoinhibition of respiration in epilithic periphyton. Can. J. Fish. Aquat. Sci. 44(Suppl. 1): 150–153.

Grapentine, L.C., and D.M. Rosenberg. 1992. Responses of the freshwater amphipod *Hyalella azteca* to environmental acidification. Can. J. Fish. Aquat. Sci. 49: 52–64.

Hendrey, G.R. 1976. Effects of pH on the growth of periphytic algae in artificial stream channels. Sur. Nedbors Virkning pa Skog eg Fisk Project, Intern. Rep. No. 25/76. Aas-NLH, Norway.

Hendrey, G.R. 1982. Effects of acidification on aquatic primary producers and decomposers. *In* Acid Rain / Fisheries: Proceedings of an International Symposium on Acid Rain and Fishery Impacts on Northeastern North America, Ithaca, N.Y., Aug. 2–5, 1981. *Edited by* R.E. Johnson. American Fisheries Society, Bethesda, Md. pp. 125–135.

Hendrey, G.R., K. Baalsrud, T.S. Traaen, M. Laake, and G. Raddum. 1976. Acid precipitation: some hydrobiological changes. Ambio, 5: 224–227.

Howell, E.T., M.A. Turner, R.L. France, M.B. Jackson, and P.M. Stokes. 1990. Comparison of Zygnematacean (*Chlorophyta*) algae in the metaphyton of two acidic lakes. Can. J. Fish. Aquat. Sci. 47: 1085–1092.

Junger, M., and D. Planas. 1993. Alteration of trophic interactions between periphyton and invertebrates in an acidified stream: a stable carbon isotope study. Hydrobiologia, 262: 97–107.

Kelly, C.A., J.W.M. Rudd, A. Furutani, and D.W. Schindler. 1984. Effects of lake acidification on rates of organic matter decomposition in sediments. Limnol. Oceanogr. 29: 687–694.

Kelly, C.A., J. Amaral, M.A. Turner, J.W.M. Rudd, D.W. Schindler, and M.P. Stainton. 1995. Disruption of sulfur cycling and acid neutralization in lakes. Biogeochemistry, 28: 115–130.

Kling, H.J., D.L. Findlay, and J. Komárek. 1994. *Aphanizomenon schindleri* sp.nov.: a new nostocacean cyanoprokaryote from the Experimental Lakes Area, northwestern Ontario. Can. J. Fish. Aquat. Sci. 51: 2267–2285.

Lazarek, S. 1982. Structure and function of a cyanophytan mat community in an acidified lake. Can. J. Bot. 60: 2235–2240.

Müller, P. 1980. Effects of artificial acidification on the growth of periphyton. Can. J. Fish. Aquat. Sci. 37: 355–363.

Odum, E.P. 1971. Fundamentals of ecology. 3rd ed. W.B. Saunders, Philadelphia, Pa.

Odum, E.P. 1985. Trends expected in stressed ecosystems. BioScience, 35: 419–422.

Riber, H.H., and R.G. Wetzel. 1987. Boundary-layer and internal diffusion effects on phosphorus fluxes in lake periphyton. Limnol. Oceanogr. 32: 1181–1194.

Rudd, J.W.M., C.A. Kelly, D.W. Schindler, and M.A. Turner. 1990. A comparison of the acidification efficiencies of nitric and sulfuric acids by two whole-lake addition experiments. Limnol. Oceanogr. 35: 663–679.

Schindler, D.W. 1987. Detecting ecosystem responses to anthropogenic stress. Can. J. Fish. Aquat. Sci. 44(Suppl. 1): 6–25.

Schindler, D.W. 1988. Effects of acid rain on freshwater ecosystems. Science (Washington, D.C.), 239: 149–157.

Schindler, D.W. 1990. Experimental perturbations of whole lakes as tests of hypotheses concerning ecosystem structure and function. Oikos, 57: 25–41.

Schindler, D.W., and M.A. Turner. 1982. Biological, chemical and physical responses of lakes to experimental acidification. Water Air Soil Pollut. 18: 259–271.

Schindler, D.W., K.H. Mills, D.F. Malley, D.L. Findlay, J.A. Shearer, I.J. Davies, M.A. Turner, G.A. Linsey, and D.R. Cruikshank. 1985. Long-term ecosystem stress: the effects of years of experimental acidification on a small lake. Science (Washington, D.C.), 228: 1395–1401.

Schindler, D.W., R.H. Hesslein, and M.A. Turner. 1987. Exchange of nutrients between sediments and water after 15 years of experimental eutrophication. Can. J. Fish. Aquat. Sci. 44(Suppl. 1): 26–33.

Schindler, D.W., T.M. Frost, K.H. Mills, P.S.S. Chang, I.J. Davies, D.L. Findlay, D.F. Malley, J.A. Shearer, M.A. Turner, P.J. Garrison, C.J. Watras, K. Webster, J.M. Gunn, P.L. Brezonik, and W.A. Swenson. 1991. Comparisons between experimentally- and atmospherically-acidified lakes during stress and recovery. Proc. R. Soc. Edinburgh, Sect. B Biol. Sci. 97: 193–226.

Shearer, J.A., and E.R. DeBruyn. 1986. Phytoplankton productivity responses to direct addition of sulfuric and nitric acids to the waters of a double-basin lake. Water Air Soil Pollut. 30: 695–702.

Shearer, J.A., E.J. Fee, E.R. DeBruyn, and D.R. DeClerq. 1987. Phytoplankton primary production and light attenuation responses to the experimental acidification of a small Canadian Shield lake. Can. J. Fish. Aquat. Sci. 44(Suppl. 1): 83–90.

Stainton, M.P., M.J. Capel, and F.A.J. Armstrong. 1977. The chemical analysis of fresh water. 2nd ed. Can. Fish. Mar. Serv. Misc. Spec. Publ. No. 25.

Stevenson, R.J., and R. Glover. 1993. Effects of algal density and current on ion transport through periphyton communities. Limnol. Oceanogr. 38: 1276–1281.

Stockner, J.G., and F.A.J. Armstrong. 1971. Periphyton of the Experimental Lakes Area, northwestern Ontario. J. Fish. Res. Board Can. 28: 215–229.

Stokes, P.M. 1986. Ecological effects of acidification on primary producers in aquatic systems. Water Air Soil Pollut. 30: 421–438.

Traaen, T.S. 1980. Effects of acidity on decomposition of organic matter in aquatic environments. *In* Ecological impact of acid precipitation. *Edited by* D. Drabløs and A. Tollan. Proceedings of an International Symposium, Sandefjord, Norway, March 1980. Sur. Nedbors Virkning pa Skog eg Fisk Project, Oslo, Norway. pp. 340–341.

Turner, M.A. 1993. The ecological effects of experimental acidification upon littoral algal associations of lakes in the boreal forest. Ph.D. thesis, University of Manitoba, Winnipeg, Man.

Turner, M.A., D.W. Schindler, and R.W. Graham. 1983. Photosynthesis–irradiance relationships of epilithic algae measured in the laboratory and in situ. *In* Periphyton of freshwater ecosystems. *Edited by* R.G. Wetzel. Dr. W. Junk, The Hague, The Netherlands. pp. 73–87.

Turner, M.A., M.B. Jackson, D.L. Findlay, R.W. Graham, E.R. DeBruyn, and E.M. Vandermeer. 1987. Early responses of periphyton to experimental lake acidification. Can. J. Fish. Aquat. Sci. 44(Suppl. 1): 135–149.

Turner, M.A., E.T. Howell, M. Summerby, R.H. Hesslein, D.L. Findlay, and M.B. Jackson. 1991. Changes in epilithon and epiphyton associated with experimental acidification of a lake to pH 5. Limnol. Oceanogr. 36: 1390–1405.

Turner, M.A., E.T. Howell, G.G.C. Robinson, P. Campbell, R.E. Hecky, and E.U. Schindler. 1994. Roles of nutrients in controlling growth of epilithon in oligotrophic lakes of low alkalinity. Can. J. Fish. Aquat. Sci. 51: 2784–2793.

Turner, M.A., E.T. Howell, G.G.C. Robinson, J.F. Brewster, L.J. Sigurdson, and D.L. Findlay. 1995*a*. Growth characteristics of bloom-forming filamentous green algae in the littoral zone of an experimentally acidified lake. Can. J. Fish. Aquat. Sci. 52: 2251–2263.

Turner, M.A., G.G.C. Robinson, B.E. Townsend, B.J. Hann, and J.A. Amaral. 1995*b*. Ecological effects of blooms of filamentous green algae in the littoral zone of an acid lake. Can. J. Fish. Aquat. Sci. 52: 2264–2275.

Webster, K.E., T.M. Frost, C.J. Watras, W.A. Swenson, M. Gonzalez, and P.J. Garrison. 1992. Complex biological responses to the experimental acidification of Little Rock Lake, Wisconsin, USA. Environ. Pollut. 78: 73–78.

Wei, Y.-X., Y.-K. Yung, M.B. Jackson, and T. Sawa. 1989. Some Zygnemataceae (Chlorophyta) of Ontario, Canada, including descriptions of two new species. Can. J. Bot. 67: 3233–3247.

Growth characteristics of bloom-forming filamentous green algae in the littoral zone of an experimentally acidified lake[1]

Michael A. Turner, E. Todd Howell, Gordon G.C. Robinson, John F. Brewster, Leif J. Sigurdson, and David L. Findlay

Abstract: Filamentous green algae, predominantly *Mougeotia* and *Zygogonium*, bloom frequently in the littoral zones of acidified lakes. Growth characteristics of *Zygogonium*-dominated filamentous green algae were studied for 4 yr in an experimentally acidified (pH 4.5) lake at the Experimental Lakes Area of northwestern Ontario. They were present in low abundance as periphyton (algal associations attached to surfaces) during spring, and as blooms of metaphyton (benthic algae unconstrained by surfaces) beginning in midsummer and reaching a maximum in early fall. Metaphytic filamentous green algae displayed high photosynthetic capacity in summer despite the oligotrophic nature of the acidified lake. The major factors controlling photosynthetic rates of *Zygogonium* were similar to those controlling *Mougeotia*, and included algal crowding, irradiance, dissolved inorganic carbon, and water temperature. Rates of photosynthesis were negatively dependent upon algal crowding, so that highest rates were associated with minimum algal crowding. Light requirements for photosynthesis were higher than those of the epilithon, which were dominant prior to acidification. The dependence of photosynthesis on ambient concentrations of dissolved inorganic carbon was partly regulated by water temperature. Anthropogenically caused releases from growth limitations (e.g., increased availability of limiting nutrients, increased water temperature, and extension of the growing season) may cause proliferation of filamentous green algae in the future.

Résumé : Les chlorophycées filamenteuses (algues vertes), surtout *Mougeotia* et *Zygogonium*, prolifèrent souvent dans les zones littorales des lacs acidifiés. Les caractéristiques de croissance des chlorophycées filamenteuses à prédominance de *Zygogonium* ont fait l'objet d'études échelonnées sur 4 ans dans un lac acidifié expérimentalement (à un pH de 4,5) dans la région des lacs expérimentaux du nord-ouest de l'Ontario. Ces algues étaient présentes en faible abondance sous forme de périphyton (associations algales fixées à des surfaces) au cours du printemps, et sous forme d'efflorescences du métaphyton (algues benthiques non liées à des surfaces), commençant à proliférer au milieu de l'été et atteignant un niveau maximal au début de l'automne. Les algues vertes du métaphyton présentaient une grande capacité photosynthétique en été malgré le caractère oligotrophe du lac acidifié. Les principaux facteurs régissant la photosynthèse de *Zygogonium* étaient semblables à ceux qui sont à la base de la photosynthèse de *Mougeotia*, notamment la densité de peuplement, l'éclairement énergétique, le carbone inorganique dissous et la température de l'eau. La photosynthèse était inversement proportionnelle à la densité des algues, le taux le plus élevé étant observé aux endroits où la densité de peuplement était minimale. Les besoins en éclairement aux fins de la photosynthèse étaient supérieurs à ceux de l'épilithon, qui dominait avant l'acidification. La dépendance de la photosynthèse à l'égard des concentrations ambiantes

Received August 5, 1993. Accepted April 28, 1995.
J12036

M.A. Turner, L.J. Sigurdson,[2] and D.L. Findlay. Department of Fisheries and Oceans, Freshwater Institute, 501 University Crescent, Winnipeg, MB R3T 2N6, Canada.
E.T. Howell.[3] Institute for Environmental Studies, University of Toronto, Toronto, ON M5S 1A4, Canada.
G.G.C. Robinson. Department of Botany, University of Manitoba, Winnipeg, MB R3T 2N2, Canada.
J.F. Brewster. Department of Statistics, University of Manitoba, Winnipeg, MB R3T 2N2, Canada.

[1] This paper is one of a series done in honor of the 25th anniversary of the Experimental Lakes Area.
[2] Present address: 144 Knudson Street, Kanata, ON K2K 2L8, Canada.
[3] Present address: Water Resources Branch, Ontario Ministry of the Environment, Toronto, ON M4V 1P5, Canada.

Can. J. Fish. Aquat. Sci. **52**: 2251–2263 (1995). Printed in Canada / Imprimé au Canada

de carbone inorganique dissous est régie en partie par la température de l'eau. La réduction anthropique de facteurs limitatifs de la croissance (p. ex., la disponibilité accrue d'éléments nutritifs limitants, l'augmentation de la température de l'eau et la prolongation de la saison de croissance) peuvent causer la prolifération future d'algues vertes.

[Traduit par la Rédaction]

Introduction

The proliferation of filamentous green algae (FGA) caused by acidification is a major change in the littoral zone of lakes. This phenomenon was first observed in Scandinavia (Hendrey et al. 1976; Almer et al. 1978) and later seen in culturally and experimentally acidified lakes of North America (Schindler and Turner 1982; Stokes 1986; Howell et al. 1990; Brezonik et al. 1993; Turner et al. 1995*b*). Yet aside from studies of artificial substrata (Müller 1980; Fairchild and Everett 1988), preliminary ecological research (Wei et al. 1989; Howell et al. 1990; France and Welbourn 1992), and recent physiological research (Graham et al. 1995), relatively little is known about the ecology of FGA growth in acid lakes.

Acid-induced growths of FGA occurred initially as epilithic waterline bands and epiphytic accumulations at pH ≥ 6.0 in experimentally acidified Lake 302S at the Experimental Lakes Area (ELA) in northwestern Ontario (Turner et al. 1987). As lake acidification progressed, the FGA began to grow as metaphyton (Howell et al. 1990), i.e., as forms that were either unattached to any substratum, or were so large that their growth form was unrestricted by the surface on which the algae initially developed. Metaphyton bloomed annually as the epilimnetic pH declined to 5.5 and below in Lake 302S (Turner et al. 1995*b*), although blooms also occurred at pH ~ 6 in lakes located on the Canadian Shield in central Ontario (France and Welbourn 1992). Blooms of *Spirogyra* and *Mougeotia* at pH 5.5–4.8 were followed by *Zygogonium* as the pH declined below 4.8 (Turner et al. 1995*b*). *Zygogonium* is the most abundant zygnematacean alga that blooms metaphytically in acidified lakes of central Ontario (Wei et al. 1989; France et al. 1992).

The metabolism of these *Mougeotia*- and *Zygogonium*-dominated metaphytic FGA differed from that of acidified periphyton (Howell et al. 1990). For example, these FGA required high light intensities for optimal photosynthesis (Graham et al. 1995), were capable of potentially high rates of photosynthesis, and demonstrated an inverse relationship between rates of biomass-normalized photosynthesis and algal biomass (Howell et al. 1990).

Despite their status as nuisance algae (SPR Associates 1986), the ecology of FGA in acid lakes is otherwise little understood for a number of reasons. First, ecological studies of acidification have focused primarily on the structure and function of the pelagic zone in lakes (Stokes 1986). Second, the littoral zone was considered unimportant to energy flow in many boreal forest lakes (Schindler et al. 1973). Last, appropriate methods were unavailable to address littoral heterogeneity and the structural complexity of benthic algal communities (Howell et al. 1990). As a result, previous whole-lake experiments (e.g., Lake 223: Schindler and Turner 1982; Schindler et al. 1985) have neglected study of the ecological factors controlling growth of FGA.

The principal objective of this study was to characterize the ecological factors controlling photosynthetic potential and biomass development of FGA in Lake 302S as it was acidified to pH 4.5 from pH 5.0. This information is useful in developing strategies for controlling nuisance growths of FGA. In addition, the information can be used to suggest physiological, laboratory-based studies and to direct future development of FGA growth models.

Methods

Study lake

Lake 302S (93°45′W, 49°40′N) was first described by Brunskill and Schindler (1971). It has a surface area of 10.9 ha, a mean depth of 5.1 m, a mean July thermocline depth of 5 m, and a median Secchi depth of 4 m (Cruikshank 1988). The nutrient chemistry of this oligotrophic lake was characterized by Howell et al. (1990), Rudd et al. (1990), and Turner et al. (1991); the trace metal chemistry was documented by Cruikshank et al. (1988). The artificial separation of Lake 302S from its downstream northern basin and the subsequent experimental acidification of Lake 302S with sulfuric acid were described by Turner et al. (1991). The lake's epilimnetic pH was lowered in annual stepwise increments beginning from ~6.7 in 1982 to ~4.5 in 1988, a level that was held through to 1991. The lake has been allowed to recover since then.

Measurement of FGA photosynthesis

Collection of algae

Duplicate composite samples of metaphytic FGA were collected near three shoreline stations known to regularly develop blooms. FGA were collected from 0–1 m water depth using a 100-μm mesh sweep net. Drained algal volume was measured, and the FGA were returned immediately to lake water in a 1-L polyethylene bottle. The pooling of 5 mL of FGA from each of the three stations yielded ~15 mL of FGA$\cdot$L^{-1} in each of the duplicate collections. Metaphyton was usually unavailable during May and early June of each year, so epiphytic samples were collected from macrophytes and submerged trees.

Aliquots of the duplicate lake collections were combined and sampled for taxonomic analysis on each sampling occasion. These samples were then preserved in a final concentration of 4% acid Lugol's solution and FAA (formalin, alcohol, and acetic acid). Turner et al. (1987, 1991) described the procedures used for subsequent taxonomic analysis.

Description of incubator

The incubator was a simple open basin (0.44 × 1.20 × 0.13 m, i.d.) constructed of grey opaque polyethylene

Table 1. Measurement terms for photosynthesis of filamentous green algae.

Symbol	Meaning	Units
α	Initial slope of $P = f(I)$	μmol C·mg dry weight^{-1}·(3600 μE·m^{-2})$^{-1}$
B	Areal concentration of biomass	g·m^{-2}
D	Algal density or crowding	g·L^{-1}
DIC	Dissolved inorganic carbon	μM
I	Irradiance or light intensity	μE·m^{-2}·s^{-1}
P_b	Biomass-normalized photosynthesis	μmol C·mg dry weight^{-1}·h^{-1}
P_g	Respiration-normalized photosynthesis	μmol C·(125 mL)$^{-1}$·h^{-1}
P_{gb}	Respiration- and biomass-normalized photosynthesis	μmol C·mg dry weight^{-1}·h^{-1}
P_{gbm}	Maximum rate of P_{gb}	μmol C·mg dry weight^{-1}·h^{-1}
R_d	Biomass-normalized respiration	μmol C·mg dry weight^{-1}·h^{-1}

(0.9 cm thick). Mirrors lined the bottom and walls of the interior. Clear acrylic replaced the grey polyethylene at one end where a single 150-W HPS sodium-vapor lamp (Sylvania type HPS-61-150-N) was placed. Water temperature within the incubator was maintained within 1–2°C of epilimnetic temperature by addition of ice as needed. Locations within the incubator that yielded the needed light intensities were determined prior to the start of the experiments. Dark bottles used to measure dark respiration were prepared by dipping Pyrex bottles in rubberized black paint.

Measurement strategy

Samples were returned to the laboratory and placed in the incubator at an irradiance of ~500 μE·m^{-2}·s^{-1} (1 μE·m^{-2}·s^{-1} = 0.217 W·m^{-2}); incubations were started within ~2 h of algal collection. Just prior to sample manipulation, the 1-L bulk samples were mixed in a Waring blender for 1–3 s at the lowest available setting and were then returned to the incubator. The blending permitted control of algal quantities and effectively standardized any temporal changes of in situ structure of the FGA, but had no discernible effect on rates of photosynthesis or cellular structure (Turner 1993).

Aliquots of the bulk algal samples were added to 125-mL Pyrex reagent bottles filled with lake water. After mixing for ~5 s, two or three water samples for analysis of initial concentrations of dissolved inorganic carbon (DIC) were withdrawn from each 125-mL suspension through a porous polyethylene frit (nominal pore size of 100 μm) connected to a 2.5-mL syringe by a 3-way valve and Tygon® tubing. Water removed for DIC analysis was replaced immediately with lake water of appropriate DIC concentration (see below). The sample bottle was then stoppered, placed in the incubator, and incubated for ~30–60 min. The initial DIC samples were placed in a dark ice bath until analysis by an infrared gas technique (Turner et al. 1987). Final DIC samples were collected in similar fashion.

Dry weight of algal suspensions was determined as a surrogate for algal biomass by filtering each 125-mL sample suspension through preweighed 45- or 25-mm Whatman GF/C filters. Filters and blanks were dried to constant weight at 60°C.

Algal photosynthesis (see Table 1 for measurement terms) was calculated as the measured change in DIC adjusted for incubation time and the amount of algal material incubated. Methodological details are described in Turner (1993).

Seasonal variation in factors controlling photosynthesis

Lake 302S was sampled approximately once every 4 wk during the open-water seasons of 1988–1991, yielding 27 sampling dates. Usually 8–10 samples were used on each date to evaluate the relationship between photosynthesis and algal crowding or density. Photosynthesis was measured in triplicate at each of at least three different levels of algal density in 1988. The algal density of the intermediate level was 47 ± 24 mg dry weight·L^{-1} (mean ± SD, n = 7). From 1989 to 1991, four levels of density were sampled in duplicate on each date. The algal density at the second lowest level, the level at which variation in responses to DIC and irradiance was examined, averaged 24 ± 7 mg dry weight·L^{-1} (n = 20).

The photosynthesis–irradiance relationship was measured from 1989 to 1991 using four levels of irradiance, each examined in duplicate. Nominal light intensities were 0, 75, 500, and 1600 μE·m^{-2}·s^{-1}. Respiration was measured in duplicate in 1988 and 1989, and in triplicate in 1990 and 1991. These samples were inoculated with FGA at the same algal density as for DIC, as described above.

To evaluate the role of DIC as a controlling factor, FGA were incubated at three nominal levels of DIC (ambient, 0.5× ambient, and 2× ambient) from 1989 to 1991. Nitrogen (N_2) gas was bubbled through a 1-L container of lake water for ~20 min to obtain low DIC (0.5× ambient) concentrations. One or two millilitres of saturated carbon dioxide (CO_2) solution was added to 1 L of lake water to obtain high DIC concentrations. Initial DIC concentrations were measured in all cases.

Several nutrient ratios were measured to determine whether N and phosphorus (P) were limiting FGA growth. This approach used the guidelines of Healey (1975) and Healey and Hendzel (1979), recognizing that both nonalgal material and algae in varying growth states could obscure the interpretation. Aliquots of FGA collections were filtered through preignited Whatman GF/C filters, which were then frozen and subsequently analysed for particulate carbon (PC), nitrogen (PN), and phosphorus (PP), according to the procedures of Stainton et al. (1977).

Fig. 1. Seasonal variation in the slope of the linear fit of respiration-normalized photosynthesis (P_g) versus incubated algal biomasses, i.e., P_g = slope × biomass. Standard errors are shown.

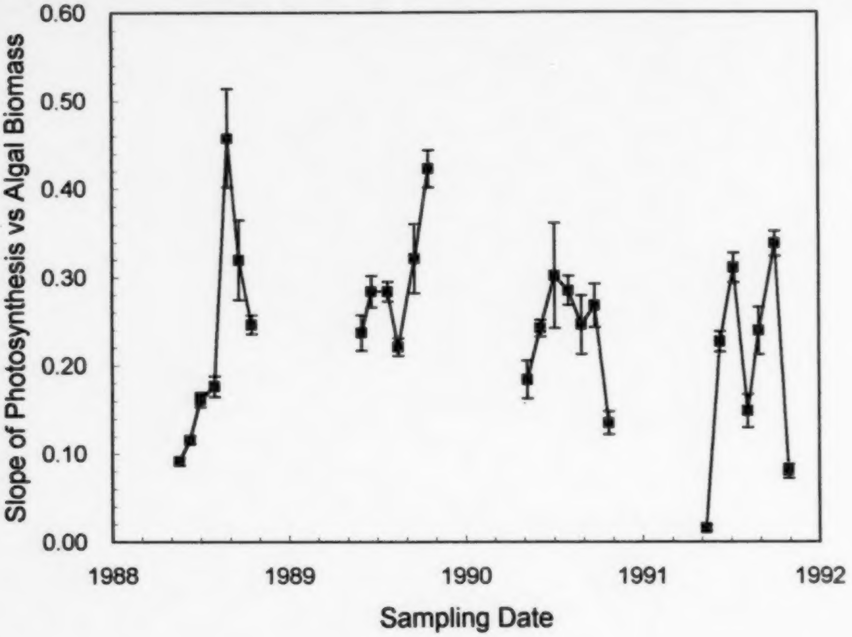

Duplicate check samples were created (and frozen) during the first sampling period of 1990 to assess the degree of analytical variation in particulate composition over time. These samples were processed along with the ones generated during the remainder of 1990. The overall percent coefficients of variation (CV) for PC, PN, and PP were 11, 16, and 9%, respectively. The duration of freezing of the check samples was not responsible for this variation.

Measurement of FGA biomass

Seasonal changes in FGA biomass at 1 m depth in the lake were measured in 1991 to evaluate the generality of the metabolism studies, and to establish the ecologically relevant bounds for variation in FGA growth. The shoreline of Lake 302S was marked every 20 m, and the total possible number of sampling sites was divided into 16 equal groups, the anticipated maximum sampling load. A single station was randomly selected from the first sampling group; the corresponding station was sampled in all other groups. The average slope of the lake bottom at these 16 stations was 31 ± 19% (range 3–88%).

The diver used a 1 × 1 m polyethylene square to sample three quadrats at each of the 16 long-term stations. Percent areal coverage and growth thickness were measured, typically 3–9 times in each quadrat.

Seasonal changes in algal density or crowding were measured by collecting adjacent to two stations on each sampling occasion. The geometric shape of the sampled growth forms was characterized (typically a box, sphere, or cylinder), and the pertinent dimensions were measured by the diver to allow calculation of the volume of the algal growth form. The entire growth form was then cleaned of debris and placed into a polyethylene bag. The sample was subsequently dried and its weight was measured to calculate algal crowding or density as grams dry weight per litre.

Depth variation (1–5 m) was measured at eight stations from August 12 to 14. Percent coverage and growth thickness were measured in three adjacent 1 × 1 m quadrats at each combination of station and depth. FGA were collected from two stations to measure depth variation in algal density.

Results

Metabolic characteristics of FGA growth

Algal density

Rates of photosynthesis, normalized only for respiration (P_g; Table 1), were linear functions of the amount of algal biomass (dry weight) incubated, i.e., P_g = slope × biomass. The linear fit averaged 94 ± 6% for the 27 seasonal observations made between 1988 and 1991. The constant of the linear relationship was set equal to zero because P_g is zero when algal biomass is zero. The slope of the linear relationship ranged from 0.02 to 0.46 (Fig. 1), with an overall mean of 0.24 ± 0.10 (n = 27). The slope of the relationship varied seasonally with annual minima in spring and fall (Fig. 1); the autumn of 1989 was an exception, possibly because of the relatively high temperatures (8°C in 1989, compared with 6 and 5°C in 1990 and 1991) at the time of collection.

Although the linear model was a reasonable descriptor of the relation between P_g and algal biomass, it was biased.

Table 2. Irradiance parameters for Lake 302S filamentous green algae as fit to Smith's (1936) equation: $P_{gb} = (P_{gbm} \times \alpha \times I) / (P_{gbm}^2 + (\alpha \times I)^2)^{0.5}$.

Year	Day	*n*	R_d	SD	*n*	P_{gbm}	ASE	α	ASE	% r^2
1988	139	2	0.03	0.01						
1988	160	2	0.08	0.02						
1988	182	2	0.09	0.01						
1988	211	2	0.06	0.01						
1988	239	2	0.11	0.01						
1988	262	2	0.07	0.02						
1988	289	2	0.06	0.03						
1989	151	2	0.06	0.11	8	0.29	0.03	9.0×10^{-4}	1.3×10^{-4}	95
1989	172	2	0.14	0.05	8	0.35	0.02	1.8×10^{-3}	1.1×10^{-4}	98
1989	206	2	0.11	0.02	8	0.27	0.02	2.0×10^{-3}	1.4×10^{-4}	98
1989	228	2	0.06	0.03	8	0.34	0.04	1.3×10^{-3}	1.6×10^{-4}	94
1989	262	2	0.11	0.03	8	1.04	0.17	2.0×10^{-3}	3.2×10^{-4}	93
1989	291	2	0.31	0.17	8	0.53	0.09	3.5×10^{-3}	1.5×10^{-3}	90
1990	129	3	0.12	0.08	9	0.18	0.06	1.3×10^{-3}	4.4×10^{-4}	60
1990	156	3	0.16	0.12	9	0.29	0.05	1.1×10^{-3}	2.2×10^{-4}	86
1990	185	3	0.10	0.08	8	0.41	0.09	1.8×10^{-3}	4.2×10^{-4}	82
1990	214	3	0.16	0.07	9	0.45	0.06	3.5×10^{-3}	1.6×10^{-3}	91
1990	240	3	0.07	0.16	9	0.86	0.18	2.1×10^{-3}	5.5×10^{-4}	83
1990	268	3	0.04	0.02	9	0.50	0.04	2.2×10^{-3}	3.2×10^{-4}	96
1990	296	3	0.07	0.08	9	0.15	—[a]	5.8×10^{-4}	—[a]	55
1991	131	3	0.00	0.02	9	0.05	—[a]	1.5×10^{-4}	—[a]	69
1991	159	3	0.08	0.04	9	0.28	0.02	1.8×10^{-3}	1.1×10^{-4}	97
1991	189	3	0.21	0.05	9	0.51	0.04	3.3×10^{-3}	9.8×10^{-4}	96
1991	218	3	0.06	0.03	9	0.55	0.27	4.2×10^{-4}	2.7×10^{-4}	96
1991	241	3	0.04	0.03	9	1.16	0.51	5.7×10^{-4}	1.4×10^{-4}	95
1991	274	3	0.21	0.10	9	0.39	0.04	6.0×10^{-3}	2.2×10^{-3}	95
1991	302	3	0.05	0.02	8	0.09	0.01	1.6×10^{-3}	2.0×10^{-4}	93
Mean			0.11	0.07		0.44		1.9×10^{-3}		88
SD			0.07	0.05		0.29		1.4×10^{-3}		13
n			20	20		20		20		20

Note: Measurement terms are described in Table 1. ASE, asymptotic standard error.

[a] Not computable.

The residuals of these fits were small, however, and they were nonzero only when algal densities were very low, a situation deemed acceptable.

Rates of photosynthesis, when normalized for the amount of algal material incubated (P_b), were nonlinear decreasing functions of algal density (D). For example, a linear relationship accounted for only 51% of variance in the 26 August 1988 experiment, when five levels of density were duplicated. Other nonlinear relationships fit better: $P_b = \log(D)$, 64%; $(-1/P_b) = \text{intercept} + (\text{slope} \times D)$, 84%; and $\log(P_b) = \log(D)$, 91%.

Light intensity

No general seasonal pattern existed in rates of respiration. The overall mean (± SE) rate of respiration for the 27 sets of seasonal observations was 0.098 ± 0.013 μmol C·mg^{-1}·h^{-1}. Correlational analysis indicated that respiration was independent of DIC, algal density, and water temperature. The lack of relationship between respiration and temperature was surprising, and may have been a result of the insufficient precision of the measurements. For example, the mean CV in biomass-normalized respiration (R_d) on any given date was 61% (calculated from Table 2).

The nonlinear dependency of biomass- and respiration-normalized photosynthesis (P_{gb}) on irradiance (I) was evaluated in detail on 30 August 1988. Each of six irradiances (0–1700 μE·m^{-2}·s^{-1}) was replicated three times. Smith's (1936) and Jassby and Platt's (1976) own hyperbolic tangent function fitted equally well (~89%) using the Marquardt convergence procedure (Wilkinson 1990). Values of the maximum rate of biomass- and respiration-normalized photosynthesis (P_{gbm}) predicted by the first two equations were within 1%. The initial slope of the photosynthesis–irradiance relationship (α) predicted by Smith's equation was 34% greater than that derived from Jassby and Platt's equation. This reasonable agreement between formulations was expected (Geider and Osborne 1991). The simpler equation of Smith was therefore chosen for use: $P_{gb} = (P_{gbm} \times \alpha \times I) / (P_{gbm}^2 + (\alpha \times I)^2)^{0.5}$.

The value of P_{gbm} was 0.44 ± 0.29 μmol C·mg^{-1}·h^{-1} (mean ± SD) for the 20 experimental cases measured from 1989 to 1991 (Table 2). The corresponding value for α

Fig. 2. Seasonal changes in the dependency of biomass- and respiration-normalized photosynthesis (P_{gb}, Table 1) upon irradiance. The photosynthetic maximum (P_{gbm}, μmol $C{\cdot}(mg{\cdot}h)^{-1}$) and α ((μmol C·mg dry weight^{-1})·(3600 $\mu E{\cdot}m^{-2})^{-1}$) were derived from fits of Smith's (1936) equation to the incubator-generated data.

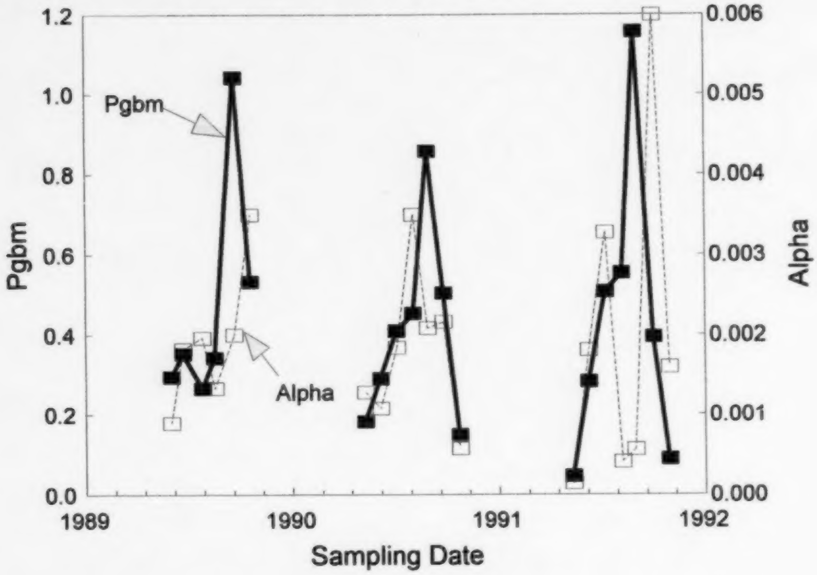

was 0.0019 ± 0.0014 μmol $C{\cdot}m^{-2}{\cdot}(3600\ \mu E{\cdot}mg)^{-1}$. The degree of fit in the seasonal studies averaged 88 ± 13% (Table 2). The degree of fit varied seasonally, being poorer in early spring and in late fall than in summer, possibly as a result of a low signal-to-noise ratio caused by the reduced photosynthetic rates at these times.

The seasonal pattern of variation in P_{gbm} was generally unimodal with annual maxima occurring typically between late August and mid September (Fig. 2). Although P_{gbm} was correlated with water temperature ($r = 0.44$, $n = 20$, $P \sim 0.05$), it appeared to lag behind water temperature. For example, the correlation was improved by allowing temperature to lag by one sampling period ($r = 0.61$, $P < 0.01$).

The degree to which FGA were readily saturated by light varied seasonally. When the overall mean values of P_{gbm} were incorporated in Smith's photosynthesis–irradiance equation, 90% of P_{gbm} was achieved at irradiances of 500 $\mu E{\cdot}m^{-2}{\cdot}s^{-1}$. This was similar to the average situation in spring, but by late August 90% of P_{gbm} was usually achieved at the much higher value of 1300 $\mu E{\cdot}m^{-2}{\cdot}s^{-1}$. By late October, in contrast, 90% was achieved below 300 $\mu E{\cdot}m^{-2}{\cdot}s^{-1}$.

No evidence of photoinhibition existed in these investigations. This was corroborated by the fact that residuals of the fits to Smith's equation, which ignores photoinhibition, were independent of irradiance. If photoinhibition had been important, residuals should have been large at high irradiances.

Nutrients: inorganic C

Photosynthesis, normalized for biomass and adjusted for respiration, was generally a linear function of DIC, i.e., P_{gb} = slope × DIC. The average r^2 was 82 ± 20% (mean ± SD, $n = 20$); when two cold-water and high-DIC observations were excluded the r^2 value increased to 88 ± 8% ($n = 18$). Standard errors of these slope estimates averaged 19%. Minima in slope values occurred in spring and fall, whereas annual maxima occurred during July and August (Fig. 3). The slope of P_{gb} as a linear function of DIC, therefore, correlated positively with water temperature (slope = 0.0018 + 0.00057 × temperature; $r = 0.69$, $n = 20$, $P \leq 0.001$). The synchrony between slope and P_{gbm} was also strong ($r = 0.59$, $n = 20$, $P \leq 0.01$), possibly because of water temperature.

The slope of P_{gb} as a linear function of DIC was negatively correlated with DIC as expected, but the correlation was weak ($r = -0.42$, $n = 20$, $P \sim 0.06$). Although this preliminary result supports the idea that affinity for CO_2 is sensitive to its availability, a multiple regression of slope with both temperature and DIC was performed. Inclusion of DIC provided no significant improvement ($P \sim 0.98$) over that contributed by temperature alone. It was concluded, therefore, that the negative relationship between the slope and DIC availability occurred indirectly through the generally negative relationship between DIC and water temperature.

Other nutrients

The indicator of N deficiency, the mass ratio of N:C, averaged 0.11 ± 0.02 (mean ± SE, sampling period = 4 yr) and showed no regular seasonal trend from 1988 to 1991. Thus, the FGA on average were moderately N deficient (0.10 < N:C < 0.13; Healey 1975).

The two indicators of P deficiency (1000 × P:C and N:P) also signified deficiency. The mass ratio of 1000 × P:C in combined samples of incubated FGA averaged 5.8 ±

Fig. 3. Seasonal variation in the slope of the linear dependence of biomass- and respiration-normalized photosynthesis on concentrations of dissolved inorganic carbon (DIC). Prevailing epilimnetic concentrations ($\mu mol \cdot L^{-1}$) of DIC are also shown.

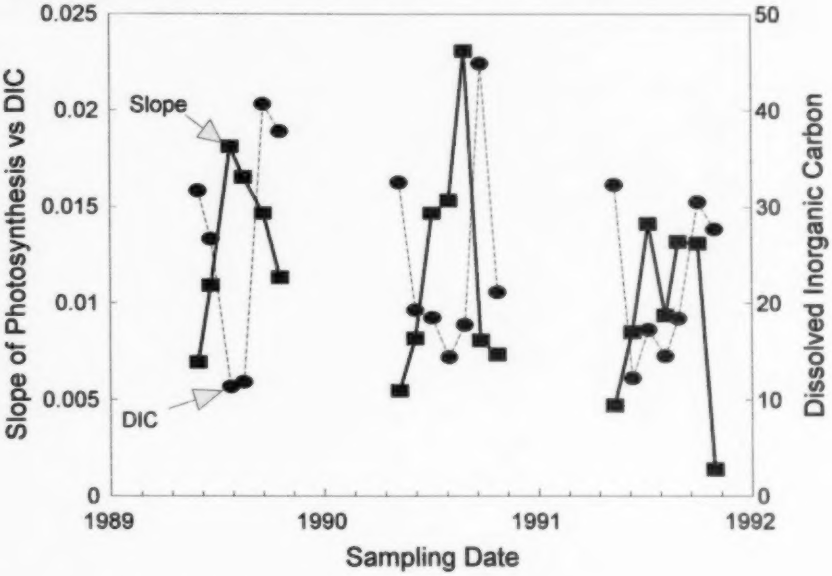

0.6 (sampling period = 3 yr), and generally remained below 10 from 1989 to 1991, which indicated extreme deficiency (Healey and Hendzel 1979). The ratio of N:P averaged 19 ± 1 (sampling period = 3 yr), suggesting borderline deficiency (Healey 1975).

Characteristics of FGA development

Algal composition

Collections of FGA were sometimes diverse when examined microscopically. Green algae dominated collections from 1989 to 1991, averaging 86 ± 24% (mean ± SD, $n = 19$) of the algal biomass. Springtime periphyton samples, however, sometimes contained a large proportion of diatoms, principally *Tabellaria quadriseptata* Knudson, *Tabellaria fenestrata* (Lyngbye) Kützing, or *Tabellaria flocculosa* (Roth) Kützing.

The abundance of *Zygogonium* as metaphyton varied somewhat among years (Fig. 4), but overall was 67 ± 31% ($n = 19$) of FGA biomass. *Mougeotia* dominated the assemblage briefly in the early summers of 1990 and 1991 and contributed 30 ± 30% ($n = 19$) of overall FGA biomass, but *Zygogonium* was dominant by midsummer and remained so subsequently. *Oedogonium* was always a small component (2 ± 2%, $n = 19$) and displayed no regular seasonal pattern.

Qualitative observations of seasonal development of FGA

Several qualitative observations of FGA development aid in understanding seasonal effects of the factors affecting FGA growth. FGA were epiphytic on submerged plants and branches in the shallows during spring; this growth form was sampled in spring for analysis. FGA were also found as highly compact, brownish mats on sediments and in some rock crevices. The brown mats, which were probably decomposing FGA, were frequently underlain by an easily disturbed black floc containing high concentrations of iron sulfide (Amaral 1991) and were sometimes covered by an orange layer, presumably enriched with iron oxides.

In the early to mid summer, previously periphytic FGA broke away in some locations to form the ‘tumbleweed’ stage. These amorphous masses settled in new areas, spreading and thickening with continued growth. In some cases, the FGA eventually blanketed large expanses of the bottom of the littoral zone.

In late summer or early fall, thick mats of FGA sometimes trapped quantities of gas bubbles produced by underlying sediments and (or) algal photosynthesis. The bubbles could cause the FGA to rise to the lake surface and drift elsewhere. Alternatively, the FGA collapsed, usually in locations where patches of the otherwise green or grey mats had begun to darken, eventually forming the brown phase or blackened sediment seen in spring.

Seasonal changes in biomass and algal density

Development of FGA varied substantially during 1991 (Fig. 5; Table 3), as expected from seasonal variation in different metabolic parameters. Coverage by FGA of the lake bottom at 1 m depth increased from 6% in May to a maximum of 74% in early September, declining to 46% in late October. The pattern of seasonal variation in algal thickness was similar to that of bottom coverage (Fig. 5). Minima occurred in spring and fall, and a maximum occurred in August. The maximum mean algal thickness was 16 ± 2 cm (mean ± SE); station means ranged from 7 to 30 cm.

Algal density, measured as the dried biomass of FGA that occupied a volume of water, varied seasonally as the

Fig. 4. The percentage composition of green algal biomass represented by *Zygogonium*, *Mougeotia*, and *Oedogonium* in samples of filamentous green algae.

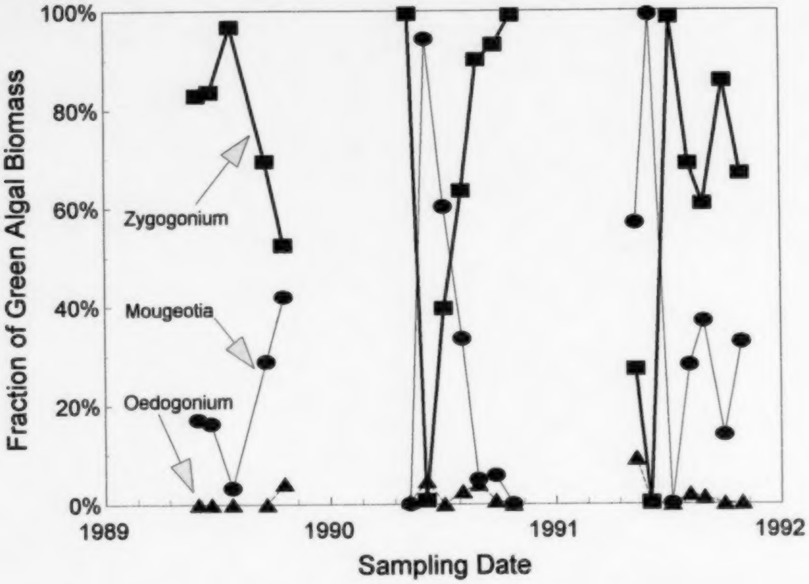

Fig. 5. Features of the development of filamentous green algal biomass at the 1-m sampling stations in 1991: areal coverage (%), algal thickness (cm), algal density ($g \cdot L^{-1}$), and areal biomass of algae ($g \cdot m^{-2}$). Standard errors are provided in Table 3.

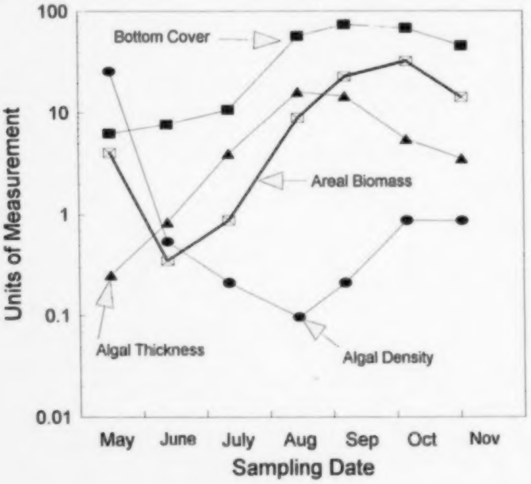

inverse of the other biomass-related measures (Fig. 5). The FGA reached a minimum of 0.1 $g \cdot L^{-1}$ in mid August, and maxima of 26 and 0.9 $g \cdot L^{-1}$ in spring and fall, respectively. The greater spring maximum corresponded to the FGA existing as periphyton rather than as metaphyton.

Seasonal variation in the areal biomass of FGA was similar to other measures of FGA coverage (Fig. 5). Areal biomass of algae was calculated by adjusting algal thickness for both bottom coverage and algal density. The maximum biomass of algae at 1 m depth occurred in early October (Fig. 5), whereas the minimum surprisingly occurred in June (rather than in May). It is possible that in 1990, FGA did not completely decompose under ice, but then decomposed after exposure to the higher water temperatures of spring.

Effect of depth and slope

The biomass of FGA also varied strongly with depth (Fig. 6). Bottom coverage, algal thickness, and biomass declined progressively with depth. Algal density, in contrast, increased with water depth. This increase was insufficient to offset the decline in algal coverage and thickness, so that algal biomass also decreased with water depth.

The slope of the lake bottom was also important to development of FGA. The average proportion of the lake bottom covered by FGA during the open-water season decreased as the slope increased (% cover = 61% − 0.61 × % slope; $r^2 = 0.44$, $n = 16$, SE of constant = 0.13, SE of coefficient = 0.18, $P < 0.01$). Algal thickness, however, was independent of slope ($r^2 = 0.09$).

Discussion

The progressive acidification of Lake 302S produced increased coverage (depth and lateral extent) and thickness of metaphytic FGA (Howell et al. 1990; Turner et al. 1995*b*). For example, FGA reached a maximum coverage of ~30 $g \cdot m^{-2}$ at 1 m depth in Lake 302S during 1991. This was much larger than the <2 $g \cdot m^{-2}$ found in less acidic Plastic Lake (Howell et al. 1990), but was similar to coverage by *Oedogonium* in neutral Lake Wingra (McCracken et al. 1974).

Table 3. Biomass of filamentous green algae at 1 m depth in Lake 302S during 1991.

	Sampling day							
	135	162	191	224	246	275	301	Mean
Stations[a]	4	16	16	16	16	16	5	
Bottom coverage (%)	6±6	8±3	11±6	57±8	74±7	68±6	46±11	39±11
Algal thickness (cm)	0.25±0.25	0.84±0.09	3.9±0.4	16.1±1.8	14.6±1.4	5.5±0.4	3.5±0.8	6.4±2.4
Areal thickness (cm)	0.02	0.06	0.42	9.2	10.9	3.7	1.6	2.5
Algal density ($g \cdot L^{-1}$)	26±9	0.54±0.13	0.21±0.07	0.10±0.02	0.21±0.12	0.87±0.63	0.87±0.25	4.1±3.6
Algal biomass ($g \cdot m^{-2}$)	4.0	0.3	0.9	8.9	22.8	32.4	14.2	11.9

Note: Values are given as the mean ± SE.

[a] Number of sites at which algal cover and thickness were measured.

Fig. 6. The vertical distribution of filamentous green algae at eight stations in August 1991. The percentage of the maximum value measured for bottom coverage, algal thickness, algal density (two stations only), and areal biomass is expressed as a function of water depth (m).

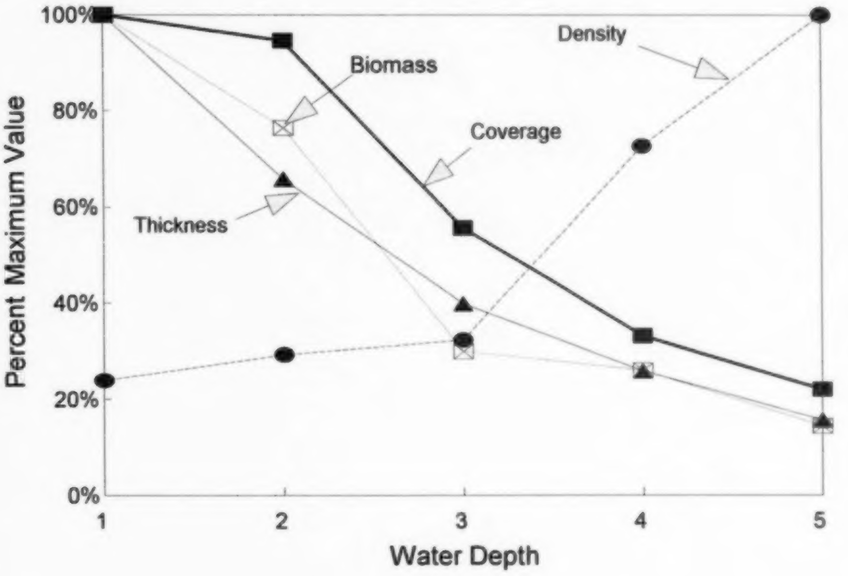

Zygogonium, the most common bloom-forming zygnematacean alga in acid lakes of central Ontario (Wei et al. 1989; France et al. 1992), became the annually dominant member of the FGA with acidification of Lake 302S to pH 4.5 (Fig. 4; Turner et al. 1995*b*). It replaced *Mougeotia*, the subject of an earlier study in Lake 302S (Howell et al. 1990). The findings of these experiments, therefore, apply principally to the FGA complex dominated in summer and fall by *Zygogonium*, and having a heterogeneous springtime complex (Fig. 4).

Low respiration rates caused the respiration:photosynthesis ratio in FGA to be much lower than that seen in acidified periphyton (Turner et al. 1987, 1991, 1995*b*). For example, respiratory losses in the FGA averaged 16% during August of 1989–1991 (Table 2), whereas average epilithic losses approached 100% during these periods (Turner et al. 1995*b*). In other words, metaphytic *Zygogonium* was able to put a greater fraction of its photosynthesis into net growth during the warm periods of the open-water season than could the previously dominant epilithon. This FGA growth also exceeded any grazing losses, resulting in appreciable accumulation of biomass (Fig. 5).

Temporal and spatial characteristics of biomass distribution

Variation in the occurrence of FGA in the lake was considerable both spatially (horizontally and vertically: Table 3, Fig. 6) and temporally (seasonally, Fig. 5; annually, Turner et al. 1995*a*). Understanding this variability aids in evaluating the reliability of the metabolic information. For example, the seasonal pattern of biomass development generally corroborated the seasonal variation in

P_{gbm} (compare Figs. 2 and 5). The springtime decline in biomass may have reflected the relatively high respiration:photosynthesis ratio at this time.

The pattern of depth distribution (Fig. 6), with most growth at shallow depths and a marked decrease between 2 and 3 m, was similar to that found for sparse growths of *Zygogonium* in Plastic Lake in August 1986 (Howell et al. 1990). This depth distribution paralleled light intensity, except for the very shallow zone (not measured quantitatively in this study) where wave erosion and displacement probably were important factors. The depth distribution was also consistent with stimulation of FGA photosynthesis by water movement (Turner 1993).

The increase in algal density with depth (Fig. 6) may have been related to increasing water pressure, which increases the solubility of oxygen and thereby reduces the formation of oxygen bubbles (Howell et al. 1990). Decreased light with increased depth contributed to lowered photosynthesis, again decreasing oxygen bubble formation, and lessening algal buoyancy. Lower rates of algal photosynthesis would be expected as a result of the increased algal density with increased water depth, on the basis of negative density-dependent feedback.

The depth distribution also confirmed that FGA growth was principally a littoral phenomenon. It is possible that the degree of depth penetration was a function of overall growth. That is, after the FGA grew and occupied optimal spaces, FGA then spread to other less favorable zones (lower light and higher pressure). This is consistent with the deepening of FGA development seen during the open-water period (M.A. Turner and B.E. Townsend, Department of Fisheries and Oceans, Winnipeg, Man., unpublished data).

Metabolic characteristics of FGA growth

Algal density

The relationship between biomass-normalized photosynthesis (P_b) and biomass (B) was earlier described mathematically by using the nonlinear relationship of P_b = slope/B + constant (Howell et al. 1990). This nonlinearity helps in understanding some of the implications of the structural character of FGA growth forms because it represents a summation of the photosynthetic relationships with irradiance, DIC, and water movement. Cells in the interior of a metaphytic mat grow in suboptimal conditions as the mat thickens and nutrient and physical limitations come into play. In contrast, when FGA densities are very low, their environment has fewer limitations and more closely resembles that of planktonic algae.

There is a mathematical complication with this nonlinear equation, however, because P_b is undefined when $B = 0$, i.e., there is no y intercept. A more serious complication arises with statistical analysis of P_b as a function of biomass given the potential for autocorrelation, because biomass is also an element of the denominator of the dependent variable, P_b. Thus, alternative descriptions of the relationship between photosynthesis and algal biomass were sought.

The effect of algal density on respiration-normalized photosynthesis (P_g), but unadjusted for the amount of algal biomass incubated, was described well by the simple linear model P_g = slope × biomass (Fig. 1), where the intercept is forced through zero. The small residuals were significant because the linear relationship underestimated rates of photosynthesis when the biomass incubated was very small, which is consistent with the nonlinear decreasing relationship of P_b with algal crowding. The bias was deemed acceptable because these low densities were uncharacteristic of benthic FGA (see below).

Substantial seasonal variation existed in the density dependence relationship (Fig. 1). The linear coefficients of the photosynthesis–biomass relationship during spring were small (Fig. 1), consistent with the observation that FGA were then growing in the less-effective periphytic form for which density-dependent feedback is high. The low springtime coefficients may also result from the more heterogeneous algal composition typical of this period (Fig. 4). The linear coefficients increased as the FGA developed into metaphyton during summer (Fig. 1) coincident with improved growth conditions (high light and temperature), although CO_2 availability declined. The coefficients declined in three of the four fall periods, consistent with qualitative observations of compression, darkening, and a decline in biomass (Fig. 5). Alternatively, the density-dependent factors controlling *Zygogonium* growth may have changed in the fall. For example, as the FGA aged, algal and detrital decay would result in increased internal DIC and other nutrients. Grazing by numerous microcrustacea could also lead to filament shortening and loss of community structure (B. Hann, University of Manitoba, Winnipeg, Man., and M.A. Turner, unpublished data), which would result in mat compression, increasing algal density, and diminishing photosynthetic capacity (Fig. 1).

Light intensity

Smith's (1936) characterization of the dependence of photosynthesis upon irradiance fit the observations well (Table 1). It was reasonable, therefore, to evaluate the relationship in terms of both α and P_{gbm}. An important feature of the relationship between light and photosynthesis for FGA was that photoinhibition was absent, which agrees with the laboratory studies of O'Grady (1987) for *Mougeotia*, and is also consistent with the initial development of the FGA in the shallows (Fig. 6; Howell et al. 1990). As a result, additions of calcite that were intended to provide alkalinity to acidified lakes, but which also reduced water clarity (Roberts and Boylen 1989), probably impeded FGA growth (reported by Jackson et al. 1990). The apparent lack of photoinhibition also simplifies measurement of P_{gbm} for those unable to examine photosynthesis over a range of irradiances. That is, simple in situ incubations of FGA in the shallows during sunny periods should suffice to characterize P_{gbm}.

The seasonal variation of P_{gbm} was regular from year to year (Fig. 2). It was similar to that in epilithon of neutral lakes (see Fig. 6 of Turner et al. 1987), but development of the FGA maximum lagged, occurring later in the open-water period than did the epilithic maximum. The pattern in FGA, however, was different from that in acidified epilithon; i.e., a mid-year maximum with minima in spring and fall contrasted sharply with the epilithic pattern of a mid-year minimum with maxima in spring and fall.

Greater uncertainty existed in estimating α (Table 2), so that its seasonal pattern was less clear than for P_{gbm}

(Fig. 2). The value of α regularly increased from its springtime minimum before the increase seen in P_{gbm}; α was also positively correlated with seasonal variation in the slope of the dependency of photosynthesis upon algal biomass ($P \leq 0.01$). Although the significance of this correlation is unclear, it may reflect the dependency of both α and the slope of $P = f$(biomass) on the physiological status of the algal association.

Nutrients: inorganic C

Dissolved inorganic carbon was a seasonally important controller of FGA photosynthesis (Fig. 3); DIC was also important to acidified epilithon and epiphyton (Turner et al. 1987, 1991, 1994), and to FGA of different composition or in different acid lakes (Howell et al. 1990). Photosynthesis within FGA mats can draw DIC down to low levels (~4 μM), which corroborates the conclusion that DIC can be limiting (Howell et al. 1990; Turner et al. 1995*a*). The laboratory experiment evaluating incubation conditions also demonstrated this limitation (M.A. Turner, unpublished data). DIC may also limit FGA photosynthesis in nonacid lakes. For example, the pH in FGA mats can become high (e.g., from 7 to 12) in neutral systems, causing low CO_2 in the interior of cells (cited in Hoshaw and McCourt 1988).

The seasonally variable dependence of FGA photosynthesis on DIC (Fig. 3) correlated positively with water temperature, which is consistent with the idea that affinity for CO_2 is controlled enzymatically. The pattern of seasonal changes in DIC dependency also supports the hypothesis that maximum need (highest P_{gbm}) coincides with midyear lows in DIC. Lessened stimulation by DIC in spring and fall, in contrast, is consistent with changes in both the life cycle of the algae and nutrient availability. Rates of FGA photosynthesis (Fig. 2) and biomass accumulation (Fig. 5) were lower during these periods, producing less need for DIC. The colder water during these periods would also contain high levels of DIC because of increased solubility of CO_2.

Photosynthetic control appeared to shift from DIC to other factors at ~30 μM (Fig. 3); self-shading and P limitation could be such factors. This low-level saturation by DIC is unlike that previously recorded in other benthic algae (Turner et al. 1991, 1994), but it has occurred in laboratory algal cultures acclimated to very low DIC concentrations (Mayo et al. 1986).

FGA appear to have been more successful than acidified periphyton in overcoming DIC limitation. In part, community architecture would increase water movement within the FGA, reducing the diffusive resistance to nutrient influx (Turner et al. 1991, 1995*a*). Mats of FGA can also be transient sources of DIC for photosynthesis given that nighttime buildup of DIC can occur (Turner et al. 1995*a*). Similarly, high DIC concentrations can occur during fall in the bottom region of FGA mats where decomposition is occurring. Alternatively, FGA may also be able to overcome low DIC by possessing an inducible C-concentrating mechanism (G.G.C. Robinson, unpublished data).

Other nutrients

The possibility that N and P were also limiting was evaluated to determine their significance to FGA growth. Two caveats were used in examining the ratios of nutrients in FGA: (*i*) these ratios are insensitive to transient changes in nutritional status (Istvanovics et al. 1992), and (*ii*) the FGA collections were impure because they included varying amounts of other algae and organisms. Hecky and Kilham (1988) believe that the latter problem is overrated in phytoplankton, but their supposition needs to be verified for benthic algal associations.

The FGA appeared to be P limited using the criteria established for both N:P and 1000 × P:C by Healey (1975) and Healey and Hendzel (1979). Phosphorus deficiency was previously demonstrated for *Oedogonium* in Lake Wingra, Wisconsin (McCracken et al. 1974), and both *Ulothrix* and *Cladophora* in the Laurentian Great Lakes (Auer et al. 1983). If P availability limits growth of *Zygogonium*, then P control measures will be important in controlling FGA growth in some circumstances. For example, cottagers would worsen nuisance blooms of FGA metaphyton that already develop in acid lakes (SPR Associates 1986) by using inadequate sewage systems.

Nitrogen limitation of the FGA appeared to be moderate using the criteria of Healey (1975). This finding is rather surprising given that epilimnetic concentrations of ammonium were much higher than in neutral lakes (Rudd et al. 1990), although only a small proportion would have been available as ammonia at pH 4.5. Disruption of nitrification by acidification (Rudd et al. 1990) would also have diminished the availability of nitrate.

Temperature

Temperature appeared to be important to FGA growth but this was examined only indirectly. This study found that temperature mainly controlled photosynthesis, although Graham et al. (1995) established that respiration of *Mougeotia* was related to temperature. Both the increase in P_{gbm} and the seasonal development of FGA biomass were related to, but lagged behind, the increase in water temperature. The effect of temperature on DIC would have impeded FGA growth because DIC levels decrease with increased temperature as the solubility of CO_2 decreases. As a result, potential for C limitation increases directly with temperature, and must be compensated for by some CO_2-concentrating mechanism, possibly explaining the lag.

Temperature may also partly explain the large interannual variability in the development of FGA biomass; maximum amounts of FGA produced from 1988 to 1991 were ~75, 2, 22, and 18 $g \cdot m^{-2}$, respectively (Turner et al. 1995*a*). Maximum development occurred in the year when epilimnetic temperatures reached 22°C by the end of May 1988. In contrast, end-of-May temperatures were only 15, 17, and 19°C from 1989 to 1991, respectively. Given that maximum FGA biomass occurred late in the year, delayed ice-out in 1989 (11 days later than in any of the other years) may also have contributed to reduced biomass development. FGA that are able to start growing early in the season will be exposed to a beneficial combination of favorable water temperatures and high spring light intensities.

Algal density was also inversely related to water temperature (Fig. 5), in part because of the inverse relationship between oxygen solubility and temperature. With rising temperatures, photosynthetic production of oxygen would probably cause bubble formation, reduce algal density or crowding, and increase photosynthetic potential. In contrast, declining water temperatures would reduce bubble formation and increase algal density. The eventual result would be the collapse of a bloom, initiated by falling water temperatures, because increased density would decrease photosynthesis by negative density-dependent feedback (Howell et al. 1990), and lowered rates of photosynthesis would reduce bubble formation, further increasing density.

Effects of anthropogenic changes on future growth of FGA

The abundance of FGA, already nuisance algae in some situations (SPR Associates 1986), may increase in the future. Growth of FGA is controlled by several factors that are now being altered by anthropogenic activities. It is clear that acidification increases FGA abundance (Stokes 1986; Turner et al. 1987; Howell et al. 1990; Turner et al. 1995*b*). Global warming will increase the open-water period, principally in the spring when irradiances are high (Schindler et al. 1990), and potentially enhance the ability of the FGA to overcome the delay in shifting from a periphytic to metaphytic growth form. Epiphytic FGA already increased in an unperturbed lake at the ELA in response to increased water temperatures (Schindler et al. 1990). Increased temperatures should also stimulate growth by improving the algal density–photosynthesis relationship by increasing the buoyancy of the FGA community. Increased concentrations of atmospheric CO_2 should alleviate C limitation. Local releases of P into acidified catchments by human activities are likely to stimulate FGA growth. Increased anthropogenic emissions of N oxides (Galloway 1989), aside from increasing rates of acidification (Rudd et al. 1990), may also remove secondary N limitations. Finally, any increase in ultraviolet radiation may destroy humic acids in lake water, increase transparency, and increase FGA growth, presuming FGA are unaffected by increased ultraviolet radiation.

Acknowledgments

Technical support was provided by S. Zettler and N. Strange. B. Townsend contributed SCUBA assistance. D. Cruikshank managed technical aspects of the Lake 302S experiment. Chemical data used to characterize Lake 302S were collected by M. Stainton and his staff at the ELA and the Freshwater Institute. L. Neden assisted in experimental design. B. Jestadt, S. Kasian, and L. Neden helped in data analysis. The manuscript improved markedly with the critiques of an anonymous reviewer, G. Fairchild, B. Hann, R. Hecky, F. Healey, N. Kenkel, and especially D. Rosenberg. Elements of this work were originally part of a Ph.D. thesis by M.A.T. at the University of Manitoba.

References

Almer, B., W. Dickson, C. Ekstrom, and E. Hornstrom. 1978. Sulfur pollution and the aquatic ecosystem. *In* Sulfur in the environment. Part 2. Ecological impacts. *Edited by* J.O. Nriagu. John Wiley and Sons, New York. pp. 271–311.

Amaral, J.A. 1991. Sulfate reduction and organic sulfur formation in lake sediments. Ph.D. thesis, University of Manitoba, Winnipeg, Man.

Auer, M.T., J.M. Graham, L.E. Graham, and J.A. Kranzfelder. 1983. Factors regulating the spatial and temporal distribution of *Cladophora* and *Ulothrix* in the Laurentian Great Lakes. *In* Periphyton of freshwater ecosystems. *Edited by* R.G. Wetzel. Dr. W. Junk, The Hague, The Netherlands. pp. 135–145.

Brezonik, P.L., J.G. Eaton, T.M. Frost, P.J. Garrison, T.K. Kratz, C.E. Mach, J.H. McCormick, J.A. Perry, W.A. Rose, C.J. Sampson, B.C.L. Shelley, W.A. Swenson, and K.E. Webster. 1993. Experimental acidification of Little Rock Lake, Wisconsin: chemical and biological changes over the pH range 6.1 to 4.7. Can. J. Fish. Aquat. Sci. 50: 1101–1121.

Brunskill, G.J., and D.W. Schindler. 1971. Geography and bathymetry of selected lake basins, Experimental Lakes Area, northwestern Ontario. J. Fish. Res. Board Can. 28: 139–155.

Cruikshank, D.R. 1988. Effects of nutrient and acid additions on Secchi depth at the Experimental Lakes Area, 1969–1986. Can. Tech. Rep. Fish. Aquat. Sci. No. 1597.

Cruikshank, D., K. Matthisen, and R. Hunt. 1988. Trace metal data in water from lakes and streams of the Experimental Lakes Area, northwestern Ontario, 1976–1986. Can. Data Rep. Fish. Aquat. Sci. No. 695.

Fairchild, G.W., and A.C. Everett. 1988. Effects of nutrient (N, P, C) enrichment upon periphyton standing crop, species composition and primary production in an oligotrophic softwater lake. Freshwater Biol. 19: 57–70.

France, R.L., and P.M. Welbourn. 1992. Influence of lake pH and macrograzers on the distribution and abundance of nuisance metaphytic algae in Ontario, Canada. Can. J. Fish. Aquat. Sci. 49: 185–195.

France, R.L., Y.-K. Yung, and P.M. Welbourn. 1992. Identification of metaphytic zygnematacean algae in acid-sensitive Canadian Shield lakes. Algol. Stud. 66: 99–103.

Galloway, J.N. 1989. Atmospheric acidification: projections for the future. Ambio, 18: 161–166.

Geider, R.J., and B.A. Osborne. 1991. Algal photosynthesis: the measurement of algal gas exchange. Chapman and Hall, New York.

Graham, J.M., P. Arancibia-Avila, and L.E. Graham. 1995. Physiological ecology of the filamentous green alga *Mougeotia* (Zygnematales, Charaophyceae) under acidic conditions: light and temperature effects on photosynthesis and respiration. Limnol. Oceanogr. In press.

Healey, F.P. 1975. Physiological indicators of nutrient deficiency in algae. Tech. Rep. Fish. Mar. Serv. Can. No. 585.

Healey, F.P., and L.L. Hendzel. 1979. Indicators of phosphorus and nitrogen deficiency in five algae in culture. J. Fish. Res. Board Can. 36: 1364–1369.

Hecky, R.E., and P. Kilham. 1988. Nutrient limitation of phytoplankton in freshwater and marine environments: a review of recent evidence on the effects of enrichment. Limnol. Oceanogr. 33: 796–822.

Hendrey, G.R., K. Baalsrud, T.S. Traaen, M. Laake, and G. Raddum. 1976. Acid precipitation: some hydrobiological changes. Ambio, 5: 224–227.

Hoshaw, R.W., and R.M. McCourt. 1988. The Zygnemataceae (Chlorophyta): a twenty-year update of research. Phycologia, 27: 511–548.

Howell, E.T., M.A. Turner, R.L. France, M.B. Jackson, and P.M. Stokes. 1990. Comparison of Zygnematacean (Chlorophyta) algae in the metaphyton of two acidic lakes. Can. J. Fish. Aquat. Sci. 47: 1085–1092.

Istvanovics, V., K. Pettersson, D. Pierson, and R. Bell. 1992. Evaluation of phosphorus deficiency indicators for summer phytoplankton in Lake Erken. Limnol. Oceanogr. 37: 890–900.

Jackson, M.B., E.M. Vandermeer, N. Lester, J.A. Booth, L. Molot, and I.M. Gray. 1990. Effects of neutralization and early reacidification on filamentous algae and macrophytes in Bowland Lake. Can. J. Fish. Aquat. Sci. 47: 432–439.

Jassby, A.D., and T. Platt. 1976. Mathematical formulation of the relationship between photosynthesis and light for phytoplankton. Limnol. Oceanogr. 21: 540–547.

Mayo, W.P., T.G. Williams, D.G. Birch, and D.H. Turpin. 1986. Photosynthetic adaptation by *Synechococcus leopoliensis* in response to exogenous dissolved inorganic carbon. Plant Physiol. 80: 1038–1040.

McCracken, M.D., T.D. Gustafson, and M.S. Adams. 1974. Productivity of *Oedogonium* in Lake Wingra, Wisconsin. Am. Midl. Nat. 92: 247–254.

Müller, P. 1980. Effects of artificial acidification on the growth of periphyton. Can. J. Fish. Aquat. Sci. 37: 355–363.

O'Grady, K.A. 1987. Light, temperature and nitrogen interactions in two freshwater algae from lakes undergoing acidification. M.Sc. thesis, University of Western Ontario, London, Ont.

Roberts, D.A., and C.W. Boylen. 1989. Effects of liming on the epipelic algal community of Woods Lake, New York. Can. J. Fish. Aquat. Sci. 46: 287–294.

Rudd, J.W.M., C.A. Kelly, D.W. Schindler, and M.A. Turner. 1990. A comparison of the acidification efficiencies of nitric and sulfuric acids by two whole-lake addition experiments. Limnol. Oceanogr. 35: 663–679.

Schindler, D.W., and M.A. Turner. 1982. Biological, chemical and physical responses of lakes to experimental acidification. Water Air Soil Pollut. 18: 259–271.

Schindler, D.W., V.E. Frost, and R.V. Schmidt. 1973. Production of epilithiphyton in two lakes of the Experimental Lakes Area, northwestern Ontario. J. Fish. Res. Board Can. 30: 1511–1524.

Schindler, D.W., K.H. Mills, D.F. Malley, D.L. Findlay, J.A. Shearer, I.J. Davies, M.A. Turner, G.A. Linsey, and D.R. Cruikshank. 1985. Long-term ecosystem stress: the effects of years of experimental acidification on a small lake. Science (Washington, D.C.), 228: 1395–1401.

Schindler, D.W., K.G. Beaty, E.J. Fee, D.R. Cruikshank, E.R. DeBruyn, D.L. Findlay, G.A. Linsey, J.A. Shearer, M.P. Stainton, and M.A. Turner. 1990. Effects of climatic warming on lakes of the central boreal forest. Science (Washington, D.C.), 250: 967–970.

Smith, E.L. 1936. Photosynthesis in relation to light and carbon dioxide. Proc. Natl. Acad. Sci. U.S.A. 22: 504–511.

SPR Associates, Inc. 1986. Estimation of the presence and impact of filamentous and odour producing algae: a survey of cottagers on 214 Ontario recreational lakes. Queen's Printer for Ontario, Toronto, Ont.

Stainton, M.P., M.J. Capel, and F.A.J. Armstrong. 1977. The chemical analysis of fresh water. 2nd ed. Can. Fish. Mar. Serv. Misc. Spec. Publ. No. 25.

Stokes, P.M. 1986. Ecological effects of acidification on primary producers in aquatic systems. Water Air Soil Pollut. 30: 421–438.

Turner, M.A. 1993. The ecological effects of experimental acidification upon littoral algal associations of lakes in the boreal forest. Ph.D. thesis, University of Manitoba, Winnipeg, Man.

Turner, M.A., M.B. Jackson, D.L. Findlay, R.W. Graham, E.R. DeBruyn, and E.M. Vandermeer. 1987. Early responses of periphyton to experimental lake acidification. Can. J. Fish. Aquat. Sci. 44(Suppl. 1): 135–149.

Turner, M.A., E.T. Howell, M. Summerby, R.H. Hesslein, D.L. Findlay, and M.B. Jackson. 1991. Changes in epilithon and epiphyton associated with experimental acidification of a lake to pH 5. Limnol. Oceanogr. 36: 1390–1405.

Turner, M.A., E.T. Howell, G.G.C. Robinson, P. Campbell, R.E. Hecky, and E.U. Schindler. 1994. Roles of nutrients in controlling growth of epilithon in oligotrophic lakes of low alkalinity. Can. J. Fish. Aquat. Sci. 51: 2784–2793.

Turner, M.A., G.G.C. Robinson, B.E. Townsend, B.J. Hann, and J.A. Amaral. 1995*a*. Ecological effects of blooms of filamentous green algae in the littoral zone of an acid lake. Can. J. Fish. Aquat. Sci. 52: 2264–2275.

Turner, M.A., D.W. Schindler, D.L. Findlay, M.B. Jackson, and G.G.C. Robinson. 1995*b*. Disruption of littoral algal associations by experimental lake acidification. Can. J. Fish. Aquat. Sci. 52: 2238–2250.

Wei, Y.-X., Y.-K. Yung, M.B. Jackson, and T. Sawa. 1989. Some Zygnemataceae (Chlorophyta) of Ontario, Canada, including descriptions of two new species. Can. J. Bot. 67: 3233–3247.

Wilkinson, L. 1990. SYSTAT: the system for statistics. SYSTAT Inc., Evanston, Ill.

Ecological effects of blooms of filamentous green algae in the littoral zone of an acid lake[1]

Michael A. Turner, Gordon G.C. Robinson, Bruce E. Townsend, Brenda J. Hann, and John A. Amaral

Abstract: Ecological effects of blooms of filamentous green algae (FGA) were studied in an experimentally acidified lake (pH 4.5) at the Experimental Lakes Area in northwestern Ontario, Canada. Blooms of FGA influenced the energy balance, chemical cycling, physical features, and biological conditions in the littoral zone. Photosynthetic capacity of the FGA, dominated by *Zygogonium*, was greater than that of acidified epilithon, the normally dominant littoral algal association, partially offsetting acidification-induced oligotrophication in the littoral zone. Intra- and inter-annual variability of FGA growth was large, however, so that FGA were an unreliable energy source for the littoral food web. Nutrient uptake varied with the degree of FGA growth; e.g., FGA were occasionally the largest phosphorus pool in the epilimnion. Nitrogen dynamics of FGA varied seasonally causing acidification in spring and summer, and alkalinization in fall. The blooms also affected epilimnetic cycling of dissolved inorganic carbon. Peak blooms prevented as much as 90% of the light from reaching the lake bottom. Local depletions of oxygen resulting from FGA decomposition also posed potential risks for animals using the FGA as habitat.

Résumé : Les effets écologiques de la prolifération d'algues vertes (chlorophycées filamenteuses) ont fait l'objet d'études dans un lac expérimentalement acidifié (pH de 4,5) dans la région des lacs expérimentaux du nord-ouest de l'Ontario (Canada). Les proliférations d'algues vertes ont eu une incidence sur le bilan énergétique, le cycle chimique, les caractéristiques physiques et les conditions biologiques de la zone littorale. La capacité de photosynthèse des algues vertes, dominées par *Zygogonium*, était supérieure à celle de l'épilithon acidifié, l'association algale qui domine normalement dans la zone littorale, compensant en partie l'oligotrophisation résultant du processus d'acidification du littoral. Cependant, on a enregistré une grande variabilité de la croissance des algues vertes au cours de l'année et d'une année à l'autre, ce qui fait de ces algues une source d'énergie peu fiable pour le réseau trophique littoral. L'absorption des éléments nutritifs varie avec le degré de croissance des algues vertes; p. ex., les algues vertes constituaient parfois la réserve de phosphore la plus importante de l'épilimnion. La dynamique de l'azote chez les algues vertes varie d'une saison à l'autre, entraînant une acidification au printemps et en été, et une alcalinisation en automne. Les proliférations ont également nui au cycle du carbone inorganique dissous dans l'épilimnion. Au cours des périodes de prolifération maximale, la proportion de l'éclairement qui ne pouvait pas atteindre le fond du lac s'élevait parfois à 90%. L'appauvrissement local en oxygène résultant de la décomposition des algues vertes posait également des risques éventuels pour les organismes utilisant les algues vertes comme habitat.
[Traduit par la Rédaction]

Received August 5, 1993. Accepted April 28, 1995.
J12037

M.A. Turner, and B.E. Townsend. Department of Fisheries and Oceans, Freshwater Institute, 501 University Crescent, Winnipeg, MB R3T 2N6, Canada.
G.G.C. Robinson. Department of Botany, University of Manitoba, Winnipeg, MB R3T 2N2, Canada.
B.J. Hann. Department of Zoology, University of Manitoba, Winnipeg, MB R3T 2N2, Canada.
J.A. Amaral.[2] Department of Microbiology, University of Manitoba, Winnipeg, MB R3T 2N2, Canada.

Introduction

Filamentous green algae (FGA) are widespread (Hoshaw and McCourt 1988), and are especially prolific in the littoral zones of acidic lakes in Scandinavia (Hendrey et al. 1976; Almer et al. 1978; Hendrey 1982) and North America (Stokes 1986; Wei et al. 1989; Howell et al. 1990; France et al. 1992). Blooms of FGA have also occurred in whole-lake acidification experiments (Müller 1980; Schindler and Turner 1982; Schindler et al. 1985; Howell et al. 1990; Webster et al. 1992; Brezonik et al. 1993). They may also become more widespread in the future because the products of human activity will provide a release from growth limitation (Turner et al. 1995*a*).

Little prior knowledge existed concerning the growth characteristics of bloom-forming FGA in acidified systems.

[1] This paper is one of a series done in honor of the 25th anniversary of the Experimental Lakes Area.

[2] Present address: Department of Microbiology, Macdonald College of McGill University, Ste. Anne de Bellevue, QC H9X 3V9, Canada.

Can. J. Fish. Aquat. Sci. **52**: 2264–2275 (1995). Printed in Canada / Imprimé au Canada

The recent experimental acidification of Lake 302S at the Experimental Lakes Area (ELA) in northwestern Ontario produced changes in the character of FGA growths as pH declined. FGA appeared initially both as a shoreline band of epilithon (the benthic algal association on rock surfaces) and as epiphyton (on plant surfaces) at pH values >6 (Turner et al. 1987). However, the FGA bloomed as metaphytic growth forms (no longer truly attached to the substratum) as the pH declined to 5.5 and below (Howell et al. 1990; Turner et al. 1995*a*, 1995*b*). These bloom-forming FGA, dominated initially by *Mougeotia* and later *Zygogonium*, successfully obtained dissolved inorganic carbon (DIC) at low concentrations, allowing them to partly overcome the carbon (C) limitation found in acidified lakes (Turner et al. 1987, 1991, 1995*a*; Howell et al. 1990). They also benefited from the warm temperatures and high light intensities of the epilimnion (Graham et al. 1996; Turner et al. 1995*a*).

Ecological effects of these FGA blooms are hardly known. Hendrey (1982) speculated that blooms of FGA might lead to overall ecosystem impoverishment by impeding the flux of nutrients. Stokes (1986) speculated that habitat modification by FGA blooms would not be trivial. Both Webster et al. (1992) and Brezonik et al. (1993) argued that many of the acidification effects on food webs were indirect effects of FGA mat formation.

The objectives of this study were to investigate the chemical, physical, and biological effects of FGA blooms in a lake acidified experimentally to a pH of 4.5. The effects examined included (*i*) variation in energy flow among littoral algae; (*ii*) alteration of nutrient cycles and internal alkalinity generation; (*iii*) changes in light transmissivity, bottom temperatures, and water movement; and (*iv*) provision of habitat for animals. The study was designed to evaluate the scale of these effects as a guide to future studies, and to provide approaches to more detailed analysis of some of them.

Methods

Turner et al. (1987, 1991, 1995*b*) and Howell et al. (1990) described the physical and chemical characteristics and recent experimental history of oligotrophic Lake 302S. During the period of this study (1988–1991), Lake 302S was held at a pH of 4.5 by additions of sulfuric acid. Studies of epilithon were also conducted in unperturbed Lake 239, a nearby neutral lake (Turner et al. 1995*b*).

Measurement of algal metabolism and biomass

Algal photosynthesis and nutrient concentrations

Turner et al. (1995*a*) described the techniques for measuring rates of FGA photosynthesis and concentrations of FGA macronutrients. Seasonal changes in maximum rates of biomass-normalized photosynthesis were determined from incubator measurements of photosynthesis–irradiance relationships. Photosynthesis and respiration were estimated by measuring changes in DIC. The photosynthetic maxima were then multiplied by the scalar coefficients derived from the corresponding measurement of the density dependence of FGA photosynthesis. Areal productivity of FGA was then derived by multiplying the adjusted maxima by the average areal amount of FGA at the corresponding sampling period.

SCUBA-based in situ techniques were used to measure rates of photosynthesis in epilithon in the middle littoral zone (1–3 m) of lakes 302S and 239 approximately every 4 wk from 1989 to 1991. To generate a photosynthesis–irradiance curve, typically 12 samples of epilithon, each 100 cm^2, were isolated with 0.4 L of overlying water inside acrylic chambers and exposed to variable light intensities. Rates of photosynthesis and respiration were estimated by measuring the rate of change in DIC concentration in the water. Samples of epilithon were collected using a scraping device (Turner et al. 1991), and were analysed for concentrations of particulate C (PC), nitrogen (PN), and phosphorus (PP; Stainton et al. 1977). Further details of these techniques are described by Turner et al. (1991, 1995*b*).

Lake-wide biomass of FGA

Lake-wide biomass of FGA was measured by a SCUBA diver using the depth-stratified transect methods of Howell et al. (1990) and Turner et al. (1995*a*). Variations in these procedures over the 4 yr of the study are described below; in part, sampling strategies were modified to compensate for year-to-year variations in FGA biomass.

The procedures in 1988 and 1989 followed Howell et al. (1990). The FGA were sampled from 8 to 26 August 1988 and from 30 July to 1 August 1989. In 1988, four transects (selected randomly from 91 equally spaced locations around the lake perimeter) were sampled, whereas 10 were sampled in 1989. Fifteen sampling sites, ranging in depth from 0.25 to 4.0 m, were selected randomly along each transect in 1988; 10 sampling sites (0.1–5 m depth) were used in 1989. The deepest collection depth was increased in 1989 after it was recognized that FGA sometimes occurred below 4 m.

A SCUBA diver measured the percent coverage by FGA of each plot area (0.5 × 0.5 m), and the median thickness of FGA growing there. The entire biomass of FGA in each plot was then collected and screened through a 102-μm mesh net. The FGA was retrieved from the net, cleaned of any visible debris, measured volumetrically, weighed wet, and dried at 60°C to a stable weight.

In 1990, FGA were sampled along eight transects during six periods from 10 June to 29 October. The stations were selected randomly as before. Fixed sampling depths of 0.5, 1.0, 1.5, 2.0, 3.0, 4.0, and 5.0 m were established along each transect, and locations for later sampling periods were predefined and marked along each depth contour to avoid disturbance by the SCUBA divers. The procedures followed were otherwise equivalent to those described above for 1988.

The 1991 sampling program was described by Turner et al. (1995*a*). Seasonal sampling was nondestructive to enhance detection of time-related trends; it focussed on the 1-m depth contour to maximize sampling effort in the growing zone. The plot area was increased to 1 × 1 m because of patchy growth of FGA during spring and early summer. Measurements were also made in three adjacent plots, increasing the area sampled 12-fold at a single site in comparison with previous years. The number of sites sampled at 1 m was also increased to 16. Algal coverage and growth thickness were measured in the sample plots as before. Algal density, equivalent to algal crowding, was measured in separate collections made next to established transects. Algal density was calculated as the dry biomass of a sample divided by its growth volume. Algal biomass was then calculated as percent bottom coverage × algal thickness × algal density. The vertical distribution of the FGA over 1 to 5 m also was evaluated along 8 of the 16 transects from 10 to 12 August.

Calculating whole-lake estimates of FGA biomass

Mean biomass found at each depth contour was multiplied by the corresponding area of lake bottom to express the observations on a whole-lake basis. The whole-lake biomass for sampling periods in 1991 was estimated using the assumption that the vertical distribution seen from 10 to 12 August applied throughout the open-water season. Filamentous green algae developed first in the shallows and later in deeper water (M.A. Turner, unpublished observations), so this assumption would likely overestimate lake-wide biomass prior to mid-August and underestimate biomass at subsequent periods.

Effects of FGA on chemical properties

Mesocosm studies

Randomized block design experiments (each consisting of six mesocosms, with two blocks of three mesocosms each) were conducted in 1989 and 1990 to evaluate the effects of FGA upon lake chemistry. The cylindrical mesocosms used in both experiments (1 m diameter, approximately 1 m depth) had polyethylene walls and bottoms. Each mesocosm was filled with water pumped through a 102-μm screen prior to algal addition. Inocula of FGA were collected using 102-μm mesh nets; inclusion of shoreline detritus was minimized.

The 1989 experiment, started 29 August, originally was intended to evaluate the effects of herbivory on FGA, but was subsequently used to provide information on nutrient chemistry instead. Originally, attempts were made to control the degree of herbivory, so macroinvertebrates were initially removed from the FGA collections and were re-added at low, medium, and high levels. Appreciable amounts of FGA were transferred along with the invertebrates, causing initial FGA densities to range from 6 to 10 g dry weight (gdw)$\cdot$m^{-2} and to covary with intensity of herbivory. Water chemistry samples were collected with an acrylic tube from the middle of each mesocosm in one block on 29 August and 9 September 1989.

The 1990 mesocosm experiment, started 4 October, was designed to evaluate changes in water chemistry accompanying FGA decomposition. Three levels of FGA (none, low, high) were used, and additions of FGA were better controlled than in 1989. Average areal densities of FGA in the low and high mesocosms were 4 and 40 gdw$\cdot$m^{-2}, respectively, on the basis of a conversion from wet to dry weight of 6% (M.A. Turner, unpublished observations). Duplicate samples for water chemistry were collected on 5 and 24 October 1990.

Other analyses of chemical effects

Vertical profiles of DIC were measured within FGA at sunset of 1 September 1988 and again at sunrise the next day. The FGA mat studied was approximately 0.4 m thick and located in approximately 0.9 m of water overlying rock. Dissolved inorganic carbon was sampled using a rigid acrylic tube with a porous (approximately 100-μm pore size) polyethylene end; this probe was connected by Tygon® tubing through a three-way valve to flushing and sampling syringes. Samples for DIC were collected at each depth within the FGA after flushing the sampling line at least three times with approximately 45 mL of lake water; this procedure sampled a sphere of 2–3 cm radius.

Release or uptake of ammonia (NH_3) by FGA was determined four times in 1991. Samples of 8–15 mgdw were incubated in 125-mL bottles for 1 d in darkness on 13 August. Incubation time was subsequently reduced after sufficient sensitivity was demonstrated. Samples were then incubated for 4 h in darkness or in light (>650 $\mu E \cdot m^{-2} \cdot s^{-1}$) ($1\ \mu E \cdot m^{-2} \cdot s^{-1} = 0.217\ W \cdot m^{-2}$) in September and October. The ammonium (NH_4^+) concentration in the water phase was measured (Stainton et al. 1977) prior to and just after incubation. The rate of change in concentration was expressed as a biomass-normalized flux.

A rudimentary three-compartment model (FGA, epilithon, and plankton) was used to estimate the proportion of epilimnetic PP accumulated within the FGA compartment. The PP of each compartment was measured during the open-water period of 1991 (Stainton et al. 1977). The amount of FGA on the lake bottom was varied over the approximate range of maximum coverage measured from 1988 to 1991 (Table 1). The following assumptions were made: (*i*) the plankton and epilithon compartments were constant in size; (*ii*) the littoral bottom was covered entirely by epilithon (an overestimation of the size of this compartment); and (*iii*) the epilimnion was 5 m deep, yielding an epilimnetic volume of 4.30×10^8 L and a corresponding epilimnetic bottom area of 4.7 ha. Other compartments such as macrophytes and their epiphyton were ignored because they were not abundant in Lake 302S (Schindler et al. 1973). Sedimentary P was also ignored because littoral sedimentary P efflux was probably unimportant (Levine and Schindler 1992).

Changes in oxygen concentration were measured in several different masses of FGA overlying sediment. An oxygen-needle probe (Flett Research Ltd., Winnipeg, Man.) was connected to an oxygen meter using waterproof cable. The probe, secured in a micromanipulator arm situated on the lake bottom, was moved by the SCUBA diver who also noted the depth of penetration into the FGA.

Pore-water samplers (Hesslein 1976) were inserted by a SCUBA diver into the sediment inside and outside an FGA mat. The sampler and its polycarbonate membranes (0.2-μm pore size) were washed in distilled water and soaked overnight in deionized water bubbled with N_2 gas to deoxygenate the sampler before use (Kelly et al. 1984). The samplers were retrieved after 20 and 21 d by a SCUBA diver who also noted locations of algae–water and sediment–algae interfaces. Samples for pH were obtained immediately by another person at the surface who carefully extracted the contents of the sampler cells into glass syringes. These samples were analysed within hours using an Orion pH meter (model 811) and an electrode.

Table 1. Approximate maximum amounts of filamentous green algal biomass found in the littoral zone (0 to approximately 5 m) of Lake 302S from 1988 to 1991.

Sampling information

Year	Date	Number of samples	Total sample area (m^2)	Water depth (m)	Bottom slope (%)
88	230	55	14	2.0±1.1	16±18
89	212	92	23	2.5±1.4	29±23
90	275	56	14	2.4±1.6	36±21
91[a]	275	120	120	3.0±1.6	36±21

Algal information

Year	Bottom coverage (%)	Algal thickness (cm)	Algal density ($g \cdot L^{-1}$)	Biomass ($g \cdot m^{-2}$)
88[b,c]	83±28	22±15	0.4±0.9	75
89[c]	5±15	7±6	0.6±0.6	2
90[d]	33±19	4±3		22
91[e,f]	41±33	3±4	1.6±1.3	18

Note: Methodological details for particular years are noted in the text. Values are given as the mean ± SD. SD, standard deviation.

[a] The sampling stations used to measure vertical distribution in 1991 were the same as those used in 1990.

[b] Areal biomass was calculated as percent coverage × algal thickness × algal density.

[c] The seasonal maximum probably occurred after this sampling period.

[d] The corresponding algal density information from 1991 was used in the biomass calculation for 1990.

[e] 1991 SD values are those measured on day 225 adjusted for the ratio of 1-m values between days 275 and 225.

[f] The maximum biomass was seen on day 275 at 1-m sites; these data are adjusted for the vertical distribution seen on day 225.

Effects of FGA on physical properties

To evaluate the rate of attenuation of light within FGA mats, *Zygogonium* was collected on 31 August 1988 and blended to create a suspension (Turner et al. 1995*a*). Transmittance of photosynthetically available radiation (400–700 nm) was measured using a flat cosine LiCor Inc. LI-192SA quantum sensor connected to an LI-1000-32 data logger. Aliquots of algal suspension were added to a beaker of lake water, and transmittance was measured repeatedly after each of four replicate additions. The contribution of FGA to the attenuation coefficient was derived using the Beer–Lambert Law (Turner et al. 1983).

The attenuation of light by FGA was examined in situ on 29 August 1990. Photosynthetically available radiation was measured by a SCUBA diver using a spherical LiCor Inc. LI-193SA quantum sensor connected to a data logger. The sensor was placed next to the FGA to measure ambient irradiance and was then placed underneath the FGA to measure the transmitted irradiance. The approximate water depth and vertical thickness of the FGA were measured.

Potential for attenuation of water movement by FGA was determined on two occasions using the techniques described by Turner et al. (1991) for measuring boundary layer thickness. On 2 September 1988, approximately 1 cm^2 of preweighed calcium sulfate ($CaSO_4$) chips were suspended at several depths both outside and inside an algal mat. The rate of dissolution of the $CaSO_4$ over the 4–5 h sampling period was determined by measuring the rate of weight loss. On 29 August 1990, chips were placed on the lake bottom by a SCUBA diver, either with or without FGA overlying the chips. Water depth, FGA thickness, and duration of incubation were recorded. Chips were retrieved after approximately 1 h, dried, and reweighed.

The possible influence of FGA on water temperature was measured on three occasions during August 1990. A SCUBA diver used a total-immersion thermometer (Fisher 15-043A), so measured temperature differences applied to large volumes rather than to specific points within the mats.

Results

Algal metabolism and biomass

Seasonal patterns in net photosynthesis of FGA and epilithon in Lake 302S were dissimilar during the period 1989–1991 (Fig. 1). Acidified epilithon exhibited relatively high rates in spring and early fall, and annual minima in midsummer. The opposite pattern was true for biomass-normalized photosynthesis of FGA, which resembled the

Fig. 1. Maximum rates of net photosynthesis in the epilithon (μmol C·m^{-2}·h^{-1}) of lakes 239 and 302S and in the filamentous green algae (FGA; μmol C·mgdw^{-1}·h^{-1}) of Lake 302S from 1989 to 1991.

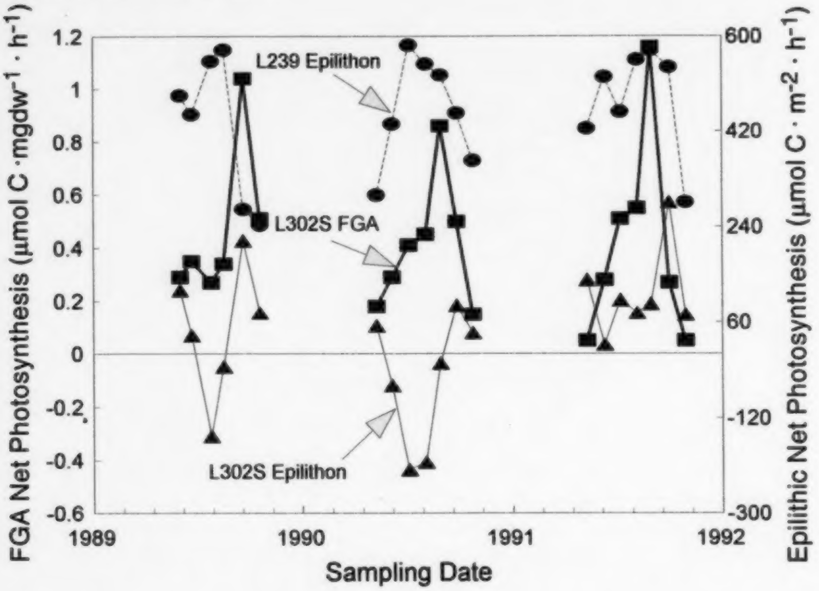

Fig. 2. Areal rates of net photosynthesis (μmol C·m^{-2}·h^{-1}) in two algal communities of Lake 302S and in epilithon of Lake 239 in 1991. Rates of filamentous green algae (FGA) are expressed per unit of occupied lake area; epilithic rates are normalized per unit of sampled lake area.

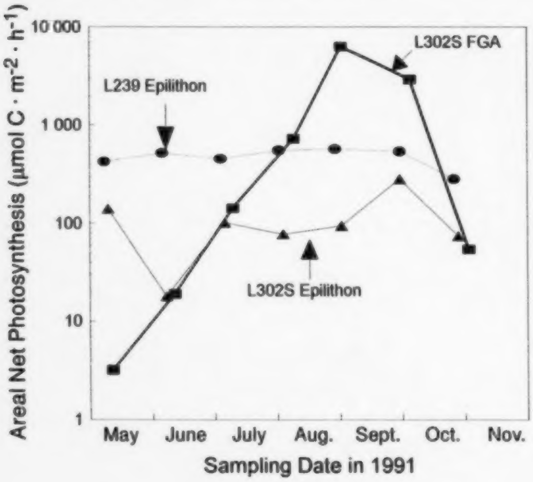

epilithic pattern in neutral Lake 239 (Fig. 1). Calculated rates of FGA areal photosynthesis during 1991 remained low until August when they were similar to rates in neutral epilithon (Fig. 2). Areal rates of FGA were much greater during August–October than in epilithon of either the acidified or neutral lake (Fig. 2).

Seasonal distributions of acidified epilithic and FGA biomass were almost mirror images in 1991 (Fig. 3). Maximum FGA biomass occurred in early October, despite a decline in areal coverage and thickness of FGA, because algal density (quantity of algae per unit of growth volume) was high. In contrast, epilithic biomass in Lake 302S was maximal in spring and fall, and low from July to September. The seasonal pattern in FGA was similar to that of epilithon in Lake 239. In spite of the substantial FGA areal photosynthesis, the 1991 sum of FGA and epilithic biomasses in Lake 302S was lower than that of epilithon in Lake 239 (Fig. 3). This was unlikely to have been true in all years (e.g., see 1988 below).

Maximum biomass of FGA distributed over the littoral bottom fluctuated markedly from 1988 to 1991, varying from 2 to 75 gdw·m^{-2} (Table 1). These measurements concurred with visual impressions. The average bottom slope at the sampling sites exceeded the 11% (0–5 m) calculated from Brunskill and Schindler (1971), so FGA biomass was probably underestimated in all years (Turner et al. 1995*a*). Maximum biomass probably would not have been measured during August surveys because maxima occurred in late September or early October during both 1990 (M.A. Turner, unpublished data) and 1991 (Fig. 3).

Effects of FGA on chemical properties

Mesocosm studies

Areal concentrations of FGA in the 1989 mesocosms (6–10 gdw·m^{-2}) resembled low to moderate annual maxima seen in the lake (Table 1). The appearance of the FGA varied markedly among the 1989 mesocosms, providing

Fig. 3. Areal biomass (g $C \cdot m^{-2}$) of epilithon and filamentous green algae (FGA) at 1-m depth in Lake 302S, and of epilithon in neutral Lake 239 during the open-water period of 1991. Biomass of FGA is expressed per unit of occupied lake area; epilithic biomass is normalized per unit of sampled lake area.

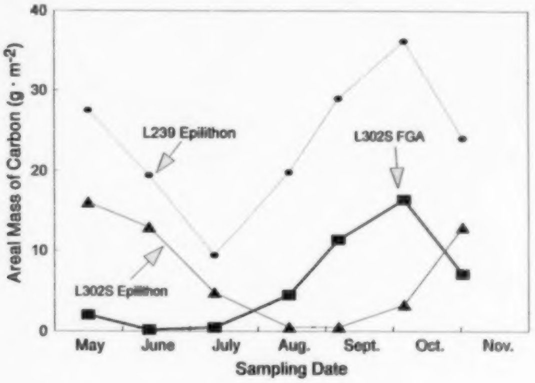

information on the growth status of the enclosed algae. Filamentous green algae were yellow–green and remained dispersed in the low-treatment mesocosms on 10 October. In contrast, FGA were clumped and brown to black in the high-treatment mesocosms. The FGA in the medium-treatment mesocosms were intermediate in appearance.

Major nutrient chemistry was sensitive to the amount of algal material (Table 2). Changes in concentrations of C, N, and P supported the interpretation that FGA in the low-treatment mesocosm were growing (accumulating C, N, and P). In contrast, FGA in the high-treatment mesocosm were decomposing (releasing N and P), partly as a result of negative density-dependent feedback (Turner et al. 1995*a*). The high concentration of total N in this mesocosm was caused almost entirely by an increase in NH_4^+. The rate of approximately 7 $\mu g\ N \cdot L^{-1} \cdot d^{-1}$ or approximately 0.05 $\mu g\ N \cdot mgdw^{-1} \cdot h^{-1}$ resembled the bioassay results obtained in 1991.

Areal concentrations in the low- (4 $gdw \cdot m^{-2}$) and high-treatment (40 $gdw \cdot m^{-2}$) mesocosms of 1990 encompassed those in the 1989 mesocosms and the lake from 1988 to 1991 (Table 1). The high-density FGA were probably in decline given the density-dependent negative feedback of FGA growth at that time of year (Howell et al. 1990; Turner et al. 1995*a*). Furthermore, the 1990 experiment was conducted in October as water temperatures declined from 11 to 6°C, when the FGA collapsed and coalesced into small clumps.

Water depth declined from 0.78 ± 0.01 to 0.71 ± 0.01 m (mean ± SD, $n = 6$ means) during the experiment, so water chemistries in the algal mesocosms and the water-only mesocosms were compared to factor out the effect of evaporation (Table 3). The major increase in NH_4^+ of 1989 occurred again in the high-density FGA enclosure of 1990 (Table 3). The average daily increase was approximately 6 $\mu g\ N \cdot L^{-1} \cdot d^{-1}$ between FGA collection and initial mesocosm sampling, followed by a slower rate of approximately 3 $\mu g\ N \cdot L^{-1} \cdot d^{-1}$. The rates were slower than in 1989 probably because water temperatures were cooler. Both pH and alkalinity increased in the high-density FGA treatment compared with the water-only treatment (Table 3), as would be expected from the observed increase in NH_4^+, a base cation. Sulfate also increased, possibly reflecting oxidation of organic sulfur (S) in the FGA. Oxidation of reduced S would be accompanied by the release of hydrogen ion and decreasing pH, and would counter the ammonium-induced pH increase. Total dissolved iron declined in the high-density FGA mesocosm, in contrast to the other cations, which increased or were unchanged.

Table 2. Nutrient chemistry in the water phase of the 1989 mesocosm experiment.

	Total C		Total N		Total P	
Mesocosm	μM	%	μM	%	μM	%
Low FGA	−39	−16	−2	−6	−0.65	−20
Medium FGA	−11	−5	3	11	0.00	0
High FGA	−1	0	30	35	0.03	11

Note: Changes in concentration of carbon (C), nitrogen (N), and phosphorus (P) are reported as percentage of the initial values. Areal concentrations of filamentous green algae (FGA) ranged from approximately 6 to 10 $gdw \cdot m^{-2}$ in the low to high FGA mesocosms.

Other chemical effects

Concentrations of DIC varied with time of day and depth within an FGA mat (Fig. 4). Concentrations within the FGA mat were below those in the overlying water in the evening, except at the very bottom of the mat, so that FGA were a daytime sink for DIC. Concentrations early next morning, however, increased strongly with mat depth and exceeded those in the overlying water, so FGA were a nighttime source of DIC. Concentrations were high near the bottom where either decomposition or animal activity were occurring. Concentrations in the water overlying the FGA paralleled those in the upper portions of the FGA mat (Fig. 4) and in epilimnetic samples.

The direction of NH_3 flux in FGA varied seasonally. Ammonia uptake occurred in mid-August of 1991 at a rate of 0.037 ± 0.005 $\mu g\ N \cdot mgdw^{-1} \cdot h^{-1}$ (mean ± SD, n = 3 samples). From 5 September to 29 October, the mean net release of NH_3 was 0.060 ± 0.013 $\mu g\ N \cdot mgdw^{-1} \cdot h^{-1}$ (mean ± SE, n = 3 means of 4 samples each). Exposure of FGA to light had no effect on NH_3 flux; the ratio of irradiated to dark rates averaged 96 ± 7% (mean ± SE, n = 3 means). Rates in both the dark and light, therefore, were included in the above estimate.

The whole-lake flux of NH_3 from FGA appeared to be large when estimated for September–October 1991 using the mean overall efflux of NH_3 (0.06 $\mu g\ N \cdot mgdw^{-1} \cdot h^{-1}$). The average biomass of FGA in the 0–5 m zone during these months was 440 kgdw (calculated from Turner et al. 1995*a*), so the resulting daily efflux of NH_4^+ from FGA equalled 0.63 kg $N \cdot d^{-1}$. This amount would yield a daily increase of about 1 $\mu g\ N \cdot L^{-1}$ when diluted into the whole lake (5.5 ×

Table 3. Nutrient and ionic chemistry of the 1990 mesocosm experiment.

	Low FGA	High FGA
Nutrient chemistry		
Total carbon (μM)	5±15	125±21
Dissolved inorganic carbon (μM)	−5±0	−5±0
Dissolved organic carbon (μM)	10±14	110±21
Suspended carbon (μM)	0±1	20±0
Total nitrogen (μM)	−1.7±0.5	9.1±1.5
Nitrate (μg N·L^{-1})	−1±0	−7±0
Ammonia (μg N·L^{-1})	−20±7	98±18
Suspended nitrogen (μg N·L^{-1})	−3±0	36±2
Total phosphorus (μM)	−0.04±0.01	0.16±0.01
Total dissolved phosphorus (μg P·L^{-1})	−1.3±0.4	0.5±0.0
Suspended phosphorus (μg P·L^{-1})	−0.2±0.0	4.7±0.4
Ionic chemistry (all μequiv.·L^{-1})		
H$^+$	0.0±0.2	8.3±1.0
Alkalinity	0±1	10±1
Sulfate	0.0±0.2	8.3±1.0
Chloride	0.4±0.0	6.1±0.0
Sodium	0.1±0.0	0.2±0.0
Calcium	0±0	0±0
Magnesium	0.6±0.0	6.6±0.3
TdFe	−1.3±0.0	−3.5±1.5

Note: Reported values are the mean differences in concentration between the filamentous green algae (FGA) and water-only mesocosms; means of the water-only mesocosms are, therefore, not shown. Total dissolved iron (TdFe) is assumed to have a valence of ±3. Values are given as the mean ± SD. SD, standard deviation.

10^8 L), an amount equal to one-third to one-half of the total increase seen in the epilimnion during the fall (M.A. Turner, unpublished data).

The PP content of FGA increased as FGA coverage was enlarged in the three-compartment epilimnetic model (Fig. 5). Only a small amount of epilimnetic PP (approximately 3%) would be in FGA at the 1989 level of coverage (approximately 2 gdw·m^{-2}), but the amount would nearly equal that in periphyton and plankton with an FGA coverage of approximately 35 gdw·m^{-2}. At the 1988 level of coverage (approximately 75 gdw·m^{-2}, Table 1), FGA would have been the largest PP-containing compartment, accumulating approximately 54% of PP in the epilimnion.

Growths of FGA could alter the vertical distribution of oxygen (O_2) near the lake bottom. Profiles of O_2 concentration were measured in various mats of FGA on 29 September 1990. Oxygen concentrations declined rapidly in the lower half of decaying masses of FGA and reached less than 20% of ambient values near the base (Fig. 6). In contrast, O_2 concentrations resembled ambient values in healthy FGA, although in one case concentrations were increased by at least 80%.

The pore-water samplers installed at a depth of 2 m on 4 October 1990 indicated that FGA increased the pH in water overlying the sediments (Fig. 7). The pH increased almost 2 units within an established FGA mat that had compressed from 11 to 6 cm in thickness during 20 d of equilibration. The increase in pH was less than 1 unit where a smaller amount of FGA had developed around the sampler during the incubation period. In both cases, the increase occurred gradually with depth in the FGA and was probably related to generation of alkalinity associated with algal decomposition (see below).

Effects of FGA on physical properties

Blooms of FGA intercepted light strongly. Transmittance of natural light through lake water was reduced from 91.4 to 72.9 ± 2.7% (mean ± SE, *n* = 4 means; SD of measurements without FGA averaged less than 0.5%) by even small amounts of FGA (equivalent to 2.6 gdw·m^{-2}). Attenuation of light by FGA was more than 90% when the biomass of FGA reached 40 gdw·m^{-2}. In situ measurements corroborated the substantial attenuation of light by FGA: 72–81% of the light was intercepted by growths of FGA ranging in thickness from 5 to 25 cm. The surprisingly high attenuation at low thicknesses may have been caused by high algal densities.

Growths of FGA also were able to decrease water movement reaching the lake bottom. The rate of weight loss in the $CaSO_4$ chips, and hence water movement, declined with water depth both inside and outside a 15 cm thick mat (2 September 1988). The rate of weight loss within the mat, however, was approximately 10 mg·h^{-1} less than that occurring at corresponding depths outside the mat. Similarly, rates of weight loss in chips placed beneath mats of FGA were 43 ± 11% (mean ± SD, *n* = 5 samples) of rates at corresponding depths outside the mats (29 August

Fig. 4. Vertical profiles of dissolved inorganic carbon (DIC) measured during the evening of 2 September 1988 and the following morning in a mat of filamentous green algae (FGA) overlying rock in Lake 302S. Absolute DIC concentrations (µmol·L^{-1}) are shown for the water phase overlying the FGA and within the mat itself at various depths (cm).

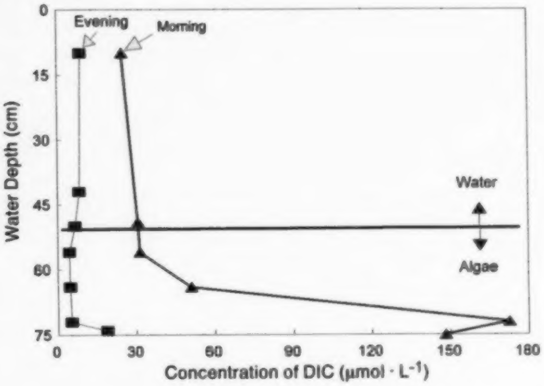

1990). The attenuation of water movement also appeared proportional to FGA thickness.

Water temperature measurements made within clouds of FGA in 0.5–1 m of water on the overcast morning of 10 August 1990 revealed that the interior temperatures were 0.4 ± 0.1°C (mean ± SD, $n = 7$ measurements) higher than the ambient temperature of 22.3°C. The temperature increase was independent of the volume of the FGA (approximately 1–100 L). The increase in temperature within growths of FGA during the cloudy afternoon of 15 August 1990 was 0.2 ± 0.1°C (mean ± SD, $n = 14$ measurements). Neither water depth (0.6–2.5 m) nor thickness of FGA (10–40 cm) were important. Similar results were obtained on the sunny afternoon of 29 August 1990.

Discussion

Consequences of FGA blooms on energy flow

Blooms of FGA affected littoral productivity in acidified Lake 302S in several ways. First, FGA sometimes helped alleviate the oligotrophication (i.e., diminished productivity of algal associations) that can occur in the littoral zone of acidified lakes (Turner et al. 1987, 1991, 1995*b*) because the potential extent of FGA productivity was sufficient to compensate for reduced epilithic productivity (Fig. 2). Peak areal productivity of Lake 302S FGA (Fig. 2) was even similar to the maximum rate (7.5 mmol C·m^{-2}·h^{-1}) measured in an *Oedogonium* mat in productive neutral Lake Wingra (McCracken et al. 1974).

Second, the seasonal pattern of FGA photosynthetic rates resembled that of epilithon in Lake 239 and counterbalanced the changes in seasonal pattern that had occurred in the acidified epilithon of Lake 302S (Fig. 1, cf. Fig. 5*a* of Turner et al. 1987 and Fig. 4 of Turner et al. 1991). Appreciable FGA photosynthesis usually coincided with maximum rates of Lake 239 epilithic photosynthesis during midsummer, so when rates of acidified epilithon were near their minima, the FGA reestablished seasonal normality in productivity within the acidified littoral zone.

Fig. 5. The potential of filamentous green algae (FGA) compared with periphyton and epilimnetic plankton to accumulate epilimnetic phosphorus, expressed as a function of FGA areal coverage (gdw·m^{-2}) in Lake 302S. See text for details of this rudimentary three-compartment model.

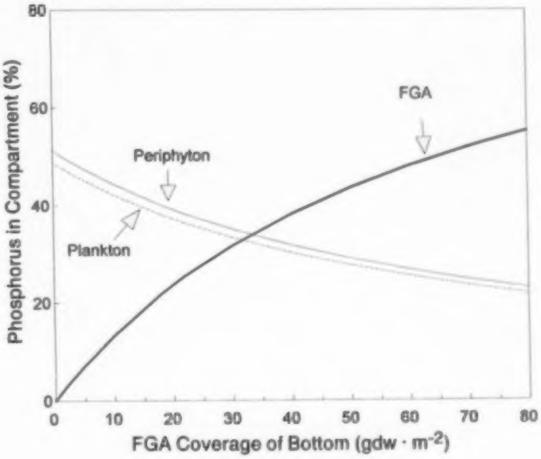

Third, the interannual variability in maximum development of FGA biomass was surprisingly large (Table 1). Although the epilimnetic pH remained stable at 4.5 over the 4 yr of the study (Turner et al. 1995*b*), maximum annual FGA biomass ranged from approximately 2 to 75 gdw·m^{-2} (Table 1). The lowest value was similar to the small amounts of *Zygogonium* that developed in less acid Plastic Lake, Ontario (summer pH of 5.5–5.8; Howell et al. 1990), whereas the maximum value resembled the 90 gdw·m^{-2} measured in neutral Lake Wingra (McCracken et al. 1974). The variability in FGA biomass of Lake 302S was probably related to climatic conditions (Turner et al. 1995*a*); Junger and Planas (1993) demonstrated in experimental stream studies that herbivory is unlikely to control FGA growth. If the annual maximum in biomass is a surrogate for net annual FGA productivity (e.g., Westlake 1965 for macrophytes), then the base of the acidified littoral food web was unstable compared with that provided by epilithon under neutral conditions (Fig. 1, cf. Fig. 5*a* of Turner et al. 1987). Seasonal variability in photosynthesis and biomass was also larger than that observed in neutral epilithon (Figs. 1 and 2; Turner et al. 1995*b*). Thus, acidification shifted the base of the littoral foodweb from that of stable epilithic production (Turner et al. 1995*b*) to the unstable irregular production of FGA. Such variability would most favor herbivores with flexible life histories and adaptable feeding strategies.

Influence of FGA on chemical properties

Effects of FGA on nutrient cycles

Growths of FGA can affect the C cycle in at least two ways. First, FGA can be both a sink and a source for DIC; effects upon DIC dynamics will vary daily and seasonally.

Fig. 6. Depth (cm) profiles of oxygen measured in mats of filamentous green algae (FGA) in Lake 302S on 29 September 1990. Algal masses *a* and *b* were decaying, whereas masses *c* and *d* were viable. Oxygen concentrations are normalized as a percentage of those in the water overlying the algae. Horizontal lines on each profile mark the algae–water interface. Algal masses *a* and *b* were located over sediment, whereas masses *c* and *d* were located on rock.

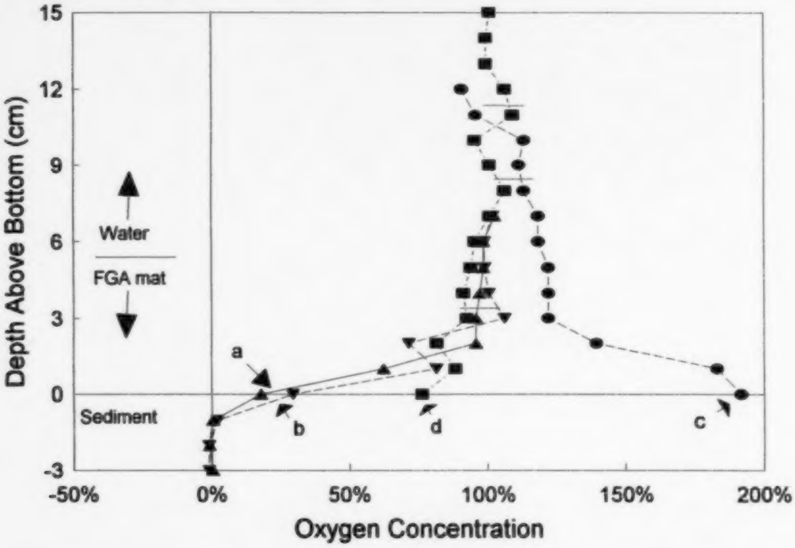

Low concentrations of DIC limit benthic algal photosynthesis (Turner et al. 1995*a*), especially in acidified lakes (Turner et al. 1987, 1991; Fairchild and Sherman 1992), so that uptake of DIC by FGA (see evening profile in Fig. 4; Howell et al. 1990; Turner et al. 1995*a*) may slow growth in other benthic algae. In contrast, DIC released during FGA respiration and decomposition (see morning profile in Fig. 4) could temporarily contribute to increased epilimnetic concentrations and enhance photosynthesis in other benthic algae.

Second, decomposing FGA can produce and release dissolved organic carbon (DOC; Tables 2, 3). The FGA also produced oil-like films on the surface of Lake 302S and in the mesocosms, possibly caused either by lipid production in healthy cells or by decomposition. Levels of DOC can become especially low in acidified lakes (Schindler et al. 1992), so DOC production by FGA may be important to the microbial loop. Filamentous green algae may also serve as a source of readily usable organic material for contaminant binding, metal chelation, and microbially mediated processes such as SO_4 reduction.

Filamentous green algae affected the N cycle principally through the flux of NH_3. The effect was bidirectional (Tables 2, 3) depending on the growth status of the algal association: NH_3 was taken up during summer growth and released during autumn and winter decomposition. Such effects have consequences for internal generation of alkalinity and acidity in the lake (see below).

The FGA were able to accumulate appreciable quantities of PP, but the major impact on the P cycle may be the mobilization of P previously located in the sediments. Phosphorus accumulation was related to FGA growth (Fig. 5), and consequently to time of year (Turner et al. 1995*a*) and to pH (Turner et al. 1994). At times, FGA were potentially the largest P-containing compartment (excluding the sediments) in the epilimnion of Lake 302S. The accumulation and potential sequestering of P is especially important, unlike C and N, because P is not stored in the atmosphere. The rudimentary model used here ignored the potential for sedimentary efflux of P. Additional research is needed to determine whether PP in the FGA was liberated by the physical–chemical conditions created by FGA overlying littoral sediments (see below), or was sequestered from the other compartments; our observations were equivocal. If mobilization of sedimentary P occurs, then FGA blooms could alleviate any potential P-related oligotrophication in the lake.

The FGA can also exert other effects upon nutrient cycling. The blooms can alter redox conditions at the sediment–water interface because of O_2 production during photosynthesis and consumption during decomposition (Fig. 6). This has been previously demonstrated for other benthic algal associations (Revsbech and Jørgensen 1981; Carlton and Wetzel 1988). Oxygen production and consumption yield markedly different results in the sediment–water exchange of chemicals (e.g., the sedimentary efflux of P by epipelic algae; see Carlton and Wetzel 1988).

Effects on internal alkalinity generation and acidification

The effects of FGA on both the N and S cycles can also affect internal generation and consumption of lake alkalinity.

Fig. 7. Depth (cm) profiles of pH in filamentous green algae (FGA), overlying water, and underlying sediment. The algae–sediment interface is shown by the light horizontal line across the figure. The shorter, darker horizontal lines on each profile denote the location of the algae–water interfaces on 24 October 1990.

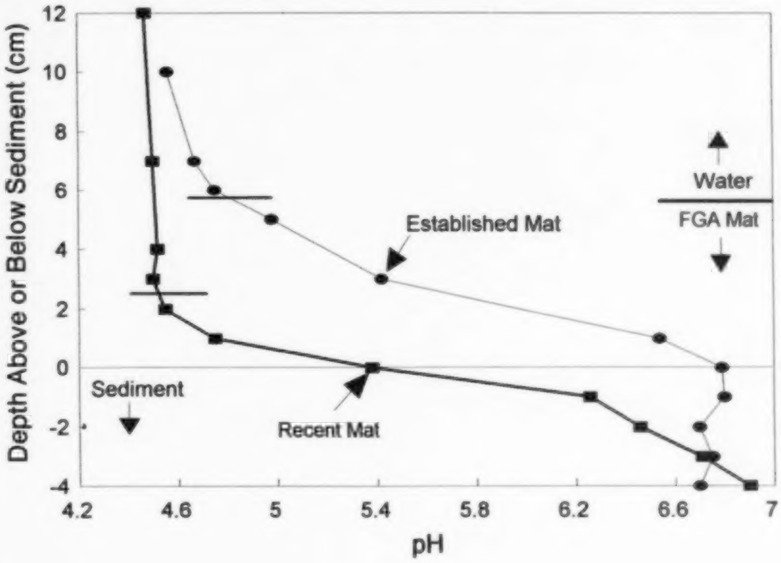

The FGA can contribute to internal lake acidification because of NH_3 uptake during their growth phase, i.e., from spring to early fall. Conversely, FGA can produce alkalinity during decomposition in fall and winter, augmenting the fall entrainment of hypolimnion-generated alkalinity into the epilimnion. Annual growths of FGA decompose each winter, so their nitrogen-related long-term net effect on alkalinity is probably negligible.

Filamentous green algae can further alter a lake's acid neutralizing capacity (Kelly et al. 1995) by disrupting the S cycle (Amaral 1991) and by shifting the depth of oxidation–reduction reactions in the sediments (Fig. 6). The site of S reduction will be shallower when anoxic conditions develop at the base of FGA blooms than with fully oxygenated water overlying the sediments. The reduced S compounds subsequently formed will then be more vulnerable to reoxidation when the FGA further decompose in fall and winter. The shifting of the site of S reduction may even occur on a daily basis because of the interplay between photosynthesis and respiration. This process will ultimately reduce the long-term effectiveness of in-lake generation of alkalinity.

Effects of FGA on physical properties

Blooms of FGA can influence several physical properties of the littoral zone. Light attenuation by FGA was sufficient at times to impair the growth of other phytobenthos, especially those that are normally light limited. The degree of attenuation was dependent upon the extent of FGA coverage, and so the impact would be seasonal. Photosynthesis in acidified epilithon displayed maxima in spring and fall (Fig. 1), so the greatest effect on epilithon would occur in the fall because surface irradiances then are lower and FGA blooms are larger than in spring. Filamentous green algae may also cause the decline of submerged macrophytes because of attenuation of light (e.g., the acidification-related loss of isoetids reported in the survey of Roelofs 1983).

The effect of FGA on bottom temperatures appeared to be minor. Increases of 1–2°C were seen by Hillebrand (1983) in "flab" comprised of Zygnematales in eutrophic alkaline ditches; temperature increases in Hillebrand's (1983) study were much larger in floating clusters of *Chara* and *Cladophora*, possibly because of greater densities. Temperature increases probably would also be transient, varying daily with light availability.

The FGA also diminished the amount of water movement reaching the littoral-zone bottom, which could diminish chemical transport at the sediment surface. The presence of FGA overlying the bottom could also slow translocation of materials from the littoral to the profundal zone.

Potential biological consequences of FGA growth

The proliferation of FGA may have other biological effects. For example, FGA may provide temporary refuge from predation for some animal taxa (Webster et al. 1992) or from the low pH of the overlying lake water (Fig. 7). However, the FGA habitat has some risks associated with O_2 depletion, which occurs with net respiration in the mats (Fig. 6). These consequences would vary spatially and temporally with the state of growth and light intensity; the latter would affect rates of photosynthetic O_2 production.

The FGA may also provide new habitat for some organisms. For example, some littoral Cladocera inhabit the

FGA in enormous numbers (B.J. Hann and M.A. Turner, unpublished data). Similarly, a littoral cladoceran and a trichopteran were associated with FGA growths in experimentally acidified Little Rock Lake (Webster et al. 1992). The FGA may provide a source of food for other taxa (Fulton 1988), material for net-spinning Trichoptera, and a substratum for chironomids. In contrast, the FGA may make spawning sites unsuitable for fish populations (Mills and Schindler 1986).

In summary, understanding the ecological effects of FGA blooms is important to understanding the functioning of acidified lakes. Several effects were potentially lakewide in scale, but this depended upon the degree of FGA bloom formation. Even small growths will probably affect local functioning of the littoral zone, thereby augmenting the heterogeneity that is characteristic of the littoral zone. The FGA blooms partially replaced the acidification-induced loss of primary production by epilithon. This positive benefit may have been offset by several negative consequences, as high biomasses of FGA transformed the chemical, physical, and biological properties of the littoral zone. Further research is needed to discover whether some of the apparent negative effects were in fact beneficial because future FGA growth may be increased by anthropogenic activities (Turner et al. 1995*a*).

Acknowledgments

Technical assistance was provided by C. Grose, B. Lonsberry, S. Richards, L. Sigurdson, S. Zettler, members of B. Townsend's 1990 research diver course (particularly R. Sigurdson and G. Bell), and L. Camarero. W. and M. Curry furnished engineering advice and fabricated the 1989 and 1990 mesocosms. The manuscript was improved by the reviews of an anonymous reviewer, G. Fairchild, F. Healey, R. Hecky, N. Kenkel, D. Schindler, E. Schindler, and especially D. Rosenberg. Elements of this work were originally part of a Ph.D. thesis by M.A.T. at the University of Manitoba.

References

Almer, B., W. Dickson, C. Ekstrom, and E. Hornstrom. 1978. Sulfur pollution and the aquatic ecosystem. *In* Sulfur in the environment: part 2. Ecological impacts. *Edited by* J.O. Nriagu. John Wiley & Sons, New York. pp. 271–311.

Amaral, J.A. 1991. Sulfate reduction and organic sulfur formation in lake sediments. Ph.D. thesis, University of Manitoba, Winnipeg, Man.

Brezonik, P.L., J.G. Eaton, T.M. Frost, P.J. Garrison, T.K. Kratz, C.E. Mach, H.H. McCormick, J.A. Perry, W.A. Rose, C.J. Sampson, B.C.L. Shelley, W.A. Swenson, and K.E. Webster. 1993. Experimental acidification of Little Rock Lake, Wisconsin: chemical and biological changes over the pH range 6.1 to 4.7. Can. J. Fish. Aquat. Sci. 50: 1101–1121.

Brunskill, G.J., and D.W. Schindler. 1971. Geography and bathymetry of selected lake basins, Experimental Lakes Area, northwestern Ontario. J. Fish. Res. Board Can. 28: 139–155.

Carlton, R.G., and R.G. Wetzel. 1988. Phosphorus flux from lake sediments: effect of epipelic algal oxygen production. Limnol. Oceanogr. 33: 562–570.

Fairchild, G.W., and J.W. Sherman. 1992. Linkage between epilithic algal growth and water column nutrients in softwater lakes. Can. J. Fish. Aquat. Sci. 49: 1641–1649.

France, R.L., Y.-K. Yung, and P.M. Welbourn. 1992. Identifiation of metaphytic zygnematacean algae in acid-sensitive Canadian Shield lakes. Arch. Hydrobiol. Suppl. 66: 99–103.

Fulton, R.S., III. 1988. Grazing on filamentous algae by herbivorous zooplankton. Freshwater Biol. 20: 263–271.

Graham, J.M., P. Arancibia-Avila, and L.E. Graham. 1996. Physiological ecology of the filamentous green alga *Mougeotia* (Zygnematales, Charaophyceae) under acidic conditions: light and temperature effects on photosynthesis and respiration. Limnol. Oceanogr. In press.

Hendrey, G.R. 1982. Effects of acidification on aquatic primary producers and decomposers. *In* Proceedings of an International Symposium on Acidic Precipitation and Fishery Impacts in northeastern North America. Cornell University, Ithaca, N.Y., August 2–5, 1981. *Edited by* R.E. Johnson. American Fisheries Society, Bethesda, Md. pp. 125–135.

Hendrey, G.R., K. Baalsrud, T.S. Traaen, M. Laake, and G. Raddum. 1976. Acid precipitation: some hydrobiological changes. Ambio, 15: 224–227.

Hesslein, R.H. 1976. An in situ sampler for close interval pore water studies. Limnol. Oceanogr. 21: 912–914.

Hillebrand, H. 1983. Development and dynamics of floating clusters of filamentous algae. *In* Periphyton of freshwater ecosystems. *Edited by* R.G. Wetzel. Dr. W. Junk, The Hague, The Netherlands. pp. 31–39.

Hoshaw, R.W., and R.M. McCourt. 1988. The Zygnemataceae (Chlorophyta): a twenty-year update of research. Phycologia, 27: 511–548.

Howell, E.T., M.A. Turner, R.L. France, M.B. Jackson, and P.M. Stokes. 1990. Comparison of Zygnematacean (Chlorophyta) algae in the metaphyton of two acidic lakes. Can. J. Fish. Aquat. Sci. 47: 1085–1092.

Junger, M., and D. Planas. 1993. Alteration of trophic interactions between periphyton and invertebrates in an acidified stream: a stable carbon isotope study. Hydrobiologia, 262: 97–107.

Kelly, C.A., J.W.M. Rudd, A. Furutani, and D.W. Schindler. 1984. Effects of lake acidification on rates of organic matter decomposition in sediments. Limnol. Oceanogr. 29: 687–694.

Kelly, C.A., J.A. Amaral, M.A. Turner, D.W. Schindler, J.W.M. Rudd, and M.P. Stainton. 1995. Impairment of in-lake alkalinity generation at low pH by disruption of sulfur cycling. Biogeochemistry, 28: 115–130.

Levine, S.N., and D.W. Schindler. 1992. Modification of the N:P ratio in lakes by in situ processes. Limnol. Oceanogr. 37: 917–935.

McCracken, M.D., T.D. Gustafson, and M.S. Adams. 1974. Productivity of *Oedogonium* in Lake Wingra, Wisconsin. Am. Midl. Nat. 92: 247–254.

Mills, K.H., and D.W. Schindler. 1986. Biological indicators of lake acidification. Water Air Soil Pollut. 30: 779–789.

Müller, P. 1980. Effects of artificial acidification on the growth of periphyton. Can. J. Fish. Aquat. Sci. 37: 355–363.

Revsbech, N.P., and B.B. Jørgensen. 1981. Primary production of microalgae in sediments measured by oxygen microprofile, $H^{14}CO_3$-fixation, and oxygen exchange methods. Limnol. Oceanogr. 26: 717–730.

Roelofs, J.G.M. 1983. Impact of acidification and eutrophication on macrophyte communities in soft waters in the Netherlands. I. Field observations. Aquat. Bot. 17: 139–155.

Schindler, D.W., and M.A. Turner. 1982. Biological, chemical and physical responses of lakes to experimental acidification. Water Air Soil Pollut. 18: 259–271.

Schindler, D.W., V.E. Frost, and R.V. Schmidt. 1973. Production of epilithiphyton in two lakes of the Experimental Lakes Area, northwestern Ontario. J. Fish. Res. Board Can. 30: 1511–1524.

Schindler, D.W., K.H. Mills, D.F. Malley, D.L. Findlay, J.A. Shearer, I.J. Davies, M.A. Turner, G.A. Linsey, and D.R. Cruikshank. 1985. Long-term ecosystem stress: the effects of years of experimental acidification on a small lake. Science (Washington, D.C.), 228: 1395–1401.

Schindler, D.W., S.E. Bayley, P.J. Curtis, B.R. Parker, M.P. Stainton, and C.A. Kelly. 1992. Natural and man-caused factors affecting the abundance and cycling of dissolved organic substances in Precambrian Shield lakes. Hydrobiologia, 229: 1–21.

Stainton, M.P., M.J. Capel, and F.A.J. Armstrong. 1977. The chemical analysis of fresh water. 2nd ed. Can. Fish. Mar. Serv. Misc. Spec. Publ. No. 25.

Stokes, P.M. 1986. Ecological effects of acidification on primary producers in aquatic systems. Water Air Soil Pollut. 30: 421–438.

Turner, M.A., D.W. Schindler, and R.W. Graham. 1983. Photosynthesis–irradiance relationships of epilithic algae measured in the laboratory and in situ. *In* Periphyton of freshwater ecosystems. *Edited by* R.G. Wetzel. Dr. W. Junk, The Hague, The Netherlands. pp. 73–87.

Turner, M.A., M.B. Jackson, D.L. Findlay, R.W. Graham, E.R. DeBruyn, and E.M. Vandermeer. 1987. Early responses of periphyton to experimental lake acidification. Can. J. Fish. Aquat. Sci. 44(Suppl. 1): 135–149.

Turner, M.A., E.T. Howell, M. Summerby, R.H. Hesslein, D.L. Findlay, and M.B. Jackson. 1991. Changes in epilithon and epiphyton associated with experimental acidification of a lake to pH 5. Limnol. Oceanogr. 36: 1390–1405.

Turner, M.A., E.T. Howell, G.G.C. Robinson, P. Campbell, R.E. Hecky, and E.U. Schindler. 1994. Roles of nutrients in controlling growth of epilithon in oligotrophic lakes of low alkalinity. Can. J. Fish. Aquat. Sci. 51: 2784–2793.

Turner, M.A., E.T. Howell, G.G.C. Robinson, J.F. Brewster, L.J. Sigurdson, and D.L. Findlay. 1995*a*. Growth characteristics of bloom-forming filamentous green algae in the littoral zone of an experimentally acidified lake. Can. J. Fish. Aquat. Sci. 52: 2251–2263.

Turner, M.A., D.W. Schindler, D.L. Findlay, M.B. Jackson, and G.G.C. Robinson. 1995*b*. Disruption of littoral algal communities by experimental lake acidification. Can. J. Fish. Aquat. Sci. 52: 2238–2250.

Webster, K.E., T.M. Frost, C.J. Watras, W.A. Swenson, M. Gonzalez, and P.J. Garrison. 1992. Complex biological responses to the experimental acidification of Little Rock Lake, Wisconsin, U.S.A. Environ. Pollut. 78: 73–78.

Wei, Y.-X., Y.-K. Yung, M.B. Jackson, and T. Sawa. 1989. Some Zygnemataceae (Chlorophyta) of Ontario, Canada, including descriptions of two new species. Can. J. Bot. 67: 3233–3247.

Westlake, D.F. 1965. Some basic data for investigations of the productivity of aquatic macrophytes. Mem. Ist. Ital. Idrobiol. 18(Suppl.): 229–248.

Fate of ^{60}Co and ^{134}Cs added to the hypolimnion of a Canadian Shield lake[1]

G.A. Bird, M. Stephenson, R. Roshon, W.J. Schwartz, and M. Motycka

Abstract: Tritium (^{3}H), cobalt-60 (^{60}Co), and cesium-134 (^{134}Cs) were added to the anaerobic hypolimnion of a Canadian Shield lake during the summer of 1989 to simulate the nuclear fuel waste disposal scenario in which nuclides are assumed to enter the bottom of a lake with deep groundwater flow. The radionuclides initially remained confined to the hypolimnion and there was little loss from the water. Lake mixing during autumn turnover resulted in the rapid loss of ^{60}Co (first order rate constant, k, is 0.036 d^{-1}) and much slower loss of ^{134}Cs ($k = 0.006\ d^{-1}$) from the water to sediment over the next 41 and 238 d, respectively. One year after the addition, <1% of the ^{60}Co and ^{134}Cs and 6% of the tritiated water added to trace water movement had been lost to the outflow. About 6% of the ^{60}Co and 19% of the ^{134}Cs remained in the water column. Loss rates to the sediment observed following autumn turnover in the present study were slower than those previously observed from the epilimnion; however, there was little difference in the amount of ^{60}Co and ^{134}Cs remaining in the water after 1 year when the input was to the hypolimnion as opposed to the epilimnion.

Résumé : Au cours de l'été de 1989, on a ajouté du tritium (^{3}H), du cobalt (^{60}Co) et du césium (^{134}Cs) radioactifs à l'hypolimnion anaérobie d'un lac du Bouclier canadien afin de simuler un scénario d'élimination de déchets de combustible nucléaire suivant des nucléides seraient censés pénétrer au fond d'un lac alimenté par des eaux souterraines. Au début, les radionucléides sont restés confinés à l'hypolimnion, et l'on n'a enregistré qu'une faible déperdition des nucléides présents dans l'eau. Le brassage des eaux du lac par la circulation d'automne a entraîné une perte rapide de ^{60}Co (constante de vitesse de premier ordre $k = 0{,}036 \cdot d^{-1}$) et une perte beaucoup plus lente de ^{134}Cs ($k = 0{,}006 \cdot d^{-1}$) de l'eau vers les sédiments, soit 41 jours pour le cobalt, et 238 jours le césium. Un an après l'addition de nucléides, moins de 1% du ^{60}Co et du ^{134}Cs et 6% de l'eau tritiée ajoutée afin de suivre les déplacements de l'eau avaient été emportés par la décharge. Il restait environ 6% du ^{60}Co et 19% du ^{134}Cs dans la colonne d'eau. La vitesse de dépôt des nucléides dans les sédiments enregistrée ici à la suite du brassage automnal était inférieure à celle observée quand l'apport avait été fait dans l'épilimnion (rapport antérieur); toutefois, il n'y avait que peu de différence dans la quantité de ^{60}Co et de ^{134}Cs qui restait dans l'eau après 1 an lorsque l'apport de nucléides était fait dans l'hypolimnion plutôt que dans l'épilimnion.

[Traduit par la Rédaction]

Introduction

The concept of permanent disposal of Canada's nuclear fuel waste deep underground in the crystalline rock of the Canadian Shield is being evaluated (Hancox and Nuttall 1991). The disposal concept incorporates natural and engineered barriers to isolate the waste from the biosphere. However, total containment of nuclear fuel wastes in an underground vault may not last indefinitely. A probable pathway for the transport of radionuclides from an underground vault to a lake or wetland is with deep groundwater flow along a fracture in the geosphere. Because this is not expected to occur until far into the future, the protection of the environment and biota cannot be demonstrated directly but must be evaluated with the help of assessment models.

A surface-water model for assessing the disposal concept (Bird et al. 1992, 1993*a*) predicts the concentration of radionuclides in water and sediments. It is a simple, probabilistic, mass-balance model with a single, well-mixed compartment representing water and a second compartment representing surficial sediment; parameter values are represented by probability density functions. The model is sensitive to the rate of radionuclide transfer from water to sediment, values for which were taken from the literature (Bird et al. 1992, 1993*a*). Data are available for the fate

Received May 31, 1993. Accepted April 28, 1995.
J11956

G.A. Bird, M. Stephenson, R. Roshon, W.J. Schwartz, and M. Motycka. Atomic Energy of Canada Limited, Whiteshell Laboratories, Pinawa, MB R0E 1L0, Canada.

---

[1] This paper is one of a series done in honour of the 25th anniversary of the Experimental Lakes Area.

of radionuclides entering lakes from atmospheric fallout (Tracy and Prantl 1983; Brunskill et al. 1984; Brunskill and Wilkinson 1987; Cornett and Chant 1988; Santschi et al. 1990; Kansanen et al. 1991) and as a result of experimental additions of radionuclides to the epilimnion of lakes (Hesslein et al. 1980; Santschi et al. 1986; Hesslein 1987; Diamond et al. 1990). However, it is not known whether the behaviour of radionuclides entering lakes with groundwater flow will be similar to their behaviour after surface addition. In particular, the behaviour of redox-sensitive nuclides, such as ^{60}Co, in an anaerobic hypolimnion may be different from their behaviour when added to the epilimnion. Thus, to validate the use of literature data for our surface-water model, it is important to test the hypothesis that the ultimate fate of radionuclides added to an anaerobic hypolimnion and the epilimnion is the same. This test is not only important for nuclear fuel waste disposal, but also for the underground storage and disposal of other hazardous substances.

Several radiotracer experiments were carried out at the Experimental Lakes Area (ELA) in northwestern Ontario during the 1970s. In one study, Hesslein (1987) added ^{60}Co, ^{134}Cs, ^{59}Fe, ^{203}Hg, ^{75}Se, ^{85}Sr, and ^{65}Zn to the epilimnion of Lake 226 (L226). To test our hypothesis, we added ^{60}Co and ^{134}Cs, and tritium (^{3}H) to trace the water movement, to the anaerobic hypolimnion of L226 during the summer of 1989. Co and Cs are lost from the water and deposited to sediments by different processes. Co is a divalent cation that readily binds to suspended organic particles, which are subject to sedimentation (Parker and Hasler 1969; Hesslein et al. 1980; Santschi et al. 1986; Hesslein 1987). Co is bound primarily to the organic fraction in sediments (Evans et al. 1988). The behaviour of Co is particularly sensitive to changes in redox potential. Under moderately reducing conditions, Co is released from sediments as Co^{2+} and is precipitated as CoS in the presence of sulfide (Balistrieri et al. 1992; Wallman 1992). Cs is a monovalent cation that does not bind readily to suspended organic particles but is lost from the water column through direct sorption to bottom sediments (Evans et al. 1983; Hesslein et al. 1980; Hesslein 1987; Kansanen et al. 1991; Santschi et al. 1986). However, Cs will readily bind to suspended clay particles (Garder and Skulberg 1964). Alberts et al. (1989) found that Cs sorption to sediments is associated with the cystalline fraction (clay) and is not readily reversible. Lake sediments containing little clay have low ^{137}Cs concentrations (Heit and Miller 1987).

This paper describes the fate of ^{60}Co and ^{134}Cs for 1 year after their addition to the anaerobic hypolimnion of ELA L226 and compares their behaviour with the fate of the same radionuclides previously added to the epilimnion of the same lake by Hesslein (1987).

Materials and methods

Study site

The ELA is located in northwestern Ontario on the Canadian Shield and was described by Brunskill and Schindler (1971) and Cleugh and Hauser (1971). Lake 226 is a small (16.1 ha) dimictic, double-basin, headwater lake (Fig. 1). It is naturally divided into two basins by a shallow channel (Findlay and Kasian 1987). The northeast basin (L226N) has an area of 8.3 ha with a maximum depth of 14 m, whereas the southwest basin (L226S) is 7.8 ha in area with a maximum depth of 10 m. No permanent streams flow into L226; it is fed by precipitation and runoff. The outflow is located at the north end of the northeast basin. Lake 226 was the site of a fertilization study from 1973 to 1980, L226S receiving annual inputs of C ($3.67\ g{\cdot}m^{-2}$) and N ($1.92\ g{\cdot}m^{-2}$), and L226N receiving equivalent quantities of C and N plus P ($0.34\ g{\cdot}m^{-2}$; Findlay and Kasian 1987). After nutrient inputs stopped, the primary production of L226 quickly returned to prefertilization levels (Shearer et al. 1987). Hesslein (1987) added 4.5 GBq each of ^{60}Co and ^{134}Cs, and between 4.5 and 13 GBq each of ^{59}Fe, ^{203}Hg, ^{75}Se, ^{85}Sr, and ^{65}Zn to the epilimnion of both basins on July 25, 1977. In addition, Bower et al. (1987) added 46 GBq of ^{14}C to the epilimnion of L226N and 11.5 GBq of ^{14}C to the epilimnion of L226S in 1978.

Radionuclide addition

For our additions, 4.6 GBq of ^{60}Co (as $CoCl_2$), 4.6 GBq of ^{134}Cs (as CsCl), and 370 GBq of ^{3}H (as ^{3}HHO) were added to an acidified solution (4 mL of 6 M HNO_3 in distilled water) in a 250-mL polypropylene sample bottle (fitted with a septum cap) in the laboratory. The bottle of radionuclides was placed into a brass insert, packaged in a B-type canister, and transported to L226 where the radionuclides were added from a raft to the anaerobic hypolimnion of L226N at 12 m depth (Fig. 1) on August 2, 1989. A depth of 12 m was chosen to place the radionuclides midway between the aerobic–anaerobic water interface and the sediments.

For safety reasons, the radionuclides were added to the lake without removing the sample bottle from the canister by using the injection system described by Bird et al. (1993*b*). Briefly, water was pumped from a depth of 12 m to the surface and then back to the 12 m depth using a peristaltic pump. The radionuclide solution was aspirated from the bottle into the outflow from the pump and into the hypolimnion. Once the bottle with the radionuclide solution was empty, as determined by the appearance of air bubbles in the outflow hose from the pump, the system was rinsed three times with 250 mL of acidified solution (4 mL of 6 M HNO_3 in distilled water).

Precautions were taken to avoid warming the hypolimnetic water during the addition, thus preventing upward convection of water returning to the hypolimnion. The uptake and return hoses were insulated to a depth of 5 m, the depth of the epilimnion. Furthermore, the water passed through a 15 m length of copper tubing immersed in an ice bath before reaching the peristaltic pump and being returned to the hypolimnion. Care was also taken to avoid mixing the radionuclides in the hypolimnion. The uptake line was located 20 m from the return outlet, which was immediately below the injection raft. A diffuser, consisting of two sheets of Plexiglas 30 cm in diameter with a 2-mm space between them, was used to assist in delivering the radionuclides at a uniform depth.

Addition of the radionuclides to the lake took 7 min; together with the three rinses, the total procedure took approximately 30 min. About 20 L of water was pumped

Fig. 1. Contour map of Lake 226 illustrating the location of the radionuclide addition and sampling locations. ⊠, radionuclide addition; ●, water samples along vertical profiles; ■, sediment core samples; and 1 to 5, sediment trap locations at 6 m depth.

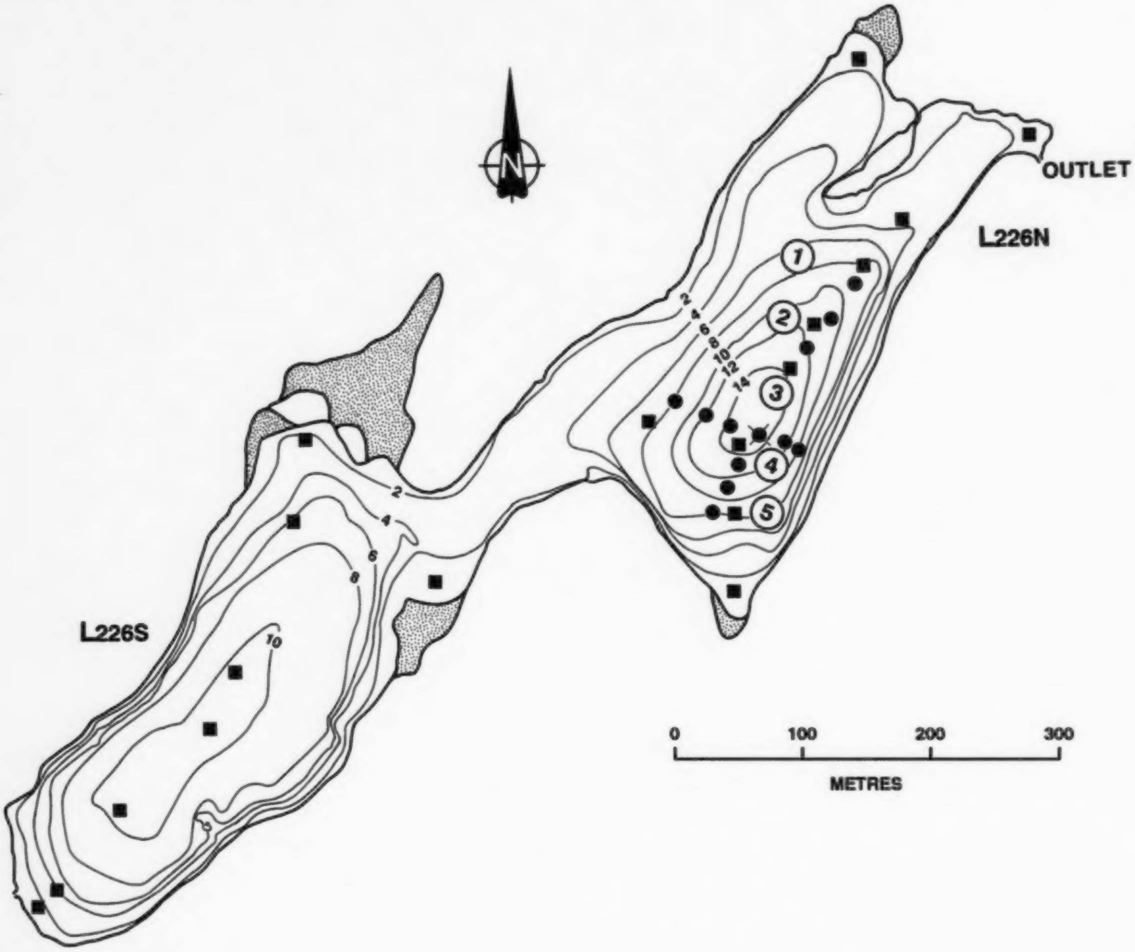

from the hypolimnion and returned during the operation. The efficiency of the system in delivering the radionuclides to the lake was >99.99% (Bird et al. 1993*b*).

Water samples

Three automatic water samplers (ISCO 2900 wastewater samplers) were placed on rafts anchored 20, 30, and 100 m from the point of injection to monitor the horizontal dispersion of the radionuclides within the hypolimnion over the first 41 d of the study. Each sampler was programmed to collect 400 mL of water from a depth of 12 m, at 12-h intervals. A fourth sampler, located on the injection raft, sampled water at 8 m, just above the aerobic–anaerobic water interface. This sampler monitored the vertical movement of the radionuclides from the hypolimnion. In addition, at weeks 1, 2, and 4, and periodically thereafter until freeze-up, vertical profiles were sampled at 25-m intervals along two transect lines from the point of injection (Fig. 1) using a peristaltic pump. Following freeze-up, vertical profiles were collected only at the deepest point of L226N and L226S at approximately monthly intervals. Initially, 1-L samples were collected, but as ^{60}Co and ^{134}Cs concentrations decreased 2-L and then 4-L samples were collected. On each sampling occasion from August 31 to freeze-up, a 22-L water sample was collected at the lake outflow to measure the loss of radionuclides from the lake. On each occasion, oxygen and temperature were measured at 1-m intervals along a vertical profile in the deepest part of L226N, and from October 18 and thereafter in L226S, using a dissolved-oxygen meter (YSI model 57). In addition, water samples along a vertical profile in L226N were collected at least once a month for chemical analysis. (Data on cations, anions, pH, and conductivity are available upon request from the senior author, G.A. Bird.)

In the laboratory, water samples were acidified with 0.5 mL of 6 M HNO_3/L of water, and stored at room temperature until processed for gamma counting. Samples were dried onto polyethylene sheets as described by Guthrie and Grummitt (1963), but no carrier was added to the sample prior to evaporation. The plastic sheeting was rolled up and inserted into a 20-mL liquid scintillation vial for gamma counting. To guard against problems with counting geometry, following counting the polyethylene sheeting was inverted in the vials and the samples were recounted. The mean of these two values, which were usually within 10% of each other, was taken as the best estimate. Close agreement was obtained between samples processed as described and a dilution series of known activity.

To measure the fraction of radionuclides bound to particles, water samples were collected at monthly intervals from the injection raft at depths of 2, 9, and 12 m and filtered through preweighed 0.45-μm cellulose nitrate filters in the field. Cellulose filters were used because of insignificant adsorption of dissolved isotopes onto these filters (Hesslein et al. 1980). To prevent contamination of samples, filtration equipment was cleaned with 1 M HCl between sampling depths. In the laboratory, the filters were dried at 65°C for 24 h, reweighed to within 0.01 mg, and digested in 6 M NaOH for gamma counting as a liquid.

Sedimentation and sediment samples

From June 1, 1989 to June 13, 1990, the sedimentation of particles from the water column was monitored using five pairs of sediment traps suspended at a depth of 6 m along a transect across L226N (Fig. 1). Two additional pairs of sediment traps were placed at depths of 9 and 12 m in the deepest part of the basin (site 3) to measure sedimentation rates with depth. Sediment traps consisted of a 40 cm length of ABS piping, 5 cm in diameter. A 15 cm length of 6 mm diameter Tygon tubing, attached to the bottom of the trap, was pinched closed while the trap was in position; it allowed for easy draining of settled particles into a 250-mL sample bottle. Samples were collected weekly during the ice-free season. They were stored on ice until returned to the laboratory, where they were refrigerated until filtered through preweighed 0.45-μm glass-fibre filters, usually within 2 d. The filters were dried at 65°C for 24 h, reweighed, and packed into a 7-mL vial for gamma counting. Because of the high concentration of particles in these samples, we assumed all the radioactivity was particle bound and that adsorption of activity from the water was insignificant.

Eight sediment cores were collected from L226N on May 11, 1989, prior to the radionuclide addition, to determine baseline levels of radioactivity from previous additions. During the study, 15 sediment cores were taken from L226N on August 17 and 3 sediment cores were collected on September 28, 1989 to determine whether sorption of radionuclides from the anaerobic water to sediment had occurred. Cores were also collected on March 22–23 and June 13, 1990 from 10 locations in L226N and 8 locations in L226S; these locations represented various depths on transects across the basins (Fig. 1).

Coarse sandy sediment from 2 m depth was collected using an acrylic tube (5 cm diameter) threaded onto a 1.9 m length of ABS tubing (3.8 cm diameter) which was carefully pushed into the sediment. Other sediment types were collected using a K–B core sampler fitted with a clear acrylic tube (5 cm diameter). The K–B core sampler was lowered slowly into the sediment; only those cores that appeared undisturbed were used. Cores were immediately sectioned into 1-cm slices, and each slice was placed in an appropriately labelled, preweighed 120-mL sample cup. Usually, 15 slices were taken from each core; however, on September 28, only the top 3 cm were taken. In the laboratory, the samples were immediately frozen. To process the samples, they were thawed, weighed, dried at 65°C, reweighed, and ground with a mortar and pestle. A weighed amount of the sediment was then placed in a 5-mL vial to a depth corresponding to a standard geometry for gamma counting.

Radiological and statistical analyses

Water, sediment trap, and core samples were analyzed using a high-purity coaxial germanium detector in conjunction with a Nuclear Data 6700 computer – multichannel analyzer to detect gamma emissions for ^{134}Cs at 796 keV (1 eV = 0.160 217 733 aJ) and for ^{60}Co at 1332 keV energies. Counts were for samples corresponding to standard geometries, assuming uniform distribution of the radioactivity throughout the sample. Analysis of samples spiked with known quantities of activity showed close agreement (generally within 90%) between observed and expected results. Tritium activity was measured by beta analysis at 18 keV with a Packard 2000 CA/LL liquid scintillation counter.

Statistical analysis of the sedimentation data was by two-way analysis of variance (ANOVA) using the SAS GLM program (SAS 1985). Loss rates of ^{60}Co and ^{134}Cs from water with time, and radionuclide inventories in sediment cores with depth in March and June were determined by regression of the ln-transformed data. Analysis of covariance was used to determine whether the regressions of radionuclide inventories in sediment cores with the covariant depth on the two sampling occasions were different from each other. We compared pairs of means by t tests. Values are given as the mean ± 1 SD unless specified otherwise. Results at or below $P = 0.05$ are deemed significant. All radionuclide data were back-dated to August 2, 1989 to account for radioactive decay.

Results

Dispersion and loss from water

It took more than 12 h for the radionuclides to travel horizontally 20 to 30 m (Figs. 2*a*, 2*b*) in the anaerobic hypolimnion. Radioactivity was not detected 100 m from the point of injection until 48 h after addition (Fig. 2*c*). This indicates a horizontal dispersal rate of about 0.057 ± 0.012 $cm \cdot s^{-1}$, assuming a straight-line travel path. The levels of radioactivity generally decreased with distance from the point of injection, but considerable variability was observed over the 6-wk sampling period (Figs. 2*a*–*c*). Variability appears to decrease after day 28 (Fig. 2), but this may actually be the result of analyzing every fourth sample from day 28 onward. During the investigation period,

Fig. 2. Concentrations of ^{60}Co, ^{134}Cs, and ^{3}H (Bq·mL^{-1}) in water samples collected at 12 m depth at (*a*) 20 m, (*b*) 30 m, and (*c*) 100 m from the point of the addition, and (*d*) at 7 or 8 m depth directly above the point of the addition over the first 41 d of the study. Broken line, ^{60}Co; dot-dashed line, ^{134}Cs; solid line, ^{3}H.

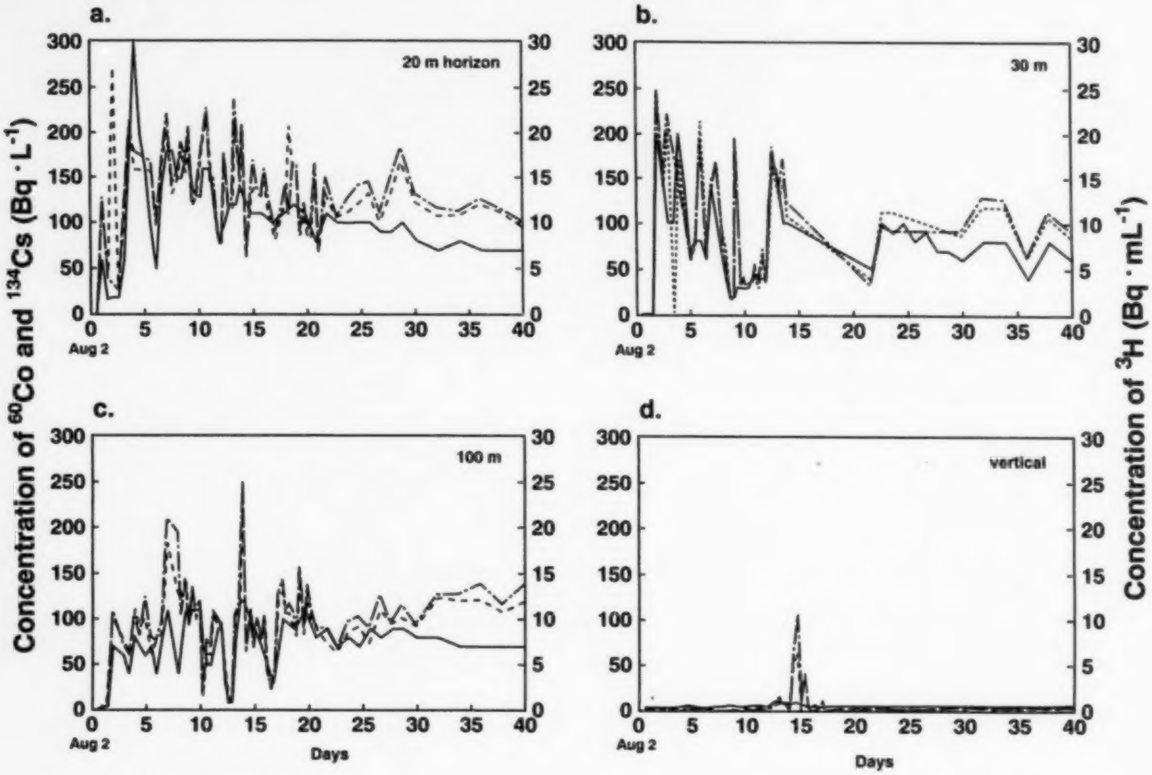

the radionuclides remained confined to the anaerobic hypolimnion (Fig. 2*d*). The marked increase in concentrations around day 15 (Fig. 2*d*) is the result of the anaerobic hypolimnion expanding upward to a depth of 8 m. As a result, we raised the uptake line to the 8-m autosampler to a depth of 7 m, so it was just above the aerobic–anaerobic water interface, which accounts for the lower concentrations observed thereafter.

Vertical ^{60}Co and ^{134}Cs profiles confirm that the radionuclides remained confined to the anaerobic hypolimnion prior to autumn turnover (Fig. 3). With the loss of summer stratification as autumn turnover progressed, the radionuclides became dispersed throughout the lake (Fig. 3). Thus, approximately 34% of the ^{60}Co, approximately 44% of the ^{134}Cs (Fig. 4*b*), and approximately 46% of the ^{3}H (data not presented) that was added to L226N was transferred to L226S; L226S accounts for 51% of the volume of L226. ^{60}Co was rapidly lost from the water with oxygenation of the hypolimnetic waters during autumn turnover (Figs. 4*a*, 4*b*), except from the water within approximately 1 m of the bottom that did not mix and remained anaerobic (Fig. 3*d*). This resulted in high concentrations of radionuclides near the bottom until spring turnover. During winter, most of the ^{60}Co in water was in the hypolimnion, whereas ^{134}Cs concentrations were more uniformly distributed with depth, except in the bottom layer of water, which did not mix (Fig. 5). Thus, most of the ^{134}Cs in water was in the epilimnion (Fig. 5), because this forms the greatest portion of the lake volume. A first-order loss rate coefficient (k) of 0.036 d^{-1} was calculated for ^{60}Co during the period of rapid loss from the water following autumn overturn (days 90 and 131); ^{134}Cs was lost from the water column at a slower rate for this period (Table 1). Spring turnover was complete and radionuclides remaining in the water were dispersed throughout the lake. This resulted in low to nondetectable ^{60}Co concentrations in the water column and ^{134}Cs concentrations of about 2.5 Bq·L^{-1}. With the development of anaerobic conditions in the hypolimnion during summer, ^{60}Co concentrations increased again in the bottom water (Fig. 3*a*). On the basis of the change in the ^{60}Co and ^{134}Cs inventory in the hypolimnion below the 12 m depth between May 30 and July 25, 1990, ^{60}Co and ^{134}Cs were released from the sediment at net rates of about 118 and 22 Bq·m^{-2}·d^{-1} respectively. The release of radionuclides from sediment was equivalent to approximately 14% of the ^{60}Co and approximately 5% of the ^{134}Cs inventory estimated to be in the sediment below 12 m using the regressions for June in Table 2.

Fig. 3. Depth–time profiles for (*a*) ^{60}Co (Bq·L^{-1}), (*b*) ^{134}Cs (Bq·L^{-1}), (*c*) ^{3}H (Bq·L^{-1}), (*d*) oxygen (mg·L^{-1}), and (*e*) temperature (°C) over the 358-d study period at the station where the radionuclides were added to the anaerobic hypolimnion of Lake 226N. The solid bar indicates ice cover.

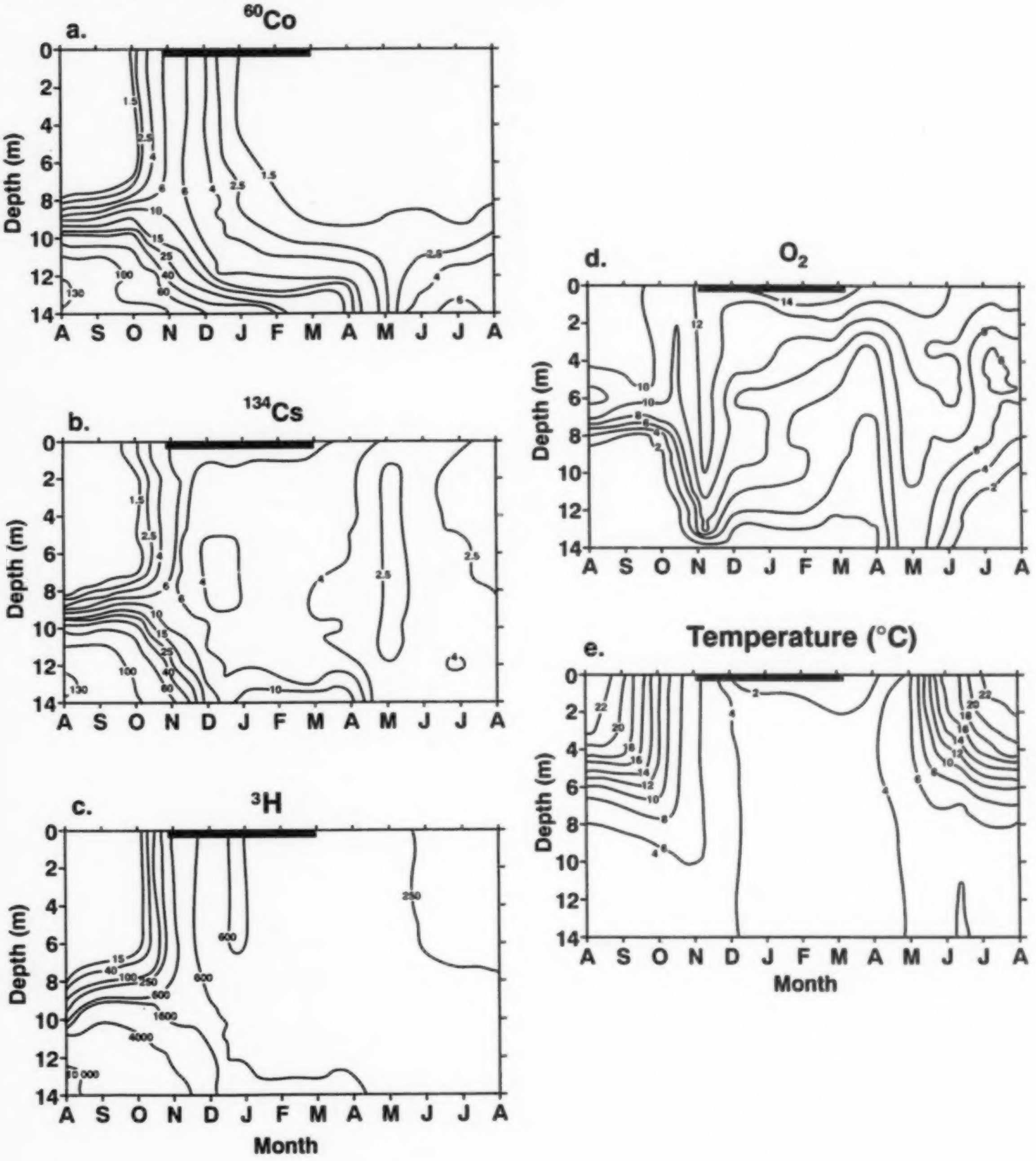

A mass balance showed that approximately 6% and approximately 19% of the initial ^{60}Co and ^{134}Cs still remained in the water column after 1 yr (Fig. 4), whereas 94% of the ^{3}H remained in the lake (data not presented). Hydrological data for L226 (K. Beaty, Department of Fisheries and Oceans, Winnipeg, Man., personal communication) showed that little discharge occurred in the latter part of 1989, and the water renewal rate for the study period was

Fig. 4. Mean percent (± SD) of ^{60}Co and ^{134}Cs remaining in the water column (*a*) in Lake 226 and (*b*) in Lake 226S over the 358-d study period following their addition to the hypolimnion of Lake 226N.

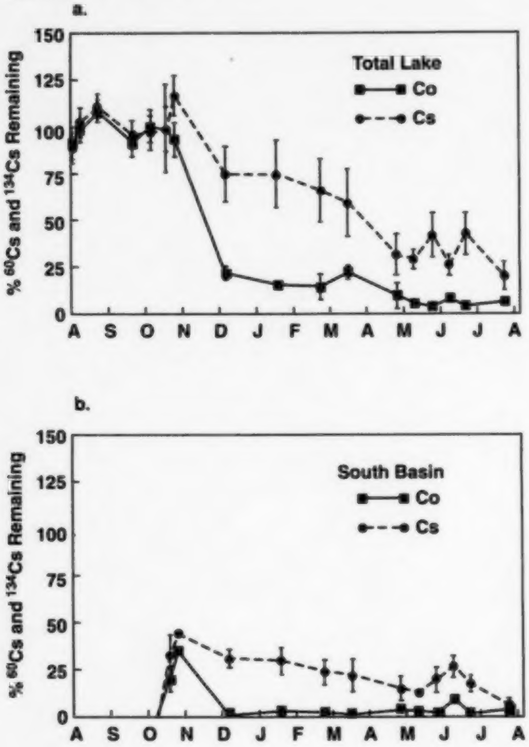

Fig. 5. Mean vertical profile (± SD) of the inventory of (*a*) ^{60}Co and (*b*) ^{134}Cs in the water column of Lake 226 shortly before (October 12, 1989) and after (January 23, 1990) autumn turnover.

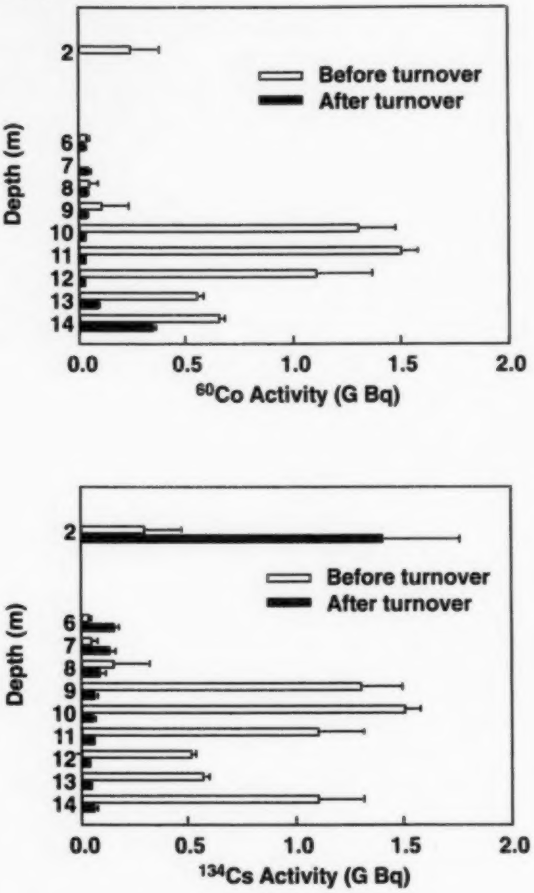

0.06 yr^{-1}. Most of the water input occurred during spring runoff. Hydrological flushing accounted for <1% of the loss of ^{60}Co and ^{134}Cs from the lake and approximately 6% of the ^{3}H; the latter is consistent with the quantity of ^{3}H remaining in the lake on day 358. Because there was little loss of the radionuclides from the lake, losses of ^{60}Co and ^{134}Cs from water were primarily to the sediment.

In general, only a small fraction (<10%) of the ^{60}Co and ^{134}Cs was particle bound (Table 3). Exceptions occurred during autumn turnover (October 25, 1989) when >86% of the ^{60}Co present was particle bound at the 2 and 9 m depths, and on initiation of spring turnover (May 1, 1990) when 83.2% of the ^{60}Co at 14 m was particle bound. The partition coefficient, K_d, for the suspended sediment had a geometric mean (GM) of 4.2×10^4 L·kg^{-1} with a geometric standard deviation (GSD) of 6.0 for ^{60}Co and a GM of 3.1×10^4 L·kg^{-1} with a GSD of 3.4 for ^{134}Cs.

Sedimentation

The quantity of sediment collected in pairs of sediment traps over the study was similar ($P > 0.05$); therefore, samples from the paired traps were pooled. Differences in sediment ^{60}Co, and ^{134}Cs collected in the sediment traps between June 1, 1989 and June 13, 1990 along the sampling transect were not significant (Table 4). The amount of sediment collected over the study period increased with depth (Table 4, Fig. 6) and was greatest at 12 m ($P < 0.05$). Differences in ^{60}Co collected in sediment traps with depth were negligible ($P > 0.05$), although slightly larger quantities were collected at the 9 m depth than at the other depths (Fig. 6). However, from October 18 to November 1 (days 291–305), significantly more ^{60}Co was collected in traps at 6 and 9 m depths than at 12 m (Table 4), with the largest amount collected on October 25 (Fig. 7). In contrast, significantly more ^{134}Cs was collected in sediment traps at 12 m depth than at 6 and 9 m, both throughout the study and during autumn turnover (Table 4).

Overall, a mean sedimentation rate of 1.19 ± 0.58 g·m^{-2}·d^{-1} and a GM deposition rate of 2.34 ± 0.59 Bq·m^{-2}·d^{-1} for ^{60}Co and 2.16 ± 0.39 Bq·m^{-2}·d^{-1} for ^{134}Cs were observed between August 2, 1989 and June 13, 1990. The quantity collected per day varied with time (Fig. 7). Quantities collected increased dramatically during autumn turnover

Table 1. Loss rate coefficients, *k* (d^{-1}), for ln-transformed data for ^{60}Co and ^{134}Cs in the water column of Lake 226 over the study period.

	^{60}Co				^{134}Cs			
Days	*k*	SE	r^2	*P*	*k*	SE	r^2	*P*
1 to 358	−0.010	0.001	0.91	0.0001	−0.004	0.001	0.82	0.0001
90 to 131	−0.036	—	—	—	−0.007	—	—	—
90 to 328	−0.010	0.002	0.79	0.0009	−0.006	0.001	0.86	0.0001
131 to 358	−0.008	0.002	0.65	0.005	−0.006	0.001	0.71	0.002
131 to 301	−0.010	0.003	0.60	0.04	−0.006	0.002	0.64	0.03

Note: —, not applicable.

Table 2. Equations for the regression of ^{60}Co and ^{134}Cs inventories in sediment core samples collected in March and June 1990 with depth (m) in Lake 226 north and south basins.

	March		June	
	Equation	r^2	Equation	r^2
L226N				
^{60}Co	6.32 depth + 14.14	0.95**	6.27 depth + 21.66	0.30
^{134}Cs	3.85 depth + 7.37	0.69**	2.11 depth + 24.82	0.15
L226S				
^{60}Co	−0.41 depth + 26.49	0.07	−0.29 depth + 27.82	0.03
^{134}Cs	−0.83 depth + 10.30	0.42*	−1.30 depth + 21.0	0.37

Note: Analysis of covariance revealed that regression equations for ^{60}Co and ^{134}Cs in March and in June are not significantly different for both basins.

* indicates a significant correlation coefficient at $P < 0.05$.

** indicates a significant correlation at $P < 0.005$.

(October 18 to November 1, 1989), when 2166 $Bq{\cdot}m^{-2}{\cdot}d^{-1}$ of ^{60}Co and 1101 $Bq{\cdot}m^{-2}{\cdot}d^{-1}$ of ^{134}Cs were deposited to the traps. It is not clear why there was a peak in ^{134}Cs activity in the traps on days 14 and 21 (Fig. 7), because ^{134}Cs activity was not detected in the water column. K_d for the sediment collected in the traps had a GM of 5.5 × 10^5 $L{\cdot}kg^{-1}$ with a GSD of 1.1 for ^{60}Co and a GM of 3.0 × 10^4 $L{\cdot}kg^{-1}$ with a GSD of 2.6 for ^{134}Cs.

Sediment cores were collected on March 22 and 23 and on June 13, 1990 to assess sediment focussing resulting from spring turnover and to measure the radionuclide inventory in sediment. In March, there was a strong correlation between the inventory of ^{60}Co ($r^2 = 0.95$, $P > 0.0001$) and ^{134}Cs ($r^2 = 0.69$, $P > 0.0028$) with depth in L226N (Table 2). In contrast, in L226S a weak negative correlation was observed between the radionuclide inventory in sediment cores and depth (Table 2). In June, following spring turnover, there was a decrease ($P > 0.05$) in the slope of the regression lines and the correlations were weaker (Table 4). This may have resulted partially from further transfer of the radionuclides from water to sediment, and partially from heterogeneity in sediment radionuclide concentrations in core samples collected from nearly the same location. On the basis of the regression equations for the inventory of radionuclides in sediment cores with depth in June (Table 2) and the area of lake sediment represented by the various depths, the total inventory of radionuclides in the sediment was 72.9 ± 50.0 and 44.6 ± 42.4% of the ^{60}Co and ^{134}Cs added to the lake, respectively.

Discussion

Loss of radionuclides from water

In our study, ^{60}Co and ^{134}Cs remained confined to the anaerobic hypolimnion under stratification, which is consistent with the findings for other nuclides (Stuiver 1967; Hooper and Imes 1971; Edmondson 1972; Schindler et al. 1980). However, there was little loss of the radionuclides from the water column to the sediment while they were confined to the hypolimnion, which is in contrast to the findings reported for P, N, and C (Schindler et al. 1980), and for S (Stuiver 1967). Autumn turnover resulted in the dispersal of the radionuclides throughout the lake and aeration of the bottom water, causing rapid loss of ^{60}Co from the water and a slower loss of ^{134}Cs (Fig. 4).

The first order loss rate coefficient of 0.036 d^{-1} for ^{60}Co between days 90 and 131 (Table 1), during and immediately following autumn turnover, is lower than the *k* value of 0.056 d^{-1} reported from the epilimnion of L226N (Hesslein 1987), but is greater than the value of 0.025 d^{-1} for ^{60}Co measured in the epilimnion of nearby Lake 224

Table 3. Percent filterable fraction of ^{60}Co and ^{134}Cs at various depths over time in Lake 226.

Depth (m)		1989						1990		
		Aug. 16	Aug. 31	Sept. 13	Sept. 28	Oct. 12	Oct. 25	May 1	June 26	July 25
2	^{134}Cs	nd	nd	nd	nd	nd	nd	nd	nd	nd
	^{60}Co	nd	nd	nd	nd	nd	86.2 (32.8)	56.9 (42.7)	nd	nd
9	^{134}Cs	nd	6.9 (4.8)	5.2 (5.2)	nd	15.4 (7.4)	nd	—	—	—
	^{60}Co	nd	nd	nd	nd	19.2 (5.4)	94.7 (5.4)	—	—	—
12	^{134}Cs	nd	2.1 (2.8)	4.3 (1.1)	5 (2.5)	4.9 (2.2)	2.5 (1.6)	—	nd	—
	^{60}Co	0.7 (0.7)	0.9 (0.5)	1 (0.5)	nd	1.6 (0.7)	1 (0.7)	—	4.8 (4.8)	—
14	^{134}Cs	nd	3.6 (1.4)	3.8 (1.1)	3.4 (2.8)	4.9 (1.1)	4 (1.4)	nd	nd	4.6 (4.1)
	^{60}Co	nd	1.4 (0.7)	1.1 (0.7)	nd	1.4 (0.7)	2.5 (0.7)	83.2 (22.5)	nd	8.1 (1.9)

Note: Values in parentheses indicate an analytical counting error of 2 standard deviations ($n = 1$); nd indicates that the filterable fraction of ^{60}Co and ^{134}Cs was not detectable (<1 Bq·L^{-1}) and in most cases constituted <1% of the radioactivity in the water column; —, data not available.

Table 4. Statistical summary of the amount of sediment, ^{60}Co, and ^{134}Cs collected in paired sediment traps along a transect and with depth in Lake 226N over the study and during autumn turnover.

(*a*) Over the study (June 1, 1989 to June 13, 1990)

	Location					Depth (m)		
Sediment	5	2	3	1	4	6	9	12
^{60}Co	5	1	3	2	4	6	12	9
^{134}Cs	5	1	3	2	4	6	9	12

(*b*) Autumn turnover (October 18 to November 1, 1989)

	Day of year			Location					Depth (m)		
Sediment	305	298	291	5	4	3	2	1	6	9	12
^{60}Co	291	305	298	5	4	1	3	2	12	6	9
^{134}Cs	305	298	291	5	3	4	2	1	6	9	12

Note: Analysis was by two-way analysis of variance in combination with Scheffé's multiple range test using (*a*) location and depth, or (*b*) location, depth, and time as independent variables and the amount of sediment, ^{60}Co, and ^{134}Cs as dependent variables. Quantities collected in sediment traps are arranged in ascending order from left to right. Locations 1 to 5 are from north to south (Fig. 1). Underlining indicates statistically homogeneous sets.

during summer (Hesslein 1987). Our k for ^{60}Co may be a slight underestimate because we were unable to collect more frequent samples under poor ice conditions during the period of rapid loss from the water column. Therefore, the k values for ^{60}Co reported from the epilimnion during summer (Hesslein 1987) and measured in our study may be more similar than the values indicate. In comparison with ^{60}Co, the loss of ^{134}Cs ($k = 0.006$ d^{-1}) from the water column following autumn turnover (days 90 to 358) was considerably slower than the loss reported from the epilimnion of L226 ($k = 0.042$) and Lake 224 ($k = 0.016$) during summer. Because the loss of ^{134}Cs from water is governed by molecular diffusion (Santschi et al. 1986; Santschi 1988), slower loss rates are expected at lower water temperatures. The slower loss of ^{60}Co and ^{134}Cs may also be partially caused by not accounting for K_d equilibrium as described by Hesslein (1987), although this probably had only a minor effect on the loss rates for ^{60}Co because of the short time frame modelled and for ^{134}Cs because k values exhibited little change when calculated over the different time periods (Table 1). An increase in the rate of removal of ^{137}Cs from water during summer was observed in Fayetteville Green Lake, New York (Brunskill et al. 1984), and at higher water temperatures in the laboratory (Bird and Evenden 1993).

The proportions of ^{60}Co and ^{134}Cs remaining in the water after 1 year were comparable for the hypolimnetic and epilimnetic additions even though in our study the loss of ^{60}Co and ^{134}Cs from the water did not begin until autumn turnover and the k for ^{134}Cs was much lower than when ^{134}Cs was added to the epilimnion. At day 358, 6% of the ^{60}Co, 19% of the ^{134}Cs, and 94% of the ^{3}H remained in the water column. This is similar to the 9% of the ^{60}Co and 10% of the ^{134}Cs in L226N, and the 6% of the ^{60}Co and the 7% of the ^{134}Cs in L226S estimated to remain in the water column at day 350 when the radionuclides were added to the epilimnion (estimated from Fig. 1 of Hesslein 1987 and morphometric data for L226). In Lake 224, 23% of the ^{60}Co and 22% of the ^{134}Cs remained in the water column 1 yr after addition to the lake (Hesslein et al. 1980). Similarities in the amount of ^{60}Co and ^{134}Cs remaining in the water column, when added to the hypolimnion versus

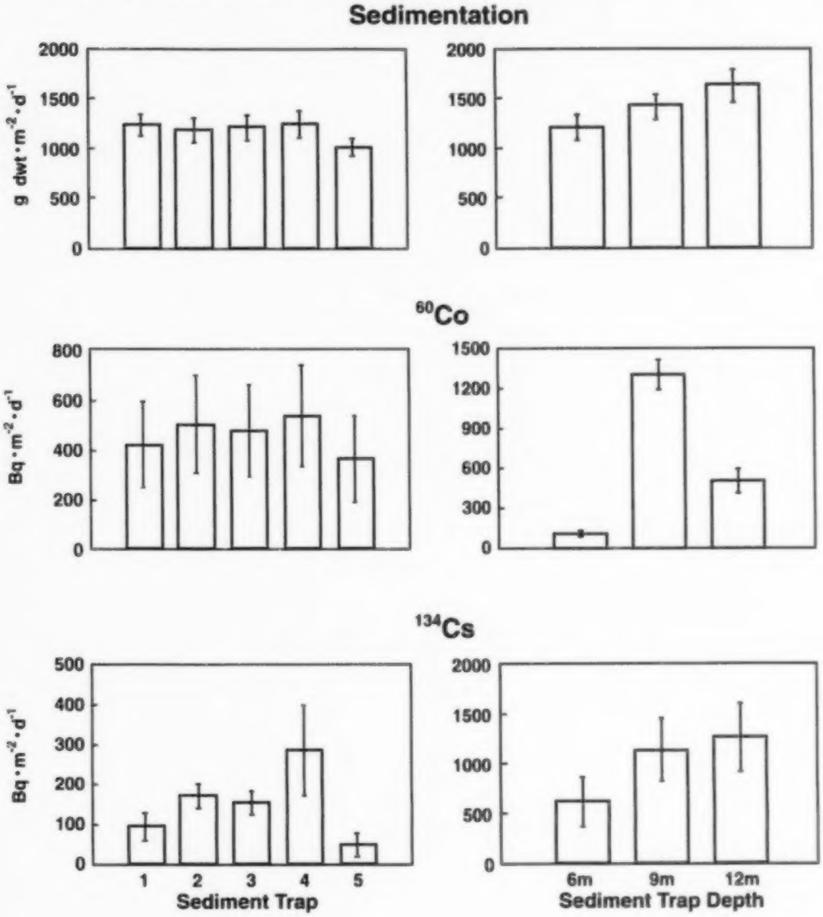

Fig. 6. The effect of sediment trap location (Fig. 1) at 6 m depth and various depths (6, 9, and 12 m) at site 3 on the mean amount (± SD) of sediment, ^{60}Co, and ^{134}Cs collected per day from June 1, 1989 to June 13, 1990.

the epilimnion, may be partially the result of dissolution or desorption of the radionuclides sedimented from the epilimnion once in the hypolimnion.

Sediments

The release of Co from sediment to water was observed here under anaerobic conditions in the summer of 1990 (Fig. 3) and previously by Hesslein (1987). Others have also reported the release of Co from sediment under anaerobic conditions (Marshall and LeRoy 1971; Wallman 1992) and at low pH (Santschi 1988). Because the hypolimnetic water had a pH of 6.3 during the summer, low pH was not a major factor governing the release of ^{60}Co from sediment in L226. In contrast to those who have reported a release of Co from sediment, Cornett and Ophel (1986), on the basis of model simulations, concluded that the release of ^{60}Co from sediments was not an important process in Perch Lake, Ontario. Whether the release of ^{60}Co from sediments in Perch Lake was masked by the continuous input and loss of ^{60}Co from the lake is not clear. Nevertheless, release of ^{60}Co from the sediments under reducing conditions seems to be an important process and will be the subject of further investigation in L226.

^{60}Co added to sediment is rapidly incorporated into the exchangeable carbonate-bound and oxide-bound fractions, with little ^{60}Co in the organic and residual fractions, which contained most of the stable cobalt (Evans et al. 1988). Therefore, ^{60}Co is available for exchange, at least initially after it is incorporated into the sediment. This applies even to softwater lakes, such as those at the ELA, where little or no carbonates are present, because of the importance of oxides in the adsorption of Co (Jenne 1968; Means et al. 1978). Sorption of Co is greatest to Mn oxides, which exhibit their greatest solubility at low pH and low Eh (Means et al. 1978). Sorption also depends on the form of Co, i.e., Co(II) and Co(III) behave similarly in sediment, whereas Co complexed to humic acid is more labile (Santschi 1988). Both ^{60}Co and ^{137}Cs activities tend to

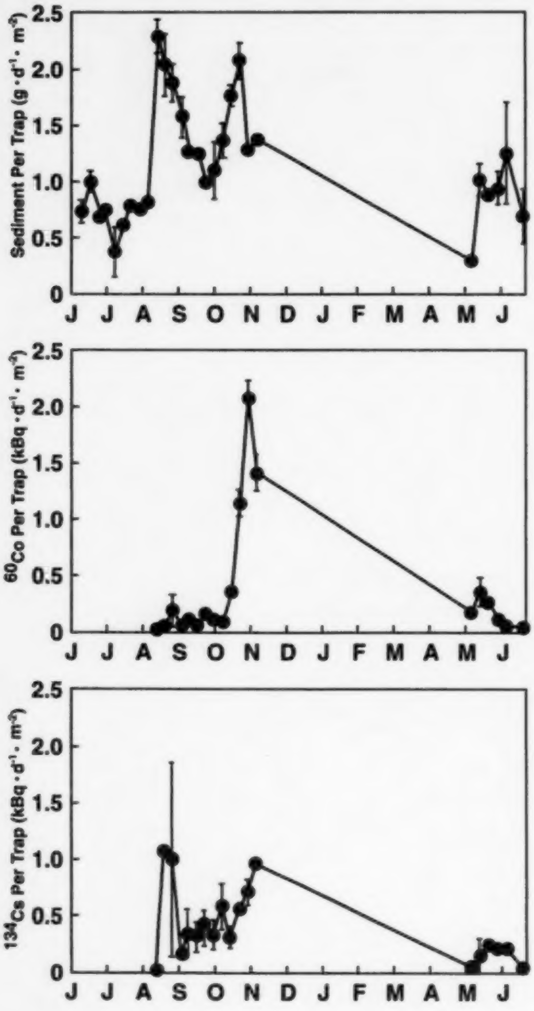

Fig. 7. Mean amounts (± SD) of sediment, ^{60}Co, and ^{134}Cs collected in sediment traps at 6 m depth over the study.

increase with decreasing particle size, suggesting a high surface-to-volume ratio effect (Means et al. 1978; Cerling et al. 1990; Voshell et al. 1985).

In the present study, a small increase in the ^{134}Cs concentration in water under anaerobic conditions suggests that ^{134}Cs was released from sediment. The release of ^{137}Cs from sediment has been reported under seasonally anaerobic conditions in Par Pond, South Carolina (Alberts et al. 1979; Evans et al. 1983), and two lakes in Britain (Davison et al. 1993). In contrast, Cerling et al. (1990) found that adsorption of ^{137}Cs was essentially irreversible and was greatest to clayey sediments. The binding of ^{137}Cs to clay involves three sites: surface sites where binding is nonselective; edge sites where ^{137}Cs is selectively fixed and effectively displaced by cations such as NH_4^+ and K^+; and interlattice sites where ^{137}Cs is not readily exchangeable with cations (Evans et al. 1983). Thus the release of ^{137}Cs is the result of ion-exchange (Evans et al. 1983) and is influenced by the seasonal buildup of NH_4^+ in sediment pore water (Alberts et al. 1979; Pardue et al. 1989).

Clay is probably not a significant component of the hypolimnetic sediment in L226, but more clay and silt may be present in the epilimnion. Low quantities of clay were reported in the sediment of four nearby lakes at the ELA (Brunskill et al. 1971; Jackson et al. 1980). The low clay content of L226 sediments may account for the slower loss rate for ^{134}Cs than ^{60}Co in L226, because ^{134}Cs is rapidly lost from water to clay sediment in the laboratory (Bird and Evenden 1993). In Lake 303, 22% of the sediment-bound ^{60}Co and 7% of the ^{134}Cs were extractable with 1 M HCl compared with 2 and 0% with 0.1 M NaOH (Jackson et al. 1980).

In the present study, about 94% of the ^{60}Co and 81% of the ^{134}Cs were retained in the sediment. Retention of Co and Cs in lakes varies considerably, with most values ranging from about 8 to 50% (Lerman and Taniguchi 1971; Carlsson 1978; Cornett and Ophel 1986; McLean and Summers 1990; Robbins et al. 1990). We estimated that 72.9 ± 50.0% of the ^{60}Co and 44.6 ± 42.3% of the ^{134}Cs were retained in the sediment, on the basis of the regressions for sediment core inventory with depth in June (Table 2). These estimates are low, but they are within measurement error of the retention of the radionuclides calculated on the basis of the inventory in the water column. Considerable spatial heterogeneity exists in sediment core samples (Hesslein et al. 1980; Hesslein 1987; Kansanen et al. 1991), which makes an acceptable mass balance difficult. On the basis of the regression models for June (Table 2), to obtain an accurate mass balance (SE ± 10%) for ^{60}Co in L226N, a small lake with a simple morphology, 21 sediment core samples would be required, whereas 36 samples would be required for ^{134}Cs. This not only demonstrates the large heterogeneity in a relatively simple system, but brings into question the frequent practice of using only a small number of samples (often one) to estimate sediment contaminant levels.

Comparison of hypolimnion and epilimnion addition

Over the short term, several minor differences occurred in the behaviour of the radionuclides when they were added to the hypolimnion rather than the epilimnion. Epilimnion inputs mix uniformly within a day or two, and losses of radionuclides from the water begin immediately; this results in ^{134}Cs being absorbed to littoral sediment, whereas more of the ^{60}Co, which binds to particles, is lost to profundal sediment. For example, in Lake 224, ^{134}Cs was 2.5 times more abundant than ^{60}Co in the littoral sediment, and ^{60}Co was 3 to 10 times more abundant in profundal sediment (Hesslein et al. 1980). In contrast, ^{60}Co, ^{134}Cs, and ^{3}H concentrations after hypolimnetic input fluctuated considerably over the first 41 d, and only small (approximately 2%) losses occurred to the sediment, presumably via diffusion. This is in contrast to the loss of about 70 to 90% of the ^{60}Co from water to sediment under anaerobic conditions in the laboratory (Mahara and Kudo 1981*a*, 1981*b*) and the substantial loss of nutrients from the anaerobic hypolimnion to sediments in Lake 302 (Schindler et al. 1980).

Transfer of a significant proportion of ^{60}Co, ^{134}Cs, and ^{3}H from L226N to L226S during autumn turnover indicates almost complete mixing of water between the two basins, despite the narrow channel separating the basins. The radionuclides were lost from the water only after mixing of the lake. Mixing of ^{60}Co and ^{134}Cs in the lake was essentially the same, and for both the epilimnion and the hypolimnion the ^{60}Co to ^{134}Cs sediment ratio ranged generally between 1.1 and 2.4.

Less than 10% of the ^{60}Co was filterable in the anaerobic hypolimnion in our study, whereas following autumn turnover approximately 80% of the ^{60}Co was filterable. The latter is in agreement with filterable fractions reported by Hesslein et al. (1980) and Hesslein (1987). Differences seen in the sorption of ^{60}Co to suspended particles between the hypolimnion and epilimnion are probably a function of redox conditions. Balistrieri et al. (1992) found that the inventories of particle-bound Co are much lower than the inventories of dissolved cobalt under anoxic conditions, whereas Parker and Hasler (1969) noted that the portion of ^{57}Co bound to suspended particles varies considerably among lakes and with seasons. Generally, <10% of the ^{134}Cs in the water column in our study was filterable, which is in agreement with the findings of Hesslein (1987) and Hesslein et al. (1980). However, we collected significantly more ^{134}Cs in sediment traps at the 12 m depth than at 6 or 9 m. It is not clear whether this is a real phenomenon or an artifact resulting from sorption of dissolved ^{134}Cs to the glass-fibre filters. There was little difference in the amount of ^{60}Co collected with depth (Table 4, Fig. 6), except during turnover. This is in contrast to the findings with epilimnetic addition. An increase in particulate material with depth is in agreement with increased organic C fluxes in sediment traps near the bottom of Lake Superior (Baker et al. 1991).

Sedimentation and sediment focussing

Our sediment trap data may underestimate actual sedimentation rates as we did not account for particle decomposition by poisoning the traps. Considerable loss of material may occur in traps placed in the epilimnion for periods greater than 2 d (Santschi et al. 1986), although Callieri et al. (1991) found no difference in catches in poisoned and nonpoisoned traps set in the hypolimnion, where our traps were located. The sedimentation rate of 0.43 $kg \cdot m^{-2} \cdot yr^{-1}$ measured in our sediment traps is higher than the 0.12 to 0.22 $kg \cdot m^{-2} \cdot yr^{-1}$ measured for L226 using the ^{210}Pb method for sediment profiles (Anderson et al. 1987; Crusius and Anderson 1990). Partition coefficients of about 10^5 $L \cdot kg^{-1}$ for ^{60}Co and 10^4 $L \cdot kg^{-1}$ for ^{134}Cs for particles collected in the sediment traps are consistent with published K_ds (Santschi et al. 1986).

Turnover of the water column may result in sediment focussing of fine particles and associated contaminants from the littoral region to deeper waters (Lehman 1975; Likens and Davis 1975). However, in the present study, little evidence of focussing was observed following spring turnover; sediment focussing of the radionuclides may become evident with time. Focussing of ^{14}C over an 11-yr period is evident in L226 and Lake 224 (M. Stephenson, Whiteshell Laboratories, Pinawa, Man., unpublished data).

Summary and conclusions

Our findings demonstrate that radionuclides added to the anaerobic hypolimnion remain in the water and confined to the hypolimnion until turnover of the water column. The mixing of the radionuclides throughout the lake with autumn turnover resulted in the loss of ^{60}Co and ^{134}Cs from the water to the sediment. Minor differences occurred in the behaviour of the radionuclides when they were added to the hypolimnion rather than the epilimnion. In particular, a greater portion of the radionuclides were deposited in profundal sediments with hypolimnetic addition. However, there is little difference in the amount of ^{60}Co and ^{134}Cs remaining in the water column after 1 yr.

We conclude that there is little difference in the fate of these radionuclides when their addition is to the anaerobic hypolimnion versus the epilimnion. Therefore, our results validate the use of literature data from epilimnetic additions to model the behaviour of radionuclides in Canadian Shield lakes for assessing Canada's nuclear fuel waste disposal concept.

Acknowledgments

The work was conducted for the Canadian Nuclear Fuel Waste Management Program, which is jointly funded by AECL Research and Ontario Hydro under the auspices of the CANDU Owners Group. We thank S. Sheppard and R. Zach, Whiteshell Laboratories (WL), Pinawa, and R. Hesslein, Department of Fisheries and Oceans, Winnipeg, for their constructive criticism of the manuscript, staff in the Analytical Science Branch, WL, for counting the samples, S. Hampshire and M. Macdonald for typing the manuscript, and staff with the Experimental Lakes Area Camp, Department of Fisheries and Oceans, for their support. M. Wilkins, M. Rochon, and J. Rosentreter provided technical assistance.

References

Alberts, J.J., L.J. Tilly, and T.J. Vigerstad. 1979. Seasonal cycling of cesium-137 in a reservoir. Science (Washington, D.C.), 203: 649–651.

Alberts, J.J., M.A. Wahlgren, K.A. Orlandini, and C.A. Durbahn. 1989. The distributions of ^{239,240}Pu, ^{238}Pu, ^{241}Am and ^{137}Cs among chemically-defined components of sediments, settling particulates and net plankton of Lake Michigan. J. Environ. Radioactivity, 9: 89–103.

Anderson, R.F., S.L. Schiff, and R.H. Hesslein. 1987. Validating the use of radiotracers as analogs of stable metal behaviour in enclosed aquatic ecosystem experiments. Can. J. Fish. Aquat. Sci. 44(Suppl. 1): 231–250.

Baker, J.E., S.J. Eisenreich, and B.J. Eadie. 1991. Sediment trap fluxes and benthic recycling of organic carbon, polycyclic aromatic hydrocarbons, and polychlorobiphenyl congeners in Lake Superior. Environ. Sci. Tech. 25: 500–509.

Balistrieri, L.S., J.W. Murray, and B. Paul. 1992. The biogeochemical cycling of trace metals in the water column of Lake Sammamish, Washington: response to seasonally anoxic conditions. Limnol. Oceanogr. 37: 529–548.

Bird, G.A., and W.G. Evenden. 1994. Effect of sediment type, temperature, and colloids on the transfer of radionuclides from water to sediment. J. Environ. Radioact. 22: 219–242.

Bird, G.A., M. Stephenson, and R.J. Cornett. 1992. The surface water submodel for the assessment of Canada's nuclear fuel waste management concept. Rep. No. AECL-10290, COG-91-193. Atomic Energy of Canada Limited, Pinawa, Man.

Bird, G.A., M. Stephenson, and R.J. Cornett. 1993*a*. The surface water model for assessing Canada's nuclear fuel waste disposal concept. Waste Manage. 13: 153–170.

Bird, G.A., W.J. Schwartz, and M. Stephenson. 1993*b*. A safe, simple method to add radionuclides to a lake. AECL Res. Tech. Rep. TR-607, COG-93-170.

Bower, P.M., C.A. Kelly, E.J. Fee, J.A. Shearer, D.R. DeClercq, and D.W. Schindler. 1987. Simultaneous measurement of primary production by whole-lake and bottle radiocarbon additions. Limnol. Oceanogr. 32: 299–312.

Brunskill, G.J., and D.W. Schindler. 1971. Geography and bathymetry of selected lake basins, Experimental Lakes Area, northwestern Ontario. J. Fish. Res. Board Can. 28: 139–155.

Brunskill, G.J., and P. Wilkinson. 1987. Annual supply of ^{238}U, ^{234}U, ^{230}Th, ^{226}Ra, ^{210}Pb, ^{210}Po, and ^{232}Th to Lake 239 (Experimental Lakes Area, Ontario) from terrestrial and atmospheric sources. Can. J. Fish. Aquat. Sci. 44(Suppl. 1): 215–230.

Brunskill, G.J., D. Povoledo, B.W. Graham, and M.P. Stainton. 1971. Chemistry of surface sediments of 16 lakes in the Experimental Lakes Area, northwestern Ontario. J. Fish. Res. Board Can. 28: 277–294.

Brunskill, G.J., S.D. Ludlam, and T.H. Peng. 1984. Fayetteville Green Lake, New York, U.S.A. VIII. Mass balance for ^{137}Cs in water, varved and nonvarved sediments. Chem. Geol. 44: 101–117.

Callieri, C., R. Bertoni, C. DeMarco, and M. Contesini. 1991. Settling flux and sinking velocity of seston in Lago di Mergozzo (northern Italy) and influence of microbial activity on the decomposition of entrapped organic material. Hydrobiologia, 213: 155–165.

Carlsson, S. 1978. A model for the movement and loss of ^{137}Cs in a small watershed. Health Phys. 34: 33–37.

Cerling, T.E., S.J. Morrison, and R.W. Sobocinski. 1990. Sediment–water interaction in a small stream: adsorption of ^{137}Cs by bed load sediments. Water Resour. Res. 26: 1165–1176.

Cleugh, T.R., and B.W. Hauser. 1971. Results of the initial survey of the Experimental Lakes Area, northwestern Ontario. J. Fish. Res. Board Can. 28: 129–137.

Cornett, R.J., and L. Chant. 1988. ^{239,240}Pu residence times in fresh waters and accumulation in Shield lake sediments. Can. J. Fish. Aquat. Sci. 45: 407–415.

Cornett, R.J., and I.L. Ophel. 1986. Transport of ^{60}Co between water and sediments in a small Shield lake. Can. J. Fish. Aquat. Sci. 43: 877–884.

Crusius, J., and R.F. Anderson. 1991. Core compression and surficial loss of lake sediments of high porosity caused by gravity coring. Limnol. Oceanogr. 36: 1021–1031.

Davison, W., J. Hilton, J. Hamilton-Taylor, M. Kelly, F. Livens, E. Riggs, T.R. Carrick, and D.L. Singleton. 1993. The transport of Chernobyl-derived radiocaesium through two freshwater lakes in Cumbria, U.K. J. Environ. Radioactivity, 19: 125–153.

Diamond, M.L., D. Mackay, R.J. Cornett, and L.A. Chant. 1990. A model of the exchange of inorganic chemicals between water and sediments. Environ. Sci. Technol. 24: 713–722.

Edmondson, W.T. 1972. Nutrients and phytoplankton in Lake Washington. Spec. Symp. Am. Soc. Limnol. Oceanogr. 1: 172–193.

Evans, D.W., J.J. Alberts, and R.A. Clark, III. 1983. Reversible ion-exchange fixation of cesium-137 leading to mobilization from reservoir sediments. Geochim. Cosmochim. Acta, 47: 1041–1049.

Evans, R.D., D. Andrews, and R.J. Cornett. 1988. Chemical fractionation and bioavailability of cobalt-60 to benthic deposit-feeders. Can. J. Fish. Aquat. Sci. 45: 228–236.

Findlay, D.L., and S.E.M. Kasian. 1987. Phytoplankton community responses to nutrient addition in Lake 226, Experimental Lakes Area, northwestern Ontario. Can. J. Fish. Aquat. Sci. 44(Suppl. 1): 35–46.

Garder, K., and O. Skulberg. 1964. Sorption phenomena of radionuclides to clay particles in river water. Int. J. Air Water Pollut. 8: 229–241.

Guthrie, J.E., and W.E. Grummitt. 1963. Manual of low activity environmental analyses. Procedures and methods for preparation and radiochemical analyses of environmental samples at AECL. Rep. No. AECL-1745. Atomic Energy of Canada Limited, Pinawa, Man.

Hancox, W.T., and K. Nuttall. 1991. The Canadian approach to safe, permanent disposal of nuclear fuel waste. Nucl. Eng. Design, 129: 109–117.

Heit, M., and K.M. Miller. 1987. Cesium-137 sediment depth profiles and inventories in Adirondack Lake sediments. Biogeochemistry, 3: 243–265.

Hesslein, R.H. 1987. Whole-lake metal radiotracer movement in fertilized lake basins. Can. J. Fish. Aquat. Sci. 44(Suppl. 1): 74–82.

Hesslein, R.H., W.S. Broecker, and D.W. Schindler. 1980. Fates of metal radiotracers added to a whole lake: sediment–water interactions. Can. J. Fish. Aquat. Sci. 37: 378–386.

Hooper, F.F., and D.G. Imes. 1971. Physical and biological dispersion of the hypolimnetic phosphorus of a bog lake system. *In* Proceedings of the Third National Symposium of Radioecology, Oak Ridge, Tenn., May 10–12, 1971. U.S. Atomic Energy Commission Rep. No. CONF-710501. pp. 401–409.

Jackson, T.A., G. Kipphut, R.H. Hesslein, and D.W. Schindler. 1980. Experimental study of trace metal chemistry in softwater lakes in different pH levels. Can. J. Fish Aquat. Sci. 37: 387–402.

Jenne, E.A. 1968. Controls on Mn, Fe, Co, Ni, Cu and Zn concentrations in soils and water: the significant role of hydrous Mn and Fe oxides. *In* Trace inorganics in water. Advances in chemistry series 73. *Edited by* R.F. Gould. American Chemical Society, Washington, D.C. pp. 337–387.

Kansanen, P.H., T. Jaakkola, S. Kulmala, and R. Suutarinen. 1991. Sedimentation and distribution of gamma-emitting radionuclides in bottom sediments of southern Lake Paijanne, Finland, after the Chernobyl accident. Hydrobiologia, 222: 121–140.

Lehman, J.T. 1975. Reconstructing the rate of accumulation of lake sediment: the effect of sediment focussing. Quat. Res. 5: 541–550.

Lerman, A., and H. Taniguchi. 1971. Strontium-90 and cesium-137 in water and deep sediments of the Great Lakes. *In* Proceedings of the Third National Symposium on Radioecology, Oak Ridge, Tenn., May 10–12, 1971. *Edited by* D.J. Nelson. U.S. Atomic Energy Commission Rep. No. CONF-710501. pp. 410–464.

Likens, G.E., and M.B. Davis. 1975. Post-glacial history of Mirror Lake and its watershed in New Hampshire, U.S.A.: an initial report. Verh. Int. Ver. Theor. Angew. Limnol. 19: 982–993.

Mahara, Y., and A. Kudo. 1981*a*. Interaction and mobility of cobalt-60 between water and sediments in marine environments. Possible effects by acid rain. J. Water Res. 15: 413–419.

Mahara, Y., and A. Kudo. 1981*b*. Fixation and mobilization of ^{60}Co on sediments in coastal environments. Health Phys. 41: 645–655.

Marshall, J.S., and J.H. LeRoy. 1971. Iron, manganese, cobalt, and zinc cycles in a South Carolina Reservoir. *In* Proceedings of the Third National Symposium on Radioecology, Oak Ridge, Tenn., May 10–12, 1971. *Edited by* D.J. Nelson. U.S. Atomic Energy Commission Rep. No. CONF-710501. pp. 465–471.

McLean, R.I., and J.K. Summers. 1990. Evaluation of transport and storage of ^{60}Co, ^{134}Cs, ^{137}Cs and ^{65}Zn by river sediments in the lower Susquehanna River. Environ. Pollut. 63: 137–153.

Means, J.L., D.A. Crear, M.P. Borcsik, and J.O. Duguid. 1978. Adsorption of Co and selected actinides by Mn and Fe oxides in soils and sediments. Geochim. Cosmochim. Acta, 42: 1763–1773.

Pardue, J.H., R.D. DeLaune, W.H. Patrick, Jr., and J.H. Whitcomb. 1989. Effect of redox potential on fixation of ^{137}Cs in lake sediment. Health Phys. 57: 781–789.

Parker, M., and A.D. Hasler. 1969. Studies on the distribution of cobalt in lakes. Limnol. Oceanogr. 14: 229–241.

Robbins, J.A., A. Mudroch, and B.G. Oliver. 1990. Transport and storage of ^{137}Cs and ^{210}Pb in sediments of Lake St. Clair. Can. J. Fish. Aquat. Sci. 47: 572–587.

Santschi, P.H. 1988. Factors controlling the biogeochemical cycles of trace elements in fresh and coastal marine waters as revealed by artificial radioisotopes. Limnol. Oceanogr. 33: 848–866.

Santschi, P.H., U.P. Nyffeler, R.F. Anderson, S.L. Schiff, P. O'Hara, and R.H. Hesslein. 1986. Response of radioactive trace metals to acid–base titrations in controlled experimental ecosystems: evaluation of transport parameters for application to whole-lake radiotracer experiments. Can. J. Fish. Aquat. Sci. 43: 60–77.

Santschi, P.H., S. Bollhalder, S. Zingg, A. Luck, and K. Farrenkothen. 1990. The self-cleaning capacity of surface waters after radioactive fallout. Evidence from European waters after Chernobyl, 1986–1988. Environ. Sci. Technol. 24: 519–527.

SAS Institute Inc. 1985. SAS user's guide: statistics version 5 ed. SAS Institute Inc., Cary, NC.

Schindler, D.W., T. Ruszczynski, and E.J. Fee. 1980. Hypolimnion injection of nutrient effluents as a method for reducing eutrophication. Can. J. Fish. Aquat. Sci. 37: 320–327.

Shearer, J.A., E.J. Fee, E.R. DeBruyn, and D.R. DeClercq. 1987. Phytoplankton productivity changes in a small double-basin lake in response to termination of experimental fertilization. Can. J. Fish. Aquat. Sci. 44(Suppl. 1): 47–54.

Stuiver, M. 1967. The sulfur cycle in lake waters during thermal stratification. Geochim. Cosmochim. Acta, 31: 2151–2167.

Tracy, B.L., and F.A. Prantl. 1983. 25 years of fission product input to Lakes Superior and Huron. Water Air Soil Pollut. 19: 15–27.

Voshell, J.R., Jr., J.S. Eldridge, and T.W. Oakes. 1985. Transfer of ^{137}Cs and ^{60}Co in a waste retention pond with emphasis on aquatic insects. Health Phys. 49: 777–789.

Wallman, K. 1992. Solubility of cadmium and cobalt in a post-oxic or sub-oxic sediment suspension. Hydrobiologia, 235–236: 611–622.

Deformities in the menta of chironomid larvae from the Experimental Lakes Area, Ontario[1]

G.A. Bird, M.J. Rosentreter, and W.J. Schwartz

Abstract: *Chironomus* spp. larvae in Experimental Lakes Area Lake 382, which received experimental additions of cadmium, were exposed to cadmium concentrations up to approximately 200 $\mathrm{ng \cdot L^{-1}}$ in water and to about 4 $\mathrm{\mu g \cdot g^{-1}}$ in dry sediment, resulting in body burdens of about 3.5 $\mathrm{\mu g \cdot (g\ dry\ weight)^{-1}}$. Mentum deformities in *Chironomus* spp. larvae in Lake 382 and five reference lakes ranged from 0 to 16%, which was within the range reported for other contaminated lakes (2 to 83%). The frequency of deformities in Lake 382 was not detectably different either in larvae collected between 1989 and 1992, or in those from reference lakes. Incidence of deformities was higher in four of the five reference lakes than in Lake 382. The constancy of the deformities (confined mainly to the median tooth, commonly with cleft or forked median teeth) is consistent with an inherited genetic effect; therefore, we consider the deformities to be natural abnormalities. We conclude that the low cadmium levels added to Lake 382 did not induce mentum deformities and that background levels of deformities are high (up to 16%) in Experimental Lakes Area lakes. The common occurrence of natural abnormalities must be considered when using chironomid mouthpart deformities as an index of environmental degradation.

Résumé : Dans le lac 382 faisant partie de la région des lacs expérimentaux, où l'on ajouté du cadmium à des fins expérimentales, on a exposé des larves de *Chironomus* sp. à des concentrations de cadmium atteignant environ 200 $\mathrm{ng \cdot L^{-1}}$ dans l'eau et d'environ 4 $\mathrm{\mu g \cdot g^{-1}}$ dans les sédiments secs; la charge corporelle résultante était d'environ 3,5 $\mathrm{\mu g \cdot (g\ de\ poids\ sec)^{-1}}$. Les malformations du mentum observées chez les larves de *Chironomus* sp. du lac 382 ainsi que de cinq lacs de référence variaient de 0 à 16%, ce qui entre dans la fourchette observée pour d'autres lacs contaminés (2 à 83%). La fréquence des malformations observées chez les chironomidés du lac 382 n'était pas non plus sensiblement différente de celle enregistrée chez les larves prélevées entre 1989 et 1992 dans les lacs de référence. Dans quatre des cinq lacs de référence, l'incidence des malformations était supérieure à celle des spécimens du lac 382. La constance des malformations (limitée surtout à la dent médiane, qui était souvent fourchue ou bifide) correspond à un effet génétique congénital; par conséquent, nous considérons ces malformations comme étant naturelles. Notre conclusion est que les faibles quantités de cadmium ajoutées au lac 382 n'ont pas donné lieu à des malformations du mentum, et que les niveaux naturels de malformations sont élevés (jusqu'à 16%) dans les lacs de la région des lacs expérimentaux. On doit tenir compte de la forte incidence des malformations naturelles lorsque l'on utilise les malformations du rostre chez les chironomidés comme indicateur de la dégradation de l'environnement.

[Traduit par la Rédaction]

Introduction

In freshwater ecosystems, chironomid larvae are considered to be ideal bioassay organisms because (*i*) they spend most of their larval stages in superficial sediments where they are exposed to toxicants in both water and sediments, (*ii*) they have a fairly restricted home range (Davies 1976), and (*iii*) they occur in a variety of habitats. Chironomid community structure is used as an index of environmental quality (Sæther 1979). Chironomid mouthpart deformities, primarily deformities of the hypostoma or mentum, a broad, sclerotized tooth structure, have been observed in polluted waters. However, the frequency of deformities reported from polluted areas varies widely: about 80% of chironomid larvae had deformed menta in two studies (Hare and Carter 1976; Warwick et al. 1987), but deformation frequency generally ranges from 1 to approximately 30% (Dickman et al. 1992; Warwick and Tisdale 1988; Warwick 1990; Wiederholm 1984) and is often <5% (Cushman 1984; Tennessen and Gottfried 1983; Warwick 1980*a*, 1980*b*).

Received May 31, 1993. Accepted April 28, 1995.
J11957

G.A. Bird, M.J. Rosentreter, and W.J. Schwartz. Atomic Energy of Canada Limited, Whiteshell Laboratories, Pinawa, MB R0E 1L0, Canada.

[1] This paper is one of a series done in honour of the 25th anniversary of the Experimental Lakes Area.

Can. J. Fish. Aquat. Sci. **52**: 2290–2295 (1995). Printed in Canada / Imprimé au Canada

Table 1. Morphometric and chemical data for the study lakes.

	Lake					
	382	224	226N	260	468	304
Area (ha)	36.9	26	8.3	32.4	295	3.62
Maximum depth (m)	13.1	27	14.7	14.6	29	6.7
Mean depth (m)	5.8	12	5.7	—	—	3.2
pH	7.01	7.04	6.79	7.34	6.96	6.49
Alkalinity (μequiv.$\cdot L^{-1}$)	99	76	79	156	125	60
DOC (μM$\cdot L^{-1}$)	870	320	770	530	470	910
DIC (μM$\cdot L^{-1}$)	100	100	90	190	120	60
NO_3-N (μg$\cdot L^{-1}$)	<1	1	<1	<1	—	<1
NO_2-N (μg$\cdot L^{-1}$)	<1	<1	<1	<1	—	1
NH_4-N (μg$\cdot L^{-1}$)	11	5	4	4	—	12
TDN (μg$\cdot L^{-1}$)	240	150	240	230	—	350
TDP (μg$\cdot L^{-1}$)	2	1	2	1	—	3
Ca (mg$\cdot L^{-1}$)	2.31	1.83	1.65	2.58	—	1.6
Fe (mg$\cdot L^{-1}$)	<0.01	0.02	0.04	<0.01	—	0.04
SO_4 (mg$\cdot L^{-1}$)	2.69	3.44	2.23	2.4	—	2.71

Note: —, no data. DOC, dissolved organic carbon; DIC, dissolved inorganic carbon; TDN, total dissolved nitrogen; TDP, total dissolved phosphorus.

The frequency of deformities at uncontaminated sites is generally <1% (Warwick 1980*b*; Weiderholm 1984; Hare and Carter 1976).

In most studies, it has not been possible to designate with certainty specific causative agents of the deformities, but agricultural and industrial pollutants have been implicated. More information is required on the incidence of chironomid mouthpart deformities in relation to various types of pollution, especially because there is continued interest in the use of chironomid deformities as an index of environmental degradation (Warwick 1991; Dickman et al. 1992; Janssens de Bisthoven et al. 1992). Our study differs from others in that we investigated the incidence of deformed *Chironomus* spp. larvae in an oligotrophic Canadian Shield lake to which low concentrations of a single pollutant, cadmium (Cd), were experimentally added. We also examined several nearby reference lakes. Only *Chironomus* larvae were examined because genera may vary in their susceptibility to deformities, and because deformities are more common in *Chironomus* than in other genera (Warwick 1988).

Stable Cd, and ^{109}Cd, which served as a tracer, were experimentally added to Experimental Lakes Area (ELA) Lake 382 in northwestern Ontario from 1987 to 1992. The objective of the experiment was to determine whether biological effects could be measured in biota of a softwater Canadian Shield lake at, or below, the Canadian Water Quality Guideline for Cd of 200 ng$\cdot L^{-1}$ in water (Malley et al. 1989). Cd accumulates in sediment (Evans et al. 1983; Stephenson and Mackie 1988), is toxic at low concentrations, and is bioaccumulated by a wide variety of aquatic organisms (Malley et al. 1989), including chironomids (Heinis et al. 1990). Chironomid deformities have been reported from areas contaminated with Cd (Wiederholm 1984; Warwick 1991), although it has not been experimentally demonstrated that Cd induces deformities. On the basis of laboratory studies, fourth-instar chironomid larvae are not very sensitive to Cd (Heinis et al. 1990; Pascoe et al. 1990): the 96-h LC_{50} for *Chironomus riparius* is between 50 and 100 mg Cd$\cdot L^{-1}$ (Pascoe et al. 1990), a concentration considerably higher than the levels reached in Lake 382. However, early instar larvae are sensitive to Cd; for example, poor survival was reported for first-instar larvae exposed to 10 μg Cd$\cdot L^{-1}$ (Timmermans et al. 1992). The Cd addition experiment gave us the opportunity to assess whether low concentrations of Cd-induced deformities in chironomid larvae over several generations in a softwater Canadian Shield lake, and to determine the background frequency of deformities in ELA lakes.

Material and methods

Study lakes

The ELA has been described by Armstrong and Schindler (1971), Brunskill and Schindler (1971), and Cleugh and Hauser (1971). Lake 382 is a 36.9-ha oligotrophic lake with a mean depth of 5.8 m, a maximum depth of 13.1 m, a volume of 21.3×10^5 m^3, a hardness of 7.0 mg$\cdot L^{-1}$ as $CaCO_3$, and a pH of 6.8 to 7.3 (Malley et al. 1989) (Table 1). Further information on Lake 382 can be found in Malley et al. (1989) and Malley and Chang (1991).

Reference lakes were chosen on the basis of their proximity and similarity to Lake 382. This meant selecting lakes that contained *Chironomus* larvae and for which lake morphology and water chemistry data were available. Because it was difficult to find nearby limnologically similar lakes that contained *Chironomus* larvae, three lakes that had been previously manipulated were included in our set of reference lakes. Thus, the reference lakes sampled (Table 1) had either never been experimentally manipulated or had recovered from past manipulation. Lake 468 (Roddy Lake) and Lake 260 are oligotrophic lake trout lakes that have never been the subject of experimental manipulation. Lake 304 was the focus of a nutrient enrichment

Table 2. Incidence of deformities in *Chironomus* spp. larvae following the addition of cadmium to Lake 382 and in five nearby reference lakes.

Lake	Date	Total number	Number deformed	% deformed ($\bar{x}$ ± SD)
382	89/09/28	27	3	11.1±6.0
	90/07/26	89	12	13.5±3.6
	91/05/02	231	13	5.6±1.5
	91/08/06	189	11	5.8±1.7
	92/09/23	136	7	5.1±1.9
226	90/06/27	55	8	14.5±4.7
260	91/08/07	149	15	10.1±2.5
468	92/09/23	74	12	16.2±4.3
304	92/09/24	115	0	0.0±0.0
224	92/09/23	97	15	15.5±3.7

study from 1970 to 1976 (Cruikshank 1984; Schindler 1988); the addition of NH_4^+ during this period resulted in acidification (Beamish et al. 1976). Lake 304 currently has a sparse fish population, and its bottom waters are anaerobic under thermally stratified conditions. Lake 224 was the subject of a whole-lake radionuclide addition experiment in which 7.4–18.5 GBq each of ^{59}Fe, ^{60}Co, ^{75}Se, ^{134}Cs, and ^{203}Hg were added in 1976 (Hesslein et al. 1980). Initial radionuclide levels in Lake 224 were well below drinking water quality guidelines and, as a result of radioactive decay, the levels of radioactivity remaining in the lake are extremely low. Lake 226 is a small dimictic headwater lake that is naturally divided into two basins by a shallow channel (Findlay and Kasian 1987). Lake 226 differs from the other lakes in that it is mesotrophic and it was the site of several whole-lake contaminant studies. The northeast basin (Lake 226N) was fertilized from 1973 to 1980; it received annual inputs of carbon ($3.67\ g\cdot m^{-2}$), nitrogen ($1.92\ g\cdot m^{-2}$), and phosphorous ($0.34\ g\cdot m^{-2}$) (Findlay and Kasian 1987). After nutrient inputs stopped, the primary production of Lake 226 quickly returned to prefertilization levels (Shearer et al. 1987). Radionuclides were also added to Lake 226. Hesslein (1987) added between 4.5 and 13 GBq of ^{59}Fe, ^{60}Co, ^{65}Zn, ^{75}Se, ^{85}Sr, ^{134}Cs, and ^{203}Hg to the epilimnion of both basins in 1977, and Bower et al. (1987) added 46 GBq of ^{14}C to the epilimnion of Lake 226N and 11.5 GBq of ^{14}C to the epilimnion of Lake 226S in 1978. In addition, Bird et al. (1994) added 4.6 GBq each of ^{60}Co and ^{134}Cs and 370 GBq of ^{3}H to Lake 226N in 1989.

Cadmium and ^{109}Cd additions to Lake 382

Starting in June 1987, the epilimnion of Lake 382 was annually loaded with Cd as $CdCl_2$, and ^{109}Cd (164 ng $Cd\cdot Bq\ ^{109}Cd^{-1}$) during the ice-free season. Target concentrations were 100, 100, 120, 160, 200, and 200 $ng\ Cd\cdot L^{-1}$ in each year from 1987 to 1992, respectively. Observed addition-season mean concentrations were 77, 54, 92, 132, 179, and 177 $ng\cdot L^{-1}$, respectively. The ^{109}Cd was added to facilitate tracing the fate and accumulation of Cd in the lake. Commencing in 1987, 975, 643, 778, 1437, 2143, and 1117 g of Cd were added to the lake in each of the 6 yr, respectively. Most of the Cd was transferred to the sediments (M. Stephenson, Whiteshell Laboratories, Pinawa, Man., unpublished data; R. Hesslein, Department of Fisheries and Oceans, Winnipeg, Man., personal communication).

Methods

On each sampling occasion (see dates in Table 2), a stainless steel Ekman grab (15.2 cm wide × 15.2 cm long × 22.9 cm high) was used to collect sediment samples at a depth of 7 to 9 m in the northeast bay of Lake 382 between transects 6 and 8 of Malley et al. (1989). In the other lakes, samples were collected from depths ranging from 3 m in Lake 304 to 20 m in Lake 224, depending on the nature of the sediments and the abundance of chironomid larvae. In all cases, the sediment sampled was a soft flocculent organic material. Each site was sampled for about 3 h, or until at least 200 red chironomid larvae were collected. This involved taking between 25 and 40 Ekman samples per site or sampling occasion. The sediments were passed through an 800-μm sieve in the field, and the larvae were removed, pooled into a single sample for each site, and preserved in 70% ethanol.

To detect gamma emissions for ^{109}Cd (22.1 keV) (1 eV = 0.160 217 733 aJ), chironomid larvae from Lake 382 were packed in standard 5-mL vials and analysed using a high-purity germanium, intrinsic, p-type well detector linked to a Nuclear Data 6700 series MCA–computer.

Mouthpart deformities were examined by clearing head capsules of chironomid larvae in 8% KOH, placing them in glacial acetic acid for 15 min to neutralize the KOH, and then rinsing twice (15-min each) in 70% ethanol. Head capsules were mounted in Hoyers medium ventral side up on microscope slides with the aid of a dissecting microscope. Gentle pressure was applied to the cover slip to extrude the mandibles and to provide a clear view of the hypostomal teeth.

Head capsules were examined under a compound microscope, generally at 400× magnification. Only larvae belonging to the genus *Chironomus* (Oliver and Roussel 1983) were examined for deformities. Emphasis was placed on examining the hypostomal teeth for deformities, although the mandibles, premandibles, and antennae were also examined. Antennae were examined only for gross deformities, such as missing or extra segments, or major differences in the size of segments between both antennae. The hypostoma was classified as deformed if it had extra or missing teeth (including gaps), or if it was asymmetric or abnormal in shape. Minor asymmetry (i.e., worn teeth or slight development of a cleft median tooth) was considered to be normal variation. The number of deformed *Chironomus* spp. larvae observed per site or sampling occasion was expressed as a percentage, and a standard deviation of the number was calculated.

Results and discussion

Types of deformities

Deformities were typically confined to the median tooth (Figs. 1B–G); an indentation or cleft (Fig. 1C) was the most common deformity observed. More extreme development of this cleft resulted in the formation of two lobes or teeth

Fig. 1. Normal mentum (A) and representative deformities (B–I) observed in *Chironomus* spp. larvae collected from the Experimental Lakes Area lakes. MT, median teeth; ILT, inner lateral teeth.

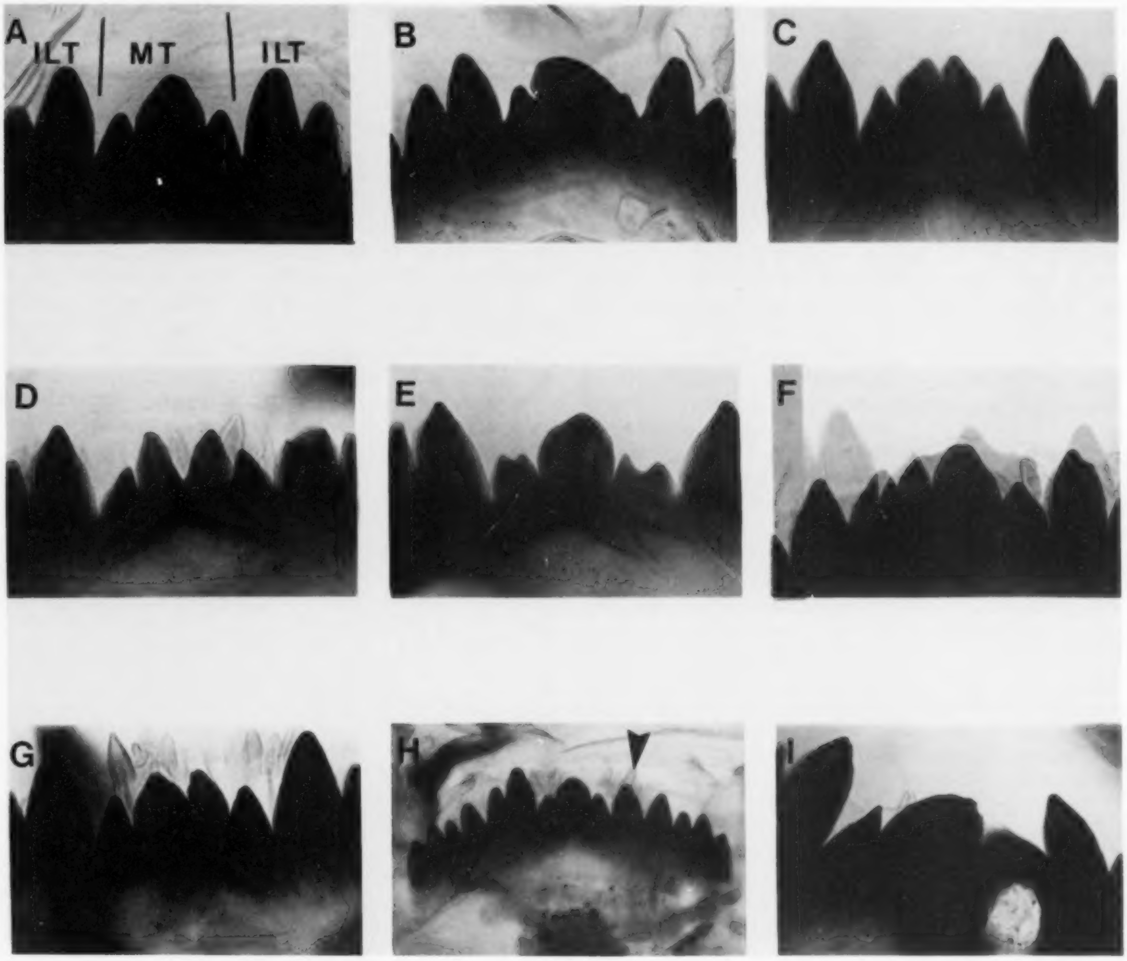

(Fig. 1D), or a forked median tooth. Forking of the outer median teeth (Fig. 1E) was rare. An occasional specimen had median teeth that were fused and lopsided (Fig. 1B) or the specimen was missing one of the paired inner lateral teeth (Fig. 1H). Other deformities such as gaps between teeth, missing teeth, or extra teeth, which were not created by forking of the median tooth, were rare. One specimen from Lake 382 had a hole in its mentum (Fig. 1I). No deformed mandibles were observed, and only a single specimen (from Lake 224) had a deformed antenna (similar to that illustrated in Fig. 12E of Warwick 1985).

Incidence of deformities

In total, 627 *Chironomus* spp. larvae from Lake 382 and 490 larvae from the five reference lakes were examined for deformities (Table 2). *Chironomus* spp. collected from the ELA include *Chironomus* (s.s.) *anthracinus*, *C.* cf. *atritibia*, *C.* (s.s.) cf. *decorus*, *C. lacunarius*, *C. pilcornis*, *C.* cf. *sororius*, and *C.* cf. *venustus*; *C.* (s.s.) cf. *decorus* is present in Lake 382 (I. Davies, Department of Fisheries and Oceans, Winnipeg, Man., personal communication). The mean frequency of deformities in the five reference lakes ranged from 0 to 16.2% (Table 2). The widespread occurrence of deformed larvae in these remote lakes is surprising because concentrations of metals and nutrients in ELA lakes are naturally extremely low (Armstrong and Schindler 1971; Beamish et al. 1976). Unmanipulated, oligotrophic, lake trout lakes had the highest frequencies of deformities (16.2% in Lake 468, and 10.2% in Lake 260), whereas no deformities were recorded from Lake 304, a lake suffering periodic anoxia. The frequency of deformities was essentially similar among all the lakes, except perhaps Lake 304 (Table 2).

The frequency of deformities did not increase over time with annual additions of Cd to Lake 382 (Table 2). Therefore, it appears that Cd was not responsible for inducing the deformities observed in *Chironomus* spp. larvae in Lake 382. Larvae were exposed to concentrations of Cd up to approximately 200 $ng \cdot L^{-1}$ in water, and to approximately 4 $\mu g \cdot g^{-1}$ of dry sediment (M. Stephenson, Whiteshell Laboratories, Pinawa, Man., unpublished data), which resulted in Cd body burdens of approximately 3.5 $\mu g \cdot (g\ dry\ weight)^{-1}$. These same low concentrations of Cd had measurable effects on metallothionein levels in mussels, on the histology of thyroid cells in fish, and on porcelain disease in crayfish, but had no effect on reducing population numbers of phytoplankton, zooplankton, or *Hyalella azteca* (Malley and Chang 1991; D. Malley, Department of Fisheries and Oceans, Freshwater Institute, Winnipeg, Man., personal communication).

The only source of anthropogenic contaminants to these lakes is from atmospheric deposition; precipitation chemistry at the ELA is influenced by soil-derived substances to the west, and by long-range transport of atmospheric emissions from the industrialized lower Great Lakes region to the southeast (Linsey et al. 1987). However, atmospheric deposition of contaminants is expected to be low; for example, the atmospheric deposition of polychlorinated biphenyls (PCBs) and atrazine is comparable to that for the upper Great Lakes, which are considered to be pristine (D. Muir, Department of Fisheries and Oceans, Winnipeg, Man., personal communication). Levels of radiation in lakes 224 and 226 were well below the lowest doses that produce effects in aquatic biota (Rose 1992; Bird et al. 1993).

The range in frequency of deformities in *Chironomus* spp. larvae from the ELA (Table 2) is generally higher than that expected for background levels, although frequencies of 9% (control site, Welland River, Ontario; Dickman et al. 1992) and 19% (Maskawa Lake, Saskatchewan; Warwick 1988) have been reported for uncontaminated sites. The frequency of deformities at uncontaminated sites is usually <1%. For example, 0.09% of the chironomid larvae collected from the Bay of Quinte, Lake Ontario, prior to European settlement (Warwick 1980*b*), 0.8% of the subfossil *Chironomus* larvae from Ekoln Bay, Sweden (Wiederholm 1984), and 1.4% of the chironomid larvae from an uncontaminated site in Georgian Bay, Lake Huron (Hare and Carter 1976), exhibited deformities. However, 3–4% of deformities in *Chironomus* larvae have also been reported from other uncontaminated sites in Lake Huron and Lake Superior (Dermott 1991; Dickman et al. 1992).

The deformed median teeth observed in the ELA are identical to many deformities observed in *Chironomus* larvae from Pasqua Lake (Fig. 3Cl of Warwick 1980*a*) and Tobin Lake (Fig. 3 of Warwick and Tisdale 1988), both in Saskatchewan; from the Dyle River, Belgium (Fig. 1B of Janssens de Bisthoven et al. 1992); and from the St. Lawrence River (Fig. 4D of Warwick 1990); and produced in the laboratory in response to dichlorodiphenyl dichloroethylene (Fig. 14.11 of Warwick 1988). Similar deformities have also been reported in studies by Dickman et al. (Fig. 2E, 1992) and Cushman (Plate 1B, 1984) in response to coal tar and coal-derived oil pollution.

The restriction of mentum deformities to the median tooth observed in our study is consistent with an inherited genetic effect, because somatic damage is usually not symmetrical (Hart et al. 1987). Similar deformities have been observed in laboratory cultures of *Chironomus tentans* (Bird 1989; Bird et al. 1993). They were attributed to inbreeding of the stock culture, which presumably resulted in an increased expression of recessive characteristics (Bird 1989; Bird et al. 1993). The suggestion that the deformities observed in field-collected *Chironomus* spp. larvae from the ELA are natural genetic abnormalities differs from those of other researchers who claim that such deformities are a somatic response to environmental contaminants (Janssens de Bisthoven et al. 1992; Dickman et al. 1992; Dermott 1991).

In summary, the addition of low levels of Cd to Lake 382 did not induce detectable increases in mentum deformities in *Chironomus* spp. larvae. Mean background levels of deformities in larvae from the six ELA lakes ranged from 0 to 16.2%. The common occurrence of natural abnormalities in *Chironomus* spp. larvae collected from the ELA raises the question: what constitutes a mouthpart deformity and what is normal variation? Greater concern should be shown for natural abnormalities when chironomid mouthpart deformities are used as an index of environmental degradation.

Acknowledgments

The study was carried out under the Canadian Nuclear Fuel Waste Management Program, which is jointly funded by AECL and Ontario Hydro under the auspices of the CANDU Owners Group. We thank M. Stephenson, C. Macdonald, and R. Zach, Whiteshell Laboratories, for their constructive criticisms of the manuscript, M.F. Motycka for his technical assistance, S. Hampshire and M. Macdonald for typing the manuscript, and staff at the Experimental Lakes Area camp, Department of Fisheries and Oceans, for their support. We also thank B. Bilyj, BIOTAX Incorporated, Weston, Ontario, for verifying our identifications.

References

Armstrong, F.A.J., and D.W. Schindler. 1971. Preliminary chemical characterization of waters in the Experimental Lakes Area, northwestern Ontario. J. Fish. Res. Board Can. 28: 171–187.

Beamish, R.J., L.M. Blouw, and G.A. McFarlane. 1976. A fish and chemical study of 109 lakes in the Experimental Lakes Area (ELA), northwestern Ontario, with appended reports on lake whitefish aging errors and the northwestern Ontario baitfish industry. Can. Fish. Mar. Serv. Tech. Rep. No. 607.

Bird, G.A. 1989. Study on the utility of chironomid deformities in the assessment of water quality. NWRI Contribution No. 89-62. Report to the Rivers Research Branch, National Water Research Institute, Burlington, Ont.

Bird, G.A., W.J. Schwartz, and D. Hoffman. 1993. The effect of ^{210}Pb and stable lead on the induction of mouthpart deformities in chironomid larvae. Res. Proj. No. 3.150.2. Rep. No. AECB INFO-0573, Atomic Energy Control Board, Ottawa, Ont.

Bird, G.A., M. Stephenson, R. Roshon, W.J. Schwartz, and M. Motycka. 1995. Fate of ^{60}Co and ^{134}Cs added to the hypolimnion of a Canadian Shield lake. Can. J. Fish. Aquat. Sci. 52: 2276–2289.

Bower, P.M., C.A. Kelly, E.J. Free, J.A. Schearer, D.R. DeClercq, and D.W. Schindler. 1987. Simultaneous measurement of primary production by whole-lake and bottle radiocarbon additions. Limnol. Oceanogr. 32: 299–312.

Brunskill, G.J., and D.W. Schindler. 1971. Geography and bathymetry of selected lake basins, Experimental Lakes Area, northwestern Ontario. J. Fish. Res. Board Can. 28: 139–155.

Cleugh, T.R., and B.W. Hauser. 1971. Results of the initial survey of the Experimental Lakes Area, northwestern Ontario. J. Fish. Res. Board Can. 28: 129–137.

Cruikshank, D.R. 1984. Whole lake chemical additions in the Experimental Lakes Area, 1969–1983. Can. Data Rep. Fish. Aquat. Sci. No. 449.

Cushman, R.M. 1984. Chironomid deformities as indicators of pollution from a synthetic, coal-derived oil. Freshwater Biol. 14: 179–182.

Davies, B.R. 1976. The dispersal of Chironomidae larvae: a review. J. Entomol. Soc. South Afr. 39: 39–62.

Dermott, R.M. 1991. Deformities in larval *Procladius* spp. and dominant Chironomini from the St. Clair River. Hydrobiologia, 219: 171–185.

Dickman, M., I. Brindle, and M. Benson. 1992. Evidence of teratogens in sediments of the Niagara River watershed as reflected by chironomid (Diptera: Chironomidae) deformities. J. Gt. Lakes Res. 18: 467–480.

Evans, H.E., P.J. Smith, and P.J. Dillon. 1983. Anthropogenic zinc and cadmium burdens in sediments of selected southern Ontario lakes. Can. J. Fish. Aquat. Sci. 40: 570–579.

Findlay, D.L., and S.E.M. Kasian. 1987. Phytoplankton community responses to nutrient addition in Lake 226, Experimental Lakes Area, northwestern Ontario. Can. J. Fish. Aquat. Sci. 44(Suppl. 1): 35–46.

Hare, L., and J.C.H. Carter. 1976. The distribution of *Chironomus* (s.s)? *cucini* (*salinarius* group) larvae (Diptera: Chironomidae) in Parry Sound, Georgian Bay, with particular reference to structural deformities. Can. J. Zool. 54: 2129–2134.

Hart, D.R., J. Fitchko, M. Brinkman, and P.M. McKee. 1987. A biological indicator system to identify genotoxicity of in-place pollutants. *In* Proceedings Technology Transfer Conference. Part D. Analytical methods, Toronto, Ont., December 8–9, 1986. The Queen's Printers for Ontario, Toronto, Ont. pp. 167–188.

Heinis, F., K.R. Timmermans, and W.R. Swain. 1990. Short-term sublethal effects of cadmium on the filter feeding chironomid larva of *Glyptotendipes pallens* (Meigen) (Diptera). Aquat. Toxicol. 16: 73–86.

Hesslein, R.H. 1987. Whole-lake metal radiotracer movement in fertilized lake basins. Can. J. Fish. Aquat. Sci. 44(Suppl. 1): 74–82.

Hesslein, R.H., W.S. Broecker, and D.W. Schindler. 1980. Fates of metal radiotracers added to a whole lake: sediment–water interactions. Can. J. Fish. Aquat. Sci. 37: 378–386.

Janssens de Bisthoven, L.G.J., K.R. Timmermans, and F. Ollevier. 1992. The concentration of cadmium, lead, copper and zinc in *Chironomus* gr. *thummi* larvae (Diptera: Chironomidae) with deformed versus normal mentum. Hydrobiologia, 239: 141–149.

Linsey, G.A., D.W. Schindler, and M.P. Stainton. 1987. Atmospheric deposition of nutrients and major ions at the Experimental Lakes Area in northwestern Ontario, 1970 to 1982. Can. J. Fish. Aquat. Sci. 44(Suppl. 1): 206–214.

Malley, D.F., and P.S.S. Chang. 1991. Early observations on the zooplankton community of a Precambrian Shield lake receiving experimental additions of cadmium. Verh. Int. Ver. Theor. Angew. Limnol. 24: 2248–2253.

Malley, D.F., P.S.S. Chang, and R.H. Hesslein. 1989. Whole lake addition of cadmium-109: radiotracer accumulation in the mussel population in the first season. Sci. Total Environ. 87–88: 397–417.

Oliver, D.R., and M.E. Roussel. 1983. The insects and arachnids of Canada. Part II. The genera of larval midges of Canada. Diptera: Chironomidae. Publ. No. 1746. Biosystematics Research Institute, Agriculture Canada, Ottawa, Ont.

Pascoe, D., A.F. Brown, B.M.J. Evans, and C. McKavanagh. 1990. Effects and fate of cadmium during toxicity tests with *Chironomus riparius*: the influence of food and artificial sediment. Arch. Environ. Contam. Toxicol. 19: 872–877.

Rose, K.S.B. 1992. Lower limits of radiosensitivity in organisms, excluding man. J. Environ. Radioact. 15: 113–133.

Sæther, O.A. 1979. Chironomid communities as water quality indicators. Holarct. Ecol. 2: 65–74.

Schindler, D.W. 1988. Experimental studies of chemical stressors on whole lake ecosystems. Verh. Int. Ver. Theor. Angew. Limnol. 23: 11–41.

Shearer, J.A., E.J. Fee, E.R. DeBruyn, and D.R. DeClercq. 1987. Phytoplankton productivity changes in a small, double-basin lake in response to termination of experimental fertilization. Can. J. Fish. Aquat. Sci. 44(Suppl. 1): 47–54.

Stephenson, M., and G.L. Mackie. 1988. Total cadmium concentrations in the water and littoral sediments of central Ontario lakes. Water Air Soil Pollut. 38: 121–136.

Tennessen, K.J., and P.K. Gottfried. 1983. Variation in structure of ligula of Tanypodinae larvae (Diptera: Chironomidae). Entomol. News, 94: 109–116.

Timmermans, K.R., W. Peeters, and M. Tonkes. 1992. Cadmium, zinc, lead and copper in *Chironomus riparius* (Meigen) larvae (Diptera: Chironomidae): uptake and effects. Hydrobiologia, 241: 119–134.

Warwick, W.F. 1980*a*. Pasqua Lake, southeastern Saskatchewan: a preliminary assessment of trophic status and contamination based on the Chironomidae (Diptera). *In* Chironomidae: ecology, systematics, cytology and physiology. *Edited by* D.A. Murray. Pergamon Press, Oxford, U.K. pp. 255–267.

Warwick, W.F. 1980*b*. Palaeolimnology of the Bay of Quinte, Lake Ontario: 2800 years of cultural influence. Can. Bull. Fish. Aquat. Sci. No. 206.

Warwick, W.F. 1985. Morphological abnormalities of Chironomidae (Diptera) larvae as measures of toxic stress in freshwater ecosystems: indexing antennal deformities in *Chironomus* Meigen. Can. J. Fish. Aquat. Sci. 42: 1881–1914.

Warwick, W.F. 1988. Morphological deformities in Chironomidae (Diptera) larvae as biological indicators of toxic stress. *In* Toxic contaminants and ecosystem health; a Great Lakes focus. *Edited by* M.S. Evans. John Wiley and Sons, New York. pp. 281–320.

Warwick, W.F. 1990. Morphological deformities in chironomids (Diptera) larvae from the Lac St. Louis and Laprairie basins of the St. Lawrence River. J. Gt. Lakes Res. 16: 185–208.

Warwick, W.F. 1991. Indexing deformities in ligulae and antennae of *Procladius* larvae (Diptera: Chironomidae): application to contaminant-stressed environments. Can. J. Fish. Aquat. Sci. 48: 1151–1166.

Warwick, W.F., and N.A. Tisdale. 1988. Morphological deformities in *Chironomus*, *Cryptochironomus*, and *Procladius* larvae (Diptera: Chironomidae) from two differentially stressed sites in Tobin Lake, Saskatchewan. Can. J. Fish. Aquat. Sci. 45: 1123–1144.

Warwick, W.F., J. Fitchko, P.M. McKee, D.R. Hart, and A.J. Burt. 1987. The incidence of deformities in *Chironomus* spp. from Port Hope Harbour, Lake Ontario. J. Gt. Lakes Res. 13: 88–92.

Wiederholm, T. 1984. Incidence of deformed chironomid larvae (Diptera: Chironomidae) in Swedish lakes. Hydrobiologia, 109: 243–249.

PERSPECTIVE

Perspectives on the relationship between otolith growth and the conversion of isotope activity ratios to fish ages

Daniel K. Kimura and Craig R. Kastelle

Abstract: Ageing of fish otoliths using radiometric methods is now becoming widely accepted. Using this methodology, one has the choice of extracting otolith cores or modeling otolith mass growth. Modeling otolith growth forgoes the difficult work of extracting cores, but one is left with the nearly equally daunting task of selecting and validating an otolith growth model and deriving the corresponding decay equations. We note that the mathematical aspects of this problem appear to have been satisfactorily resolved. However, problems of interpretation remain, and it is not clear whether practitioners fully appreciate the sensitivity of their results to growth model selection and interpretation. We note that the two-stage linear growth model appears to be generally misapplied in the literature. Also, we present evidence that the process of using otolith growth curves estimated from annular ring counts to validate the method of counting annular rings can constitute circular reasoning. Although tedious work, extracting otolith cores seems the most valid way to avoid some serious problems in radiometric age determination work.

Résumé : La mesure de l'âge par les otolithes de poisson au moyen de méthodes radiométriques est de plus en plus répandue. Dans cette méthode, on peut choisir entre l'extraction du noyau de l'otolithe et la modélisation de la croissance de la masse de l'otolithe. Le recours au modèle de croissance de l'otolithe permet d'éviter le travail difficile que représente l'extraction du noyau, mais on se retrouve avec la tâche presque aussi accablante de choisir et de valider un modèle de croissance des otolithes, et d'en dériver les équations de décroissance correspondantes. Nous constatons que les aspects mathématiques de ce problème semblent résolus de façon satisfaisante. Toutefois, certains problèmes d'interprétation demeurent, et il n'est pas certain que les praticiens mesurent entièrement la sensibilité de leurs résultats au choix et à l'interprétation du modèle de croissance. D'après les documents consultés, le modèle de croissance linéaire en deux stades semble généralement appliqué d'un façon inadéquate. Nous montrons également que le procédé qui consiste à utiliser des courbes de croissance des otolithes estimées d'après le décompte des anneaux de croissance annuels pour valider la méthode de décompte des anneaux de croissance peut être un cercle vicieux. Bien qu'il s'agisse d'un travail fastidieux, l'extraction du noyau de l'otolithe semble le moyen le plus valable pour éviter de graves problèmes lors des travaux de détermination de l'âge par radiométrie.

[Traduit par la Rédaction]

Introduction

Radiometric validation of ages calculated from counting growth rings on otoliths has been described by Bennett et al. (1982), Campana et al. (1990), and Fenton and Short (1992). In general, otoliths are first separated into groups on the basis of presumed annular ring counts. Either the otolith's core (e.g., first year's, or first 5 years' growth) is removed by mechanical grinding, or the otoliths are analyzed whole. Subsequently, the activity ratio (^{210}Pb/^{226}Ra) is determined for each group of otoliths. These ratios are compared with curves expected on the basis of radioactive decay, which are solely a function of the age of each group.

The basic method of radiometric age determination we consider in this paper is based on the activity ratio of radioisotope pairs: usually ^{210}Pb/^{226}Ra is used, but ^{228}Th/^{228}Ra has also been used to age fish otoliths (Smith et al.

Received October 12, 1994. Accepted May 5, 1995.
J12601

D.K. Kimura and C.R. Kastelle. Alaska Fisheries Science Center, National Marine Fisheries Service, National Oceanic and Atmospheric Administration, 7600 Sand Point Way Northeast, Seattle, WA 98115-0070, U.S.A.

1991; Campana et al. 1993). Because nearly all radiometric fish work has used the ^{210}Pb/^{226}Ra isotope pair, we shall deal mainly with this case. The theory is not affected by using different radioisotope pairs, but the exponential decay constants appearing in the equations do change.

Since the earliest days of nuclear physics, nuclear decay has been known to be governed by the exponential decay law: $N^t = N^0 \exp(-\lambda t)$. Here, N^t is the number of atoms of the radioisotope in the sample at time t, $\lambda = \ln(2)/t_{1/2}$ is the exponential decay constant, and $t_{1/2}$ is the half-life of the radioisotope being considered. The analysis presented here considers implications of this basic law as they have been used to age fish otoliths. The introductory material is therefore classical; the new material is the equations describing the expected isotope ratio when whole otoliths are used for radiometric ageing. These equations derived by Bennett et al. (1982) and further refined by Campana et al. (1993) are fundamental, and we have used them as our basic tools of evaluation in this paper. Previously, there have been analogies to otolith growth published in radiometric applications to geology (e.g., Gascoyne and Schwarcz 1982).

The parent isotope ^{226}Ra ($t_{1/2}$ = 1600 years) is a Ca analog naturally incorporated into the fish otolith while it is growing. ^{226}Ra spontaneously decays through ^{210}Pb ($t_{1/2}$ = 22.3 years) as part of the ^{238}U decay chain. The activity ratio ^{210}Pb/^{226}Ra increases with the elapsed time between deposition and time of activity measurements and thus correlates with fish age. The curve describing this correlation, which we call the activity ratio curve, is the subject of this paper. The activity ratio curve is always dependent on the initial ratio (R_0) of ^{210}Pb/^{226}Ra in the material incorporated in the otolith as it is being formed. R_0 is generally unknown, but can often be inferred from the ratio of ^{210}Pb/^{226}Ra found in the youngest age group. Therefore, validation for the youngest age group is sometimes sacrificed in radiometric analysis. Because the age of the young group can often be determined by ancillary age determination methods (e.g., modal length analysis) other than that being validated, the potential for circularity in the age validation caused by estimating R_0 can be reduced. However, if whole otoliths rather than otolith cores are being used in the age validation, then the otolith mass growth curve must be known. This involves either a strong assumption concerning otolith growth, or the use of otolith growth data arrived at from direct ages (we use the term direct ages to mean the ages obtained from annular ring counts). The latter use of direct ages is again potentially circular when the goal is age validation.

The goal of this paper is to examine the validity of current methods to estimate fish ages from isotope activity ratios and in particular to address whether radiometric age validation based on the activity ratio curve constitutes circular reasoning when the direct ages being validated are themselves used to establish the activity ratio curve. We start by reviewing the derivation of decay equations that are currently being used to estimate radiometric ages in the literature. In a brief Results section, we compare results using these equations with selected results from the literature. We also explore the implication of using inaccurate ages when modeling otolith growth. In the Discussion section we review findings of significance from the previous sections and present some general statistical considerations and our principal conclusions.

Derivation of decay equations

Let N_1 and N_2 refer to the number of atoms of the parent and daughter isotopes present in the sample at some moment in time, and let λ_1 and λ_2 refer to their respective exponential decay constants. If the sample initially ($t = 0$) contains N_1^0, N_2^0 atoms of these isotopes, respectively, then the quantities of these isotopes found in the sample in the future are a function only of the time lapse since the sample was formed. This is an inescapable result of the exponential law of radioactive decay, in which radioactivity decreases exponentially with time: $N_1 = N_1^0 \exp(-\lambda_1 t)$ so that the activity level at time t must be $A_1 = -\mathrm{d}N_1/\mathrm{d}t = \lambda_1 N_1$. In fish otolith work, radioisotope activity is usually measured in (disintegrations per second) per gram of otolith.

Concerning the daughter isotope N_2, the differential equation governing its evolution is

$$[1] \qquad \begin{aligned} \frac{\mathrm{d}N_2}{\mathrm{d}t} &= \lambda_1 N_1 - \lambda_2 N_2 \\ &= \lambda_1 N_1^0 \exp(-\lambda_1 t) - \lambda_2 N_2 \end{aligned}$$

The solution to this differential equation was first given by Bateman (1910):

$$[2] \qquad N_2 = \left(\frac{\lambda_1}{\lambda_2 - \lambda_1}\right) N_1^0 \left(\exp(-\lambda_1 t) - \exp(-\lambda_2 t)\right) + N_2^0 \exp(-\lambda_2 t)$$

The validity of eq. 2 can be verified by differentiation and substitution into eq. 1. The activity ratio (A_2/A_1) at time t is calculated as

$$[3] \qquad \begin{aligned} \frac{A_2}{A_1} &= \frac{\lambda_2 N_2}{\lambda_1 N_1^0 \exp(-\lambda_1 t)} \\ &= \left(\frac{\lambda_2}{\lambda_2 - \lambda_1}\right)\left(1 - \exp\left(-(\lambda_2 - \lambda_1)t\right)\right) + R_0 \exp\left(-(\lambda_2 - \lambda_1)t\right) \end{aligned}$$

Here, $R_0 = (\lambda_2 N_2^0)/(\lambda_1 N_1^0)$ is the initial activity ratio, and t is the elapsed time since the sample was formed. Equation 3 is essentially identical to eq. 11 of Campana et al. (1993).

Equation 3 gives the relationship between the activity ratio and the elapsed time between core formation and the time of analysis, when otolith cores are used for radiometric ageing and otolith growth does not need to be taken into account. Here, we assume that the otolith core is formed instantaneously. Campana et al. (1990) were the first to use otolith cores in radiochemical assays, thus avoiding the need to model otolith growth. In the case where $\lambda_2 >> \lambda_1$ and $\lambda_1 \approx 0$, as is the case with ^{210}Pb/^{226}Ra, the equation simplifies to (Kastelle et al. 1994)

$$[4] \qquad A_2/A_1 = 1 - \exp(-\lambda_2 t) + R_0 \exp(-\lambda_2 t)$$

Material newly incorporated into the otolith core has the lowest activity ratio (R_0). As the material ages, the activity ratio of this material increases, approaching one asymptotically.

Fig. 1. Activity ratio curves assuming core and one-stage linear otolith growth (i.e., constant growth) models: (*a*) $R_0 = 0.0$; (*b*) $R_0 = 0.3$.

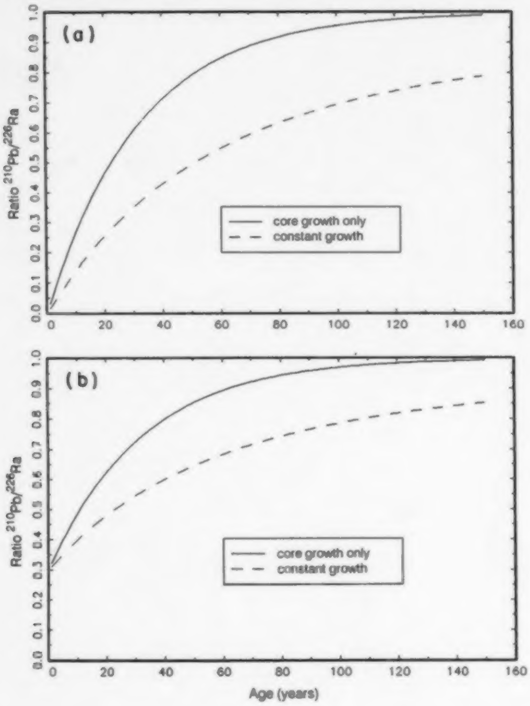

When whole otoliths are used, the continued growth and deposition of new material must be taken into account. Generally an otolith would be expected to show rapid growth when the fish is young, followed by slower growth especially following maturity. Two-stage linear growth and von Bertalanffy growth are two ways of describing the slowing of growth. If otolith growth slows with age, then relatively more of the otolith is older material, so for a given age the activity ratio in the whole otolith would be higher than if growth had not slowed. This means that for a given observed activity ratio (S_r), the predicted age would be lower than if growth had not slowed. If growth remained constant in an otolith, then relatively more of the material in the otolith would be young, which means that the activity ratio for a given age otolith would be lower than when growth slows, and the predicted age at a given observed activity ratio would be higher than when growth slows.

With the above argument in mind, we have two extreme scenarios for otolith growth. The first is the case in which the otolith completes growth in the first year, which would be unusual but is equivalent to the case when we take an otolith core. This maximizes the relative amount of older material found in an otolith. The second extreme case is the constant growth scenario, which for practical purposes maximizes the relative amount of young material found in an otolith. Therefore, for an observed S_r, the curves generated by using eqs. 4 and 10 (eq. 10 is derived later) bracket the possible age range for the otolith(s) (Fig. 1). Figure 1*a* is plotted assuming $R_0 = 0$, and Fig. 1*b* shows the shift in the *y*-axis intercept when $R_0 = 0.3$. R_0 describes the position of the *y*-axis intercept, and also the slope of the activity curve because this curve is bounded by one.

In their pioneering paper, Bennett et al. (1982) radiometrically aged *Sebastes diploproa* using whole otoliths. Because whole otoliths were used it was necessary to model the growth by the change in mass of the otolith to arrive at the expected isotope ratio at a given sample age. They recognized that the activity of the daughter product ^{210}Pb could be predicted for whole otoliths by integrating the product of the growth rate of the otolith, $G(t) = \mathrm{d}g(t)/\mathrm{d}t$, where $g(t)$ is some function describing the growth in mass of the otolith, with the Bateman equation. Bennett et al. (1982) examined models assuming one- and two-stage linear growth.

Campana et al. (1993) recognized an error in Bennett et al.'s (1982) paper and, in principle, all other papers modeling otolith growth in fisheries radiometric ageing and provided the corrected equations that we believe should be standard for whole fish otolith radiometric work:

$$[5] \qquad A_1 = \int_0^a G(t) A_1^{\,0} \exp(-\lambda_1(a-t))\, \mathrm{d}t$$

$$[6] \qquad A_2 = \int_0^a G(t)\left(A_1^{\,0}\left(\frac{\lambda_2}{\lambda_2-\lambda_1}\right)\left(\exp(-\lambda_1(a-t)) - \exp(-\lambda_2(a-t))\right) + A_2^{\,0}\exp(-\lambda_2(a-t))\right)\mathrm{d}t$$

In eqs. 5 and 6, a is a constant that represents the otolith age at the time of collection (i.e., capture). Campana et al.'s (1993) correction was to recognize that t should be $a - t$ in the exponential expressions in eqs. 5 and 6. The reason for this correction is that $a - t$ gives the proper period of decay for material laid down at any time t. For example, material laid down at time $t = 0$ has decayed a years at the time of otolith collection, and material laid down at time $t = a$ has not undergone any decay at the time of collection a.

In the following sections we derive the activity ratio curves for the principal otolith growth models that have been used in the literature.

One-stage linear growth

Campana et al. (1993) noted that the corrections given in eqs. 5 and 6 were inconsequential for the one-stage linear growth model (note that we often call this constant growth). We can easily verify this by assuming $G(t) \equiv G_0$ and performing the integration in eqs. 5 and 6, resulting in

$$[7] \qquad A_1 = \frac{G_0 A_1^{\,0}}{\lambda_1}(1-\exp(-\lambda_1 a))$$

$$[8] \qquad A_2 = G_0 A_1^{\,0}\left(\frac{\lambda_2}{\lambda_2-\lambda_1}\right)\left(\left(\frac{1}{\lambda_1}\right)(1-\exp(-\lambda_1 a)) - \left(\frac{1}{\lambda_2}\right)(1-\exp(-\lambda_2 a))\right) + G_0 A_2^{\,0}\left(\frac{1}{\lambda_2}\right)(1-\exp(-\lambda_2 a))$$

The activity ratio in this case becomes

$$[9]\qquad \frac{A_2}{A_1}=\left(\frac{\lambda_2}{\lambda_2-\lambda_1}\right)\left(1-\frac{\lambda_1(1-\exp(-\lambda_2 a))}{\lambda_2(1-\exp(-\lambda_1 a))}\right)+R_0\left(\frac{\lambda_1(1-\exp(-\lambda_2 a))}{\lambda_2(1-\exp(-\lambda_1 a))}\right)$$

If $\lambda_2 >> \lambda_1$ and $\lambda_1 \approx 0$, we can use the approximations $\lambda_2/(\lambda_2 - \lambda_1) \approx 1$ and $\exp(-\lambda_1 a) = 1 - \lambda_1 a$ to arrive at

$$[10]\qquad \frac{A_2}{A_1}=1-(1-R_0)\,\frac{(1-\exp(-\lambda_2 a))}{\lambda_2 a}$$

Note that the expected isotope ratio at age is not dependent on the actual value of G_0. Equation 10 is identical to Bennett et al.'s eq. 3 (1982) and is not affected by Campana et al.'s (1993) correction. This result is due to the symmetry assumed under the linear growth model.

Two-stage linear growth

Bennett et al. (1982) recognized that assuming constant otolith growth throughout the life of a fish would often prove to be too stringent an assumption. Therefore, they also considered a two-stage linear model in which growth was assumed to slow at some age a_1, usually the age at maturity. Assume a constant growth rate $G(t) = G_1$ up to some age a_1, which is then reduced to $G(t) = G_2$ from age a_1, up to the total age of the otolith, for instance age a. Using these constants in eqs. 5 and 6, we have, after integration and taking ratios, the following:

$$[11]\qquad \frac{A_2}{A_1}=\left(\frac{\lambda_2}{\lambda_2-\lambda_1}\right)\left(1-\left(\frac{\lambda_1}{\lambda_2}\right)\left(\frac{G_1\big(\exp(-\lambda_2(a-a_1))-\exp(-\lambda_2 a)\big)+G_2\big(1-\exp(-\lambda_2(a-a_1))\big)}{G_1\big(\exp(-\lambda_1(a-a_1))-\exp(-\lambda_1 a)\big)+G_2\big(1-\exp(-\lambda_1(a-a_1))\big)}\right)\right)$$
$$+R_0\left(\frac{\lambda_1}{\lambda_2}\right)\left(\frac{G_1\big(\exp(-\lambda_2(a-a_1))-\exp(-\lambda_2 a)\big)+G_2\big(1-\exp(-\lambda_2(a-a_1))\big)}{G_1\big(\exp(-\lambda_1(a-a_1))-\exp(-\lambda_1 a)\big)+G_2\big(1-\exp(-\lambda_1(a-a_1))\big)}\right)$$

For ages $t < a_1$, or when $G_1 = G_2$, eq. 11 becomes identical to eq. 9. The two-stage linear growth model is not dependent on the actual values of G_1 and G_2, but only on their ratio (G_2/G_1).

If $\lambda_2 >> \lambda_1$ and $\lambda_1 \approx 0$, we can again use the approximations $\lambda_2/(\lambda_2 - \lambda_1) \approx 1$ and $\exp(-\lambda_1 a) = 1 - \lambda_1 a$ to arrive at

$$[12]\qquad A_2/A_1$$
$$=\left(\frac{G_1 a_1}{M_a}\right)\left(1-(1-R_0)\left(\frac{(1-\exp(-\lambda_2 a_1))}{\lambda_2 a_1}\right)\exp(-\lambda_2(a-a_1))\right)$$
$$+\left(\frac{G_2(a-a_1)}{M_a}\right)\left(1-(1-R_0)\left(\frac{(1-\exp(-\lambda_2(a-a_1)))}{\lambda_2(a-a_1)}\right)\right)$$

where $M_a = G_1 a_1 + G_2(a - a_1)$ is the mass of otolith at age a. Equation 12 is identical to the expression derived by Bennett et al. (1982; see also Fenton and Short 1992). Because the results would be incorrect for the two-stage growth model without Campana et al.'s (1993) correction, it seems probable that Bennett et al. derived eq. 12 heuristically, rather than by direct integration of eqs. 5 and 6.

von Bertalanffy growth

The case of von Bertalanffy growth is covered by Campana et al. (1993). In this case, $G(t) = 3kW_\infty((1 - \exp(-k(t - t_0)))^2 - (1 - \exp(-k(t - t_0)))^3)$, and results can be obtained by integrating eqs. 5 and 6.

When using any otolith growth model, and time elapses between the completion of otolith growth and the time of radiometric analysis, the sample undergoes further radioactive decay. Campana et al. (1993) noted that this further decay, say t_p time units, should be governed by a slightly modified version of eq. 3:

$$[13]\qquad \frac{A_2}{A_1}=\left(\frac{\lambda_2}{\lambda_2-\lambda_1}\right)\big(1-\exp(-(\lambda_2-\lambda_1)t_p)\big)+R_a\exp\big(-(\lambda_2-\lambda_1)t_p\big)$$

Here, A_2/A_1 is now the activity ratio at time $a + t_p$, and R_a is the activity ratio at the end of growth (i.e., time a). Equation 13 is the appropriate equation to use if decay correction (i.e., estimating R_a) is desired.

The simplicity of eqs. 5 and 6 contrasts with the complexity of eq. 11 and Campana et al.'s (1993) results for the von Bertalanffy curve, suggesting that things might be simpler if we derive $G(t)$ and simply let the computer do the integrations in eqs. 5 and 6. This is the approach we used in this paper. However, when using numerical integration on the two-stage growth model, we provided continuity for $G(t)$ by connecting the points $(a_1 - 1, G_1)$, $(a_1, (G_1 + G_2)/2)$, and $(a_1 + 1, G_2)$ with a straight line. The period of transition, which is 2 years in our paper, can be adjusted to suit the desires of the modeler. Numerical integration should not introduce significant error into the results, but it will keep the analysis simple.

Generally, we will have measured some activity ratio (S_r) and know the elapsed time (t_p) between the cessation of growth and measurement of activity. The way we arrive at a fish age (a) depends on whether we made radiometric measurements on otolith cores or whole otoliths and, if we used whole otoliths, which growth model we assume. For otolith cores, the total age ($a + t_p$) of the sample is determined to be that t, such that the predicted activity ratio given by eq. 3 is equal to S_r. The age of the fish is then $a = t - t_p$. For whole otoliths, the age of the fish is that a, such that the predicted activity ratio at the end of growth ($R_a = A_2(a)/A_1(a)$), further decayed for time t_p

Table 1. A comparison of radiometric ages estimated using methods presented in this paper with those published by other authors.

Otolith growth model	Reference	Species	Radionuclide pair	t_p (years)	Ratio	Reported age (years)	Our age (years)	Initial ratio (R_0)	Growth parameters	Comments
Core	Campana et al. 1990	Redfish (*Sebastes mentella*)	$^{210}Pb/^{226}Ra$	0.0[a]	0.552 0.812	28 57	25.6 52.5	0.0		Assumed linear growth during 5-year core formation. Radiometric ages were not calculated, but we estimated ages from their Fig. 1.
	Campana et al. 1993	Flyingfish (*Hirundichthys affinis*)	$^{228}Th/^{228}Ra$	1.1	0.36	0.22	0.03	0.0		Initial ratio was not discussed in cited text, but it appears from the figures that the authors used $R_0 = 0.0$.
	Kastelle et al. 1994	Sablefish (*Anoplopoma fimbria*)	$^{210}Pb/^{226}Ra$	4.5	0.500 0.570	17.83 22.66	17.6 22.4	0.0		Used ^{226}Ra from individual measurements.
One-stage linear growth	Bennett et al. 1982	Splitnose rockfish (*Sebastes diploproa*)	$^{210}Pb/^{226}Ra$	0.0[b]	0.13	2.6	2.2	0.1		We used the following information from Bennett et al. (1982): $R_0 = 0.1$, ^{226}Ra from individual measurements, and estimated the age from their Fig. 4.
	Fenton et al. 1991	Orange roughy (*Hoplostethus atlanticus*)	$^{210}Pb/^{226}Ra$	0.0[b]	0.193 0.499 0.830	10.7 46.7 179	10.8 46.4 173.8	0.05		
Two-stage linear growth	Bennett et al. 1982	Splitnose rockfish (*Sebastes diploproa*)	$^{210}Pb/^{226}Ra$	0.0[b]	0.35 0.76	19 93	18.5 87.8	0.1	$a_1 = 12$ $G_2/G_1 = 0.42$ $a_1 = 14$ $G_2/G_1 = 0.30$	We used the following information from Bennett et al. (1982): $R_0 = 0.1$, ^{226}Ra from individual measurements, and estimated the age from their Figs. 5 and 6 (rounding to the nearest year).
	Fenton et al. 1991	Orange roughy (*Hoplostethus atlanticus*)	$^{210}Pb/^{226}Ra$	0.0[b]	0.499 0.830	47 94	40.4 136.7	0.05	$a_1 = 32$ $G_2/G_1 = 0.45$	
von Bertalanffy growth	Campana et al. 1993	Flyingfish (*Hirundichthys affinis*)	$^{228}Th/^{228}Ra$	0.23	0.28 0.14	1.04 0.45	1.04 0.45	0.0	$W_\infty = 40$ mm^3 $k = 0.0126$ d^{-1} $t_0 = 11.0$ d	Initial ratio was not discussed in cited text, but it appears from the figures that the authors used $R_0 = 0.0$. von Bertalanffy parameters used otolith volume as a proxy for otolith mass.

[a] The authors presented data in which the fish age included the time between capture and analysis.

[b] The authors presented activity data corrected to the time of capture.

Fig. 2. Comparison of activity ratio curves when $\bar{M}_{\mathrm{obs}}$ is substituted for M_a in eq. 12. For illustrative purposes we used data from orange roughy: G_1 = 3.94 mg/year, G_2 = 1.77 mg/year, a_1 = 32 year, and $\bar{M}_{\mathrm{obs}}$ = 224 mg (from Fenton et al. 1991).

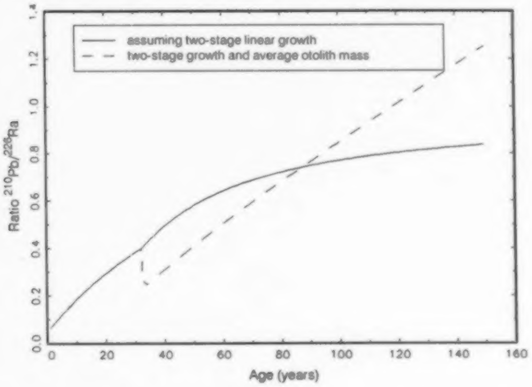

(using eq. 13), is equal to S_r. The numerical method of bisection was used to find the solution (Press et al. 1986).

The ratio of isotopes incorporated into the otolith, R_0, can be inferred from the youngest age group being radiometrically aged. Simply substitute the known age a in the above procedure and pick the R_0 that yields the observed S_r for the youngest age group. Depending on the method used to determine the age of this youngest group, we may forgo its radiometric validation.

Results

Predicting ages using the methods described above, from activity ratios previously published in other age validation papers, gives results both similar to and strikingly different from the ages previously reported (Table 1). We do not think that Campana et al.'s (1993) correction affected our results, because the activity ratio curves for the single- and two-stage linear growth models published by Bennett et al. (1982) were in fact correct. Most of the small differences can probably be attributed to interpolation of ages from published figures, decay correction methods, and approximations such as eq. 4 that are commonly used. The latter two suggest that standardization of methodology using methods described here (basically the methods of Campana et al. 1993) might be helpful. This method is mathematically exact and avoids the need for decay correction.

However, for the two-stage linear growth model the differences between our predicted ages and those presented in the literature are sufficient to cause alarm (Table 1; 94 versus 136.7 years). We feel that the problem stems from Bennett et al.'s (1982) interpretation of eq. 12. Although we agree with Bennett et al. (1982) on the form of eq. 12, it appears that they suggest substituting the observed mean sample otolith mass $\bar{M}_{\mathrm{obs}}$ for $M_a = G_1a_1 + G_2(a - a_1)$. We believe this to be incorrect. This is equivalent to assuming $\bar{M}_{\mathrm{obs}} = G_1a_1 + G_2(a - a_1)$, which may or may not be true. In fact a correct G_1 and G_2 can be estimated by solving the following simultaneous equations: $G_2/G_1 = c_0$ and $\bar{M}_{\mathrm{obs}} = G_1a_1 + G_2(a - a_1)$, where c_0 is a known constant. However, the resulting G_1 and G_2 estimates will give the same activity ratio curve as that assuming a value for a_1 and $G_2/G_1 = c_0$. The average mass of the otolith and the actual values of G_1 and G_2 are irrelevant in the two-stage linear growth model.

Fig. 3. Activity ratio curves assuming the two-stage linear otolith growth model. (*a*) Different ratios of G_2/G_1 for a fixed age at maturity a_1 = 32 years. (*b*) Different ages at maturity (a_1) for G_2/G_1 = 0.5.

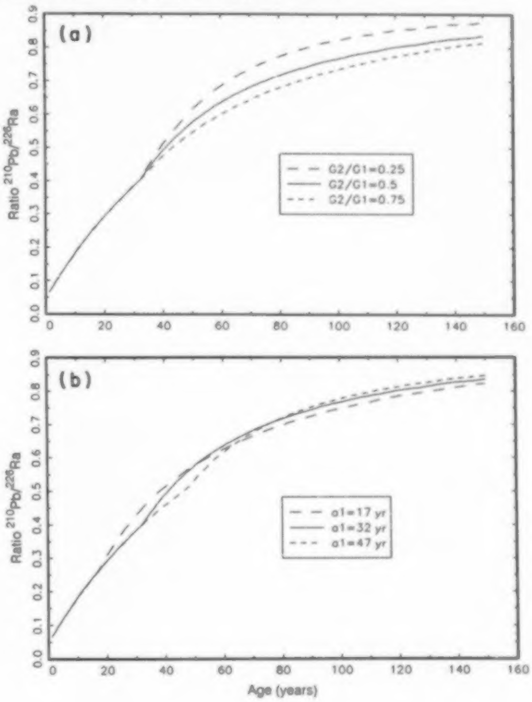

The activity ratio curve can be strongly distorted by substituting $\bar{M}_{\mathrm{obs}}$ for M_a (Fig. 2). This may be true even in the neighborhood where the two activity ratios coincide (i.e., that point where $\bar{M}_{\mathrm{obs}} = G_1a_1 + G_2(a - a_1)$). We cannot think of a valid argument for substituting $\bar{M}_{\mathrm{obs}}$ for M_a in eq. 12.

We provide two examples, based on the two-stage and von Bertalanffy growth models, showing how otolith growth curve assumptions can influence estimated radiometric ages. The two-stage growth model results are roughly based on the work by Fenton et al. (1991) on orange roughy (*Hoplostethus atlanticus*). These authors used an age of maturity of a_1 = 32 years, with G_2/G_1 = 0.45.

As stated earlier, the two-stage linear growth model (eq. 11) is not dependent on the actual values of G_1 and G_2, but only on their ratio (G_2/G_1). For a fixed age at maturity, the smaller the ratio, the more sharply the age versus activity ratio plot moves toward the core growth model (Fig. 3*a*). Figure 3*b* traces the two-stage linear growth model for different ages of maturity (i.e., ages where

Fig. 4. Fit of Pacific Ocean perch otolith growth data to the von Bertalanffy growth model (eq. 14). Estimated parameters were $W_\infty = 0.306$ mg, $k = 0.101$ years^{-1}, $t_0 = -5.76$ years.

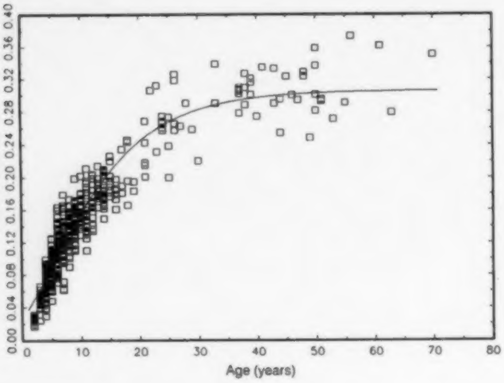

growth slows to $G_2/G_1 = 0.5$). Note that the curves representing different ages of maturity cross so that no single curve gives the youngest or oldest age for all observed activity ratios.

We analyzed otolith growth data for Pacific Ocean perch (*Sebastes alutus*) otolith growth data (Fig. 4), assuming the von Bertalanffy growth curve:

$$[14] \quad W_t = W_\infty(1 - \exp(-k(t - t_0)))^3$$

Parameters were estimated for eq. 14 using nonlinear least squares. The original age data (multiplier = 1.0) were then halved (multiplier = 0.5) and doubled (multiplier = 2.0) and the von Bertalanffy parameters reestimated. The resulting relationships between age and expected activity ratio for ^{210}Pb/^{226}Ra are shown in Fig. 5*a*. The same exercise was carried out for the translation of ages (±10 years), which is equivalent to shifting t_0 (±10 years in the opposite direction) (Fig. 5*b*). For all von Bertalanffy scenarios, when more growth occurred earlier in the life history, the activity ratio curve behaved as expected, resulting in lower predicted ages for a given isotope activity ratio (S_r). Adding 10 years to the growth data introduced an artifact in Fig. 4*b*, because the growth curve becomes negative at young ages. Integrating over only the domain of positive growth is equivalent to assuming zero growth at young ages, causing this S_r curve to fall below the constant growth curve.

Discussion

Unless otolith cores are used for radiometric ageing, otolith growth must be modeled. As shown in Fig. 1, much of the uncertainty in radiometric age determination is contained in the modeling of growth. This is an important reason for using otolith cores instead of whole otoliths.

However, otolith growth can be modeled simply by weighing otoliths that have been aged by counting presumed annuli and fitting the resulting data to a growth model. A problem arises if the direct ages determined by counting annuli are incorrect. Might the radiometric method validate an incorrect ageing method? We think this problem can best be considered as a classic hypothesis-testing problem in statistics. Under the null hypothesis, if the assumptions of the radiometric theory hold and the direct ages are correct, then the radiometric ages should compare well with the direct ages. Using statistical interpretation we cannot prove the null hypothesis but only report that it was not rejected. If something is in error with the radiometric theory, or the direct ageing method, one would hope that the null hypothesis will be rejected.

Fig. 5. Activity ratio curves assuming the von Bertalanffy otolith growth model. (*a*) The effect of halving (mult = 0.5) or doubling (mult = 2.0) the direct ages used to fit the otolith growth model. (*b*) The effect of subtracting or adding 10 years to the direct ages before fitting the von Bertalanffy model.

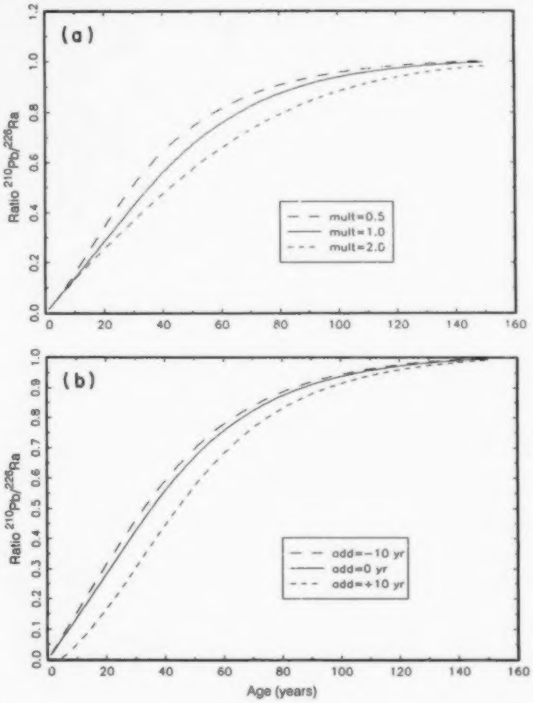

The question then becomes the following: does the radiometric method have statistical power sufficient to reject the null hypothesis when it is not true? What we do not wish to see is the same direction bias in direct and radiometric ages. That is, if direct ages are biased low, we do not want radiometric ages also to be biased low. This could lead to an undesirable false validation. In fact, the two-stage model (Fig. 3*b*) shows that when the assumed age at maturity is lowered, the predicted age can also be lowered.

Assuming von Bertalanffy otolith growth, a similar potential for false validation emerges. If we halve (double) the original age in the otolith growth data and refit the von Bertalanffy growth parameters, then the resulting radiometric ages will actually be younger (older) (Fig. 5*a*). Similarly, subtracting or adding 10 years to the growth data moves the radiometric age in the same direction (Fig. 5*b*). This suggests that biased direct ages would tend to be validated.

There appears to be a serious potential for circularity in radiometric age validation when otolith growth is being estimated using the method of direct ageing that is being validated. Also, it seems clear that radiometric ages from whole otoliths are very sensitive to the choice of growth model so that when whole otoliths are used for radiometric ageing, strong evidence should be provided to support the particular growth model that is used.

The preferable situation is to use otolith cores, because then the problem of modeling otolith growth is totally eliminated. As a result of the current study, our laboratory plans to base radiometric age validation on otolith cores. Also, when using otolith cores, one need worry less about the radiometric assumption that the specific activities of ^{226}Ra and ^{210}Pb in material incorporated into the otolith are constant (Kastelle et al. 1994).

Still, in some situations, there may be no alternative to using whole otoliths. For example, some species may have extremely tiny or fragile otoliths. Nevertheless, even for those species the radiometric method of age validation must be considered suspect unless the presumed otolith growth has a basis for support.

The effect of $R_0 > 0$ need not be minimal. This parameter has traditionally been estimated using a young group of fish whose ages are thought to be relatively well known. The role of R_0 in age validation is very much like the intercept in regression models, suggesting that R_0 be estimated using nonlinear regression and all of the radiometric data instead of just the youngest age group. For example, fit eq. 4 to the radiometric data. In this equation, t would be the direct ages, an independent variable; the observed activity ratios would be the dependent variable; and R_0 would be the parameter to be estimated. Such an approach will provide the best fit between observed and predicted activity ratios. Once R_0 is estimated, the radiometric ages can be estimated and compared with the direct ages. This method would seem to be most attractive when the radiometric ages compare well with the direct ages over all age groups. Use of the youngest age group offers an advantage in that often researchers believe that the youngest direct ages are the most accurate, and young ages can often be corroborated by ancillary ageing methods.

We have shown that the two-stage linear growth model has been generally misapplied in the literature. There does not appear to be a basis for substituting observed otolith mass into the activity ratio curve.

One reviewer took strong exception to our modeling of the otolith growth of Pacific Ocean perch by using the von Bertalanffy curve. This reviewer suggested that the correct growth curve is probably the two-stage linear growth model, hinting that our direct ageing shows too great a decrease in otolith growth. The reviewer's comments underscored the difficulty of arriving at an appropriate otolith growth curve on the basis of direct ages.

Following the journal's review of our paper, we became aware of the paper by West and Gauldie (1994). These authors conclude that radiometric age validation is invalid because of the possibility of ^{222}Rn emanating from the otoliths and the circularity involved with using otolith growth models based on direct ages. Although the present paper did not touch on the possible problem of ^{222}Rn emanation, we agree that further research needs to be done to test this hypothesis. It should be clear that we also agree with these authors that circularity is involved when estimating radiometric ages using otolith growth models based on direct ages.

Acknowledgments

We acknowledge the publications of our colleagues on which this paper is based. These pioneering papers brought us new applications of radiometric ageing methodology and showed how it could be useful, and without them we would not have radiometric fish age validation. We thank Dr. Steven Campana and an anonymous reviewer for some very helpful and insightful comments.

References

Bateman, H. 1910. Solution of a system of differential equations occurring in the theory of radioactive transformations. Proc. Cambridge Philos. Soc. Vol. 15.

Bennett, J.T., G.W. Boehlert, and K.K. Turekian. 1982. Confirmation of longevity in *Sebastes diploproa* (Pisces: Scorpaenidae) from ^{210}Pb/^{226}Ra measurements in otoliths. Mar. Biol. (Berlin), 71: 209–215.

Campana, S.E., K.C.T. Zwanenburg, and J.N. Smith. 1990. ^{210}Pb/^{226}Ra determination of longevity in redfish. Can. J. Fish. Aquat. Sci. 47: 163–165.

Campana, S.E., H.A. Oxenford, and J.N. Smith. 1993. Radiochemical determination of longevity in flying fish *Hirundichthys affinis* using ^{228}Th/^{228}Ra. Mar. Ecol. Prog. Ser. 100: 211–219.

Fenton, G.E., and S.A. Short. 1992. Fish age validation by radiometric analysis of otoliths. Aust. J. Mar. Freshwater Res. 43: 913–922.

Fenton, G.E., S.A. Short, and D.A. Ritz. 1991. Age determination of orange roughy, *Hoplostethus atlanticus* (Pisces: Trachichthyidae) using ^{210}Pb:^{226}Ra disequilibria. Mar. Biol. (Berlin), 109: 197–202.

Gascoyne M., and H.P. Schwarcz. 1982. Carbonate and sulphate precipitates. *In* Uranium series disequilibrium: applications to environmental problems. *Edited by* M. Ivanovich and R.S. Harmon. Oxford University Press, New York. pp. 268–301.

Kastelle, C.R., D.K. Kimura, A.E. Nevissi, and D.R. Gunderson. 1994. Using ^{210}Pb/^{226}Ra disequilibria for sablefish, *Anoplopoma fimbria*, age validation. Fish. Bull. 92: 292–301.

Press, W.H., B.P. Flannery, S.A. Teukolsky, and W.T. Vetterling. 1986. Numerical recipes (the art of scientific computing). Cambridge University Press, Cambridge, U.K.

Smith, J.N., R. Nelson, and S.E. Campana. 1991. The use of ^{210}Pb/^{226}Ra and ^{228}Th/^{228}Ra dis-equilibria in the ageing of otoliths of marine fish. *In* Radionuclides in the study of marine processes. *Edited by* P.J. Kershaw and D.S. Woodhead. Elsevier Applied Science, New York. pp. 350–359.

West, I.F., and R.W. Gauldie. 1994. Determination of fish age using ^{210}Pb : ^{226}Ra disequilibrium methods. Can. J. Fish. Aquat. Sci. 51: 2333–2340.

ERRATUM

Erratum: Density-dependent survival as a function of size in juvenile salmonids in streams

Elizabeth A. Marschall and Larry B. Crowder

Ref.: Can. J. Fish. Aquat. Sci. 52: 136–140 (1995).

In the Model comparison section on page 137, the correct relationship between m (mass in g) and FL (fork length in cm) is

$$m = 0.0117\ (FL)^{3.03}$$

(Grant and Kramer 1990). Then the correct relationship to convert between ℓ (total length in cm) and m is

$$m = 0.0107\ell^{3.03}$$

Finally, the relationship between ℓ and n_F (density of age-0 fish in the food-limitation model) is

$$n_F = \rho_F F \frac{1}{\alpha}(0.0107\ell^{3.03)^{-\beta}} = \rho_F F \cdot 823\ell^{-2.33}$$

such that, when we assume $\rho_F = 1$,

$$\log(n_F) = \log(823F) - 2.33\ \log(\ell)$$

These corrections cause no further changes and do not affect the printed final equation describing n_F as a function of ℓ.

Received at NRC September 13, 1995.
J12630

E.A. Marshall. Department of Zoology, 1735 Neil Avenue, Ohio State University, Columbus, OH 43210, U.S.A.
L.B. Crowder.[1] Department of Zoology, North Carolina State University, Raleigh, NC 27965-7617, U.S.A.

[1] Present address: Duke University Marine Lab, 135 Duke Marine Lab Road, Beaufort, NC 28516-9721, U.S.A.

Can. J. Fish. Aquat. Sci. **52**: 2304 (1995). Printed in Canada / Imprimé au Canada

ANNOUNCEMENTS / ANNONCES

Ecohydraulics 2000

The second international symposium on hydraulics and habitats of the International Association for Hydraulic Research (IAHR) will be held at Hotel Loews Le Concorde in Quebec City, Canada, from June 11 to 14, 1996. All communications are to be presented in either English or French; bi-directional simultaneous translation will be provided for all lectures.

The main objective of the symposium is to make available new scientific knowledge, state of the art analysis tools and advantageous technical solutions to prevent or limit the negative impacts that hydraulic works could have on aquatic fauna and habitats.

For more information, please contact:

Secretariat Ecohydraulics 2000
M. Ronald Greendale
c/o INRS-Eau
2800 Einstein Street
P.O. Box 7500
Ste.Foy (Québec)
Canada G1V 4C7
Tel.: (418) 654-3822, Fax: (418) 654-2600
E-Mail: Greendro@inrs-eau.uquebec.ca

Écohydraulique 2000

Le deuxième symposium international sur l'hydraulique et les habitats, de l'Association International de Recherches en Hydrauliques (AIRH), sera tenu à l'hôtel Loews Le Concorde, à Québec, Canada, du 11 au 14 juin 1996. Les présentations seront faites en français on en anglais; la traduction simultanée bi-directionnelle sera offerte pour toutes les communications orales.

L'objectif du symposium est de partager des connaissances, des outils d'analyse et des solutions techniques avantageuses pour prévenir ou atténuer les impacts négatifs des interventions hydrauliques sur la faune et les habitats aquatiques.

Pour de plus amples informations, veuillez communiquer avec :

Secrétariat Écohydraulique 2000
M. Ronald Greendale
a/s INRS-Eau
2800 rue Einstein
C.P. 7500
Sainte-Foy (Québec)
Canada G1V 4C7
Tél.: (418) 654-3822, Fax: (418) 654-2600
Courrier électronique : Greendro@inrs-eau.uquebec.ca

Back in 1869,
it took a great deal of ingenuity
to get your picture in the paper.

Before 1869, it was literally impossible to get your picture in the paper no matter how famous, infamous, or accomplished you were. It was then that Canadian Georges-Édouard Desbarats (ironically, not shown here) invented the revolutionary halftone photographic printing process, still being used today.

It is this sort of ingenuity and innovation that the Manning Awards have been recognizing and honouring for over 14 years. Awards range from the $5,000 Innovation Award to the $100,000 Principal Award.

So regardless of how big or small your innovations are (the IMAX film system was invented by a Canadian, as was the zipper), we encourage you to submit them. And who knows, you may even get your picture in the paper.

To receive a nomination form or further information, please call or write:
The Manning Awards, 3900, 421 - 7 Avenue S.W., Calgary, Alberta T2P 4K9
Telephone: (403) 266-7571, Fax: (403) 266-8154
Or visit us on the Internet at: http://www.manningawards.ca
Nominations close February 15 of each year.

PRIX MANNING
MANNING AWARDS

OUR RESEARCH JOURNALS SPEAK VOLUMES

Scientific journals shouldn't simply meet a researcher's expectations... they should *exceed* them!

The National Research Council of Canada (NRC) is Canada's leading *international* scientific press. We publish 14 scientific and technical journals — filled with the latest research studies, discoveries and reviews from around the world.

Readers will appreciate the high standard of quality and credibility. The journals have achieved an international reputation in the fields of physical sciences, engineering, biomedical and life sciences.

Keep your researchers at the forefront of their disciplines. Subscribe to NRC Research Journals, today.

For a complete list of titles and subscription information, contact:

NRC Research Press, National Research Council of Canada
Montreal Road, Ottawa, Canada K1A 0R6
Tel: (613) 993-9085, Fax: (613) 952-7656, or E-mail: research.journals@nrc.ca

To access our complete catalogue online:

World Wide Web site: http://www.cisti.nrc.ca/journals/rj.html

NRC·CNRC

National Research Council Canada
Conseil national de recherches Canada

Canada

NOS REVUES SCIENTIFIQUES NE MANQUENT PAS DE VOLUME

Les périodiques scientifiques ne doivent pas simplement répondre aux attentes des chercheurs et chercheuses, ils doivent les *surpasser*.

Le Conseil national de recherches du Canada (CNRC) est le plus important éditeur canadien de publications scientifiques *internationales*. Nous publions 14 revues scientifiques et techniques, qui rendent compte des plus récentes études, découvertes et synthèses savantes du monde entier.

Nos lecteurs apprécient nos normes élevées de qualité ainsi que notre crédibilité. Nos revues scientifiques jouissent d'une solide réputation à l'échelle mondiale dans les domaines des sciences physiques, du génie, ainsi que des sciences biomédicales et de la vie.

Vos scientifiques se doivent de rester au fait du progrès dans leur discipline. Facilitez-leur la tâche : abonnez-vous aux Revues scientifiques du CNRC dès aujourd'hui.

Pour obtenir une liste complète de nos titres ainsi que des renseignements quant à l'abonnement, communiquez avec :

Presses scientifiques du CNRC, Conseil national de recherches Canada
Chemin Montréal, Ottawa, Canada K1A 0R6
Téléphone : (613) 993-9085 Télécopieur : (613) 952-7656
Internet : research.journals@nrc.ca

Accès à notre catalogue en direct sur le World Wide Web :

http://www.cisti.nrc.ca/journals/rj.html

CNRC·NRC

Conseil national de recherches Canada
National Research Council Canada

Canada

1996
Annual Subscription Rates / Abonnements annuels[*][†][‡]

Publication	Volume	Code	Canada ($CAN) Institutional/ Collectif (CI)	Canada ($CAN) Personal/ Personnel (CP)	Foreign / Étranger ($US) Institutional/ Collectif (FI)	Foreign / Étranger ($US) Personal/ Personnel (FP)	Foreign / Étranger ($US) Airmail / Par avion Add / ajouter
Monthly / Mensuelle							
Canadian Journal of Botany / Revue canadienne de botanique	74	45	475	176	475	186	150
Canadian Journal of Chemistry / Revue canadienne de chimie	74	46	545	172	545	182	150
Canadian Journal of Earth Sciences / Revue canadienne des sciences de la Terre	33	47	455	152	455	162	150
Canadian Journal of Fisheries and Aquatic Sciences / Journal canadien des sciences halieutiques et aquatiques	53	261	419	154	419	164	150
Canadian Journal of Forest Research / Revue canadienne de recherche forestière	26	54	420	155	420	165	75
Canadian Journal of Microbiology / Revue canadienne de microbiologie	42	48	320	128	320	138	75
Canadian Journal of Physics / Revue canadienne de physique	74	49	325	108	325	118	75
Canadian Journal of Physiology and Pharmacology / Revue canadienne de physiologie et pharmacologie	74	50	390	142	390	152	75
Canadian Journal of Zoology / Revue canadienne de zoologie	74	51	515	188	515	198	150
Bimonthly / Bimestrielle							
Biochemistry and Cell Biology / Biochimie et biologie cellulaire	74	44	265	98	265	108	75
Canadian Journal of Civil Engineering / Revue canadienne de génie civil	23	52	330	110	330	120	75
Genome / Génome	39	70	300	120	300	130	75
Canadian Geotechnical Journal / Revue canadienne de géotechnique	33	53	259	104	259	114	50
Quarterly / Trimestrielle							
Environmental Reviews/ Dossiers environnement	4	244	170	68	170	74	25

[*] Price of regular single issues of all journals: institutional, $60.00; personal, $25.00. Special issues and supplements will be individually priced. For all orders outside Canada, rates are in U.S. dollars. / Prix des numéros réguliers de toutes les revues : collectif, 60,00 $; personnel, 25,00 $. Les prix varient pour les numéros spéciaux et les suppléments. Pour les commandes de l'étranger, les tarifs sont en dollars américains.

[†] Rates include second-class postage. Canadian customers please include additional 7% GST (GST No. R121491807). In Quebec please add a further 6.5% QST to the total price including GST (QST No. 1006178088). / Affranchissement de deuxième classe compris. Clients canadiens veuillez ajouter 7% pour la TPS (No de TPS R121491807). Au Québec veuillez ajouter un 6,5% de plus pour la TVQ au montant total incluant la TPS (No de TVQ 1006178088).

[‡] Special rates apply for members of Canadian scientific and engineering societies if they subscribe through their respective societies. / Les tarifs spéciaux sont offerts aux membres des sociétés scientifiques et des sociétés de génie au Canada, s'ils s'abonnent par l'intermédiaire de leur société respective.

Subscriptions, renewals, requests for single or back numbers, and all remittances should be sent to Subscription Office, NRC Research Press, National Research Council Canada, Ottawa, ON K1A 0R6, Canada. Remittances should be made payable to the Receiver General for Canada, credit National Research Council of Canada.
Enquiries: Helen Goulet: 613-993-9084; Fax No.: 613-952-7656; E-mail: research.journals@nrc.ca.

Subscriptions are entered for the calendar year. There are no refunds on cancelled subscriptions once delivery has begun.

Change of address - Send change of address information (complete old address, customer code, and new address) to Subscription Office, NRC Research Press, National Research Council Canada, Ottawa, ON K1A 0R6, Canada.

Claims for missing numbers should be made within four months (North America) or six months (outside North America) following the date of publication. The publisher expects to supply missing numbers only when losses have been sustained in transit and when the reserve stock will permit.

Abonnements - Pour toutes les questions d'abonnements, paiements, demandes de vieux numéros de la revue, etc., on doit s'adresser au Bureau d'abonnements, Presses scientifiques du CNRC, Conseil national de recherches Canada, Ottawa, ON K1A 0R6, Canada. Les chèques et mandats seront formulés à l'ordre du Receveur général du Canada, au crédit du Conseil national de recherches du Canada.
Renseignements : Helen Goulet : 613-993-9084; N° de télécopieur : 613-952-7656 ; Courrier électronique : research.journals@nrc.ca.

La durée des abonnements correspond à l'année civile. Les abonnements annulés ne pourront être remboursés une fois que le premier numéro sera envoyé.

Changement d'adresse - Faire parvenir tous renseignements (ancienne adresse, code du client et nouvelle adresse) au Bureau d'abonnements, Presses scientifiques du CNRC, Conseil national de recherches Canada, Ottawa, ON K1A 0R6, Canada.

Les réclamations de numéros manquants doivent être adressées dans les quatre mois (en Amérique du Nord) ou les six mois (à l'étranger) suivant la date de publication. L'éditeur s'engage à remplacer les numéros manquants seulement lorsque les pertes ont été subies en transit et lorsque ses réserves le permettent.

Tor Næsje, Bror Jonsson, and Jostein Skurdal	**2190–2196**	Spring flood: a primary cue for hatching of river spawning Coregoninae
Richard S. Stemberger	**2197–2210**	Pleistocene refuge areas and postglacial dispersal of copepods of the northeastern United States

25TH ANNIVERSARY OF THE EXPERIMENTAL LAKES AREA

25° ANNIVERSAIRE DE LA RÉGION DES LACS EXPÉRIMENTAUX

D.M. Rosenberg, R.E. Hecky, and P. Campbell	**2211–2212**	Introduction to contaminants research at the Experimental Lakes Area
Craig J. Allan	**2213–2228**	Hydrochemical response of upland Precambrian Shield catchments to additions of H_2SO_4 and NH_4NO_3 during snowmelt
David M. Rosenberg, Allen P. Wiens, Bohdan Bilyj, and Llwellyn Armstrong	**2229–2237**	Experimental acidification of a poor fen in northwestern Ontario: effects on emergence of Chironomidae (Diptera)
Michael A. Turner, David W. Schindler, David L. Findlay, Michael B. Jackson, and Gordon G.C. Robinson	**2238–2250**	Disruption of littoral algal associations by Experimental Lake acidification
Michael A. Turner, E. Todd Howell, Gordon G.C. Robinson, John F. Brewster, Leif J. Sigurdson, and David L. Findlay	**2251–2263**	Growth characteristics of bloom-forming filamentous green algae in the littoral zone of an experimentally acidified lake
Michael A. Turner, Gordon G.C. Robinson, Bruce E. Townsend, Brenda J. Hann, and John A. Amaral	**2264–2275**	Ecological effects of blooms of filamentous green algae in the littoral zone of an acid lake
G.A. Bird, M. Stephenson, R. Roshon, W.J. Schwartz, and M. Motycka	**2276–2289**	Fate of ^{60}Co and ^{134}Cs added to the hypolimnion of a Canadian Shield lake
G.A. Bird, M.J. Rosentreter, and W.J. Schwartz	**2290–2295**	Deformities in the menta of chironomid larvae from the Experimental Lakes Area, Ontario

PERSPECTIVE

Daniel K. Kimura and Craig R. Kastelle	**2296–2303**	Perspectives on the relationship between otolith growth and the conversion of isotope activity ratios to fish ages

ERRATUM

Elizabeth A. Marschall and Larry B. Crowder	**2304**	Erratum: Density-dependent survival as a function of size in juvenile salmonids in streams

National Research Council Canada
Ottawa, Canada
K1A 0R6

Conseil national de recherches Canada
Ottawa, Canada
K1A 0R6

Canadian Journal of Fisheries and Aquatic Sciences

Journal canadien des sciences halieutiques et aquatiques

Volume 52, Number 10, October 1995

Volume 52, numéro 10, octobre 1995

ARTICLES

Jon T. Schnute and Laura J. Richards	**2063–2077**	The influence of error on population estimates from catch-age models
G.T. Ankley, M.K. Schubauer-Berigan, and P.D. Monson	**2078–2083**	Influence of pH and hardness on toxicity of ammonia to the amphipod *Hyalella azteca*
Janine Gibert, Pierre Marmonier, Vladimir Vanek, and Sandrine Plénet	**2084–2097**	Hydrological exchange and sediment characteristics in a riverbank: relationship between heavy metals and invertebrate community structure
Robert W. Hannah, Stephen A. Jones, and Michele R. Long	**2098–2107**	Fecundity of the ocean shrimp (*Pandalus jordani*)
Adrian P. Spidle, Edward L. Mills, and Bernie May	**2108–2119**	Limits to tolerance of temperature and salinity in the quagga mussel (*Dreissena bugensis*) and the zebra mussel (*Dreissena polymorpha*)
J. Bruce Wallace, Jackson R. Webster, and Judith L. Meyer	**2120–2137**	Influence of log additions on physical and biotic characteristics of a mountain stream
Ming Tang and Daniel Boisclair	**2138–2145**	Relationship between respiration rate of juvenile brook trout (*Salvelinus fontinalis*), water temperature, and swimming characteristics
David J. Rowan, Joseph B. Rasmussen, and Jacob Kalff	**2146–2158**	Optimal allocation of sampling effort in lake sediment studies
T. Hesthagen, O. Hegge, J. Skurdal, and B.K. Dervo	**2159–2167**	Differences in habitat utilization among native, native stocked, and non-native stocked brown trout (*Salmo trutta*) in a hydroelectric reservoir
Judith S. Weis and Peddrick Weis	**2168–2173**	Swimming performance and predator avoidance by mummichog (*Fundulus heteroclitus*) larvae after embryonic or larval exposure to methylmercury
Josh Korman, Randall M. Peterman, and Carl J. Walters	**2174–2189**	Empirical and theoretical analyses of correction of time-series bias in stock-recruitment relationships of sockeye salmon (*Oncorhynchus nerka*)

Continued on inside back cover / Suite au verso

Canada

Printed in Canada by / Imprimé au Canada par
University of Toronto Press, Inc.
Typesetting by / Typographie par
Aubut & Nadeau Services Inc.

0706-652X(199510)52:10;1-2